ESCUELA DE DOCTORADO
INTERNACIONAL DE LA USC

Xandro
Vidal Pereira

Tesis doctoral

Azaheterocycles through Pd(II)-catalyzed formal cycloadditions involving C–H activation

Santiago de Compostela, 2022

Programa de doctorado en Ciencia y Tecnología Química

TESIS DE DOCTORADO

AZAHETEROCYCLES THROUGH Pd(II)–CATALYZED FORMAL CYCLOADDITIONS INVOLVING C–H ACTIVATION

Xandro Vidal Pereira

ESCUELA DE DOCTORADO INTERNACIONAL DE LA UNIVERSIDAD DE SANTIAGO DE COMPOSTELA

PROGRAMA DE DOCTORADO EN CIENCIA Y TECNOLOGÍA QUÍMICA

SANTIAGO DE COMPOSTELA

AÑO 2022

DECLARACIÓN DEL AUTOR DE LA TESIS

AZAHETEROCYCLES THROUGH Pd(II)–CATALYZED FORMAL CYCLOADDITIONS INVOLVING C–H ACTIVATION

D. Xandro Vidal Pereira

Presento mi tesis, siguiendo el procedimiento adecuado al Reglamento, y declaro que:

1) *La tesis abarca los resultados de la elaboración de mi trabajo.*
2) *En su caso, en la tesis se hace referencia a las colaboraciones que tuvo este trabajo.*
3) *La tesis es la versión definitiva presentada para su defensa y coincide con la versión enviada en formato electrónico.*
4) *Confirmo que la tesis no incurre en ningún tipo de plagio de otros autores ni de trabajos presentados por mí para la obtención de otros títulos.*

En **Santiago de Compostela**, **27 de enero de 2022**

Firmado

Xandro Vidal Pereira

AUTORIZACIÓN DEL DIRECTOR / TUTOR DE LA TESIS

Azaheterocycles through Pd(II)-catalyzed formal cycloadditions involving C–H activation

D. José Luis Mascareñas Cid y D. Moisés Gulías Costa
En condición de: Tutor y director En condición de: Director

INFORMAN:

Que la presente tesis, se corresponde con el trabajo realizado por D. Xandro Vidal Pereira, bajo mi dirección/tutorización, y autorizo su presentación, considerando que reúne los requisitos exigidos en el Reglamento de Estudios de Doctorado de la USC, y que como director de esta no incurre en las causas de abstención establecidas en la Ley 40/2015.

De acuerdo con lo indicado en el Reglamento de Estudios de Doctorado, declara también que la presente tesis doctoral es idónea para ser defendida en base a la modalidad de Monográfica con reproducción de publicaciones, en los que la participación del doctorando fue decisiva para su elaboración y las publicaciones se ajustan al Plan de Investigación.

En Santiago de Compostela, 28 de enero de 2022

El modo de dar una vez en el clavo

es dar cien veces en la herradura

-Miguel de Unamuno

Agradecimientos

Me gustaría empezar dando las gracias a mis directores de tesis por todo el apoyo que me han brindado a lo largo de estos casi seis años en el grupo. Gracias, José Luis, por haber hecho posible el que pudiese hacer ciencia en un grupo de investigación puntero en el mundo sin tener que salir, no ya de España, sino de Galicia. Lo que has construido a lo largo de tantos años merece, y mucho, la pena. Gracias, Moisés, por todos los proyectos en los que me has incluido, por todas las discusiones fructíferas, las buenas ideas y, como no, las charlas distendidas sobre tantos temas. Gracias a los dos, pues sin vosotros, esta tesis no hubiese sido posible.

Agradezco al programa FPU (2016) del Ministerio de Universidades por haber financiado mi contrato de tesis doctoral y mi estancia de tres meses en la Universidad de Estocolmo.

I would like to thank Prof. Abraham Mendoza for giving me the opportunity of being part of his research group in Stockholm during my brief stay. I would also like to thank Rajdip, Stefanie, Stefano, and, of course, Matteo (one of the most prepared PhD candidates that I have ever seen), for the warm welcome in the group. Also, thanks to Vivek, Sam, Prabodha and Sneha for showing me the wonders of Indian cuisine.

La química ha definido mi vida desde que era un renacuajo. De niño observaba embobado el material de laboratorio, perteneciente a mi tío Roberto, que reposaba en una estantería alta de casa de mis abuelos. Mis padres, buenos observadores, me compraron un juego de química con el que me pasaba horas y horas practicando. Tanta era mi pasión por la química que memoricé la tabla periódica a los diez años, e incluso acabe llevando experimentos de química a mi clase de primaria para hacerlos delante de mis compañeros. En el instituto soñaba con ser químico, y apenas tuve dudas de qué carrera quería estudiar. Durante la carrera, soñaba con ser investigador, ayudar a la humanidad descubriendo algo nuevo, y, la verdad, nunca me planteé que significaba un doctorado hasta que estuve metido de lleno en él.

El Xandro que entró con el programa de *Summer Fellowships* del CiQUS allá por el verano de 2016 dista bastante del Xandro que escribe estas palabras. Durante estos casi seis años trabajando en el P3L3 no solo he investigado, sino también he crecido como persona. Un doctorado es aprender a conocerse a uno mismo, disfrutar de los éxitos personales, compartir los momentos (buenos y malos) con tus compañeros, viajar a un país extranjero a hacer una estancia mientras descubres otra cultura, y, sobre todo, sentir que cuando descubres algo nuevo, eres la primera persona en hacerlo. Sin embargo, un doctorado también es un reto personal y profesional. Durante este tiempo he aprendido a lidiar con la frustración, con la autoexigencia, con los plazos y también con la perspectiva de un futuro incierto. En resumen, un doctorado es una auténtica lección de vida, pero afortunadamente, una lección compartida.

Gracias a todos los que habéis compartido esta etapa conmigo. Borja, gracias por los buenos momentos y por transmitir orden y cordura al P3L3 cuando se ha necesitado (y se ha necesitado). José Manuel, gracias por reinfundirme esa pasión por la química cuando empezaba a decaer. Edu, siempre *trancuilo*, con clase y buen compañero, gracias por estar ahí cuando lo he necesitado. Ricardo, eterno despistado, tu buen humor y positivismo me han animado más de una vez. Andy, tienes el alma traviesa, a veces demasiado, pero reconozco que también un buen corazón. Alex, mi vecino de vitrina, espero compartir alguna otra partida de ajedrez contigo. Andrés, pocas personas tan positivas he conocido nunca, gracias por transmitir ese buen rollo y echar broncas cuando es necesario, gracias por todas las tardes de juegos de mesa y charlas de videojuegos. Lara V., gracias por todos los momentos compartidos, charlas agradables y buenos consejos. Xuli, Cinzia, Fernando, Alejandro, Soraya, Dani, Ana, Sara y los

demás “cañitas”, gracias por amenizarme el congreso de Alcalá. Fue magnífico. Marc, gracias por las discusiones de química. Iván, buena suerte con la tesis, que sé que a veces puede atragantarse. Joan, compartir el período de escritura contigo ha sido un placer, gracias por descubrirme Måneskin. María Rey y Adrián, gracias por organizar el grupo de forma tan eficiente (y aguantarnos, que se dice pronto). Sin vosotros, el grupo no funcionaría, sois realmente imprescindibles. Gracias también a Fernando López, María Tomás, Pablo, Sergio, Rebeca, Natalia, Arcadio, Mencha y siento si me he dejado a alguien en el tintero.

Y cómo olvidarme de los que ya han volado del grupo a nuevos horizontes. Ronald, gracias por tu infinito saber de síntesis orgánica, por tus fascinantes historias sobre Chile y por cohesionar el grupo. Noelia, gracias por iniciarme en el P3L3 durante las becas de verano. Felipe, gracias por tu compañía y buenas anécdotas. Iván V., gracias por ser el DJ oficial del P3L3 tanto tiempo. David F., gracias por recordarme la importancia del gallego en la ciencia. Marcote, gracias por tantas y buenas risas y por tu gran lista de reproducción de Spotify. Catarina, mi compañera de vitrina con más *mau feitio*, gracias por los buenos momentos. Gracias también a Paolo, Cibrán, Renata, Jaime, Miguel, José, Cristian, Ramón, Marta y, de nuevo, siento si me olvido de alguien.

Agradecer también a todos aquellos que me habéis acompañado en mi período de tesis. Dicen que los buenos amigos son los que traspasan la criba del tiempo, y casi cinco años dan para mucho. Gracias, Adán, Maló y Pablo, por incontables “juegues” (y “miércogues”) de mesa y por hacerme sonreír al menos un poquito en los malos momentos (y mucho más en los buenos). Gracias, Alba, por escuchar mis movidas y brindarme muy buenos consejos. Gracias a “los buenos” (Eloy, Sonia, David, Henar, Andrés, Nuria, Pablo, Teresa, Nerea) pues, aunque con tantas responsabilidades cuesta juntarnos todos, lo acabamos haciendo (y ya son muchos años haciéndolo). Gracias a mi equipo de Quidditch (Lucus Centauri) y particularmente a su núcleo duro (Ana, Andrés, Eli, Cecilia y Albert) por haber estado ahí estos casi cinco años, compartiendo tantos momentos vitales, alegrías y derrotas, y en definitiva enseñarme lo que es pertenecer a un equipo (*we all we got, we all we need*). Ana, Celia, gracias por todos los buenos momentos compartidos. En esta tesis hay un pedacito de cada una. Gracias a todos a los que no menciono pero que, de un modo u otro, han contribuido a que sea quién soy.

Y finalmente, terminar agradeciendo a mi familia por haber estado ahí siempre. Gracias, muchas gracias, de verdad, a mis padres, mis abuelos, mis tíos, mis primos, a todos vosotros por apoyarme desde siempre. Dedico esta tesis a mi madre, Paula, por el amor incondicional que siempre me ha dado, y por confiar en mí, en mis decisiones y dejar que me equivocase. Y se la dedico a mis abuelos, Chus y Lolo, por tantísimo cariño, cuidados, buena comida, y amor.

Muchísimas gracias por todo.

Table of content

Abbreviations and acronyms

Ac Acetate

Ad Adamantyl

Ala Alanine

APAO *N*-acyl-protected aminomethyl oxazoline

APAQ *N*-acyl-protected aminoethyl quinoline

APCI Atmospheric pressure chemical ionization

BDE Bond dissociation energy

BINAP 2,2'-bis(diphenylphosphino)-1,1'-binaphthyl

BINOL 1,1'-Bi-2-naphthol

Bn Benzyl

Boc *tert*-Butyloxycarbonyl

BQ *p*-Benzoquinone

brs Broad singlet

Bz Benzoyl

Cat Catalytic amount

CMD Concerted metalation-deprotonation

cod 1,5-Cyclooctadiene

Cp cyclopentadienyl

Cy Cyclohexyl

d Doublet

dba Dibenzylideneacetone

DCE 1,2-Dichloroethane

DCM Dichloromethane

de Diasteroisomeric excess

DEAD Diethylazodicarboxylate

DEPT Distortionless Enhancement by polarization transfer

DG Directing group

DIAD Diisopropylazodicarboxylate

DMAP *N*,*N*-Dimethylaminopyridine

DMF *N,N*-Dimethyl formamide

DMSO Dimethyl sulfoxide

DOPA Dihydroxyphenylalanine

dppp 1,4-Bis(diphenylphosphino) propane

ee Enantiomeric excess

equiv Equivalent

er Enantiomeric ratio

ESI Electrospray

Et Ethyl

Fmoc Fluorenylmethyloxycarbonyl

Gly Glycine

hfacac Hexafluoroacetylacetone

HFIP Hexafluoroisopropanol

HOMO Highest occupied molecular orbital

HRMS High resolution mass spectroscopy

HSQC Heteronuclear single quantum correlation

^{i}Pr Isopropyl

J Coupling constant

KIE Kinetic isotopic effect

Leu Leucine

LUMO Lowest unoccupied molecular orbital

m Multiplet

Me Methyl

Meas. Measured

MPAA Mono-protected amino acid

MPAAM Mono *N*-protected aminoethyl amine

MPAThio Mono *N*-protected aminoethyl thioether

Ms Mesyl

Naph Naphtyl

^{n}Bu n-Butyl

NFSI *N*-fluorobenzenesulfonimide

^{n}Hex n-Hexyl

NMR Nuclear magnetic resonance

nOe Nuclear Overhauser effect

Ns 4-Nitrobenzenesulfonyl

PG Protecting group

Ph Phenyl

Phe Phenylalanine

Phth Phthaloyl

pin Pinacolate

PIP Pyridyl isopropylamine group

Piv 2,2-Dimethylpropionate

Pro Propyl

q Quadruplet

rr Regioisomeric ratio

rt Room temperature

s Singlet

SIPr 1,3-Bis(2,6-diisopropylphenyl)-4,5-dihydro-*1H*-imidazol-3-ium-2-ide

SN_2 Bimolecular nucleophilic substitution

t Triplet

^{t}AmOH 2-Methyl-2-butanol

TBHP *tert*-Butyl hydrogen peroxide

TBS *tert*-Butyldimethylsilyl

^{t}Bu *tert*-Butyl

TCE Trichloroethylene

Tf Trifluoromethylsulfonyl

TFA Trifluoroacetic acid

THF Tetrahydrofuran

THIQ Tetrahydroisoquinoline

THQ Tetrahydroquinoline

TM Transition metal

TMEDA *N,N,N',N'*-Tetramethylethylenediamine

TMS Trimethylsilyl

Tol Toluene

TS Transition state

Ts 4-Methylbenzenesulfonyl

Val Valine

Chapter I

Introduction

1- Organic synthesis: building molecules for life

1.1 Introduction

Chemistry is, arguably, one of the scientific disciplines that has contributed more to the progress of humankind. Traditionally defined as "the branch of science that studies the nature, properties, and composition of matter, and the transformations in which matter is involved",[1] chemistry has progressively become a more transversal discipline, interfacing with many others fields like physics, biology or medicine. Owing to their widespread presence in almost any aspect of the natural world, and their easiness to combine with the rest of central sciences (biochemistry, physical chemistry and medicinal chemistry among others), the study of chemistry is vital for the development of the society.

Organic synthesis is the branch of chemistry that, in words of one of its most representative ambassadors, K. C. Nicolaou, deals with the construction of organic molecules from atoms and/or simpler molecules. As he states,[2] "the chemical synthesis of nature's molecules without the aid of enzymes often presents formidable challenges to human ingenuity and skill". The humankind, in its inherent eagerness, has pursued the dream of mimicking nature in its ability to create molecules of relevance for daily life. By developing this discipline, organic chemists have been able to synthesize not only natural occurring molecules, but many others never considered by nature. In fact, organic chemistry has played a relevant role in the development of our modern way of life, and human-made organic molecules are widely spread in our society: medicine, plastic industry, cosmetics, food industry and much more.

The field of organic synthesis has evolved since the first rational synthesis of urea by Wöhler in 1828.[3] Through the XX century, the capability and power of this field experienced a dramatic increase, so that today's synthetic chemists are in the position to construct molecules of impressive complexity.[4] Examples of these complex molecules made using synthetic chemistry are depicted in Figure 1.[2]

[1] Russell, J. B., *General Chemistry,* McGraw-Hill International Book Company, **1980**.
[2] Nicolaou, K. C.; Sorensen, E. J. *Classics in total synthesis: Targets, strategies, methods,* Wiley-VCH, **1996**.
[3] Wöhler, F. *Ann. Phys.* **1828**, *88*, 253.
[4] Gaich, T., Baran, P. S. *Journal of Organic Chemistry* **2010,** *75,* 4657.

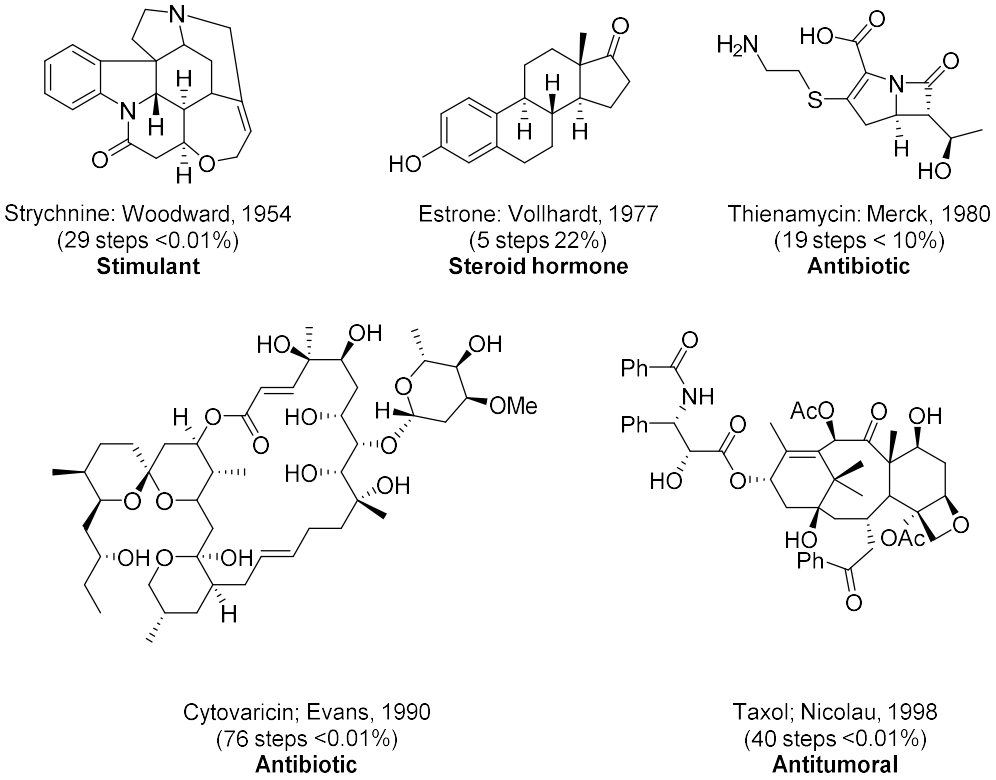

Figure 1. *Examples of classic total syntheses and their number of steps and total yield.*

As a result of these advances, the aim of organic synthesis has changed from "capability" (to be able to make molecules) to "ideality" (make the molecules in the most efficient way). Hendrickson describes ideality in organic synthesis as the creation of a complex molecule in a sequence that only involves construction reactions, without intermediary refunctionalizations, and leading directly to the target, not only its skeleton but also its correctly placed functionality.[5]

1.2 Modern organic synthesis

Epitomized by the "ideality" of Hendrickson, modern organic synthesis moved from the aim of obtaining the final molecule with any possible, available method towards the careful selection of the methods involved in the synthesis of the target. New concepts were introduced, like *atom economy,*[6] simply defined by Trost as "how much of the reactants end up in the product"; *step economy,*[7] introduced by Wender, meaning the minimization of the transformations needed to obtain the target; *redox economy*, concept introduced by Evans[8] and later by Baran and Hoffmann[9] that refers to the reduction of the number of nonstrategic steps (those that do not set stereochemistry or are not skeleton-building) or corrective oxidation and reduction steps during the synthesis; *pot economy,*[10] stated by Hayashi, regarding the minimization of the

[5] Hendrickson, J. B. *J. Am. Chem. Soc.* **1975**, *97*, 5784.
[6] (a) Trost, B. M. *Science* **1991**, *254*, 1471. (b) Trost, B. M. *Angew. Chem. Int. Ed.* **1995**, *34*, 259.
[7] (a) Wender, P. A.; Croatt, M. P.; Witulski, B. *Tetrahedron* **2006**, *62*, 7505. (b) Wender, P. A.; Verma, V. A.; Paxton, T. J.; Pillow, T. H. *Acc. Chem. Res.* **2008**, *41*, 40. (c) Wender, P. A.; Miller, B. L. *Nature,* **2009**, *460*, 197.
[8] D. A. Evans, oral presentation at *The Scripps Research Institute*, 12 February **2004**.
[9] Burns, N. Z.; Baran, P. S.; Hoffmann, R. W. *Angew. Chem. Int. Ed.* **2009**, *48*, 2854.
[10] Hayashi, Y. *Chem. Sci.* **2016**, *7*, 866.

number of pots required for each reaction method, by the elimination of unnecessary workups and isolations of intermediates; and indubitably *green chemistry,*[11] defined by Anastas and Warner with their famous twelve principles, as a guide of how to reduce the environmental impact of chemical production.

All these concepts define the field of modern organic synthesis, and set the stage for the invention and development of new synthetic methods.

2- Organometallic catalysis: a key tool in synthetic chemistry

2.1 Introduction

The development of new methodologies that can fit with the above concepts represents a major scientific aim. In this context, the use of metal complexes as reagents in organic synthesis has always been highly attractive. Despite the fact that the first organometallic compound, the Cadet's fuming liquid, was synthesized in 1760,[12] it was not until the first years of XX century when Barbier and his famous student, Grignard, started the development of the organometallic chemistry.[13] During the second half of the century, with the discovery of ferrocene by Woodward and Wilkinson,[14] Fischer[15] and Eiland and Pepinsky,[16] dozens of synthetic chemistry groups became interested in organometallic chemistry. These discoveries set the stage for the beginning of organometallic catalysis over one decade later.

2.2 Catalysis: when fewer is better

Even though the production of alcohol by fermentation of sugar is known from the beginning of human history,[17] representing one of the first examples of human-made catalysis reactions, it was not until 1835 when Berzelius[18] coined the term *catalysis* to define reactions that are accelerated by a substance that remain unchanged after the reaction. By the end of XIX century, the research of Ostwald and Sabatier about catalysis was rewarded with both Nobel Prizes in 1909 and 1912 respectively.[19] When organometallic stoichiometric reactions started to show its limitations at industrial scale, especially when precious metals where involved, the importance of metal catalysis became clearer. The idea of transforming large amounts of reactants using small amounts of organometallic reagents looked highly attractive.

[11] Anastas P. T.; Warner, J. C. *Green chemistry: Theory and practice,* Oxford university press, **1998**.
[12] Seyferth, D. *Organometallics* **2001**, *20*, 1488.
[13] Zanda, M. *Synform,* **2018***, 10*, A155.
[14] Wilkinson, G.; Rosenblum, M.; Whiting, M. C.; Woodward, R. B. *J. Am. Chem. Soc.* **1952**, *74*, 2125.
[15] Fischer, E. O.; Pfab, W. *Zeitschrift für Anorganische und Allgemeine Chemie* **1952**, *7*, 377.
[16] Eiland, P. F.; Pepinsky, R. *J. Am. Chem. Soc.* **1952**, *74*, 4971.
[17] Wisniak, J. *Educ. Química*, **2010**, *21*, 60.
[18] Berzelius, J.J. *Årsberättelsen om framsteg i fysik och kemi* [Annual report on progress in physics and chemistry] *Royal Swedish Academy of Sciences*, **1835**.
[19] (a) *The Nobel Prize in Chemistry 1909*. https://www.nobelprize.org/prizes/chemistry/1909/summary/ (accessed 2022-01-05). (b) *The Nobel Prize in Chemistry 1912* https://www.nobelprize.org/prizes /chemistry/1912/summary/ (accessed 2022-01-05).

2.3 Transition-metal catalyzed reactions: cycloadditions

After the *boom* of organometallic chemistry in the mid-XX century, metal-catalyzed reactions become among the more useful tools in organic synthesis. Representative examples are the catalytic asymmetric hydrogenations which led to Noyori and Knowles to receive the Nobel Prize in 2001[20], or the very useful cross-coupling reactions whose discovery awarded the Nobel prize in 2010 to Suzuki, Negishi and Heck[21]. Another type of reactions in which organometallic catalysis led to a great impact are cycloaddition reactions.

According to the IUPAC Gold Book, a cycloaddition, sometimes called annulation, is "a reaction in which two or more unsaturated molecules (or parts of the same molecule) combine with the formation of a cyclic adduct in which there is a net reduction in bond multiplicity".[22] An inherent capability of this type of reaction is the perfect conservation of *atom economy*, as every atom in the substrate molecule is found in the product. Given that rings are a very common motif in bioactive molecules, cycloadditions have proven to be particularly useful in total synthesis, providing novel disconnections to afford the desired compounds in fewer steps.[23] The Diels-Alder reaction[24] is probably the most relevant cycloaddition in the organic synthesis history. It is a (4+2) cycloaddition, which means that a 6-membered ring is formed from two acyclic reactants, one providing four of the six carbons, and the other one the two remaining carbons.[25] These two partners involved in the Diels-Alder reaction are called diene and dienophile (Scheme 1).

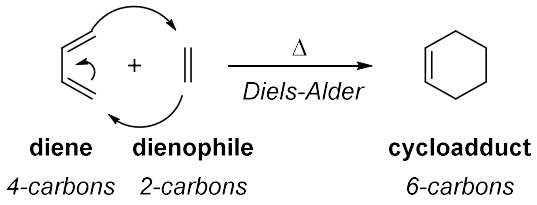

Scheme 1. *Model of the Diels-Alder reaction.*

Classic, thermal cycloadditions are limited to those that fulfill the Woodward and Hoffmann rules,[26] so the substrates need to be appropriately matched from an electronic point of view. The employment of transition-metals can overcome these limitations, as their reactions work

[20] *The Nobel Prize in Chemistry 2001*. https://www.nobelprize.org/prizes/chemistry/2001/summary/ (accessed 2022-01-05).
[21] *The Nobel Prize in Chemistry 2010*. https://www.nobelprize.org/prizes/chemistry/2010/summary/ (accessed 2022-01-05).
[22] McNaught, A. D.; Wilkinson, A. *IUPAC compendium of chemical terminology 2nd Ed. (The "gold" book),* Oxford, **1997**.
[23] Selected examples of reviews about cycloadditions applied to natural product synthesis: (a) Gao, K.; Zhang, Y. G.; Wang, Z.; Ding, H. *Chem. Commun.* **2019**, *55*, 1859. (b) Poplata, S.; Tröster, A.; Zou, Y. Q.; Bach, T. *Chem. Rev.* **2016**, *116*, 9748. Battiste, M. A.; Pelphrey, P. M.; Wright, D. L. *Chem. Eur. J.* **2006**, *12*, 3438.
[24] Diels, O.; Alder, K. *Justus Liebigs Ann. Chem.* **1928**, *460*, 98.
[25] In this doctoral thesis, we use Huisgen notation for cycloadditions, where numbers between parenthesis mean the atoms involved in the ring formation. This differs with Woodward-Hoffman notation, which uses numbers between brackets meaning the electrons involved in the cyclization.
[26] (a) Woodward, R.; Hoffmann, R. *J. Am. Chem. Soc.* **1965**, *87*, 395. (b) Woodward, R.; Hoffmann, R. J. Am. Chem. Soc. **1965**, *87*, 2046. (c) Woodward, R.; Hoffmann, R. *J. Am. Chem. Soc.* **1965**, *87*, 2511.

with different mechanisms that are not subjected to the restrictions of the Woodward and Hoffman rules. Furthermore, transition-metal catalyzed cycloadditions can allow reactions at lower temperatures than thermal cycloadditions. Another clear advantage of metal-catalyzed cycloadditions is that the metal can accommodate ligands, and therefore they can be used to induce enantioselectivity. Illustrative examples are the enantioselective Pd-catalyzed (3+2) and (4+3) intramolecular cycloadditions of alkylidene cyclopropanes reported by our research group (Scheme 2).[27]

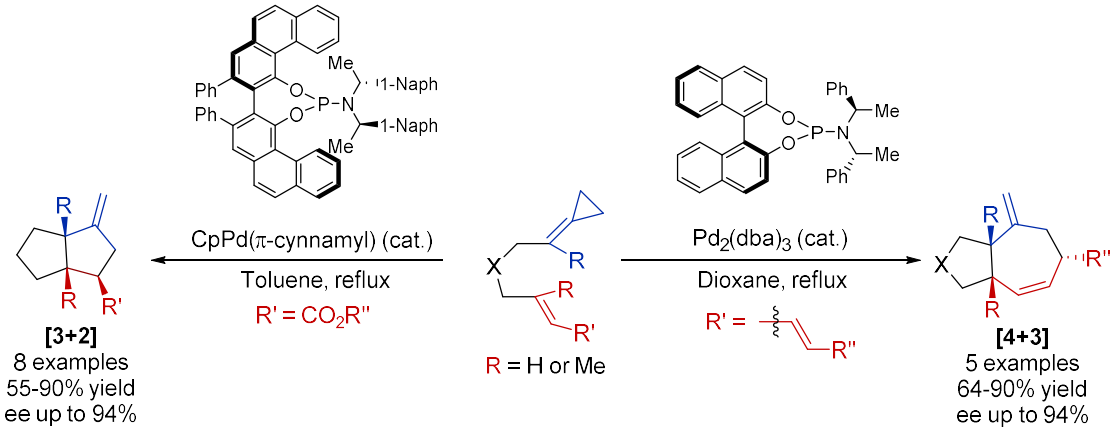

Scheme 2. *Enantioselective palladium-catalyzed (3+2) and (4+3) cycloadditions reported by Gulías, Mascareñas, López and co-workers.*

Furthermore, transition-metals can catalyze multicomponent annulations in a single step, which convey a very significant increase in complexity. An example on these types of transformations, also developed by our laboratory, is the Rh(I)-catalyzed (3+2+2) cycloaddition shown in Scheme 3.[28]

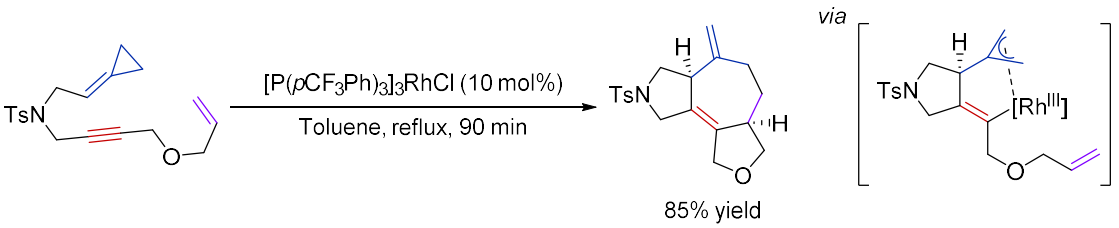

Scheme 3. *Rh(I)-catalyzed (3+2+2) cycloaddition, and key intermediate.*

These types of metal-promoted cycloadditions have proven to be very useful; however, as they rely on the presence of π-bonds, the substrates need to be appropriately functionalized. Moreover, the scope of these reactions is usually limited to the assembly of carbocycles, with heterocycles being more difficult to build using these technologies.

[27] Verdugo, F.; Villarino, L.; Durán, J.; Gulías, M.; Mascareñas, J. L.; López, F. *ACS Catal.* **2018**, *8*, 6100.
[28] Araya, M.; Gulías, M.; Fernández, I.; Bhargava, G.; Castedo, L.; Mascareñas, J. L.; López, F. *Chem. Eur. J.* **2014**, *20*, 10255.

2.4 Transition-metal catalyzed reactions: cross-coupling

Together with transition-metal catalyzed cycloadditions, cross-coupling reactions have been extremely important in organic synthesis.[29] In fact, the 2010 Nobel Prize of Chemistry was awarded to Richard Heck, Ei-ichi Negishi and Akira Suzuki for their "palladium-catalyzed cross couplings in organic synthesis".[21] The generally accepted mechanisms for these transformations are depicted in Scheme 4.[30]

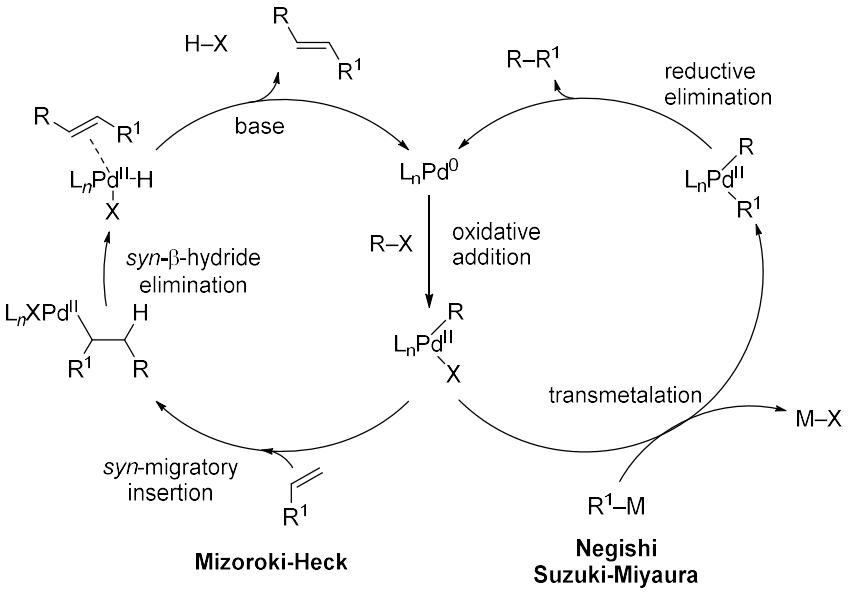

Scheme 4. *General catalytic cycles for Heck-Mizoroki, Negishi and Suzuki-Miyaura reactions.*

Common to both types of coupling reactions is the starting point of the catalytic cycle, with the oxidative addition of the aryl halide (or pseudohalide) to the Pd^0 catalyst. At this point, the processes diverge. In the Mizoroki-Heck reaction, the mechanism goes through a first coordination of an alkene to the catalyst, followed by a *syn*-migratory insertion/*syn*-β-hydride elimination pathway to make the C-C bond. In the Negishi and the Suzuki-Miyaura reactions (and other related reactions such as Corriu–Kumada, Stille, or Hiyama coupling processes), the oxidative addition is followed by a transmetalation to the catalyst. In this process, R^1 is provided by a metal-containing species (such as a borate in Suzuki-Miyaura coupling, zincate in Negishi coupling, etc.). Subsequent reductive elimination results in the C-C bond formation.

[29] Nicolaou, K. C.; Bulger, P. G.; Sarlah, D. *Angew. Chem. Int. Ed.* **2005**, *44*, 4442.
[30] (a) Johansson Seechurn, C. C. C.; Kitching, M. O.; Colacot, T. J.; Snieckus, V. *Angew. Chem. Int. Ed.* **2012**, *51*, 5062 (b) Meijere, A. de; Diederich, F. *Metal-Catalyzed Cross-Coupling Reactions*, Wiley-VCH, **2004** (c) Meijere, A. de; Negishi, E. *Handbook of Organopalladium Chemistry for Organic Synthesis* Wiley, **2002**.

The synthetic applications of these processes encouraged organic chemists to research to broad the scope of these transformations. One of the key developments was the employment of ligands with different steric and electronic properties. The resulting modified catalysts made possible to perform cross-coupling transformations under milder conditions and with lower catalyst loadings. For example, Heck demonstrated that, by adding phosphines to the reaction media, the range of reactive alkenes could be expanded (Scheme 5).[31]

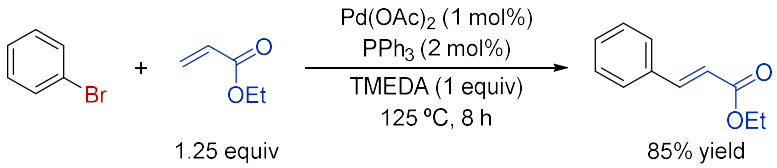

Scheme 5. *Use of phosphines as ligands to improve the Heck reaction.*

Playing with ligands, it was possible to perform cross-coupling reactions which generate heteroatom bonds, instead of C–C bonds. Hartwig-Buchwald amination is probably one of the most important reactions in this context.[32] It has been used in numerous synthetic processes, for example, in the Novartis route for the synthesis of Imatinib, a medication used to treat cancer (Scheme 6).[33]

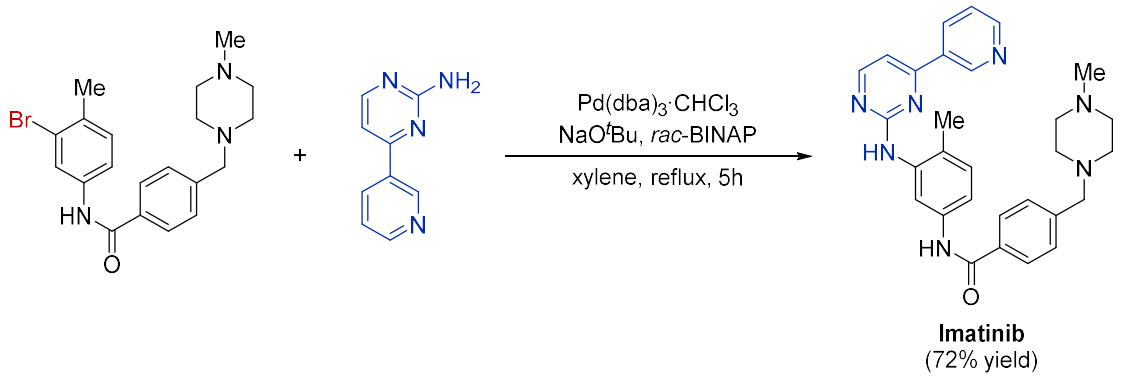

Scheme 6. *Last step of the Novartis route for the synthesis of Imatinib.*

Even though cross-couplings have proved to be very powerful tools for synthetic chemists, there are still some inherent limitations. Particularly, the need of prefunctionalized substrates such aryl halides, pseudohalides and organometallic reagents, which requires of additional synthetic steps to install the corresponding functional groups, with its subsequent waste of stoichiometric reactants. In the pursuit of greater *atom and step economy*, the dream of any synthetic chemist is the invention of other methodologies to form C–C or C–X bonds without the need of prefunctionalization. And at this point, it is where C−H activation has taken the stage.

[31] Dieck, H. A.; Heck, R. F. *J. Am. Chem. Soc.* **1974**, *96*, 1133.
[32] Dorel, R.; Grugel, C. P.; Haydl, A. M. *Angew. Chem. Int. Ed.* **2019**, *58*, 17118.
[33] O. Loiseleur, D. Kaufmann, S. Abel, H. M. Buerger, M. Meisenbach, B. Schmitz and G. Sedelmeier, *World Pat.*, 03066613, **2003**.

3- Organometallic catalysis triggered by C–H activation: initial developments

Carbon-hydrogen bonds have been generally considered "inert". In fact, one of the old names of alkanes, "paraffines", came from Latin *parum affinis*, which means "without affinity". By having a look at bond dissociation energies (BDE), the strength of C–H bonds is evident. Whereas the weakly polarized C–H bond of methane presents a BDE of 105 kcal mol^{-1}, its brominated counterpart, the more polarized C–Br bond of bromomethane, has a lower BDE of 70.3 kcal mol^{-1}.[34]

Despite the challenge of its inertness, the activation of C–H bonds is a major research topic in modern synthetic chemistry. The ubiquity of this type of bonds in organic molecules makes this field very attractive to transform widely-available hydrocarbon feedstocks. However, this ubiquity is a double-edge sword. The little difference of energies among the several C–H bonds of organic molecules makes very difficult to control selectivity. In fact, classic reactions with alkanes, based on radical (autoxidation, halogenation) or carbene chemistry are characterized by a lack of selectivity. This is due to the fact that these reactions are based on very reactive species that are able to overcome the inherent inertness of alkanes, but that give rise to the formation of many products due to their indiscriminate attack to different C–H bonds.[35] Therefore, the development of novel procedures to selectively activate carbon-hydrogen bonds represents a challenging issue in the field of synthetic chemistry.

In the 1960's, during the *boom* of organometallic chemistry, several research groups started to study the activation of carbon-hydrogen bonds by the employment of transition-metals, with the objective of creating organometallic complexes from hydrocarbons through the processed that was called "C–H activation". The first examples in this field can be traced back to the work of Kleiman and Dubech (Scheme 7)[36] in 1963, describing the cyclometalation of aromatic compounds with a Ni(0) complex, and the work of Chatt[37] on 1965, on the addition of C–H bonds of naphthalene to Ru(0) complexes.

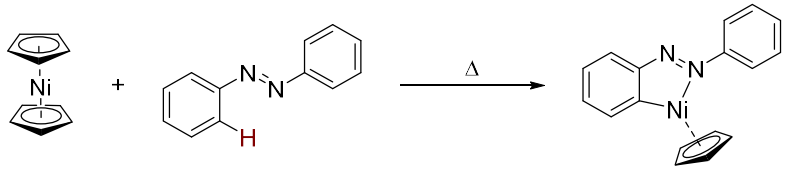

Scheme 7. *First example of stoichiometric C–H activation by Kleiman and Dubech.*

[34] Y. R. Luo, *Comprehensive Handbook of Chemical Bond Energies*, CRC Press, Boca Raton, **2007**.
[35] Shilov, A. E.; Shul'pin, G. B. *Chem. Rev.* **1997**, *97*, 2879.
[36] Kleiman, J. P.; Dubeck, M.; *J. Am. Chem. Soc.* **1963**, *85*, 1544.
[37] Chatt, J.; Davidson, J. M. *J. Chem. Soc.* **1965**, 843.

Palladium soon took protagonism as one of the mosts active metals in C–H activation. In 1965, Verberg[38] published a method of oxidative coupling of aromatic compounds with palladium salts. A key discovery was the catalytic arylation of alkenes reported by Fujiwara and Moritani in 1969 by the employment of palladium catalysts (Scheme 8).[39]

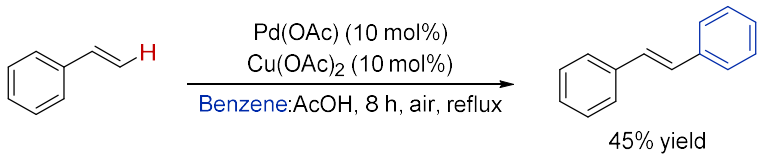

Scheme 8. *Fujiwara-Moritani reaction.*

It is important to notice that, even though this reaction proceeds through a very similar mechanism that the Mizoroki-Heck reaction (vide supra), the oxidative addition of the Ar–X bond to a Pd(0) complex is substituted by the C–H activation of the Ar–H bond with a Pd(II) catalyst, which overcomes one of the main disadvantages of cross-coupling reactions: the need of a prefunctionalized substrate. Curiously, the Heck reaction was published three years after the Fujiwara-Moritani reaction.

In 1969, the first transition-metal C(sp^3)–H bond activation was discovered. Shilov[40] reported that K_2PtCl_4 catalyze the H–D exchange of methane with heavy water at room temperature. The group later developed a method to catalytically convert methane to methanol. It was called the Shilov system (Scheme 9).[41] The need to use stoichiometric platinum as oxidant was its mayor drawback. However, it is, even today, one of the few catalytic systems that allows selective alkane functionalizations under mild conditions.[42]

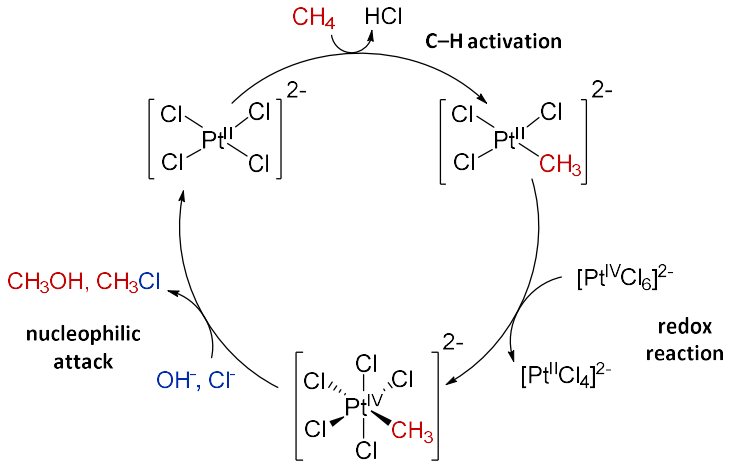

Scheme 9. *Shilov system to convert methane into methanol.*

[38] van Helden, R.; Verberg, G. *Recl. Trav. Chim. Pays-Bas* **1965**, *84*, 1263.
[39] Fujiwara, Y.; Moritani, I.; Danno, S.; Asano, R.; Teranishi, S. *J. Am. Chem. Soc.* **1969**, *91*, 7166.
[40] Gol'dshleger, N. F.; Tyabin, M. B.; Shilov, A. E.; Shteinman, A. A. *Zh. Fiz. Khim.* **1969**, *43*, 2174.
[41] (a) Gol'dshleger, N. F.; Es'kova, V. V.; Shilov, A. E.; Shteinman, A. A. *Zh. Fiz. Khim.* **1972**, 46, 1353. (b) Crabtree, R. H. *J. Chem. Soc. Dalt. Trans.* **2001**, 17, 2437.
[42] Goldman, A. S.; Goldberg, K. I. Organometallic C–H Bond Activation: An Introduction. In *ACS Symposium Series Vol. 885*, **2004**.

The next breakthrough had to wait nearly a decade until, in 1982, Bergman[43] and Graham[44] independently published a photochemical C–H activation of alkanes with an iridium complex (Scheme 10).

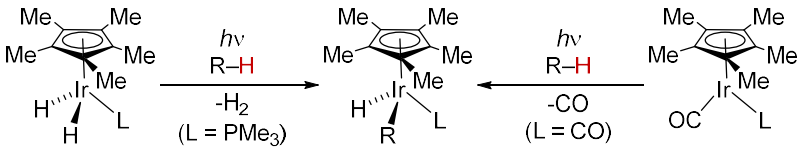

Scheme 10. *C–H activation by Bergman et al. (left) and Graham et al. (right).*

It was not until 1993 that the field experimented a new boost, with the outstanding discovery by Murai and co-workers of a ruthenium-catalyzed selective *ortho*-directed C–H functionalization of aryl ketones (Scheme 11).[45] The use of a carbonyl as directing group for the metal complex was key in the success of the reaction. This development revigorated the field, which is still in relentless ascension.

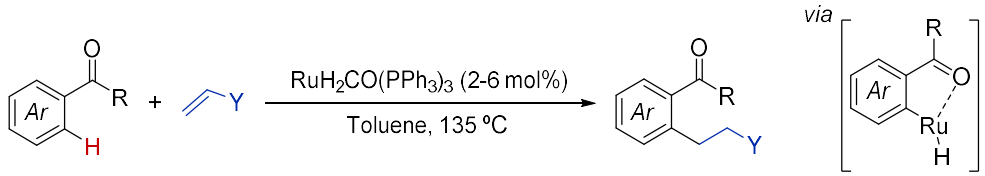

Scheme 11. *Ruthenium-catalyzed C–H functionalization of aryl ketones by Murai.*

At this point, it is important to mention that the term C–H functionalization includes any transformation that converts a C–H bond into a C–FG bond (FG ≠ H) via C–H activation. The work of Murai can be considered as the spark that ignited the C–H activation field using metal catalysis. Since its publication, the number of references of "C–H activation" has experienced an exponential grow,[46] evidencing the importance of this topic in contemporary organic chemistry. The vast majority of the publications rely on the activation of C(sp^2)–H bonds, due to the fact that this type of bond is easier to cleave (see section 1 of Chapter III for further explanation), even though the field of C(sp^3)–H activation has been growing in recent years.

[43] Janowicz, A. H.; Bergman, R. G. *J. Am. Chem. Soc.* **1982**, *104,* 352.
[44] Hoyano, J. K.; Graham, W. A. G. *J. Am. Chem. Soc.* **1982**, *104*, 3723.
[45] Murai, S.; Kakiuchi, F.; Sekine, S.; Tanaka, Y.; Kamatani, A.; Sonoda, M.; N. Chatani, N. *Nature* **1993**, *366*, 529.
[46] Source: *Scifinder*, by searching "C–H activation" as keyword (searched 2022-01-05) there were 31 references in 1993 and 760 in 2021.

Asymmetric functionalizations have also been developed by taking advantage of the employment of chiral ligands. One example is the work of Shibata in the enantioselective iridium-catalyzed C(sp^3)–H alkylation of ɣ-butyrolactam for the synthesis of ɣ-amino acids, with the enantioselectivity induced by a chiral phosphine. The presence of the pyridine directing group in the substrate is key for the reaction (Scheme 12).[47]

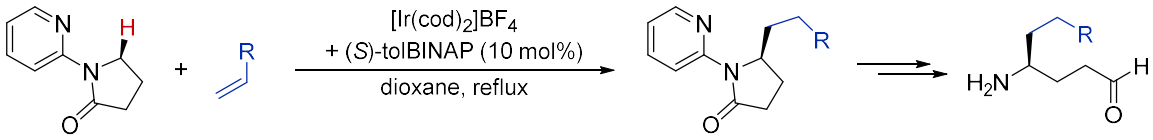

Scheme 12. *Iridium-catalyzed C(sp^3)–H alkylation of ɣ-butyrolactam by Shibata.*

As can be deduced from the above reactions, the use of directing groups seems critical to allow the C–H activation chemistry.[48] These moieties can control site-selectivity by approximating the reactive metal center to the desired C–H bond (Scheme 13), and accelerate the reactions by decreasing the entropic cost of C–H activation process.

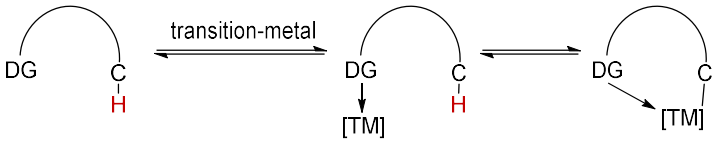

Scheme 13. *Site selective controlled by the employment of a directing group. TM = transition metal.*

In fact, it was thanks to a ketone acting as a chelation-assisted directing group that Murai could achieve that important milestone in C–H activation chemistry that ignited the spark of this field (vide supra). During these two last decades, several directing groups have been employed to functionalize C–H bonds,[48] some of which are depicted in Figure 2.

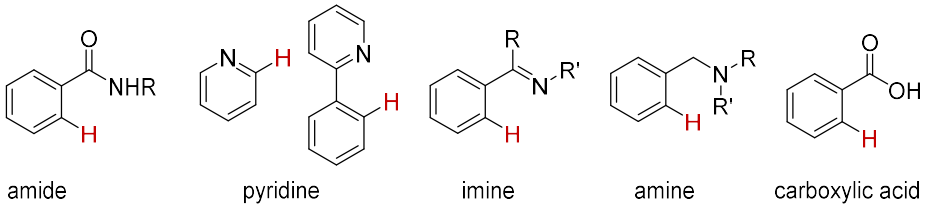

Figure 2. *Common directing groups, with indication (in red) of the C–H bond that is activated.*

Most directing groups are employed to functionalize aryl C–H bonds in *ortho* position, like Murai's work (vide supra), but there is an increasing effort to develop novel strategies that allow *meta*[49] and *para*[50] functionalizations in aromatic systems.

[47] Tahara, Y. K.; Michino, M.; Ito, M.; Kanyiva, K. S.; Shibata, T. *Chem. Commun.* **2015**, *51*, 16660.
[48] Chen, Z.; Wang, B.; Zhang, J.; Yu, W.; Liu, Z.; Zhang, Y. *Org. Chem. Front.* **2015**, *2*, 1107.
[49] Xu, H. J.; Kang, Y. S.; Shi, H.; Zhang, P.; Chen, Y. K.; Zhang, B.; Liu, Z. Q.; Zhao, J.; Sun, W. Y.; Yu, J. Q.; Lu, Y. *J. Am. Chem. Soc.* **2019**, *141*, 76.
[50] (a) Bag, S.; Patra, T.; Modak, A.; Deb, A.; Maity, S.; Dutta, U.; Dey, A.; Kancherla, R.; Maji, A.; Hazra, A.; Bera, M.; Maiti, D. *J. Am. Chem. Soc.* **2015**, *137*, 11888. (b) Li, M.; Shang, M.; Xu, H.; Wang, X.; Dai, H. X.; Yu, J. Q. *Org. Lett.* **2019**, *21*, 540.

4- Palladium: a noble metal that waived the field of catalytic C–H functionalizations

4.1 Introduction

Palladium, named after the Greek goddess Pallas Athenea, is one of the most used transition-metals in organic chemistry. From cross-coupling reactions (vide supra) to the Tsuji-Trost reaction,[51] palladium reagents have played a critical role in the development of novel organic transformations.

Regarding the C–H activation field, palladium catalysts are particularly attractive for several reasons. First, there is a relatively low barrier between the oxidation states of 0 and +2 corresponding to the d^{10} and d^8 configuration, which favors reversibility. As a consequence, oxidative insertions and reductive eliminations occur rapidly, leading to faster catalytic cycles. Second, the inherent square planar geometries of palladium complexes offer more versatility than linear geometries, characteristic of gold complexes, but are also relatively simple and sterically accessible, and easier to control than octahedral geometries where *fac* and *mer* stereoisomerism may appear. Palladium also shows a good affinity for electron donating ligands and unsaturated moieties, which further favors reactivity.[52]

4.2 Mechanisms of palladium-catalyzed C–H activations. The introduction of amino acids as ligands

As stated in the previous section, the employment of directing groups is essential to boost reactivity and control selectivity in C–H functionalization reactions (vide supra). After coordination to these groups, the palladium complex can effectively perform the required C–H activation, usually through concerted metalation-deprotonation (CMD) processes (Scheme 14). In this mechanism, the palladium weakens the C–H bond, while a base, generally coordinated to the metal, abstracts the proton, all occurring in a concerted manner.[53] The base is generally a carboxylate, like the acetate of $Pd(OAc)_2$.

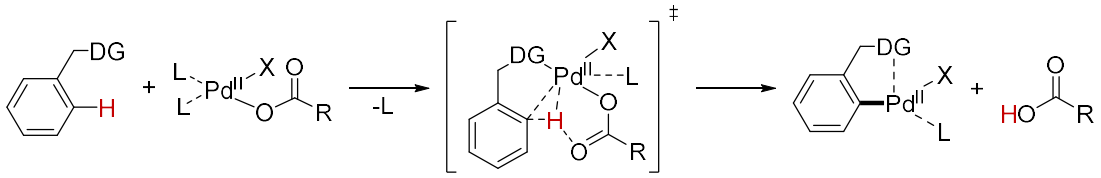

Scheme 14. *Scheme of a CMD mechanism for a Pd(II) complex.*

The ligands coordinated to the palladium center can modify the electronic properties and steric environment of the metal, and thus the performance of the catalyst in C–H activation reactions. Depending on the type of catalytic cycle that is present in the reaction, some ligands are

[51] (a) Tsuji, J.; Takahashi, H.; Morikawa, M. *Tetrahedron Lett.* **1965**, *6*, 4387. (b) Trost, B. M.; Fullerton, T. J. *J. Am. Chem. Soc.* **1973**, *95*, 292.

[52] (a) Hegedus, L. S. *Transition metals in the synthesis of complex organic molecules* University Science Books, **1994**. (b) Crabtree, R. H. *The organometallic chemistry of the transition metals.* Wiley-VCH, **2014**.

[53] Lapointe, D.; Fagnou, K. *Chem. Lett.* **2010**, *39*, 1118.

preferred over the others.[54] For example, in Pd(II)/Pd(0) catalytic cycles, pyridines can be used as monodentate ligands for the reaction. These ligands are not only capable of tuning the electronics of the catalyst, but also of driving the formation of active monomeric catalytic species.[55]

The idea of employing chiral ligands in C–H activation reactions is very appealing as a way to introduce asymmetry in organic molecules. As early as in 1979, Sokolov hypothesized that a chiral carboxylate acting as a monodentate ligand could induce enantioselectivity during the C−H activation step (Figure 3, mechanism **A**). With this idea, his group developed the first stoichiometric asymmetric cyclopalladation by the employment of a *N*-acyl-α-amino acid as a chiral carboxylate.[56] However, this mechanism, later studied by Richards,[57] was inconsistent with some data reported by Yu's group years later, such as the fact that C2-symmetric amino acids or diprotected amino acids give racemic mixtures.

In 2008, Yu reported the first catalytic enantioselective C−H activation mediated by mono-protected amino acids (MPAA), a series of amino acids where the amine is monoprotected with an acyl group.[58] He proposed in this publication an alternative mechanism for the C–H activation (Figure 3, mechanism **B**), with the amino acid coordinate in a bidentate fashion to the metal center, and with an external base activating the C−H bond. In this model, the nitrogen would coordinate as a neutral donor ligand. The problem with this hypothesis is that the N–H bond is more acidic than the C−H bond, thus the external base should deprotonate the N–H before attacking the C−H bond.

Yu and Musaev discussed in 2012 a modification in the mechanism (Figure 3, mechanism **C**),[59] in which the N–H deprotonation would occur first, generating an anionic palladium. This mechanism was supported by computational studies. However, some experimental data were still inconsistent. The employment of electron withdrawing protecting groups in the amine suppresses the reactivity in some particular cases. The mechanism **C** suggests exactly the opposite, as the inductive effect may stabilize the anionic palladium complex. Therefore, Houk, Yu and Musaev proposed an alternative mechanism (Figure 3, mechanism **D**),[60] in which the external base is substituted with an inner-sphere C−H cleavage performed by the amidate group of the amino acid, in an overall ligand-assist CMD mechanism. This model is more consistent with all the reactivity and selectivity data reported to date, and it is generally proposed for Pd-catalyzed reactions using MPAAs as ligands.

[54] Engle, K.M.; Yu, J.-Q. *J. Org. Chem.* **2013**, *78*, 8927.
[55] Cendón, B.; Font, M.; Mascareñas, J. L.; Gulías, M. *ACS Catal.* **2020**, *10*, 3425.
[56] Sokolov, V. I.; Troitskaya, L. L.; Reutov, O. A *J. Organomet. Chem.* **1979**, *182*, 537.
[57] Günay, M. E.; Ilyashenko, G.; Richards, C. J. *Tetrahedron Asymmetry* **2010**, *21*, 2782.
[58] Shi, B. F.; Maugel, N.; Zhang, Y. H.; Yu, J.-Q. *Angew. Chem., Int. Ed.* **2008**, *47*, 4882.
[59] Musaev, D. G.; Kaledin, A.; Shi, B. F.; Yu, J.-Q. *J. Am. Chem. Soc.* **2012**, *134*, 1690.
[60] (a) Cheng, G. J.; Yang, Y. F.; Liu, P.; Chen, P.; Sun, T. Y.; Li, G.; Zhang, X.; Houk, K. N.; Yu, J.-Q.; Wu, Y. D. *J. Am. Chem. Soc.* **2014**, *136*, 894. (b) Cheng, G. J.; Chen, P.; Sun, T. Y.; Zhang, X.; Yu, J.-Q.; Wu, Y. D. *Chem. Eur. J.* **2015**, *21*, 11180.

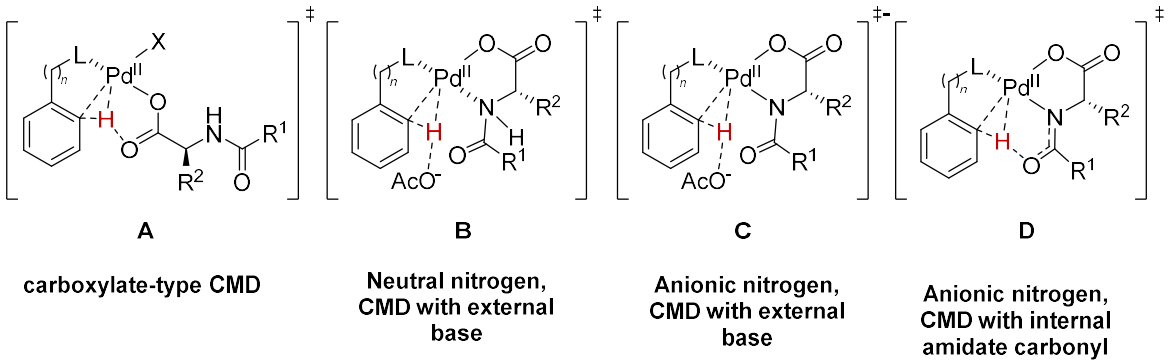

Figure 3. *Transition-state structures proposed for the Pd-catalyzed C–H activation assisted by MPAAs.*

MPAAs ligands have demonstrated to improve yields and broaden the scope of C–H functionalization reactions. [61] One example is the Pd(II)-catalyzed C–H olefination of phenylacetic acids reported by Yu and co-workers and depicted in Scheme 15, where the employment of Boc-Val-OH resulted in an increase in the reaction rate and in the efficiency of the reaction.[62] The yield of the reaction increased from 12% to 90% when using a MPAA ligand, and kinetic studies determined that there is a 36-fold increase in the reaction rate in the ligand-assisted olefination.

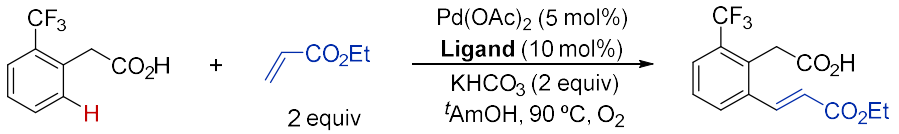

No ligand: Rate = 1.3 x 10^{-4} M/min (12% yield after 48 h)
Ligand (Boc-Val-OH): Rate = 4.7 x 10^{-3} M/min (90% yield after 48 h)

Scheme 15. *Ligand acceleration in the Pd(II)-catalyzed C–H olefination of phenylacetic acids reported by Yu and co-workers.*

The reactivity enhancement can be explaining considering several aspects contemplated in mechanism **D**:[61a]

- The basicity of the carbonyl group of the amidate is higher compared to acetate.
- A less steric hindrance environment for coordination of the directing group due to the smaller bite angle of the MPAA compared to two acetate ligands.
- The favorable coplanar orientation of the *N*-acyl carbonyl group and the C–H bond, due to the planar structure of the bidentate MPAA and the square planar geometry of the palladium (II) center.
- The stabilization of active monomeric palladium species in solution.
- For this particular reaction, a change in the reaction mechanism, from electrophilic palladation to ligand-assisted CMD.

[61] Selected reviews of mono-protected amino acid as ligands in Pd-catalyzed C-H activation: (a) Engle, K. M. *Pure Appl. Chem.* **2016**, *88*, 119. (b) Shao, Q.; Wu, K.; Zhuang, Z.; Qian, S.; Yu, J.-Q. *Acc. Chem. Res.* **2020**, *53*, 833–851.

[62] (a) Wang, D. H.; Engle, K. M., Shi, B. F.; Yu. J.-Q. *Science,* **2010**, *327*, 315. (b) Engle, K. M.; Wang, D. H.; Yu, J.-Q. *J. Am. Chem. Soc.* **2010**, *132*, 14137.

An additional, important advantage of MPAAs is that they are chiral, and thefore can have enantio-inducting effects, especially if mechanism **D** is operating. The chelating ligand creates a semirigid framework that can differentiate the two diastereomeric transition states, as it is depicted in Scheme 16.[61b]

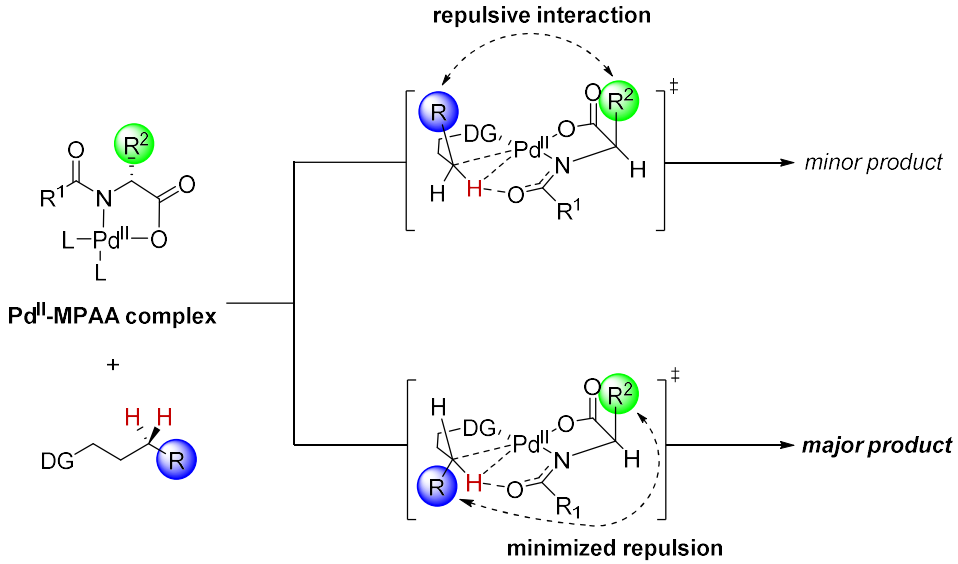

Scheme 16. *Stereomodel for bidentate internal amidate MPAA enantioselective C–H activation. The model is illustrated with a D-MPAA.*

The side chain of the amino acid (R^2) is placed in an axial position due to the steric repulsion with the *N*-acyl protecting group (R^1). Therefore, steric interactions of R^2 with the R group of the substrate help to differentiate between the two diastereomeric transition states. The election of proper R^1 and R^2 moieties is crucial for achieving a good enantioselectivity. Besides, interactions with the directing group can also influence the relative energies of the transition states.

Mechanistic studies of the behavior of mono-protected amino acids in palladium-catalyzed C–H activation reactions have shed a light on the influence of each structural feature of the ligand in these types of reactions. The conclusions are summarized in Figure 4.

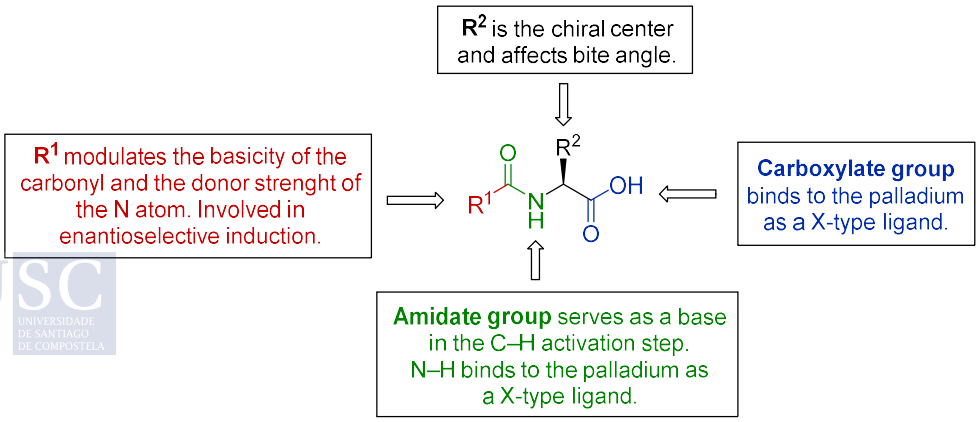

Figure 4. *Structural features of MPAAs and its influence in C–H activation reactions.*

The employment of MPAAs as both promoters and chiral inductors has been very successful in different types of metal-catalyzed reactions, from remote C−H functionalizations to late stage postfunctionalizations.[61] However, it is usually needed to screen for the more appropriate MPAA for each reaction. Therefore, the discovery of a more general set of ligands that could be successfully employed in any type of palladium-catalyzed C−H functionalization would be extremely relevant. Yu's group has also designed a new generation of ligands which preserve the key features of the MPAAs, but replace the carboxylate moiety for an L type ligand, preserving a bidentate coordination (Figure 5). Each ligand needs to be optimized for different types of C−H activation reactions. *N*-acyl-protected aminomethyl oxazoline (APAO) ligands induce high enantioselectivity in C−H desymmetrizations of prochiral methyl groups in isobutyramides.[63] *N*-acyl-protected aminoethyl quinoline (APAQ) ligands have been employed in enantioselective arylation of methylene C(sp^3)−H bonds.[64] Mono *N*-protected aminoethyl amine (MPAAM) ligands have demonstrated to be useful in enantioselective C−H arylation of cyclopropanecarboxylic and 2-aminoisobutyric acids.[65] Finally, mono *N*-protected aminoethyl thioether (MPAThio) ligands enable C−H olefination of simple free carboxylic acids.[66]

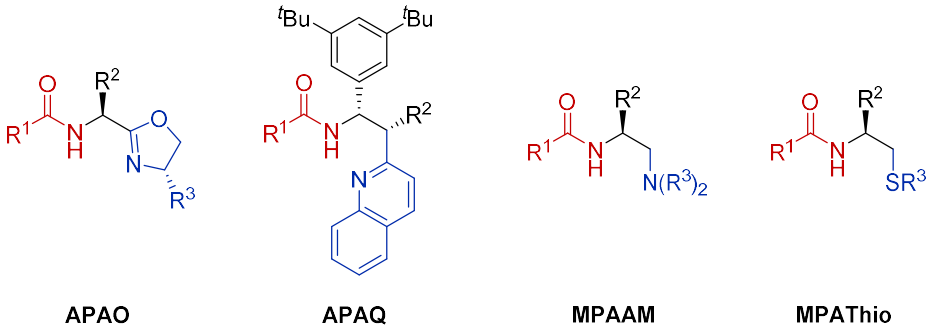

Figure 5. *New generation of ligands inspired by MPAA mechanistic understanding.*

[63] Wu, Q. F.; Shen, P. X.; He, J.; Wang, X. B.; Zhang, F.; Shao, Q.; Zhu, R. Y.; Mapelli, C.; Qiao, J. X.; Poss, M. A.; Yu, J.-Q. *Science* **2017**, *355*, 499.
[64] Chen, G.; Gong, W.; Zhuang, Z.; Andrä, M. S.; Chen, Y. Q.; Hong, X.; Yang, Y. F.; Liu, T.; Houk, K. N.; Yu, J.-Q. *Science* **2016**, *353*, 1023.
[65] Shen, P. X.; Hu, L.; Shao, Q.; Hong, K.; Yu, J.-Q. *J. Am. Chem. Soc.* **2018**, *140*, 6545.
[66] Zhuang, Z.; Yu, C. Bin; Chen, G.; Wu, Q. F.; Hsiao, Y.; Joe, C. L.; Qiao, J. X.; Poss, M. A.; Yu, J.-Q. *J. Am. Chem. Soc.* **2018**, *140*, 10363.

4.3 Types of reactions based on Pd-catalyzed C–H activation

Before commenting on specific type of Pd-promoted transformations involving C–H activation, it is important to note that in general, the cleavage of Ar–H and other C(sp^2)–H bonds is usually easier and more common than of C(sp^3)–H bonds. This will be later further discussed in the introduction of Chapter III.

4.3.1 C–H functionalizations

When the activated C–H bond is exchanged for a C–FG bond where FG ≠ H, the overall process is generally considered as a C–H functionalization. This is the most developed are in the field of palladium-catalyzed C–H activation-based reactions, and several methods have been reported for the construction of different type of bonds.

4.3.1.1 Formation of carbon-carbon (C–C) bonds

The formation of carbon-carbon bonds is the most widely studied area in the field of C−H functionalizations. In fact, one of the first reactions of this field was the Fujiwara-Moritani reaction (vide supra), involving the arylation of activated alkenes. The most common C−C bond formations entail aromatic rings, and tend to take place in the *ortho*-position to a directing group (DG),[67] as it happened in the Murai reaction with ruthenium (vide supra). Palladium is not an exception, and a large number of Pd-catalyzed C–H functionalization reactions controlled by a DG, including asymmetric processes, have been developed. For instance, the Yu's group reported a Pd(II)-catalyzed desymmetrizing cross-coupling of prochiral pyridines with alkylboronic acids promoted by an amino acid protected as menthyl ester, affording alkylated products with enantiomeric excesses up to 95% (Scheme 17a).[58] They also included a preliminary example of desymmetrizing C(sp^3)–H butylation of 2-isopropylpyridine assisted by a cyclopropyl-amino acid ligand, obtaining the product in modest yield and enantioselectivity (Scheme 17b).

[67] Rao, Y.; Shan, G.; Yang, X. *Sci. China Chem.* **2014**, *57*, 930.

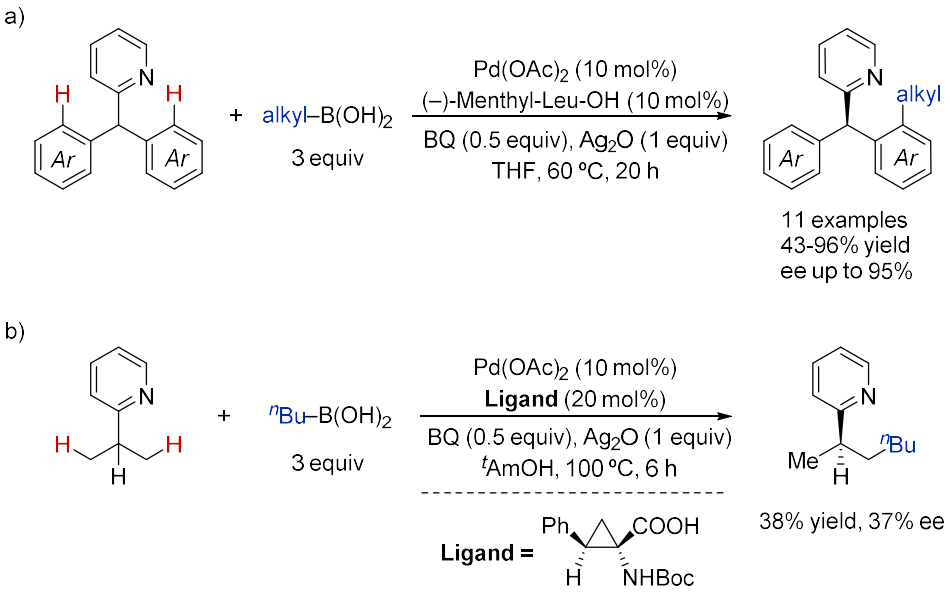

Scheme 17. *Pd(II)-catalyzed desymmetrizing cross-coupling of prochiral pyridines with alkylboronic acids developed by Yu and co-workers.*

Another notably example of activating C(sp^3)–H bonds was reported by the Sanford´s group (Scheme 18),[68] consisting on a transannular arylation of alicyclic amines. In this case the reaction does not need additional ligands, as it relies on a bidentate directing group.

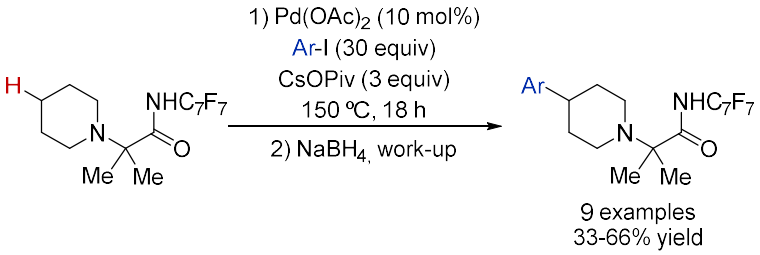

Scheme 18. *Pd-catalyzed transannular C(sp^3)–H arylation of alicyclic amines reported by Sanford and co-workers.*

To overcome the challenge of selectivity in *para* position to the directing group, plus the high activation barrier of cleaving a C(sp^3)–H bond, the group took advantage of the preferred ring conformation of the alicyclic amines, as it is depicted in Scheme 19.

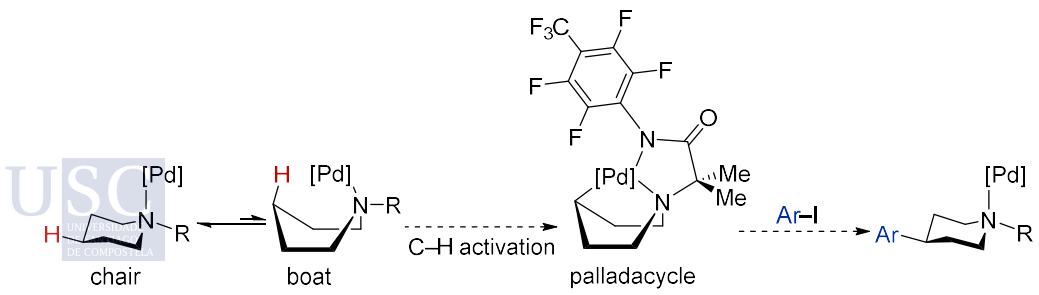

Scheme 19. *Conceptual approach for a distal C(sp^3)–H activation of alicyclic amines.*

[68] Topczewski, J. J.; Cabrera, P. J.; Saper, N. I.; Sanford, M. S. *Nature* **2016**, *531*, 220.

The metal center is close to the desired C−H bond owing to the boat conformation of the alicyclic amines. The authors applied this methodology to the late-stage derivatization of bioactive molecules. Two years later, the group of Sanford published a second-generation palladium catalyst system for this reaction, which enhances reactivity by the employment of quinoline/pyridine-carboxylate ligands.[69]

4.3.1.2 Formation of carbon-nitrogen (C−N) bonds

The formation of C−N bonds via C−H activation reactions have been mostly developed in an intramolecular fashion to synthesize azaheterocycles.[70] One example of this type of chemistry is the preparation of carbazole derivatives from *o*-arylanilines reported by Buchwald and co-workers in 2011 (Scheme 20).[71] After the C–H activation at the aryl moiety through a CMD mechanism, the resulting pallacyclic species evolves by reductive elimination of the C–N bond, which leads to the formation of the carbazole. The Pd(0) species is reoxidized to Pd (II) thanks to a combined action of copper acetate and oxygen.

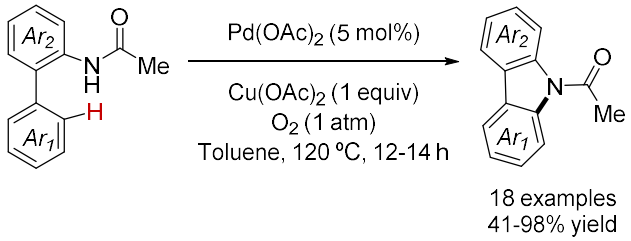

Scheme 20. *Pd(II)-catalyzed intramolecular amination of o-arylanilines reported by Buchwald and co-workers.*

There are also a few examples of intermolecular C–N coupling reactions, such as that shown in Scheme 21, also reported by the group of Buchwald.[72]

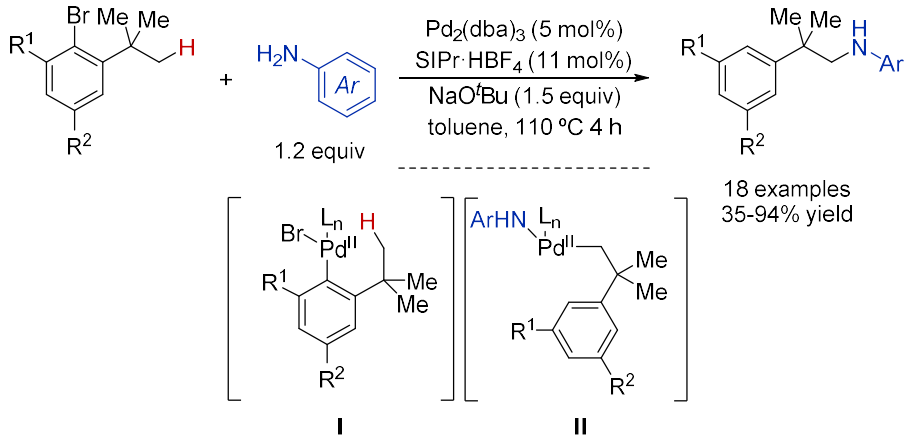

Scheme 21. *Pd(0)-catalyzed C(sp³)–H amination with aryl amines developed by Buchwald and collaborators, and key intermediates.*

[69] Cabrera, P. J.; Lee, M.; Sanford, M. S. *J. Am. Chem. Soc.* **2018**, *140*, 5599.
[70] Park, Y.; Kim, Y.; Chang, S. *Chem. Rev.* **2017**, *117*, 9247.
[71] Tsang, W. C. P.; Zheng, N.; Buchwald, S. L. *J. Am. Chem. Soc.* **2005**, *127*, 14560.
[72] Pan, J.; Su, M.; Buchwald, S. L. *Angew. Chem. Int. Ed.* **2011**, *50*, 8647.

In this reaction, the catalytic cycle starts with a Pd(0) catalyst. This happens because the first step is the oxidative addition of the palladium to the aryl bromide, so the metal center is now located close to the activated C−H bond (intermediate **I**). This approach, complementary to the directing group strategy for Pd(II) catalysts, is also often seen in Pd-catalyzed C−H activation chemistry.[73] After the C−H activation, the palladacycle undergoes a protodemetalation, followed by the activation of the N–H bond of the aniline (intermediate **II**), and a reductive elimination to give the product.

4.3.1.3 Formation of carbon-oxygen (C−O) bonds

Most of these reactions have focused on acetoxylations, and involve Pd(II)/Pd(IV) mechanisms.[74] Among all these examples, the most employed oxidants are based on iodine(III) reagents, particularly (diacetoxyiodo)benzene ($PhI(OAc)_2$). An illustrative example from the group of Sanford is depicted in Scheme 22.[75]

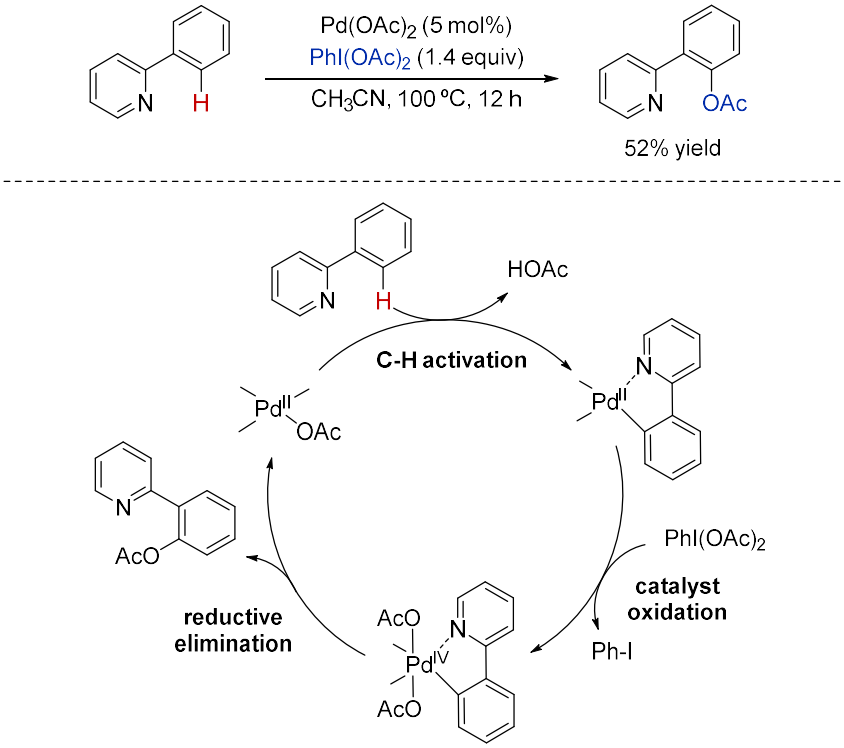

Scheme 22. *Pd-catalyzed C−H acetoxylation directed by a pyridine group, and mechanistic proposal.*

[73] (a) Baudoin, O. *Acc. Chem. Res.* **2017**, *50*, 1114. (b) Chen, X.; Engle, K. M.; Wang, D. H.; Yu, J.-Q. *Angew. Chem. Int. Ed.* **2009**, *48*, 5094. (c) He, J.; Wasa, M.; Chan, K. S. L.; Shao, Q.; Yu, J.-Q. *Chem. Rev.* **2017**, *117*, 8754.

[74] Lyons, T. W.; Sanford, M. S. *Chem. Rev.* **2010**, *110*, 1147.

[75] Dick, A. R.; Hull, K. L.; Sanford, M. S. *J. Am. Chem. Soc.* **2004**, *126*, 2300.

The mechanism starts with the coordination of the pyridine to the metal center, followed by a C–H activation. Then, the metal is oxidized from Pd(II) to Pd(IV), with the addition of two acetates. Finally, a reductive elimination yields the product. This mechanism has been extensively discussed by several authors due to the unusual nature of palladium (IV) complexes.[76]

Other example of acetoxylations can be found in the work developed in parallel by Yu[77] and van Gemmeren[78] for the β-C(sp^3)–H acetoxylation of aliphatic carboxylic acids. Yu's reaction entails the use of mono-protected amino acid ligands and *tert*-butyl hydroperoxide (TBHP) as oxidant (Scheme 23). It is important to notice the essential role of the base in this reaction. Its employment favors the coordination of the Na^+ to the carboxylate, preventing the poisoning of the catalyst and allowing the C(sp^3)–H activation to take place. After that, the catalyst is oxidized from Pd(II) to Pd(IV) by TBHP. Then, a ligand exchange places two acetate ligands in the catalyst and, after a reductive elimination, the product is formed. However, a SN_2-type reductive elimination cannon be ruled out.

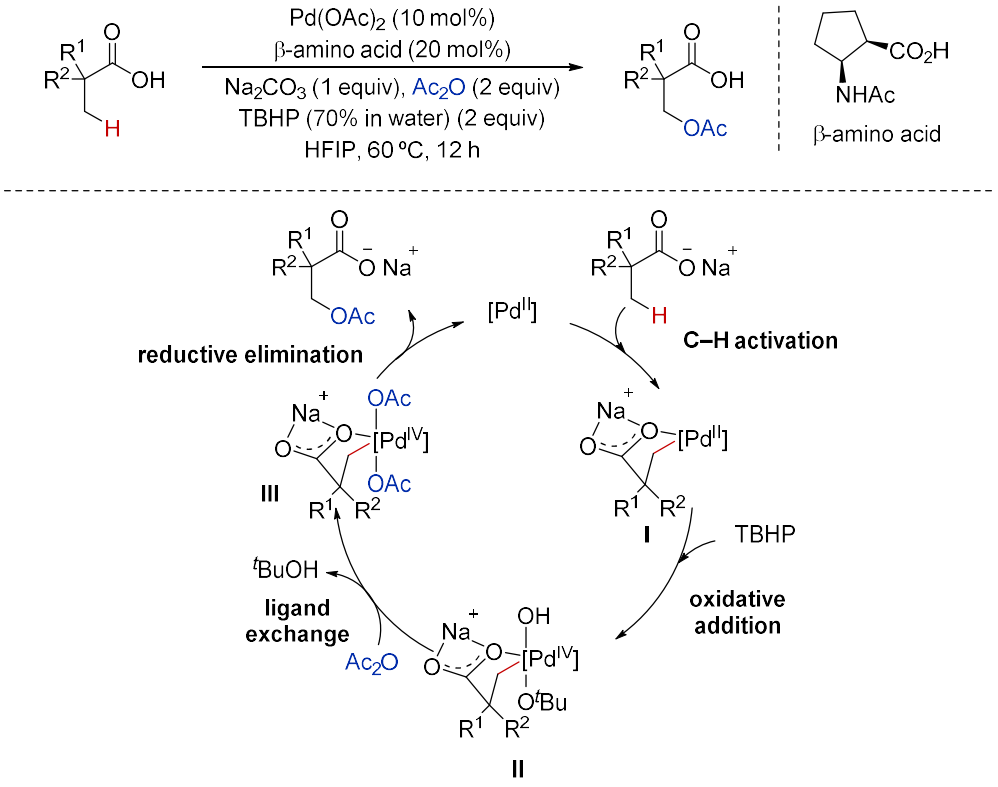

Scheme 23. *Pd-catalyzed β-C(sp^3)–H acetoxylation of aliphatic carboxylic acids reported by Yu and co-workers, and mechanistic proposal.*

[76] (a) Dick, A. R.; Kampf, J. W.; Sanford, M. S. *J. Am. Chem. Soc.* **2005**, *127*, 12790. (b) Racowski, J. M.; Dick, A. R.; Sanford, M. S. *J. Am. Chem. Soc.* **2009**, *131*, 10974. (c) Powers, D. C.; Xiao, D. Y.; Geibel, M. A. L.; Ritter, T. *J. Am. Chem. Soc.* **2010**, *132*, 14530. (d) Guo, L.; Xu, Y.; Wang, X.; Liu, W.; Lu, D. *Organometallics* **2013**, *32*, 3780. (e) Le Bras, J.; Muzart, J. *Eur. J. Org. Chem.* **2017**, 3528.

[77] Zhuang, Z.; Herron, A. N.; Fan, Z.; Yu, J.-Q. *J. Am. Chem. Soc.* **2020**, *142*, 6769.

[78] Ghosh, K. K.; Uttry, A.; Koldemir, A.; Ong, M.; Van Gemmeren, M. *Org. Lett.* **2019**, *21*, 7154.

It is important to remark the relevance of the ligand in this reaction. The six-membered chelation by the β-amino acid is crucial to form the palladacycle by C(sp^3)−H activation (Figure 6). The authors claim this because of the higher bite angle and rigidity of this ligand.

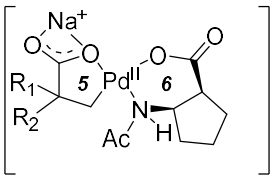

Figure 6. *Intermediate **I** of the catalytic cycle of Yu´s acetoxylation.*

4.3.1.4 Formation of carbon-halogen (C–X) bonds

The introduction of halides is highly relevant from the synthetic and functional point of view. For instance, the introduction of fluorine groups[79] has attracted an increasing interest in the field of medicinal chemistry due to their dramatic influence in the lipophilicity, conformational flexibility and metabolic stability of the compounds.[80] Besides, ^{18}F-labeled molecules can be employed as radiotracers in positron emission tomography (PET).[81]

Pd-catalyzed C−H functionalization reactions have been seen as an ideal tool to introduce fluorine atoms in organic compounds. For instance, in a parallel work developed by Yu[82] and Shi[83], they reported a methodology for the synthesis of chiral β-fluoro α-amino acids. In both works, they perform a C(sp^3)−H activation of a methylene, followed by the introduction of the fluorine moiety with the aid of Selectfluor©, an electrophilic fluorine-donor reagent (Scheme 24). As indicated in the scheme, in this case the reaction was better carried out using a quinoline type of ligand, which probably plays a role in avoiding the formation of inactive palladium species.

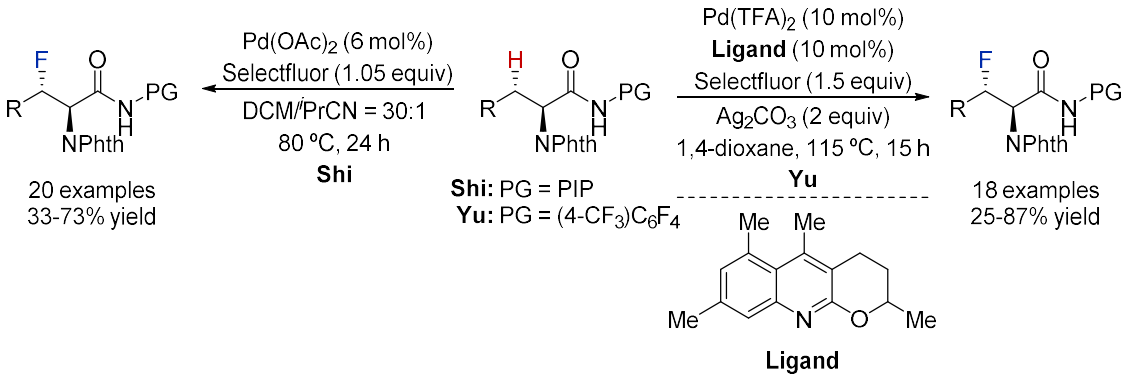

Scheme 24. *Pd-catalyzed β-C(sp^3)−H fluorination of α-amino acids developed by Shi, Yu and co-workers.*

[79] Szpera, R.; Moseley, D. F. J.; Smith, L. B.; Sterling, A. J.; Gouverneur, V. *Angew. Chem. Int. Ed.* **2019**, *58*, 14824.

[80] (a) Müller, K.; Faeh, C.; Diederich, F. *Science* **2007**, *317*, 1881. (b) Purser, S.; Moore, P. R.; Swallow, S.; Gouverneur, V. *Chem. Soc. Rev.* **2008**, 37, 320. (c) Swallow, S. *Progress in Medicinal Chemistry*, Vol. 54, Elsevier B.V., **2015**, 65.

[81] Bailey, D.L; D.W. Townsend; P.E. Valk; M.N. Maisey *Positron Emission Tomography*, Springer, **2005**.

[82] Zhu, R. Y.; Tanaka, K.; Li, G. C.; He, J.; Fu, H. Y.; Li, S. H.; Yu, J.-Q. *J. Am. Chem. Soc.* **2015**, *137*, 7067.

[83] Zhang, Q.; Yin, X. S.; Chen, K.; Zhang, S. Q.; Shi, B. F. *J. Am. Chem. Soc.* **2015**, *137*, 8219.

Other halogens can also be introduced using Pd-catalyzed C−H activation reactions.[84] For instance, Yu developed in 2017 a β-C(sp^3)−H iodination of ketones using a removable directing group auxiliary that works as an L,X ligand (Scheme 25).[85] After the palladacycle is formed, the iodination takes places through a Pd(II)/Pd(IV) mechanism, employing molecular iodine as oxidant, in a similar fashion to the acetoxylation reactions reported above (vide supra).

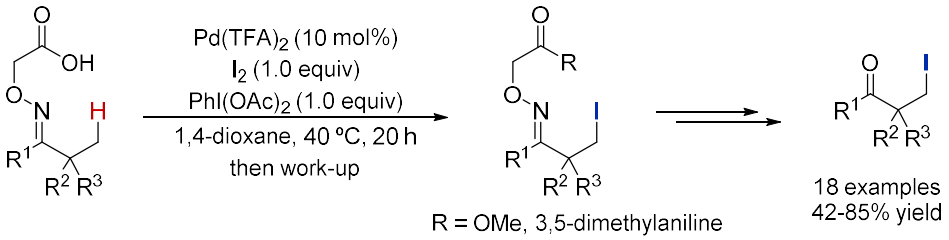

Scheme 25. *Pd-catalyzed β-C(sp^3)−H iodination of ketones reported by Yu and co-workers.*

The intermediate which likely undergoes reductive elimination of the C–I bond is depicted in Figure 7. After the formation of the iodinated product, the oxime directing group can be easily removed to obtain the β-iodinated ketone.

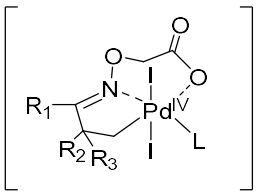

Figure 7. *Proposed intermediate of the catalytic cycle.*

[84] Petrone, D. A.; Ye, J.; Lautens, M. *Chem. Rev.* **2016**, *116*, 8003.
[85] Zhu, R. Y.; Liu, L. Y.; Yu, J.-Q. *J. Am. Chem. Soc.* **2017**, *139*, 12394.

4.3.2 Formal cycloadditions involving the activation of C−H bonds

4.3.2.1 Introduction

As it explained in previous sections, the use of directing groups tends to be mandatory in many transition-metal mediated C−H functionalization processes, including palladium-catalyzed reactions. In most of the cases, the directing group is only used as a coordinating motif to achieve the C−H functionalization, so it is not usually needed in the final structure, and it has to be removed afterwards. Thus, it is somewhat contradictory to employ C−H activation reactions as a way to pursue total *atom* and *step economy*, when the introduction and subsequent removal of structural motifs is often mandatory for this methodology. Additional strategies, like the employment of transient directing groups that are only present in the C−H functionalization step[86], avoid these extra actions, but they only can be implemented in certain cases.

Another alternative consists of engineering reactions in which the directing group could be part of the product, something that is feasible in formal cycloaddition processes. Classical metal-catalyzed cycloadditions involve the formation of metalacyclic intermediates via oxidative cyclometalations (Scheme 26a). Assembling related metalacycles using C–H activations could provide an alternative, step economical way to build cyclic products from acyclic starting materials in an atom economical manner. This strategy provides a new, different approach for the synthesis of cyclic molecules, particularly heterocyclic rings, which are a common motif in bioactive products (Scheme 26b). [87]

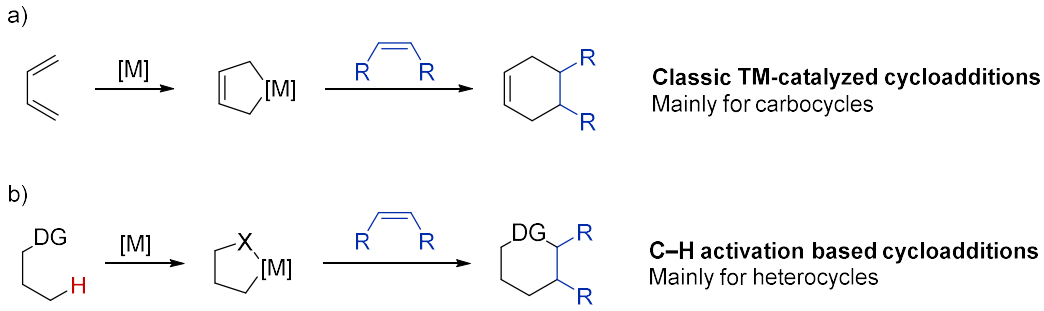

Scheme 26. *Comparison between classic transition-metal catalyzed cycloadditions and C−H activation-based cycloadditions.*

Most of the C−H activation-based formal cycloadditions rely on the same mechanistic framework, namely C−H activation, migratory insertion and reductive elimination. An illustrative example for a general Pd-catalyzed C(sp^2)–H activation-based cycloaddition with alkenes is depicted in Scheme 27.[88]

The mechanism starts with the formation of the palladacycle via C−H activation assisted by the directing group. Then, the coupling partner, in this case an alkene, coordinates to the palladium center and undergoes a migratory insertion to form a larger palladacycle, that suffers a reductive elimination to form the product. The Pd(0) is reoxidized to Pd(II) with the aid of an oxidant. It is

[86] Gandeepan, P.; Ackermann, L. *Chem* **2018**, *4*, 199.
[87] (a) Majumdar, K. C.; Chattopadyay, S. K. *Heterocycles in natural product synthesis* Wiley-VCH, **2011**. (b) Lamberth, C.; Dinges, J. *Bioactive heterocyclic compound classes: Pharmaceuticals* Wiley-VCH, **2012**.
[88] For further information about Pd-catalyzed C–H activation-based cycloadditions, among other metals: Gulías, M.; Mascareñas, J. L. *Angew. Chem. Int. Ed.* **2016**, *55*, 1100.

important to mention that, if there are available hydrogens at the β position, an undesired β-hydride elimination could take place after the migratory insertion.

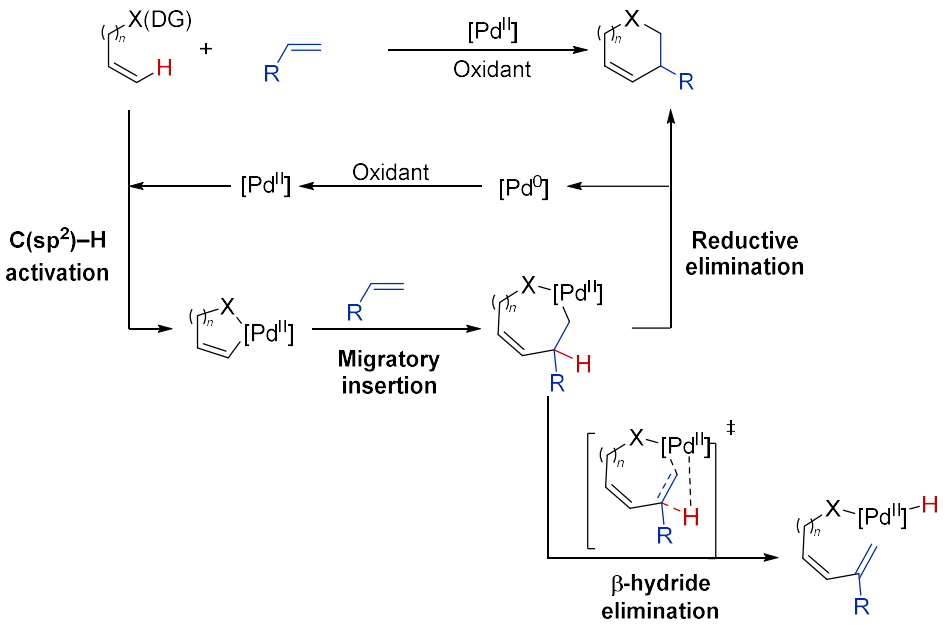

Scheme 27. *General mechanism for a Pd-catalyzed cycloaddition with alkenes via C(sp^2)–H activation.*

In the following sections, examples of different palladium-catalyzed cycloadditions engaging C(sp^2)−H activation will be depicted. Only a few examples of formal cycloadditions entailing C(sp^3)−H activations have been reported, and they will be covered in section 1.4 of Chapter III.

4.3.2.2 (n+1) cycloadditions

In these types of formal cycloadditions, the coupling partner provides one carbon to the final ring. The most common reagent for this purpose is carbon monoxide. A representative example of this chemistry is the work of Shi and collaborators, describing the Pd(II)-catalyzed carbonylation of 2-arylphenols (formal (5+1) annulation).[89] Mechanistic studies suggested that the C–H activation goes through an electrophilic cyclopalladation rather than a CMD. After this step, a Pd-carbonyl intermediate is formed. In a same way that the aforementioned general mechanism, this intermediate evolves by migratory insertion of the CO group followed by reductive elimination to afford the lactone-derived cycloadducts. The resulting Pd^0 species is reoxidized to Pd^{II} by a combination of $Cu(OAc)_2$ and oxygen from the air atmosphere (Scheme 28).

[89] Luo, S.; Luo, F.-X.; Zhang, X.-S.; Shi, Z.-J. *Angew. Chem. Int. Ed.* **2013**, *125*, 10792.

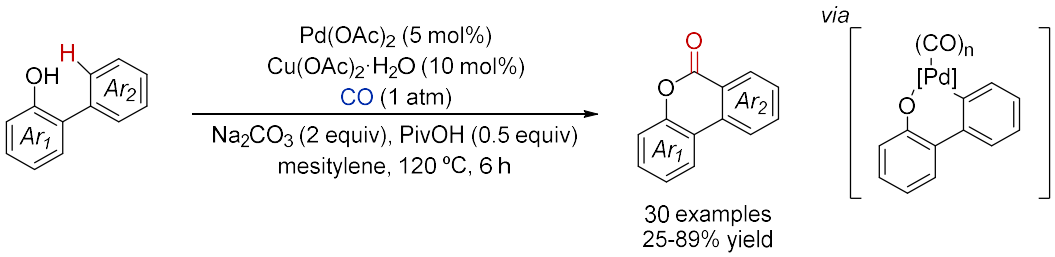

Scheme 28. *Pd(II)-catalyzed (5+1) carbonylation of 2-arylphenols developed by Shi and co-workers, and key intermediate.*

4.3.2.3 (n+2) cycloadditions

In these reactions, the unsaturated coupling partners are 2-carbon donors, which usually coordinate well to the metal center through their π-bonds. A variety of methodologies based on these types of formal annulations have been described, especially using rhodium catalysis.[90] Palladium catalysts have been scarcely reported. Our research group has published several formal (4+2) cycloadditions,[91] e.g., the annulation between triflyl protected vinylanilines and allenes to give benzazepine skeletons (Scheme 29).[91a] Allenes are especially valuable as partners owing to their intrinsic reactivity and the viability of generating π-allyl intermediates that stabilize metalacycles and favor reductive elimination over β-hydride elimination. Besides, they are not as coordinating as alkynes, avoiding the saturation of the metal coordination sphere to give nonactive complexes.

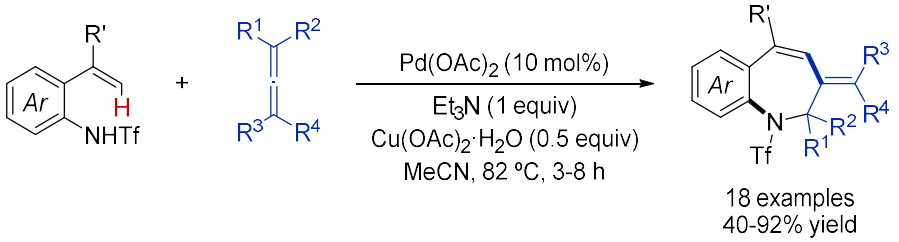

Scheme 29. *Pd(II)-catalyzed (4+2) cycloaddition of vinylanilides and allenes reported by Gulías, Mascareñas and collaborators.*

4.3.2.4 (n+n+n) cycloadditions

Multicomponent cycloadditions are very interesting transformations as they can lead to a rapid increase in complexity in a single step. However, they are not as common as other types of C–H activation-based cycloadditions. Examples of these kind of transformations employing palladium complexes as catalysts are the (3+2+1) annulation reported by Wu[92], and the (3+2+2) annulation reported by Wang (Scheme 30).[93]

[90] Satoh, T.; Miura, M. *Chem. Eur. J.* **2010**, *16*, 11212.
[91] (a) Casanova, N.; Del Rio, K. P.; García-Fandiño, R.; Mascareñas, J. L.; Gulías, M. *ACS Catal.* **2016**, *6*, 3349. (b) Cendón, B.; Casanova, N.; Comanescu, C. C.; García-Fandiño, R.; Seoane, A.; Gulías, M.; Mascareñas, J. L *Org. Lett.* **2017**, *19*, 1674. (c) González, J. M.; Cendón, B.; Mascareñas, J. L.; Gulías, M. *J. Am. Chem. Soc.* **2021**, *143*, 3747.
[92] Chen, J.; Natte, K.; Spannenberg, A.; Neumann, H.; Beller, M.; Wu, X. F. *Chem. Eur. J.* **2014**, *20*, 14189.
[93] Wang, L.; Huang, J.; Peng, S.; Liu, H.; Jiang, X.; Wang, J. *Angew. Chem. Int. Ed.* **2013**, *52*, 1768.

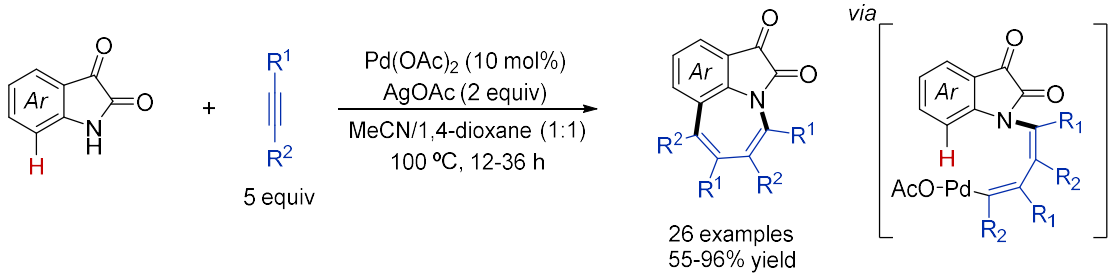

Scheme 30. *Pd(II)-catalyzed (3+2+2) cycloaddition of isatin derivatives and alkynes developed by Wang and co-workers, and intermediate prior to C–H activation.*

The mechanism proposed for this reaction starts with an initial tandem amination of two alkyne moieties, followed by a C−H activation step and a reductive elimination. With this methodology, it is possible to build these interesting scaffolds in a single step from simple and readily available starting materials.

Even though classic palladium-catalyzed cycloadditions of unsaturated precursors are still predominant, it is a matter of time that palladium-catalyzed C−H activation-based cycloadditions become a common method for the synthesis of cycles and heterocycles in organic synthesis.

4.4 Current challenges and future outlook

With the global concern of climate change and other environmental challenges, it is now more important than ever to develop synthetic methodologies that follow the green chemistry precepts. The principles of *atom* and *step economy* should guide many of the future developments in synthetic chemistry.

In this context, the metal-mediated C–H activation field, by avoiding the need of functionalized precursors, will provide some of the most relevant solutions. However, there are still important challenges to be solved, for instance, the requirement of stoichiometric amounts of inorganic oxidants to regenerate the metal catalysts. There is a notable interest in substituting the inorganic oxidants of C–H activation reactions for organic oxidants or, ultimately, by electricity.[94] Another problem is the need to have directing groups, which are not relevant beyond their role as activating moiety.

Additionally, as chirality is inherent to most of the bioactive molecules in nature, asymmetric methods that enable the synthesis of enantiopure compounds are highly desirable to avoid complex, costly enantiomeric resolutions that introduce extra steps in the overall procedure. Even though there have been important contributions in the field of enantioselective C–H functionalization, this area is yet starting to be developed.

Another current challenge is the functionalization of C(sp^3)–H bonds. This field is still underdeveloped, due to the inherent inertness of these types of bonds, which hampers its selective activation. Related to this, the field of formal cycloadditions based on the activation of C(sp^3)–H bonds is still in its complete infancy, and only a few methods have been reported, none of them being enantioselective (see Chapter III).

[94] Jiao, K. J.; Xing, Y. K.; Yang, Q. L.; Qiu, H.; Mei, T. S. *Acc. Chem. Res.* **2020**, *53*, 300.

General objectives

General objectives

Considering all the precedents and current challenges in the field of palladium-catalyzed C–H activation, discussed in the Chapter I, we have focused on the development of novel methodologies based on this area of research. Specifically, we have focused on the following objectives:

- Development of novel formal cycloadditions based on palladium-catalyzed C–H activation: among all the reactions reported in the field of palladium-catalyzed C–H activation, formal cycloadditions are still underdeveloped. These types of reactions are especially useful for the assembly of azaheterocycles, whose synthesis is not straightforward using classic metal-catalyzed formal-cycloadditions. Our research group has published several formal (4+2) cycloadditions using allenes as coupling partners,[91] and therefore this previous experience could be particularly useful for the accomplishment of this objective.

- Exploring the asymmetric version of the aforementioned formal cycloadditions: heterocycles in nature often present several stereocenters due to the inherent chirality of life. Precedents in the employment of chiral ligands, like mono-protected amino acids, has demonstrated the possibility of performing asymmetric C–H activation reactions based on palladium catalysis. Therefore, it is of high interest to explore the use of chiral ligands to induce enantioselectivity in the novel formal cycloadditions based on C–H activation.

- Development of novel transformations based on the activation of $C(sp^3)$–H bonds: the activation of $C(sp^3)$–H presents important challenges compared with the activation of $C(sp^2)$–H bonds. In fact, palladium-catalyzed formal cycloadditions based on this type of activation are scarce, none of them being enantioselective. Therefore, development of novel methodologies, like formal cycloadditions or cyclizations, is of high interest as an elegant, efficient way to access cyclic structures like azaheterocycles.

Chapter II

Synthesis of tetrahydroisoquinoline skeletons via enantioselective formal cycloadditions of benzyltriflamides with allenes

This chapter includes work published in *Journal of the American Chemical Society* as:

Vidal, X.;[a] Mascareñas, J. L.;[a] Gulías, M.[a] *J. Am. Chem. Soc.* **2019**, *141*, 1862.

[a] Centro Singular de Investigacion en Química Bioloxica e Materiais Moleculares (CIQUS) and Departamento de Química Organica, Universidade de Santiago de Compostela, 15782 Santiago de Compostela, Spain

DOI: 10.1021/jacs.8b12636, Open Access article (ACS AutorChoice)

1- Introduction

1.1 Tetrahydroisoquinolines as important scaffolds in nature

Tetrahydroisoquinoline (THIQ) alkaloids are common in nature and present a wide variety of biological activities. Among all of them, those who present antitumor and antimicrobial activity have drawn a particular interest on the field of medicinal chemistry (Figure 8).[95]

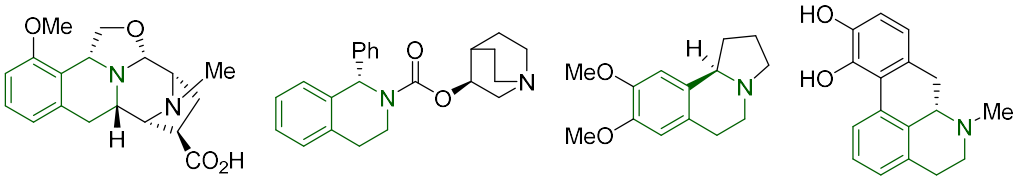

Quinocarcin (antitumoral) | **Solifenacin** (antimuscarinic) | **Crispine A** (antitumoral) | **Apomorphine** (Parkinson treatment)

Figure 8. *Examples of tetrahydroisoquinoline alkaloids and their medical application.*

As it can be deduced from the figure above, most of the bioactive THIQ alkaloids are complex, chiral molecules, bearing several stereocenters. Thus, development of efficient, enantioselective methods to assemble those skeletons is of primary relevance.

1.2 Classical methods for the synthesis of optically active tetrahydroisoquinolines

Due to their potential use as drugs, tetrahydroisoquinolines have been important synthetic targets over the last decades.[96] In this section, the three main synthetic strategies that have been classically employed to synthesize optically active THIQ alkaloids are going to be disclosed: the Picted–Spengler cyclization, the Bischler−Napieralski cyclization/reduction and the Pomeranz−Fritsch−Bobbitt cyclization.

1.2.1 Picted–Spengler cyclization

The Picted–Spengler cyclization was discovered in 1911 by Amé Picted and Theodor Spengler.[97] Sometimes considered as a special variation of the Mannich reaction, it consists in an acid-catalyzed condensation between β-arylethylamines and aldehydes or their synthetic equivalents. Despite its antiquity, this reaction is still frequently employed in modern synthesis of THIQ alkaloids. In the case of the asymmetric variant, it is usual to employ chiral β-arylethylamines, mostly obtained from natural α-amino acids like L-phenylalanine, L-tyrosine or L-DOPA, as amine component and source of chirality. Following this strategy, the group of Herr synthesize the (*S*)-enantiomer of the natural anti-tumor alkaloid (*R*)-Crispine A using commercially available L-DOPA methyl ester.[98] Their condensation with 4-chloro-1,1-dimethoxybutane afforded the Picted-Spengler product in a 98% yield and a 4.5:1 diasteroisomeric ratio. The synthesis was completed by radical decarboxylation of the

[95] Scott, J. D.; Williams, R. M. *Chem. Rev.* **2002**, *102*, 1669.
[96] Chrzanowska, M.; Grajewska, A.; Rozwadowska, M. D. *Chem. Rev.* **2016**, *116*, 12369.
[97] Pictet, A.; Spengler, T. *Berichte der Dtsch. Chem. Gesellschaft* **1911**, *44*, 2030.
[98] Gurram, M.; Gyimóthy, B.; Wang, R.; Lam, S. Q.; Ahmed, F.; Herr, R. J. *J. Org. Chem.* **2011**, *76*, 1605.

corresponding methylselenyl ester group, leading to the formation of the (*S*)-(-)-Crispine A in a 31% overall yield (Scheme 31).

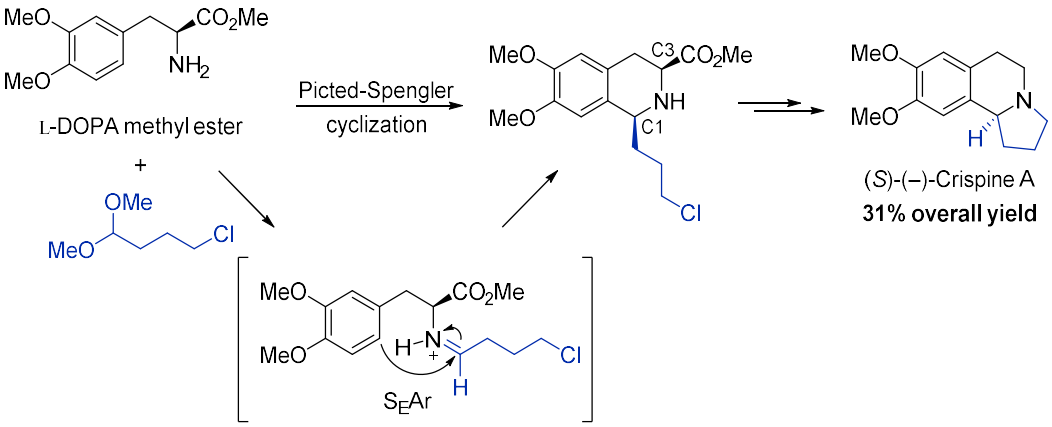

Scheme 31. *Diastereoselective synthesis of (S)-(–)-Crispine A from L-DOPA methyl ester developed by Herr and co-workers, and key intermediate.*

The C1 chiral center is formed in a diastereoselective fashion because of the influence of the C3 stereocenter in the iminium cation conformation.

There are also several reports of β-arylethylamines bearing a chiral auxiliary attached to the nitrogen atom that can be later removed. As in the previous case, the diastereoselectivity is determined by the conformation of the iminium cation, which is affected by the electronic and steric features of the chiral auxiliary.[99]

1.2.2 Bischler–Napieralski cyclization/reduction

The Bischler–Napieralski cyclization was discovered in 1893 by August Bischler and Bernard Napieralski as a method for the synthesis of dihydroisoquinolines from β-arylethylamides using condensation agents, mostly phosphoryl chloride ($POCl_3$).[100] This reaction can be combined with a subsequent stereoselective reduction of the imine group for the synthesis of optically active tetrahydroisoquinolines. To control the stereoselectivity, a chiral auxiliary-based strategy is employed in most cases. The auxiliary can be placed either in the β-arylethylamide or at the *N*-acyl moiety, so the chiral imine intermediate can be diastereoselectively reduced with hydride-based reductants or by catalytic hydrogenation. An illustrative example of this methodology is the synthesis of both enantiomers of the minor opium alkaloid *N*-Norlaudanidine reported by Georghiou and co-workers.[101] They prepared the Bischler–Napieralski precursor with the proper enantiomer of the popular chiral auxiliary α-methylbenzylamine. After the cyclization, the dihydroisoquinoline was stereoselectively reduced with $NaBH_4$ to afford the corresponding THIQ in a 95% diasteroisomeric excess (*de*). Finally, the corresponding enantiomer of *N*-Norlaudanidine was obtained after the auxiliary removal via catalytic hydrogenolysis in an overall yield of 28% (Scheme 32).

[99] Sánchez-Obregón, R.; Ortiz, B.; Mastranzo, V. M.; Yuste, F.; Ruano, J. L. G. *Tetrahedron Lett.* **2013**, *54*, 1893.
[100] Bischler, A; Napieralski, B. *Berichte der Dtsch. Chem. Gesellschaft* **1893**, 1903.
[101] Zein, A. L.; Dakhil, O. O.; Dawe, L. N.; Georghiou, P. E. *Tetrahedron Lett.* **2010**, *51*, 177.

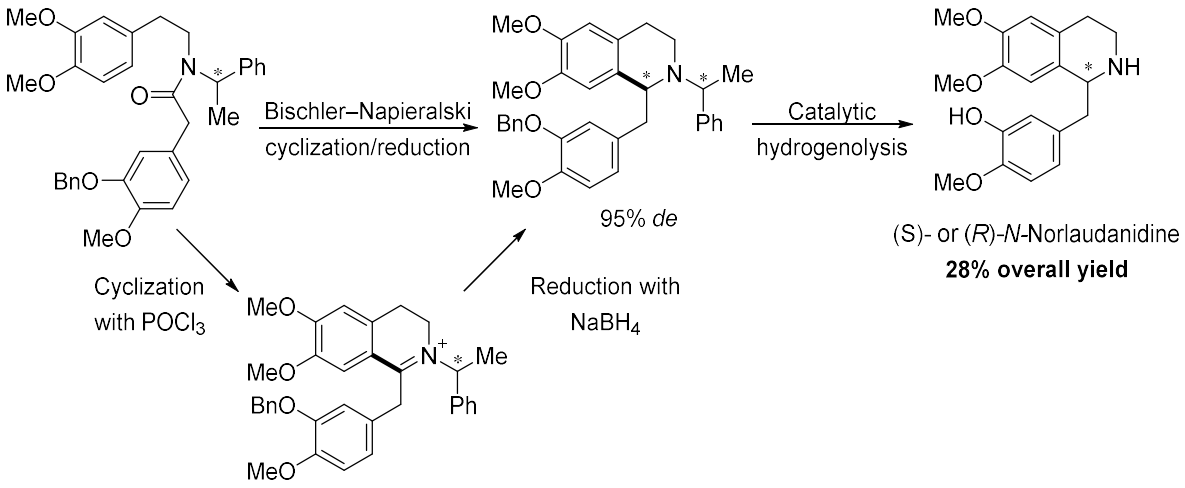

Scheme 32. *Diastereoselective synthesis of both enantiomers of N-Norlaudanidine using α-methylbenzylamine as chiral auxiliary developed by Georghiou and co-workers.*

In the pursue of *step economy*, the focus of the asymmetric Bischler−Napieralski cyclization/ reduction has shifted towards development of transition-metal catalyzed enantioselective reduction of prochiral isoquinolines, either by catalytic hydrogenation with Ir, Rh or Ru complexes, or by transfer hydrogenation, mostly with Ru complexes like Noyori´s catalyst.

1.2.3 Pomeranz−Fritsch−Bobbitt synthesis

The Pomeranz−Fritsch−Bobbitt synthesis of tetrahydroisoquinolines is a modification of the Pomeranz−Fritsch cyclization developed in 1893.[102] The original method described the synthesis of isoquinolines by condensation of aldehydes and 2,2-dialkoxyethylamines, followed by the acid-catalyzed cyclization of the corresponding benzylidenoacetals. Bobbitt and co-workers reported in 1965 a modification of this methodology.[103] It consists of the hydrogenation or the nucleophilic addition to the imine group of the benzylidenoacetal prior to the cyclization, which eventually leads to the formation of THIQ instead of isoquinolines.

In order to obtain enantioenriched THIQs, the benzylidenoacetal precursor has to be chiral. This could be done by employing asymmetric nucleophilic addition over chiral imine precursors or by the use of alternative synthesis that lead to the same chiral intermediate. An illustrative example of the first method is the synthesis of the aporphine alkaloid (*S*)-(+)-Laudanosine from (*S*)-phenylglycinol derived imine and the proper Grignard reagent reported by Badía and co-workers in 2004.[104] The chiral auxiliary was removed after the nucleophilic addition and the proper diethylacetal moiety was introduced to perform the Pomeranz–Fritsch cyclization, that lead to the formation of the (*S*)-Laudanosine (Scheme 33).

[102] (a) Pomeranz, C. *Monatshefte für Chemie* **1893**, *14*, 116. (b) Fritsch, P. *Berichte der Dtsch. Chem. Gesellschaft* **1893**, *26*, 419.
[103] Bobbitt, J. M.; Kiely, J. M. N.; Khanna, K. L.; Ebermann, R. *J. Org. Chem.* **1965**, *30*, 2247.
[104] Anakabe, E.; Carrillo, L.; Badía, D.; Vicario, J. L.; Villegas, M. *Synthesis* **2004**, 1093.

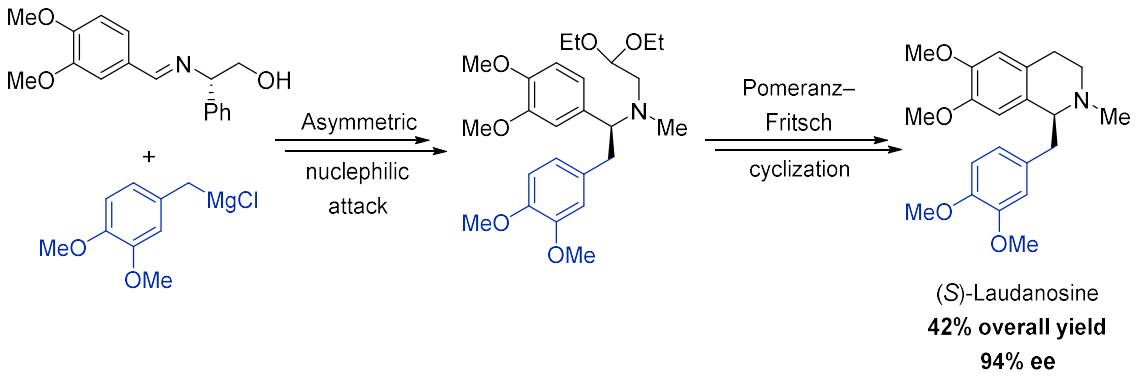

Scheme 33. *General mechanism of the Pomeranz–Fritsch–Bobbitt synthesis of tetrahydroisoquinolines.*

1.3 Synthesis of tetrahydroisoquinoline skeletons relying on Pd-catalyzed C–H activations

Even though classic methods for the synthesis of THIQ are well-stablished, more efficient methods based on catalytic processes are clearly needed. Often, these classic methods require nonstrategic steps, like attachment and removal of chiral auxiliaries. Besides, several methodologies employ chiral precursors, e.g., natural amino acids, in order to build asymmetric skeletons, being limited to only obtain the natural enantiomer of the precursor. It is also important to mention that classic methods are limited to electron-rich arenes, as the cyclizations are based on S_EAr reactions. Hence, the development of novel protocols based on different strategies is of high importance. Among all the possibilities, organometallic methodologies involving the activation of C–H bonds are especially attractive.

However, to the best of our knowledge, only two methods based on this technology had been reported when we started our work. In 2008, Yu and co-workers reported the synthesis of tetrahydroisoquinoline skeletons, as part of a larger study about the synthesis of indolines. The method employs triflyl-protected arylethylamine precursors and a Pd(II)-catalyzed C–H alkenylation/intramolecular Michael-addition process.[105] The reaction tolerates electron-withdrawing groups in the aryl moiety. This tolerance contrasts with classic arylations, which need electron-rich systems (Scheme 34).

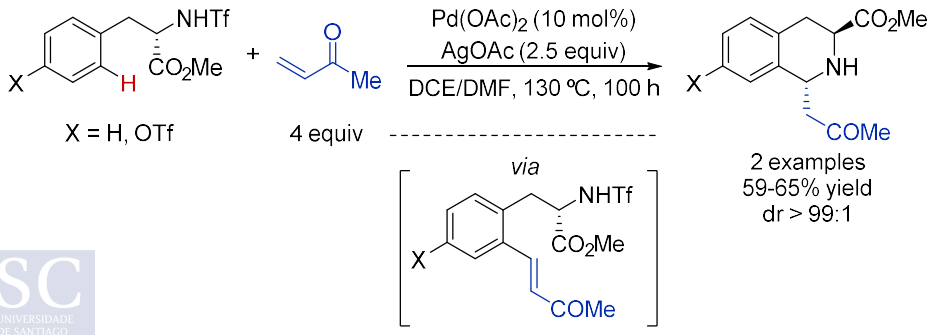

Scheme 34. *Pd(II)-catalyzed alkenylation/Michael-addition of triflyl-protected arylethylamines disclosed by Yu and co-workers, and key intermediate.*

[105] Li, J.-J.; Mei, T.-S.; Yu, J.-Q. *Angew. Chem. Int. Ed.* **2008**, *120*, 6552.

The methodology is clever, but in some cases dialkenylation side products resulting from a double C–H activation of the precursor are obtained. Furthermore, the synthesis of the products in an asymmetric fashion relies on the use of chiral precursors.

In 2014, the group of Nicolás published a formal (4+2) cycloaddition of α-disubstituted benzylamines and phenylethylamines with allenes (Scheme 36), a method that allows a direct assembly of the azaheterocyclic skeletons and is based on a Pd-catalyzed C–H activation.[106]

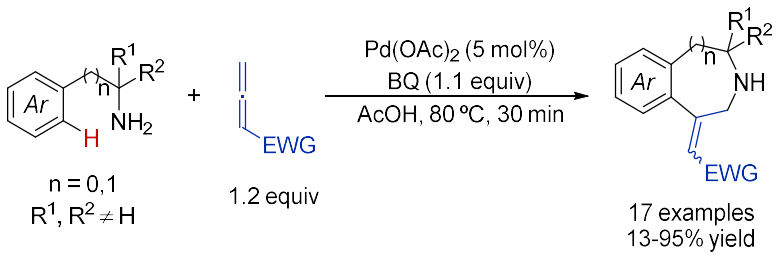

Scheme 35. *Pd(II)-catalyzed formal (4+2) annulation of benzylamines and phenylethylamines with allenes reported by Nicolás and co-workers.*

While the strategy is very attractive, the reaction presents important limitations. First, the protocol only works with substrates bearing two substituents at the α-position of the amine to prevent benzylic oxidation. Second, the methodology is limited to the use of electron-poor primary allenes. Third, the resulting tetrahydroisoquinolines and benzazepines were obtained as regio- and stereoisomeric mixtures. And last but not least, the method is racemic, and therefore chiral THIQ cannot be obtained. In this context, performing asymmetric C–H activations of benzylamine precursors can open interesting opportunities.

1.4 Palladium-catalyzed enantioselective C–H functionalization of benzylamine derivatives

The generation of asymmetry in C–H activation reactions has been an area of increasingly intensive research during the last decade.[107] Several strategies can be used in order to make enantioenriched products using this chemistry. When in a racemic mixture, one of the enantiomers is selectively recognized by a chiral catalyst, we can achieve a kinetic resolution process. Alternatively, when there are symmetry elements in the molecule prior to the C–H activation, and the reaction results in the loss of one or more of them, we can promote desymmetrization processes.

Both strategies have been employed for palladium-catalyzed C–H functionalizations of benzylamines. These types of substrates present an amino functionality that acts as a directing group, placing the palladium close to the desired C–H bond, often located in *ortho* position. However, the employment of substrates with unprotected amino groups usually limits the reactivity, in part because of the formation of highly stable cyclometalated intermediates, that are less reactive in subsequent functionalization steps. Indeed, amines are known to form stable,

[106] Rodríguez, A.; Albert, J.; Ariza, X.; Garcia, J.; Granell, J.; Farràs, J.; La Mela, A.; Nicolás, E. *J. Org. Chem.* **2014**, *79*, 9578.
[107] Newton, C. G.; Wang, S. G.; Oliveira, C. C.; Cramer, N. *Chem. Rev.* **2017**, *117*, 8908.

unreactive bis(amine)-Pd(II) species.[108] Besides, free amines are susceptible to oxidative degradation through β-hydride elimination to give imines, and N-substitution reactions toward electrophiles. Additionally, amines coordinated to transition-metal catalysts have a strong donor effect that decreases the electrophilicity of the metal, thus, hampering the C–H activation based on electrophilic addition or CMD mechanisms.

One strategy to address these problems consists of using electron-poor protecting groups that withdraw charge from the nitrogen, making it less reactive towards degradation and N-substitution reactions. However, these groups may also decrease the coordination ability of the amine to the catalyst. Therefore, they are usually combined with a base, that deprotonates the remaining hydrogen of the amine group in order to ease the coordination with the metal center. Besides, the base could also participate in the C–H activation step by triggering the CMD mechanism.[109]

In 2013, the Yu´s group disclosed the first palladium-catalyzed enantioselective C–H functionalization of benzylamides. They published a desymmetrization based on the *ortho* C–H iodination of triflyl-protected diarylmethylamines. Bz-Leu-OH was employed as chiral ligand, allowing the formation of the iodinated diarylmethylamines with *ees* up to 99% (Scheme 36).[110]

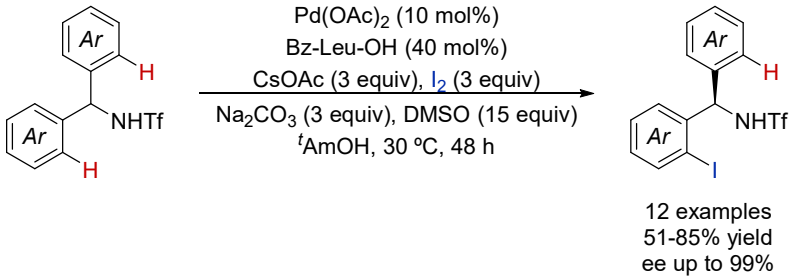

Scheme 36. *Pd(II)-catalyzed desymmetric C–H iodination of diarylmethylamines reported by Yu and co-workers.*

One year later, the same group published a kinetic resolution of α-substituted benzyltriflamides under similar reaction conditions.[111] The desymmetrizing *ortho* C–H arylation of diarylmethylamines with organoborons was described by the same group in 2015.[112] In this case, they use a nosyl protecting group, which is easier to remove than the triflate, and Fmoc-Leu-NHOMe as chiral ligand (Scheme 37). One year later, they published the kinetic resolution of α-substituted benzylnosylamides employing similar reaction conditions.[113]

[108] Zhuang, Z.; Yu, J.-Q. *J. Am. Chem. Soc.* **2020**, *142*, 12015.
[109] Engle, K. M.; Mei, T.; Wasa, M.; Yu, J.-Q. *Acc. Chem. Res.* **2012**, *45*, 788.
[110] Chu, L.; Wang, X. C.; Moore, C. E.; Rheingold, A. L.; Yu, J.-Q. *J. Am. Chem. Soc.* **2013**, *135*, 16344.
[111] Chu L.; Xiao, K.-J.; Yu, J.-Q. *Science* **2014**, *346*, 451.
[112] Laforteza, B. N.; Chan, K. S. L.; Yu, J.-Q. *Angew. Chem. Int. Ed.* **2015**, *54*, 11143.
[113] Xiao, K. J.; Chu, L.; Chen, G.; Yu, J.-Q. *J. Am. Chem. Soc.* **2016**, *138*, 7796.

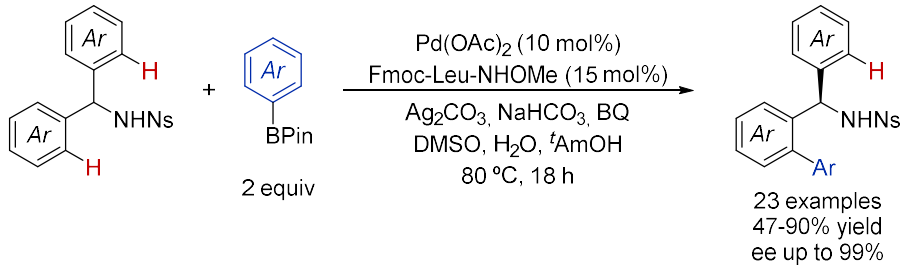

Scheme 37. *Pd(II)-catalyzed desymmetric C–H arylation of diarylmethylamines disclosed by Yu and co-workers.*

In 2019, after we published the results of our work, included in this thesis (vide infra), the group of Xu reported the desymmetrizing C–H carbonylation of benzyltosylamides to make enantioenriched isoindolinones. Boc-protected valine was employed as chiral ligand, and the reaction was performed by using a balloon with a mixture of carbon monoxide and oxygen (Scheme 38).

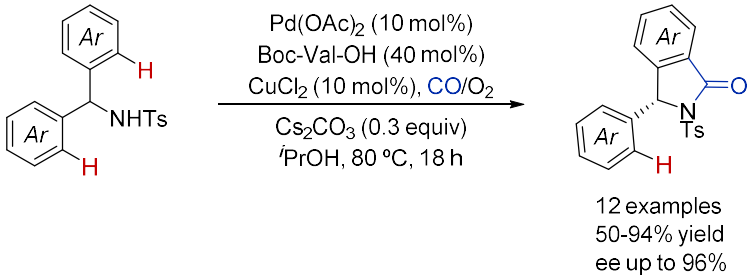

Scheme 38. *Pd(II)-catalyzed desymmetric C–H carbonylation of benzyltosylamides reported by Xu and co-workers.*

2- Objectives

Considering these precedents, and the need to develop practical, enantioselective entries to THIQs skeletons, we proposed as one of the main objectives of this doctoral thesis the development of a (4+2) formal cycloaddition between benzylamines and unsaturated two-carbon partners, mediated by a Pd-catalyzed C–H activation process (Scheme 39a). While we might explore different unsaturated partners, the precedents of the group on the use of allenes in other related cycloadditions[91] led us to select these types of reactants as primary choices. Allenes might be advantageous over alkenes in terms of reactivity (migratory insertion), as well as because of the resulting π-allyl intermediates (Scheme 40) might easily undergo the required reductive elimination.

We also intended to explore the viability of extending the annulation to alkenylamide precursors, which would lead to piperidine and azepine skeletons (Scheme 39b).

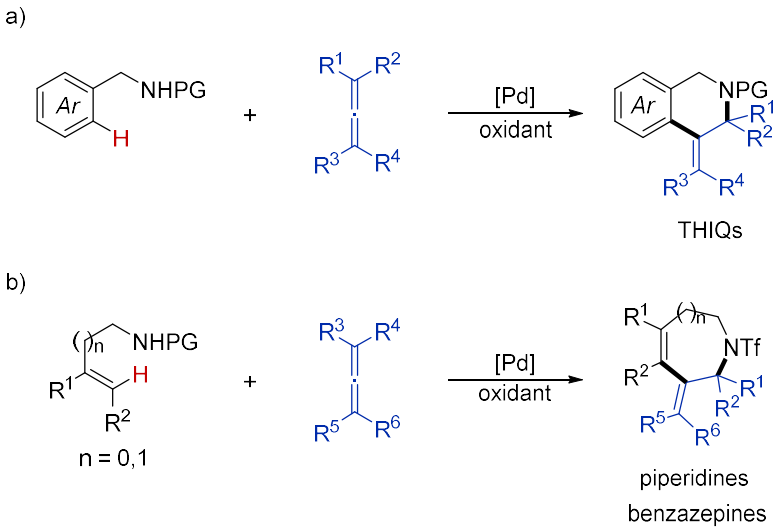

Scheme 39. *General objective of the (4+2) formal cycloaddition between benzylamines or alkenylamines and allenes.*

The proposed reactions should proceed though the general mechanism indicated below (Scheme 40). First, a C–H activation step would produce the metalacycle **I**, which could then react with the unsaturated partner through a migratory insertion step. When using allenes, this would produce π-allylic palladium species **II** that upon reductive elimination should yield the desired product.

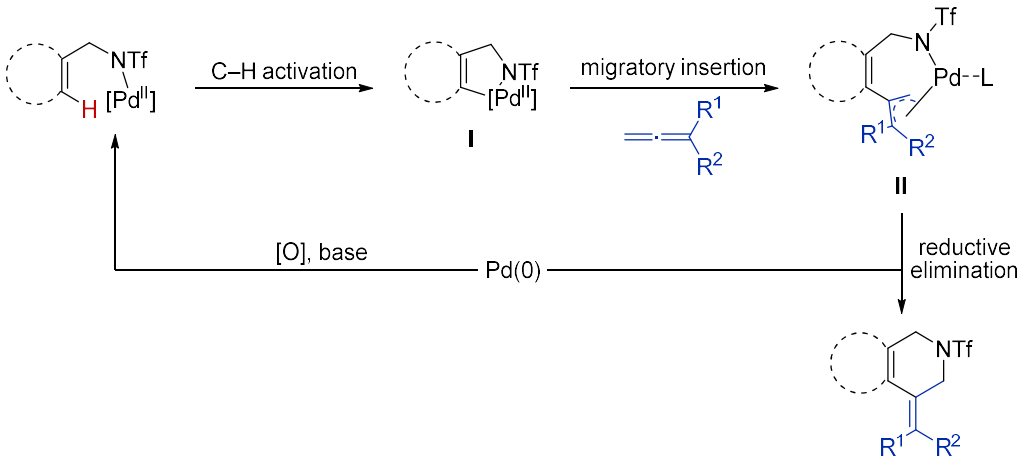

Scheme 40. *General mechanistic proposal of the (4+2) formal cycloaddition between benzyl-or alkenylamides and allenes.*

The strategy should allow the development of asymmetric variants, by using chiral palladium ligands. This would be an important advantage over other classical methods for the asymmetric synthesis of THIQs, as they often rely on the employment of chiral auxiliaries that have to be attached and removed. Particularly attractive is the possibility of implementing desymmetrizing cycloadditions as those indicated in Scheme 41. A chiral ligand coordinated to the palladium during the C–H activation step should favor the formation of one palladacycle over the other.

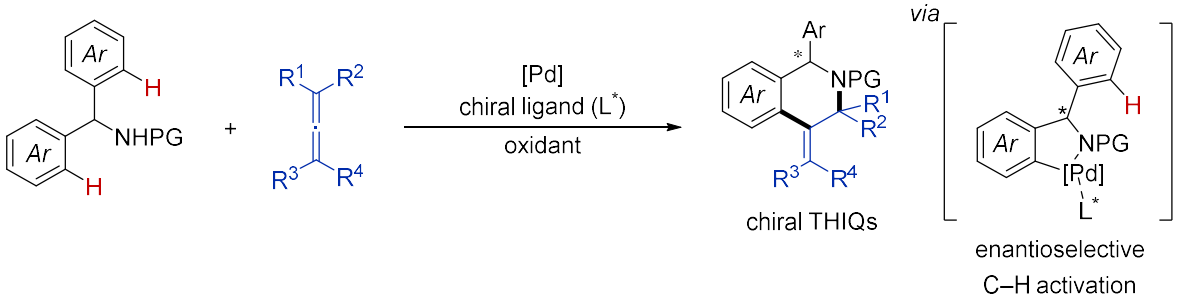

Scheme 41. *General objective of the desymmetrizing (4+2) formal cycloaddition between diarylbenzylamines and allenes.*

3- Results and discussion

3.1 Preliminary studies to identify the best reaction conditions

To begin our research, we decided to use benzyltriflamide **1a** as model substrate. We selected the triflyl protecting group because it notably increases the acidity of the N–H bond, which should facilitate the formation of the Pd–N bond, while the palladium remains electrophilic enough to promote C–H activation. Benzyltriflamide **1a** was readily synthesized by treatment of benzylamine with triflic anhydride in the presence of Et_3N.

As cycloaddition partners we focused on allenes, owing to the previous results in the group with other type of annulations.[91] In particular, the initial assays were performed with the commercially available vinilidenecyclohexane **2a**. We decided to employ $Pd(OAc)_2$ as catalyst, $Cu(OAc)_2{\cdot}H_2O$ as oxidant for the catalyst and cesium carbonate as base, as it could help both the N–H deprotonation of the triflamide and the C–H activation step. The reaction was performed under air atmosphere as there are no oxygen- or moisture-sensitive reactants. In fact, oxygen could help to reoxidize the copper acetate.

Using ^{t}AmOH as solvent, at 80 °C the expected product **3aa** was obtained in a modest 15% yield, after 16 hours. It is worth to highlight that only one regioisomer was observed, which demonstrate the selectivity of this transformation. This regioselectivity may be related with the formation of a π-allyl intermediate (see section 3.4 for a mechanistic proposal). The reaction was carried out with 2 equivalents of benzyltriflamide **1a**. However, full conversion of both **1a** and allene **2a** was observed. We detected significant amounts of benzaldehyde as an undesired side-product, presumably as a result of some benzylic oxidation and hydrolysis of the corresponding imine in the work-up conditions. Besides, allenes tend to decompose or polymerize in presence of transition-metals. After this initial result, we decided to make a screening of different conditions (Table 1). The reaction works in different solvents, being toluene the most suitable in terms of yield (25% at 90 °C, entry 5).

Table 1. *Screening of solvents.*

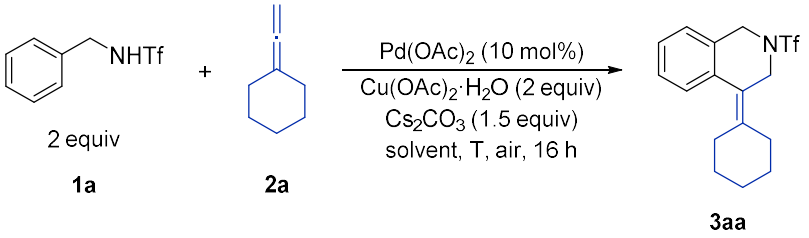

Entry	Solvent	Temp.	Yield[b]
1	^{t}AmyOH	80 °C	15%
2	Dioxane	80 °C	23%
3	DCE	80 °C	24%
4	CH_3CN	80 °C	9%
5	Toluene	90 °C	25%

[a] Conditions: 0.333 mmol **1a**, 0.167 mmol of allene **2a**, 2 mL of solvent. [c] Yields calculated by using an internal standard.

Then, we started to test the effect of adding external ligands, in particular mono-protected amino acids (MPAA ligands) as they could facilitate C–H activation reactions (see section 4.2 of Chapter I), and might also allow asymmetric processes. These results are summarized in Table 2. The use of Boc-protected amino acids, or derivatives with methoxyamide groups, as ligands allowed to increase the yield (entries 1-4). But the important change came by using 2,6-F,F-Bz-Leu-OH as ligand, which allowed to obtain the cycloadduct **3aa** in an 85% yield (entry 5). The reason for using this benzoate with two fluorides in *ortho* positions is to avoid internal C–H activations in the ligand. The addition of 15 equivalents of DMSO allowed to further rise the yield to 95% (entry 6). The reason behind the positive effect of this additive on the reaction is not clear; some studies[114] suggest that DMSO can prevent the aggregation of palladium black via S–bound coordination to Pd(0) species, thus easing the reoxidation process. It may also act as a co-solvent, helping to solubilize salts in non-polar solvents like toluene. Besides, it could also have a positive effect on the enantioselectivity of asymmetric processes as well, by sequestering the small amount of free Pd(II) species not coordinated to the chiral ligand, thus inhibiting the racemic reaction.[110]

The amount of copper acetate can be decreased to 50 mol% without significantly affecting the yield (entry 7). Besides, it was discovered that the reaction can be performed with full conversion in only 40 minutes without compromising the yield (entry 8). In the absence of DMSO, under these conditions, the yield decreased to 31% (after 40 minutes, entry 9).

[114] Diao, T.; White, P.; Guzei, I.; Stahl, S. S. *Inorg. Chem.* **2012**, *51*, 11898.

Table 2. *Screening of mono-protected amino acids.*

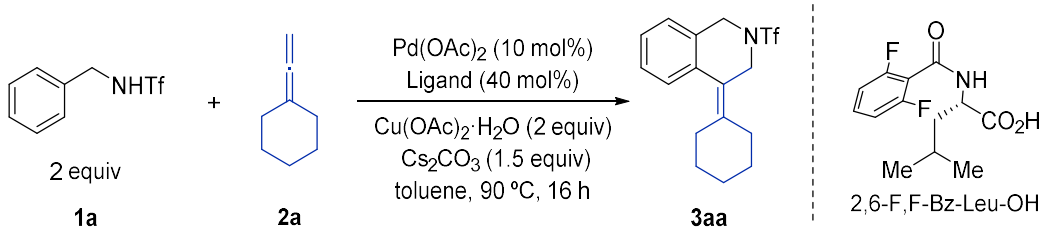

Entry	Ligand (40 mol%)	Yield[b]
1	Boc-Ala-OH	58%
2	Boc-Val-OH	69%
3	Boc-Leu-NHOMe	37%
4	Boc-Phe-NHOMe	31%
5	2,6-F,F-Bz-Leu-OH	85%
6[c]	2,6-F,F-Bz-Leu-OH	95%[d]
7[c]	2,6-F,F-Bz-Leu-OH	86%[d,e]
8[c]	2,6-F,F-Bz-Leu-OH	95%[f]
9	2,6-F,F-Bz-Leu-OH	31%[f]

[a] Conditions: 0.333 mmol **1a**, 0.167 mmol of allene **2a**, 2 mL of solvent. [b] Yields calculated by using an internal standard. [c] 15 equiv of DMSO added [d] Isolated yield based on **2a**. [e] 0.5 equiv. of $Cu(OAc)_2 \cdot H_2O$. [f] Reaction performed during 40 minutes.

As an additional test, acetyl- methyl- and nosyl- protected benzylamines were submitted to the optimized reaction conditions, but the formation of the expected cycloadduct was not observed. Again, full conversion of both the protected benzylamine and the allene was observed, likely due to the same decomposition pathways previously observed with benzyltrilamide **1a**. These results evidenced the key role of the triflyl protecting group in the cycloaddition.

Other coupling partners were tested for the reaction. Diphenylacetylene was essentially unreactive, whereas with benzyl acrylate or styrene, we observed low conversions of the alkenes and traces of olefination products. These results highlight the relevance of using allenes as coupling partners for the cycloaddition.

3.2 Scope of the annulation

With the optimized conditions in our hands, we studied the scope of the reaction. For that purpose, we synthesized several allenes bearing different substitution patterns, following previously reported synthetic procedures. The 1,1-disubstituted allenes **2b** (5-vinylidenenonane) and **2c** ((4-methylpenta-1,2-dien-3-yl)benzene) were synthesized from their corresponding propargylic alcohols in a two-step procedure that involves the tosylation of the

alcohol and the subsequent SN_2' reaction of the tosylate with the corresponding alkylmagnesium bromide and Cu(I) (Scheme 42a).[115] 1,3-disubstituted allene **2d** (1,3-diphenylpropa-1,2-diene) was synthesized from phenylacetylene and benzaldehyde, using a zinc-catalyzed process (Scheme 42b).[116] 1,3-disubstituted allene **2e** (buta-1,2-dien-1-ylbenzene) and trisubstituted allenes **2g** ((3-methylbuta-1,2-dien-1-yl)benzene) and **2h** ((3-methylhepta-1,2-dien-1-yl)benzene) were synthesized from their corresponding propargylic alcohols in a two-step procedure that involves the acetylation of the alcohol and the subsequent SN_2' reaction of the acetoxylate with the corresponding alkylmagnesium bromide and Cu(I) (Scheme 42c).[117] Allene **2f** ((1,2-propadienyl)cyclohexane) was commercially available.

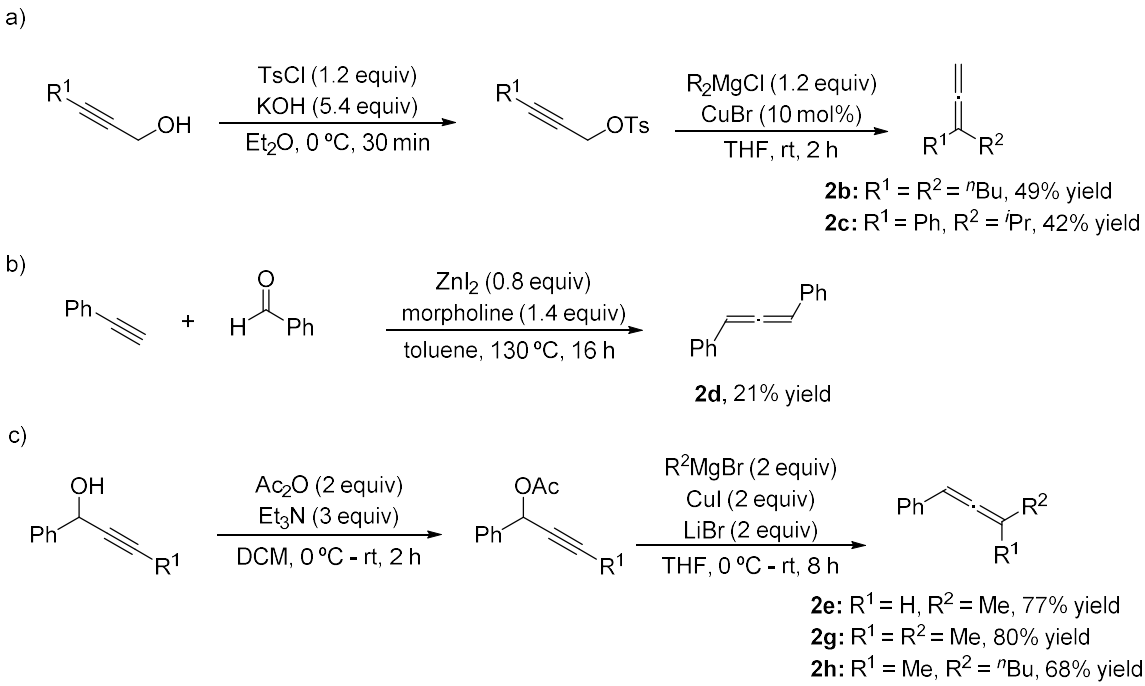

Scheme 42. *Synthetic procedures for the allenes **2a**-**2h**.*

The results of the annulations with all these allenes are indicated in Scheme 43. As shown, 1,1-disubstituted allenes other than **2a**, like **2b** or **2c**, were good reactions partners, affording the corresponding cycloadducts in 85% and 86% yield, respectively. The reaction also tolerates 1,3-disubstituted allenes, like **2d** and **2e**, providing the tetrahydroisoquinolines **3ad** and **3ae** as single stereo- and regioisomers (80% yield and 74% yield respectively). The explanation of this selectivity may be related with the steric hindrance of the phenyl group, which favors one of the possible conformations of the π-allyl intermediate over the other (see section 3.4 for the proposed mechanism). Monosubstituted allenes, like **2f**, can also engage in the cycloaddition, leading to the formation of the corresponding product **3af** in a 85% yield, albeit as a 1.1:1 mixture of *E:Z* steroisomers. Notably, trisubstituted allenes, like **2g** and **2h**, afford the corresponding cycloadducts as a single stereo- and regioisomer (80% yield and 90% yield respectively). Overall, the reaction presents a good scope with respect to the allenyl partner.

[115] Kippo, T.; Fukuyama, T.; Ryu, I. *Org. Lett.* **2011**, *13*, 3864.
[116] Zhao, Z.; Racicot, L.; Murphy, G. K. *Angew. Chem. Int. Ed.* **2017**, *56*, 11620.
[117] Ting, C.-H.; Hsu, Y.-L.; Liu, R.-S., *Chem. Commun.* **2012**, *48*, 6577.

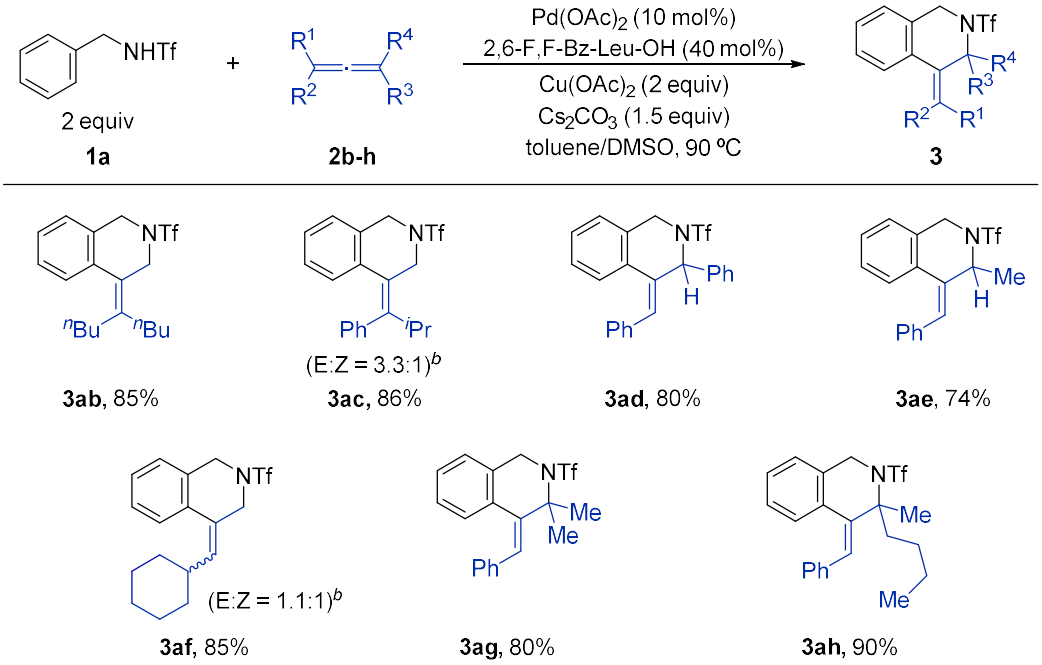

[a] Conditions: 0.333 mmol of amide **1a**, 0.167 mmol of allenes **2**, 2 mL toluene, 15 equiv DMSO, under air, 16 h. Isolated yields based on **2**. *E:Z* and regioisomeric ratios are >20:1, unless otherwise noted. [b] Inseparable isomers. Regioisomeric ratio determined by crude ^{1}H NMR.

Scheme 43. *Scope of the (4+2) cycloaddition between benzyltriflamides and allenes.*

In general, reactions initiated by the activation of C–H bonds in aromatic precursors tend to be much easier than those requiring the activation of alkenyl C–H bonds. Nonetheless, given our good results in the annulation, we wondered whether we could perform similar formal cycloadditions using alkenyl instead of aryl precursors. There are relatively few reports on palladium-catalyzed activation of olefinic C–H bonds, presumably because alkenes could engage in secondary reactions like additions or oxidations.[118] The extension of our annulation to alkenyl substrates is challenging, but very attractive, as it would allow the formation of highly interesting piperidine and eventually azepine products in a single step.

For evaluating the reaction, several alkenyltriflamides were synthesized using either a triflation reaction from their corresponding free amines or a Mitsunobu reaction from their corresponding alcohols (Scheme 44).

[118] For recent examples of Pd-catalyzed C–H functionalization of olefins, see: (a) Schreib, B. S.; Carreira, E. M. *J. Am. Chem. Soc.* **2019**, *141*, 8758. (b) Liu, M.; Yang, P.; Karunananda, M. K.; Wang, Y.; Liu, P.; Engle, K. M. *J. Am. Chem. Soc.* **2018**, *140*, 5805. (c) Luo, Y.-C.; Yang, C.; Qiu, S.-Q.; Liang, Q.-J.; Xu, Y.-H.; Loh, T.-P. *ACS Catal.* **2019**, 9, 4271.

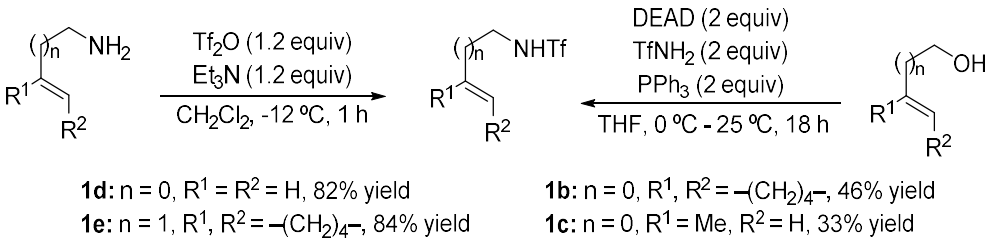

Scheme 44. *Synthetic procedures for the alkenyltriflamides **1b**-**1e**.*

We then tested the viability of the annulation. Gratifyingly, using the conditions optimized for the benzylamides, we found that the cycloaddition works efficiently with several alkenyltriflamides. The results with some selected substrates are summarized in Scheme 45. Allylamides **1b** (with a trisubstituted alkene moiety) and **1c** (*N*-(2-methylallyltriflamide)) react efficiently with allene **2a**, affording the corresponding tetrahydropyridines **3ba** and **3ca** with 71% and 88% yield respectively. Unfortunately, using allyltriflamide (**1d**), we observed a complex mixture of products and partial decomposition of the starting material. These results suggest that for a successful outcome it is important that the most internal position of the alkene is substituted, which avoids side reactions.

Trisubstituted allene **2g** efficiently engaged in the reaction with the cyclohexenyl triflamide **1b**, leading to the product **3bg** in 90% yield as a single stereo- and regioisomer. Notably, the methodology can be extended to homoallylic amines, in a rare example of a formal (5+2) cycloaddition. Therefore, azepine **3ea** was synthesized from the corresponding homoallylamide in an 83% yield. Besides, whereas with allylamides we use excess of these reactants owing to their lability, likely due to α-oxidation, in the case of homoallylamides the α-oxidation is much slower. Therefore, the reaction can be performed with equimolar amounts of the reacting partners.

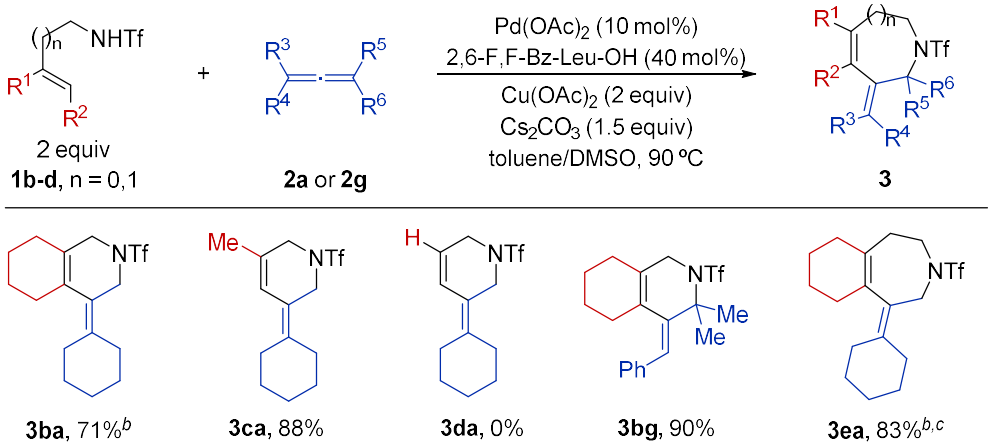

[a] Conditions: 0.333 mmol of amides **1**, 0.167 mmol of allenes **2**, 2 mL toluene, 15 equiv DMSO, under air, 16 h. Isolated yields based on **2**. *E:Z* and regioisomeric ratios are >20:1, unless otherwise noted. [b] 105 °C. [c] An equimolar amount of **1e** and **2a** was used.

Scheme 45. *Scope of the cycloaddition between alkenyltriflamides and allenes.*

Those results regarding the formal cycloaddition of protected alkenylamines and allenes warranted studies to further extend the scope. In fact, our group has recently published a kinetic resolution of alkenyltriflamides and allenes that includes some additional substrates.[91c]

3.3 Asymmetric annulations

Given that the annulation is accelerated by the use of amino acid ligands, it makes sense to explore the viability of performing asymmetric versions. Toward this end, we synthesized the α-ethyl substituted benzyltriflamide **1f** in racemic form through a standard triflation from commercially available 1-phenylethylamine, and we analyzed its performance in the reaction with allene **2a** using the optimized conditions, in order to achieve a kinetic resolution. Delightfully, cycloadduct **3fa** was obtained in a 91% yield (45% yield based on the triflimide **1f**) with a promising 93:7 enantiomeric ratio (er*)*. The enantioenriched starting amide was recovered in an 80% yield (40% yield based on the triflimide **1f**) with an 86:14 er (Scheme 46).

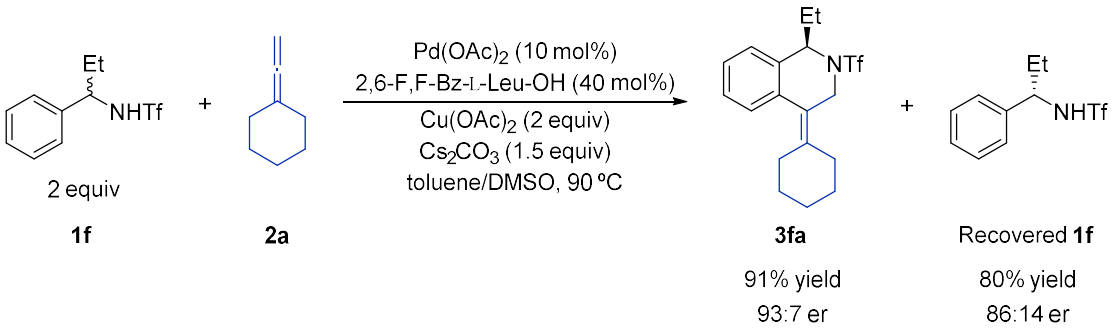

Scheme 46. *Kinetic resolution of α-ethyl substituted benzyltriflamide, and X-ray diffraction structure.*

Moreover, the absolute configuration of cycloadduct **3fa** was determined by X-ray diffraction analysis (Figure 9).

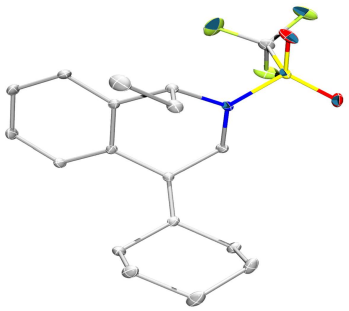

Figure 9. *Structure of compound **3fa** determined by X-Ray diffraction analysis. Hydrogens omitted for clarity.*

Owing to this positive result, we next wondered if symmetrical diarylbenzylamines could engage in a desymmetrizing process to afford enantioenriched THIQs. For that purpose, we synthesized diarylmethyltriflamides **1g-1m**, featuring different electronic and steric properties. The amine precursors were commercially available or synthesized from their corresponding nitriles through addition of arylmagnesium reagents and a subsequent reduction of the imine, following a previously reported one-pot procedure (Scheme 47).[119]

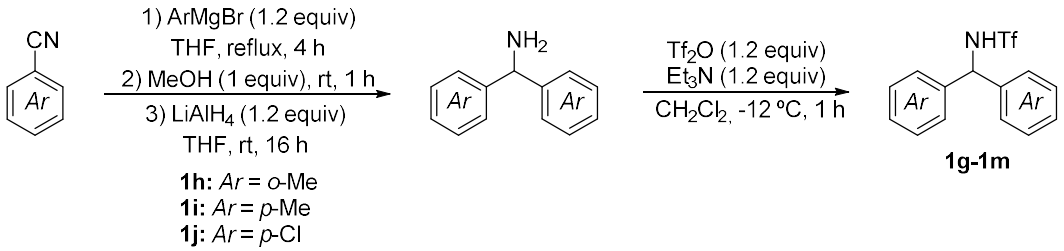

Scheme 47. *Synthetic procedures for the diarylbenzylamides **1g**-**1m**.*

With the precursors in our hands, we evaluated the cycloaddition reactivity using different types of allenes. The results are depicted in Scheme 48. We were glad to find that under standard conditions, the cycloaddition of diarylmethyltriflamide **1g** with model allene **2a** gives the expected optically active tetrahydroisoquinoline **3ga** in an 85% yield and a 94:6 enantiomeric ratio.[120] Very good results were also obtained with other disubstituted allenes, such as **2b** and **2c**, that gave the corresponding products **3gb** and **3gc** with 95% and 66% yield respectively, and 95:5 *ers* in both cases. Notably, the use of monosubstituted allene **2f** lead to the cycloadduct **3gf** as a single isomer (*Z* isomer) with an 81% yield and a 93:7 *er*. This contrasts with the reaction with the unsubstituted benzyltriflamide **1a** to give the product **3af** as a mixture of E/Z isomers.

[119] Zhang, Y.; Lu, Z.; Desai, A.; Wulff, W. D. *Org. Lett.* **2008**, *10*, 5429.

[120] Enantiomeric ratios were measured using either HPLC-DAD or SFC-PDA analysis (see Experimental Section)

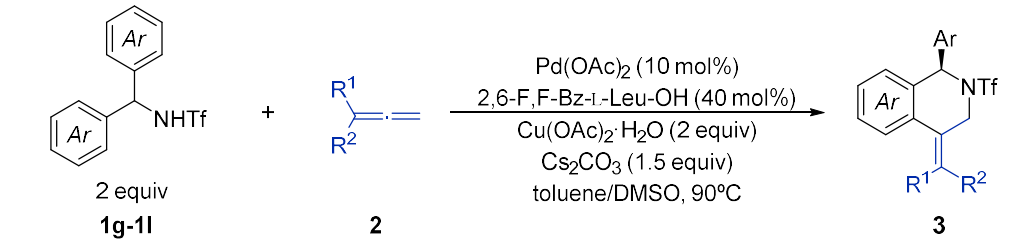

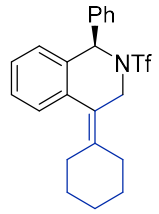

3ga, 85% yield
94:6 *er*

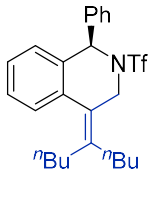

3gb, 95% yield
95:5 *er*

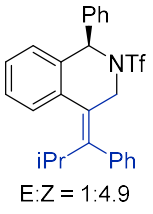

E:Z = 1:4.9

3gc,[b] 66% yield
95:5 *er*

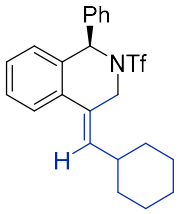

3gf, 81% yield
93:7 *er*

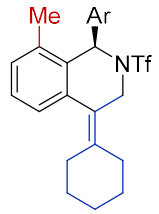

3ha,[c] 66% yield
97:3 *er*

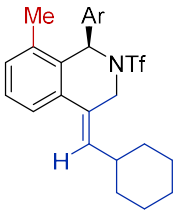

3hf,[c] 95% yield
98:2 *er*

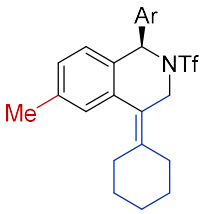

3ia, 95% yield
94:6 *er*

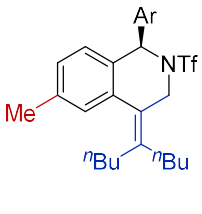

3ib, 92% yield
95:5 *er*

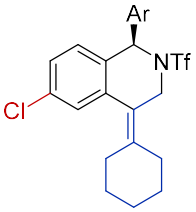

3ja, 93% yield
91:9 *er*

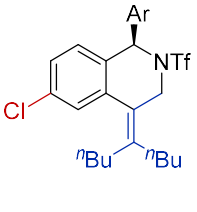

3jb, 86% yield
91:9 *er*

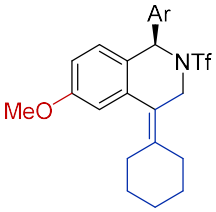

3ka, 93% yield
94:6 *er*

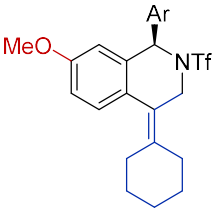

3la, 90% yield
90:10 *er*

[a] Conditions: 0.333 mmol of amides **1**, 0.167 mmol of allenes **2**, 2 mL toluene, 15 equiv DMSO, under air, 16 h. Isolated yields based on **2**. *E:Z* and regioisomeric ratios are >20:1, unless otherwise noted. Structure of the major product shown. [b] 70 °C, 3 days. [c] 0.167 mmol of triflamide **1h**, 0.333 mmol of allenes **2a** and **2f**. Yield based on **1h**. Note: Ar represents the same aromatic ring that is undergoing the transformation.

Scheme 48. *Scope of the enantioselective cycloaddition between diarylmethyltriflamides and allenes.*

Then, other prochiral substrates bearing different substitution patterns were also evaluated. We observed that the reaction works with substrates exhibiting *ortho*, *meta* and *para* substitution, affording the corresponding cycloadducts in 66-95% yields and enantiomeric ratios up to 98:2. *Ortho* and *para* substituted precursors gave very good results, whereas the *meta* substitution resulted in slightly worse enantiomeric ratios (90:10 for product **3la**). The absolute configuration of the compound **3ha** was determined by X-Ray diffraction analysis (Figure 10), and should be the same in all cases.

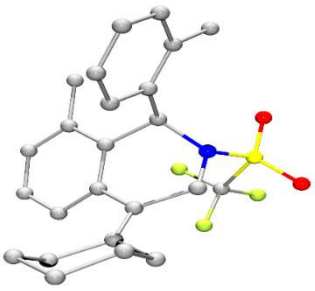

Figure 10. *Structure of compound **3ha** determined by X-ray diffraction analysis. Hydrogens omitted for clarity.*

An additional test to determine the chemoselectivity of the reaction was carried out with a substrate bearing two different aryl rings. Therefore, benzyltriflamide **1m** was synthesized from *p*-tolunitrileand 4-chlorophenylmagnesium bromide, following the general procedure for diarylbenzylamides described above, and it was submitted to the cycloaddition with allene **2a** under standard conditions. The outcome of the reaction, depicted in Scheme 49, consisted in a 1.6:1 inseparable mixture of two products, obtained in a total 90% yield. Therefore, only slight regioselectivity was observed towards the least hindered ring.

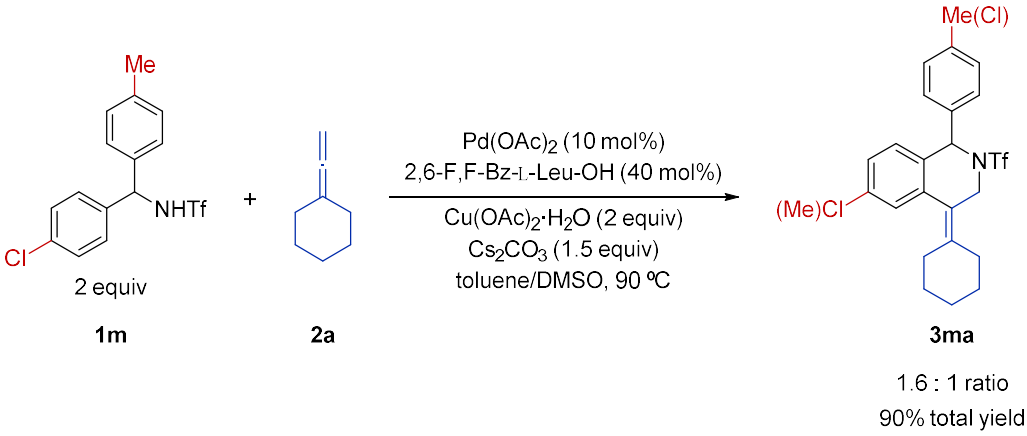

Scheme 49. *Pd-catalyzed cycloaddition of benzyltriflimide **1m** (bearing two different aryl rings) with allene **2a**. Substituents in brackets belong to the minor isomer.*

Overall, the asymmetric methodology is quite powerful and versatile.

3.4 Mechanistic proposal

The proposed mechanism for the formal cycloaddition is depicted in Scheme 50a. Considering the current state of the art in the field of C–H activation using palladium catalysis, it is highly probable that the active catalyst is formed in situ by an exchange between the palladium acetate salt (it could exist in form of a dimer or trimer in solution) and the amino acid ligand, assisted by the base. Afterward, the intermediate **I** is formed by deprotonation of the nitrogen of the amide, which is favored by the presence of the electron withdrawing triflyl group. In this intermediate, β-hydride eliminations entailing benzylic hydrogens might be slower, due to the coordination of the nitrogen to the palladium. The presence of the amino acid ligand is key for the next step, the C–H activation to give palladacycle **IIb**. This step should consist of a CMD, promoted by the internal amidate carbonyl (see section 4.2 of Chapter I). After the formation of the intermediate

III by coordination of the allene to the metal center, there is a regioselective migratory insertion of the allene to give a π-allylic palladacycle **IV**, whose exact structure may well be directly influenced by the substituents of the allene. A subsequent C–N–reductive elimination, favored by the presence of the olefin in the coordination sphere of the palladium, would lead to the products **3**. An outer-sphere mechanism cannot be ruled out, but in that situation, we might have observed alkenyl side products arising from β-hydride elimination processes, which were not detected (Scheme 50b). Finally, Pd(0), likely stabilized by complexation with DMSO, is reoxidized to the active Pd(II) catalyst by the $Cu(OAc)_2$ and, to a lesser extent, by the oxygen present in the air atmosphere.

In the case of the desymmetrization process, the substrate features a chiral or prochiral center, and therefore an intermediate like **II** would be chiral, with the formation of one of the enantiomers preferred over the other, due to steric clashing effects in the C–H activation step (see Scheme 16 of Chapter I).

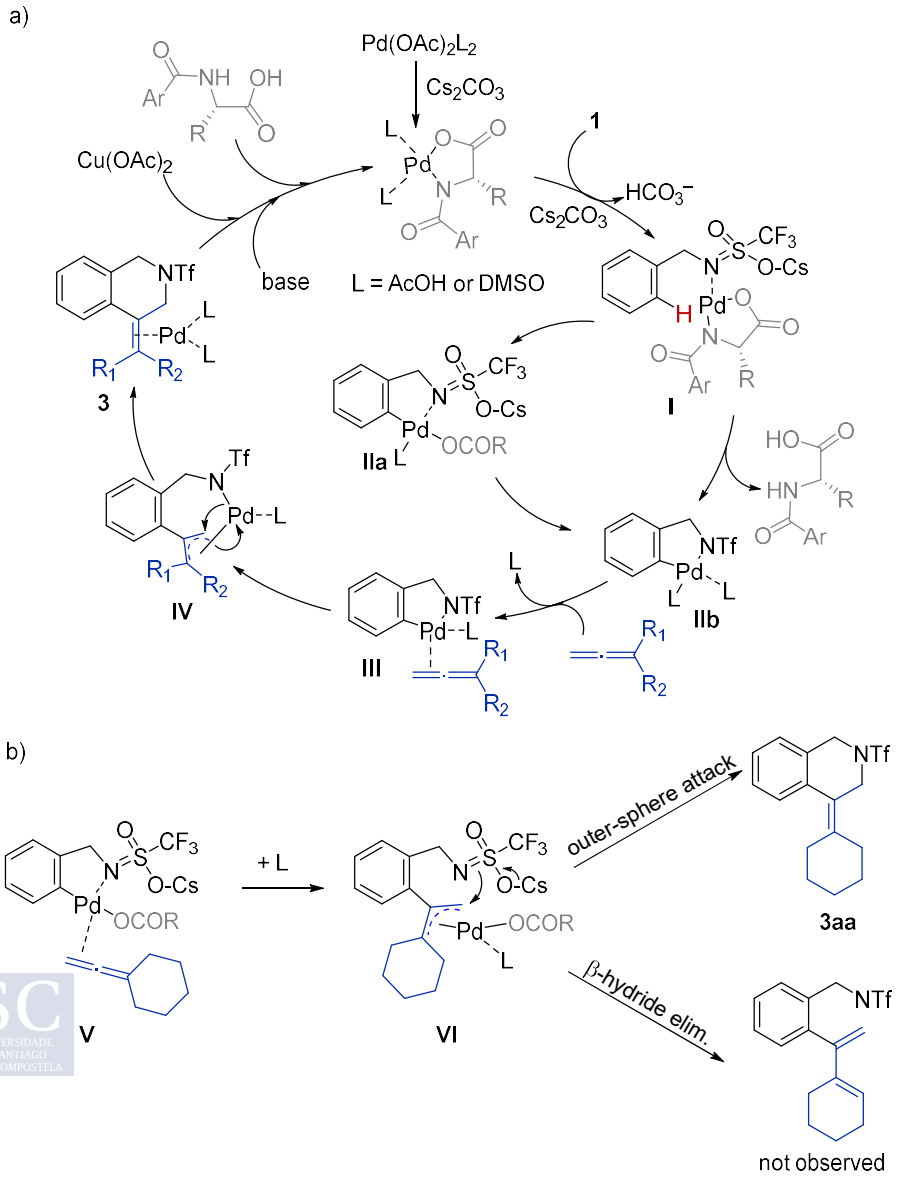

Scheme 50. *Proposed mechanism for the formal (4+2) cycloaddition and alternative outer-sphere pathway.*

4- Conclusions

In conclusion, we have developed a methodology that allows a straightforward access to highly valuable tetrahydroisoquinoline (THIQ) skeletons through a formal (4+2) cycloaddition between benzyl triflamides and allenes. We have optimized the reaction conditions so that it is possible to obtain excellent yields of the cycloadducts. The reaction presents excellent levels of chemo- and regioselectivity. We successfully demonstrated the possibility of extending the methodology to triflamides bearing alkenyl instead of aryl pendants to afford tetrahydropyridine skeletons. In these reactions, the presence of a substituent in the most internal position of the alkene is necessary to avoid decomposition of the substrate. Furthermore, we reported one example of a rare formal (5+2) cycloaddition of homoallylamines, to give an azepine skeleton (Scheme 51).

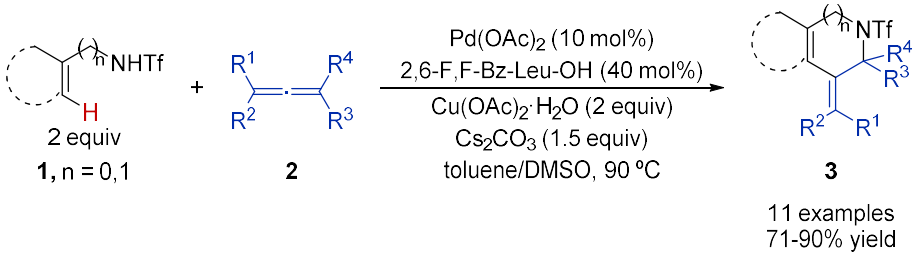

Scheme 51. *Pd-catalyzed formal cycloaddition between benzyl- and alkenyltriflamides and allenes.*

Moreover, this methodology can be used to promote asymmetric processes. A desymmetrization of prochiral diarylmethylamines allows to obtain enantioenriched tetrahydroisoquinolines with enantiomeric ratios up to 98:2. This represents the first palladium-catalyzed annulative C–H activation/desymmetrization process that has been reported. Thus, it is an important addition to the portfolio of catalytic asymmetric methods (Scheme 52). We also demonstrate the viability of a kinetic resolution process which can increase the scope of products in a significant manner.

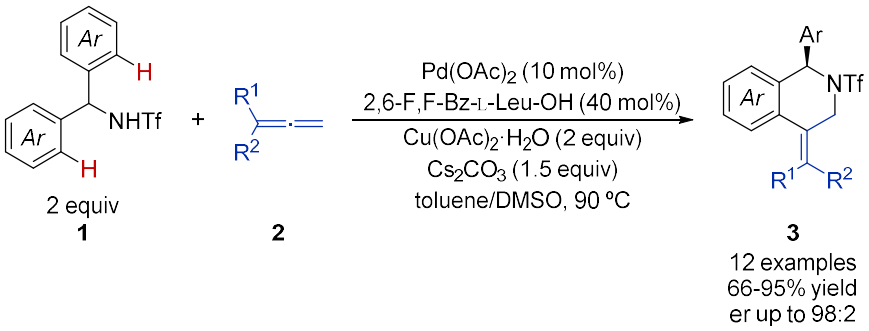

Scheme 52. *Desymmetrizing Pd-catalyzed (4+2) formal cycloaddition between diarylmethyltriflamides and allenes.*

Chapter III

Assembly of azaheterocycles by Pd(II)-catalyzed cycloadditions involving the activation of C(sp^3)-H bonds

This chapter includes work published in *Organic Letters* as:

Vidal, X.;[a] Mascareñas, J. L.;[a] Gulías, M.[a] *Org. Lett.* **2021**, *23*, 5323.

[a] Centro Singular de Investigacion en Química Bioloxica e Materiais Moleculares (CIQUS) and Departamento de Química Organica, Universidade de Santiago de Compostela, 15782 Santiago de Compostela, Spain

DOI: 10.1021/acs.orglett.1c01594, Open Access article (ACS AutorChoice)

1- Introduction

1.1 Challenges in the activation of C(sp^3)–H bonds

As it has been stated in the introduction of this manuscript, the topic of metal-mediated C–H activation has become a well-stablished field of research, with hundreds of articles published every year. However, most of them are still based on the activation of C(sp^2)–H bonds, as these types of bonds are easier to break than those found in their full-saturated counterparts. The reasons beyond the difficulties in activating C(sp^3)–H bonds include: a high bond dissociation energy (BDE), lack of ''active'' orbitals (HOMO or LUMO) to interact with transition metal catalytic centers, the lower strength of the resulting C–M bonds, and the difficulties to control the regioselectivity (Figure 11a).[121] As in the case of the activation of C(sp^2)–H bonds, the most employed strategy to overcome these limitations is the use of directing groups,[122] although indirect activations by other C(sp^2)–M bonds generated from oxidative additions to C–X functionalities, has also been exploited (vide infra, Scheme 53).

An interesting exception to this limitation can be found in allylic systems. In this special case, the adjacent olefin can coordinate the metal center and facilitate the C–H activation. Besides, the presence of the double bond also decreases the BDE of the C–H bond (88 kcal mol^{-1} versus 105 kcal mol^{-1} of methane).[34] The subsequent reactivity of the system will be analogous to that of π-allyl intermediates obtained using the Tsuji-Trost reaction.[51] Benzylic C(sp^3)–H bonds, despite the structural similarity, do not show the same reactivity than their allylic counterparts, in part because the π-cloud of the double bound located in the vicinal position is participating in the aromaticity of the benzene ring. However, the benzylic position is also benefiting from the decrease in the BDE due to the presence of a double bond (Figure 11b).

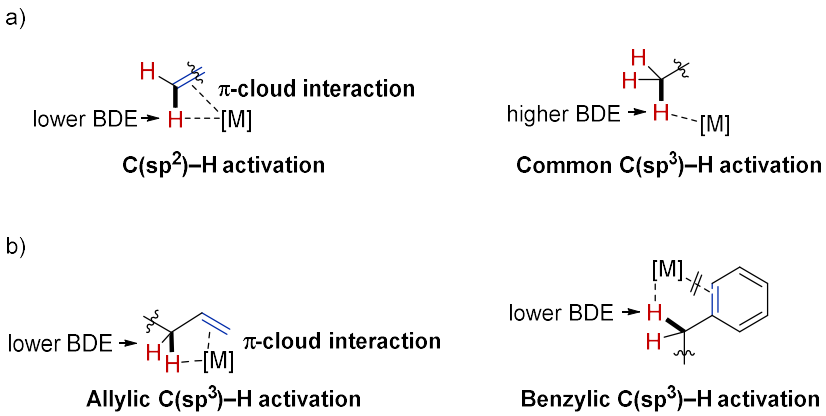

Figure 11. *Comparisons among different types of C–H activation.*

The activation of allylic and benzylic positions is thus a very interesting strategy to overcome the challenges of cleaving C(sp^3)–H bonds. Between both of them, the activation and functionalization of benzylic methyl groups is especially appealing due to the accessibility of the precursors and the possibility of obtaining important products.

[121] Li, H.; Li, B. J.; Shi, Z. J. *Catal. Sci. Technol.* **2011**, *1*, 191.
[122] Xie, J.; Chengjian, Z. Transition Metal-Catalyzed, Directing Group-Assisted C(sp^3)–H Bond Functionalization. In *Sustainable C(sp^3)–H Bond Functionalization,* Springer, **2016**.

1.2 Palladium-catalyzed functionalization of benzylic methyl groups

The first example of palladium-catalyzed benzylic C(sp^3)–H activations was reported in 2000 by Catellani and co-workers.[123] They discovered a method for the construction of cyclopentene rings by activating benzylic methyl groups in the presence of norbornene. The reaction was initiated by the oxidative addition of the C–I bond to the Pd(0) catalyst, followed by migratory insertion of norbornene. Then, a C(sp^3)–H activation of the benzylic methyl group and a subsequent reductive elimination led to the formation of the product in a 65% yield (Scheme 53).

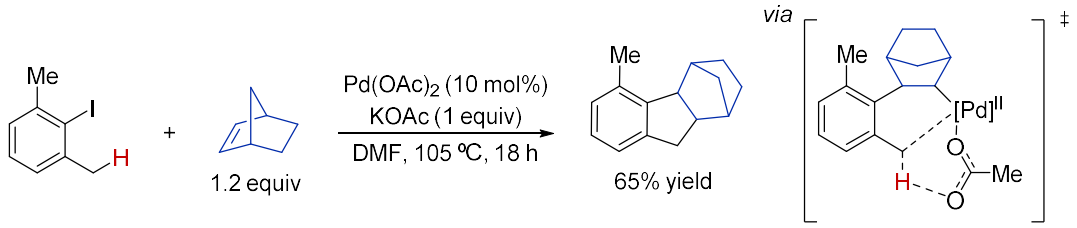

Scheme 53. *Pd(0)-catalyzed benzylic C(sp^3)–H functionalization of* o,o'*-dimethyliodobenzene with norbornene for the construction of cyclopentene rings reported by Catellani and co-workers.*

In 2004, Sanford and co-workers published the first example of a palladium-catalyzed acetoxylation of benzylic C–H bonds.[75] They employed quinolines as substrates, which exhibit an intrinsic directing group, affording the acetoxylated products with excellent levels of regio- and chemoselectivity (Scheme 54). The reaction proceeds through a Pd(II)/Pd(IV) catalytic cycle, in a similar manner to that of other aforementioned acetoxylation reactions with $PdI(OAc_2)$ (see section 4.3.1.3 of Chapter I).

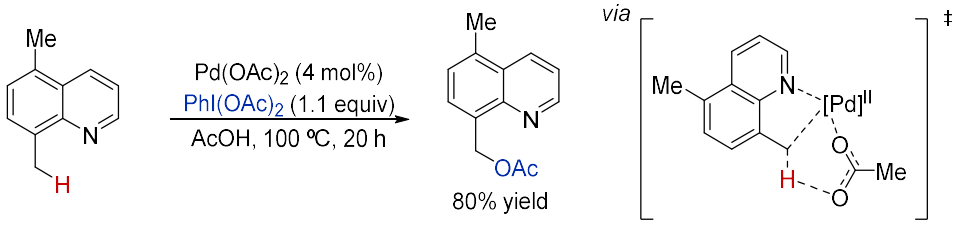

Scheme 54. *Pd(II)-catalyzed C(sp^3)–H acetoxylation of benzylic bonds directed by quinolines reported by Sanford and co-workers.*

The Sanford´s group explored further these quinoline-type precursors. The following year they reported the C(sp^3)–H arylation of 8-methylquinoline derivatives with hypervalent iodine(III) arylating reagents.[124] Mechanistic experiments evidenced an unusual Pd(II)/Pd(IV) catalytic cycle involving a bimetallic intermediate.[125] The same year, in 2006, Sanford and co-workers also published the C(sp^3)–H fluorination of the same substrates with electrophilic *N*-fluoropyridinium reagents, further promoted by microwave radiation (Scheme 55).[126]

[123] Catellani, M.; Motti, E.; Ghelli, S. *Chem. Commun.* **2000**, *20*, 2003.
[124] Kalyani, D.; Deprez, N. R.; Desai, L. V.; Sanford, M. S. *J. Am. Chem. Soc.* **2005**, *127*, 7330.
[125] Deprez, N. R.; Sanford, M. S. *J. Am. Chem. Soc.* **2009**, *131*, 11234.
[126] Hull, K. L.; Anani, W. Q.; Sanford, M. S. *J. Am. Chem. Soc.* **2006**, *128*, 7134.

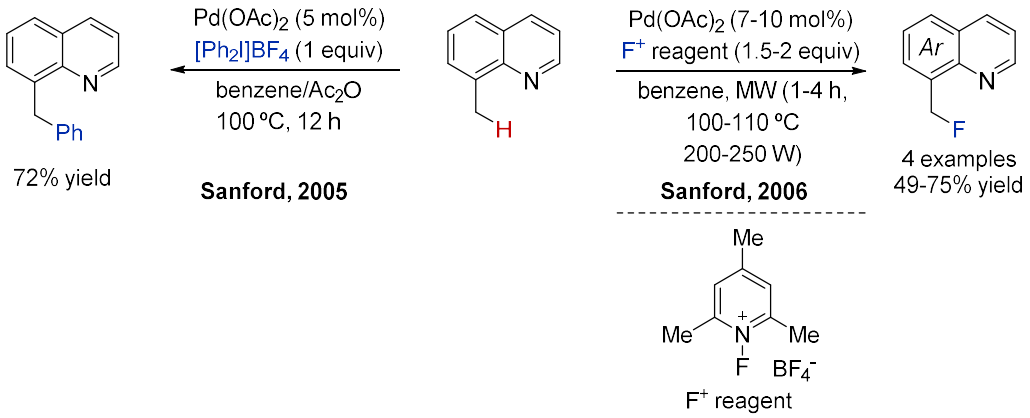

Scheme 55. *Pd(II)-catalyzed benzylic C(sp³)–H functionalizations of 8-methylquinoline derivatives reported by Sanford and co-workers.*

This system has also been explored by other research groups. Daugulis and Shabashov disclosed in 2005 a benzylic C(sp³)–H arylation of 8-methylquinolines complementary to Sanford's work, employing aryl iodides as coupling partners.[127] In 2012, the group of Muñiz published the C(sp³)–H oxidate amidation of the same substrates.[128] The use of NSFI as oxidant played a key role for the reductive C–N bond formation (Scheme 56). Yu´s group also reported some examples of benzylic C(sp³)–H alkylation of 8-methylquinolines as part of a larger study about the functionalization of sp² and sp³ C–H bonds.[129]

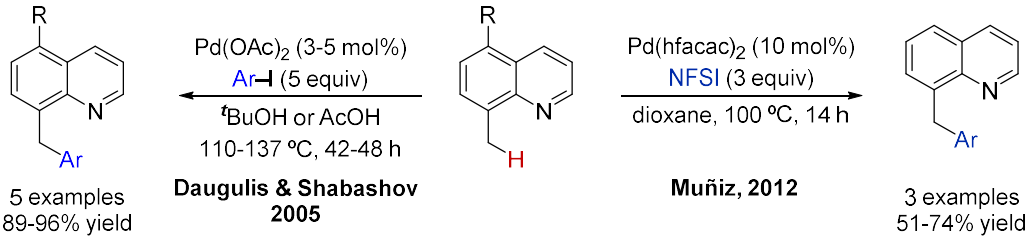

Scheme 56. *Pd(II)-catalyzed benzylic C(sp³)–H functionalizations of 8-methylquinoline derivatives developed by Daugulis, Shabashov, Muñiz and co-workers.*

There have been reports on benzylic C(sp³)–H functionalizations where the heteroatom-based directing group is placed in the same aromatic ring that bears the activated benzylic position. In 2008, Fagnou and co-workers published a palladium-catalyzed site-selective arylation of benzylic C(sp³)–H bonds of azine and diazine *N*-oxide substrates.[130] The choice of a proper base was key for achieving the desired selectivity. Two years later, Huang´s group reported a novel protocol for the functionalization of 2-methylsubstituted azaheterocycles with *N*-sulfonyl aldimines.[131] The proposed mechanism proceeds through a nucleophilic addition of the benzylic position over the coupling partner (Scheme 57).

[127] Shabashov, D.; Daugulis, O. *Org. Lett.* **2005**, *7*, 3657.
[128] Iglesias, Á.; Álvarez, R.; De-Lera, Á. R.; Muñiz, K. *Angew. Chem. Int. Ed.* **2012**, *51*, 2225.
[129] Chen, X.; Goodhue, C. E.; Yu, J.-Q. *J. Am. Chem. Soc.* **2006**, *128*, 12634.
[130] Campeau, L.-C.; Schipper, D. J.; Fagnou, K. *J. Am. Chem. Soc.* **2008**, *130*, 3266.
[131] Qian, B.; Guo, S.; Shao, J.; Zhu, Q.; Yang, L.; Xia, C.; Huang, H. *J. Am. Chem. Soc.* **2010**, *132*, 3650.

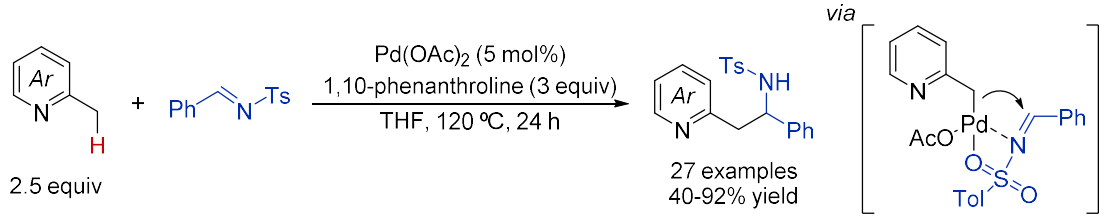

Scheme 57. *Pd(II)-catalyzed benzylic addition of C(sp³)–H bonds to* N*-sulfonyl aldimines developed by Huang and co-workers, and key intermediate.*

1.3 Palladium-catalyzed benzylic C(sp³)–H functionalization of o-methylaniline and o-methylbenzylamine precursors

A particular case of Pd-catalyzed benzylic C(sp³)–H functionalizations is the activation of methyl groups located in the *ortho* position of anilines or benzylamines. The challenges of employing free amines as directing groups were previously discussed (see section 1.4 of Chapter II). Therefore, it is not surprising that all the methodologies related to this particular activation employ appropriately protected amines.

The first example of benzylic C(sp³)–H functionalization of aniline type of precursors was published in 2012 by Takemoto and co-workers.[132] They describe the Pd(0)-catalyzed construction of oxindole skeletons from carbamoyl chloride precursors. The employment of Ad_2PBu as palladium ligand and PivNHOH as an additive under a CO atmosphere allowed to achieve the chemoselective C(sp³)–H activation over competitive C(sp²)–H activation (Scheme 58). The process starts by oxidative addition of Pd(0) to the C–Cl bond, followed by the activation of the benzylic hydrogen.

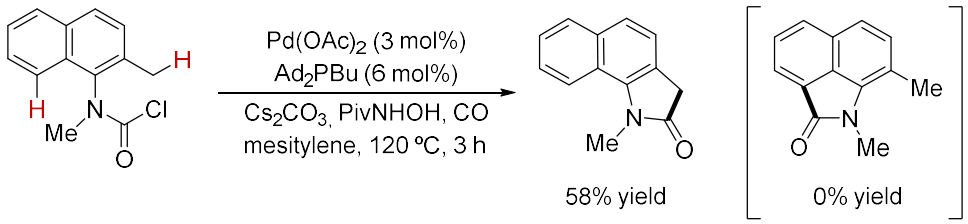

Scheme 58. *Pd(0)-catalyzed chemoselective C(sp³)–H activation of carbamoyl protected* o*-methylanilines reported by Takemoto and co-workers.*

The same year, the group of Zhang disclosed a benzylic C(sp³)–H arylation/oxidation of *o*-methylanilines equipped with a bidentate chelating group, employing aryl iodides as coupling partner and molecular oxygen as oxidant (Scheme 59).[133] Substrates equipped with monodentate directing groups failed to react, which confirms the key role of the chelating system. This methodology was further established by Zhang and Huang, when they concurrently reported the C–H acetoxylation of the same substrates.[134]

[132] Tsukano, C.; Okuno, M.; Takemoto, Y. *Angew. Chem. Int. Ed.* **2012**, *51*, 2763.
[133] Xie, Y.; Yang, Y.; Huang, L.; Zhang, X.; Zhang, Y. *Org. Lett.* **2012**, *14*, 1238.
[134] (a) Ju, L.; Yao, J.; Wu, Z.; Liu, Z.; Zhang, Y. *J. Org. Chem.* **2013**, *78*, 10821. (b) Cheng, T.; Yin, W.; Zhang, Y.; Zhang, Y.; Huang, Y. *Org. Biomol. Chem.* **2014**, *12*, 1405.

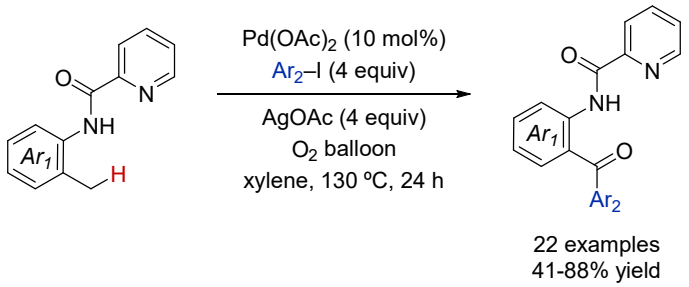

Scheme 59. *Pd(II)-catalyzed C(sp^3)–H arylation/oxidation of o-methylanilides assisted by a chelating directing group reported by Zhang and co-workers.*

In 2014, Yu and co-workers reported an example of benzylic C(sp^3)–H arylation of triflyl-protected *o*-methylanilines with organoboron reagents, as part of a larger study on amine-directed C(sp^3)–H activation of aliphatic chains.[135] The amide moiety was used as directing group by itself, and MPAA ligands were also employed to promote the reactivity (Scheme 60). In 2019, the group of Babu published the C–H arylation and acetoxylation of *o*-methylanilines using 5-methylisoxazole-3-carboxamide as directing group, which can be easily removed afterwards.[136]

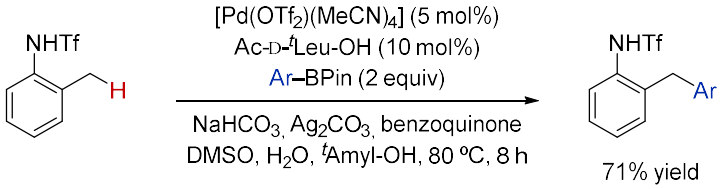

Scheme 60. *Pd(II)-catalyzed C(sp^3)–H arylation of triflyl protected* o*-methylanilines with organoboron reagents reported by Yu and co-workers.*

Regarding the Pd-catalyzed benzylic C(sp^3)–H activation of *o*-methylbenzylamines, there are very few reports. Chen and co-workers disclosed in 2012 the intramolecular amination of a single *o*-methylbenzylamine derivative as part of a larger research on the synthesis of azaheterocycles through intramolecular amination of C(sp^2)–H and C(sp^3)–H bonds.[137] The amine group was equipped with a bidentate chelating group. Two years later, Zhao, Yao and co-workers published a similar protocol with the same substrate, but assisted by an oxalyl amide auxiliary, also as part of a larger piece of research (Scheme 61).[138]

[135] Chan, K. S. L.; Wasa, M.; Chu, L.; Laforteza, B. N.; Miura, M.; Yu, J.-Q. *Nat. Chem.* **2014**, *6*, 146.
[136] Singh, P.; Dalal, A.; Babu, S. A. *Asian J. Org. Chem.* **2019**, *8*, 877.
[137] He, G.; Zhao, Y.; Zhang, S.; Lu, C.; Chen, G. *J. Am. Chem. Soc.* **2012**, *134*, 3.
[138] Wang, C.; Chen, C.; Zhang, J.; Han, J.; Wang, Q.; Guo, K.; Liu, P.; Guan, M.; Yao, Y.; Zhao, Y. *Angew. Chem. Int. Ed.* **2014**, *53*, 9884.

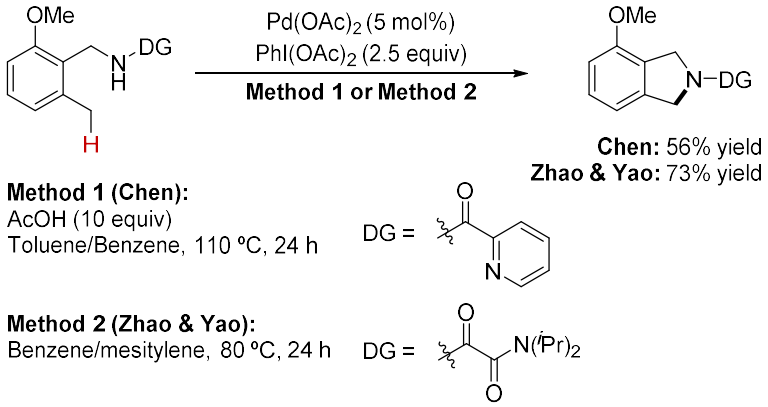

Scheme 61. *Pd(II)-catalyzed intramolecular C(sp³)–H amination of* o*-methylbenzylamines assisted by chelating directing groups reported by Chen, Zhao, Yao and co-workers.*

1.4 Formal cycloadditions involving Pd-catalyzed C(sp³)–H activations

1.4.1 Introduction

The importance of cycloadditions in the context of *atom* and *step* economy for the synthesis of cyclic products has been already commented in Chapter I. Several examples of formal cycloadditions based on palladium-catalyzed C(sp²)–H activations have been reviewed in section 4.3.2 of that chapter. It is worth to highlight that despite the high relevance of this transformation, the number of reports entailing annulation processes through metal-catalyzed C(sp³)–H activations is very limited.[139]

There are several reasons for this shortage (Scheme 62). In the first place, the aforementioned difficulty of activating C(sp³)–H bonds. Second, the competition of β-hydride elimination side processes, either after the C(sp³)–H activation or the migratory insertion of the unsaturated partners. In fact, there are several methodologies that take advantage of this undesired pathway, relying in a sequence of functionalization/cyclization reactions (mostly alkenylation/Michael-addition).[140] Third, reductive eliminations from sp³ carbons are slower and more difficult than from sp² carbons, owing to the absence of coordinating π-bonds.[141] Furthermore, the absence of a π-cloud on the substrates makes the approximation of the substrate to the catalyst more difficult. In fact, the metal center could be inactivated by coordinative saturation with the unsaturated coupling partner.

[139]For further information about Pd-catalyzed C(sp³)–H activation-based cycloadditions, among other metals: Font, M.; Gulías, M.; Mascareñas, J.L. *Angew. Chem. Int. Ed.* **2021**, Accepted article, DOI: 10.1002/anie.202112848.

[140] (a) Wasa, M.; Engle, K. M.; Yu, J.-Q. *J. Am. Chem. Soc.* **2010**, *132*, 3680. (b) Ghosh, K. K.; Uttry, A.; Mondal, A.; Ghiringhelli, F.; Wedi, P.; van Gemmeren, M. *Angew. Chem. Int. Ed.* **2020**, *59*, 12848. (c) Calleja, J.; Pla, D.; Gorman, T. W.; Domingo, V.; Haffemayer, B.; Gaunt, M. J. *Nat. Chem.* **2015**, *7*, 1009.

[141] Yu, Z. X.; Cheong, P. H. Y.; Liu, P.; Legault, C. Y.; Wender, P. A.; Houk, K. N. *J. Am. Chem. Soc.* **2008**, *130*, 2378.

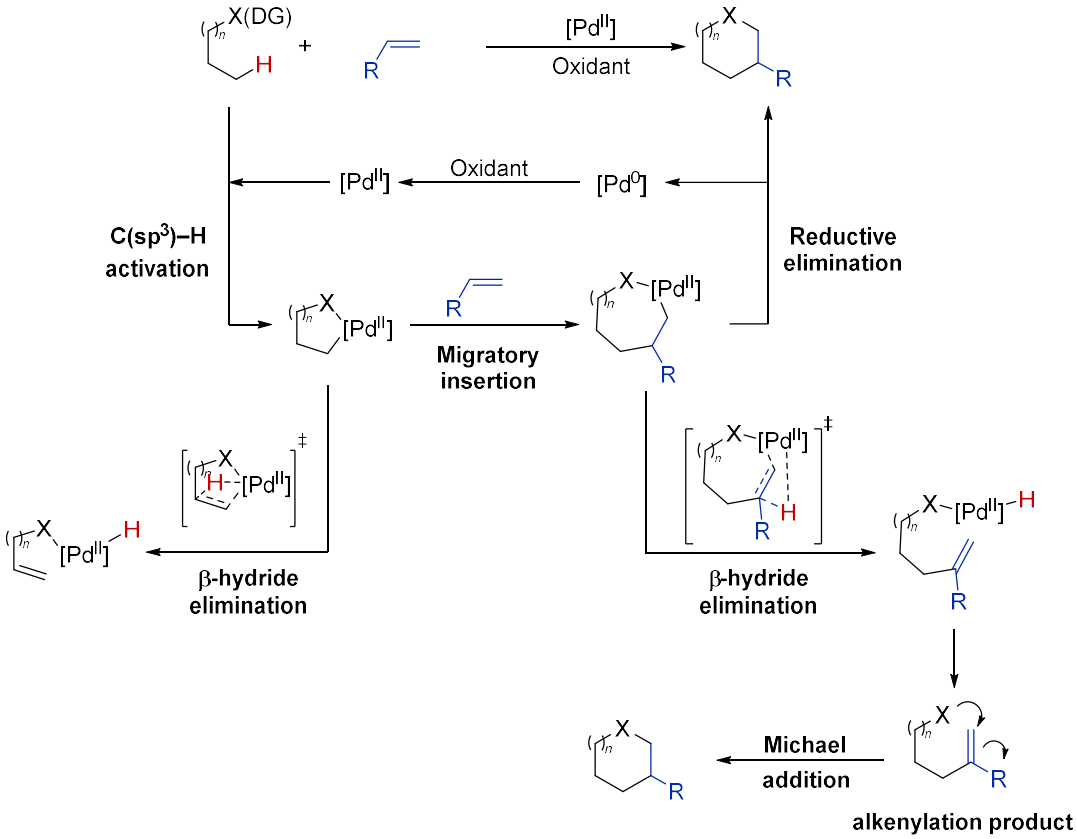

Scheme 62. *Challenges in Pd-promoted C(sp³)–H activation-based cycloadditions.*

Only very limited progress in formal one-step cycloadditions where the metal is involved in the whole process has been done. More relevant results are summarized in the following sections.

1.4.2 (n+1) cycloadditions

Carbonylations are the most common formal (n+1) cycloadditions. This is due to the fact that Pd–acyl intermediates that are formed after the migratory insertion of the CO unit can undergo easier reductive elimination than their precursor palladium complexes. An illustrative example of this kind was published in 2017 by the group of Gaunt. They developed a diastereoselective Pd(II)-catalyzed (3+1) carbonylation of β-C(sp³)−H bonds in aliphatic amines (Scheme 63).[142] The employment of Xantphos as ligand seemed critical for the efficiency of the process. As Gaunt proposed, the phosphine likely stabilizes the Pd(0) at the end of the catalytic cycle, prior to the reoxidation to Pd(II), and so preventing the formation of inactive Pd(0)-carbonyl adducts.

[142] Cabrera-Pardo, J. R.; Trowbridge, A.; Nappi, M.; Ozaki, K.; Gaunt, M. J. *Angew. Chem. Int. Ed.* **2017**, *56*, 11958.

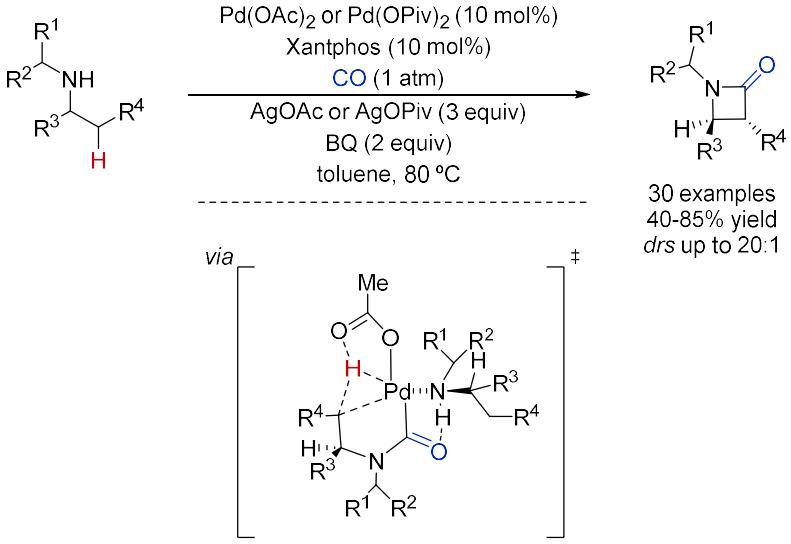

Scheme 63. *Pd(II)-catalyzed diastereoselective (3+1) carbonylation of aliphatic amines developed by Gaunt and collaborators, and transition state proposed for the C–H activation.*

The selectivity observed for this reaction is explained by the formation of a carbamoyl intermediate, which undergoes the C–H activation step. Thus, the CO insertion in the palladium center is prior to the selective C−H activation. After the formation of the palladacycle, it evolves via reductive elimination to form the β-lactam.

There are examples of (n+1) annulations where the one-carbon surrogate is not carbon monoxide. This is the case of methodologies based on functionalization/aza-Waker cyclization processes. In contrast with the aforementioned functionalization/Michael addition reactions, the palladium catalyst is involved in the whole process. One example of this type of chemistry is the asymmetric construction of γ-lactams developed by Shi and co-workers.[143] Alkyl amides bearing a pyridyl isopropylamine group (PIP) can undergo an enantioselective Pd(II)-catalyzed C(sp^3)−H alkenylation assisted by BINOL chiral ligands, followed by an aza-Waker cyclization to afford a variety of enantioenriched γ-lactams with ees up to 98% (Scheme 64). This methodology was extended to the construction of α,β-contiguous stereocenters in a follow-up paper published by the same group.[144]

[143] Ding, Y.; Han, Y. Q.; Wu, L. S.; Zhou, T.; Yao, Q. J.; Feng, Y. L.; Li, Y.; Kong, K. X.; Shi, B. F. *Angew. Chem. Int. Ed.* **2020**, *59*, 14060.
[144] Wu, L. S.; Ding, Y.; Han, Y. Q.; Shi, B. F. *Org. Lett.* **2021**, *23*, 2048.

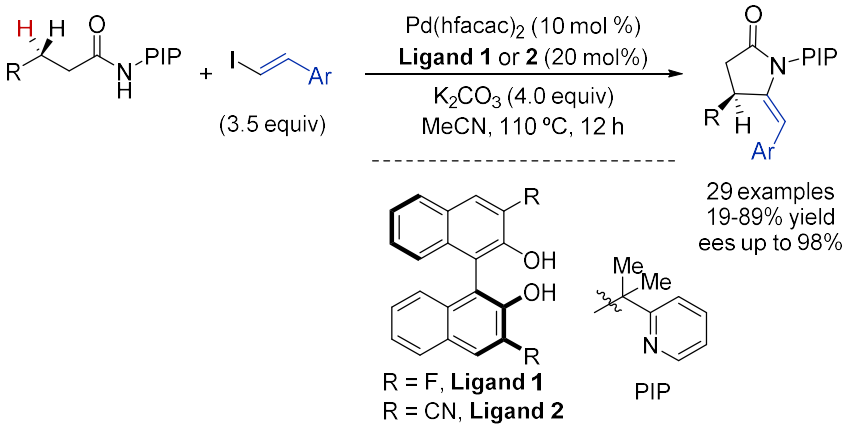

Scheme 64. *Pd(II)-catalyzed enantioselective γ-alkenylation/aza-Wacker cyclization of alkyl amides and vinyl iodides reported by Shi and co-workers.*

The proposed mechanism for this reaction is depicted in Scheme 65. In the first place, an enantioselective C(sp^3)–H activation of the substrate, assisted by the BINOL chiral ligand, affords chiral palladacycle **I**. After the oxidative addition of the vinyl iodide over the palladium catalyst, the Pd(IV) species **II** evolves via reductive elimination to generate the alkenylation product **III**. The coordination of the directing group and the alkene facilitates the intramolecular *syn*-aminopalladation to form the intermediate **IV**. Finally, β-hydride elimination gives the cyclic product, and the catalyst is regenerated to Pd(II) by a oxidative addition/reductive elimination sequence with two units of vinyl iodide.

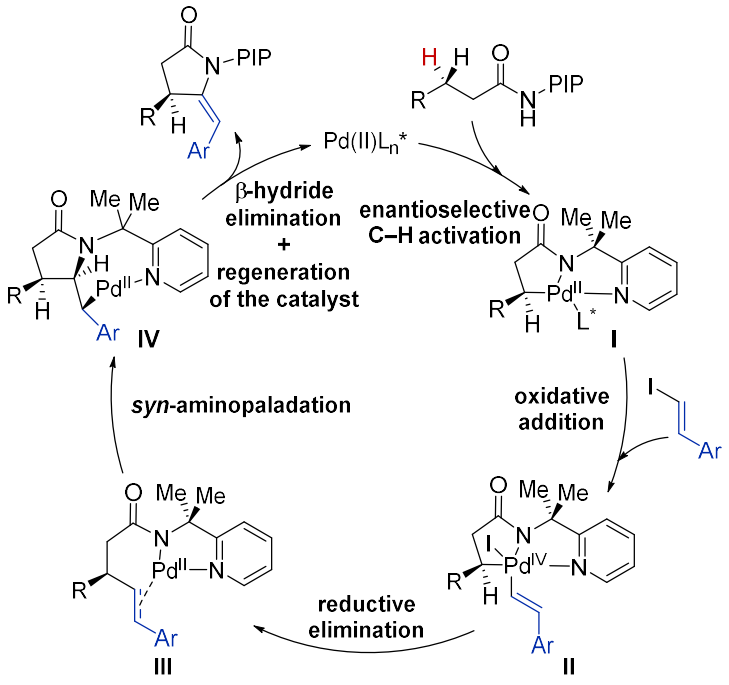

Scheme 65. *Proposed mechanism for the Pd(II)-catalyzed enantioselective γ-alkenylation/aza-Wacker cyclization.*

1.4.3 (n+2) cycloadditions

Formal cycloadditions using alkenyl type of unsaturated partners instead of carbon monoxide are more challenging. As commented in the introduction, the palladacycle intermediates resulting from the migratory insertion are more prone to suffer undesired β-hydride elimination processes, and subsequent intramolecular Michael additions. This is why most of the (n+2) formal cycloadditions based on C(sp^3)–H activation are in fact alkenylation/Michael-addition processes. Related reactions where the palladium is involved in the whole mechanism are indeed very scarce. The first example of a formal cycloaddition of this kind was published in 2020 by our research group. A Pd-catalyzed (4+2) cycloaddition between nosyl-protected alkylamides and dienes allowed the synthesis of a variety of saturated lactams (Scheme 66).[55] Mechanistic studies revealed the key role of the directing group and the quinaldine ligand in the reactivity, as well as the importance of the presence of a conjugated double bond in the alkene partner.

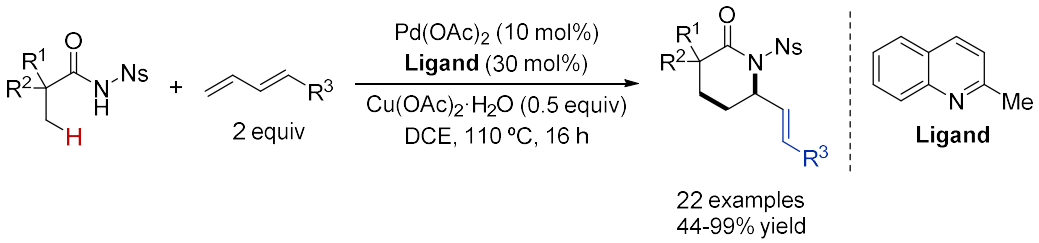

Scheme 66. *Pd(II)-catalyzed formal (4+2) cycloaddition between alkyl amides and dienes reported by Gulías, Mascareñas and co-workers.*

The same year, Yu and Park described a formal (3+2) cycloaddition between alkyl amides and maleimides based on a twofold C(sp^3)–H activation.[145] The reaction is limited to the use of maleimides as coupling partner, likely to prevent the undesired β-hydride elimination pathway and favor the second C(sp^3)–H activation. The use of a weak-coordinating amide directing group proved to be also essential to prevent Heck additions or alkylation products (Scheme 67).

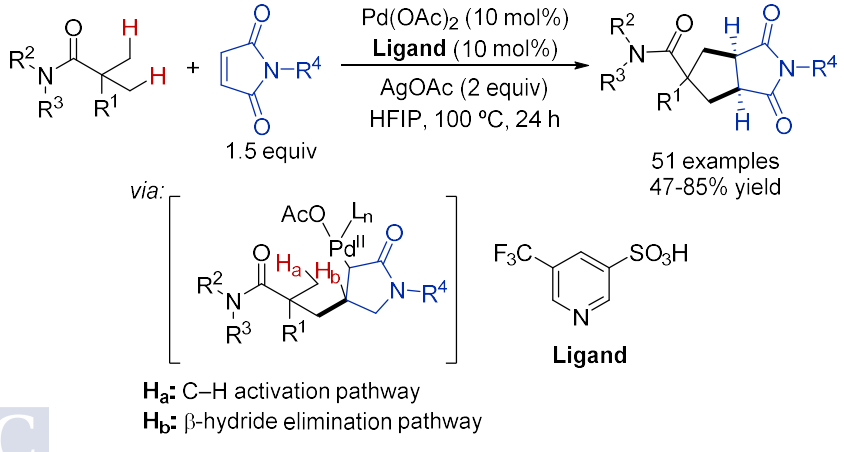

Scheme 67. *Pd(II)-catalyzed formal (3+2) cycloaddition between alkyl amides and maleimides based on a twofold C(sp^3)–H activation developed by Yu and Park.*

[145] Park, H.; Yu, J.-Q. *J. Am. Chem. Soc.* **2020**, *142*, 16552.

A similar strategy was followed by Chatani and He. In 2021, they published a site-selective formal (3+2) cycloaddition between aromatic amides and maleimides based on a twofold C(sp^3)–H activation at high temperature.[146] It is worth to mention that it is the first cycloaddition that involves a benzylic C(sp^3)–H activation of protected *o*-methylanilines (Scheme 68). The amide protecting/chelating group, containing both N–H and SMe moieties, proved to be essential for the reaction.

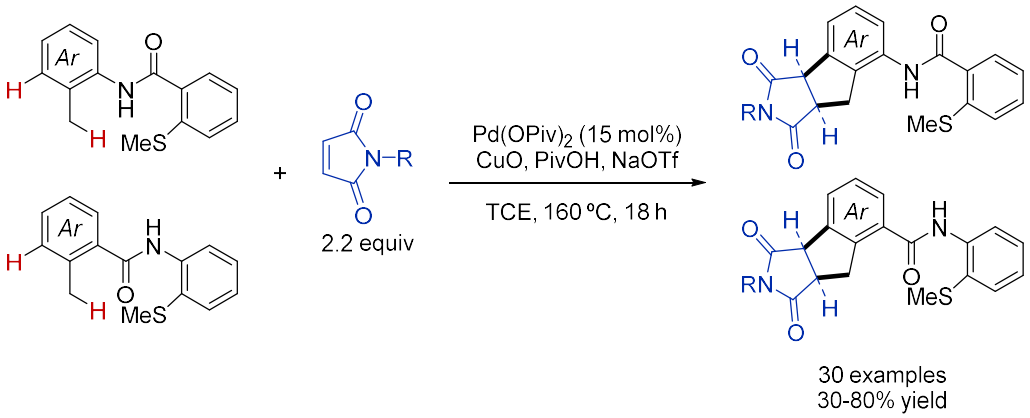

Scheme 68. *Pd(II)-catalyzed formal (3+2) cycloaddition between aromatic amides and maleimides based on a twofold C(sp^3)–H activation reported by Chatani and He.*

Cycloadditions based on the activation of C(sp^3)–H bonds are an elegant and efficient way to build complexity from barely-functionalized, readily-available acyclic starting materials. This field is still in its infancy, and even though there have been important breakthroughs in the last years, there are plenty of room for new developments, including the use of less engineered substrates or the implementation of asymmetric transformations.

[146] He, Q.; Chatani, N. *Angew. Chem. Int. Ed.* **2021**, *60*, 5189.

2- Objectives

Considering the current challenges in the metal-promoted activation of C(sp^3)–H bonds, and the scarce number of precedents in formal cycloadditions involving the cleavage of these bonds, we traced as main aim of the work included in this chapter the development of (4+2) annulations between *ortho*-methyl aromatic amines and unsaturated moieties, in principle allenyl derivatives, owing to our previous work with these types of partners (Scheme 69).

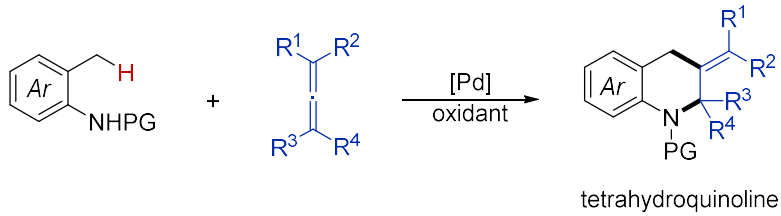

Scheme 69. *General objective of the formal (4+2) cycloaddition between* o*-methyl aromatic amines and allenes.*

This strategy would provide a direct entry to tetrahydroquinoline (THQ) skeletons, which are valuable backbones in natural alkaloids and are prominently represented in medicinal chemistry (Figure 12).[147]

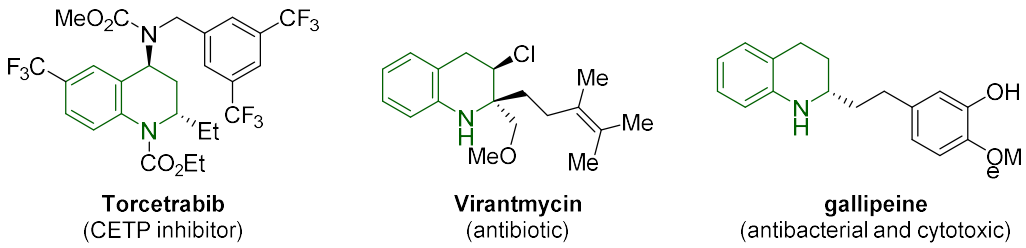

Figure 12. *Bioactive compounds featuring tetrahydroquinoline scaffolds.*

Moreover, we envisioned that protected *o*-methylbenzylamines might also engage in these types of cycloadditions, but to deliver seven-membered tetrahydro-2-benzazepines through an unprecedented type of formal (5+2) annulation (Scheme 70). This transformation is far from be straightforward, as the amide directing group is further apart from the methyl substituent and sensitive to oxidation. Additionally, an asymmetric version of these cycloadditions could be explored, by employing α-substituted *o*-methylbenzylamines as racemic precursors and the adequate chiral ligands.

[147] Muthukrishnan, I.; Sridharan, V.; Menéndez, J. C. *Chem. Rev.* **2019**, *119*, 5057.

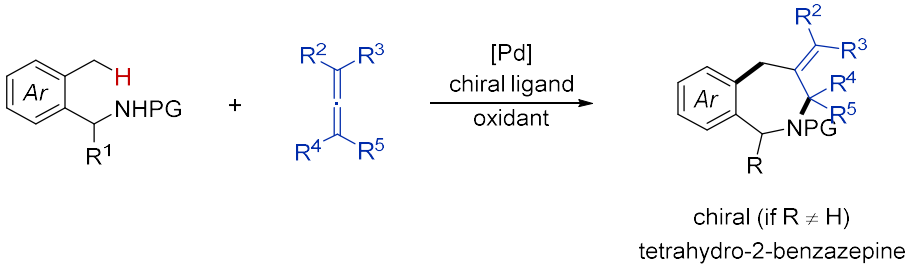

Scheme 70. *General objective of the formal (5+2) cycloaddition between o-methylbenzylamines and allenes.*

These methodologies would represent a substantial addition to the scarce set of cycloadditions based on the activation of C(sp^3)–H bonds, allowing the straightforward construction of highly valuable tetrahydroquinoline and tetrahydro-2-benzazepine scaffolds from readily available starting materials.

3- Results and discussion

3.1 Formal (4+2) cycloaddition between o-methylanilines and allenes: initial assays and optimization

For the initial screening we selected 1,1,1-trifluoro-*N*-(*o*-tolyl)methanesulfonamide **4a** as model substrate. Again, we decided to use the triflyl protecting group for the same reason that in our previous project: increasing the acidity of the N–H bond without compromising the electrophilicity of the palladium, that will be coordinated by the nitrogen atom. Substrate **4a** was synthetized from commercially available *o*-methylaniline, by reaction with triflic anhydride in the presence of triethylamine.

As initial coupling cycloaddition partner, we decided to select the 1,1,-disubstituted allene 5-vinylidenenonane (**2b**). We started by testing the reaction conditions optimized in our previous project: $Pd(OAc)_2$ as catalyst, 2,6-F,F-Bz-Leu-OH as mono-protected amino acid (MPAA) ligand, $Cu(OAc)_2 \cdot H_2O$ as oxidant, cesium carbonate as base, toluene as solvent and DMSO as additive. Again, the reaction was performed under air atmosphere, as there are no oxygen-sensitive reactants and oxygen can further help in closing the catalyst cycle. Gratifyingly, the expected product **5ab** was obtained in a 45% yield, after heating at 105 °C for 16 hours. Complete conversions were observed in both the allene and the starting anilide. As comented in Chapter II, allenes tend to decompose or polymerize in the presence of transition-metals. A control experiment in which only the substrate **4a** was heated at 105 °C in toluene in presence of Cs_2CO_3 revealed that the base can partially decompose the anilide. This result led us to employ an excess of anilide in the ensuing experiments.

With the initial promising result, we performed a thorough screening of conditions. First, we started by testing several natural amino acid ligands bearing different protecting groups. The reaction results, indicated in Table 3, confirm that the acetyl protecting group is the one leading to the best results (entries 10-14). In every case, complete conversion of both the allene and the starting anilide was observed, presumably due to decomposition in the reaction media. Among all the side chains of the amino acids, valine led to the best yield (60%, entry 10). Valine amino acids featuring Boc, pivaloyl or propionyl protecting groups gave worse yields than when protected with acetyl, suggesting that large protecting groups in the nitrogen atom of the amino acid hamper the reaction. However, a formyl group, which is smaller than acetyl, also gave a low yield. This might be explained in terms of the lower basicity of the amidate carbonyl of the formyl-protected amino acid. Nonetheless, it is very difficult to interpret the effect of the protecting group or the side chain of the ligands in the reactivity of the system.

Table 3. *Screening of amino acid ligands.*

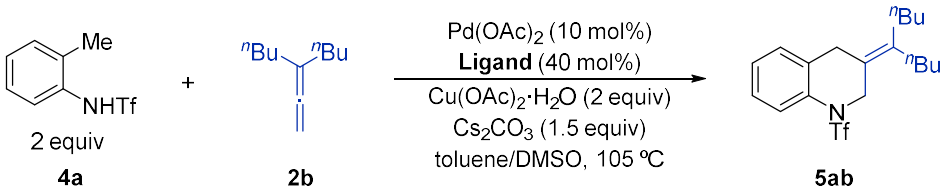

Entry	Ligand	Yield[b]	Entry	Ligand	Yield[b]
1	2,6-F,F,-Bz-Leu-OH	45%	8	Pro-Val-OH	52%
2	Boc-Val-OH	25%	9	Formyl-Val-OH	37%
3	Boc-Gly-OH	10%	10	Ac-Val-OH	60%
4	Boc-Cyclohexylglycine-OH	30%	11	Ac-Leu-OH	55%
5	Boc-Leu-NHOMe	18%	12	Ac-Ala-OH	55%
6	Fmoc-Leu-OH	10%	13	Ac-Phe-OH	35%
7	Piv-Val-OH	<5%	14	Ac-Gly-OH	42%

[a] Conditions: 0.333 mmol **4a**, 0.167 mmol of allene **2b**, 15 equiv of DMSO, 2 mL of toluene, under air, 16 h. [b] Yields calculated based on **2b**. Calculated by using 1,3,5-trimethoxybenzene as ^{1}H NMR internal standard.

Once Ac-Val-OH was selected as the best amino acid ligand for the reaction, we explored the effect of the oxidant. The results are summarized in Table 4. The yield dropped dramatically when no oxidant was employed (entry 1). Copper acetate cannot be used in substoichiometric amounts without compromising the yield (entry 2). It was observed that performing the reaction under a O_2 atmosphere slightly increases the yield for the substoichiometric test (entry 3), evidencing that there is an underlying reoxidation mechanism based on molecular oxygen. Other oxidants, like *p*-benzoquinone (BQ), silver salts or potassium persulfate gave worse results (entries 4-7) in terms of yield. After the screening, it was determined that the initial conditions were the most suitable for obtaining the best yields.

Table 4. *Screening of oxidants.*

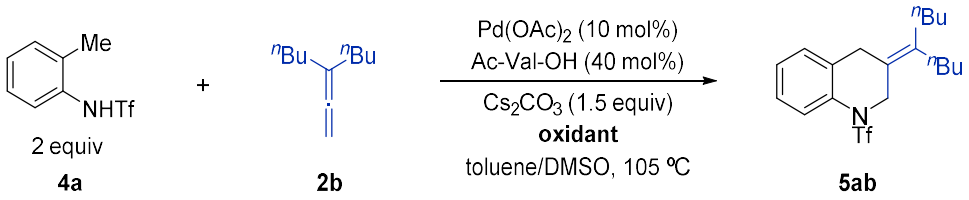

Entry	oxidant	Yield[b]
1	-	7%
2	$Cu(OAc)_2 \cdot H_2O$ (0.5 equiv)	37%
3	$Cu(OAc)_2 \cdot H_2O$ (0.5 equiv)	47%[c]
4	BQ (2 equiv)	4%
5	Ag_2CO_3 (1.5 equiv)	8%
6	Ag_2PO_4 (1.5 equiv)	24%
7	$K_2S_2O_8$ (2 equiv)	27%

[a] Conditions: 0.333 mmol **4a**, 0.167 mmol of allene **2b**, 15 equiv of DMSO, 2 mL of toluene, under air, 16 h. [b] Yields calculated based on **2b**. Calculated by using 1,3,5-trimethoxybenzene as ^{1}H NMR internal standard. [c] Reaction performed under O_2 atmosphere.

We then evaluated the effect of different bases in the reaction. The results are described in Table 5. The reaction does not work without base (entry 1). It was observed that the use of substoichiometric amounts of cesium carbonate decreased the yield (entry 2). With different carbonate bases we observed that the larger the size of the cation, the better the yield (entries 3-5). The role of the cation is going to be discussed later during the mechanistic proposal (section 3.3.3). Potassium phosphate was also effective for the reaction, leading to similar yields than cesium carbonate (entry 6). However, cesium acetate was not as effective, probably because of the less basicity of the acetate group compared to phosphate or carbonate groups (entry 7). It is important to highlight that in all the experiments with different bases we observed complete conversion of the starting material, demonstrating that the decomposition is not only caused by cesium carbonate, but by other inorganic bases.

Table 5. *Screening of bases.*

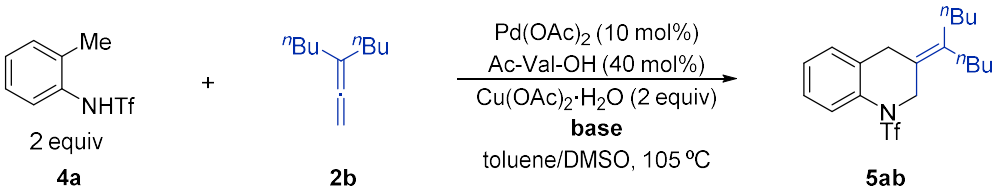

Entry	base	Yield[b]
1	-	<5%
2	Cs_2CO_3 (0.5 equiv)	49%
3	Li_2CO_3 (2 equiv)	<5%
4	Na_2CO_3 (1.5 equiv)	31%
5	K_2CO_3 (1.5 equiv)	53%
6	K_3PO_4 (1.5 equiv)	58%
7	CsOAc (1 equiv)	38%

[a] Conditions: 0.333 mmol **4a**, 0.167 mmol of allene **2b**, 15 equiv of DMSO, 2 mL of toluene, under air, 16 h. [b] Yields calculated based on **2b**. Calculated by using 1,3,5-trimethoxybenzene as ^{1}H NMR internal standard.

We next studied the effect of the solvents. The results are illustrated in Table 6. The reaction worked in most of the solvents so far tested, albeit with lower yields than in toluene. The best result was obtained with 2-methyl THF, with a 58% yield (entry 8), very close to the 60% with toluene. 2-Methyl THF is environmentally friendly, as it is obtained from furfural, an agriculture byproduct, and therefore it is a very convenient solvent for the reaction from a sustainability perspective.[148]

[148] Leal Silva, J. F.; Mariano, A. P.; Maciel Filho, R. *Biomass and Bioenergy* **2018**, *119*, 492.

Table 6. *Screening of solvents.*

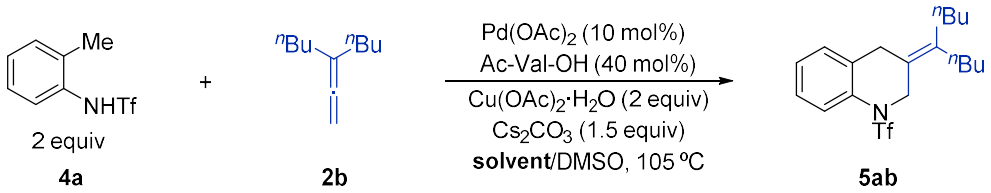

Entry	Solvent	Yield[b]
1	Trifluorotoluene	42%
2[d]	Hexafluorobenzene	32%
3	*p*-Xylene	49%
4	Dioxane	38%
5[d]	Acetonitrile	28%
6[d]	DCE	<5%
7[d]	THF	53%[c]
8[d]	2-methyl THF	58%[c]

[a] Conditions: 0.333 mmol **4a**, 0.167 mmol of allene **2b**, 15 equiv of DMSO, 2 mL of solvent, under air, 16 h. [b] Yields calculated based on **2b**. Calculated by using 1,3,5-trimethoxybenzene as ^{1}H NMR internal standard. [c] Isolated yield based on a **2b**. [d] Reaction performed in sealed tube.

By using 2-methyl THF as solvent, it is possible to decrease the temperature to 85 °C without compromising the yield (entry 1, Table 7), which enables to perform the reaction without employing a sealed tube. Additionally, as 2-methyl THF is more polar than toluene, salts like copper acetate or cesium carbonate are more soluble. This may explain why it is possible to decrease the amount of oxidant and base to 1 equivalent each, even observing a slight increase in the yield (entry 2).

The reaction was tested without DMSO, and it was evidenced that the effect of the additive is not as important as in apolar solvents like toluene (entry 3). However, its absence led to a slight decrease in the yield, so it was still used for the optimization. We found that equimolar amounts of both substrates **4a** and **2b** led to lower yields (entry 4), as when using excess of allene (entry 5). The reason behind these results is the decomposition of both the allene and the anilide in the reaction media, with the latter being more labile. Therefore, we decided to keep the excess of anilide and we performed a slow addition of the allene over the reaction media in 1 hour. That experiment gave a boost in the yield up to 71% (entry 6).

Table 7. *Tests using 2-methyl THF as solvent.*

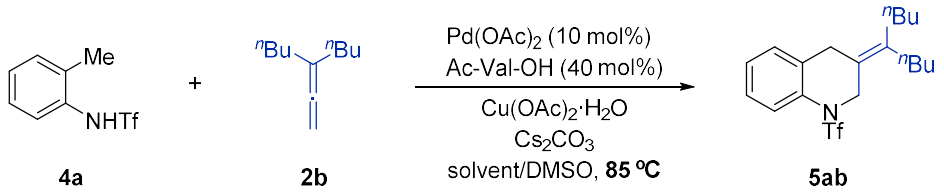

Entry	mmol **4a**	mmol **2b**	equiv $Cu(OAc)_2 \cdot H_2O$	equiv Cs_2CO_3	Yield[b]
1	0.333	0.167	2	1.5	54%[c]
2	0.333	0.167	1	1	61%[c]
3[d]	0.333	0.167	1	1	56%
4	0.167	0.167	1	1	56%
5	0.167	0.333	1	1	55%
6[e]	0.333	0.167	1	1	71%[c]

[a] Conditions: 40 mol% of Ac-Val-OH, 15 equiv of DMSO, 2 mL of 2-methyl THF, under air, 16 h. [b] Yields calculated based on **2b**. Calculated by using 1,3,5-trimethoxybenzene as ^{1}H NMR internal standard. [c] Isolated yield based on a **2b**. [d] Without DMSO. [e] Slow addition over 1 h of 0.167 mmol of allene **2b** in 1.5 mL of 2-methyl THF to the reaction instead of mixing it before heating.

The reaction did not proceed in absence of palladium acetate, whereas the use of 5 mol% instead of 10 mol% led to incomplete conversion and 23% yield. The reaction was also tested using several protecting groups in the amine moiety, employing conditions of entry 10 of Table 3 (toluene, 105 °C, Method A) or entry 2 of Table 7 (2-methyl THF, 85 °C, Method B) for experimental simplicity. The results are depicted in Scheme 71. Among all tested, triflate was still the most adequate for the transformations, followed by mesyl, probably because of their structure similarity.

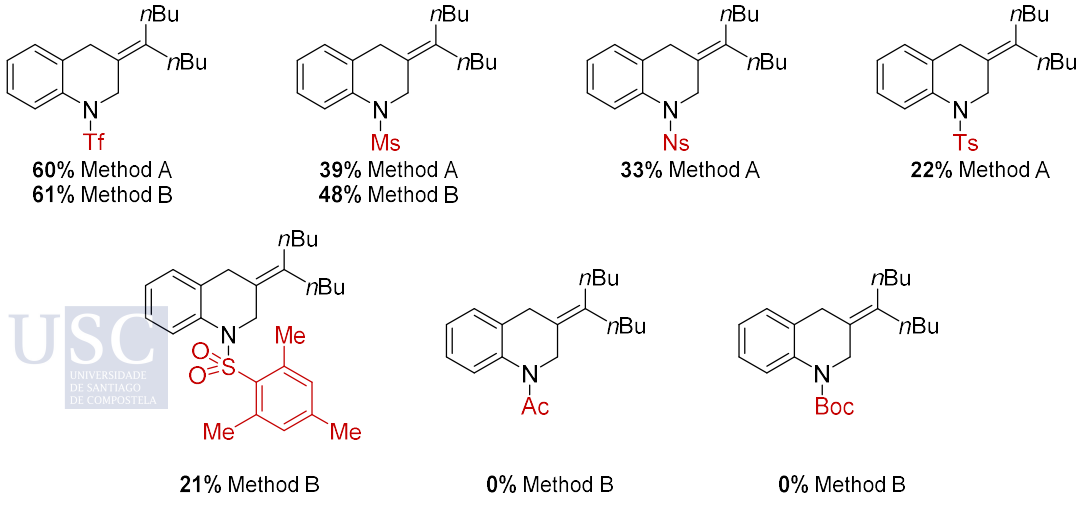

Scheme 71. *Screening of different protecting groups for the amine.*

3.2 Scope of the (4+2) cycloaddition between o-methylanilides and allenes

Using the optimized conditions, we explored the scope of the reaction. For that purpose, we synthesized allenes bearing different substitution patterns, following previously reported synthetic procedures. The synthesis of allenes **2a**-**2h** were described in the previous chapter (section 3.2). Allene **2i** (nona-4,5-diene) was made from trans-4-octene in a two-step procedure which involves a cyclopropanation with bromoform and a second step of elimination using methyllithium as base (Scheme 72a).[115] Allene **2j** (penta-1,2-diene-1,5-diyldibenzene) was synthesized from 3-phenylpropanal and phenylacetylene following also a two-step procedure (Scheme 72b). The first step was the reaction of the aldehyde with p-tosyhidrazine to form a hydrazone derivative that was reacted with phenylacetylene in a copper-catalyzed process.[149] Allene **2k** (1-(propa-1,2-dien-1-yl)-4-(trifluoromethyl)benzene) was synthesized from 4-ethynyl-α,α,α-trifluorotoluene following a standard Crabbé reaction with formaldehyde (Scheme 72c).[150] Meanwhile, allene **2l** (2-methyldeca-2,3-diene) was synthesized from 2-methyl-3-butyn-2-ol in a one-pot procedure that involves mesylation of 2-methylbut-3-yn-2-ol and then a SN_2' reaction with hexylmagnesium bromide and copper(I) (Scheme 72d).[151]

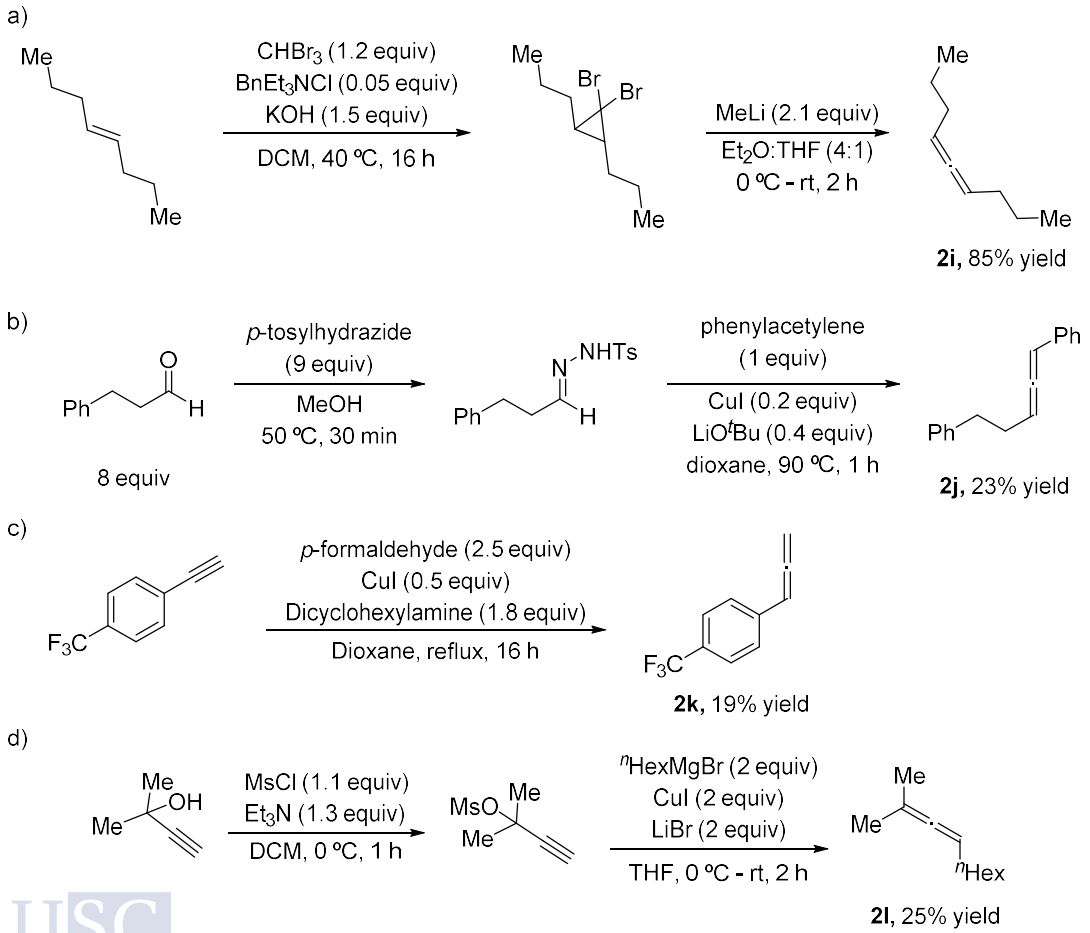

Scheme 72. *Synthetic procedures for the allenes **2i**-**2l**.*

[149] Ghosh, C.; Nagtilak, P. J.; Kapur, M. *Org. Lett.* **2019**, *21*, 3237.
[150] Kuang, J.; Shengming, M. *J. Org. Chem.* **2009**, *74*, 1763.
[151] Ahmar, M.; Barieux, J.-J.; Cazes, B.; Gore, J. *Tetrahedron* **1987**, *43*, 513.

We also prepared *o*-methylanilides featuring different electronic and steric characteristics. All of them were synthesized from their corresponding free amines through the same triflation procedure applied for the model substrate. Most of them were commercially available, except for 3-methyl-[1,1'-biphenyl]-4-amine (precursor of **4g**) and 3,5-dimethyl-[1,1'-biphenyl]-4-amine (precursor of **4n**), which were synthesized from their corresponding 4-bromoanilines through a Suzuki coupling with phenylboronic acid;[152] and 3-methylnaphthalen-2-amine (precursor of **4p**), which was synthesized from 2-amino-3-naphtoic acid by reduction with Red-Al® (Scheme 73).[153]

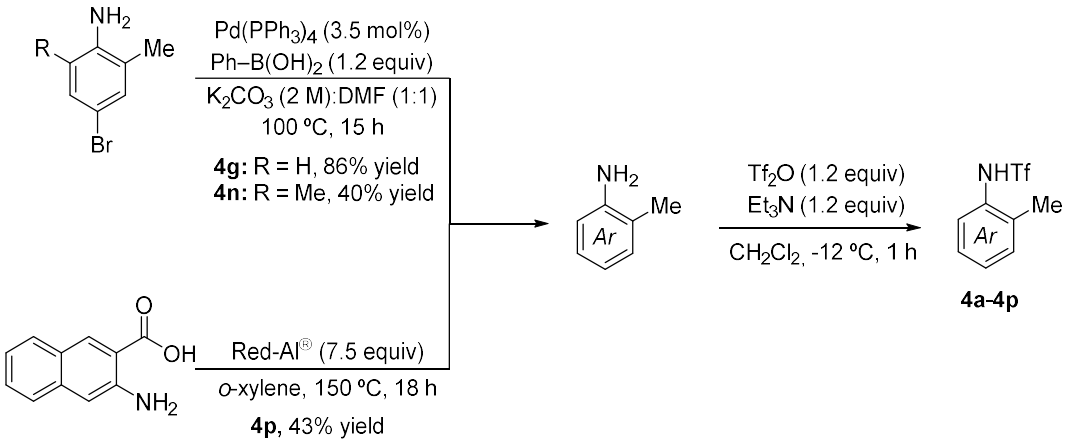

Scheme 73. *Synthetic procedures for the* o*-methylanilides **4a**-**4p***.

We were happy to observe that the annulation works using different types of allenes. The results are summarized in Scheme 74. 1,1,-disubstituted allenes like commercially available vinylidenecyclohexane **2a** gave the expected product with 61% yield. Symmetrical 1,3-disubstituted allenes such as **2i** also led to good yields (61%). Gratifyingly, non-symmetrical 1,3-disubstituted allenes **2e** and **2j** afforded the expected cycloadducts with excellent regio- and stereoselectivities and good yields (66% and 76% respectively).

As it was commented in section 3.2 of Chapter II, the preferential formation of the regioisomer depicted in the Scheme 74 is associated to a thermodynamic effect, with the double bond conjugated with the phenyl ring. Monosubstituted allenes, like **2f** and **2k**, can also engage in the reaction, albeit leading to mixtures of E:Z isomers. In the case of product **5ak** the selectivity was good but the yield was low, probably as a result of the instability of the allene partner under the reaction conditions. Notably, trisubstituted allenes also led to the tetrahydroquinoline products, and therefore cycloadducts **5ag**, **5ah** and **5al** equipped with quaternary centers were obtained in moderate to good yields (42%-73%).

[152] J. Liu, R. Ma, F. Bi, F. Zhang, C. Hu, H. Venter, S. J. Semple, S. Ma, *Bioorganic and Medicinal Chemistry Letters* **2018**, 1825.
[153] G. Q. Li, H. Gao, C. Keene, M. Devonas, D. H. Ess, L. Kürti, *J. Am. Chem. Soc.* **2013**, *135*, 7414.

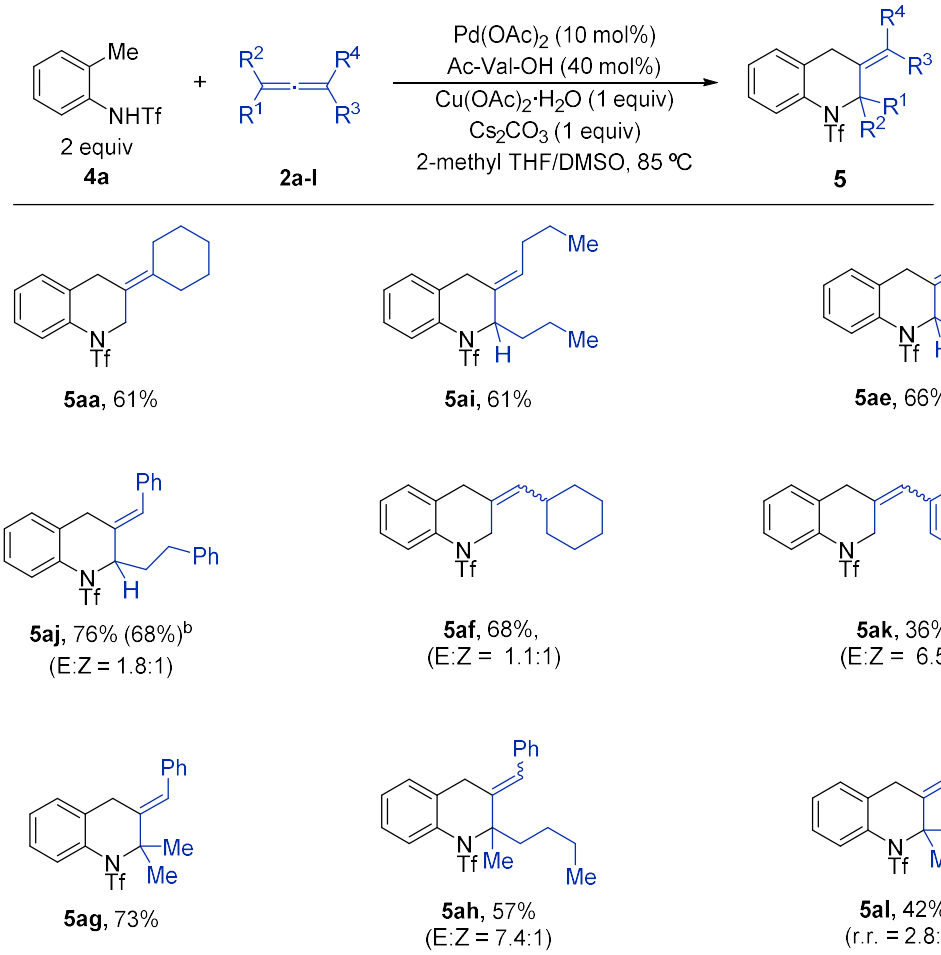

[a] Conditions: 0.333 mmol of **4a**, 0.167 mmol of allene **2**, 2.5 mL of Me-THF, 15 equiv DMSO, under air, 16 h. Slow addition over 1 h of allene in 1.5 mL of 2-methyl THF to the reaction instead of mixing it before heating. Regioisomeric ratios >20:1 and E/Z ratios >20:1, unless otherwise stated. Structure of the major product shown. Isolated yields based on **2**. [b] Yield after a gram-scale experiment.

Scheme 74. *Scope of the (4+2) cycloaddition regarding the allene coupling partner.*

In the same way indicated in the previous chapter, the use of allenes as 2-carbon partners was key for the success of the cycloaddition. Alkynes, like diphenylacetylene, were unreactive and no conversion was observed. This might be due to the higher coordination ability of alkynes, which can lead to the saturation of the metal coordination sphere to give nonactive complexes. Alkenes, such as ethyl acrylate, failed to give annulation products, providing just traces of olefination products, resulted from migratory insertion/β-hydride elimination processes (see section 1.4).

The next step was to evaluate how substitution in the aryl ring of the *o*-methylanilide affected the reaction. The results are illustrated in Scheme 75. Substitution in *ortho* position to the methyl group is tolerated, as well as the presence of diverse functional groups, like methoxy (**4b**), halogen (**4c**) or trifluoromethyl (**4d**). The corresponding products **5bb**, **5cb** and **5db** were obtained in 69%, 50% and 34% yield respectively. *Ortho*-methylanilides bearing substituents in *meta* position to the methyl group, such as phenyl, methoxy or halogens, can also engage in the reaction, affording the cycloadducts in moderate yields (**5eb-5ib**, 16-73% yield).

The reaction is also compatible with a variety of substituents *para* to the methyl group (chloride, ester, methoxy and fluoride were tested) giving the expected products in moderate to good yields (**5jb-5mb**, 50-69% yield). Aryl-disubstituted substrates such as **4n** and **4o** were also tested, as well as naphthylanilide **4p**, resulting in effective reactions (**5nb-5pb**, 52-67% yield). Finally, a mixed product **5gg** was synthesized in a 82% yield to demonstrate that the reaction is general for other allenes.

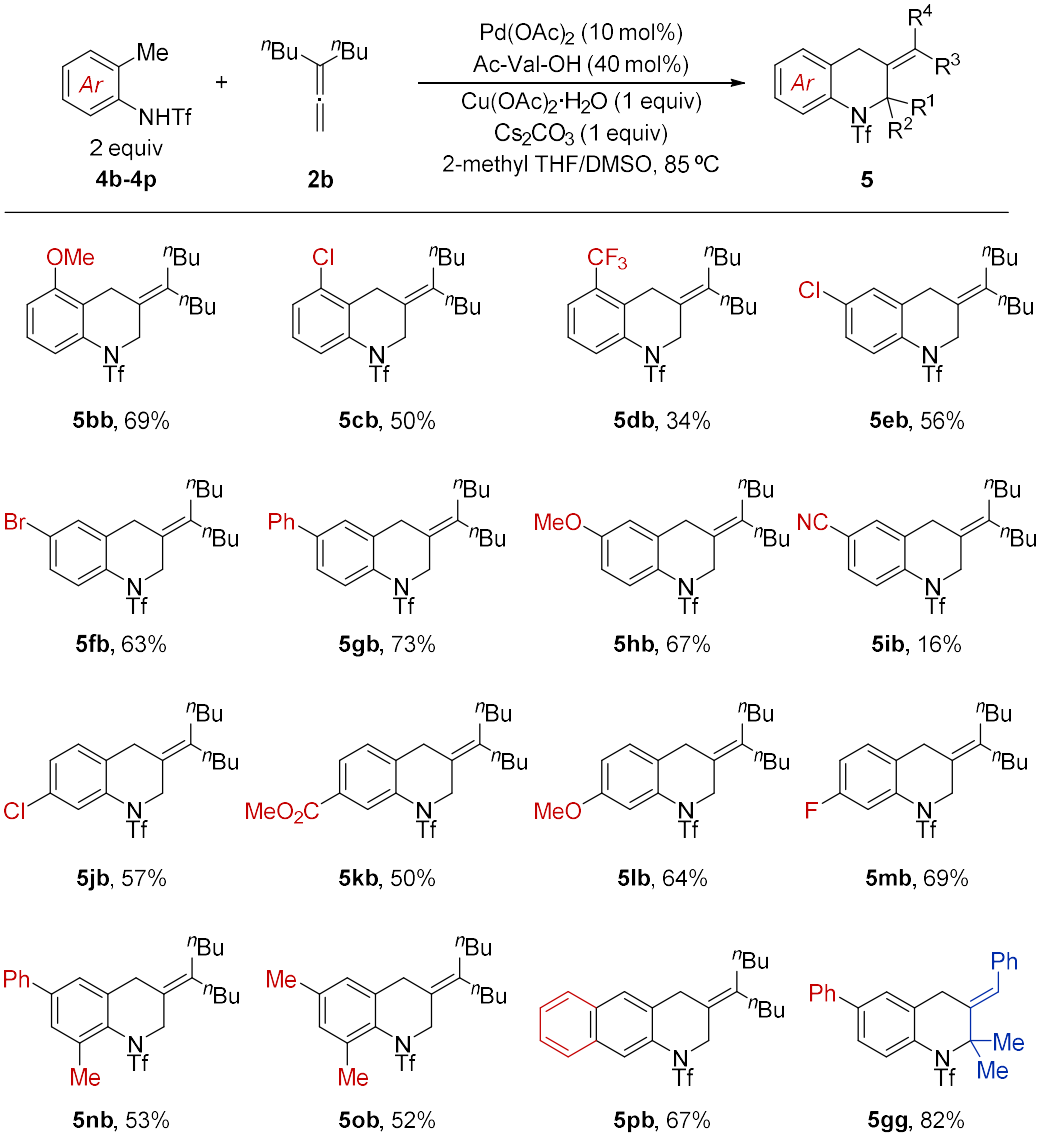

[a] Conditions: 0.333 mmol of amides **4**, 0.167 mmol of allene **2b** or **2g**, 2.5 mL of Me-THF, 15 equiv DMSO, under air, 16 h. Slow addition over 1 h of allene in 1.5 mL of 2-methyl THF to the reaction instead of mixing it before heating. Regioisomeric ratios >20:1 and E/Z ratios >20:1, unless otherwise stated. Isolated yields based on **2**.

Scheme 75. *Scope of the (4+2) cycloaddition regarding the* o*-methylanilide.*

It can be deduced from the results than *o*-methylanilides bearing electron-donating groups (like –OMe) gave better results than when bearing electron-withdrawing groups (like $–CF_3$), probably due to the greater instability of the latter under reaction conditions. Besides, *o*-methylanilides substituted in *ortho* position to the triflamide gave worse results, probably because steric reasons. Finally, product **5ib** was obtained with an unusual low yield. This could be explained

because of the coordinating character of the nitrile group, which could trap the catalyst, thus hampering the reactivity.

3.3 Mechanistic experiments

In order to obtain some information about the mechanism of the formal (4+2) cycloaddition between o-methylanilides and allenes, several experiments were performed.

3.3.1 Deuterium labeling experiments

Running the (4+2) cycloaddition between *o*-methylanilide **4a** and allene **2b** in the presence of 100 equivalents of deuterium oxide (D_2O) or 30 equivalents of Ac(d_3)–OD, under standard conditions, resulted in no deuterium incorporation in neither the starting material nor the product. This outcome suggests that the C–H activation step is irreversible (Scheme 76).

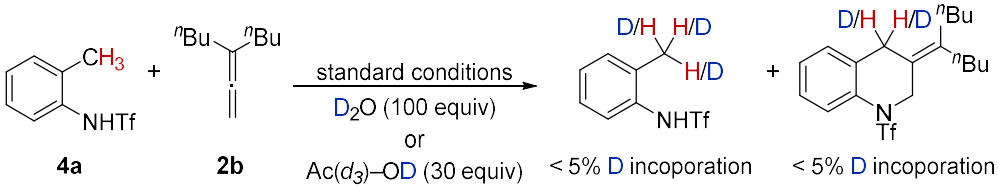

Scheme 76. *Deuterium incorporation test with substrate **4a**.*

With the intention of measuring the kinetic isotope effect (KIE), the deuterated analogue in the methyl group of model substrate **4a** was synthesized following the synthetic route depicted in Scheme 77. This route starts with the protection of the amine with Boc, followed by the nickel-catalyzed cross coupling with CD_3I to introduce the deuterated methyl group. Finally, deprotection of the Boc and triflation of the amine lead to the formation of the deuterated analogue **4a**-d_3. Details are described in the Experimental Section.

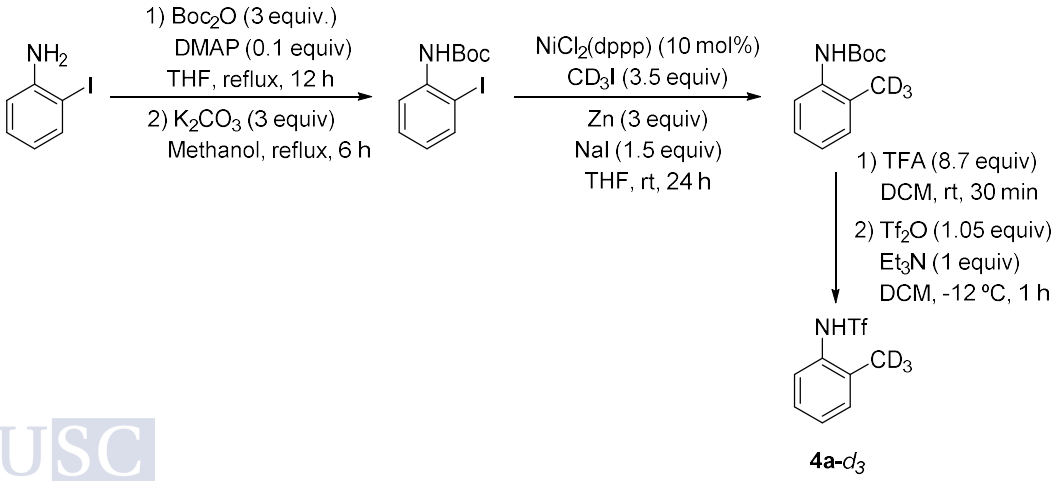

Scheme 77. *Synthetic route for the synthesis of the deuterated analogue **4a**-d_3.*

We then carried out a competition cycloaddition experiment using **4a** and the deuterated analogue in the methyl group (**4a**-d_3) (Scheme 78). In the same reaction vessel, both substrates were added in equimolar amounts, and the cycloaddition with allene **2b** was performed under standard conditions. The cycloadduct **5ab** was isolated as a mixture of both deuterated and non-deuterated products. By ^{1}H-NMR analysis, we calculated a KIE value of approximately 7.3, evidencing a primary kinetic isotope effect.[154]

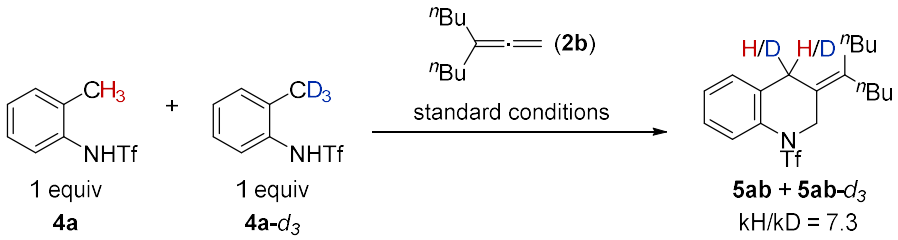

Scheme 78. *Competition experiment with substrate **4a** and **4a**-d_3 to measure the KIE of the reaction.*

An additional study of the KIE was carried out using parallel reactivity experiments. Two reaction vessels, one with substrate **4a** and other with deuterated substrate **4a**-d_3, were subjected to identical treatments with allene **2b**, under standard catalytic conditions (Scheme 79).

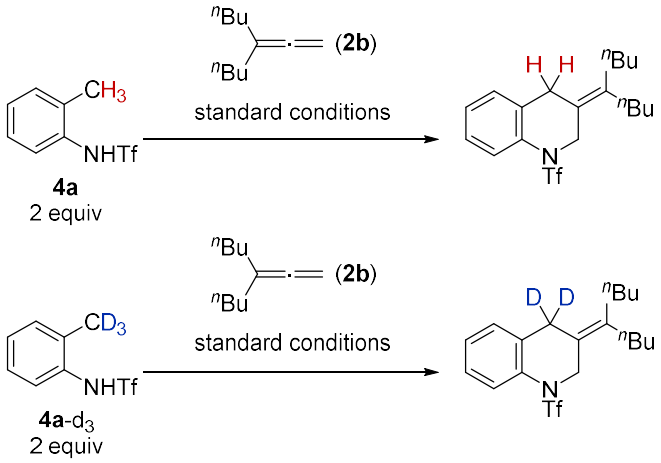

Scheme 79. *Parallel experiment with substrate **4a** and **4a**-d_3 to measure the KIE of the reaction.*

Aliquots of both reaction crudes were taken at different times and analyzed by ^{19}F-NMR to measure the conversion of the anilide, by comparing the NMR signal of the product and the remaining substrate. After collecting all data from different runs, the proportion of integral areas was plotted to calculate by least squares regression the gradient of the straight lines (Figure 13).

[154] Simmons, E. M.; Hartwig, J. F. *Angew. Chem. Int. Ed.* **2012**, *51*, 3066.

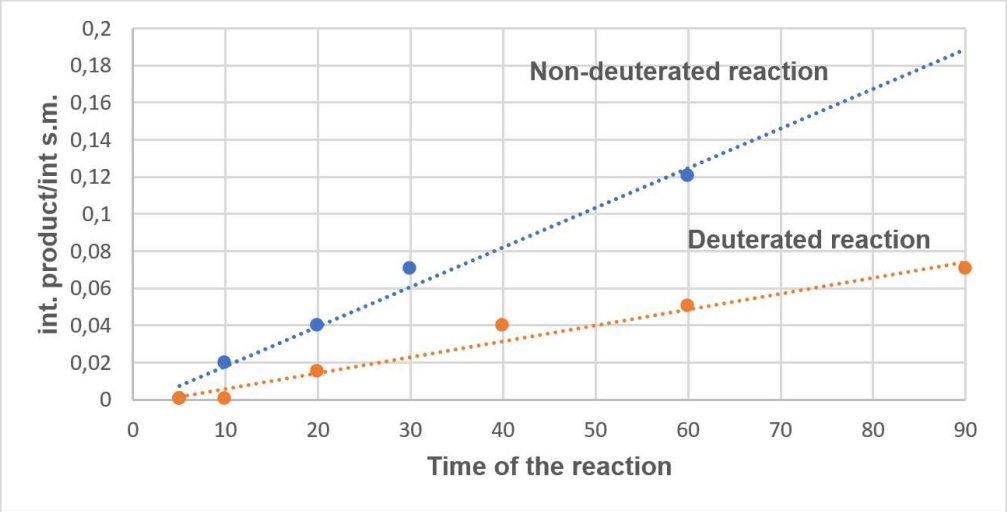

Figure 13. *Plot of the quotient between the integral of signal of the product and the remaining substrate at different times, and straight lines calculated by least squares regression. Blue line: reaction with* ***4a****. Orange line: reaction with* ***4a***-d_3.

The KIE value obtained by dividing both gradients was 2.3, which is also consistent with a primary kinetic isotopic effect. This means that the C–H activation is very probably the turnover-limiting step, albeit it is plausible that there are other high-energy steps in the reaction, which might become rate determining depending on the substrates.[154]

3.3.2 Experiments with an optically active, chiral allene

We next evaluated whether the chirality of an optically-pure allene could be transferred to the cycloaddition product. If the reaction proceeds through a π-allyl intermediate, the chirality of the allene may be conserved and transferred, depending of the nature of the reductive elimination step of the catalytic cycle. If palladium is coordinated to the nitrogen during the whole catalytic cycle (inner-sphere attack), the π-allyl intermediate may remain chiral, as the palladacycle would have a fixed conformation that would not allow the π-allyl to racemize. However, if the palladium is no longer coordinated to the nitrogen prior to the reductive elimination step (outer-sphere attack), the π-allyl intermediate could racemize (Figure 14).

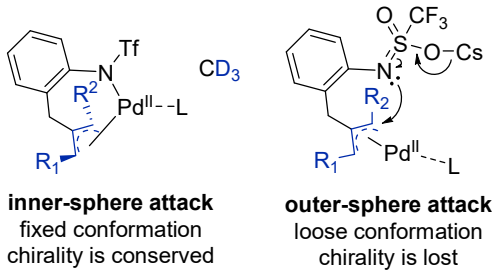

Figure 14. *Inner-sphere attack vs outer-sphere attack using a chiral allene.*

Therefore, we synthesized the chiral allene **(*S*)-2e** and we performed the cycloaddition under standard conditions with model substrate **4a**. We observed that the cycloadduct preserves some of the chiral information, as it was formed with a 62:38 enantiomeric ratio (entry 1, Table 8). Using a racemic amino acid ligand (entry 2) or a different amino acid (entry 3) gave lower enantiomeric ratios. This suggests that the amino acid could be playing a role in the racemization. DMSO is also playing a role, as enantioselectivity decreased dramatically in its absence (entry 4). Changing the solvent to toluene did not make significant changes in the enantiomeric ratio (entry 5).

Table 8. *Preliminary tests using chiral allene **(S)-2e** for the (4+2) cycloaddition.*

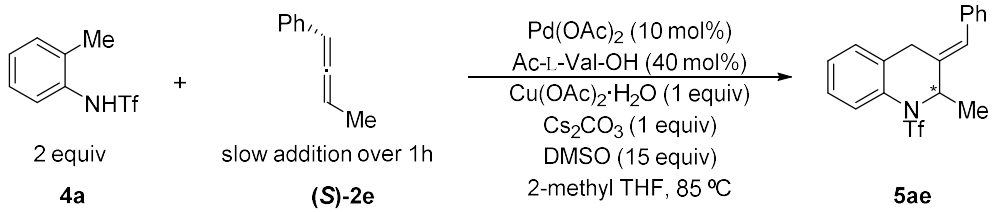

Entry	Variation in the conditions	Yield[b]	er **5ae**
1	-	67%	62:38
2	Racemic Ac-Val-OH as ligand	71%	57:43
3	Ac-Leu-OH as ligand	49%	58:42
4	Without DMSO	48%	52:48
5[c]	Toluene as solvent	65%	61:39
6	Without slow addition	43%	54:46
7	Slow addition during 4 h	73%	56:44

[a] Conditions: 0.333 mmol of amide **4a**, 0.167 mmol of allene **(*S*)-2e**, 2.5 mL of 2-methyl THF, under air, 16 h. Slow addition over 1 h of allene in 1.5 mL of 2-methyl THF to the reaction instead of mixing it before heating. [b] Yields calculated based on **(*S*)-2e**. Calculated by using 1,3,5-trimethoxybenzene as ^{1}H NMR internal standard. [c] 2 equiv of $Cu(OAc)_2{\cdot}H_2O$, 1.5 equiv of Cs_2CO_3.

These results are fairly inconclusive. Perhaps both inner and outer sphere mechanisms may operate, but it could also be that other racemization processes of the allene are also taking place. To shed some light, we performed the reaction in absence of aniline. After one hour, we discovered that part of the allene racemized, very likely in a palladium-mediated reaction in presence of nucleophiles (Scheme 81).[155]

[155] Horváth, A.; Bäckvall, J. E. *Chem. Commun.* **2004**, *4*, 964.

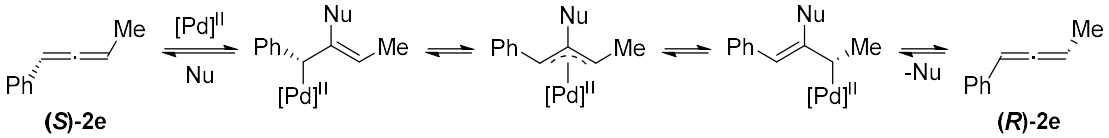

Scheme 81. *General mechanism proposed for the Pd-catalyzed racemization of chiral allene* ***(S)-2e****.*

Thus, the mechanistic test is not conclusive, as we cannot distinguish between an inner and an outer-sphere attack in the ring-closing step.

3.3.3 Mechanistic hypothesis

Considering the above results, we can propose a mechanism for the formal (4+2) cycloaddition (Scheme 80). The active Pd catalyst may be formed *in situ* by an exchange between the palladium acetate salt and the amino acid ligand, likely assisted by the base. The next step is the deprotonation of the nitrogen of substrate **4**, favored by the electron withdrawing triflyl group, to form the intermediate **I**. It is probably in this step when the cation of the base plays a role, as it is supposed to bind the oxygen of the sulfonamide. Afterward, the palladacycle **IIb** is formed through the amino acid-assisted C(sp^3)–H activation of the methyl group of the anilide. The presence of a primary kinetic isotope effect is consistent with this step being turnover-limiting. After the formation of the palladacycle, the allene coordinates to the metal center to form the intermediate **III**, which undergoes a regioselective migratory insertion to generate the putative π-allylic intermediate **IV**, whose exact structure might depend on the substituents of the allene. The next step is the C–N reductive elimination to form the product **5**, which is favored by the presence of the olefin in the coordination sphere of the catalyst. Finally, the catalyst is regenerated by the action of the $Cu(OAc)_2$ and, to a lesser extent, by the oxygen present in the air atmosphere.

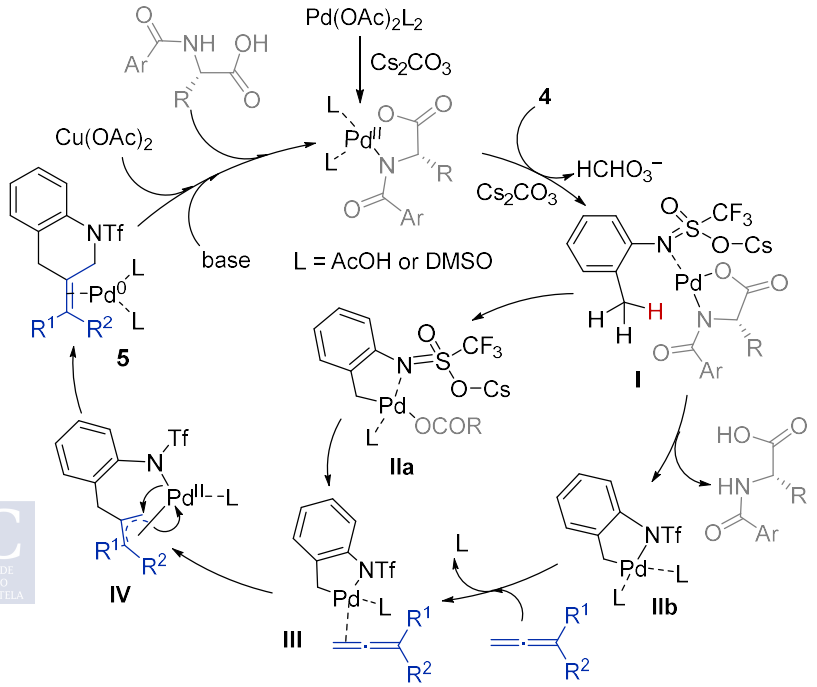

Scheme 80. *Proposed mechanism for the formal (4+2) cycloaddition and alternative outer-sphere pathway.*

Nevertheless, an outer-sphere mechanism cannot be ruled out, although in that situation we might have observed products arising from β-hydride elimination side pathways, which were not detected (Scheme 81). Experiments using chiral allene were inconclusive to settle the actual mechanism of reductive elimination, as the allene partially racemizes under the reaction conditions.

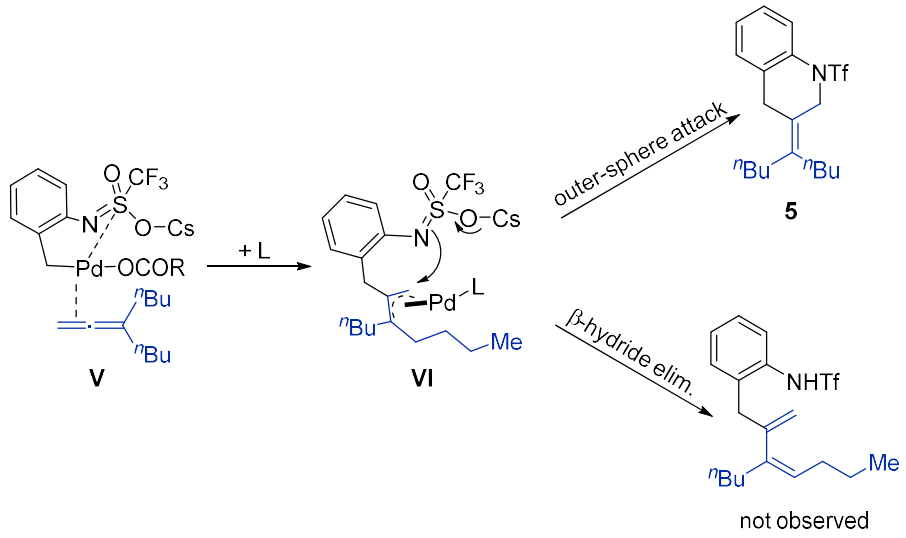

Scheme 81. *Alternative outer-sphere mechanism for the ring-closing step.*

3.4 Formal (5+2) cycloaddition between o-methylbenzyltriflamides and allenes: initial assays

At this stage, we wondered whether this methodology could be extended to more challenging *o*-methylbenzyltriflamides as annulation precursors. In these substrates, the directing group is one bond further apart from the methyl substituent, and therefore the C(sp^3)–H activation is not warranted. However, this cycloaddition would be of high interest, as it would allow to assemble synthetically relevant seven-membered heterocycles in a novel type of formal (5+2) annulation. One important issue that needs to be taken into account is that the methodology may require the employment of *ortho* disubstituted benzyltriflamides in order to avoid the competitive activation of the C(sp^2)–H bond of the aromatic ring.

We first performed a brief re-screening of reaction conditions for the (5+2) cycloaddition starting from the optimized conditions of the (4+2) cycloaddition. For that purpose, we synthesized the 2,6-dimethylbenzyltriflamide **6a** from commercially available 2,6-dimethylbenzylamine and triflic anhydride, using triethylamine as base. The remaining *ortho* position was blocked to prevent the C(sp^2)–H activation of the aryl ring (vide infra).

The results of the annulation experiments are summarized in Table 9. Using the optimized conditions for the (4+2) cycloaddition, the reaction gave low yield (entry 1, 29% yield). Complete conversion of the allene was observed after 16 hours. However, remaining substrate **6a** was detected, even though its exact conversion was not measured. In toluene at 105 °C, the yield boosted to 60%. The efficiency of these conditions might be explained in terms of the structural similarity of the substrate **6a** with the benzyltriflamides employed in the previous project (see Chapter II). Other amino acid ligands were tested for the reaction, but none of them enhanced

the yield (entries 3-6). During these assays, a side product coming from the ring closure of substrate **6a** was detected, meaning that the amide substrate might evolve by other undesired pathways in which the allene is not involved. However, the presence of unreacted **6a** suggested that this side reaction is slower than the decomposition of the allene, and therefore excess of the benzyltriflamides was not needed. This was evidenced when the reaction was performed using almost equimolar amounts of the reacting partners (entry 7), and especially with 2 equivalents of allene (entry 8), that allowed to increase the yield up to 86%.

Table 9. *Screening of conditions for the (5+2) cycloaddition.*

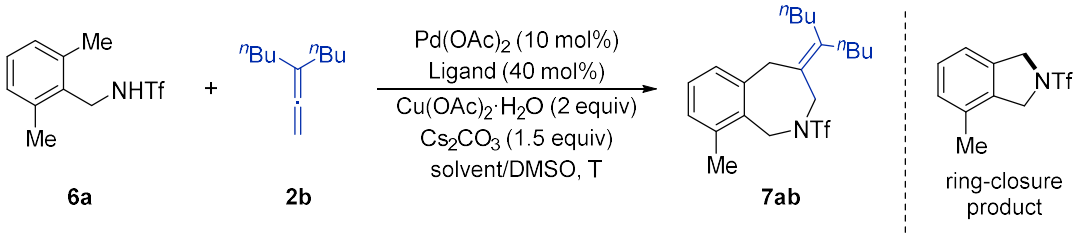

Entry	Ligand	Solvent	Temp.	Yield[b]
1[c]	Ac-Val-OH	2-methyl THF	85 °C	29%[d]
2	Ac-Val-OH	Toluene	105 °C	60%[d]
3	Ac-Ala-OH	Toluene	105 °C	58%
4	Ac-Leu-OH	Toluene	105 °C	58%
5	Ac-Gly-OH	Toluene	105 °C	47%
6	Formyl-Val-OH	Toluene	105 °C	54%
7[e]	Ac-Val-OH	Toluene	105 °C	58%[d]
8[f]	Ac-Val-OH	Toluene	105 °C	86%[d]

[a] Conditions: 0.333 mmol **6a**, 0.167 mmol of allene **2b**, 15 equiv of DMSO, 2 mL of solvent, under air, 16 h. [b] Yields calculated based on **2b**. Calculated by using 1,3,5-trimethoxybenzene as ^{1}H NMR internal standard. [c] 1 equiv of $Cu(OAc)_2{\cdot}H_2O$ and 1 equiv of Cs_2CO_3. Slow addition over 1 h of 0.167 mmol of allene **2b** in 1.5 mL of 2-methyl THF to the reaction instead of mixing it before heating. [d] Isolated yield. [e] 0.167 mmol **6a**, 0.184 mmol of allene **2b**. [f] 0.167 mmol **6a**, 0.333 mmol of allene **2b**.

3.5 Scope of the (5+2) cycloaddition between o-methylbenzylamides and allenes

With the optimized conditions in our hand, we explored the scope of the cycloaddition. We synthesized several *o*-methylbenzyltriflamides bearing different substitution patterns. Most of them were made from their corresponding free amines using a standard triflation procedure. The starting free amines were commercially available or synthesized from their corresponding nitriles and subsequent reduction of the imine following previously reported procedures. [119,156] However, **6c** and **6d** were synthesized from their corresponding alcohols using a Mitsunobu reaction (Scheme 82).

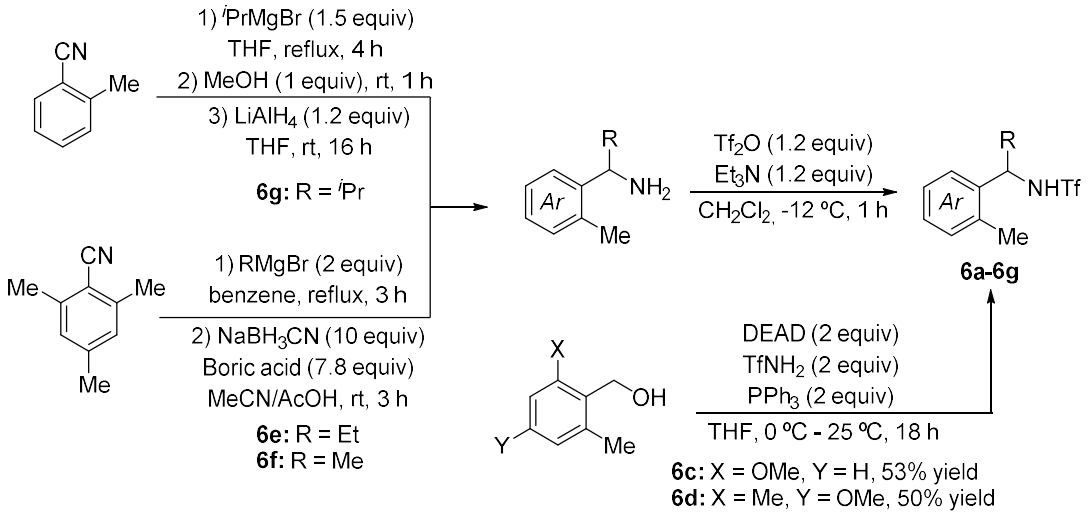

Scheme 82. *Synthetic procedures for the* o*-methylbenzyltriflamides **6a**-**6g**.*

We then assayed the cycloaddition with different allenes. The results are illustrated in Scheme 83. The reaction works in a very efficient manner, and even leads to better yields than the homologous anilides. Interesting tetrahydro-2-benzazepines cycloadducts (**7bb**-**7db**) were obtained in good to excellent yields (71%-90% yield), evidencing the tolerance to functional groups like fluorine or methoxy. Substitution in α-position to the amino group is also tolerated (**7eb** and **7fb**, 71% and 68% respectively). Other allenes, like trisubstituted allene **2g**, can also engage in the cycloaddition, affording the tetrahydro-2-benzazepine **7cg** in a 61% yield.

[156] S. Levinger, S, R. Nair, A. Hassner, *Beilstein J. Org. Chem.* **2008**, *4*, 1.

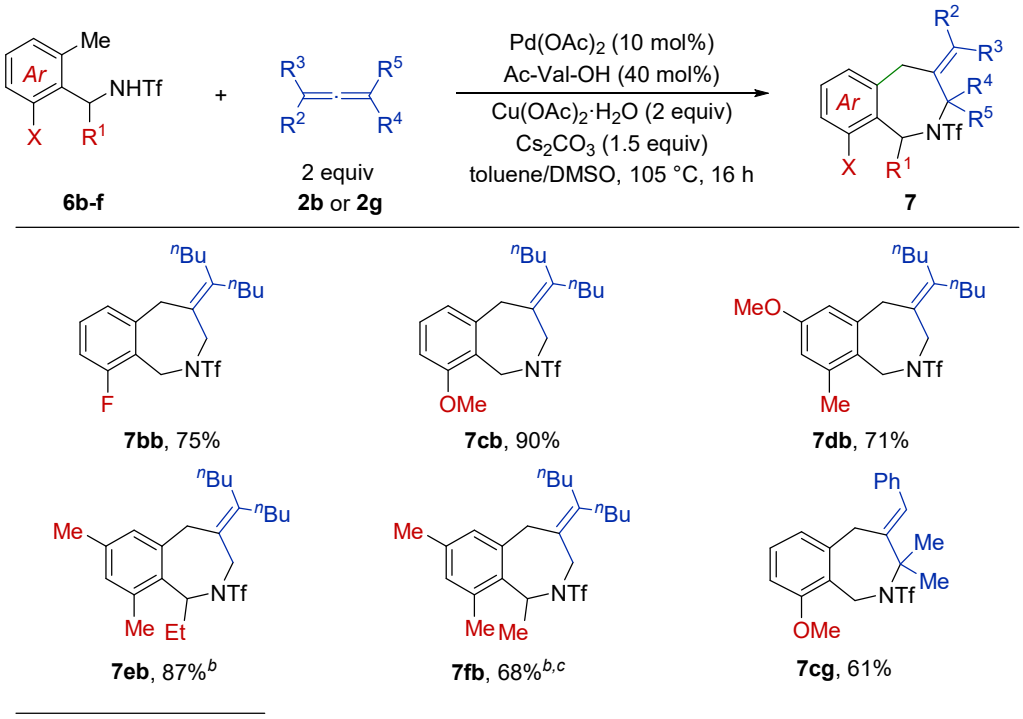

[a] Conditions: 0.167 mmol of amides **6**, 0.333 mmol of allenes **2**, 2 mL of toluene, 15 equiv DMSO, under air, 16 h. Regioisomeric ratios >20:1 and E/Z ratios >20:1, unless otherwise stated. Isolated yields based on **6**. [b] Racemic Ac-Val-OH was used. [c] 0.167 mmol of amide **6f**, 0.167 mmol of allene **2b**.

Scheme 83. *Scope of the (5+2) cycloaddition between* o*-methylbenzylamines and allenes.*

As an additional test, the *o*-methylbenzyltriflamide **6g**, that lacks on substitution in the *ortho* position, was assayed under optimized reaction conditions with racemic Ac-Val-OH and allene **2b** (Scheme 92). As expected, the formation of the cycloadduct **7gb** was not observed, whereas the product **8**, result of the C(sp^2)–H activation of the aryl ring, was isolated in an 89% yield. This demonstrates the importance of the disubstitution at the *ortho* position of the benzyltriflamide to prevent the more favorable C(sp^2)–H activation, and points out an important future challenge, promoting the preferential activation of the methyl group over the aryl C–H bond.

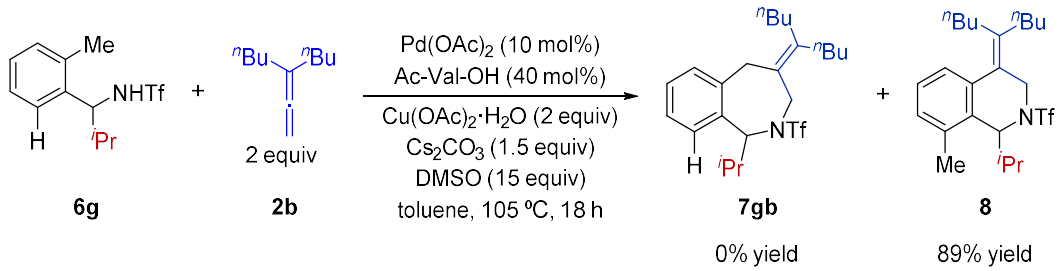

Scheme 84. *Test with the monomethylated benzyltriflamide* ***6g****.*

3.6 Preliminary tests on a (5+2) enantioselective cycloaddition based on a kinetic resolution strategy

With the above examples demonstrating the viability of employing α-substituted *o*-methylbenzyltriflamides, we envisioned the possibility of developing an enantioselective version of the cycloaddition. For that purpose, we subjected the *o*-methylbenzyltriflamide **6e** to a brief screening of conditions, as illustrated in Table 10. The use of Ac-Val-OH led to a very poor enantioselectivity at 70 °C, affording the cycloadduct **7eb** with only a 59:41 enantiomeric ratio (entry 1). When the amino acid was protected with a larger group, like Boc, the result was slightly better (73:21 er, entry 2), while with the Boc-protected amino methyl ester of phenylalanine (Boc-Phe-NHOMe), the enantiomeric ratios increased to 83:17 (entry 3). It is important to highlight the strong influence of the temperature in the kinetic resolution. At 70 °C and employing Boc-Leu-NHOMe as ligand, the product was obtained in only an 8% yield with an 88:12 er (entry 4). However, increasing the temperature in 10 °C, the yield boosted up to 48%, but the er decreased to 78:22.

Table 10. *Preliminary tests for the kinetic resolution of* ***6e****.*

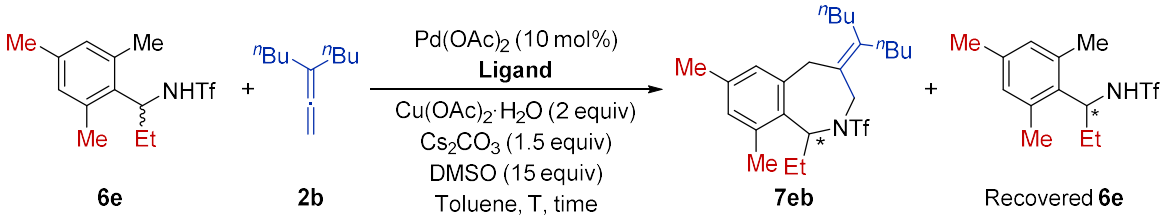

Entry	Ligand (mol%)	Temp.	Time	Yield[b]	Conversion[b]	er **7eb**	er rec. **6e**
1	Ac-Val-OH (40)	70 °C	4 h	17%	not meas.	59:41	not meas.
2	Boc-Val-OH (40)	70 °C	24 h	38%	not meas.	73:21	not meas.
3	Boc-Phe-NHOMe (15)	70 °C	48 h	33%	42%	83:17	69:31
4	Boc-Leu-NHOMe (15)	70 °C	48 h	8%	34%	88:12	52:48
5	Boc-Leu-NHOMe (15)	80 °C	48 h	48%	57%	78:22	82:18

[a] Conditions: 0.1 mmol of amide **6e**, 0.1 mmol of allene **2b**, 2 mL of toluene, under air. [b] Isolated yields, conversion based on recovered **6e**.

o-Methylbenzyltriflamide **6f** was also tested in this reaction using mono-protected amino methyl ester ligands. The results are summarized in Table 11. At 70 °C, both Boc-Phe-NHOMe and Boc-Leu-NHOMe ligands gave similar results (entries 1-2, 38-42% yield, 86:14-88:12 er). By decreasing the temperature 10 °C, the cycloadduct **7fb** was obtained with a promising 90:10 enantiomeric ratio, albeit with a moderate 20% yield (entry 3).

Table 11. *Preliminary tests for the kinetic resolution of **6f**.*

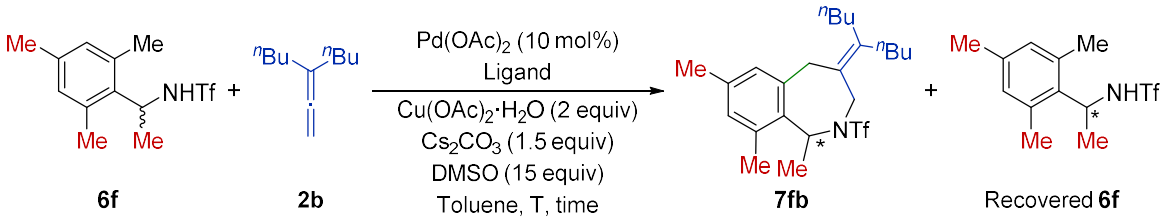

Entry	Ligand (mol%)	Temp.	Time	Yield[b]	Conversion[b]	er **7fa**	er rec. **6f**
1	Boc-Phe-NHOMe (15)	70 °C	48 h	38%	43%	86:14	75:25
2[c]	Boc-Leu-NHOMe (15)	70 °C	72 h	42%	59%	88:12	78:22
3[d]	Boc-Leu-NHOMe (15)	60 °C	72 h	20%	21%	90:10	60:40

[a] Conditions: 0.1 mmol of amide **6f**, 0.1 mmol of allene **2b**, 2 mL of toluene, under air. [b] Isolated yields, conversion based on recovered **6f**. [c] **7fb:** $[\alpha]_D^{19.8}$ = -19.3 (c 1.0, CH_2Cl_2); recovered **6f**: $[\alpha]_D^{19.8}$ = -10.3 (c 1.0, CH_2Cl_2) [d] 0.2 mmol of allene **2b**.

These preliminary results confirm that it is possible to generate optically active tetrahydro-2-benzazepine skeletons by employing the novel (5+2) cycloaddition, and warrant further studies to optimize the process.

3.7 Derivatization of the cycloadducts

The products obtained in the cycloaddition are susceptible of synthetic manipulation. For instance, the exocyclic double bond in product **7cg** was successfully hydrogenated with H_2 over Pd/C to give a fully saturated tetrahydro-2-benzazepine skeleton (**9**) in a 73% yield. The structure of compound **9** was determined by X-ray diffraction analysis. Moreover, the triflyl protecting group can be removed by treatment with Red-Al©, affording the unprotected tetrahydro-2-benzazepine **10** in 76% yield (Scheme 85). Removal of the methoxy group of **6** was also attempted using a hydrogenation procedure reported by Hartwig with Ni(0).[157] This would be very interesting, as methoxy group could be employed as a temporary moiety to block the *o*-position of the *o*-methylbenzyltriflamide. However, no reactivity was observed, and therefore the starting material was recovered.

[157] Sergeev, A. G.; Hartwig, J.F. *Science,* **2011**, *332*, 439

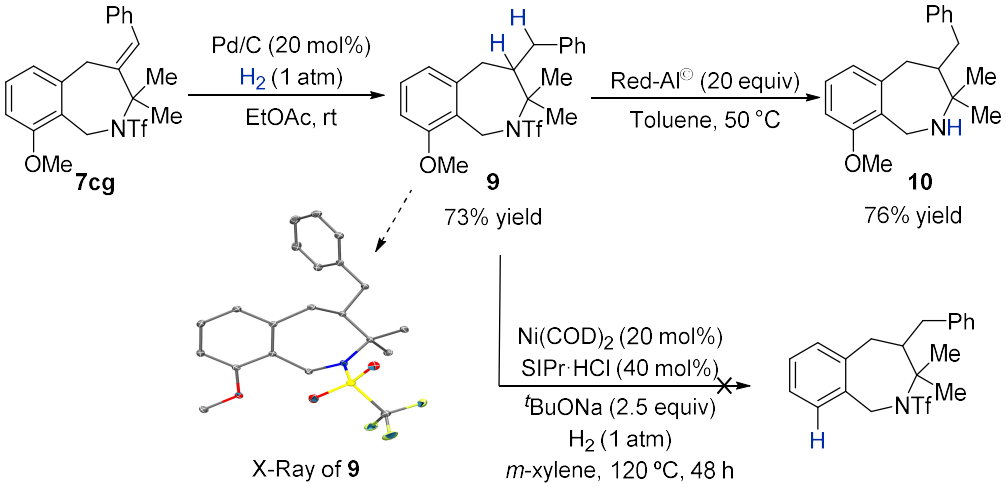

Scheme 85. *Synthetic manipulation of compound **7cg**.*

Hydrogenation of the quaternary double bond of product **5aa** was tested using a balloon of hydrogen (1 atm) over Pd/C. However, there was no reaction, and the starting material was recovered (Scheme 86a). It is possible that increasing the hydrogen pressure we could achieve the desired reactivity but it was not tested. We also tried to break the double bond of **5aj** with an ozonolysis reaction using dimethylsulfide or triphenylphosphine as reductants. However, only decomposition of the starting material was observed in both assays (Scheme 86b), probably due to an excessive fragmentation of the molecule.

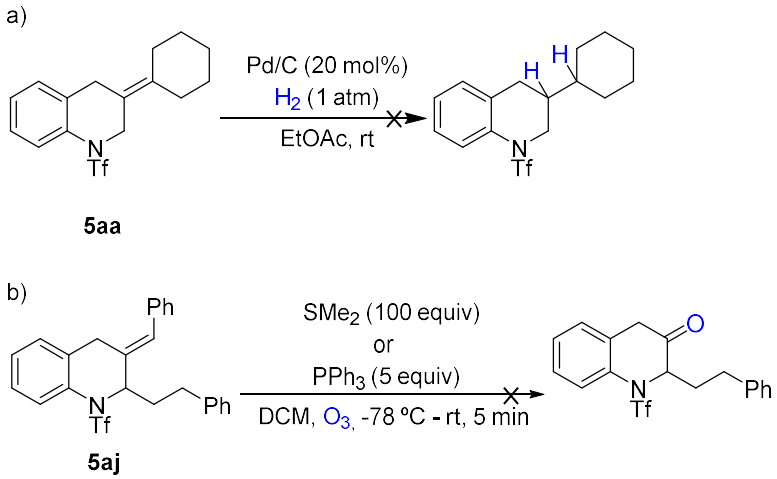

Scheme 86. *Unsuccessful derivatization assays.*

4- Conclusions

In conclusion, we have developed a palladium-catalyzed formal (4+2) cycloaddition between *ortho*-methyl anilides and allenes, relying on the activation of a benzylic C(sp^3)–H bond. This methodology allows the straightforward assembly of highly substituted tetrahydroquinoline skeletons. After a thorough screening of reaction conditions, we were able to obtain good reaction yields. The cycloaddition presents good levels of chemo- and regioselectivity, and tolerates different substitution patterns in both the anilide and the allene coupling partner (Scheme 87). This reaction is one of the first examples of cycloadditions based on benzylic C(sp^3)–H activation.

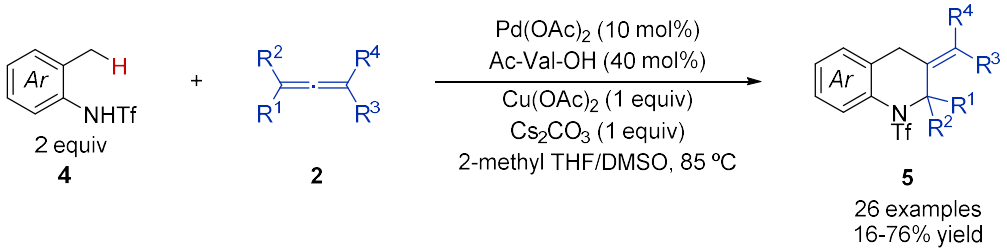

Scheme 87. *Palladium-catalyzed formal (4+2) cycloaddition between* o*-methylanilides and allenes.*

Some mechanistic tests have been performed in order to unravel more information about the mechanism. Kinetic isotope effect experiments manifested that the C(sp^3)–H activation is the turnover-limiting step of the catalytic cycle. Experiments employing chiral allenes resulted in partially-racemized cycloadducts, which reinforces the hypothesis that the reaction involves π-allyl intermediates.

Moreover, this methodology has been applied to more challenging *o*-methylbenzyl triflamide substrates, in an unprecedented example of formal (5+2) cycloaddition. Tetrahydro-2-benzazepine skeletons can be assembled through this annulation, as demonstrated by the examples reported in the scope, with yields up to 90% (Scheme 88). Besides, the cycloadducts obtained with this methodology can be synthetically manipulated, as demonstrated with the hydrogenation of product **7cg**, and the subsequent deprotection of the amino group.

Furthermore, in a preliminary study, it has been demonstrated that optically active tetrahydro-2-benzazepines can be synthesized through a kinetic resolution strategy from racemic α-substituted *o*-methylbenzyltriflamides, affording the corresponding enantioenriched cycloadducts in enantiomeric ratios up to 90:10.

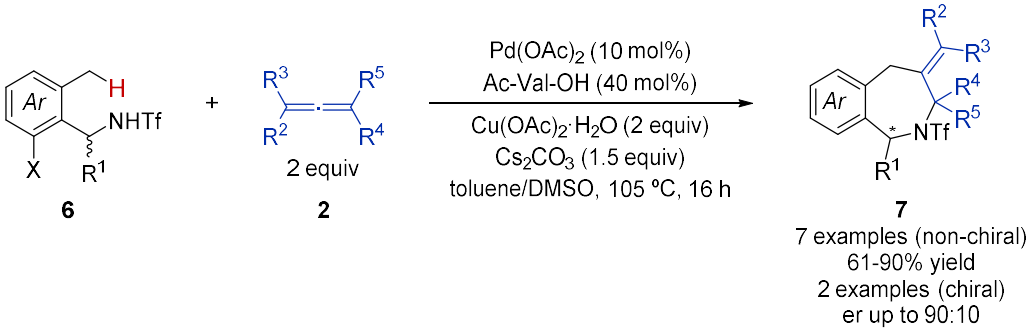

Scheme 88. *Palladium-catalyzed formal (5+2) cycloaddition between* o*-methylbenzyltriflamides and allenes.*

Addendum

Preliminary studies on Pd-catalyzed cyclization of *o*-methylbenzylamines to isoindolines involving a C(sp^3)–H activation

1- Introduction

1.1 Features of Pd(II)/Pd(IV) based catalytic cycles

The work discussed in the previous chapters entails Pd-promoted C–H activation reactions and mechanisms involving Pd(0)/Pd(II) cycles. But, as commented in the introduction, there have been numerous reports on C–H functionalization reactions that take place through alternative mechanisms based on Pd(II)/Pd(IV) catalytic cycles. This type of catalytic processes present certain advantages, such as the fact that Pd(IV) intermediates are often resistant to β-hydride elimination process, but undergo facile reductive eliminations. They are also more tolerant to the presence of O_2 or functional groups like halogens. Therefore, the range of functionalizations that can be achieved in reactions involving Pd(II)/Pd(IV) catalytic cycles is notably wider than when using Pd(II)/Pd(0) cycles.

The first Pd(IV) complexes were isolated and characterized in the 1970s, but these early investigations were limited to explore stoichiometric transformations. It was not until recent years, with the discovery of reagents capable to oxidize the palladium to its highest oxidation-state, when Pd(II)/Pd(IV) catalytic cycles were developed. This type of cycles are especially relevant in the field of C–H activation chemistry, although demonstrating the presence of Pd(IV) species is far from obvious, and there are several reports of palladium-catalyzed C–H activations where there is not enough evidence to distinguish between Pd(II)/Pd(IV) and P(II)/Pd(0) catalytic cycles.[158]

The general mechanism of the Pd(II)/Pd(IV) catalytic cycle starts with the C–H activation promoted by the Pd(II) reagent, usually via a CMD mechanism, to form the Pd–C bond. After that, there is an oxidation step, and eventually a ligand transfer to produce Pd(IV) intermediates. Finally, a reductive elimination delivers the product and regenerates the Pd(II) catalyst (Scheme 89).

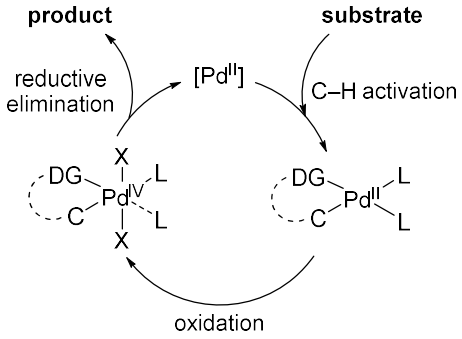

Scheme 89. *General mechanism scheme for a Pd(II)/Pd(IV) catalytic cycle.*

[158] For more information about Pd(IV)/Pd(II) catalysis, see Xu, L. M.; Li, B. J.; Yang, Z.; Shi, Z. J. *Chem. Soc. Rev.* **2010**, *39*, 712.

The oxidation step can be performed using different strategies, including an oxidative addition of aryl or alkyl halides to the complex, the addition of electrophilic fluorine species,[159] the employment of hypervalent iodine reagents or the oxidation with strong inorganic oxidants like $Ce(SO_4)_2$ or Oxone©. The election of a proper oxidant is key to obtain an efficient catalytic cycle without coping with the challenges of undesired reductive eliminations of the ligands coming from the oxidant (i.e., acetoxylation due to the acetoxy group coming from the $PhI(OAc)_2$) or the undesired oxidation of other functional groups present in the molecule.

1.2 Synthesis of indole-type skeletons through Pd(II)/Pd(IV) catalysis

The above C–H activation mechanisms are pertinent not only for intermolecular functionalizations but also for cyclization reactions. Indeed, they have been used for construction of azaheterocycles, providing a complementary approach to the Buchwald-Hartwig amination reaction[32]. Among all different azaheterocycles, those containing 5-membered rings (indole-type skeletons) are especially appealing because there is a large variety of bioactive molecules containing these cores.

One of the first examples of this kind, based on Pd(II)/Pd(IV) catalytic cycles, was reported by Yu and co-workers in 2008. They reported the synthesis of γ-lactams from aryl amides using a combination of AgOAc and $CuCl_2$ as oxidant (Scheme 90).[160] Even though the proposed mechanism goes through a Pd(II)/Pd(IV) catalytic cycle, there is not strong evidence to support the sufficient oxidation of Pd(II) to Pd (IV) by either Ag^+ or Cu^{2+}.

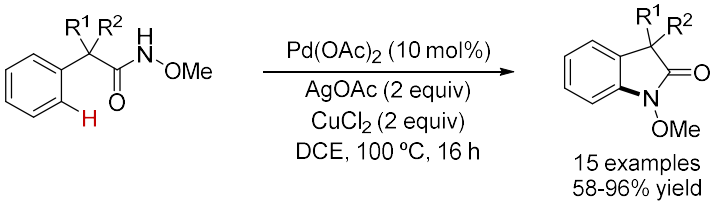

Scheme 90. *Pd(II)-catalyzed cyclization of aryl amides to synthesize γ-lactams reported by Yu and co-workers.*

The same year, the group of Gaunt developed a Pd(II)-catalyzed intramolecular amination of *o*-phenylanilines for the synthesis of carbazoles (Scheme 91).[161] $PhI(OAc)_2$ was elected as the most suitable oxidant for the reaction, allowing it to proceed under mild conditions. The isolation of a stable carbopalladation complex that can successfully give the coupling product when treated with the oxidant suggests the involvement of a Pd(IV) intermediate.

[159] Engle, K. M.; Mei, T. S.; Wang, X.; Yu, J.-Q. *Angew. Chem. Int. Ed.* **2011**, *50*, 1478.
[160] Wasa, M.; Yu, J.-Q. *J. Am. Chem. Soc.* **2008**, *130*, 14058.
[161] Jordan-Hore, J. A.; Johansson, C. C. C.; Gulias, M.; Beck, E. M.; Gaunt, M. J. *J. Am. Chem. Soc.* **2008**, *130*, 16184.

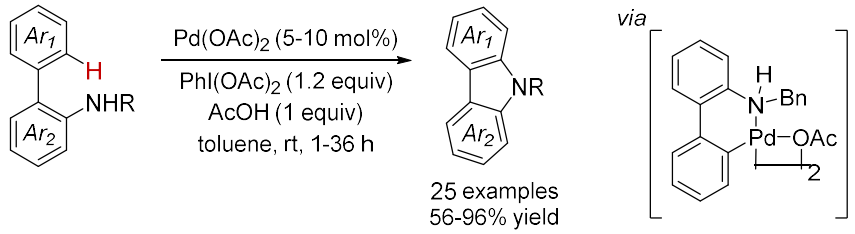

Scheme 91. *Pd(II)-catalyzed intramolecular amination of* o*-phenylanilines reported by Gaunt and co-workers.*

In 2009, the group of Yu reported the synthesis of indolines from triflyl-protected phenylethylamines with the use of a fluorine-donor reagent (F^+) as oxidant (Scheme 92).[162] Other oxidants tested failed, probably because of the presence of a strong electron withdrawing group at the nitrogen. Only 1-fluoro-2,4,6-trimethylpyridinium triflate worked effectively. It is interesting to discuss the mechanism of this reaction, particularly in comparison with the synthesis of β-fluoro α-amino acids reported by Yu and Shi (see section 4.3.1.4 of Chapter I). In both reactions, a fluorine-donor reagent is employed to oxidize the Pd(II) catalyst to Pd(IV). In the synthesis of indolines, the reductive elimination of the substrate (C–N) is favored over the reductive elimination of the fluorine (C–F), due to the strength of the Pd–F bond.

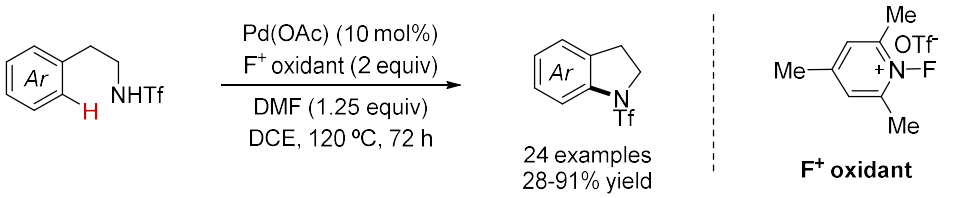

Scheme 92. *Pd(II)-catalyzed intramolecular C–H amination of phenylethyltriflamides using a F^+ oxidant.*

However, in the synthesis of β-fluoro α-amino acids, the reductive elimination of the substrate would lead to a high-strained β-lactam, and therefore the reaction prefers to evolve by formation of a C–F bond (Scheme 93)[163]. These examples remarks the idea of selecting a proper oxidant for C–H activation reactions by taking into account not only the oxidant, but also the substrates where the C–H activation takes place, in order to avoid undesired side reactions.

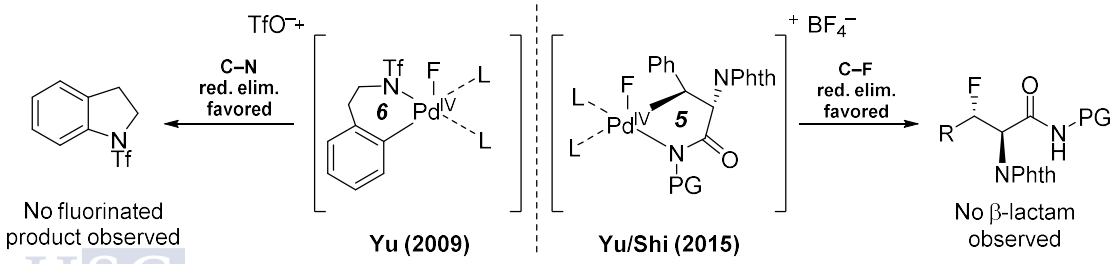

Scheme 93. *Dependence of the palladacycle size in C–F reductive elimination.*

[162] Mei, T. S.; Wang, X.; Yu, J.-Q. *J. Am. Chem. Soc.* **2009**, *131*, 10806.

[163] For further information about C–F reductive elimination mechanisms from Pd(IV) complexes: (a) Furuya, T.; Benitez, D.; Tkatchouk, E.; Strom, A. E.; Tang, P.; Goddard, W. A.; Ritter, T. *J. Am. Chem. Soc.* **2010**, *132*, 3793. (b) Racowski, J. M.; Gary, J. B.; Sanford, M. S. *Angew. Chem. Int. Ed.* **2012**, *51*, 3414.

In 2014, Zhao, Yao and co-workers reported several examples of the construction of indole-type skeletons through intramolecular amination of phenylethylamines protected with an oxalyl amide directing group, as part of a larger piece of research. $PhI(OAc)_2$ was employed as oxidant for the catalyst (Scheme 94a).[138] Additionally, they also present some examples of the construction of indole-type skeletons through C(sp^3)–H activation (Scheme 94b, Scheme 61 of section 1.3 of Chapter III).

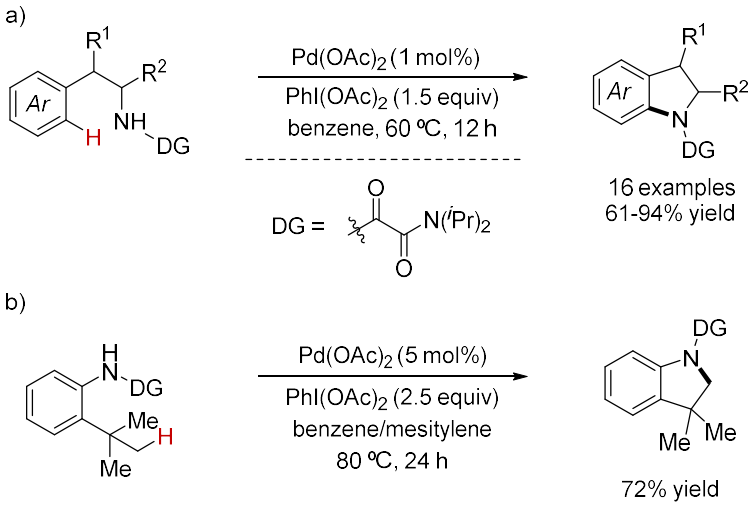

Scheme 94. *Pd(II)-catalyzed intramolecular aminations assisted by a chelating directing group reported by Zhao, Yao and co-workers.*

2- Objectives

Considering the advantages of Pd(II)/Pd(IV) catalytic cycles to cope with difficult reductive eliminations, and taking into account the precedents for the synthesis of indole-type skeletons by the employment of these types of catalytic cycles, we envisioned that a cyclization strategy via C(sp^3)–H activation of *o*-methylbenzylamines could be feasible. Additionally, the isolation of a small proportion of isoindolines in the cycloaddition experiments indicated in section 3.4 of Chapter III further supported the viability of this transformation. The development of this method would allow to build isoindoline skeletons in a quite straightforward manner. Moreover, if chiral ligands, like mono-protected amino acids, were employed for the C–H activation step, an asymmetric version of the cyclization might also be developed (Scheme 95). The election of the proper oxidant to form Pd(IV) intermediates would be crucial for the success of the intramolecular amination.

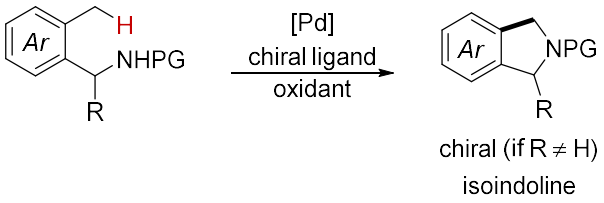

Scheme 95. *General objective: intramolecular amination of* o*-methylbenzylamines.*

3- Results and discussion

In collaboration with Dr. Marc Font, a thorough investigation of reaction conditions for the cyclization of o-methylbenzylamines was performed. For the screening, 2,6-dimethylbenzyltriflamide **6a**, which was synthesized for the project described in Chapter III, was selected as the model substrate. The election of an *ortho* disubstituted benzyltriflamides is not casual, as it can prevent undesired resting states involving the formation of palladacycles after the C(sp^2)–H activation of the aryl ring, which may make the optimization more difficult.

To begin our research, preliminary tests were performed by using the optimized conditions for the (5+2) cycloaddition, with the aim of determining the best oxidant for the reaction. The results are summarized in

Table **12**. By using (diacetoxyiodo)benzene, a very common oxidant in Pd(IV)/Pd(IV) catalysis, the product **11** was detected, but only in traces (entry 1). The conversion of the starting material is 22%, being 2,6-dimethylbenzaldehyde (**12**) the major product of the reaction, presumably as a result of benzylic oxidation and hydrolysis of the corresponding imine in the work-up.

By employing another one-electron oxidant, cerium sulfate (entry 2), the reaction did not improve in terms of yield. The use $Cu(OAc)_2$, the standard oxidant for Pd(II)/Pd(0) catalysis, did not allow to increase the yield either (entry 3). However, in combination with *p*-benzoquinone (BQ), which is known to ease kinetically difficult reductive elimination steps,[164] the reaction yield rose to 13% (entry 4). The conversion of the starting material (86%) is very high, very likely because the copper salt is promoting side reactions (benzylic oxidations). Modifications in the loadings of both oxidants did not make significative differences in the yield (entries 5-6). Besides, BQ by itself cannot promote the reaction, affording the product in traces (entry 7). The combination of BQ with other copper salts (entry 8) or (diacetoxyiodo)benzene (entry 9) did not lead to better results.

[164] Salazar, C. A.; Flesch, K. N.; Haines, B. E.; Zhou, P. S.; Musaev, D. G.; Stahl, S. S. *Science,* **2020**, *370,* 1454.

Table 12. *Screening of oxidants for the cyclization.*

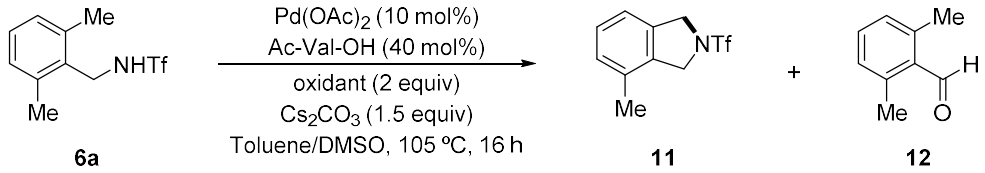

Entry	Oxidant (equiv)	Conversion	Yield (**11**)[b]
1	$PhI(OAc)_2$ (2)	22%	2%
2	$Ce(SO4)_2$ (2)	65%	3%
3	$Cu(OAc)_2$ (2)	75%	5%
4	$Cu(OAc)_2{\cdot}H_2O$ (2) / BQ (1)	86%	13%
5	$Cu(OAc)_2{\cdot}H_2O$ (2) / BQ (0.5)	81%	8%
6	$Cu(OAc)_2{\cdot}H_2O$ (1) / BQ (0.5)	79%	11%
7	BQ (2)	56%	1%
8	$Cu(acac)_2$ (2)/ BQ (1)	89%	5%
9	$PhI(OAc)_2$ (2)/BQ (1)	21%	<1%

[a] Conditions: 0.1 mmol **6a**, 40 mol% of Ac-Val-OH, 15 equiv of DMSO, 2 mL of toluene, under air, 16 h. [b] Yields calculated based on **6a**. Calculated by using 2.4-dichlorobenzotrifluoride as ^{19}F NMR internal standard.

After selecting the combination of copper acetate and BQ as the best oxidants for the reaction, a screening of different ligands was performed. The results are described in Table 13. Other acetyl-protected amino acids, as well as propionyl-protected amino acids, gave similar results (entries 1-2). The rest of the amino-acids tested as ligands gave even worse results (entries 3-6), evidencing the importance of the ligand for the cyclization.

Table 13. *Screening of ligands for the cyclization.*

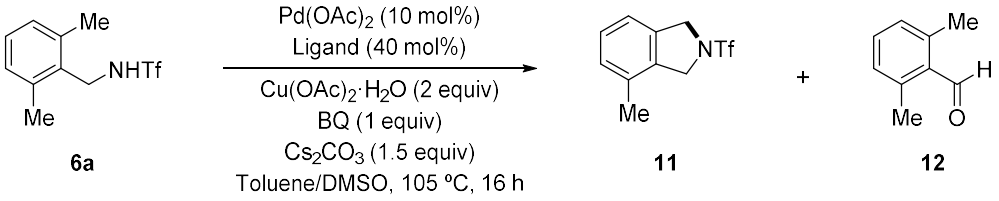

Entry	Ligand	Conversion	Yield (**11**)[b]
1	Ac-Leu-OH	89%	11%
2	Pro-Val-OH	82%	12%
3	2,6-F,F-Bz-Leu-OH	77%	5%
4	Fmoc-Leu-OH	80%	7%
5	Boc-Phe-OH	57%	5%
6[c]	Boc-Phe-NHOMe[d]	82%	10%

[a] Conditions: 0.1 mmol **6a**, 40 mol% of ligand, 15 equiv of DMSO, 2 mL of toluene, under air, 16 h. [b] Yields calculated based on **6a**. Calculated by using 2.4-dichlorobenzotrifluoride as ^{19}F NMR internal standard. [c] Reaction performed by Dr. Marc Font. [d] 15 mol% of ligand.

Some control tests were carried out in order to figure out the effect of the different components. The reaction does not work without catalyst, and neither without a base. Besides, acetyl and nosyl protecting groups for the benzylamine were also tested. Unfortunately, the formation of the cyclic product was not detected, and only benzylic oxidation of the starting material was observed.

The lack of efficiency in the cyclization reaction may be related with a kinetically challenging reductive elimination step, with the difficulty of carrying out the required oxidation from Pd(II) to Pd(IV). Besides, there is a significant decomposition of the starting material because of the benzylic oxidation. In order to avoid this oxidation problem, we assayed the reaction with substrate **6e** using different oxidants. The results are illustrated in Table 14. Unfortunately, the product **13** was not obtained, and only low amounts of 2,4,6-trimethylbenzaldehyde (**14**) were detected as a result of some benzylic oxidation of the starting material (entries 1-2). However, by using the nosyl-protected benzyltriflamide **6e'**, the product **13'** is obtained in a 10% yield. Notably, the conversions are low, evidencing that α-substituted benzyltriflamides are more stable towards benzylic oxidation, but the cyclization is still difficult. The use of other oxidants, like Selectfluor© or $PhI(OAc)_2$ did not lead to better results (entries 4-5).

Table 14. *Screening of conditions for the cyclization using α-substituted benzyltriflamide **6e**.*

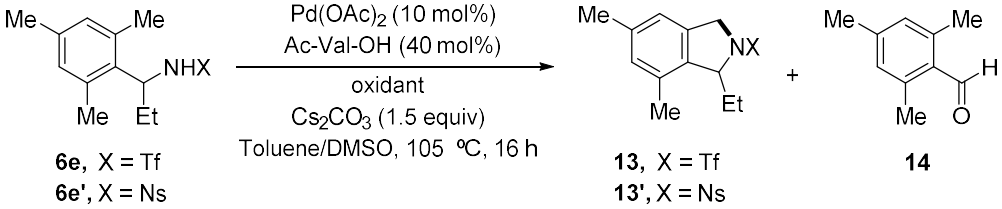

6e, X = Tf
6e', X = Ns

13, X = Tf
13', X = Ns

14

Entry	Substrate	Oxidant (equiv)	Conversion	Yield (**8**)[b]
1[c]	6e	$Cu(OAc)_2.H_2O$ (2) / BQ (1)	21%	0%
2[c, d]	6e	Ag_2CO_3 (1) / BQ (1)	20%	0%
3[c]	6e'	$Cu(OAc)_2.H_2O$ (1) / BQ (1)	15%	10%
4[c]	6e'	Selectfluor (1.5)	0%	0%
5[c]	6e'	$PhI(OAc)_2$ (1.5)	0%	0%

[a] Conditions: 0.1 mmol **6e**, 40 mol% of Ac-Val-OH, 15 equiv of DMSO, 2 mL of toluene, under air, 16 h. [b] Yields calculated based on **6e**. Calculated by using 2.4-dichlorobenzotrifluoride as ^{19}F NMR internal standard. [c] Reaction performed by Dr. Marc Font. [d] Reaction performed without Cs_2CO_3.

Overall, performing this cyclization is represents an important challenge that needs to be further addressed.

4- Conclusions

In conclusion, we have made a preliminary study of reaction conditions to promote the cyclization of *o*-methylbenzyltriflamides to isoindolines. The results suggests that the selection of a proper oxidant is key, but the efficiency of the reaction is low. We are not yet sure which is the key problem that hampers the process, and further research is clearly needed. Reductive elimination involving sp^3 carbons is more difficult, especially when the nitrogen is attached to electron withdrawing groups. It is probable that the lack of success is associated to the formation of Pd(IV) species and the reductive elimination step.

General conclusions

As general conclusions of this doctoral thesis:

1. We have developed a palladium-catalyzed formal (4+2) cycloaddition between benzyltriflamides and allenes that allows the synthesis of highly valuable tetrahydroisoquinolines skeletons in excellent yields and selectivities. We managed to extend the reaction to alkenyltriflamides to synthesize tetrahydropyridine and azepine skeletons. We have developed an asymmetric version of the reaction: a desymmetrization of diarybenzyltriflamides that affords enantioenriched tetrahydroisoquinolines in high yields and enantioselectivities. This represents the first palladium-catalyzed annulative C–H activation/desymmetrization process that has been reported.

2. We have developed a palladium-catalyzed formal (4+2) cycloaddition between *o*-methylanilides and allenes based on a C(sp^3)–H activation. This methodology makes possible to synthesize tetrahydroquinoline skeletons in good yields from trivial starting materials. Several mechanistic assays have been performed in order to unravel more information about the reaction mechanism.

3. We have developed a palladium-catalyzed formal (5+2) cycloaddition between *o*-methylbenzyltriflamides and allenes based on a C(sp^3)–H activation. This methodology allows the synthesis of tetrahydro-2-benzoazepines in good yields. We have demonstrated the viability of an asymmetric version of the reaction with a preliminary exploration of different chiral ligands. Additionally, we have synthetically manipulated the annulation products.

4. We have performed some preliminary assays on a potential palladium-catalyzed cyclization of *o*-methylbenzyltriflamides, presumably based on Pd(II)/Pd(IV) catalytic cycles. The reaction is viable, but the yields are very low.

Resumo da tese doutoral

A síntese de compostos orgánicos relativamente complexos a partir de precursores simples e baratos é un dos desafíos máis importantes en síntese orgánica. Unha das aproximacións máis interesantes para lograr este obxectivo baséase na funcionalización selectiva de ligazóns carbono-hidróxeno. Nesta tese doutoral recóllense os resultados obtidos nos estudos sobre a activación de ligazóns carbono-hidróxeno catalizadas por complexos de paladio, e a súa aplicación no desenvolvemento de novas metodoloxías baseadas en cicloadicións formais co obxectivo de construír heterociclos.

Capítulo I- Introdución

O primeiro capítulo serve como introdución e contextualización ás metodoloxías desenvolvidas durante o transcurso desta tese doutoral, e que serán descritas nos seguintes capítulos. En primeiro lugar, comézase destacando a importancia da síntese orgánica no mundo actual, en campos tan diversos como o medicamento ou a industria. Faise fincapé en que a síntese orgánica moderna busca a idealidade, desenvolvendo métodos cada vez máis eficientes e menos daniños para co medio ambiente, é dicir, que se adapten aos principios da *química verde*.

A continuación, introdúcese o concepto de química organometálica e destácase o seu papel fundamental na química sintética. O uso de complexos metálicos permitiu o desenvolvemento de novas reaccións até ese momento descoñecidas. Con todo, unha das súas limitacións principais era que o uso en cantidades estequiométricas dos reactivos organometálicos era moi custoso, sobre todo cando estes reactivos estaban formados por metais preciosos. Introdúcese, pois, o concepto de catálise, e destácase como os procesos catalíticos permitiron que os métodos baseados en reactivos organometálicos puidesen ser aplicados en procesos industriais.

En seguinte lugar, descríbese unha das reaccións catalizadas por metais de transición que maior importancia tomaron para a síntese de compostos bioactivos: as cicloadicións. Introdúcese a cicloadición clásica máis importante, a Diels-Alder, e destácanse as vantaxes que a catálise metálica ofrece ao desenvolvemento de novos métodos baseados en cicloadicións, como a indución de enantioselectividade, ou as anulacións multicompoñente. Preséntanse exemplos diso.

A continuación, descríbese outra reacción catalizada por metais de transición de gran importancia en química sintética: o acomplamiento cruzado. Introdúcense os diferentes tipos e detállanse algúns mecanismos. Destácase a posibilidade de utilizar ligandos para modificar a reactividade e preséntanse varios exemplos.

Posteriormente, introdúcese o termo de activación C–H. Destácanse as características principais deste tipo de ligazóns: a súa ubicuidade en moléculas orgánicas e a súa dificultade para ser activadas, así como as vantaxes de devandita activación no campo da síntese orgánica. Descríbense o contexto histórico e as primeiras reaccións desenvolvidas neste campo. Tamén se menciona o uso de grupos directores para superar os retos na activación de ligazóns C–H.

Seguidamente, acóutase o campo da activación C–H a aquelas reaccións catalizadas por paladio. Destácanse as vantaxes do uso deste metal fronte aos seus análogos. Introdúcense os aminoácidos mono-protexidos como ligandos de gran importancia neste campo, describindo o seu contexto histórico, mecanismo de acción e aplicacións, tanto de acelerador da reacción como de indutor de quiralidade. Tamén se menciona a nova xeración de ligandos que xorde na

actualidade a partir da estrutura xeral e modo de actuación dos aminoácidos mono-protexidos. Ademais, descríbense diversas reaccións de activación C–H catalizadas paladio, tanto funcionalizacións como cicloadicións.

En último lugar, descríbense os retos actuais no campo da activación C–H e as estratexias que se están seguindo na actualidade para superar estes retos.

Capítulo II- Síntese de tetrahidroisoquinolinas mediante cicloadicións formais enantioselectivas de benciltriflamidas e alenos

O segundo capítulo describe a primeira reacción de cicloadición formal catalizada por paladio desenvolvida durante o transcurso desta tese doutoral: a cicloadición formal (4+2) entre benciltriflamidas e alenos.

En primeiro lugar, introdúcense as tetrahidroisoquinolinas como unha estrutura presente en moléculas bioactivas. Descríbense os métodos clásicos de síntese deste tipo de esqueletos: a ciclación de Picted-Spengler, a ciclación de Bischler-Napieralski e a síntese de Pomeranz-Fritsch-Bobbitt. Seguidamente, menciónanse os métodos de síntese baseados en activación C–H, destacando as súas vantaxes sobre os métodos clásicos, así como as reaccións de funcionalización C–H enantioselectiva de bencilaminas.

Tras esta introdución, preséntanse os obxectivos deste capítulo: o desenvolvemento dunha cicloadición formal (4+2) catalizada por paladio entre bencilaminas e alenos, co obxectivo de construír esqueletos de tipo tetrahidroisoquinolina. Contémplase a posibilidade de estender a reacción a alquenilaminas para obter esqueletos de tipo piperidina ou azepina. Ademais, exponse o desenvolvemento dunha variante enantioselectiva da reacción, mediante o uso de substratos proquirais de tipo diarilbencilamina. As cicloadicións enantioselectivas baseadas en activación C–H catalizada por paladio non foran reportadas até a data, polo que constituiría o primeiro exemplo deste tipo.

Comézase describindo a investigación inicial da reacción entre a bencilamina protexida cun grupo triflato (benciltriflamida) e o aleno vinilidenociclohexano. Utilízase acetato de cobre como oxidante e carbonato de cesio como base. Primeiro atópase que o tolueno e o disolvente máis axeitado para a reacción. Descóbrese además durante a optimización da reacción que o uso de aminoácidos mono-protexidos como ligandos para o paladio acelera a reacción, mellorando así a súa eficiencia e permitindo obter o cicloaducto de tipo tetrahidroisoquinolina en rendementos en torno ao 95% co uso da 2,6-F,F-Bz-Leu-OH como ligando. Tamén se descobre o efecto do DMSO con acelerante da reacción, permitindo que se complete en tan só 40 minutos.

En seguinte lugar, demóstrase a compatibilidade da reacción con alenos con patróns de substitución diferentes. Obsérvanse mesturas de isómeros E/Z no caso dos alenos 1,1-disustituidos asimétricos e dos monosustituidos, pero notablemente os alenos trisustituidos producen o seu correspondente cicloaducto como un único estéreo- e rexioisómero. A reacción é avaliada tamén en substratos de tipo alqueniltriflamida, demostrándose que é compatible tanto con alilaminas como con homo allilaminas, permitindo por tanto a síntese de esqueletos de tipo piperidina e azepina.

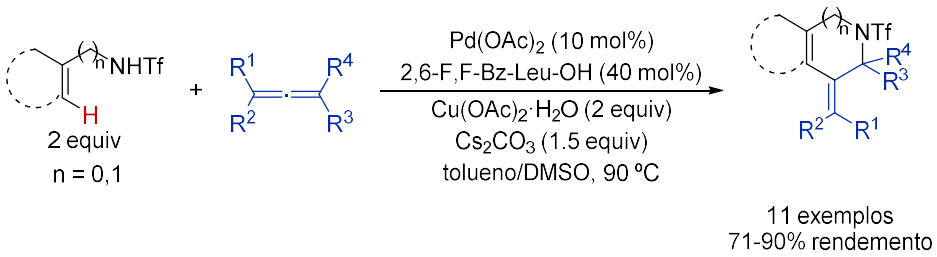

A continuación, descríbese a proba preliminar para avaliar a viabilidade da versión enantioselectiva desta reacción. Para iso, próbase a resolución cinética da benciltriflamida substituída na posición α cun etilo usando o mesmo ligando aminoácido mono-protexido como indutor quiral. Obsérvase unha proporción enantiomérica de 93:7, demostrado así a súa viabilidade, e abrindo a porta ao desenvolvemento da desimetrización de diarilbencilaminas proquirais proposta nos obxectivos. Avalíanse diferentes diarilbenciltriflamidas con substituíntes en diferentes posicións do anel, e alenos con diferentes patróns de substitución. Obtéñense resultados moi positivos, con rendementos excelentes e enantioselectividades superiores ao 90:10. A reacción demostra tolerancia á substitución en diferentes posicións nos arilos (*orto*, *meta* e *para*, sendo *meta* a menos eficaz) e a alenos mono-, di- e trisustituidos). Ademais, é eficaz na presenza de grupos funcionais tales como halóxenos ou metoxilos. Realízase tamén unha proba nun substrato que presenta dous aneis aromáticos diferentes, observando tan só unha lixeira selectividade dun anel fronte ao outro (1.6:1).

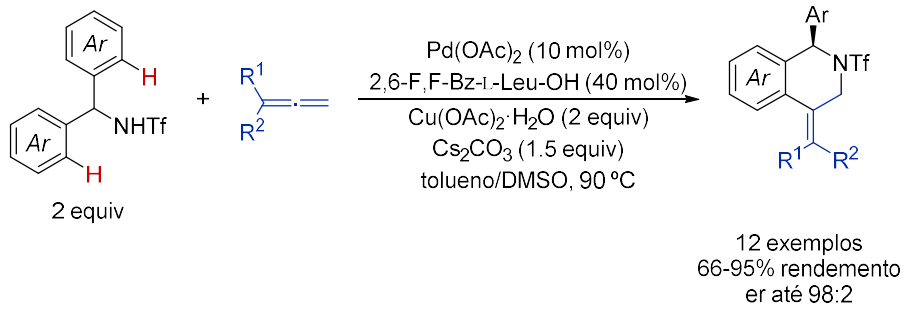

Finalmente, proponse un mecanismo para a reacción, no que se destaca o rol fundamental do ligando tipo aminoácido mono-protexido na activación C–H. Tamén se propón a formación dun intermedio paladacíclico de tipo π-alilo, cuxa conformación podería estar influenciada polos substituíntes do aleno, o que explicaría a estéreo- e rexioselectividade obtida na reacción. Ademais, aínda que se propón a evolución dese intermedio mediante unha eliminación reductora N–C, indícase que non se pode descartar un mecanismo de tipo esfera externa no que o ataque nucleófilo da amina sobre o complexo de paladio sexa a responsable da construción do ciclo.

As conclusións deste capítulo son que se desenvolveu unha cicloadición formal (4+2) catalizada por paladio de benciltriflamidas con alenos para construír esqueletos de tipo tetrahidroisoquinolina, utilizando un aminoácido mono-protexido como ligando para acelerar a reacción. Estendeuse esta metodoloxía á síntese de piperidinas e azepinas mediante a cicloadición formal de alqueniltriflamidas e alenos. Avaliouse con éxito a posibilidade de realizar unha versión enantioselectiva da reacción mediante unha proba preliminar de resolución cinética cunha benciltriflamida substituída na posición α. Desenvolveuse a desimetrización de

diarilbenciltriflamidas con alenos baseada na cicloadición formal (4+2) análoga, usando para iso o mesmo ligando de tipo aminoácido mono-protexido, obténdose rendementos e enantioselectividades excelentes. Esta desimetrización constitúe o primeiro exemplo de cicloadición formal enantioselectiva baseada na activación de ligazóns C–H catalizada por paladio que se reporta.

Capítulo III- Ensamblado de azaheterociclos mediante cicloadicións catalizadas por Pd(II) que implican a activación de ligazóns C(sp^3)–H

O terceiro capítulo describe a segunda e a terceira cicloadición formal catalizada por paladio desenvolvida durante o transcurso desta tese doutoral: a cicloadición formal (4+2) entre *o*-metilanilidas e alenos e a cicloadición formal (5+2) entre *o*-metilbenciltriflamidas e alenos. Ambas as cicloadicións presentan un punto en común, a activación de ligazóns C(sp^3)–H.

En primeiro lugar, introdúcense os retos e dificultades presentes inherentemente na activación de ligazóns C(sp^3)–H. Entre outros, menciónanse a súa maior enerxía de activación respecto das ligazóns C(sp^2)–H e as dificultades para alcanzar rexioselectividade nas reaccións que implican a súa activación. Destácanse o uso de grupos directores como a principal estratexia para tentar superar esas dificultades. A continuación, fálase sobre dous casos especiais de activación de ligazóns C(sp^3)–H: as ligazóns alílicos e bencílicos. En ambos os casos, a presenza da dobre ligazón na posición adxacente á ligazón activada diminúe a enerxía de activación da ligazón, o que mellora a súa reactividade.

En segundo lugar, preséntanse reaccións de funcionalización C–H de posicións bencílicas catalizadas por paladio. A maior parte destas reaccións utilizan grupos amino como grupos directores para o metal, destacando entre eles as quinolinas. A continuación, descríbense particularmente as reaccións de funcionalización C–H catalizadas por paladio de posicións bencílicas presentes en *o*-metilanilinas e *o*-metilbencilaminas, destacando que todas elas utilizan aminas protexidas como grupo director.

Na seguinte sección, comézase falando das cicloadicións formais baseadas na activación de ligazóns C(sp^3)–H catalizada por paladio. Destácase que, a pesar de ser un campo moi atractivo desde o punto de vista da *química verde*, o número de reportes deste tipo de metodoloxías é moi reducido, denotando que este campo está aínda nas súas primeiras etapas. Enuméranse os principais motivos polos que o desenvolvemento deste tipo de reaccións é tan desafiante, entre os que se atopan desde a propia dificultade inherente da activación de ligazóns C(sp^3)–H até nas posibles reaccións secundarias que se poden producir debido a eliminacións tipo β-hidruro competitivas. Finalmente, descríbense exemplos deste tipo de cicloadicións formais, clasificándoas polo número de átomos que forman parte das mesmas.

Tras esta introdución, preséntanse os obxectivos do presente capítulo: o desenvolvemento de dúas reaccións de cicloadición formal catalizadas por paladio e baseadas na activación de ligazóns C(sp^3)–H bencílicos. En primeiro lugar, unha cicloadición formal (4+2) entre *o*-metilanilinas e alenos, que permitiría a síntese de esqueletos de tipo tetrahidroquinolina. Este tipo de esqueletos están presentes en compostos bioactivos. En segundo lugar, unha cicloadición formal (5+2) entre *o*-metilbencilaminas e alenos, que permitiría a construción de esqueletos de tipo tetrahidro-2-benzoazepina. Ademais, se se utilizasen como substratos *o*-

metilbencilaminas substituídas na posición α respecto da amina, esta reacción podería facerse de forma asimétrica utilizando ligandos quirais, como aminoácidos mono-protexidos.

Comézase describindo os ensaios iniciais e a optimización da primeira cicloadición formal descrita neste capítulo: a cicloadición formal (4+2) entre *o*-metilanilidas e alenos. Para iso, sintetízase a *o*-metilanilina protexida cun triflato e avalíase a súa reacción co aleno 5-vinilidenonano. Durante a optimización, descóbrese que o uso de ligandos de tipo aminoácido mono-protexido mellora a reactividade. Establécese o acetato de cobre como o mellor oxidante para a reacción, e o carbonato de cesio como a mellor base, atopándose neste último caso que o tamaño do catión da base e determinante para o funcionamento da cicloadición. Ademais, a reacción funciona en 2-metiltetrahidrofurano, que é un disolvente verde, é dicir, que provén dunha fonte sustentable, en concreto o furfural, un subproduto da agricultura. Finalmente, coa adición lenta do aleno sobre a reacción, conséguese un rendemento do 71%. Outros grupos protectores para a amina resultan menos eficaces que o triflato.

Unha vez descritas as condicións optimizadas, demóstrase a viabilidade da reacción utilizando alenos con diferentes patróns de substitución. Para iso, sintetízanse unha serie de alenos e avalíanse na anulación. A reacción resulta compatible con outros alenos 1,1-disustituidos, 1,3-disustituidos, monosustituidos e trisustituidos, dando nalgúns casos mesturas de isómeros E/Z. A maiores, avalíanse na cicloadición *o*-metilanilidas con diferentes patróns de substitución e grupos funcionais. A reacción demostra ser compatible cunha variedade de substituíntes en *orto*, *meta* e *para*, así como grupos funcionais como halóxenos, metoxilos ou mesmo ésteres. A tendencia xeral parece indicar que a presenza de grupos electrodadores no anel mellora a reactividade.

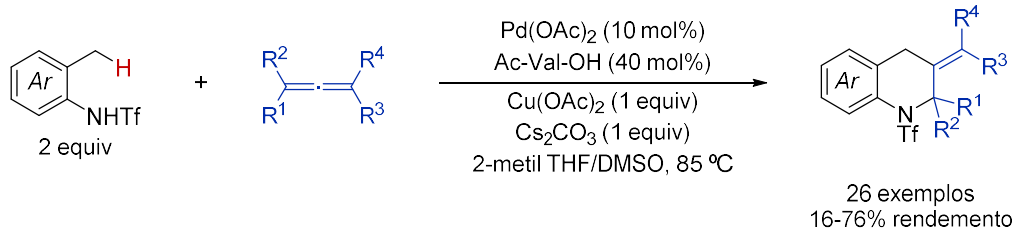

En seguinte lugar, descríbense unha serie de experimentos mecanísticos que teñen como obxectivo desvelar algunhas incógnitas sobre o mecanismo da cicloadición formal. En primeiro lugar, realízase un experimento de incorporación de deuterio, que suxire que a etapa de activación da ligazón C–H é irreversible. Posteriormente, realízanse dous experimentos para medir o efecto isotópico cinético utilizando o análogo deuterado na posición bencílica da *o*-metilanilina triflada. En concreto, un experimento de competición e outro paralelo. Tras a análise dos resultados, inférese que existe un efecto isotópico cinético primario, o que parece indicar que a activación C–H é a etapa limitante do ciclo catalítico. A continuación, realizáronse experimentos utilizando un aleno quiral, nos que se pretendía manter a quiralidade do aleno no producto final, co obxectivo de construir cicloaductos enantioenriquecidos. Con todo, estes experimentos non resultan concluíntes ao descubrirse que este aleno racemiza nas condicións de reacción. Con todos estes experimentos mecanísticos, proponse un mecanismo de reacción para a cicloadición formal (4+2), que resulta similar ao descrito no capítulo anterior.

A continuación, descríbese a segunda reacción descrita neste capítulo: a cicloadición formal (5+2) entre *o*-metilbencilaminas e alenos. En primeiro lugar, sintetízase a *o*-dimetilbencilamina protexida con triflato e descríbese a reoptimización partindo das condicións de reacción da cicloadición formal (4+2). Neste caso, o tolueno e o mellor disolvente para a reacción, e o uso de exceso de aleno fronte a anilida permite aumentar o rendemento de forma notable.

A continuación, avalíase o alcance da cicloadición con outras *o*-metilbencilaminas. A reacción demostra tolerancia a grupos funcionais tales como flúor ou metoxi, así como substitución na posición α respecto da amina. Avalíase de forma preliminar a posibilidade de realizar unha versión asimétrica da cicloadición. Os resultados utilizando diversos aminoácidos mono-protexidos como ligandos quirais, en concreto aminoácidos nos que o grupo carboxilo e substituído por un grupo amino metil éster, indican que si é posible realizar unha resolución cinética de *o*-metilbencilaminas, chegando a obter proporcións enantioméricas no cicloaducto de 90:10.

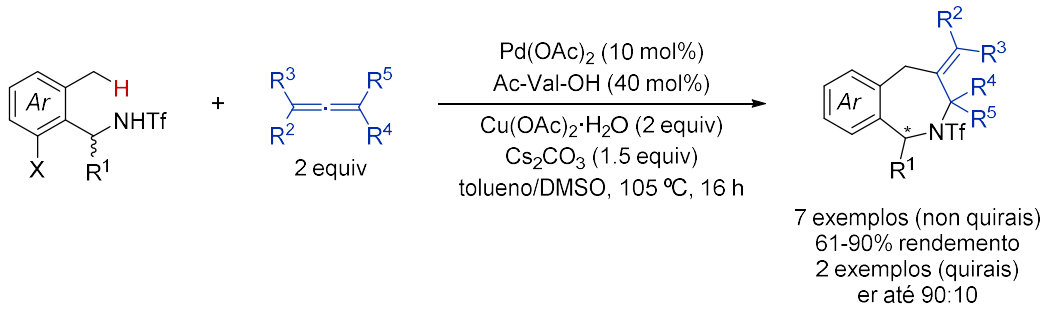

Finalmente, avalíase a posibilidade de manipular sintéticamente os produtos obtidos en ambas as cicloadiciones formais. Demóstrase que un cicloaducto proveniente da cicloadición formal (5+2) pode ser hidroxenado para obter unha tetrahidro-2-benzoazepina triflada totalmente saturada. Ademais, este mesmo triflato pode ser eliminado para obter a tetrahidro-2-benzoazepina sen protexer. Con todo, a manipulación sintética dos produtos provenientes da cicloadición formal (4+2), como por exemplo a ozonólise ou a hidroxenación, non resulta frutífera.

As conclusións deste capítulo é que se desenvolveron dúas reaccións de activación C(sp^3)–H catalizadas por paladio: unha cicloadición formal (4+2) entre *o*-metilanilidas e alenos e unha cicloadición formal (5+2) entre *o*-metilbenciltriflamidas e alenos. Realizouse unha optimización das condicións de reacción e avaliouse o seu alcance e limitacións. Tamén se realizaron estudos mecanísticos para desvelar información sobre o seu mecanismo. Ademais, desenvolveuse un estudo preliminar da versión asimétrica da cicloadición formal (5+2), demostrando a súa viabilidade. Finalmente, realizáronse experimentos de manipulación sintética dos cicloaductos obtidos nas reaccións. Estas reaccións constitúen dúas dos escasos exemplos de cicloadiciones formais baseadas na activación de ligazóns C(sp^3)–H.

Anexo- Ciclación de *o*-metilbencilaminas cara a isoindolinas catalizada por paladio e que implica activación C(sp^3)–H

Neste anexo descríbense os resultados preliminares da ciclación de *o*-metilbencilaminas baseada na activación de ligazóns C(sp^3)–H.

En primeiro lugar, introdúcense brevemente as características dos ciclos catalíticos Pd(II)/Pd(IV). Coméntase o seu esquema xeral e as súas vantaxes respecto doutros ciclos catalíticos de paladio, tales como a súa resistencia a procesos de eliminación de β-hidruro, a súa facilidade para sufrir procesos de eliminación reductora ou a súa tolerancia á presenza de osíxeno na reacción.

A continuación, descríbese unha serie de síntese de esqueletos de tipo indol mediante o uso de activación C–H catalizada por ciclos catalíticos Pd(II)/Pd(IV). Destácase que o uso deste tipo de catálisis facilita a etapa de eliminación reductora para xerar ciclos de 5 membros, que aínda que resultan complicados de sintetizar debido á tension anular, son de interese pola súa presencia en moléculas bioactivas.

Tras esta breve introdución, preséntase o obxectivo deste anexo: a síntese de esqueletos de tipo isoindolina mediante unha reacción de ciclación de *o*-metilbencilaminas baseada en activación C–H mediada por ciclos catalíticos de Pd(II)/Pd(IV). Destácase que no caso de utilizar *o*-metilbencilaminas substituídas na posición β respecto da amina, poderíase desenvolver tamén a versión asimétrica da ciclación co uso de ligandos quirais, de modo análogo ao que ocorría coa cicloadición formal (5+2) do capítulo anterior.

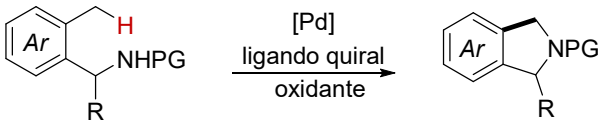

isoindolina
quiral (se R ≠ H)

A continuación, descríbense os resultados preliminares obtidos en colaboración co Dr. Marc Font. Os experimentos realizados coa *o*-dimethylbenciltriflamida usando oxidantes típicos dos ciclos catalíticos de Pd(II)/Pd(IV) non lograron rendementos superiores ao 3%. O uso de acetato de cobre como oxidante, máis relacionado con ciclos Pd(II)/Pd(0), aumentou o rendemento da reacción até o 13% ao usarse en combinación con benzoquinona, aínda que tamén levou a conversións case totais da sustancia de partida, evidenciando a oxidación bencílica mediada por cobre que se detectou con anterioridade neste tipo de substratos durante os capítulos II e III. A avaliación de diferentes tipos de aminoácidos mono-protexidos como promotores da reacción non permitiu mellorar o rendemento. Finalmente, probouse un substrato con substitución en α, que dificultaba a oxidación de devandita posición. Aínda que as conversións reducíronse, tan só se obtivo o produto esperado cando se utilizou nosilo como grupo protector da amina en lugar de triflato.A conclusión deste anexo é que a elección do oxidante adecuado resulta clave para obter mellores rendementos, xa que a etapa de eliminación reductora parece a etapa limitante da reacción. Os resultados preliminares resultan insuficientes para determinar a viabilidade da reacción, polo que é necesaria unha maior exploración nas condicións de reacción, sobre todo mediante o uso de oxidantes típicos de ciclos catalíticos de Pd(II)/Pd(IV).

Conclusión xeral

Como conclusión xeral, nesta tese doutoral descríbense varios procesos de cicloadición formal catalizados por paladio e baseados en activación de ligazóns C–H, ben de natureza sp^2 ou sp^3, dando lugar a diferentes azaheterociclos, sendo algúns deles ópticamente activos.

Experimental Section

1- General experimental procedures

Reactions were conducted in dry solvents under argon atmosphere unless otherwise stated. Dry solvents were obtained from Aldrich and used without further purification. $Pd(OAc)_2$ (98%) [3375-31-3] was obtained from Strem. All other chemicals, were purchased from Aldrich and used without further purification.

All the amino acids ligands (except 2,6-F,F-Bz-Leu-OH) were commercially available. They were purchased from Aldrich and used without further purification.

The abbreviation "rt" refers to reactions carried out at a temperature between 21-25 °C. Reaction mixtures were stirred using Teflon-coated magnetic stir bars. High reaction temperatures were maintained using Thermowatch-controlled heating blocks. Thin-layer chromatography (TLC) was performed on silica gel plates and components were visualized by observation under UV light, and/or by treating the plates with p-anisaldehyde, ninhydrin, phosphomolybdic or potassium permanganate solutions, followed by heating. Flash chromatography was carried out on silica gel. Dryings were performed with anhydrous Na_2SO_4.

Concentration refers to the removal of volatile solvents via distillation using a Büchi rotary evaporator followed by high vacuum.

All palladium-catalyzed reactions were carried out without particular precautions to extrude moisture or oxygen.

^{1}H-NMR spectra were recorded at room temperature on a Varian 300 MHz or 500 MHz spectrometer in $CDCl_3$ [using $CDCl_3$ (for ^{1}H, δ = 7.26) as internal standard]. ^{19}F-NMR (282 MHz) spectra were recorded at room temperature on a Varian 300 MHz or 500 MHz spectrometer in $CDCl_3$. ^{13}C NMR spectra were recorded at room temperature on a Varian spectrometer in $CDCl_3$ [using $CDCl_3$ (for ^{13}C, δ = 77.160) as internal standard]. The following abbreviations were used to explain the multiplicities: s = singlet, d = doublet, t = triplet, q = quartet, m = multiplet, brs = broad singlet. Carbon types and structure assignments were determined from DEPT-NMR and two-dimensional experiments (HSQC and NOESY). NMR spectra were analyzed using MestReNova© NMR data processing software (www.mestrelab.com). Mass spectra were acquired using electrospray ionization (ESI, ion polarity positive) or atmospheric pressure chemical ionization (APCI) and were recorded at the CACTUS facility of the University of Santiago de Compostela on Bruker micrOTOF. Melting points were measured on a Büchi Melting Point B-560 apparatus.

Enantiomeric ratios (er) were determined on an Agilent HPLC 1100 Series or on a Jasco SFC 4000 series using commercially available chiral columns. All racemic products were prepared under the same procedure than the chiral products but with the employment of a racemic amino acid.

X-ray crystallographic analysis was done at the CACTUS facility of the University of Santiago de Compostela. The measurements were performed with a Bruker D8 Venture Photon III-14 using a microfocus sealed tube as diffraction source.

Amounts of isolated products are indicated independently of the scale used.

2- Chapter II: Synthesis of tetrahydroisoquinoline skeletons via enantioselective formal cycloadditions of benzyltriflamides with allenes

2.1 General procedure for the synthesis of diarylbenzylamines 1h, 1i and 1j

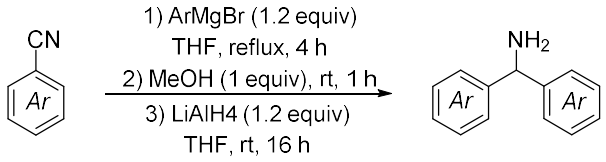

1h: *Ar* = *o*-Me
1i: *Ar* = *p*-Me
1j: *Ar* = *p*-Cl

Following a previously reported procedure,[119] to a solution of arylmagnesium bromide (1.25 equiv) in THF (0.2 M) was added the nitrile (1 equiv) at room temperature, with the resulting mixture being refluxed for 4 h. After cool, anhydrous MeOH (1 equiv) was added (vigorous reaction) and the reaction stirred for 1 h at rt. Then, $LiAlH_4$ (2 equiv) was added, and the reaction was stirred overnight at rt. After that, the reaction was quenched with the careful addition of water. The aqueous layer was extracted with diethyl ether three times. The combined organic phases were washed with aqueous $NaHCO_3$ (sat.) and dried over Na_2SO_4. The crude was used in the next step without further purification.

2.2 General procedure for the synthesis of triflyl-protected benzylamines and alkenylamines from the precursor amines, exemplified for 1a

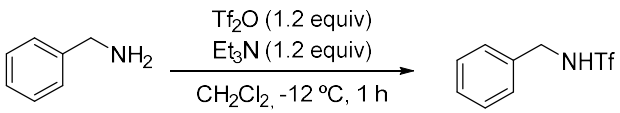

1a

To a solution of benzylamine (2 mL, 18.31 mmol) in dichloromethane (36.6 mL) under argon atmosphere was added triethylamine (2.55 mL, 18.31 mmol) at -12 °C. After the solution was stirred 5 minutes at that temperature, trifluoromethanesulfonic anhydride (3.23 mL, 19.22 mmol) was added dropwise. The reaction was stirred for 1 h at that temperature before being quenched with water. The organic layer was separated and the aqueous layer extracted with dichloromethane. The combined organic phase was washed with brine and then dried over Na_2SO_4. Evaporation and column chromatography on silica gel (hexanes:diethylether; 80:20) afforded **N-benzyl-1,1,1-trifluoromethanesulfonamide** (**1a**) as a white solid (3.97g, 91% yield). Mp: 43-44 °C. **^{1}H NMR** (300 MHz, $CDCl_3$) δ 7.34 – 7.18 (m, 5H), 5.10 (brs, 1H), 4.33 (d, *J* = 5.8 Hz, 2H). **^{19}F NMR** (282 MHz, $CDCl_3$) δ -77.64. **^{13}C NMR** (75 MHz, $CDCl_3$) δ 135.3 (C), 129.2 (CH), 128.8 (CH), 128.0 (CH), 119.8 (q, *J* = 320.9 Hz, C), 48.3 (CH_2). **HRMS** [APCI]: *m/z* calculated for $C_8H_7F_3NO_2S$ $[M+H]^+$: 238.0144, found 238.0145.

N-allyl-1,1,1-trifluoromethanesulfonamide (1d)

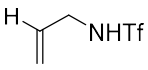

1d

(1.35 g, 82% yield), obtained as a yellow oil. **^{1}H NMR** (300 MHz, $CDCl_3$) δ 5.96 – 5.78 (m, 1H), 5.39 – 5.23 (m, 2H), 4.89 (brs, 1H), 3.92 (d, *J* = 5.8 Hz, 2H). **^{19}F NMR** (282 MHz, $CDCl_3$) δ -77.90. **^{13}C NMR** (75 MHz, $CDCl_3$) δ 132.1 (CH), 119.8 (q, *J* = 321.1 Hz, C), 119.1 (CH_2), 46.8 (CH_2). **HRMS** [ESI]: *m/z* calculated for $C_4H_7F_3NO_2S$ $[M+H]^+$: 190.0150, found 190.0148.

***N*-(2-(cyclohex-1-en-1-yl)ethyl)-1,1,1-trifluoromethanesulfonamide (1e)**

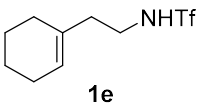

1e

(433 mg, 84% yield), obtained as a yellow oil. **^{1}H NMR** (300 MHz, $CDCl_3$) δ 5.46 (brs, 1H), 5.03 (brs, 1H), 3.28 (q, *J* = 6.3 Hz, 2H), 2.14 (t, *J* = 13.5 Hz, 2H), 2.06 – 1.97 (m, 2H), 1.93 – 1.83 (m, 2H), 1.70 – 1.49 (m, 4H). **^{19}F NMR** (282 MHz, $CDCl_3$) δ -78.00. **^{13}C NMR** (75 MHz, $CDCl_3$) δ 132.8 (C), 125.7 (CH), 119.8 (q, *J* = 321.2 Hz, C), 42.1 (CH_2), 38.2 (CH_2), 27.7 (CH_2), 25.2 (CH_2), 22.7 (CH_2), 22.2 (CH_2). **HRMS** [ESI]: *m/z* calculated for $C_9H_{15}F_3NO_2S$ $[M+H]^+$: 258.0770, found 258.0769.

1,1,1-trifluoro-*N*-(1-phenylpropyl)methanesulfonamide (1f)

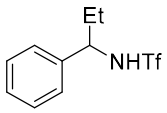

1f

(836 mg, 84% yield), obtained as a white solid. **^{1}H NMR** (300 MHz, $CDCl_3$) δ 7.34 – 7.19 (m, 3H), 7.19 – 7.12 (m, 2H), 5.50 (d, *J* = 8.8 Hz, 1H), 4.40 (q, *J* = 7.7 Hz, 1H), 1.91 – 1.70 (m, 2H), 0.84 (t, *J* = 7.4 Hz, 3H). **^{19}F NMR** (282 MHz, $CDCl_3$) δ -78.03. **^{13}C NMR** (75 MHz, $CDCl_3$) δ 140.2 (C), 129.1 (CH), 128.4 (CH), 126.3 (CH), 120.0 (d, *J* = 320.9 Hz, C), 61.6 (CH), 31.0 (CH_2), 10.6 (CH_3). **HRMS** [ESI]: *m/z* calculated for $C_{10}H_{12}F_3NNaO_2S$ $[M+Na]^+$: 290.0433, found 290.0433. Data in agreement with those reported in literature.[165]

***N*-benzhydryl-1,1,1-trifluoromethanesulfonamide (1g)**

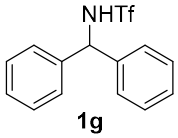

1g

(1.62 g, 63% yield), obtained as a white solid. **^{1}H NMR** (300 MHz, $CDCl_3$) δ 7.31 – 7.11 (m, 10H), 5.77 (d, *J* = 8.9 Hz, 1H), 5.68 (d, *J* = 9.0 Hz, 1H). **^{19}F NMR** (282 MHz, $CDCl_3$) δ -77.31. **^{13}C NMR** (75 MHz, $CDCl_3$) δ 139.7 (C), 129.1 (CH), 128.4 (CH), 127.3 (CH), 119.5 (q, *J* = 321.1 Hz, CF_3) 62.5 (CH). **HRMS** [ESI]: *m/z* calculated for $C_{14}H_{12}F_3NNaO_2S$ $[M+Na]^+$: 338.0443, found 338.0440. Data in agreement with those reported in literature.[110]

***N*-(di-*o*-tolylmethyl)-1,1,1-trifluoromethanesulfonamide (1h)**

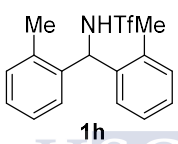

1h

(2.60 g, 80% yield), obtained as a white solid. **^{1}H NMR** (300 MHz, $CDCl_3$) δ 7.17 – 7.02 (m, 8H), 6.09 (d, *J* = 8.2 Hz, 1H), 5.27 (d, *J* = 8.2 Hz, 1H), 2.21 (s, 6H). **^{19}F NMR** (282 MHz, $CDCl_3$) δ -77.42. **^{13}C NMR** (75 MHz, $CDCl_3$) δ 137.2 (C), 136.0 (C), 131.2 (CH), 128.5 (CH), 127.0 (CH), 126.5 (CH, 119.4 (q, *J* = 321.2 Hz, C), 56.7 (CH), 19.1 (CH_3). **HRMS** [ESI]: *m/z* calculated for $C_{16}H_{16}F_3NNaO_2S$ $[M+Na]^+$: 366.0746, found 336.0749. Data in agreement with those reported in literature.[165]

[165] Miyamoto, K.; Hoque, M. M.; Ogasa, S. *J. Org. Chem.* **2012**, *77*, 8317.

***N*-(di-*p*-tolylmethyl)-1,1,1-trifluoromethanesulfonamide (1i)**

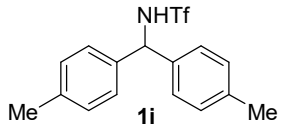

1i

(1.95 g, 70% yield), obtained as a white solid. **^{1}H NMR** (300 MHz, $CDCl_3$) δ 7.09 – 6.97 (m, 8H), 5.75 – 5.54 (m, 2H), 2.22 (s, 6H). **^{19}F NMR** (282 MHz, $CDCl_3$) δ -77.69. **^{13}C NMR** (75 MHz, $CDCl_3$) δ 138.2 (C), 137.1 (C), 129.7 (CH), 127.1 (CH), 119.6 (d, *J* = 321.0 Hz, C), 62.2 (CH), 21.2 (CH_3). **HRMS** [ESI]: *m/z* calculated for $C_{16}H_{16}F_3NNaO_2S$ $[M+Na]^+$: 366.0746, found 336.0743. Data in agreement with those reported in literature.[165]

***N*-(bis(4-chlorophenyl)methyl)-1,1,1-trifluoromethanesulfonamide (1j)**

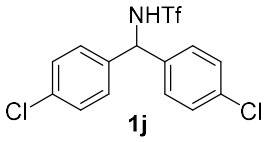

1j

(2.92 g, 74% yield), obtained as a white solid. Mp: 105-107 °C. **^{1}H NMR** (300 MHz, $CDCl_3$) δ 7.31 – 7.24 (m, 4H), 7.12 – 7.04 (m, 4H), 5.73 (d, *J* = 8.8 Hz, 1H), 5.64 (d, *J* = 8.9 Hz, 1H). **^{19}F NMR** (282 MHz, $CDCl_3$) δ -77.64. **^{13}C NMR** (75 MHz, $CDCl_3$) δ 137.7 (C), 134.8 (C), 129.5 (CH), 128.6 (CH), 119.5 (q, *J* = 321.0 Hz, C), 61.4 (CH). **HRMS** [ESI]: *m/z* calculated for $C_{14}H_{10}Cl_2F_3NNaO_2S$ $[M+Na]^+$: 405.9654, found 405.9656.

***N*-(bis(4-methoxyphenyl)methyl)-1,1,1-trifluoromethanesulfonamide (1k)**

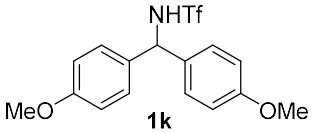

1k

(302 mg, 24% yield), obtained as a white solid. **^{1}H NMR** (300 MHz, $CDCl_3$) δ 7.09 – 7.02 (m, 4H), 6.81 – 6.73 (m, 4H), 5.69 (s, 2H), 3.70 (s, 6H). **^{19}F NMR** (282 MHz, $CDCl_3$) δ -77.90. **^{13}C NMR** (75 MHz, $CDCl_3$) δ 159.5 (C), 132.2 (C), 128.5 (CH), 119.6 (d, *J* = 321.1 Hz, C), 114.4 (C), 61.67 (C), 55.5 (CH_3). **HRMS** [ESI]: *m/z* calculated for $C_{16}H_{16}F_3NNaO_4S$ $[M+Na]^+$: 398.0644, found 398.0641. Data in agreement with those reported in literature.[165]

***N*-(bis(3-methoxyphenyl)methyl)-1,1,1-trifluoromethanesulfonamide (1l)**

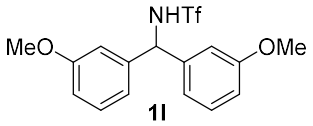

1l

(325 mg, 84% yield), obtained as a white solid. Mp: 86-87 °C. **^{1}H NMR** (300 MHz, $CDCl_3$) δ 7.20 – 7.11 (m, 3H), 6.78 – 6.65 (m, 5H), 6.00 (d, *J* = 9.0 Hz, 1H), 5.68 (d, *J* = 8.8 Hz, 1H), 3.63 (s, 6H). **^{19}F NMR** (282 MHz, $CDCl_3$) δ -77.82. **^{13}C NMR** (75 MHz, $CDCl_3$) δ 160.0 (C), 141.2 (C), 130.1 (CH), 119.6 (d, *J* = 321.1 Hz), 119.6 (CH), 113.6 (CH), 113.2 (CH), 62.3 (CH), 55.4 (CH_3). **HRMS** [ESI]: *m/z* calculated for $C_{16}H_{17}F_3NO_4S$ $[M+H]^+$: 376.0825, found 376.0825.

2.3 General procedure for the synthesis of triflyl-protected alkenylamines from the precursor alcohols, exemplified for 1b.

2-methylprop-2-en-1-ol was commercially available. Cyclohex-1-en-1-ylmethanol was synthesized with a method previously reported in literature.[166] All spectral data recorded were in agreement with those in the corresponding literature.[167]

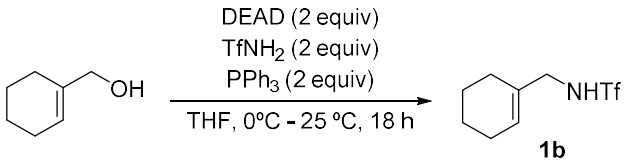

1b

To a solution of cyclohex-1-en-1-ylmethanol (801.4 mg, 7.145 mmol), trifluoromethane sulfonamide (2.13 g, 2 equiv.), and triphenylphosphine (3.75 g, 2 equiv.) in THF (25 mL) at 0 °C was added DEAD (5.6 mL, 40% in toluene, 2 equiv.). The reaction mixture was stirred at room temperature overnight, and was quenched with water, then diluted with ethyl acetate. The combined organic phases were washed with brine and then dried over Na_2SO_4. Evaporation and column chromatography on silica gel (hexanes:diethylether; 90:10) afforded ***N*-(cyclohex-1-en-1-ylmethyl)-1,1,1-trifluoromethanesulfonamide 1b** as a yellow oil (0.80 g, 46% yield). **^{1}H NMR** (300 MHz, $CDCl_3$) δ 5.65 (brs, 1H), 4.98 (brs, 1H), 3.67 (d, *J* = 5.9 Hz, 2H), 2.01 – 1.86 (m, 4H), 1.66 – 1.44 (m, 4H). **^{19}F NMR** (282 MHz, $CDCl_3$) δ -77.84. **^{13}C NMR** (75 MHz, $CDCl_3$) δ 132.2 (C), 126.9 (CH), 119.8 (q, *J* = 321.2 Hz, C), 50.8 (CH_2), 26.0 (CH_2), 25.1 (CH_2), 22.4 (CH_2), 22.1 (CH_2). **HRMS** [ESI]: *m/z* calculated for $C_8H_{12}F_3NNaO_2S$ [M+Na]$^+$: 266.0433, found 266.0432.

1,1,1-trifluoro-*N*-(2-methylallyl)methanesulfonamide (1c)

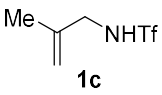

1c

(0.94 g, 33% yield), obtained as a transparent oil. **^{1}H NMR** (300 MHz, $CDCl_3$) δ 5.01 (brs, 1H), 4.94 – 4.90 (m, 2H), 3.74 (d, *J* = 6.1 Hz, 2H), 1.72 (s, 3H). **^{19}F NMR** (282 MHz, $CDCl_3$) δ -77.83. **^{13}C NMR** (75 MHz, $CDCl_3$) δ 139.6 (C), 119.8 (d, *J* = 321.2 Hz, C), 113.9 (CH_2), 50.1 (CH_2), 19.8 (CH_3). **HRMS** [ESI]: *m/z* calculated $C_5H_9F_3NO_2S$ [M+H]$^+$: 204.0301, found 204.0300.

[166] Karaki, F.; Ohgane, K.; Fukuda, H.; Nakamura, M.; Dodo, K.; Hashimoto, Y. *Bioorganic Med. Chem.* **2014**, *22*, 3587.
[167] Hanessian, S.; Szychowski, J.; Pablo Maianti, J. *Org. Lett.* **2009**, *11*, 429.

2.4 Procedure for the synthesis of N-(2,6-difluorobenzoyl)-*L*-leucine

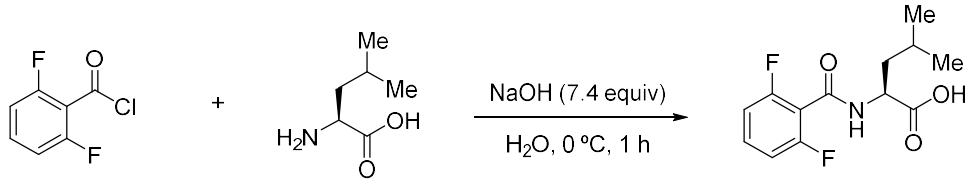

Following a previously reported procedure,[168] to a 25 mL round bottom flask with stir bar was added *L*-leucine (1.11 g, 8.496 mmol), sodium hydroxide (2.52 g, 7.4 equiv), and water (15.5 mL). The mixture was stirred at room temperature until homogeneous before cooling to 0 °C in an ice bath. Upon cooling, 2,6-difluorobenzoyl chloride (1.07 mL, 8.496 mmol) was added dropwise to the mixture. After 1 h, the reaction mixture was allowed to warm to room temperature and pH adjusted to ≈3.0 with hydrochloric acid (36% w/w). The precipitate was filtered and washed with cold water and then dried with a high-vacuum pump to give ***N*-(2,6-difluorobenzoyl)-L-leucine** as a white solid (2.10 g, 91 % yield). Spectral data recorded were in agreement with those found in the corresponding literature. **^{1}H NMR** (300 MHz, DMSO-d_6) δ 12.63 (brs, 1H), 8.97 (d, *J* = 8.1 Hz, 1H), 7.74 – 7.38 (m, 1H), 7.38 – 7.02 (m, 2H), 4.52 – 4.27 (m, 1H), 1.92 – 1.41 (m, 3H), 0.89 (t, *J* = 6.0 Hz, 6H).

2.5 Synthesis of allenes

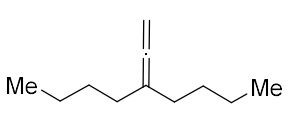

2b

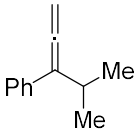

2c

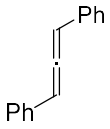

2d

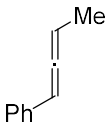

2e

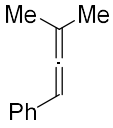

2g

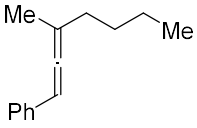

2h

*2.5.1 General procedure for the synthesis of allenes **2b** and **2c***

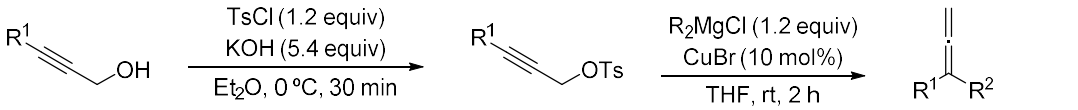

2b: $R^1 = R^2 = {}^n$Bu
2c: R^1 = Ph, $R^2 = {}^i$Pr

Following a previously reported procedure,[115] to a stirred solution of the propargylic alcohol (1 equiv) in Et_2O (0.6 M) was added *p*-toluenesulfonyl chloride (1.2 equiv). The reaction mixture was cooled to 0 °C. Then, crushed KOH (5.4 equiv) was added in small portions, and the reaction

[168] Plata, R. E.; Hill, D. E.; Haines, B. E.; Musaev, D. G.; Chu, L.; Hickey, D. P.; Sigman, M. S.; Yu, J.-Q.; Blackmond, D. G. *J. Am. Chem. Soc.* **2017**, *139*, 9238.

was stirred for 30 minutes at that temperature. After that, cold water was added to the reaction mixture. The organic layer was separated and the aqueous layer extracted with diethyl ether. The combined organic phases were washed with brine and then dried over Na_2SO_4. The solvent was removed under reduced pressure, and the crude was used for the next step without further purification.

CuBr (10 mol%), the tosylate obtained in the previous rection (1 equiv) and THF (0.5 M) were added to a purged two-neck round-bottom flask filled with Ar. Then, the corresponding Grignard reagent (2 equiv) was added dropwise. The reaction mixture was stirred for 2 h at room temperature. After that, the reaction was quenched with NH_4Cl (sat.). The organic layer was separated and the aqueous layer extracted with diethyl ether. The combined organic phases were washed with brine and then dried over Na_2SO_4. The solvent was removed under reduced pressure, and the crude was purified by column chromatography (pentane) to afford the corresponding allene. Spectral data recorded were in agreement with those found in the corresponding literature.

5-vinylidenenonane (2b)

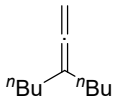

2b

(1.67 g, 49% yield) obtained as a transparent oil. **^{1}H NMR** (300 MHz, $CDCl_3$) δ 4.63 (m, 2H), 2.01 – 1.85 (m, 4H), 1.47 – 1.22 (m, 8H), 0.90 (t, *J* = 7.1 Hz, 6H).

(4-methylpenta-1,2-dien-3-yl)benzene (2c)

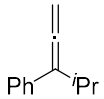

2c

(464 mg, 42% yield), obtained as a transparent oil. **^{1}H NMR** (300 MHz, $CDCl_3$) δ 7.47 – 7.15 (m, 5H), 5.16 – 5.07 (m, 2H), 2.92 – 2.77 (m, 1H), 1.17 (d, *J* = 6.5 Hz, 6H).

*2.5.2 Procedure for the synthesis of allene **2d***

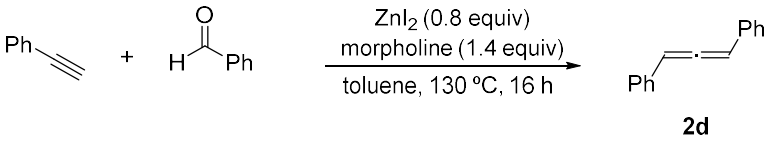

2d

Following a previously reported procedure,[116] ZnI_2 (2.50 g, 0.8 equiv) was added a reaction flask and dried under vacuum. Benzaldehyde (1.87 g, 1.8 equiv), phenylacetylene (1.00 g, 1.1 mL, 1.0 mmol), morpholine (1.19 g, 1.4 equiv) and toluene (50 mL) were added sequentially into this dried reaction flask under Ar. The reaction mixture was stirred at 130 °C overnight. After competition, the reaction mixture was cooled to room temperature and then filtered through Celite© and eluted with diethyl ether. The solvent was removed under reduced pressure, and the crude was purified by column chromatography on silica gel (hexanes) affording **1,3-diphenylpropa-1,2-diene** (**2d**) as a pale-yellow oil (402 mg, 21% yield). **^{1}H NMR** (300 MHz, $CDCl_3$) δ 7.39 – 7.20 (m, 10H), 6.60 (s, 2H). Spectral data recorded were in agreement with those found in the literature.

*2.5.3 Procedure for the synthesis of allenes **2e**, **2g** and **2h***

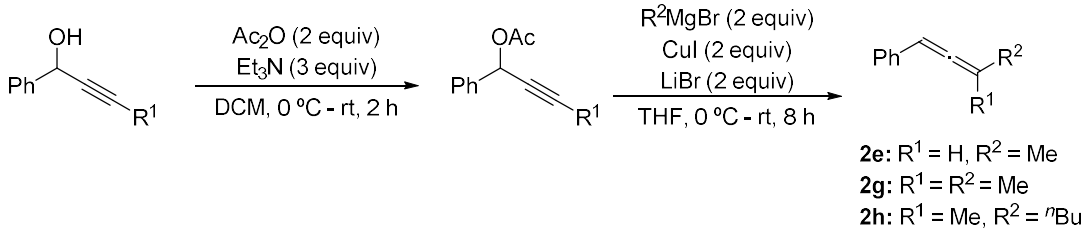

Following a previously reported procedure,[117] to a stirred solution of the propargylic alcohol (1 equiv) in DCM (0.25 M) at 0 °C was added sequentially triethylamine (3 equiv) and acetic anhydride (2 equiv). The reaction was warmed to rt and stirred at that temperature during 2 h. After competition, water was added to the reaction. The organic layer was separated and the aqueous layer extracted with DCM. The combined organic phases were washed with brine and then dried over Na_2SO_4. The solvent was removed under reduced pressure, and the crude was used for the next step without further purification.

CuI (2 equiv), LiBr (2 equiv) and THF (0.3 M) were added to a purged two-neck round-bottom flask filled with Ar. The solution was cooled to 0 °C, and then the corresponding Grignard reagent (2 equiv) was added dropwise. The solution was stirred for 1 h to form the cuprate. After that, the acetate obtained in the previous reaction (1 equiv) was added. The reaction was warmed to room temperature and stirred for 8 h. After that, the reaction was quenched with Na_2CO_3 (sat.). The organic layer was separated and the aqueous layer extracted with diethyl ether. The combined organic phases were washed with brine and then dried over Na_2SO_4. The solvent was removed under reduced pressure, and the crude was purified by column chromatography (pentane) to afford the corresponding allene. Spectral data recorded were in agreement with those found in the corresponding literature.

buta-1,2-dien-1-ylbenzene (2e)

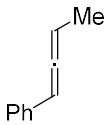

2e

(759 mg, 77% yield), obtained as a transparent oil. **^{1}H NMR** (300 MHz, $CDCl_3$) δ 7.38 – 7.26 (m, 4H), 7.26 – 7.15 (m, 1H), 6.16 – 6.07 (m, 1H), 5.62 – 5.50 (m, 1H), 1.85 – 1.78 (m, 3H).

(3-methylbuta-1,2-dien-1-yl)benzene (2g)

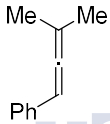

2g

(721 mg, 80% yield), obtained as a transparent oil. **^{1}H NMR** (300 MHz, $CDCl_3$) δ 7.33 – 7.23 (m, 5H), 7.22 – 7.12 (m, 1H), 6.03 – 5.95 (m, 1H), 1.82 (d, *J* = 3.0 Hz, 6H).

(3-methylhepta-1,2-dien-1-yl)benzene (2h)

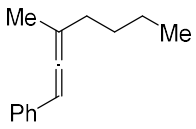

2h

(407 mg, 68% yield), obtained as a transparent oil. ^{1}H NMR (300 MHz, $CDCl_3$) δ 7.33 – 7.23 (m, 4H), 7.21 – 7.12 (m, 1H), 6.08 – 6.01 (m, 1H), 2.15 – 2.03 (m, 2H), 1.81 (t, *J* = 2.9 Hz, 3H), 1.57 – 1.29 (m, 4H), 0.89 (t, *J* = 7.1 Hz, 3H).

2.6 General procedure for the non-chiral Pd-catalyzed annulation of triflyl-protected benzylamines and alkenylamines with allenes, exemplified for 3aa:

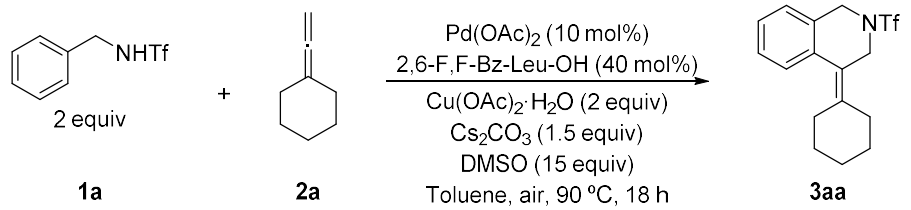

To a solution of $Pd(OAc)_2$ (3.7 mg, 10 mol%), 2,6-F,F-Bz-Leu-OH (18.1 mg, 40 mol%), $Cu(OAc)_2{\cdot}H_2O$ (66.7 mg, 2 equiv), Cs_2CO_3 (81.6 mg, 1.5 equiv) and **1a** (79.9 mg, 0.333 mmol, 2 equiv) in toluene (2 mL), under air atmosphere, in a Schlenk tube was added the allene **2a** (18.0 mg, 0.167 mmol). The tube was sealed with a rubber septum and an air atmosphere was injected in the flask with a balloon and a needle. The reaction was heated at 90 °C, stirred during 18 h and then cooled to room temperature. Evaporation and column chromatography on silica gel (hexanes:diethylether; 99:1) afforded **4-cyclohexylidene-2-(trifluoromethyl)sulfonyl)-1,2,3,4-tetrahydroisoquinoline** (**3aa**) as a white solid (54.8 mg, 95% yield) Mp: 66-67 °C. **^{1}H NMR** (300 MHz, $CDCl_3$) δ 7.28 – 7.04 (m, 4H), 4.44 (s, 2H), 4.22 (s, 2H), 2.45 – 2.34 (m, 2H), 2.32 – 2.24 (m, 2H), 1.66 – 1.49 (m, 6H).**^{19}F NMR** (282 MHz, $CDCl_3$) δ -75.78. **^{13}C NMR** (75 MHz, $CDCl_3$**)** δ 141.7 (C), 135.9 (C), 133.3 (C), 129.0 (CH), 127.3 (CH), 126.1 (CH), 120.4 (C), 120.3 (d, *J* = 324.0 Hz, C), 48.2 (CH_2), 46.8 (CH_2), 32.1 (CH_2), 31.3 (CH_2), 28.6 (CH_2), 28.3 (CH_2), 26.7 (CH_2). **HRMS** [ESI]: *m/z* calculated for $C_{16}H_{19}F_3NO_2S$ $[M+H]^+$: 346.1083, found 346.1085.

4-(nonan-5-ylidene)-2-((trifluoromethyl)sulfonyl)-1,2,3,4-tetrahydroisoquinoline (3ab)

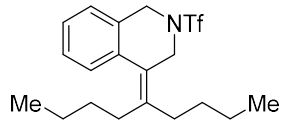

3ab

(55.3 mg, 85% yield), obtained as a transparent oil. **^{1}H NMR** (300 MHz, $CDCl_3$) δ 7.26 – 7.07 (m, 4H), 4.38 (s, 2H), 4.18 (s, 2H), 2.35 – 2.06 (m, 4H), 1.53 – 1.09 (m, 8H), 0.94 – 0.85 (m, 3H), 0.85 – 0.76 (m, 3H). **^{19}F NMR** (282 MHz, $CDCl_3$) δ -75.22. **^{13}C NMR** (75 MHz, Chloroform-*d*) δ 143.1 (C), 136.1 (C), 133.4 (C), 128.3 (CH), 127.5 (CH), 127.3 (CH), 126.1 (CH), 123.6 (C), 120.4 (d, *J* = 324.2 Hz, C), 48.2 (CH_2), 47.2 (CH_2), 33.1 (CH_2), 31.8 (CH_2), 31.6 (CH_2), 31.2 (CH_2), 23.1 (CH_2), 22.8 (CH_2), 14.1 (CH_3), 14.0 (CH_3). **HRMS** [ESI]: *m/z* calculated $C_{19}H_{27}F_3NO_2S$ $[M+H]^+$: 390.1709, found 390.1711.

4-(2-methyl-1-phenylpropylidene)-2-((trifluoromethyl)sulfonyl)-1,2,3,4-tetrahydroisoquinoline (3ac and 3ac')

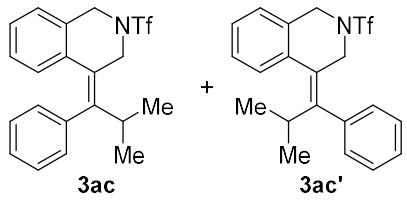

(3.3:1 E/Z ratio of **3ac** and **3ac'**, inseparable mixture (56.8 mg, 86% yield, white solid. Mp: 79-81 °C)). **^{1}H NMR** (500 MHz, $CDCl_3$) δ 7.44 (d, *J* = 7.6 Hz, 0.23H), 7.36 – 7.22 (m, 1.15H), 7.21 – 7.13 (m, 2.54H), 7.03 – 6.98 (m, 0.45H), 6.99 – 6.89 (m, 3.08H), 6.74 – 6.66 (m, 0.77H), 6.54 (d, *J* = 8.1 Hz, 0.77H), 4.55 (s, 1.54H), 4.42 (s, 2.00H), 3.75 (s, 0.46H), 3.35 (hept, *J* = 6.8 Hz, 0.23H), 3.16 (hept, *J* = 6.9 Hz, 0.77H), 0.97 (d, *J* = 6.9 Hz, 4.62H), 0.92 (d, *J* = 6.8 Hz, 1.38H). **^{19}F NMR** (470 MHz, $CDCl_3$) δ -75.50, -75.72. **^{13}C NMR** (75 MHz, $CDCl_3$) δ 149.0 (C), 147.4 (C), 139.3 (C), 137.1 (C), 135.3 (C), 135.2 (C), 134.0 (C), 132.4 (C), 130.0 (CH), 129.9 (CH), 129.5 (CH), 128.4 (CH), 128.2 (CH), 128.1 (CH), 127.9 (CH), 127.8 (CH), 127.5 (CH), 127.1 (CH), 126.9 (CH), 126.6 (CH), 126.3 (CH), 125.5 (CH), 124.66 (C), 124.46 (C), 120.29 (d, *J* = 324.1 Hz, C), 48.80 (CH_2), 48.49 (CH_2), 48.23 (CH_2), 46.42 (CH_2), 30.98 (CH), 30.60 (CH), 21.82 (CH_3), 21.71 (CH_3). **HRMS** [ESI]: *m/z* calculated $C_{20}H_{20}F_3NNaO_2S$ $[M+Na]^+$: 418.1059, found 418.1056.

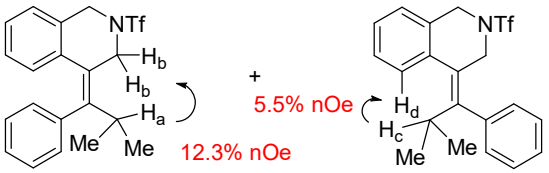

Assignment of stereochemistry based on the observed nOe between the H_a (3.16 ppm, 100%) with H_b (4.42 ppm, 12.3%) and between the H_c (3.35 ppm, 100%) with H_d (7.44 ppm, 5.5%).

(*E*)-4-benzylidene-3-phenyl-2-((trifluoromethyl)sulfonyl)-1,2,3,4-tetrahydroisoquinoline (3ad)

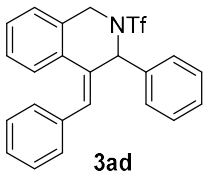

(57.9 mg, 80% yield), obtained as a white solid. Mp: 100-102 °C. **^{1}H NMR** (300 MHz, $CDCl_3$) δ 7.28 – 6.98 (m, 12H), 6.87 (d, *J* = 7.9 Hz, 2H), 6.75 (s, 1H), 5.74 (s, 1H), 4.85 (d, *J* = 17.3 Hz, 1H), 4.30 (d, *J* = 17.3 Hz, 1H). **^{19}F NMR** (282 MHz, $CDCl_3$) δ -75.65. **^{13}C NMR** (75 MHz, $CDCl_3$) δ 136.4 (C), 136.1 (C), 131.2 (C), 130.9 (CH), 130.7 (C), 130.5 (C), 129.8 (CH), 129.0 (CH), 128.9 (CH), 128.8 (CH), 128.4 (CH), 128.2 (CH), 127.9 (CH), 127.2 (CH), 126.7 (CH), 125.8 (CH), 120.2 (d, J = 323.5 Hz, C), 64.9 (CH), 45.8 (CH_2). **HRMS** [ESI]: *m/z* calculated for $C_{23}H_{18}F_3NNaO_2S$ $[M+Na]^+$: 452.0903, found 452.0901.

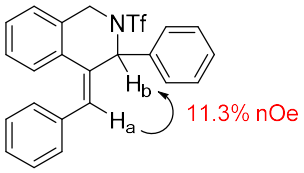

Assignment of stereochemistry based on the observed nOe between the H_a (6.75 ppm, 100%) with H_b (5.74 ppm, 11.3%).

(*E*)-4-benzylidene-3-methyl-2-((trifluoromethyl)sulfonyl)-1,2,3,4-tetrahydroisoquinoline

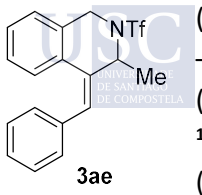

(46.2 mg, 74% yield), obtained as a yellow oil. **^{1}H NMR** (300 MHz, $CDCl_3$) δ 7.40 – 6.85 (m, 9H), 6.58 (s, 1H), 4.98 – 4.42 (m, 3H), 1.27 (d, *J* = 6.8 Hz, 3H). **^{19}F NMR** (282 MHz, $CDCl_3$) δ -77.16. **^{13}C NMR** (75 MHz, $CDCl_3$) δ 136.4 (C), 133.7 (C), 131.0 (C), 130.2 (C), 130.0 (CH), 129.0 (CH), 128.6 (CH), 128.4 (CH), 127.7 (CH), 127.5 (CH), 126.8 (CH), 125.9 (CH), 120.2 (d, *J*

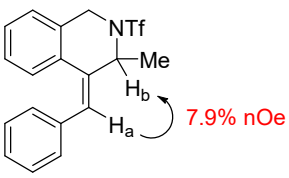

= 323.6 Hz, C), 58.8 (CH), 45.3 (CH_2), 19.7 (CH_3, brs identified by HSQC experiment). **HRMS** [ESI]: *m/z* calculated for $C_{18}H_{16}F_3NNaO_2S$ $[M+Na]^+$: 390.0746, found 390.0745.

Assignment of stereochemistry based on the observed nOe between the H_a (6.58 ppm, 100%) with H_b (4.94 – 4.88 ppm, 7.9%).

4-(cyclohexylmethylene)-2-((trifluoromethyl)sulfonyl)-1,2,3,4-tetrahydroisoquinoline (3af and 3af')

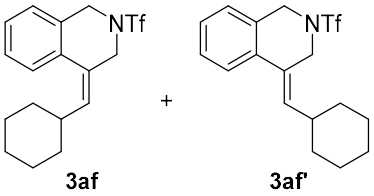

(1.1:1 E/Z rr of **3af** and **3af'**, inseparable mixture (50.8 mg, 85% yield, transparent oil)) **^{1}H NMR** (300 %MHz, $CDCl_3$) δ 7.58 – 7.47 (m, 0.47H), 7.36 – 7.06 (m, 3.06H), 7.05 – 6.95 (m, 0.47H), 5.95 (d, *J* = 9.6 Hz, 0.47H), 5.46 (d, *J* = 10.3 Hz, 0.53H), 4.65 – 4.50 (m, 2H), 4.33 (s, 0.94H), 4.05 (s, 1.06H), 2.60 – 2.44 (m, 0.47H), 2.35 – 2.16 (m, 0.53H), 1.74 – 1.55 (m, 5H), 1.32 – 0.99 (m, 5H). **^{19}F NMR** (282 MHz, $CDCl_3$) δ -75.81, -76.20. **^{13}C NMR** (75 MHz, $CDCl_3$) δ 138.1 (CH), 133.6 (C), 133.4 (CH), 133.1 (C), 132.2 (C), 130.3 (C), 128.0 (CH), 127.93 (CH), 127.87 (CH), 127.6 (CH), 127.5 (CH), 126.12 (CH), 126.05 (CH), 125.8 (C), 125.4 (C), 124.0 (CH), 120.13 (d, *J* = 332.4 Hz, C), 120.12 (d, *J* = 315.2 Hz, C), 52.9 (CH_2), 48.5 (CH_2), 48.3 (CH_2), 45.7 (CH_2), 37.4 (CH), 37.22 (CH), 33.15 (CH_2), 33.0 (CH_2), 26.0 (CH_2), 25.8 (CH_2), 25.6 (CH_2). **HRMS** [ESI]: *m/z* calculated $C_{17}H_{21}F_3NO_2S$ $[M+H]^+$: 360.1240, found 360.1238.

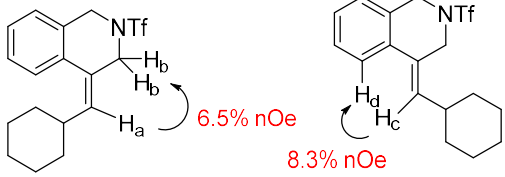

Assignment of stereochemistry based on the observed nOe between the H_a (5.46 ppm, 100%) with H_b (4.05 ppm, 6.5%) and between the H_c (5.95 ppm, 100%) with H_d (7.58 – 7.47, 8.3%).

(*E*)-4-benzylidene-3,3-dimethyl-2-((trifluoromethyl)sulfonyl)-1,2,3,4-tetrahydroisoquinoline (3ag)

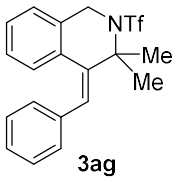

(50.7 mg, 80% yield), obtained as a white solid. Mp: 91-92 °C. **^{1}H NMR** (300 MHz, $CDCl_3$) δ 7.22 – 6.87 (m, 9H), 6.74 (s, 1H), 4.45 (s, 2H), 1.69 (s, 6H). **^{19}F NMR** (282 MHz, $CDCl_3$) δ -76.10. **^{13}C NMR** (75 MHz, $CDCl_3$) δ 141.8 (C), 136.3 (C), 135.0 (C), 134.8 (C), 129.5 (CH), 129.4 (CH), 128.29 (CH), 128.26 (CH), 128.0 (CH), 127.5 (CH), 125.7 (CH), 125.5 (CH), 119.7 (d, *J* = 324.4 Hz, C), 67.6 (C), 49.4 (CH_2), 27.9 (CH_3, brs). **HRMS** [ESI]: *m/z* calculated for $C_{19}H_{19}F_3NO_2S$ $[M+H]^+$: 382.1083, found 382.1085.

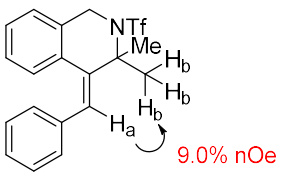

Assignment of stereochemistry based on the observed nOe between the H_a (6.74 ppm 100%) with H_b (1.69 ppm, 9.0%).

(*E*)-4-benzylidene-3-butyl-3-methyl-2-((trifluoromethyl)sulfonyl)-1,2,3,4-tetrahydroisoquinoline (3ah)

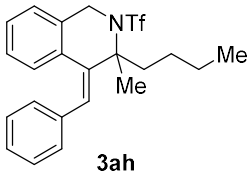

3ah

(63.8 mg, 90% yield), obtained as a transparent oil. **^{1}H NMR** (300 MHz, $CDCl_3$) δ 7.23 – 6.83 (m, 9H), 6.67 (s, 1H), 4.46 (s, 2H), 2.15 – 1.97 (m, 1H), 1.70 (s, 3H), 1.36 – 1.07 (m, 4H), 0.77 (t, *J* = 7.1 Hz, 3H). **^{19}F NMR** (282 MHz, $CDCl_3$) δ -75.93. **^{13}C NMR** (75 MHz, $CDCl_3$) δ 138.9 (C), 136.4 (C), 135.2 (C), 134.6 (C), 129.5 (CH), 129.2 (CH), 128.7 (CH), 128.3 (CH), 128.0 (CH), 127.5 (CH), 127.3 (CH), 125.4 (CH), 119.8 (d, *J* = 324.9 Hz, C), 71.2 (C), 50.2 (CH_2), 26.8 (CH_2), 25.0 (CH_3, brs), 22.8 (CH_2), 14.0 (CH_3). **HRMS** [ESI]: *m/z* calculated for $C_{22}H_{25}F_3NO_2S$ $[M+H]^+$: 424.1553, found 424.1553.

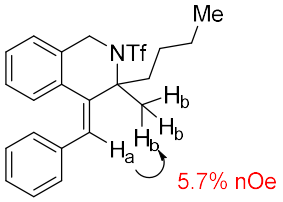

Assignment of stereochemistry based on the observed nOe between the H_a (6.67 ppm, 100%) with H_b (0.77 ppm, 5.7%).

4-cyclohexylidene-2-((trifluoromethyl)sulfonyl)-1,2,3,4,5,6,7,8-octahydroisoquinoline (3ba)

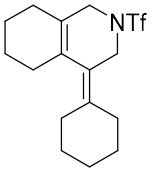

3ba

Reaction performed at 105 °C. (41.5 mg, 71% yield), obtained as a transparent oil. **^{1}H NMR** (300 MHz, $CDCl_3$) δ 4.03 (s, 2H), 3.84 (s, 2H), 2.36 – 2.17 (m, 6H), 2.09 – 1.97 (m, 2H), 1.78 – 1.65 (m, 2H), 1.65 – 1.51 (m, 8H). **^{19}F NMR** (282 MHz, $CDCl_3$) δ -76.01. **^{13}C NMR** (75 MHz, $CDCl_3$) δ 139.6 (C), 132.0 (C), 128.4 (C), 123.0 (C), 120.3 (d, *J* = 324.0 Hz, C), 49.3 (CH_2), 46.4 (CH_2), 33.4 (CH_2), 32.1 (CH_2), 31.4 (CH_2), 28.33 (CH_2), 28.28 (CH_2), 27.8 (CH_2), 26.7 (CH_2), 23.7 (CH_2), 22.4 (CH_2). **HRMS** [ESI]: *m/z* calculated for $C_{16}H_{23}F_3NO_2S$ $[M+H]^+$: 350.1396, found 350.1399.

3-cyclohexylidene-5-methyl-1-((trifluoromethyl)sulfonyl)-1,2,3,6-tetrahydropyridine (3ca)

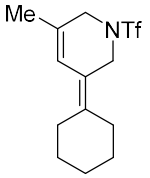

3ca

(45.7 mg, 88% yield), obtained as a transparent oil. **^{1}H NMR** (300 MHz, $CDCl_3$) δ 6.33 – 6.28 (m, 1H), 4.10 (s, 2H), 3.88 (s, 2H), 2.32 – 2.08 (m, 4H), 1.74 (s, 3H), 1.55 – 1.43 (m, 6H). **^{19}F NMR** (282 MHz, $CDCl_3$) δ -76.34. **^{13}C NMR** (75 MHz, $CDCl_3$) δ 137.4 (C), 129.3 (C), 120.6 (CH), 120.2 (d, *J* = 324.0 Hz, C), 118.6 (C), 49.1 (CH_2), 44.9 (CH_2), 30.7 (CH_2), 29.7 (CH_2), 28.11 (CH_2), 28.08 (CH_2), 26.8 (CH_2), 20.8 (CH_2). **HRMS** [APCI]: *m/z* calculated for $C_{13}H_{19}F_3NO_2S$ $[M+H]^+$: 310.1083, found 310.1083.

(*E*)-4-benzylidene-3,3-dimethyl-2-((trifluoromethyl)sulfonyl)-1,2,3,4,5,6,7,8-octahydroisoquinoline (3bg)

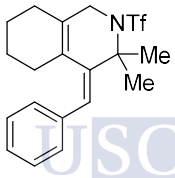

3bg

(58.2 mg, 90% yield), obtained as a transparent oil. **^{1}H NMR** (300 MHz, $CDCl_3$) δ 7.27 – 7.10 (m, 5H), 6.48 (s, 1H), 3.84 (s, 2H), 2.12 – 2.02 (m, 2H), 1.73 – 1.65 (m, 2H), 1.64 (s, 6H), 1.62 – 1.52 (m, 2H), 1.46 – 1.35 (m, 2H). **^{19}F NMR** (282 MHz, $CDCl_3$) δ -75.94. **^{13}C NMR** (75 MHz, $CDCl_3$) δ 142.6 (C), 137.7 (C), 132.7 (C), 132.5 (C), 129.0 (CH), 128.2 (CH), 127.4 (CH), 123.2 (CH), 120.0 (d, *J* = 325.1 Hz, C), 65.8 (C), 49.9 (CH_2), 28.0 (CH_2), 27.6 (CH_2), 27.3 (brs, CH_3), 22.8 (CH_2), 22.4 (CH_2). **HRMS** [APCI]: *m/z* calculated for $C_{19}H_{22}F_3NO_2S$ $[M+H]^+$: 386.1396, found 386.1395.

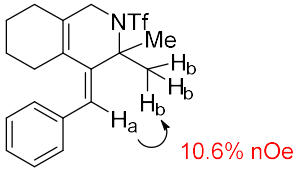

Assignment of stereochemistry based on the observed nOe between the H_a (6.48 ppm, 100%) with H_b (1.64 ppm).

1-cyclohexylidene-3-((trifluoromethyl)sulfonyl)-2,3,4,5,6,7,8,9-octahydro-1*H*-benzo[*d*]azepine (3ea)

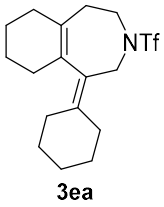

3ea

Reaction performed at 105 °C with one equivalent of alkenylamide **1e**. (50.4 mg, 83% yield), obtained as a yellow oil. NMR characterization performed at 110 °C due to the presence of conformers. **^{1}H NMR** (500 MHz, DMSO-d_6) δ 3.68 (s, 2H), 3.09 (t, *J* = 6.2 Hz, 2H), 1.87 – 1.76 (m, 4H), 1.69 (t, *J* = 6.3 Hz, 2H), 1.66 – 1.55 (m, 4H), 1.24 – 1.09 (m, 10H). **^{19}F NMR** (470 MHz, DMSO-d_6) δ -76.03. **^{13}C NMR** (126 MHz, DMSO-*d*6) δ 139.6 (C), 132.5 (C), 130.2 (C), 125.8 (C), 119.4 (q, *J* = 324.7 Hz, C), 48.2 (CH_2), 44.4 (CH_2), 33.6 (CH_2), 31.4 (CH_2), 29.4 (CH_2), 29.2 (CH_2), 28.7 (CH_2), 27.1 (CH_2), 26.6 (CH_2), 25.3 (CH_2), 21.9 (CH_2), 21.8 (CH_2). **HRMS** [ESI]: *m/z* calculated for $C_{17}H_{25}F_3NO_2S$ $[M+H]^+$: 364.1553, found 364.1549.

2.7 Procedure for the kinetic resolution of α-ethyl substituted benzyltriflamide

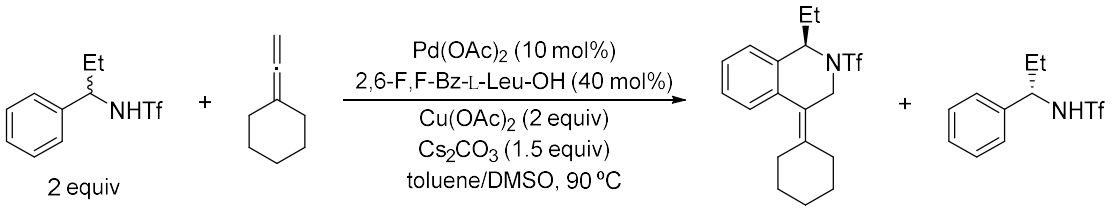

To a solution of $Pd(OAc)_2$ (3.7 mg, 10 mol%), 2,6-F,F-Bz-L-Leu-OH (18.1 mg, 40 mol%), $Cu(OAc)_2{\cdot}H_2O$ (66.7 mg, 2 equiv.), Cs_2CO_3 (81.6 mg, 1.5 equiv) and **1f** (89.3 mg, 0.333 mmol, 2 equiv) in toluene (2 mL) under air atmosphere in a Schlenk tube was added the allene **2a** (18.0 mg, 0.167 mmol).The tube was sealed with a rubber septum and an air atmosphere was injected in the flask with a balloon and a needle. The reaction was heated at 90 °C, stirred during 18 h and then cooled to room temperature. Evaporation and column chromatography on silica gel (hexanes:diethylether; 99:1) afforded **4-cyclohexylidene-1-ethyl-2-((trifluoromethyl)sulfonyl)-1,2,3,4-tetrahydroisoquinoline** (**3fa**) as a white solid (56.6 mg, 91% yield, Mp: 88-90 °C) and remaining **1f** as a white solid (39.0 mg, 80% recovered based on reaction yield). **^{1}H NMR** (300 MHz, $CDCl_3$) δ 7.28 – 7.10 (m, 3H), 7.03 (d, J = 7.3 Hz, 1H), 4.62 – 4.44 (m, 2H), 4.07 (d, *J* = 13.4 Hz, 1H), 2.45 – 2.34 (m, 2H), 2.34 – 2.11 (m, 2H), 1.92 – 1.37 (m, 9H), 0.84 (t, *J* = 7.4 Hz, 3H). **^{19}F NMR** (282 MHz, $CDCl_3$) δ -75.54. **^{13}C NMR** (75 MHz, $CDCl_3$) δ 140.5 (C), 137.8 (C), 133.9 (C), 129.5 (CH), 127.4 (CH), 127.0 (CH), 126.6 (CH), 120.2 (d, *J* = 324.4 Hz, C), 119.8 (C), 62.3 (CH), 46.3 (CH_2), 32.2 (CH_2), 31.0 (CH_2), 28.5 (CH_2), 28.0 (CH_2), 26.7 (CH_2), 11.2 (CH). **HRMS** [ESI]: *m/z* calculated for $C_{18}H_{23}F_3NO_2S$ $[M+H]^+$: 374.1396, found 374.1398.

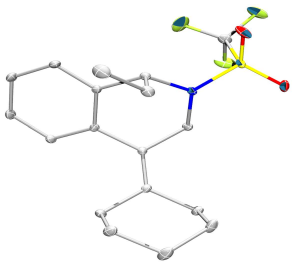

The structure of **3fa** was confirmed by X-ray diffraction analysis (CCDC: 1880116, hydrogens omitted for clarity).

Enantioselectivity was determined by chiral SFC analysis on Chiralpak IF-3 at 40 °C (CO_2, 2 mL/min).

Racemic sample

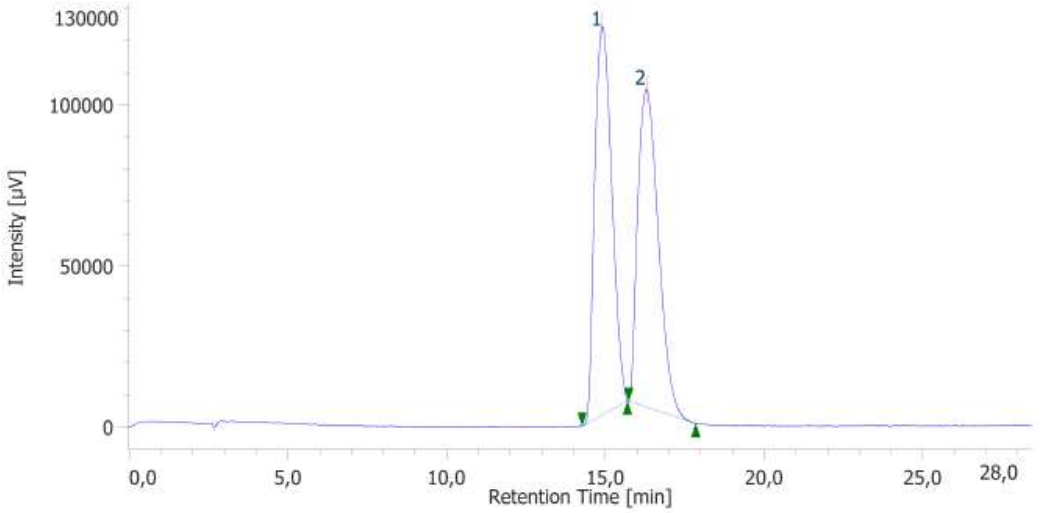

Channel Name 254,0nm Sampling Interval 200 [msec]

#	Peak Name	CH	tR [min]	Area [μV·sec]	Height [μV]	Area%	Height%	Quantity	NTP	Resolution	Symmetry Factor	Warning
1	Unknown	5	14,907	4535366	120606	50,574	54,988	N/A	3234	1,214	1,259	
2	Unknown	5	16,287	4432385	98727	49,426	45,012	N/A	2804	N/A	1,445	

Asymmetric sample (93 :7 er)

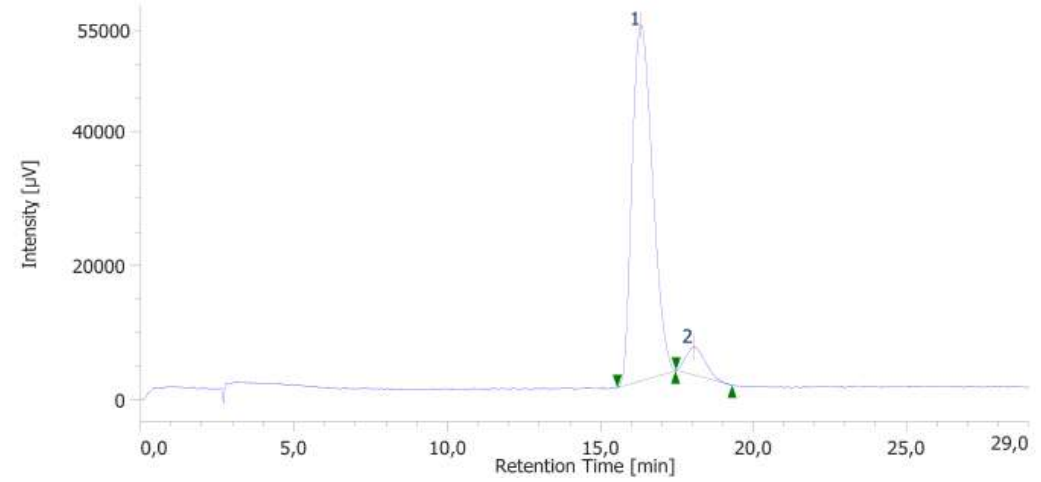

Channel Name 254,0nm Sampling Interval 200 [msec]

#	Peak Name	CH	tR [min]	Area [μV·sec]	Height [μV]	Area%	Height%	Quantity	NTP	Resolution	Symmetry Factor	Warning
1	Unknown	9	16,320	2467749	52800	93,060	92,707	N/A	2635	1,376	1,288	
2	Unknown	9	18,030	184031	4154	6,940	7,293	N/A	3487	N/A	1,353	

2.8 Procedure for the derivatization of recovered triflimide 1f to measure the enantiomeric ratio

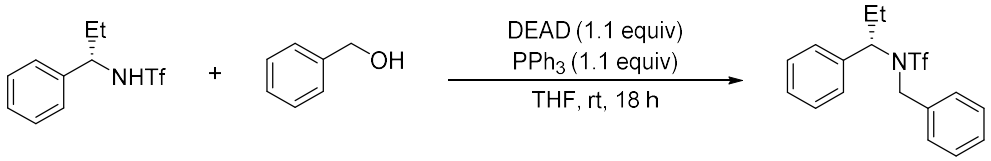

Following a previously reported procedure,[169] to a solution of recovered **1,1,1-trifluoro-N-(1-phenylpropyl)methanesulfonamide** (**1f**, 39.0 mg, 0.146 mmol), benzyl alcohol (15.8 mg, 1 equiv), and triphenylphosphine (42.1 mg, 1.1 equiv) in THF (0.15 mL) was added DEAD (63 µL, 40% in toluene, 1.1 equiv). The reaction mixture was stirred at room temperature overnight. Evaporation of the solvent and column chromatography on silica gel (hexanes:diethylether; 90:10) afforded **N-benzyl-1,1,1-trifluoro-N-(1-phenylpropyl)methanesulfonamide** as a transparent oil (22.8 mg, 44%). **^{1}H NMR** (300 MHz, $CDCl_3$) δ 7.36 – 6.99 (m, 10H), 4.87 (t, J = 7.9 Hz, 1H), 4.46 (d, J = 16.1 Hz, 1H), 3.92 (brs, 1H), 1.77 (d, J = 10.4 Hz, 2H), 0.69 (t, J = 7.3 Hz, 3H). **HRMS** [ESI]: *m/z* calculated for $C_{17}H_{18}F_3NO_2S$ $[M+H]^+$: 357.1005, found 357.1001.

Enantioselectivity was determined by chiral SFC analysis on Phenomenex Cellulose-1 at 40 °C (CO_2 : MeOH = 99:01, 0.5 mL/min).

Racemic sample

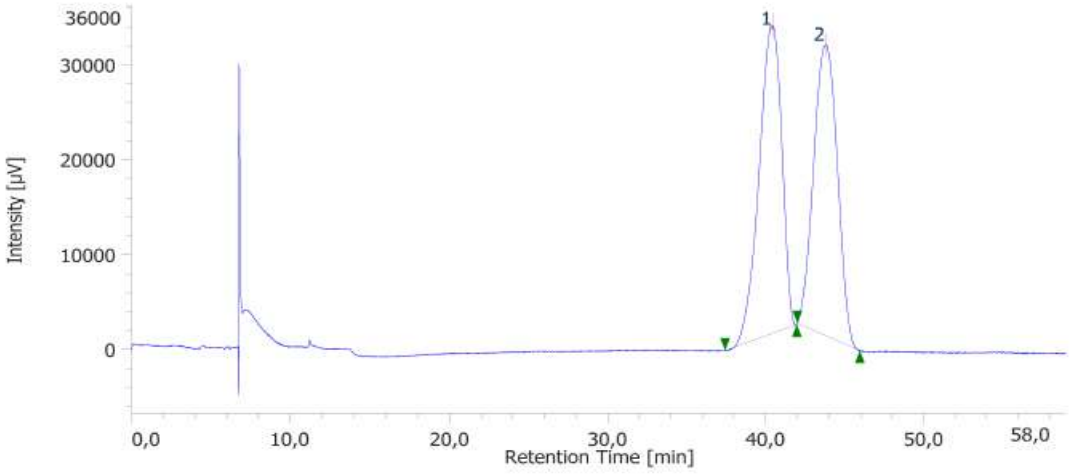

Channel Name 222,0nm Sampling Interval 200 [msec]

#	Peak Name	CH	tR [min]	Area [µV·sec]	Height [µV]	Area%	Height%	Quantity	NTP	Resolution	Symmetry Factor	Warning
1	Unknown	10	40,423	3235516	32453	50,331	51,475	N/A	3633	1,208	0,818	
2	Unknown	10	43,773	3192986	30593	49,669	48,525	N/A	3705	N/A	1,010	

[169] Bell, E.; Knight, D. W.; Uk, N. G. Z. R. D.; Gravestock, B. *Org. Lett.* **1995**, *36*, 8681.

Asymmetric sample (86 :14 er)

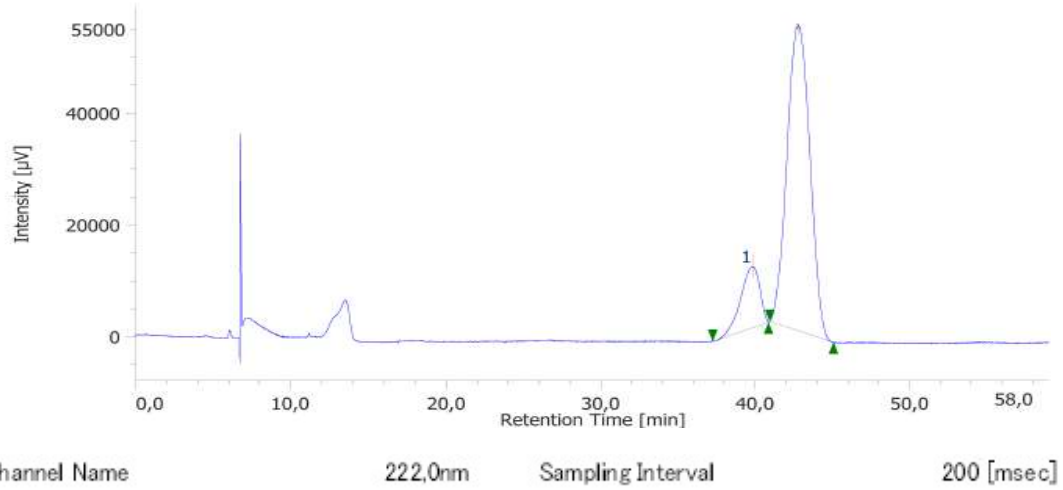

#	Peak Name	CH	tR [min]	Area [μV·sec]	Height [μV]	Area%	Height%	Quantity	NTP	Resolution	Symmetry Factor	Warning
1	Unknown	10	39,810	938742	10978	14,309	16,707	N/A	4680	1,175	0,767	
2	Unknown	10	42,817	5621613	54731	85,691	83,293	N/A	3734	N/A	0,998	

2.9 General procedure for the desymmetrizing Pd-catalyzed annulation of triflyl-protected diarylbenzylamines with allenes

Method A (using excess of amide)

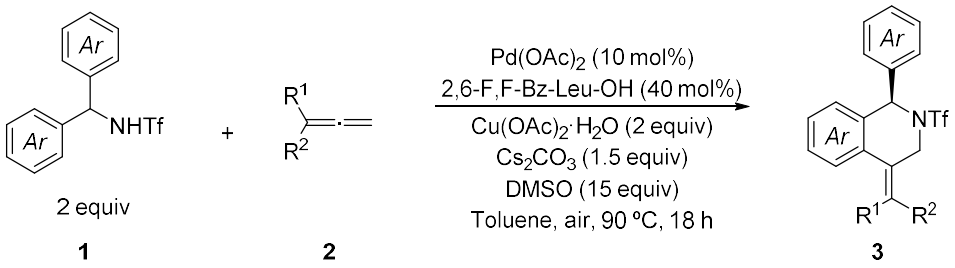

To a solution of $Pd(OAc)_2$ (3.7 mg, 10 mol%), 2,6-F,F-Bz-L-Leu-OH (18.1 mg, 40 mol%), $Cu(OAc)_2{\cdot}H_2O$ (66.7 mg, 2 equiv), Cs_2CO_3 (81.6 mg, 1.5 equiv) and triflamides **1** (0.333 mmol, 2 equiv) in toluene (2 mL) under air atmosphere in a Schlenk tube was added the allene **2** (0.167 mmol). The tube was sealed with a rubber septum and an air atmosphere was injected in the flask with a balloon and a needle. The reaction was heated at 90 °C, stirred during 18 h and then cooled to room temperature. Evaporation and column chromatography on silica gel (hexanes:diethylether; 99:1) afforded cycloadducts **3**.

Method B (using excess of allene)

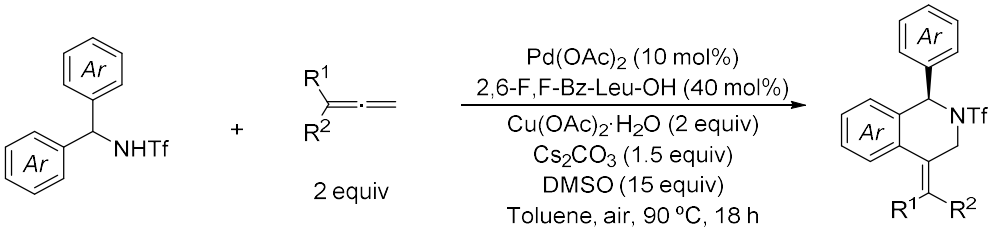

1 **2** **3**

To a solution of $Pd(OAc)_2$ (3.7 mg, 10 mol%), 2,6-F,F-Bz-L-Leu-OH (18.1 mg, 40 mol%), $Cu(OAc)_2{\cdot}H_2O$ (66.7 mg, 2 equiv), Cs_2CO_3 (81.6 mg, 1.5 equiv) and triflamides **1** (0.167 mmol, 2 equiv) in toluene (2 mL) under air atmosphere in a Schlenk tube was added the allene **2** (0.333 mmol).The tube was sealed with a rubber septum and an air atmosphere was injected in the flask with a balloon and a needle. The reaction was heated at 90 °C, stirred during 18 h and then cooled to room temperature. Evaporation and column chromatography on silica gel (hexanes:diethylether; 99:1) afforded cyloadducts **3**.

Racemic products were obtained using the racemic 2,6-F,F-Bz-Leu-OH.

4-cyclohexylidene-1-phenyl-2-((trifluoromethyl) sulfonyl)-1,2,3,4-tetrahydroisoquinoline (3ga)

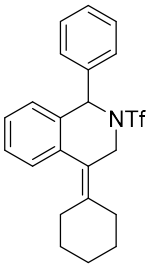

3ga

Method A: (60.1 mg, 85% yield), obtained as a white solid. Mp: 97-99 °C. **^{1}H NMR** (300 MHz, $CDCl_3$) δ 7.35 – 7.05 (m, 9H), 5.92 (s, 1H), 4.40 (d, *J* = 13.6 Hz, 1H), 4.10 (d, *J* = 13.4 Hz, 1H), 2.38 – 2.25 (m, 1H), 2.18 – 2.02 (m, 2H), 1.96 – 1.79 (m, 1H), 1.50 – 1.28 (m, 4H), 1.00 – 0.75 (m, 2H). **^{19}F NMR** (282 MHz, $CDCl_3$) δ -75.18. **^{13}C NMR** (75 MHz, $CDCl_3$) δ 140.9 (C), 138.5 (C), 137.3(C), 135.2(C), 129.8 (CH), 128.4 (CH), 127.9 (CH), 127.7 (CH), 127.31 (CH), 127.26 (CH), 127.2 (CH), 120.1 (q, *J* = 324.4 Hz, C), 119.7 (C), 62.4 (CH), 46.5 (CH_2), 31.9 (CH_2), 30.6 (CH_2), 27.8 (CH_2), 27.2 (CH_2), 26.4 (CH_2). **HRMS** [ESI]: *m/z* calculated for $C_{22}H_{23}F_3NO_2S$ $[M+H]^+$: 422.1396, found 422.1386.

Enantioselectivity was determined by chiral HPLC analysis on Chiralpak IB at rt (Hexane, 0.5 mL/min).

Racemic sample

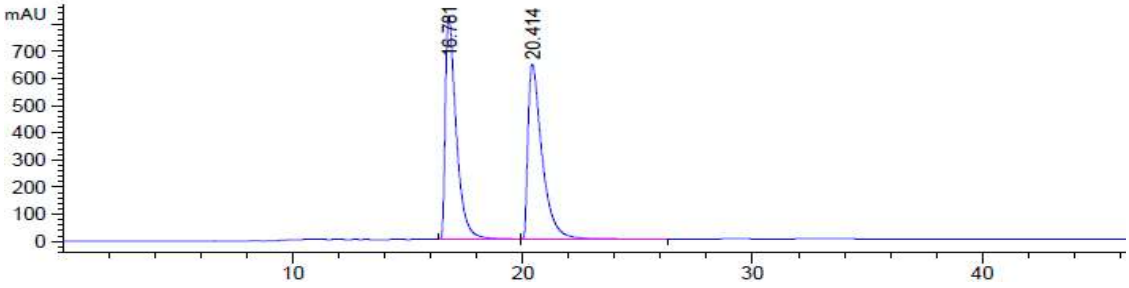

Signal 2: DAD1 B, Sig=254,4 Ref=off

Peak #	RetTime [min]	Type	Width [min]	Area [mAU*s]	Height [mAU]	Area %
1	16.781	BB	0.4998	2.72435e4	823.86963	49.7619
2	20.414	BB	0.6477	2.75042e4	644.70233	50.2381
Totals :				5.47478e4	1468.57196	

Asymmetric sample (94 : 6 er)

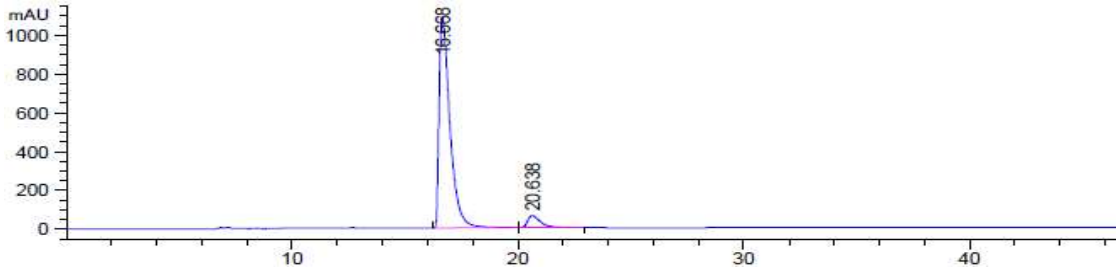

Signal 2: DAD1 B, Sig=254,4 Ref=off

Peak #	RetTime [min]	Type	Width [min]	Area [mAU*s]	Height [mAU]	Area %
1	16.668	BB	0.5091	3.63547e4	1090.09351	93.6232
2	20.638	BB	0.5843	2476.17505	63.03621	6.3768
Totals :				3.88308e4	1153.12972	

4-(nonan-5-ylidene)-1-phenyl-2-((trifluoromethyl)sulfonyl)-1,2,3,4-tetrahydroisoquinoline (3gb)

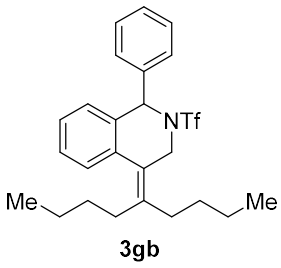

3gb

Method A: (73.2 mg, 94% yield), obtained as a yellow oil. **^{1}H NMR** (300 MHz, $CDCl_3$) δ 7.36 – 7.02 (m, 10H), 5.90 (s, 1H), 4.29 (d, *J* = 13.8 Hz, 1H), 4.11 (d, *J* = 13.9 Hz, 1H), 2.16 – 1.99 (m, 1H), 1.92 – 1.75 (m, 3H), 1.25 – 0.82 (m, 8H), 0.80 – 0.68 (m, 6H). **^{19}F NMR** (282 MHz, $CDCl_3$) δ -75.62. **^{13}C NMR** (75 MHz, $CDCl_3$) δ 141.9 (C), 138.2 (C), 136.8 (C), 135.3 (C), 129.1 (CH), 128.4 (CH), 128.1 (CH), 127.8 (CH), 127.4 (CH), 127.3 (CH), 127.2 (CH), 122.5 (C), 120.1 (d, *J* = 324.4 Hz, C), 62.3 (CH), 46.7 (CH_2), 32.9 (CH_2), 31.2 (CH_2), 31.0 (CH_2), 29.7 (CH_2), 23.03 (CH_2), 22.97 (CH_2), 14.13 (CH_3), 14.07 (CH_3). **HRMS** [ESI]: *m/z* calculated for $C_{25}H_{31}F_3NO_2S$ $[M+H]^+$: 466.2022, found 466.2015.

Enantioselectivity was determined by chiral SFC analysis on Phenomenex i-Cellulose-5 at 40 °C (CO_2 : MeOH = 98:02, 0.5 mL/min).

Racemic sample

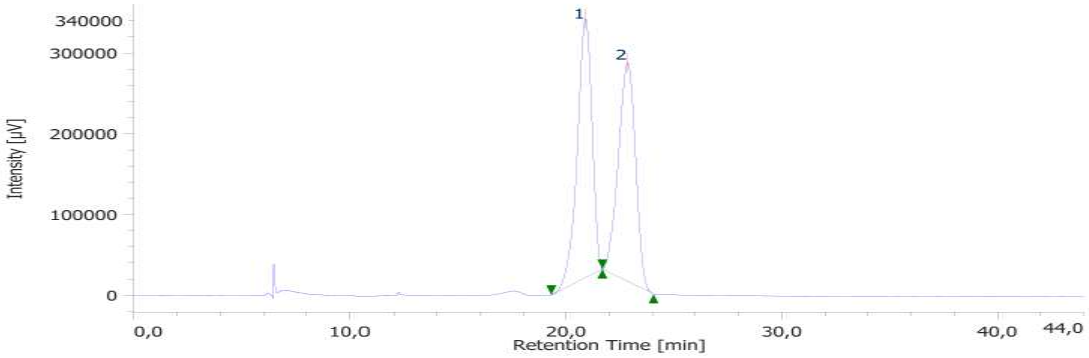

Channel Name 222,0nm Sampling Interval 200 [msec]

#	Peak Name	CH	tR [min]	Area [μV·sec]	Height [μV]	Area%	Height%	Quantity	NTP	Resolution	Symmetry Factor	Warning
1	Unknown	9	20,887	15244033	319865	50,484	54,195	N/A	4537	1,436	0,826	
2	Unknown	9	22,833	14951856	270352	49,516	45,805	N/A	3821	N/A	0,909	

Asymmetric sample (95 : 5 er)

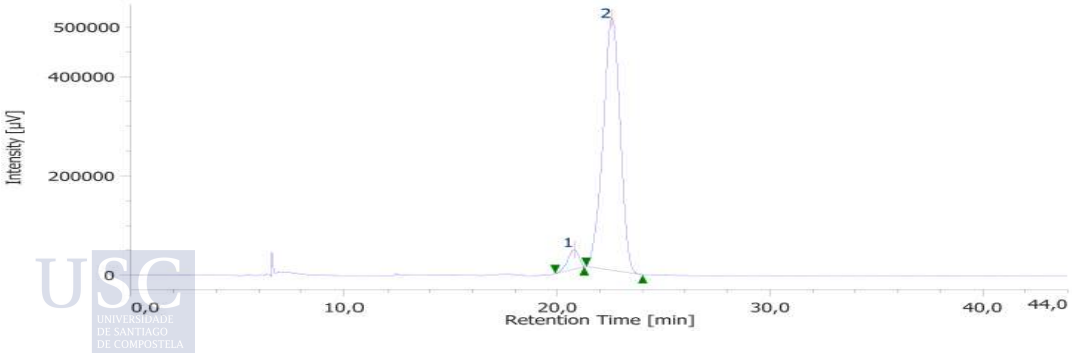

Channel Name 222,0nm Sampling Interval 200 [msec]

#	Peak Name	CH	tR [min]	Area [μV·sec]	Height [μV]	Area%	Height%	Quantity	NTP	Resolution	Symmetry Factor	Warning
1	Unknown	9	20,790	1419800	38483	4,739	7,048	N/A	6876	1,423	0,786	
2	Unknown	9	22,560	28540687	507501	95,261	92,952	N/A	3665	N/A	0,922	

4-(2-methyl-1-phenylpropylidene)-1-phenyl-2-((trifluoromethyl)sulfonyl)-1,2,3,4-tetrahydroisoquinoline (3gc)

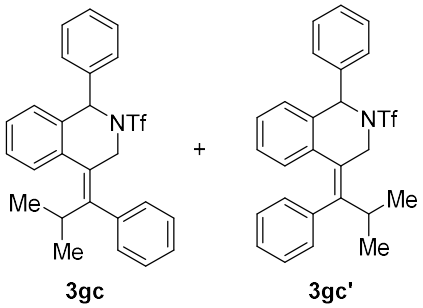

3gc 3gc'

Method A performed at 70 °C over 72h: (1:4.9 E/Z ratio of **3gc** and **3gc'**, inseparable mixture (51.8 mg, 66% yield, white solid, Mp: 143-145 °C)). **^{1}H NMR** (300 MHz, $CDCl_3$) δ 7.46 – 6.57 (m, 14H), 5.98 – 5.86 (m, 2H), 4.58 – 4.32 (m, 0.34 H), 3.76 (s, 1.66H), 3.09 (hept, *J* = 6.8 Hz, 0.83H), 2.81 (hept, *J* = 7.0 Hz, 0.17H), 0.93 (d, *J* = 6.9 Hz, 3H), 0.41 (d, *J* = 6.8 Hz, 0.51H), 0.30 (d, *J* = 6.7 Hz, 2.49H). **^{19}F NMR** (282 MHz, $CDCl_3$) δ -75.34. **^{13}C NMR** (75 MHz, $CDCl_3$) δ 147.5 (C), 138.5 (C), 137.0 (C), 134.6 (C), 130.6 (C), 129.8 (C), 129.2 (CH), 128.64 (CH), 128.55 (CH), 128.4 (CH), 128.2 (CH), 128.1 (CH), 127.9 (CH), 127.8 (CH), 127.6 (CH), 127.4 (CH), 127.3 (CH), 123.8 (C), 120.1 (d, *J* = 324.3 Hz, C), 62.4 (CH), 62.2 (CH), 48.3 (CH_2), 45.7 (CH_2), 30.5 (CH), 22.3 (CH_3), 21.5 (CH_3), 20.1 (CH_3), 19.9 (CH_3). **HRMS** [ESI]: *m/z* calculated for $C_{26}H_{25}F_3NO_2S$ $[M+H]^+$: 472.1555, found 472.1549.

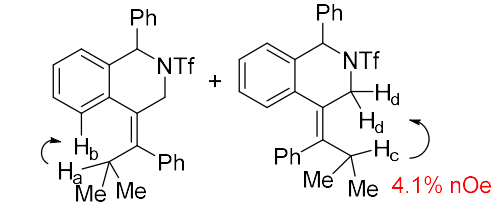

Assignment of stereochemistry based on the observed nOe between the H_a (3.09 ppm, 100%) with H_b (7.45 – 7.28 ppm, 9.4%) and the H_c (2.81 ppm, 100%) with the H_d (4.58 – 4.32 ppm, 4.1%).

Enantioselectivity was determined by chiral SFC analysis on Phenomenex Cellulose-2 at 40 °C (CO_2 : MeOH = 98:02, 1 mL/min).

Racemic sample

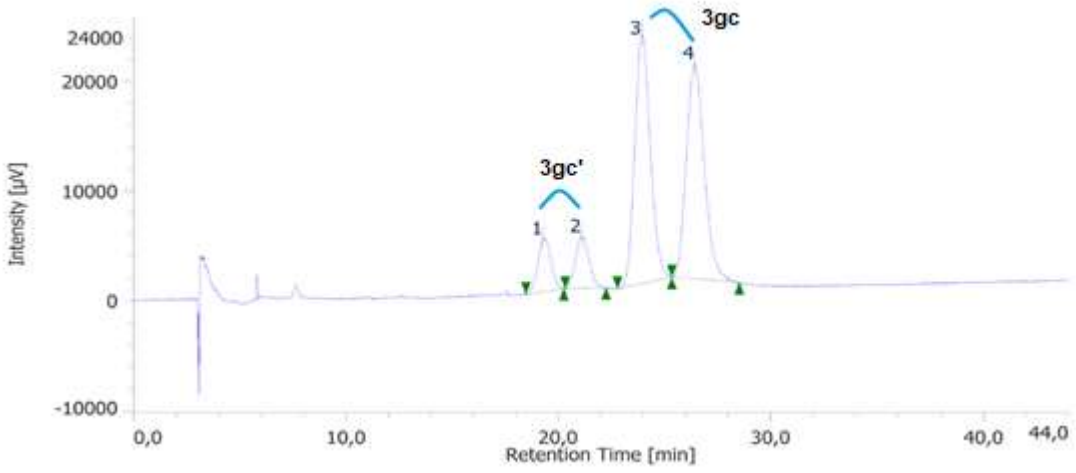

Channel Name 254,0nm Sampling Interval 200 [msec]

#	Peak Name	CH	tR [min]	Area [μV·sec]	Height [μV]	Area%	Height%	Quantity	NTP	Resolution	Symmetry Factor	Warning
1	Unknown	11	19,283	210552	4866	7,704	9,360	N/A	4391	1,550	1,087	
2	Unknown	11	21,100	207639	4747	7,598	9,132	N/A	5065	2,240	1,126	
3	Unknown	11	23,933	1165726	22705	42,656	43,678	N/A	5023	1,728	1,176	
4	Unknown	11	26,410	1148947	19664	42,042	37,829	N/A	4808	N/A	1,208	

Asymmetric sample (**3gc**, 95 : 5 er, **3gc'**, 94 : 6 er)

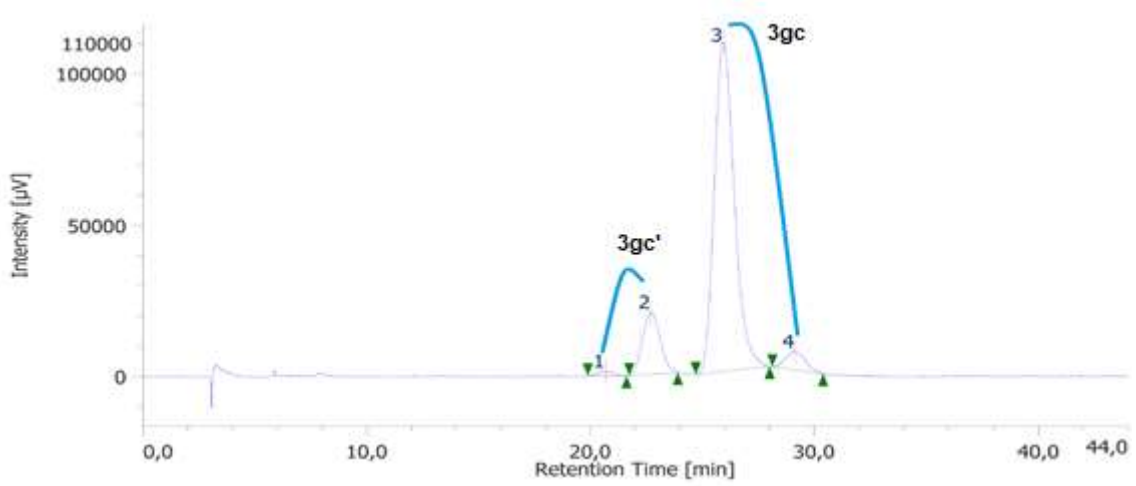

Channel Name 254,0nm Sampling Interval 200 [msec]

#	Peak Name	CH	tR [min]	Area [μV·sec]	Height [μV]	Area%	Height%	Quantity	NTP	Resolution	Symmetry Factor	Warning
1	Unknown	11	20,670	70695	1474	0,846	1,081	N/A	3968	1,455	1,069	
2	Unknown	11	22,703	1117247	20266	13,362	14,862	N/A	3715	2,079	1,107	
3	Unknown	11	25,937	6805087	108729	81,388	79,732	N/A	4059	1,910	1,266	
4	Unknown	11	29,137	368302	5898	4,405	4,325	N/A	4529	N/A	1,108	

(Z)-4-(cyclohexylmethylene)-1-phenyl-2-((trifluoromethyl)sulfonyl)-1,2,3,4-tetrahydroisoquinoline (3gf)

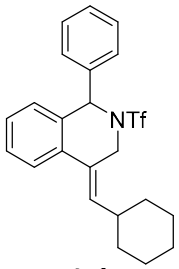

3gf

Method A: (58.9 mg, 81% yield), obtained as a transparent oil. **^{1}H NMR** (300 MHz, $CDCl_3$) δ 7.65 (d, *J* = 8.0 Hz, 1H), 7.29 – 7.09 (m, 7H), 6.98 (d, *J* = 7.1 Hz, 1H), 6.07 (s, 1H), 5.97 (d, *J* = 9.6 Hz, 1H), 4.60 (d, *J* = 16.6 Hz, 1H), 3.80 (d, *J* = 16.6 Hz, 1H), 2.23 – 2.01 (m, 1H), 1.76 – 0.89 (m, 10H). **^{19}F NMR** (282 MHz, $CDCl_3$) δ -76.64. **^{13}C NMR** (75 MHz, $CDCl_3$) δ 138.3 (C), 133.2 (C), 132.9 (CH), 128.83 (CH), 128.76 (CH), 128.6 (CH), 128.4 (CH), 128.0 (CH), 127.4 (CH), 125.0 (C), 123.9 (CH), 119.8 (q, *J* = 323.2 Hz, C), 61.2 (CH), 42.3 (CH_2), 37.1 (CH), 32.7 (CH_2), 32.6 (CH_2), 26.0 (CH_2), 25.8 (CH_2), 25.8 (CH_2). **HRMS** [ESI]: *m/z* calculated for $C_{23}H_{25}F_3NO_2S$ $[M+H]^+$: 436.1553, found 436.1550.

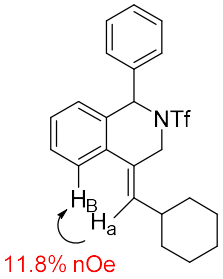

Assignment of stereochemistry based on the observed nOe between the H_a (5.97 ppm, 100%) with H_b (7.65 ppm, 11.8%).

Enantioselectivity was determined by chiral SFC analysis on Phenomenex Cellulose-1 at 40 °C (CO_2 : MeOH = 98:02, 1 mL/min).

Racemic sample

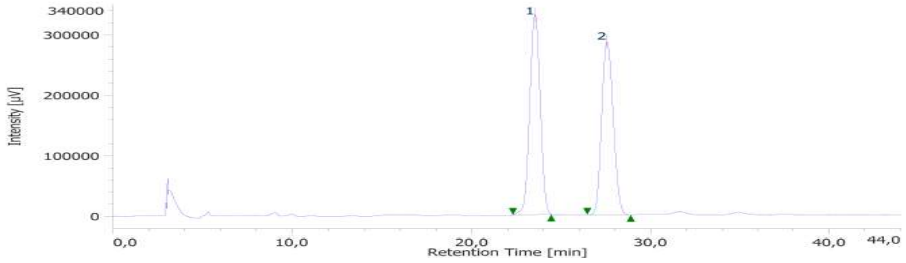

Channel Name 210,0nm Sampling Interval 200 [msec]

#	Peak Name	CH	tR [min]	Area [μV·sec]	Height [μV]	Area%	Height%	Quantity	NTP	Resolution	Symmetry Factor	Warning
1	Unknown	5	23,537	13523659	330453	51,207	53,629	N/A	7432	3,505	0,995	
2	Unknown	5	27,570	12886049	285726	48,793	46,371	N/A	8227	N/A	1,115	

Asymmetric sample (93 : 7 er)

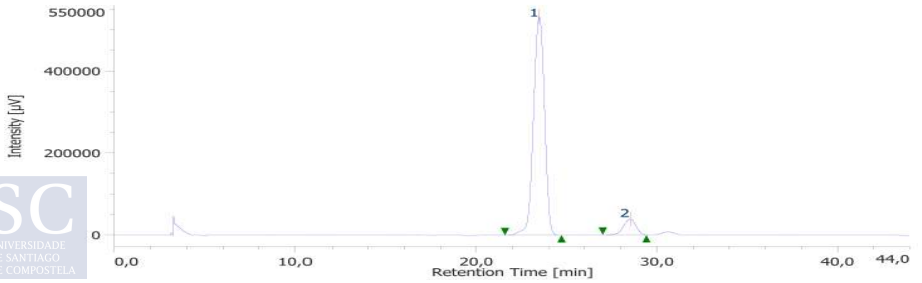

Channel Name 210,0nm Sampling Interval 200 [msec]

#	Peak Name	CH	tR [min]	Area [μV·sec]	Height [μV]	Area%	Height%	Quantity	NTP	Resolution	Symmetry Factor	Warning
1	Unknown	5	23,467	22591968	532175	92,535	93,358	N/A	6934	4,194	0,959	
2	Unknown	5	28,507	1822624	37862	7,465	6,642	N/A	7906	N/A	0,912	

4-cyclohexylidene-8-methyl-1-(*o*-tolyl)-2-((trifluoromethyl)sulfonyl)-1,2,3,4-tetrahydroisoquinoline (3ha)

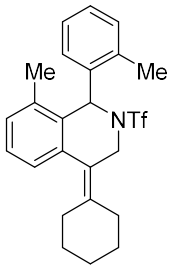

3ha

Method B: (44.9 mg, 66% yield), obtained as a white solid. Mp: 145-147 °C. **^{1}H NMR** (300 MHz, $CDCl_3$) δ 7.20 – 7.08 (m, 4H), 7.03 (d, *J* = 6.9 Hz, 1H), 6.88 (t, *J* = 7.0 Hz, 1H), 6.74 (d, *J* = 7.8 Hz, 1H), 6.29 (s, 1H), 4.41 (d, *J* = 16.4 Hz, 1H), 3.84 (d, *J* = 16.4 Hz, 1H), 2.55 (s, 3H), 2.28 (t, *J* = 11.7 Hz, 1H), 2.15 (s, 3H), 2.04 – 1.75 (m, 2H), 1.65 – 1.26 (m, 7H). **^{19}F NMR** (282 MHz, $CDCl_3$) δ -75.78. **^{13}C NMR** (75 MHz, $CDCl_3$) δ 138.7 (C), 136.5 (C), 134.4 (C), 134.1 (C), 131.9 (C), 131.5 (CH), 130.0 (CH), 128.9 (CH), 128.5 (CH), 128.2 (CH), 127.3 (CH), 125.6 (CH), 121.0 (C), 119.6 (d, *J* = 325.2 Hz, C), 57.9 (CH), 46.2 (CH_2), 32.4 (CH_2), 30.8 (CH_2), 28.1 (CH_2), 26.9 (CH_2), 26.6 (CH_2), 20.5 (CH_3), 18.6 (CH_3). **HRMS** [ESI]: *m/z* calculated for $C_{24}H_{27}F_3NO_2S$ $[M+H]^+$: 450.1709, found 450.1715.

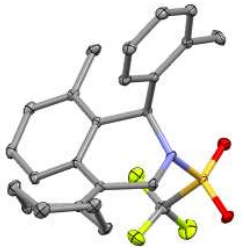

The structure of this compound was confirmed by X-Ray diffraction analysis (CCDC: 1877409).

Enantioselectivity was determined by chiral HPLC analysis on Chiralpak IB at rt (Hexane, 0.5 mL/min).

Racemic sample

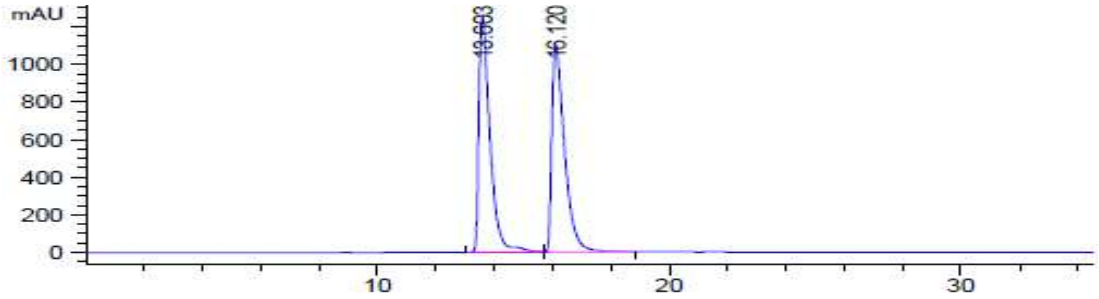

Signal 2: DAD1 B, Sig=254,4 Ref=off

Peak #	RetTime [min]	Type	Width [min]	Area [mAU*s]	Height [mAU]	Area %
1	13.603	BV R	0.3945	3.35972e4	1252.76074	50.2071
2	16.120	VB	0.4492	3.33200e4	1100.64124	49.7929
Totals :				6.69172e4	2353.40198	

Asymmetric sample (97 : 3 er)

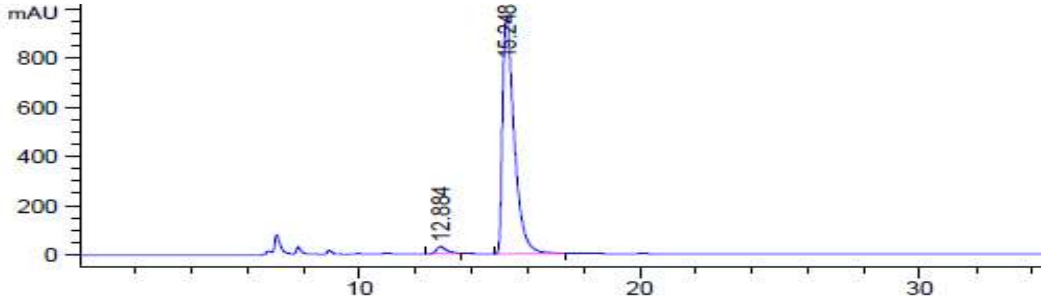

Signal 2: DAD1 B, Sig=254,4 Ref=off

Peak #	RetTime [min]	Type	Width [min]	Area [mAU*s]	Height [mAU]	Area %
1	12.884	BB	0.3744	776.70538	30.16767	2.7075
2	15.248	BB	0.4320	2.79104e4	969.03998	97.2925
Totals :				2.86871e4	999.20765	

(*Z*)-4-(cyclohexylmethylene)-8-methyl-1-(*o*-tolyl)-2-((trifluoromethyl)sulfonyl)-1,2,3,4-tetrahydroisoquinoline (3hf)

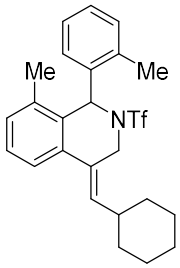

3hf

Method B: (73.5 mg, 95% yield), obtained as a transparent oil. **^{1}H NMR** (300 MHz, $CDCl_3$) δ 7.52 (d, *J* = 8.0 Hz, 1H), 7.22 – 7.07 (m, 3H), 7.03 – 6.83 (m, 2H), 6.65 (d, *J* = 7.8 Hz, 1H), 6.30 (s, 1H), 5.97 (d, *J* = 9.7 Hz, 1H), 4.61 (d, *J* = 17.6 Hz, 1H), 3.88 (d, *J* = 17.6 Hz, 1H), 2.57 (s, 3H), 2.05 (m, 1H), 1.98 (s, 3H), 1.77 – 1.53 (m, 4H), 1.49 – 1.38 (m, 1H), 1.24 – 1.01 (m, 5H). **^{19}F NMR** (282 MHz, $CDCl_3$) δ -75.74. **^{13}C NMR** (75 MHz, $CDCl_3$) δ 138.4 (C), 134.3 (C), 133.6 (C), 133.4 (C), 132.9 (C), 132.6 (CH), 131.7 (CH), 129.7 (CH), 129.3 (CH), 129.0 (CH), 128.1 (CH), 125.9 (C), 125.8 (CH), 121.5 (CH), 119.7 (d, *J* = 324.8 Hz, C), 56.5 (CH), 42.9 (CH_2), 37.2 (CH), 32.6 (CH_2), 32.3 (CH_2), 26.0 (CH_2), 25.9 (CH_2), 25.8 (CH_2), 20.0 (CH_3), 18.7 (CH_3). **HRMS** [ESI]: *m/z* calculated for $C_{25}H_{29}F_3NO_2S$ $[M+H]^+$: 464.1866, found 464.1862. Assignment of stereochemistry based on the observed nOe between the H_a (5.97 ppm, 100%) with H_b (7.52 ppm, 13.1%).

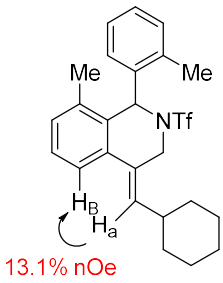

Enantioselectivity was determined by chiral SFC analysis on Phenomenex Cellulose-1 at 40 °C (CO_2 : MeOH = 99:01, 1 mL/min).

Racemic sample

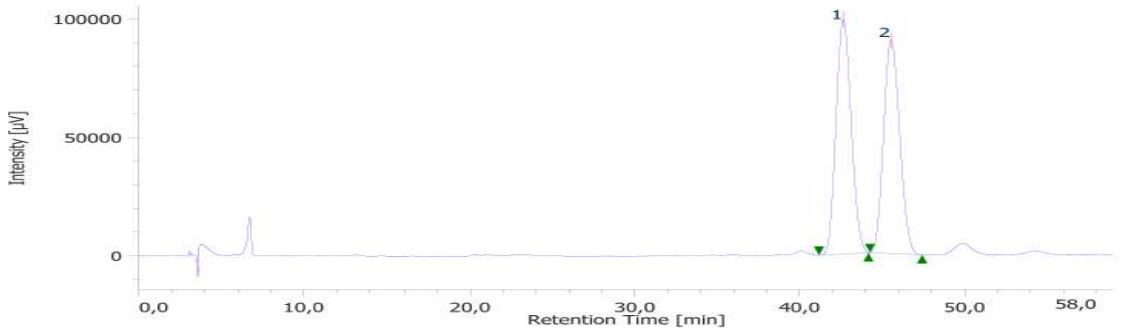

Channel Name 222,0nm Sampling Interval 200 [msec]

#	Peak Name	CH	tR [min]	Area [μV·sec]	Height [μV]	Area%	Height%	Quantity	NTP	Resolution	Symmetry Factor	Warning
1	Unknown	10	42,633	6308646	98969	50,828	52,326	N/A	9955	1,647	1,094	
2	Unknown	10	45,530	6103049	90169	49,172	47,674	N/A	10037	N/A	1,121	

Asymmetric sample (98 : 2 er)

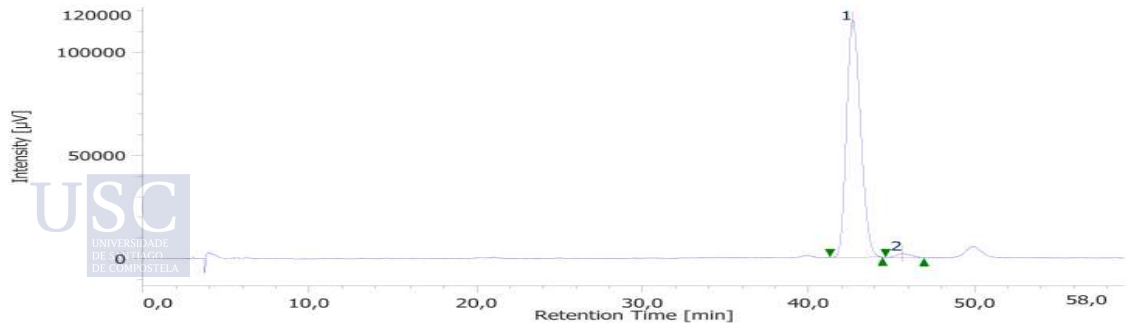

Channel Name 222,0nm Sampling Interval 200 [msec]

#	Peak Name	CH	tR [min]	Area [μV·sec]	Height [μV]	Area%	Height%	Quantity	NTP	Resolution	Symmetry Factor	Warning
1	Unknown	10	42,663	6737805	114745	98,233	98,191	N/A	11900	1,881	1,194	
2	Unknown	10	45,673	121172	2115	1,767	1,809	N/A	12349	N/A	1,267	

4-cyclohexylidene-6-methyl-1-(*p*-tolyl)-2-((trifluoromethyl)sulfonyl)-1,2,3,4-tetrahydroisoquinoline (3ia)

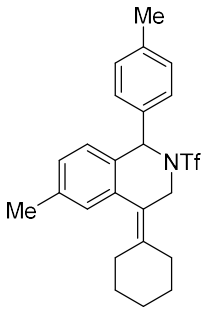

3ia

Method A: (71.2 mg, 95% yield), obtained as a transparent oil. **^{1}H NMR** (300 MHz, $CDCl_3$) δ 7.22 – 6.87 (m, 7H), 5.85 (s, 1H), 4.35 (d, *J* = 13.5 Hz, 1H), 4.08 (d, *J* = 14.0 Hz, 1H), 2.31 (s, 4H), 2.24 (s, 3H), 2.12 (d, *J* = 13.0 Hz, 2H), 1.90 (t, *J* = 11.6 Hz, 1H), 1.53 – 1.28 (m, 4H), 0.96 (brs, 2H). **^{19}F NMR** (282 MHz, $CDCl_3$) δ -75.16. **^{13}C NMR** (75 MHz, $CDCl_3$) δ 140.4 (C), 137.4 (C), 137.4 (C), 135.9 (C), 134.9 (C), 134.5 (C), 130.3 (CH), 129.0 (CH), 127.8 (CH), 127.4 (CH), 127.1 (CH), 120.2 (d, *J* = 324.2 Hz, C), 120.0 (C), 62.1 (CH), 46.3 (CH_2), 32.0 (CH_2), 30.7 (CH_2), 27.9 (CH_2), 27.3 (CH_2), 26.5 (CH_2), 21.6 (CH_3), 21.1 (CH_3). **HRMS** [ESI]: *m/z* calculated for $C_{24}H_{27}F_3NO_2S$ $[M+H]^+$: 450.1709, found 450.1707.

Enantioselectivity was determined by chiral SFC analysis on Phenomenex Cellulose-1 at 40 °C (CO_2 : MeOH = 98:02, 1 mL/min).

Racemic sample

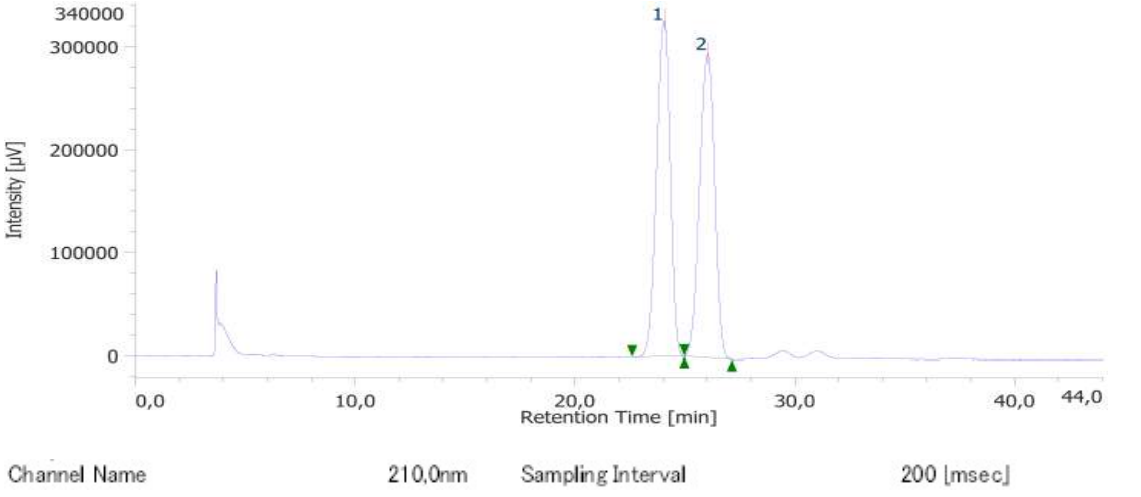

#	Peak Name	CH	tR [min]	Area [μV·sec]	Height [μV]	Area%	Height%	Quantity	NTP	Resolution	Symmetry Factor	Warning
1	Unknown	5	24,047	14221311	326263	50,358	52,512	N/A	6651	1,611	0,913	
2	Unknown	5	26,030	14019082	295054	49,642	47,488	N/A	6526	N/A	0,935	

Asymmetric sample (94 : 6 er)

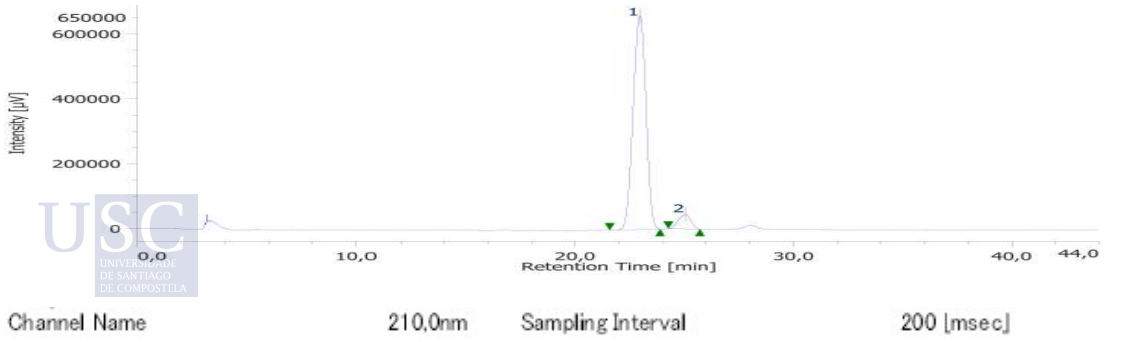

#	Peak Name	CH	tR [min]	Area [μV·sec]	Height [μV]	Area%	Height%	Quantity	NTP	Resolution	Symmetry Factor	Warning
1	Unknown	5	22,953	26775063	657766	93,968	93,772	N/A	6934	1,893	0,955	
2	Unknown	5	25,017	1718772	43685	6,032	6,228	N/A	8536	N/A	0,941	

6-methyl-4-(nonan-5-ylidene)-1-(p-tolyl)-2-((trifluoromethyl)sulfonyl)-1,2,3,4-tetrahydroisoquinoline (3ib)

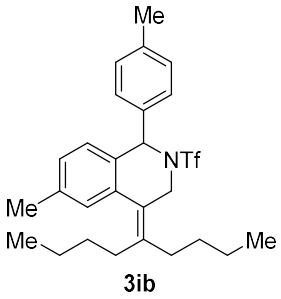

3ib

Method A: (76.2 mg, 92% yield), obtained as a white solid. Mp: 56-58 °C. **^{1}H NMR** (300 MHz, $CDCl_3$) δ 7.20 – 6.89 (m, 7H), 5.84 (s, 1H), 4.25 (d, *J* = 13.8 Hz, 1H), 4.08 (d, *J* = 14.0 Hz, 1H), 2.32 (s, 3H), 2.20 (s, 3H), 1.91 – 1.76 (m, 3H), 1.31 – 1.11 (m, 7H), 1.11 – 0.97 (m, 2H), 0.80 (t, *J* = 6.9 Hz, 3H), 0.71 (t, *J* = 7.1 Hz, 3H). **^{19}F NMR** (282 MHz, $CDCl_3$) δ -75.52. **^{13}C NMR** (75 MHz, $CDCl_3$) δ 141.4 (C), 137.50 (C), 137.46 (C), 135.4 (C), 135.0 (C), 134.1 (C) 129.7 (CH), 129.0 (CH), 127.7 (CH), 127.4 (CH), 127.0 (CH), 122.7 (C), 120.1 (d, *J* = 324.4 Hz, C), 62.0 (CH), 46.6 (CH_2), 32.9 (CH_2), 31.2 (CH_2), 31.1 (CH_2), 29.7 (CH_2), 23.00 (CH_2), 22.97 (CH_2), 21.6 (CH_3), 21.1 (CH_3), 14.2 (CH_3), 14.1 (CH_3). **HRMS** [ESI]: calculated for $C_{27}H_{35}F_3NO_2S$ $[M+H]^+$: 494.2335, found 494.2337.

Enantioselectivity was determined by chiral SFC analysis on Phenomenex Cellulose-2 at 40 °C (CO_2 : MeOH = 98:02, 1 mL/min).

Racemic sample

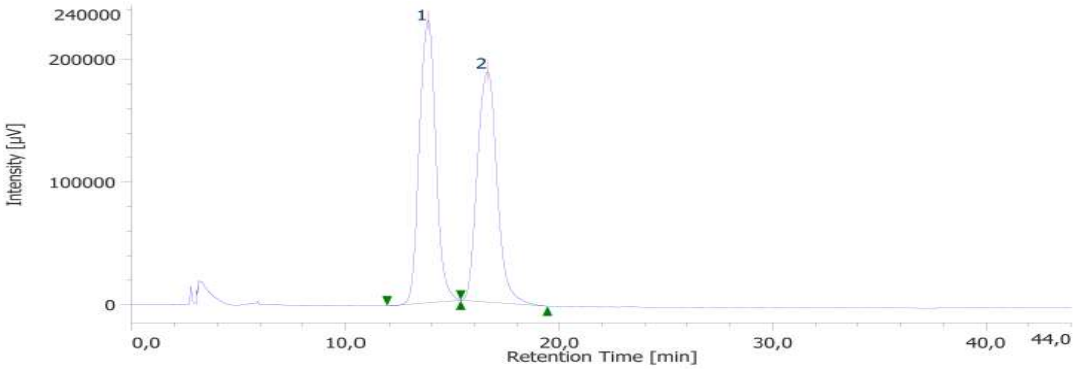

Channel Name 210,0nm Sampling Interval 200 [msec]

#	Peak Name	CH	tR [min]	Area [μV·sec]	Height [μV]	Area%	Height%	Quantity	NTP	Resolution	Symmetry Factor	Warning
1	Unknown	5	13,827	12282853	229944	50,397	55,069	N/A	1512	1,783	1,054	
2	Unknown	5	16,610	12089469	187611	49,603	44,931	N/A	1512	N/A	1,130	

Asymmetric sample (95 : 5 er)

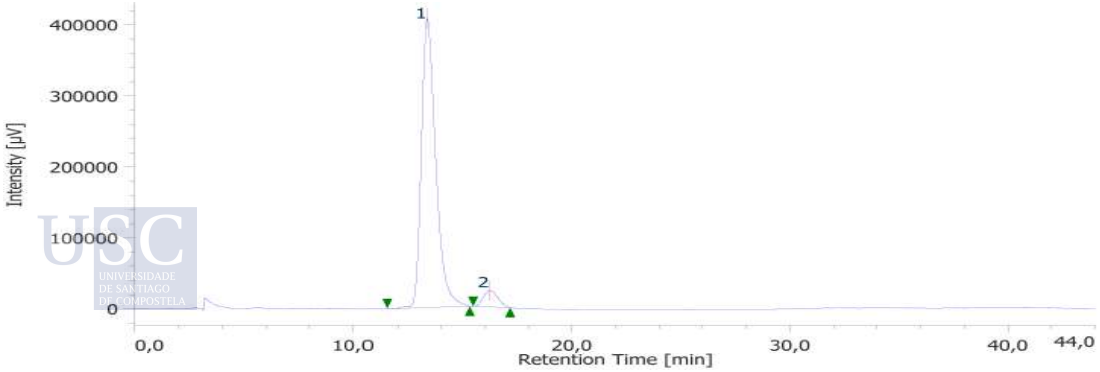

Channel Name 210,0nm Sampling Interval 200 [msec]

#	Peak Name	CH	tR [min]	Area [μV·sec]	Height [μV]	Area%	Height%	Quantity	NTP	Resolution	Symmetry Factor	Warning
1	Unknown	5	13,347	18751014	406458	94,741	94,670	N/A	2063	2,378	1,411	
2	Unknown	5	16,220	1040795	22882	5,259	5,330	N/A	2705	N/A	1,149	

6-chloro-1-(4-chlorophenyl)-4-cyclohexylidene-2-((trifluoromethyl)sulfonyl)-1,2,3,4-tetrahydroisoquinoline(3ja)

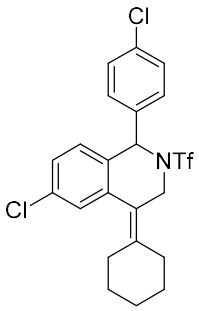

3ja

Method A: (75.9 mg, 93% yield), obtained as a white solid. Mp: 47-49 °C. **^{1}H NMR** (300 MHz, $CDCl_3$) δ 7.27 – 6.97 (m, 7H), 5.86 (s, 1H), 4.36 (d, *J* = 13.5 Hz, 1H), 4.07 (d, *J* = 13.8 Hz, 1H), 2.39 – 2.22 (m, 1H), 2.22 – 2.03 (m, 2H), 2.03 – 1.84 (m, 1H), 1.56 – 1.30 (m, 4H), 1.08 – 0.84 (m, 2H). **^{19}F NMR** (282 MHz, $CDCl_3$) δ -75.38. **^{13}C NMR** (75 MHz, $CDCl_3$) δ 142.7 (C), 136.8 (C), 135.2 (C), 134.1 (C), 134.0 (C), 129.8 (CH), 128.70 (CH), 128.65 (CH), 128.5 (CH), 127.4 (CH), 120.0 (q, *J* = 324.0 Hz, C), 118.7 (C), 77.4 (CH), 61.2 (CH_2), 46.1 (CH_2), 31.9 (CH_2), 30.7 (CH_2), 27.9 (CH_2), 27.3 (CH_2), 26.2 (CH_2). **HRMS** [ESI]: *m/z* calculated for $C_{22}H_{21}Cl_2F_3NO_2S$ $[M+H]^+$: 490.0617, found 490.0616.

Enantioselectivity was determined by chiral SFC analysis on Phenomenex i-Cellulose-5 at 40 °C (CO_2 : MeOH = 97:03, 0.5 mL/min).

Racemic sample

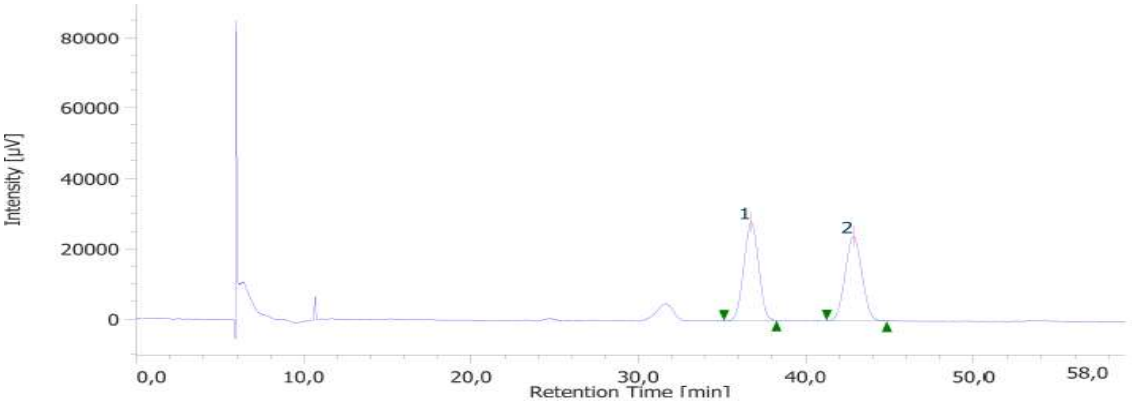

Channel Name 254,0nm Sampling Interval 200 [msec]

#	Peak Name	CH	tR [min]	Area [μV·sec]	Height [μV]	Area%	Height%	Quantity	NTP	Resolution	Symmetry Factor	Warning
1	Unknown	11	36,737	1718634	27961	50,611	53,843	N/A	7956	3,486	1,000	
2	Unknown	11	42,853	1677171	23970	49,389	46,157	N/A	8392	N/A	1,024	

Asymmetric sample (91 : 9 er)

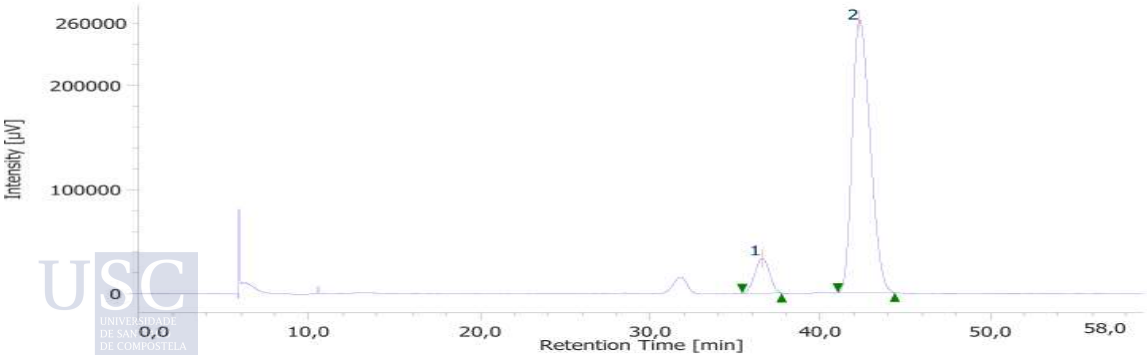

Channel Name 254,0nm Sampling Interval 200 [msec]

#	Peak Name	CH	tR [min]	Area [μV·sec]	Height [μV]	Area%	Height%	Quantity	NTP	Resolution	Symmetry Factor	Warning
1	Unknown	11	36,557	2014371	33391	9,462	11,308	N/A	7997	3,192	1,018	
2	Unknown	11	42,313	19274230	261900	90,538	88,692	N/A	7299	N/A	1,258	

6-chloro-1-(4-chlorophenyl)-4-(nonan-5-ylidene)-2-((trifluoromethyl)sulfonyl)-1,2,3,4-tetrahydroisoquinoline (3jb)

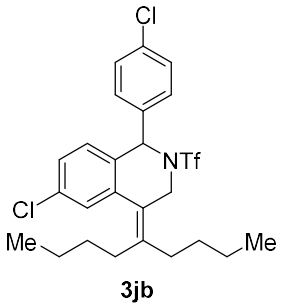

3jb

Method A: (76.8 mg, 86% yield), obtained as a transparent oil. **^{1}H NMR** (300 MHz, $CDCl_3$) δ 7.29 – 7.10 (m, 5H), 7.01 – 6.94 (m, 2H), 5.84 (s, 1H), 4.26 (d, *J* = 14.0 Hz, 1H), 4.08 (d, *J* = 14.0 Hz, 1H), 2.17 – 2.00 (m, 1H), 1.93 – 1.78 (m, 3H), 1.26 – 0.87 (m, 8H), 0.86 – 0.69 (m, 6H). **^{19}F NMR** (282 MHz, $CDCl_3$) δ -75.39. **^{13}C NMR** (75 MHz, $CDCl_3$) δ 143.9 (C), 136.9 (C), 136.4 (C), 134.8 (C), 134.2 (C), 134.1 (C), 129.3 (CH), 128.7 (CH), 128.7 (CH), 128.4 (CH), 127.4 (CH), 121.4 (C), 120.1 (d, *J* = 324.4 Hz, C), 61.2 (CH), 46.3 (CH_2), 32.9 (CH_2), 31.4 (CH_2), 30.1 (CH_2), 29.8 (CH_2), 22.95 (CH_2), 22.92 (CH_2), 14.1 (CH_3), 14.0 (CH_3). **HRMS** [ESI]: *m/z* calculated for $C_{25}H_{29}Cl_2F_3NO_2S$ $[M+H]^+$: 534.1243, found 534.1237.

Enantioselectivity was determined by chiral SFC analysis on Phenomenex i-Cellulose-5 at 40 °C (CO_2 : MeOH = 96:04, 0.5 mL/min).

Racemic sample

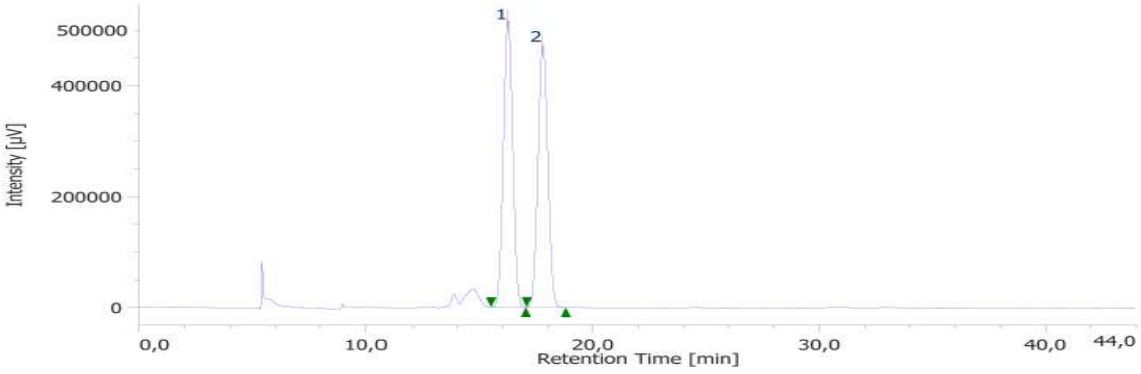

Channel Name 220,0nm Sampling Interval 200 [msec]

#	Peak Name	CH	tR [min]	Area [μV·sec]	Height [μV]	Area%	Height%	Quantity	NTP	Resolution	Symmetry Factor	Warning
1	Unknown	5	16,227	14829939	517718	50,967	52,294	N/A	7113	1,955	1,014	
2	Unknown	5	17,767	14266975	472301	49,033	47,706	N/A	7697	N/A	1,039	

Asymmetric sample (91 : 9 er)

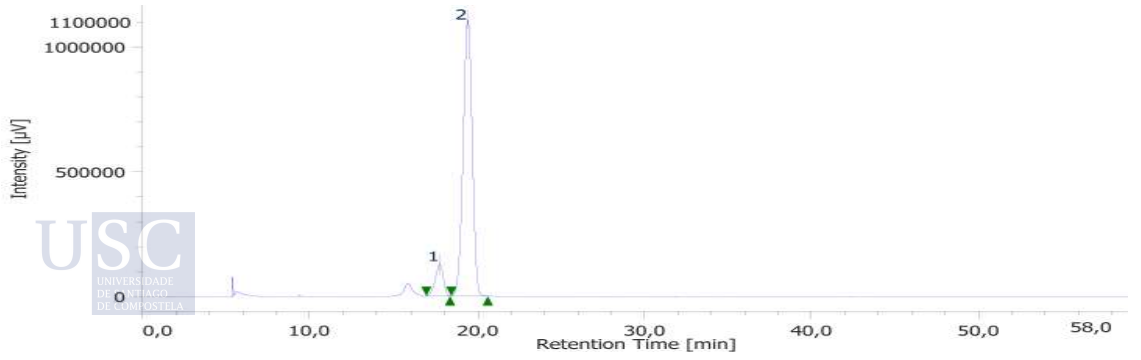

Channel Name 220,0nm Sampling Interval 200 [msec]

#	Peak Name	CH	tR [min]	Area [μV·sec]	Height [μV]	Area%	Height%	Quantity	NTP	Resolution	Symmetry Factor	Warning
1	Unknown	5	17,717	4367855	127345	9,485	10,328	N/A	6027	1,751	0,866	
2	Unknown	5	19,387	41683416	1105637	90,515	89,672	N/A	6021	N/A	0,959	

4-cyclohexylidene-6-methoxy-1-(4-methoxyphenyl)-2-((trifluoromethyl)sulfonyl)-1,2,3,4-tetrahydroisoquinoline (3ka)

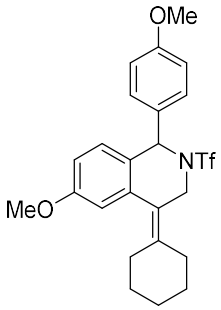

3ka

Method A: (74.8 mg, 93% yield), obtained as a yellow oil. **^{1}H NMR** (300 MHz, $CDCl_3$) δ 7.13 – 7.06 (m, 1H), 7.03 – 6.98 (m, 2H), 6.78 – 6.68 (m, 4H), 5.85 (s, 1H), 4.30 (d, *J* = 13.7 Hz, 1H), 4.10 (d, *J* = 13.8 Hz, 1H), 3.76 (s, 3H), 3.69 (s, 3H), 2.53 – 1.78 (m, 4H), 1.56 – 1.31 (m, 4H), 1.13 – 0.95 (m, 2H). **^{19}F NMR** (282 MHz, $CDCl_3$) δ -75.59. **^{13}C NMR** (75 MHz, $CDCl_3$) δ 159.2 (C), 158.9 (C), 140.8 (C), 136.2 (C), 131.0 (C), 129.8 (C), 128.8 (CH), 128.2 (CH), 120.1 (d, *J* = 324.0 Hz, C), 120.0 (C), 115.6 (CH), 113.7 (CH), 112.1 (CH), 61.5 (CH), 55.5 (CH_3), 55.4 (CH_3), 46.0 (CH_2), 32.0 (CH_2), 30.8 (CH_2), 27.9 (CH_2), 27.4 (CH_2), 26.4 (CH_2). **HRMS** [ESI]: *m/z* calculated for $C_{24}H_{27}F_3NO_4S$ $[M+H]^+$: 482.1607, found 482.1612.

Enantioselectivity was determined by chiral SFC analysis on Phenomenex Cellulose-1 at 40 °C (CO_2 : MeOH = 95:05, 1 mL/min).

Racemic sample

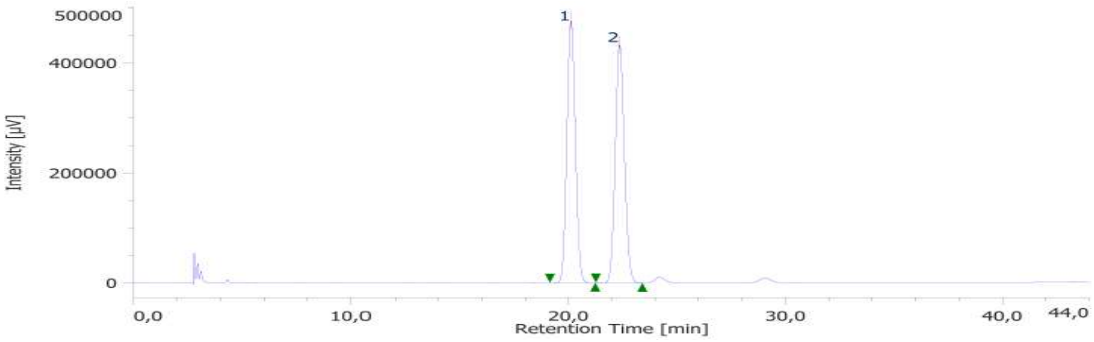

Channel Name 222,0nm Sampling Interval 200 [msec]

#	Peak Name	CH	tR [min]	Area [μV·sec]	Height [μV]	Area%	Height%	Quantity	NTP	Resolution	Symmetry Factor	Warning
1	Unknown	10	20,093	12979419	476051	50,142	52,401	N/A	12311	2,976	1,087	
2	Unknown	10	22,343	12905703	432425	49,858	47,599	N/A	12735	N/A	1,088	

Asymmetric sample (94 : 6 er)

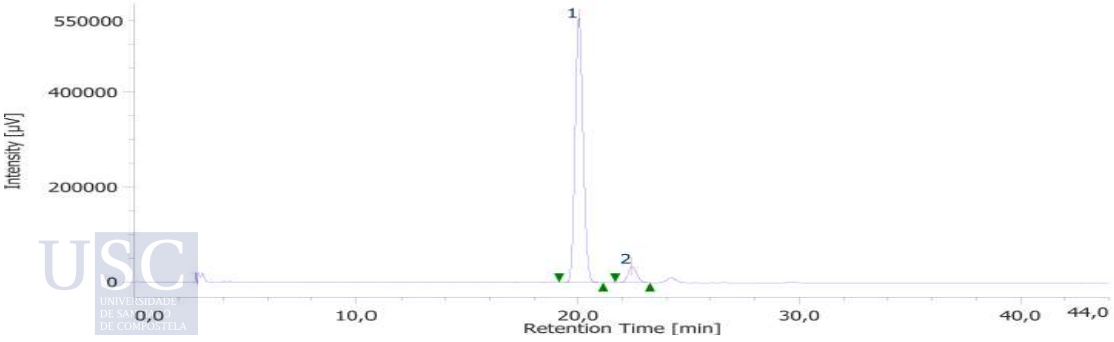

Channel Name 222,0nm Sampling Interval 200 [msec]

#	Peak Name	CH	tR [min]	Area [μV·sec]	Height [μV]	Area%	Height%	Quantity	NTP	Resolution	Symmetry Factor	Warning
1	Unknown	10	20,017	13956839	557304	93,685	94,256	N/A	14680	3,483	1,127	
2	Unknown	10	22,437	940851	33965	6,315	5,744	N/A	15014	N/A	1,098	

4-cyclohexylidene-7-methoxy-1-(3-methoxyphenyl)-2-((trifluoromethyl)sulfonyl)-1,2,3,4-tetrahydroisoquinoline (3la)

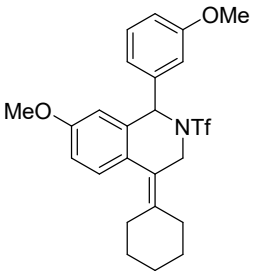

3la

Method A: (72.4 mg, 90% yield), obtained as a white solid. Mp: 125-127 °C. **^{1}H NMR** (500 MHz, $CDCl_3$) δ 7.13 (d, *J* = 8.4 Hz, 1H), 7.11 – 7.08 (m, 1H), 6.82 (dd, *J* = 8.4, 2.7 Hz, 1H), 6.75 (d, *J* = 2.7 Hz, 1H), 6.72 – 6.70 (m, 1H), 6.70 – 6.68 (m, 1H), 6.68 – 6.65 (m, 1H), 5.83 (s, 1H), 4.34 (d, *J* = 13.6 Hz, 1H), 4.11 (d, *J* = 12.7 Hz, 1H), 3.75 (s, 3H), 3.66 (s, 3H), 2.43 – 2.22 (m, 1H), 2.18 – 2.01 (m, 2H), 2.01 – 1.77 (m, 1H), 1.52 – 1.28 (m, 4H), 1.05 – 0.85 (m, 2H). **^{19}F NMR** (470 MHz, $CDCl_3$) δ -75.58. **^{13}C NMR** (76 MHz, $CDCl_3$) δ 159.8 (C), 158.6 (C), 139.9 (C), 139.4 (C), 138.3 (C), 131.0 (CH), 129.5 (CH), 127.4 (C), 120.1 (d, *J* = 323.9 Hz, C), 119.9 (CH), 119.2 (C), 113.7 (CH), 113.4 (CH), 112.8 (CH), 112.6 (CH), 62.3 (CH), 55.5 (CH_3), 55.4 (CH_3), 46.6 (CH_2), 32.0 (CH_2), 30.6 (CH_2), 27.8 (CH_2), 27.3 (CH_2), 26.5 (CH_2). **HRMS** [ESI]: *m/z* calculated for $C_{24}H_{27}F_3NO_4S$ $[M+H]^+$: 482.1607, found 482.1619.

Enantioselectivity was determined by chiral SFC analysis on Phenomenex Amylose-2 at 40 °C (CO_2 : MeOH = 96:04, 0.5 mL/min).

Racemic sample

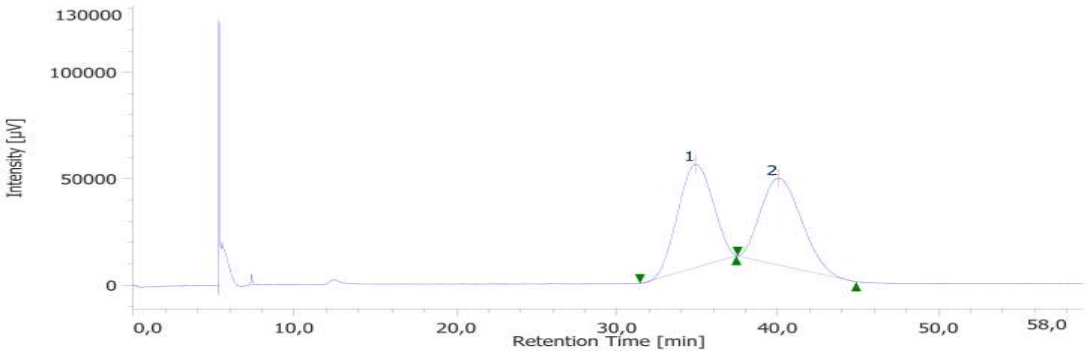

Channel Name 254,0nm Sampling Interval 200 [msec]

#	Peak Name	CH	tR [min]	Area [μV·sec]	Height [μV]	Area%	Height%	Quantity	NTP	Resolution	Symmetry Factor	Warning
1	Unknown	5	34,880	7340802	48615	50,471	54,400	N/A	1114	1,148	0,986	
2	Unknown	5	40,047	7203868	40750	49,529	45,600	N/A	1094	N/A	1,233	

Asymmetric sample (90 :10 er)

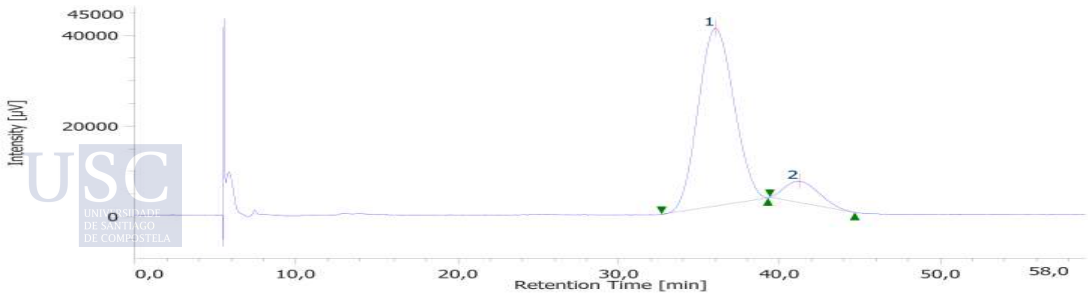

Channel Name 254,0nm Sampling Interval 200 [msec]

#	Peak Name	CH	tR [min]	Area [μV·sec]	Height [μV]	Area%	Height%	Quantity	NTP	Resolution	Symmetry Factor	Warning
1	Unknown	5	36,020	6055247	39232	89,702	89,352	N/A	1185	1,251	1,061	
2	Unknown	5	41,210	695179	4675	10,298	10,648	N/A	1589	N/A	1,321	

2.10 Procedure for the Pd-catalyzed annulation of triflimide 1m (with two different aryl rings) with allene 2a

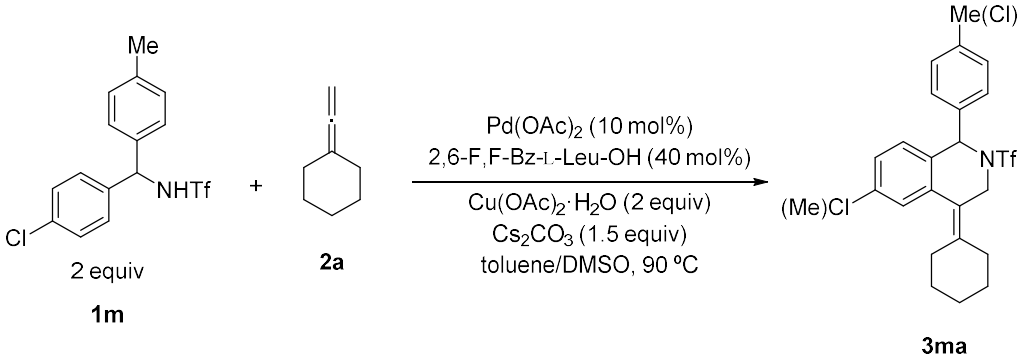

To a solution of $Pd(OAc)_2$ (3.7 mg, 10 mol%), 2,6-F,F-Bz-L-Leu-OH (18.1 mg, 40 mol%), $Cu(OAc)_2{\cdot}H_2O$ (66.7 mg, 2 equiv), Cs_2CO_3 (81.6 mg, 1.5 equiv) and **1m** (121.5 mg, 0.333 mmol, 2 equiv) in toluene (2 mL), under air atmosphere, in a Schlenk tube was added the allene **2a** (18.0 mg, 0.167 mmol). The tube was sealed with a rubber septum and an air atmosphere was injected in the flask with a balloon and a needle. The reaction was heated at 90 °C, stirred during 18 h and then cooled to room temperature. Evaporation and column chromatography on silica gel (hexanes:diethylether; 99:1). Obtained as a 1.6:1 inseparable mixture (70.4 mg, 90% yield, white solid). **^{1}H NMR** (300 MHz, $CDCl_3$) δ 7.31 – 6.87 (m, 8H), 5.88 (s, 0.39H), 5.83 (s, 0.61H), 4.52 – 3.88 (m, 2H), 2.41 – 2.03 (m, 6H), 1.98 – 1.82 (m, 1H), 1.54 – 1.25 (m, 4H), 1.10 – 0.69 (m, 2H). **^{19}F NMR** (282 MHz, $CDCl_3$) δ -75.42. **^{13}C NMR** (75 MHz, $CDCl_3$) δ 141.0 (C), 140.6 (C), 137.9 (C), 137.8 (C), 137.7 (C), 135.0 (C), 133.8 (C), 133.7 (C), 133.5 (C), 130.4 (CH) 129.80 (C), 129.7 (CH), 129.2 (CH), 129.1 (CH), 128.7 (CH), 128.5 (CH), 128.4 (CH), 128.0 (C), 127.8 (C), 127.6 (C), 127.4 (CH), 127.3 8 (CH), 127.1 (CH), 127.1 (CH), 118.8 (d, *J* = 125.7 Hz, C), 61.7 (CH), 61.6 (CH), 46.5 (CH_2), 46.0 (CH_2), 31.94 (CH_2), 31.89 (CH_2), 30.8 (CH_2), 30.6 (CH_2), 27.9 (CH_2), 27.8 (CH_2), 27.4 (CH_2), 27.2 (CH_2), 26.4 (CH_2), 26.3 (CH_2), 21.6 (CH_3), 21.1 (CH_3).

3- Chapter III: Assembly of azaheterocycles by Pd(II)-Catalyzed cycloadditions involving the activation of C(sp^3)–H Bonds

3.1 Synthesis of o-methylanilines

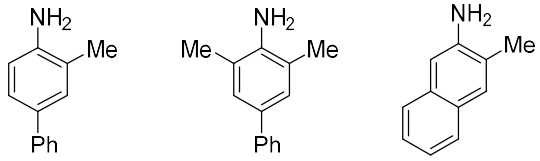

3.1.1 General procedure for the synthesis of 4-phenyl-o-methylanilines

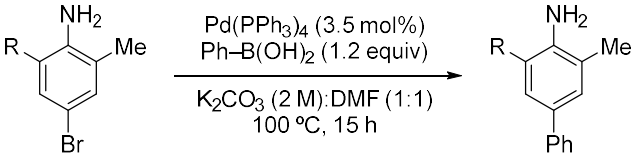

Following a reported procedure,[152] in a purged two-neck round-bottom flask under Ar, the corresponding 4-bromoaniline (1 equiv) was dissolved in the mixture of solvents (K_2CO_3 (2 M) : DMF (1:1), 0.5 M). Then, phenylboronic acid (1.2 equiv) and $Pd(PPh_3)_4$ (3.5 mol%) were added to the solution. The reaction mixture was heated at 100 °C for 15 h. The reaction was then cooled to room temperature. To the solution was added 10 times the amount of water and extracted with ethyl acetate. The organic layer was washed with brine, concentrated under reduced pressure, and purified by column chromatography on silica gel (hexanes:ethyl acetate 80:20 to 50:50) to afford the corresponding 4-phenylanilines.

3-methyl-[1,1'-biphenyl]-4-amine

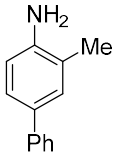

(1.01 g, 86% yield), obtained as a yellow oil. **^{1}H NMR** (300 MHz, $CDCl_3$) δ 7.57 – 7.50 (m, 2H), 7.43 – 7.36 (m, 2H), 7.36 – 7.23 (m, 3H), 6.81 (d, *J* = 7.9 Hz, 1H), 4.29 (brs, 2H), 2.27 (s, 3H). Spectral data in agreement with those found in the literature.[170]

3,5-dimethyl-[1,1'-biphenyl]-4-amine

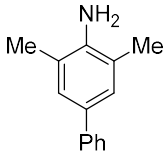

(231 mg, 40% yield), obtained as a colorless oil. **^{1}H NMR** (300 MHz, $CDCl_3$) δ 7.59 – 7.49 (m, 2H), 7.44 – 7.33 (m, 2H), 7.32 – 7.18 (m, 3H), 4.40 (s, 2H), 2.30 (s, 6H). Spectral data in agreement with those found in the literature.[171]

[170] Durgun, G.; Aksin, Ö.; Artok, L. *J. Mol. Catal. A Chem.* **2007**, *278*, 189.
[171] Rayner, P. Norcott, K. M. Appleby, W. Iali, R. O. John, S. J. Hart, A. C. Whitwood, S. B. Duckett, *Nat. Commun.* **2018**, *9*, 1

3.1.2 Procedure for the synthesis of 3-methylnaphthalen-2-amine

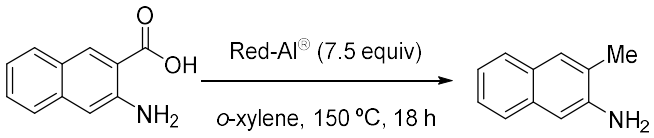

Following a reported procedure,[153] to a solution of 2-amino-3-naphtoic acid (2.34 g, 80% purity, 10.0 mmol) in *o*-xylene was added bis(2-methoxyethoxy)-aluminum dihydride (22.5 mL, 7.5 equiv., 65% wt in toluene) at room temperature under argon atmosphere. The reaction was stirred at 150 °C for 18 h. After that, the reaction was cooled to 0 °C and carefully quenched with a 3M solution of NaOH (aq.). Next, the reaction was filtered through a Celite® pad and eluted with DCM. The filtrate was concentrated under reduced pressure and purified by column chromatography on silica gel (hexanes:ethyl acetate 70:30), affording **3-methylnaphthalen-2-amine** as an orange solid (682 mg, 43% yield). **^{1}H NMR** (300 MHz, $CDCl_3$) δ 7.68 – 7.51 (m, 3H), 7.37 – 7.14 (m, 2H), 3.82 (s, 2H), 2.35 (s, 3H). Spectral data in agreement with those found in the literature.

3.2 Synthesis of o-methylbenzylamines

3.2.1 Procedure for the synthesis of 2-methyl-1-(o-tolyl)propan-1-amine

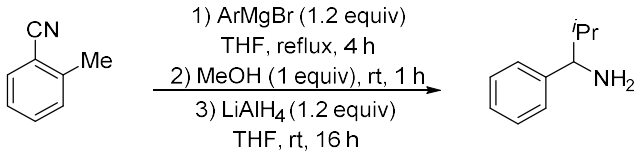

Following a reported procedure,[119] to a solution of isopropylmagnesium bromide (2 M, 6.4 mL, 1.5 equiv) in THF (0.2 M) was added the nitrile (1.00 g, 8.54 mmol) at room temperature, with the resulting mixture being refluxed for 4 h. After cool, anhydrous MeOH (0.35 mL, 1 equiv) was added (vigorous reaction) and the reaction stirred for 1 h at rt. Then, $LiAlH_4$ (0.65 g, 2 equiv) was added, and the reaction was stirred overnight at rt. After that, the reaction was quenched with the careful addition of water. The aqueous layer was extracted with diethyl ether three times. The combined organic phases were washed with $NaHCO_3$ (sat.) and dried over Na_2SO_4. The crude was used in the next step without further purification.

3.2.2 General procedure for the synthesis of α-substituted o-methylbenzylamines

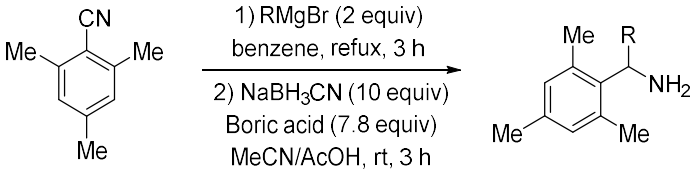

Following a reported procedure,[156] to a solution of the Grignard reagent (2 equiv) in benzene (1.5 M) under Ar was added the nitrile (1 equiv) at room temperature, with the resulting mixture being refluxed for 3 h. After that, the reaction was cooled to 0 °C and quenched with the careful

addition of NH_4Cl (sat). The aqueous layer was extracted with DCM. The combined organic phases were washed with aqueous brine and dried over Na_2SO_4. The crude was purified by column chromatography (hexanes:ethyl acetate 60:40) affording the corresponding bench-stable imine, which was used directly in the next step of the synthesis.

The imine synthesized in the previous step (1 equiv) was dissolved, under Ar atmosphere, in acetonitrile (1.5 M). To this stirred solution was added sodium cyanoborohydride (10 equiv) dissolved in acetonitrile (1.5 M), followed by boric acid (7.8 equiv). A mixture of glacial acetic acid (3.5 equiv) and acetonitrile (1:1) was slowly added to the reaction mixture, followed by another dose of the same mixture after 2 h. After 1 h, the reaction was cooled to 0 °C and carefully quenched with an aqueous solution of NaOH (60% wt). The aqueous layer was extracted with $CHCl_3$. The combined organic phases were washed with $NaHCO_3$ (sat.) and dried over Na_2SO_4. The crude was used for the next step without further purification.

3.3 General procedure for the synthesis of triflyl-protected o-methylanilines and o-methylbenzylamines from the precursor amines, exemplified for 4a

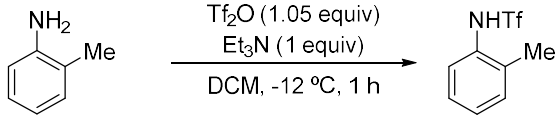

4a

To a solution of *o*-toludine (2.00 g, 18.66 mmol) in dichloromethane (37 mL) under argon atmosphere was added triethylamine (2.6 mL, 1 equiv) at -12 ℃. After the solution was stirred 5 minutes at that temperature, trifluoromethanesulfonic anhydride (3.3 mL, 1.05 equiv) was added dropwise. The reaction was stirred for 1 h at that temperature before being quenched with water. The organic layer was separated and the aqueous layer extracted with dichloromethane. The combined organic phases were washed with brine and then dried over Na_2SO_4. Evaporation and column chromatography on silica gel (hexanes:diethylether; 80:20) afforded **1,1,1-trifluoro-N-(o-tolyl)methanesulfonamide** (**4a**) as a pale yellow solid (3.61 g, 81% yield). **^{1}H NMR** (300 MHz, $CDCl_3$) δ 7.44 – 7.36 (m, 1H), 7.29 – 7.19 (m, 3H), 6.71 (brs, 1H), 2.38 (s, 3H). **^{19}F NMR** (282 MHz, $CDCl_3$) δ -76.50. **^{13}C NMR** (75 MHz, $CDCl_3$) δ 133.9 (C), 132.1 (C), 131.4 (CH), 128.6 (CH), 127.4 (CH), 126.4 (CH), 119.9 (d, *J* = 322.3 Hz, C), 17.9 (CH_3). **HRMS** [APCI]: *m/z* calculated for $C_8H_8F_3NO_2S$ $[M]^+$: 239.0222, found 239.0225. Data in agreement with those reported in literature.[172]

1,1,1-Trifluoro-*N*-(3-methoxy-2-methylphenyl)methanesulfonamide (4b)

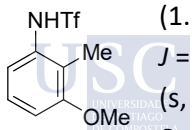

4b

(1.28 g, 81% yield), obtained as a white solid. **^{1}H NMR** (300 MHz, $CDCl_3$) δ 7.19 (t, *J* = 8.0 Hz, 1H), 7.02 (d, *J* = 8.1 Hz, 1H), 6.85 (d, *J* = 8.2 Hz, 1H), 6.57 (brs, 1H), 3.84 (s, 3H), 2.22 (s, 3H). **^{19}F NMR** (282 MHz, $CDCl_3$) δ -76.41. **^{13}C NMR** (75 MHz, $CDCl_3$) δ 158.4 (C), 132.7 (C), 127.0 (CH), 123.3 (C), 119.9 (d, *J* = 322.4 Hz, C), 118.6 (CH), 110.2 (CH), 55.9 (CH_3), 10.7 (CH_3). **HRMS** [APCI]: *m/z* calculated for $C_9H_{11}F_3NO_3S$ $[M+H]^+$: 270.0406, found 270.0407.

[172] J. Wang, F. Li, W. Pei, M. Yang, Y. Wu, D. Ma, F. Zhang, J. Wang, *Tetrahedron Lett.* **2018**, 59, 1902.

_N_-(3-Chloro-2-methylphenyl)-1,1,1-trifluoromethanesulfonamide (4c)

4c

(1.70 g, 88% yield), obtained as a white solid. **^{1}H NMR** (300 MHz, $CDCl_3$) δ 7.40 (d, *J* = 8.0 Hz, 1H), 7.33 (d, *J* = 8.0 Hz, 1H), 7.18 (t, *J* = 8.0 Hz, 1H), 6.77 (brs, 1H), 2.43 (s, 3H). **^{19}F NMR** (282 MHz, $CDCl_3$) δ -76.20. **^{13}C NMR** (75 MHz, $CDCl_3$) δ 135.9 (C), 133.2 (C), 133.1 (C), 129.8 (CH), 127.5 (CH), 125.6 (CH), 119.8 (d, *J* = 322.2 Hz, C), 15.4 (CH_3). **HRMS** [APCI]: *m/z* calculated for $C_8H_7ClF_3NO_2S$ $[M]^+$: 272.9833, found 272.9832.

1,1,1-trifluoro-N-(2-methyl-3-(trifluoromethyl)phenyl)methanesulfonamide (4d)

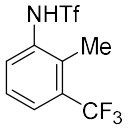

4d

(0.65 g, 64% yield), obtained as a white solid. **^{1}H NMR** (300 MHz, $CDCl_3$) δ 7.67 (d, *J* = 7.9 Hz, 1H), 7.61 (d, *J* = 8.1 Hz, 1H), 7.37 (t, *J* = 8.0 Hz, 1H), 2.49 (s, 3H). **^{19}F NMR** (282 MHz, $CDCl_3$) δ -61.09, -75.98. **^{13}C NMR** (75 MHz, $CDCl_3$) δ 133.7 (C), 133.4 (C), 131.0 (d, *J* = 30.4 Hz, C), 130.5 (CH), 127.1 (CH), 126.3 (q, *J* = 5.8 Hz, CH), 123.9 (d, *J* = 274.0 Hz, C), 119.8 (d, *J* = 322.0 Hz, C), 14.0 (CH_3). **HRMS** [APCI]: *m/z* calculated for $C_9H_7F_6NO_2S$ $[M]^+$: 307.0102, found 307.0105.

_N_-(4-Chloro-2-methylphenyl)-1,1,1-trifluoromethanesulfonamide (4e)

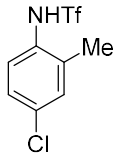

4e

(1.82 g, 94% yield), obtained as a white solid. **^{1}H NMR** (300 MHz, $CDCl_3$) δ 7.39 – 7.22 (m, 3H), 6.70 (brs, 1H), 2.39 (s, 3H). **^{19}F NMR** (282 MHz, $CDCl_3$) δ -76.43. **^{13}C NMR** (75 MHz, $CDCl_3$) δ 135.9 (C), 134.3 (C), 131.3 (CH), 130.6 (C), 127.8 (CH), 127.5 (CH), 119.8 (d, *J* = 322.1 Hz, C), 17.9 (CH_3). **HRMS** [APCI]: *m/z* calculated for $C_8H_7ClF_3NO_2S$ $[M]^+$: 272.9833, found 272.9830.

_N_-(4-Bromo-2-methylphenyl)-1,1,1-trifluoromethanesulfonamide (4f)

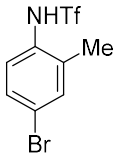

4f

(1.67 g, 81% yield), obtained as a white solid. **^{1}H NMR** (300 MHz, $CDCl_3$) δ 7.43 (d, *J* = 2.3 Hz, 1H), 7.37 (dd, *J* = 8.6, 2.4 Hz, 1H), 7.26 (d, *J* = 8.5 Hz, 1H), 6.68 (s, 1H), 2.35 (s, 3H). **^{19}F NMR** (282 MHz, $CDCl_3$) δ -76.44. **^{13}C NMR** (75 MHz, $CDCl_3$) δ 136.0 (C), 134.2 (CH), 131.2 (C), 130.5 (CH), 127.9 (CH), 122.3 (C), 119.8 (d, *J* = 322.2 Hz, C), 17.8 (CH_3). **HRMS** [APCI]: *m/z* calculated for $C_8H_7BrF_3NO_2S$ $[M]^+$: 316.9327, found 316.9327.

1,1,1-Trifluoro-_N_-(3-methyl-[1,1'-biphenyl]-4-yl)methanesulfonamide (4g)

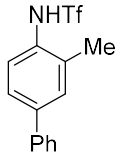

4g

(1.16 g, 84% yield), obtained as a white solid. **^{1}H NMR** (300 MHz, $CDCl_3$) δ 7.57 (d, *J* = 7.7 Hz, 2H), 7.52 – 7.33 (m, 7H), 2.45 (s, 3H). **^{19}F NMR** (282 MHz, $CDCl_3$) δ -76.39. **^{13}C NMR** (75 MHz, $CDCl_3$) δ 141.5 (C), 139.9 (C), 134.3 (C), 131.2 (C), 130.0 (CH), 129.0 (CH), 127.9 (CH), 127.2 (CH), 126.8 (CH), 126.0 (CH), 119.9 (d, *J* = 322.1 Hz, C), 18.1 (CH_3). **HRMS** [APCI]: *m/z* calculated for $C_{14}H_{13}F_3NO_2S$ $[M+H]^+$: 316.0614, found 316.0612.

1,1,1-Trifluoro-*N*-(4-methoxy-2-methylphenyl)methanesulfonamide (4h)

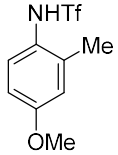

4h

(1.49 g, 71% yield), obtained as a white solid. **^{1}H NMR** (300 MHz, $CDCl_3$) δ 7.18 (d, *J* = 8.5 Hz, 1H), 6.73 – 6.63 (m, 2H), 6.40 (brs, 1H), 3.72 (s, 3H), 2.28 (s, 3H). **^{19}F NMR** (282 MHz, $CDCl_3$) δ -76.41. **^{13}C NMR** (75 MHz, $CDCl_3$) δ 159.7 (C), 137.3 (C), 129.3 (CH), 124.4 (C), 119.9 (d, *J* = 321.9 Hz, C), 116.5 (CH), 112.3 (CH), 55.6 (CH_3), 18.4 (CH_3). **HRMS** [APCI]: *m/z* calculated for $C_9H_{10}F_3NO_3S$ $[M]^+$: 269.0328, found 269.0327.

N-(4-cyano-2-methylphenyl)-1,1,1-trifluoromethanesulfonamide (4i)

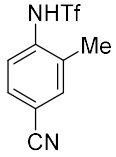

4i

(0.41 g, 41% yield) obtained as a white sold. **^{1}H NMR** (300 MHz, $CDCl_3$) δ 7.59 – 7.55 (m, 2H), 2.40 (s, 3H). **^{19}F NMR** (282 MHz, cdcl$_3$) δ -76.07. ^{13}C NMR (75 MHz, $CDCl_3$) δ 136.8 (C), 134.8 (CH), 132.8 (C), 131.3 (CH), 124.7 (CH), 119.6 (q, *J* = 322.4 Hz, C), 117.9 (C), 111.1 (C), 17.7 (CH_3). **HRMS** [APCI]: *m/z* calculated for $C_9H_7F_3N_2O_2S$ $[M]^+$: 264.0180, found 264.0178.

***N*-(5-Chloro-2-methylphenyl)-1,1,1-trifluoromethanesulfonamide (4j)**

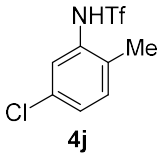

4j

(1.37 g, 71% yield), obtained as a white solid. **^{1}H NMR** (300 MHz, $CDCl_3$) δ 7.48 (s, 1H), 7.32 – 7.22 (m, 2H), 6.75 (brs, 1H), 2.39 (s, 3H). **^{19}F NMR** (282 MHz, $CDCl_3$) δ -76.48. **^{13}C NMR** (75 MHz, $CDCl_3$) δ 133.0 (C), 132.6 (C), 132.2 (CH), 131.8 (C), 128.6 (CH), 126.0 (CH), 119.8 (q, *J* = 322.0 Hz, C), 17.4 (CH_3). **HRMS** [APCI]: *m/z* calculated for $C_8H_7ClF_3NO_2S$ $[M]^+$: 272.9833, found 272.9833.

Methyl 4-methyl-3-((trifluoromethyl)sulfonamido)benzoate (4k)

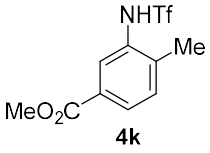

4k

(1.32 g, 73% yield), obtained as a white solid. **^{1}H NMR** (300 MHz, $CDCl_3$) δ 8.01 (s, 1H), 7.90 (d, *J* = 8.0 Hz, 1H), 7.59 (s, 1H), 7.34 (d, *J* = 8.0 Hz, 1H), 3.91 (s, 3H), 2.45 (s, 3H). **^{19}F NMR** (282 MHz, $CDCl_3$) δ -76.60. **^{13}C NMR** (75 MHz, $CDCl_3$) δ 166.7 (C), 140.4 (C), 132.6 (C), 131.6 (CH), 129.6 (CH), 129.3 (C), 128.2 (CH), 119.9 (d, *J* = 322.2 Hz, C), 52.7 (CH_3), 18.3 (CH_3). **HRMS** [APCI]: *m/z* calculated for $C_{10}H_{11}F_3NO_4S$ $[M+H]^+$: 298.0355, found 298.0358.

1,1,1-Trifluoro-*N*-(5-methoxy-2-methylphenyl)methanesulfonamide (4l)

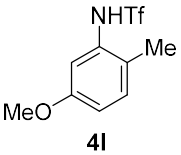

4l

(1.13 g, 72% yield), obtained as a white solid. **^{1}H NMR** (300 MHz, $CDCl_3$) δ 7.15 (d, *J* = 8.4 Hz, 1H), 6.97 (s, 1H), 6.80 (d, *J* = 8.5 Hz, 1H), 6.63 (brs, 1H), 3.79 (s, 3H), 2.28 (s, 3H). **^{19}F NMR** (282 MHz, $CDCl_3$) δ -76.52. **^{13}C NMR** (75 MHz, $CDCl_3$) δ 158.6 (C), 132.7 (C), 131.8 (CH), 124.9 (C), 119.9 (d, *J* = 322.0 Hz, C), 114.1 (CH), 111.5 (CH), 55.6 (CH_3), 16.9 (CH_3). **HRMS** [APCI]: *m/z* calculated for $C_9H_{10}F_3NO_3S$ $[M]^+$: 269.0328, found 269.0331.

1,1,1-Trifluoro-*N*-(5-fluoro-2-methylphenyl)methanesulfonamide (4m)

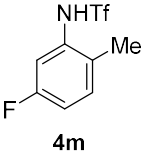

4m

(1.63 g, 79% yield), obtained as a white solid. **^{1}H NMR** (300 MHz, $CDCl_3$) δ 7.33 – 7.20 (m, 2H), 7.02 (td, *J* = 8.3, 2.6 Hz, 1H), 6.92 (brs, 1H), 2.38 (s, 3H). **^{19}F NMR** (282 MHz, $CDCl_3$) δ -76.57, -114.59 (q, *J* = 8.1 Hz). **^{13}C NMR** (75 MHz, $CDCl_3$) δ 161.3 (d, *J* = 246.0 Hz, C), 133.0 (d, *J* = 10.2 Hz, C), 132.2 (d, *J* = 8.7 Hz, CH), 128.3 (d, *J* = 3.7

Hz, C), 119.8 (d, *J* = 322.2 Hz, C), 115.2 (d, *J* = 20.9 Hz, CH), 112.8 (d, *J* = 25.0 Hz, CH), 17.2 (CH_3). **HRMS** [APCI]: *m/z* calculated for $C_8H_7F_4NO_2S$ $[M]^+$: 257.0128, found 257.0126.

_N_-(3,5-Dimethyl-[1,1'-biphenyl]-4-yl)-1,1,1-trifluoromethanesulfonamide (4n)

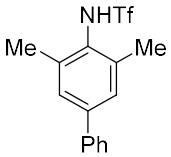

4n

(0.28 g, 74% yield), obtained as a white solid. **^{1}H NMR** (300 MHz, $CDCl_3$) δ 7.62 – 7.52 (m, 2H), 7.51 – 7.31 (m, 5H), 6.38 (s, 1H), 2.47 (s, 6H). **^{19}F NMR** (282 MHz, $CDCl_3$) δ -76.77. **^{13}C NMR** (75 MHz, $CDCl_3$) δ 142.2 (C), 139.9 (C), 138.5 (C), 129.8 (C), 129.0 (CH), 128.0 (CH), 127.9 (CH), 127.3 (CH), 119.7 (d, *J* = 321.9 Hz, C), 19.2 (CH_3). **HRMS** [APCI]: *m/z* calculated for $C_{15}H_{14}F_3NO_2S$ $[M]^+$: 329.0692, found 329.0691.

1,1,1-Trifluoro-_N_-mesitylmethanesulfonamide (4o)

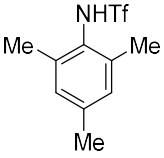

4o

(2.10g, 93% yield), obtained as a white solid. **^{1}H NMR** (300 MHz, $CDCl_3$) δ 6.94 (s, 2H), 6.37 (s, 1H), 2.36 (s, 6H), 2.29 (s, 3H). **^{19}F NMR** (282 MHz, $CDCl_3$) δ -76.89. **^{13}C NMR** (75 MHz, $CDCl_3$) δ 139.4 (C), 137.8 (C), 129.9 (CH), 128.0 (C), 119.7 (d, *J* = 321.8 Hz, C), 21.0 (CH_3), 18.8 (CH_3). **HRMS** [APCI]: *m/z* calculated for $C_{10}H_{12}F_3NO_2S$ $[M]^+$: 267.0535, found 267.0536.

1,1,1-Trifluoro-_N_-(3-methylnaphthalen-2-yl)methanesulfonamide (4p)

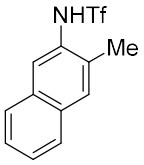

4p

(0.80 g, 87% yield), obtained as a white solid. **^{1}H NMR** (300 MHz, $CDCl_3$) δ 7.91 (s, 1H), 7.87 – 7.74 (m, 2H), 7.73 (s, 1H), 7.54 – 7.44 (m, 2H), 6.58 (brs, 1H), 2.53 (s, 3H). **^{19}F NMR** (282 MHz, $CDCl_3$) δ -76.31. **^{13}C NMR** (75 MHz, $CDCl_3$) δ 132.8 (C), 132.3 (C), 130.9 (C), 130.5 (C), 129.8 (CH), 128.0 (CH), 127.1 (CH), 126.4 (CH), 124.6 (CH), 120.0 (d, *J* = 322.5 Hz, C), 18.4 (CH_3). **HRMS** [APCI]: *m/z* calculated for $C_{12}H_{10}F_3NO_2S$ $[M]^+$: 289.0379, found 289.0376.

_N_-(2,6-Dimethylbenzyl)-1,1,1-trifluoromethanesulfonamide (6a)

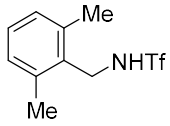

6a

(1.63 g, 82% yield), obtained as a white solid. **^{1}H NMR** (300 MHz, $CDCl_3$) δ 7.20 – 7.02 (m, 3H), 4.67 (brs, 1H), 4.48 (d, *J* = 4.6 Hz, 2H), 2.40 (s, 6H). **^{19}F NMR** (282 MHz, $CDCl_3$) δ -77.26. **^{13}C NMR** (75 MHz, $CDCl_3$) δ 137.8 (C), 130.8 (C), 129.2 (CH), 128.9 (CH), 119.9 (d, *J* = 321.6 Hz, C), 42.7 (CH_2), 19.5 (CH_3). **HRMS** [APCI]: *m/z* calculated for $C_{10}H_{12}F_3NO_2S$ $[M]^+$: 267.0535, found 267.0539.

1,1,1-Trifluoro-_N_-(2-fluoro-6-methylbenzyl)methanesulfonamide (6b)

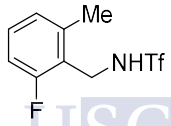

6b

(1.58 g, 86% yield), obtained as a yellow solid. **^{1}H NMR** (300 MHz, $CDCl_3$) δ 7.33 – 7.19 (m, 1H), 7.09 – 6.92 (m, 2H), 5.18 (s, 1H), 4.54 (d, *J* = 5.6 Hz, 2H), 2.44 (s, 3H). **^{19}F NMR** (282 MHz, $CDCl_3$) δ -77.75, 118.51 (m). **^{13}C NMR** (75 MHz, $CDCl_3$) δ 161.9 (d, *J* = 246.0 Hz, C), 139.4 (d, *J* = 3.1 Hz, C), 130.4 (d, *J* = 9.5 Hz, CH), 126.6 (d, *J* = 3.1 Hz, CH), 120.9 (d, *J* = 13.9 Hz, C), 119.7 (d, *J* = 321.2 Hz, C), 113.3 (d, *J* = 22.0 Hz, CH), 39.3 (d, *J* = 5.2 Hz, CH_2), 18.9 (d, *J* = 2.7 Hz, CH_3). **HRMS** [APCI]: *m/z* calculated for $C_9H_9F_4NO_2S$ $[M]^+$: 271.0285, found 271.0284. Data in agreement with those reported in literature.[173]

[173] X. Wang, T. S. Mei, J.-Q. Yu, *J. Am. Chem. Soc.* **2009**, *131*, 7520.

1,1,1-Trifluoro-*N*-(1-mesitylpropyl)methanesulfonamide (6e)

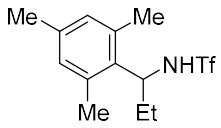

6e

(1.93 g, 55% yield), obtained as a white solid. **^{1}H NMR** (300 MHz, $CDCl_3$) δ 6.85 (s, 2H), 5.54 (d, *J* = 8.3 Hz, 1H), 5.00 (q, *J* = 8.1 Hz, 1H), 2.37 (s, 6H), 2.26 (s, 3H), 2.15 – 1.82 (m, 2H), 0.99 (t, *J* = 7.4 Hz, 3H). **^{19}F NMR** (282 MHz, $CDCl_3$) δ -78.27. **^{13}C NMR** (75 MHz, $CDCl_3$) δ 137.4 (C), 133.2 (C), 119.6 (q, *J* = 321.1 Hz, C), 57.5 (CH), 28.4 (CH_2), 20.9 (CH_3), 20.8 (CH_3), 11.2 (CH_3). **HRMS** [APCI]: *m/z* calculated for $C_{13}H_{18}F_3NO_2S$ $[M]^+$: 309.1005, found 309.1003.

1,1,1-trifluoro-N-(1-mesitylethyl)methanesulfonamide (6f)

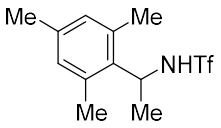

6f

(0.41 g, 33% yield), obtained as a white solid. **^{1}H NMR** (300 MHz, $CDCl_3$) δ 6.85 (s, 2H), 5.44 – 5.32 (m, 1H), 5.32 – 5.19 (m, 1H), 2.39 (s, 6H), 2.26 (s, 3H), 1.63 (d, *J* = 6.5 Hz, 3H). **^{19}F NMR** (282 MHz, $CDCl_3$) δ -77.88. **^{13}C NMR** (75 MHz, $CDCl_3$) δ 137.6 (C), 134.9 (C), 134.2 (C), 130.7 (CH), 119.6 (d, *J* = 321.1 Hz), 51.6 (CH), 21.5 (CH_3), 20.9 (CH_3), 20.7 (CH_3). **HRMS** [APCI]: *m/z* calculated for $C_{12}H_{16}F_3NO_2S$ $[M]^+$: 295.0848, found 295.0850.

1,1,1-trifluoro-N-(2-methyl-1-(o-tolyl)propyl)methanesulfonamide (6g)

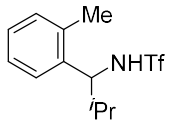

6g

(0.45 g, 91% yield), obtained as a white solid. **^{1}H NMR** (300 MHz, $CDCl_3$) δ 7.33 – 7.06 (m, 4H), 5.73 (brs, 1H), 4.61 (t, *J* = 9.0 Hz, 1H), 2.37 (s, 3H), 2.11 – 1.89 (m, *J* = 6.7 Hz, 1H), 1.09 (d, *J* = 6.7 Hz, 3H), 0.89 (d, *J* = 6.8 Hz, 3H). **^{19}F NMR** (282 MHz, $CDCl_3$) δ -77.69. **^{13}C NMR** (75 MHz, $CDCl_3$) δ 138.8 (C), 135.0 (C), 130.8 (CH), 127.7 (CH), 126.6 (CH), 125.4 (CH), 119.5 (d, *J* = 321.2 Hz, C), 61.5 (CH), 34.7 (CH), 19.5 (CH_3), 19.4 (CH_3), 18.5 (CH_3). **HRMS** [APCI]: *m/z* calculated for $C_{12}H_{16}F_3NO_2S$ $[M]^+$: 295.0848, found 295.0855.

3.4 General procedure for the synthesis of triflyl-protected o-methylbenzyamines and from the precursor alcohols, exemplified for 6c

(2-methoxy-6-methylphenyl)methanol was commercially available. (4-methoxy-2,6-dimethylphenyl)methanol was synthesized from 4-methoxy-2,6-dimethylbenzaldehyde with a method previously reported in literature. All spectral data recorded were in agreement with those reported in the literature.[174]

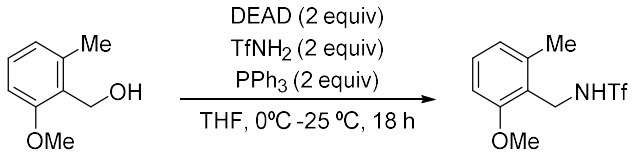

6c

To a solution of (2-methoxy-6-methylphenyl)methanol (600.0 mg, 3.94 mmol), trifluoro-methane sulfonamide (1.17 g, 2 equiv), and triphenylphosphine (2.07 g, 2 equiv) in THF (20 mL) at 0 °C was added DEAD (3.1 mL, 40% in toluene, 2 equiv). The reaction mixture was stirred at

[174] M. Nakatani, K. Takahashi, S. Watanabe, A. Shintokii, T. Hase, *Bulletin of the Chemical Society of Japan* **1984**, 1510.

room temperature overnight, and was quenched with water, then diluted with ethyl acetate. The combined organic phases were washed with brine and then dried over Na_2SO_4. Evaporation and column chromatography on silica gel (hexanes:diethylether; 90:10) afforded **1,1,1-trifluoro-N-(2-methoxy-6-methylbenzyl)methanesulfonamide 6c** as a white solid (589 mg, 53%). **^{1}H NMR** (300 MHz, $CDCl_3$) δ 7.22 (t, *J* = 8.0 Hz, 1H), 6.83 (d, *J* = 7.7 Hz, 1H), 6.78 (d, *J* = 8.4 Hz, 1H), 5.59 (t, *J* = 5.9 Hz, 1H), 4.48 (d, *J* = 5.8 Hz, 2H), 3.87 (s, 3H), 2.40 (s, 3H). **^{19}F NMR** (282 MHz, $CDCl_3$) δ -77.96. **^{13}C NMR** (75 MHz, $CDCl_3$) δ 158.1 (C), 137.9 (C), 129.5 (CH), 123.3 (CH), 122.2 (C), 119.8 (d, *J* = 321.4 Hz, C), 108.3 (CH), 55.6 (CH_3), 40.7 (CH_2), 19.2 (CH_3). **HRMS** [APCI]: *m/z* calculated for $C_{10}H_{12}F_3NO_3S$ $[M]^+$: 283.0485, found 283.0487.

1,1,1-Trifluoro-N-(4-methoxy-2,6-dimethylbenzyl)methanesulfonamide (6d)

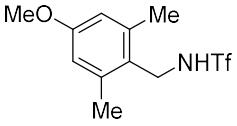

6d

(0.54 g, 50% yield), obtained as a white solid. **^{1}H NMR** (300 MHz, $CDCl_3$) δ 6.56 (s, 2H), 4.87 (brs, 1H), 4.42 (d, *J* = 4.5 Hz, 2H), 3.76 (s, 3H), 2.35 (s, 6H). **^{19}F NMR** (282 MHz, $CDCl_3$) δ -77.28. **^{13}C NMR** (75 MHz, $CDCl_3$) δ 159.5 (C), 139.3 (C), 123.2 (C), 120.0 (d, *J* = 321.8 Hz, C), 114.2 (CH), 55.3 (CH_3), 42.4 (CH_2), 19.7 (CH_3). **HRMS** [APCI]: *m/z* calculated for $C_{11}H_{15}F_3NO_3S$ $[M+H]^+$: 298.0719, found 298.0701.

3.5 Synthesis of allenes

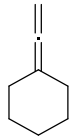
2a

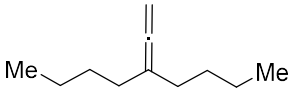

2b

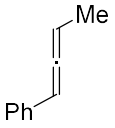

2e

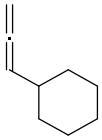
2f

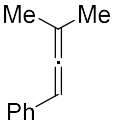

2g

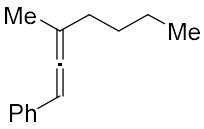

2h

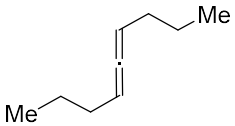

2i

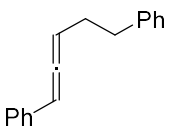

2j

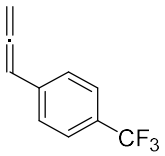

2k

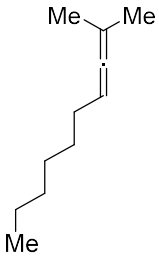

2l

The synthesis of allenes **2a**-**2h** is described in section 2.5.

*3.5.1 Procedure for the synthesis of allene **2i***

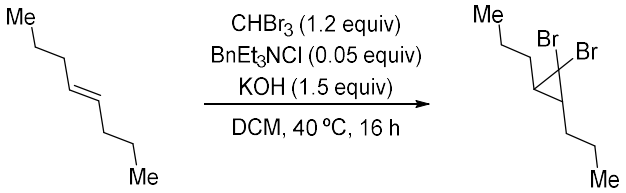

Following a reported procedure,[115] trans-4-octene (1.6 g, 14.26 mmol), benzyl-triethylammonium chloride (162 mg, 0.05 equiv) and crushed KOH (2.5 g, 1.5 equiv) were added to a round-bottom flask purged and filed with Ar and disolved in DCM (7 mL). Then, bromoform (4.32 g, 1.5 mL, 1.2 equiv) was added dropwise with a syringe pump over 1 h at 40 °C. The reaction was cooled to room temperature and stirred overnight. The mixture was filtered through a short plug of silica gel and eluted with diethyl ether. The filtrate was concentrated under reduced presure and purified by column chromatography on silica gel (hexanes) to give **1,1-dibromo-2,3-dipropylcyclopropane** as a colorless liquid (1.85 g, 46% yield). **^{1}H NMR** (300 MHz, $CDCL_3$) δ 1.68 – 1.35 (m, 9H), 1.09 (t, *J* = 4.4 Hz, 2H), 0.97 (t, *J* = 7.0 Hz, 6H).

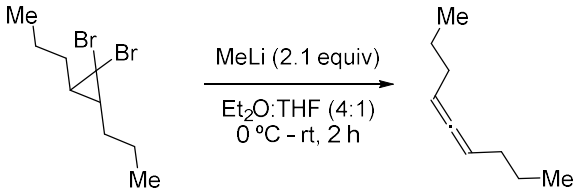

2i

To a stirred solution of 1,1-dibromo-2,3-dipropylcyclopropane (1.8 g, 6.34 mmol) in 4:1 diethyl ether:THF (28 mL) at 0 °C was added methyl lithium (1.6 M, 8.3 mL, 2.1 equiv). The reaction was stirred at this temperature for thirty minutes, warmed to room temperature and then stirred for another hour at this temperature. The reaction was quenched with a pH 7 phosphate buffer and extracted with diethyl ether. The combined organic layers were washed with brine, dried with anhydrous sodium sulfate, filtered, and concentrated under reduced presure (caution: volatile product). The crude material was purified by column chromatography on silica gel (pentane) to give **nona-4,5-diene** (**2i**) as a transparent oil (0.67 g, 85% yield). **^{1}H NMR** (300 MHz, $CDCL_3$) δ 5.10 – 5.01 (m, 2H), 2.01 – 1.89 (m, 4H), 1.42 (q, *J* = 7.4 Hz, 4H), 0.92 (t, *J* = 7.3 Hz, 6H). Spectral data were in agreement with those found in the literature.[175]

[175] Y. Pfeiffer, S. I. Gorelsky, A. M. Beauchemin, *Org. Lett.* **2009**, *11*, 1895.

*3.5.2 Procedure for the synthesis of allene **2j***

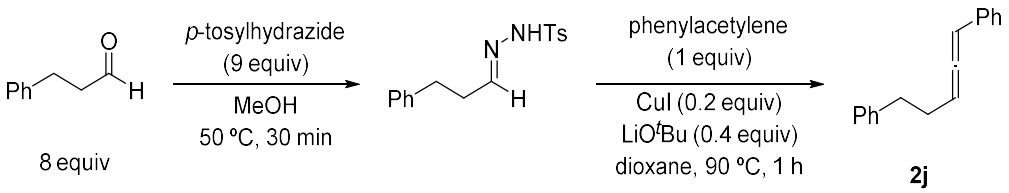

Following a reported procedure,[149] under an argon atmosphere, *p*-tosylhydrazide (5.02 g, 9 equiv) was added to a stirring solution of the aldehyde (3.57 g, 8 equiv) in MeOH (60 mL), and the resulting mixture was stirred at 50 °C for 30 minutes. The reaction mixture was concentrated and washed with pentane, and the crude product obtained was used for the next step without any purification.

Phenylacetylene (0.31 g, 3 mmol) was added to a solution of CuI (114 mg, 0.2 equiv), LiO^{t}Bu (95 mg, 0.4 equiv) and the *N*-tosylhydrazone obtained in the previous step in dioxane (150 mL). This solution was heated at 90 °C during 1 h. The reaction was cooled to room temperature and filtered through a short pad of silica, eluting with ethyl acetate. The filtered was concentrated under reduced pressure and purified by column chromatography on silica gel (hexanes) to give **penta-1,2-diene-1,5-diyldibenzene** (**2j**) as a pale-yellow oil (154 mg, 23% yield). ^{1}H NMR (300 MHz, $CDCL_3$) δ 7.36 – 7.14 (m, 10H), 6.14 (dt, *J* = 6.2, 2.9 Hz, 1H), 5.61 (q, *J* = 6.6 Hz, 1H), 2.90 – 2.78 (m, 2H), 2.57 – 2.41 (m, 2H).

*3.5.3 Procedure for the synthesis of allene **2k***

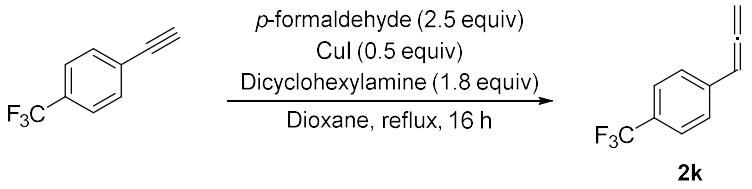

Following a reported procedure,[150] to a two-neck round-bottom flask, purged and filled with Ar, *p*-formaldehyde (0.44 g, 2.5 equiv) and CuI (0.56 g, 0.5 equiv) were added. The solids were dissolved in dioxane (9.8 mL) and, after that, 4-ethynyl-α,α,α-trifluorotoluene (1 g, 5.88 mmol) and dicyclohexylamine (1.92 g, 9.8 mL, 1.8 equiv) were sequentially added. The solution was refluxed overnight. The reaction was cooled to room temperature and filtered through Celite© to remove the CuI. The filtered was concentrated under reduced pressured. After that, water was added to protonate the amine, and the solution was extracted with diethyl ether. The combined organic phases were washed with brine, dried with anhydrous sodium sulfate, filtered, and concentrated under reduced presure. Purification by column chromatography on silica gel afforded **1-(propa-1,2-dien-1-yl)-4-(trifluoromethyl)benzene** (**2k**) as a transparent oil (200 mg, 19% yield). **^{1}H NMR** (300 MHz, $CDCL_3$) δ 7.55 (d, *J* = 8.1 Hz, 2H), 7.39 (d, *J* = 7.9 Hz, 2H), 6.19 (t, *J* = 6.7 Hz, 1H), 5.22 (d, *J* = 6.8 Hz, 2H). **^{19}F NMR** (282 MHz, $CDCL_3$) δ -62.55.

*3.5.4 Procedure for the synthesis of allene **2l***

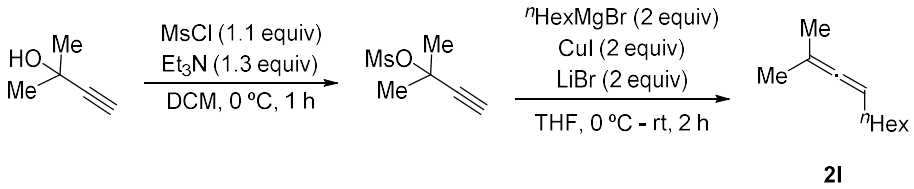

2l

Following a reported procedure,[151] to a purged two-neck round-bottom flask filled with Ar, 2-methylbut-3-yn-2-ol (0.20 g, 2.38 mmol) and DCM (24 mL) were added. The solution was cooled to 0 °C and Et_3N (0.31 g, 0.43 mL, 1.3 equiv) and MsCl (0.3 g, 0.2 mL, 1.1 equiv) were sequentially added. The reaction was stirred at that temperature during 1 h. After that time, water was added to quench the reaction. The organic layer was separated and the aqueous layer extracted with dichloromethane. The combined organic phases were washed with brine and then dried over Na_2SO_4. The solvent was removed under reduced pressure, and the crude was used for the next step without further purification.

To a purged two-neck round-bottom flask filled with Ar, CuI (0.91 g, 2 equiv) and LiBr (0.41 g, 2 equiv) were added and then dissolved with THF (15 mL). The solution was cooled to -78 °C and then ^{n}HexMgBr (2.0 M, 0.90 g, 2.4 mL, 2 equiv) was added dropwise. The reaction was stirred at room temperature during 2 h. After competition, the reaction was quenched with NH_4Cl (sat.). The organic layer was separated and the aqueous layer extracted with diethyl ether. The combined organic phases were washed with brine and then dried over Na_2SO_4. The solvent was removed under reduced pressure, and the crude was purified by column chromatography (pentane) to afford **2-methyldeca-2,3-diene** (**2l**) as a transparent oil (91.8 mg, 25% yield). **^{1}H NMR** (300 MHz, $CDCl_3$) δ 4.97 – 4.88 (m, 1H), 1.93 (q, *J* = 6.7 Hz, 2H), 1.67 (d, *J* = 2.7 Hz, 6H), 1.40 – 1.20 (m, 8H), 0.88 (t, *J* = 6.1 Hz, 3H).

*3.5.5 Synthesis of the chiral allene (S)-Buta-1,2-dien-1-ylbenzene (**(S)-2e**)*

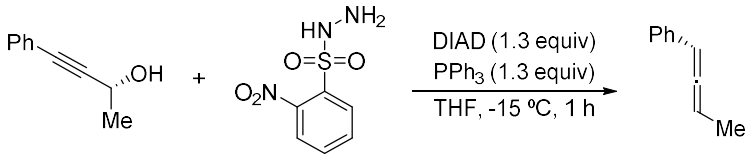

(*S*)-2e

Following a reported procedure,[176] to a solution of triphenylphosphine (3.59 g, 1.3 equiv) in THF (40 mL) at -15 °C was added DIAD (2.7 mL, 1.3 equiv). After 10 min, a solution of (*R*)-4-phenylbut-3-yn-2-ol (1.54 g, 10.53 mmol) in THF (31 mL) was added to the yellow reaction mixture, followed 10 min later by a solution of 2-nitrobenzenesulfonylhydrazide (3.20 g, 1.4 equiv) in THF (40 mL). The resulting suspension was held at -15 °C for 1 h, warmed to room temperature and left to stand overnight and then concentrated. The concentrated mixture was purified by column chromatography (pentane), affording **(*S*)-Buta-1,2-dien-1-ylbenzene ((*S*)-2e)** as a transparent oil

[176] Sutherland, D. R.; Kinsman, L.; Angiolini, S. M.; Rosair, G. M.; Lee, A. L. *Chem. A Eur. J.* **2018**, *24*, 7002.

(0.74 g, 54% yield). **^{1}H NMR** (300 MHz, $CDCl_3$) δ 7.31 – 7.23 (m, 4H), 6.07 (dq, *J* = 6.4, 3.2 Hz, 1H), 5.51 (p, *J* = 6.9 Hz, 1H), 1.76 (dd, *J* = 7.1, 3.2 Hz, 3H).

Enantiomeric purity of (*S*)-2d was determined via chiral GC analysis on Chiraldex G-TA.

Racemic sample (**2e**)

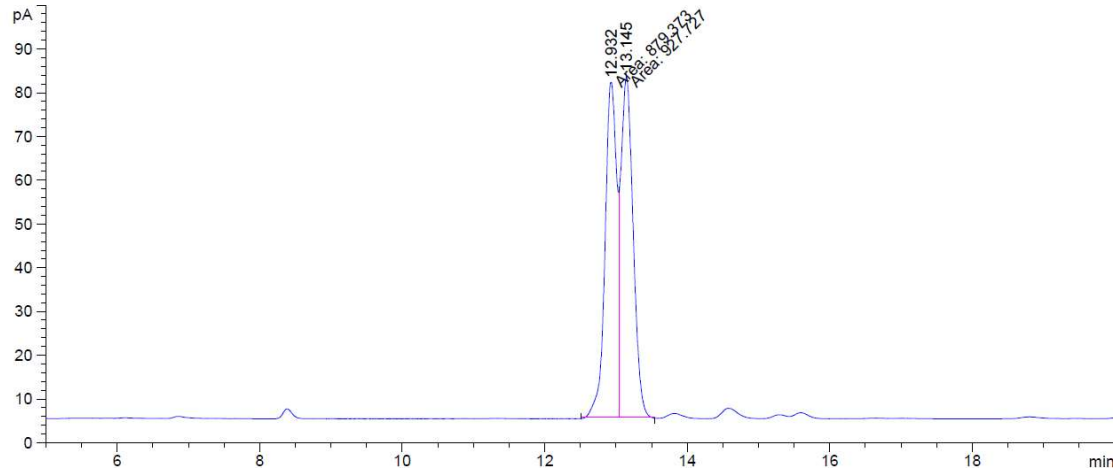

Peak #	RetTime [min]	Type	Width [min]	Area [pA*s]	Height [pA]	Area %
1	12.932	MF	0.1913	879.37335	76.61613	48.66211
2	13.145	FM	0.1979	927.72723	78.14651	51.33789
Totals :				1807.10059	154.76264	

Asymmetric sample (>99% ee)

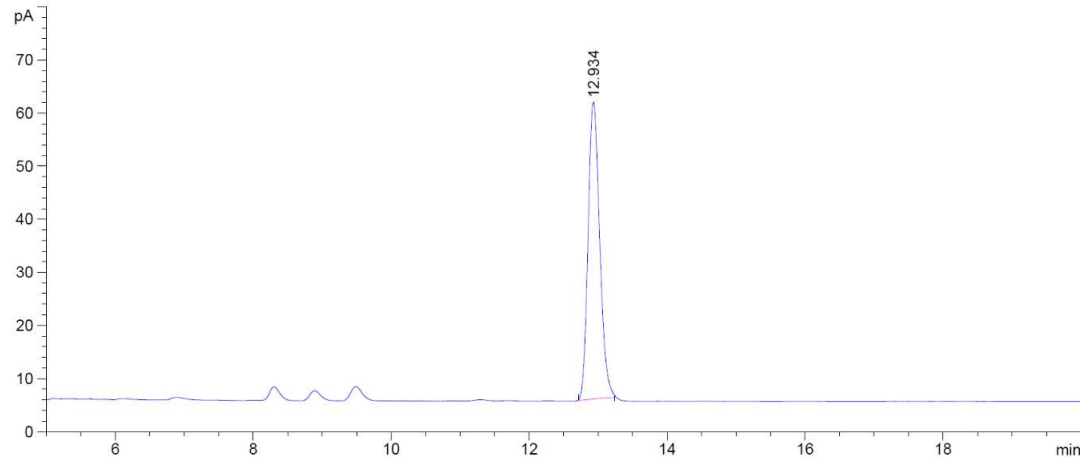

Peak #	RetTime [min]	Type	Width [min]	Area [pA*s]	Height [pA]	Area %
1	12.934	BB	0.1409	652.41986	55.91862	1.000e2
Totals :				652.41986	55.91862	

3.6 General procedure for the Pd-catalyzed formal (4+2) annulation of triflyl-protected *o*-methylanilines with allenes, exemplified with 5ab

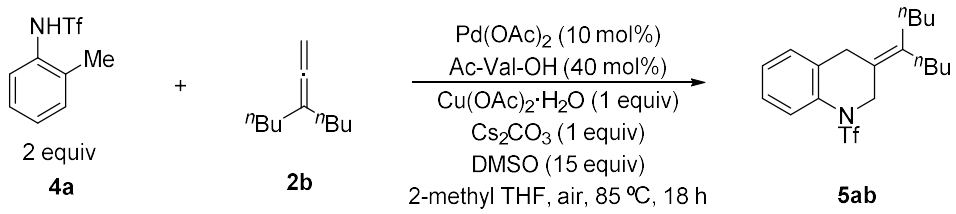

To a solution of $Pd(OAc)_2$ (3.7 mg, 10 mol%), Ac-Val-OH (10.6 mg, 40 mol%), $Cu(OAc)_2{\cdot}H_2O$ (33.3 mg, 1 equiv), Cs_2CO_3 (54.4 mg, 1 equiv) and **4a** (79.9 mg, 0.333 mmol, 2 equiv) in 2-methyl THF (1 mL) and DMSO (0.178 μL, 15 equiv), under air atmosphere, heated at 85 °C, in a Schlenk tube sealed with a rubber septum was slowly added the allene **2b** (25.4 mg, 0.167 mmol) with a syringe pump during 1h. The reaction was stirred at 85 °C during 18 h and then cooled to room temperature. Evaporation and column chromatography on silica gel (hexanes:diethylether; 99:1) afforded **3-(nonan-5-ylidene)-1-((trifluoromethyl)sulfonyl)-1,2,3,4-tetrahydroquinoline** (**5ab**) as a pale orange oil (46.4 mg, 71% yield). **^{1}H NMR** (300 MHz, $CDCl_3$) δ 7.61 – 7.49 (m, 1H), 7.31 – 7.21 (m, 3H), 4.46 (s, 2H), 3.58 (s, 2H), 2.18 – 2.02 (m, 4H), 1.46 – 1.26 (m, 8H), 1.04 – 0.86 (m, 6H). **^{19}F NMR** (282 MHz, $CDCl_3$) δ -75.61. **^{13}C NMR** (75 MHz, $CDCl_3$) δ 137.0 (C), 136.3 (C), 133.1 (C), 129.0 (CH), 127.4 (CH), 127.0 (CH), 124.7 (CH), 123.3 (C), 120.2 (d, *J* = 324.9 Hz, C), 50.1 (CH_2), 32.03 (CH_2), 31.96 (CH_2), 30.9 (CH_2), 30.8 (CH_2), 30.1 (CH_2), 23.1 (CH_2), 23.0 (CH_2), 14.2 (CH_3), 14.1 (CH_3). **HRMS** [APCI]: *m/z* calculated for $C_{19}H_{27}F_3NO_2S$ $[M+H]^+$: 298.0719, found 298.0701.

3-Cyclohexylidene-1-((trifluoromethyl)sulfonyl)-1,2,3,4-tetrahydroquinoline (5aa)

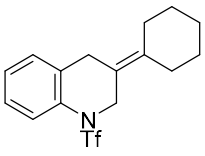

5aa

(37.8 mg, 61% yield), obtained as a transparent oil. **^{1}H NMR** (300 MHz, $CDCl_3$) δ 7.49 – 7.38 (m, 1H), 7.21 – 7.11 (m, 3H), 4.37 (s, 2H), 3.51 (s, 2H), 2.21 – 2.05 (m, 4H), 1.56 – 1.43 (m, 6H). **^{19}F NMR** (282 MHz, $CDCl_3$) δ -75.68. **^{13}C NMR** (75 MHz, $CDCl_3$) δ 136.3 (C), 135.8 (C), 132.9 (C), 129.1 (CH), 127.3 (CH), 126.9 (CH), 124.6 (CH), 120.1 (d, *J* = 324.6 Hz, C), 119.5 (C), 49.9 (CH_2), 30.7 (CH_2), 30.5 (CH_2), 30.3 (CH_2), 27.7 (CH_2), 27.6 (CH_2), 26.7 (CH_2). **HRMS** [APCI]: *m/z* calculated for $C_{16}H_{19}F_3NO_2S$ $[M+H]^+$: 346.1083, found 346.1076.

(*E*)-3-Butylidene-2-propyl-1-((trifluoromethyl)sulfonyl)-1,2,3,4-tetrahydroquinoline (5ai)

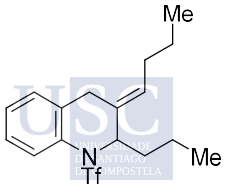

5ai

(36.8 mg, 61% yield), obtained as a transparent oil. **^{1}H NMR** (500 MHz, $CDCl_3$) δ 7.51 – 7.43 (m, 1H), 7.20 – 7.07 (m, 3H), 5.37 (t, *J* = 7.3 Hz, 1H), 4.64 – 4.55 (m, 1H), 3.50 (dd, *J* = 64.4, 20.9 Hz, 2H), 2.09 – 1.90 (m, 2H), 1.42 – 1.19 (m, 6H), 0.87 (t, *J* = 7.4 Hz, 3H), 0.78 (t, *J* = 7.0 Hz, 3H). **^{19}F NMR** (282 MHz, $CDCl_3$) δ -74.61. **^{13}C NMR** (126 MHz, $CDCl_3$) δ 133.3 (C), 131.9 (C), 131. 1 (C), 129.2 (CH), 127.7 (CH), 127.3 (CH), 127.0 (CH), 126.2 (CH), 120.2 (q, *J* = 325.6 Hz, C), 64.2 (CH_2), 36.1 (CH_2),

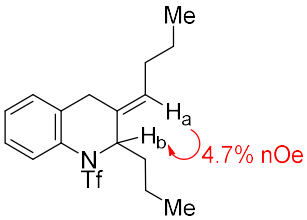

29.5 (CH_2), 28.1 (CH_2), 22.3 (CH_2), 19.2 (CH_2), 13.9 (CH_3), 13.5 (CH_3). **HRMS** [APCI]: *m/z* calculated for $C_{17}H_{22}F_3NO_2S$ $[M]^+$: 361.1323, found 361.1322.

Assignment of structure of **5ai** was based on the observed nOe between the H_a (5.37 ppm, 100%) with H_b (4.64 – 4.55 ppm, 4.7%).

(*E*)-3-Benzylidene-2-methyl-1-((trifluoromethyl)sulfonyl)-1,2,3,4-tetrahydroquinoline (5ae)

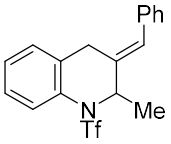

5ae

(40.5 mg, 66% yield), obtained as a white solid. **^{1}H NMR** (500 MHz, $CDCl_3$) δ 7.47 (d, *J* = 7.6 Hz, 1H), 7.32 (t, *J* = 7.7 Hz, 2H), 7.28 – 7.09 (m, 6H), 6.44 (s, 1H), 5.03 (q, *J* = 6.9 Hz, 1H), 3.81 (s, 2H), 1.28 (d, *J* = 6.9 Hz, 3H). **^{19}F NMR** (282 MHz, $CDCl_3$) δ -74.87. **^{13}C NMR** (126 MHz, $CDCl_3$) δ 136.3 (C), 135.8 (C), 133.0 (C), 130.4 (C), 129.1 (CH), 129.0 (CH), 128.6 (CH), 127.43 (CH), 127.42 (CH), 127.37 (CH), 126.3 (CH), 126.1 (CH), 120.2 (q, *J* = 324.9 Hz, C), 60.4 (CH), 29.7 (CH_2), 21.3 (CH_3). **HRMS** [APCI]: *m/z* calculated for $C_{18}H_{17}F_3NO_2S$ $[M+H]^+$: 368.0927, found 368.0928.

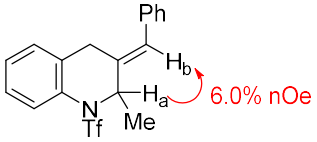

Assignment of structure of **5ae** based on the observed nOe between the H_a (5.03 ppm, 100%) with H_b (6.44 ppm, 6.0%).

3-Benzylidene-2-phenethyl-1-((trifluoromethyl)sulfonyl)-1,2,3,4-tetrahydroquinoline (5aj and 5aj')

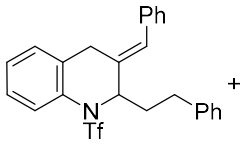

5aj

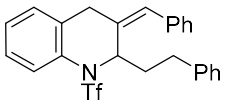

5aj'

(1.8:1 E/Z ratio of **5aj** and **5aj'**, inseparable mixture (58.1 mg, 76% yield), obtained as a yellow solid). **^{1}H NMR** (500 MHz, $CDCl_3$) δ 7.59 (d, *J* = 7.3 Hz, 0.54H), 7.49 (d, *J* = 7.8 Hz, 0.31H), 7.43 – 6.98 (m, 13H), 6.51 (s, 0.65H), 5.88 (s, 0.36H), 5.64 (t, *J* = 7.1 Hz, 0.39H), 4.92 (t, *J* = 7.7 Hz, 0.66H), 3.94 (d, *J* = 20.9 Hz, 0.68H), 3.82 (dd, *J* = 21.0, 2.2 Hz, 0.70H), 3.62 (d, *J* = 20.4 Hz, 0.41H), 3.37 (d, *J* = 20.3 Hz, 0.40H), 2.91 – 2.69 (m, 2 H), 2.57 (q, *J* = 7.4 Hz, 0.83H), 1.85 (q, *J* = 7.8 Hz, 1.40H). **^{19}F NMR** (282 MHz, $CDCl_3$) δ -74.32. **^{13}C NMR** (126 MHz, $CDCl_3$) δ 141.4 (C), 140.7 (C), 137.6 (C), 136.2 (C), 134.0 (C), 133.8 (C), 132.9 (C), 131.2 (C), 130.7 (C), 130.4 (C), 129.9 (CH), 129.3 (CH), 129.1 (CH), 129.0 (CH), 128.64 (CH), 128.62 (CH), 128.57 (CH), 128.5 (CH), 127.8 (CH), 127.6 (CH), 127.5 (CH), 127.4 (CH), 127.2 (CH), 127.1 (CH), 126.9 (CH), 126.31 (CH), 126.26 (CH), 126.13 (CH), 126.10 (CH), 120.2 (q, *J* = 325.7 Hz, C), 66.6 (CH), 64.6 (CH), 35.5 (CH_2), 35.2 (CH_2), 32.4 (CH_2), 29.7 (CH_2), 29.6 (CH_2), 28.5 (CH_2). **HRMS** [APCI]: *m/z* calculated for $C_{25}H_{23}F_3NO_2S$ $[M+H]^+$: 458.1396, found 458.1395.

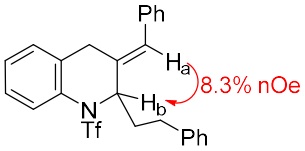

Assignment of structure of **5aj** based on the observed nOe between the H_a (6.51 ppm, 100%) with H_b (4.92 ppm, 8.3%).

3-(Cyclohexylmethylene)-1-((trifluoromethyl)sulfonyl)-1,2,3,4-tetrahydroquinoline (5af and 5af')

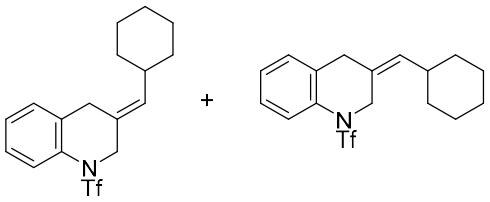

5af **5af'**

(1.1:1 E/Z ratio of **3af** and **3af'**, inseparable mixture (41.2 mg, 68% yield), obtained as a transparent oil). **^{1}H NMR** (500 MHz, $CDCl_3$) δ 7.51 – 7.40 (m, 1H), 7.20 – 7.07 (m, 3H), 5.28 (d, *J* = 9.5 Hz, 0.51), 5.19 (d, *J* = 9.6 Hz, 0.48H), 4.40 (s, 1.01H), 4.22 (s, 1.11H), 3.55 (s, 1.24H), 3.38 (s, 1.05H), 2.25 – 2.12 (m, 0.64H), 2.06 – 1.94 (m, 0.59H), 1.71 – 1.42 (m, 7H), 1.31 – 0.91 (m, 7H). **^{19}F NMR** (282 MHz, $CDCl_3$) δ -74.80, -75.77. **^{13}C NMR** (126 MHz, $CDCl_3$) δ 136.2 (C), 135.7 (C), 133.9 (CH), 133.8 (C), 132.2 (CH), 131.3 (C), 129.4 (CH), 128.5 (C), 128.2 (CH), 127.6 (CH), 127.3 (CH), 127.2 (CH), 127.0 (CH), 126.8 (C), 124.9 (CH), 124.8 (CH), 120.2 (q, *J* = 324.2 Hz, C), 120.1 (q, *J* = 325.2 Hz, C), 54.6 (CH_2), 49.5 (CH_2), 37.2 (CH_2), 36.8 (CH), 35.7 (CH), 32.9 (CH_2), 32.5 (CH_2), 29.6 (CH_2), 26.1 (CH_2), 26.0 (CH_2), 25.94 (CH_2), 25.86 (CH_2). **HRMS** [APCI]: *m/z* calculated for $C_{17}H_{20}F_3NO_2S$ $[M]^+$: 359.1161, found 359.1164.

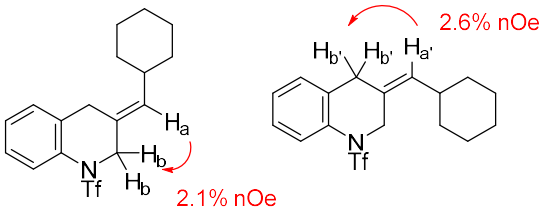

Assignment of stereochemistry of **5af** and **5af'** was based on the observed nOe between the H_a (5.28 ppm, 100%) with H_b (4.22 ppm, 2.1%) and between the $H_{a'}$ (5.19 ppm, 100%) with $H_{b'}$ (3.38 ppm, 2.6%).

3-(4-(trifluoromethyl)benzylidene)-1-((trifluoromethyl)sulfonyl)-1,2,3,4-tetrahydroquinoline (5ak and 5ak')

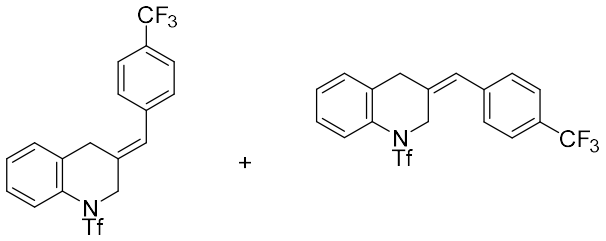

5ak **5ak'**

(6.5:1 E/Z ratio of **5ak** and **5ak'**, inseparable mixture (25.5 mg, 36% yield), obtained as a white solid). **^{1}H NMR** (500 MHz, $CDCl_3$) δ 7.53 (d, J = 7.8 Hz, 2H), 7.49 – 7.41 (m, 1H), 7.26 (d, J = 7.9 Hz, 2H), 7.24 – 7.13 (m, 3H), 7.06 – 7.00 (m, 1H), 6.49 (s, 0.13H), 6.18 (s, 0.85H), 4.62 (s, 0.30H), 4.19 (s, 1.85H), 3.63 (s, 0.31H), 3.54 (s, 1.96H). **^{19}F NMR** (282 MHz, $CDCl_3$) δ -62.25, -62.37, -74.74, -74.98. **^{13}C NMR** (126 MHz, $CDCl_3$) δ 140.7 (C), 139.6 (C), 136.8 (C), 136.1 (C), 135.4 (C), 133.1 (C), 132.2 (C), 129.8 (C), 129.74 (C), 129.67 (CH), 129.5 (C), 128.8 (CH), 128.14 (CH), 128.12 (CH), 128.07 (CH), 127.8 (CH), 127.7 (CH), 126.9 (CH), 125.9 (q, J = 3.8 Hz, CH), 125.7 (q, J = 3.8 Hz, CH), 125.1 (CH), 125.0 (CH), 124.33 (CH), 124.27 (q, J = 271.9 Hz), 123.0 (CH), 120.3 (q, J = 324.9 Hz), 50.4 (CH_2), 49.6 (CH_2), 41.0 (CH_2), 36.7 (CH_2). **HRMS** [APCI]: *m/z* calculated for $C_{18}H_{13}F_6NO_2S$ $[M]^+$: 421.0571, found 421.0574.

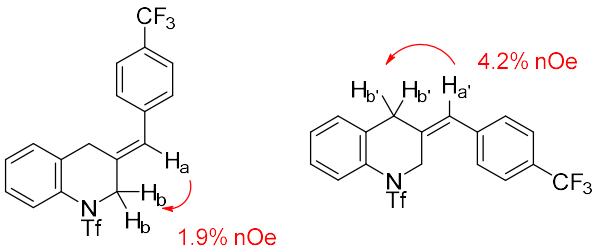

Assignment of stereochemistry of **5ak** and **5ak'** was based on the observed nOe between the H_a (6.18 ppm, 100%) with H_b (4.19 ppm, 1.9%) and between the $H_{a'}$ (6.49 ppm, 100%) with $H_{b'}$ (3.63 ppm, 4.2%).

(E)-3-Benzylidene-2,2-dimethyl-1-((trifluoromethyl)sulfonyl)-1,2,3,4-tetrahydroquinoline (5ag)

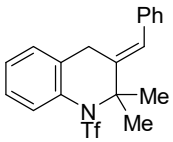

5ag

(46.6 mg, 73% yield), obtained as a white solid. **^{1}H NMR** (300 MHz, $CDCl_3$) δ 7.41 – 7.25 (m, 3H), 7.27 – 7.11 (m, 5H), 7.08 – 7.00 (m, 1H), 6.40 (s, 1H), 3.68 (s, 2H), 1.62 (s, 6H). **^{19}F NMR** (282 MHz, $CDCl_3$) δ -75.27. **^{13}C NMR** (75 MHz, $CDCl_3$) δ 143.1 (C), 137.0 (C), 136.8 (C), 134.4 (C), 129.0 (CH), 128.6 (CH), 128.2 (CH), 128.0 (CH), 127.6 (CH), 127.2 (CH), 127.1 (CH), 123.5 (CH), 120.0 (d, *J* = 324.8 Hz, C), 68.6 (C), 31.4 (CH_2), 29.7 (CH_3). **HRMS** [APCI]: *m/z* calculated for $C_{19}H_{19}F_3NO_2S$ $[M+H]^+$: 382.1083, found 382.1083.

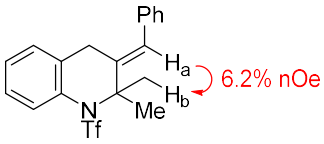

Assignment of stereochemistry of **5ag** was based on the observed nOe between the H_a (6.40 ppm, 100%) with the H_b (1.62 ppm, 6.2%).

(*E*)-3-Benzylidene-2-butyl-2-methyl-1-((trifluoromethyl)sulfonyl)-1,2,3,4-tetrahydroquinoline (5ah)

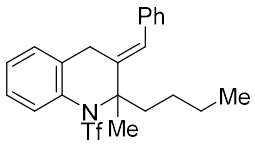

5ah

(40.2 mg, 57% yield, 7.4:1 E/Z ratio, only E isomer was characterized), obtained as a white solid. **^{1}H NMR** (300 MHz, $CDCl_3$) δ 7.42 – 6.95 (m, 9H), 6.40 (s, 1H), 3.70 (s, 2H), 1.91 (s, 3H), 1.43 – 0.81 (m, 6H), 0.68 (t, *J* = 7.3 Hz, 3H). **^{19}F NMR** (282 MHz, $CDCl_3$) δ -75.15. **^{13}C NMR** (75 MHz, $CDCl_3$) δ 143.1 (C), 137.0 (C), 136.7 (C), 134.3 (C), 129.0 (CH), 128.5 (CH), 128.2 (CH), 127.9 (CH), 127.7 (CH), 127.2 (CH), 127.0 (CH), 124.3 (CH), 120.0 (d, *J* = 324.6 Hz, C), 71.2 (C), 42.9 (CH_2), 31.5 (CH_2), 25.7 (CH_2), 23.8 (CH_3), 22.6 (CH_2), 13.9 (CH_3). **HRMS** [APCI]: *m/z* calculated for $C_{22}H_{25}F_3NO_2S$ $[M+H]^+$: 424.1553, found 424.1558.

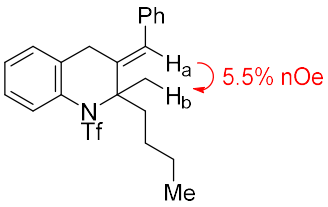

Assignment of stereochemistry of **5ah** was based on the observed nOe between the H_a (6.40 ppm, 100%) with the H_b (1.91 ppm, 5.5%).

(E)-3-heptylidene-2,2-dimethyl-1-((trifluoromethyl)sulfonyl)-1,2,3,4-tetrahydroquinoline (5al) and 2-hexyl-3-(propan-2-ylidene)-1-((trifluoromethyl)sulfonyl)-1,2,3,4-tetrahydroquinoline (5al')

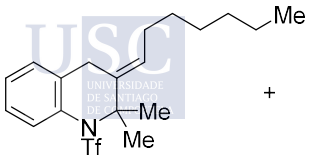

5al

+

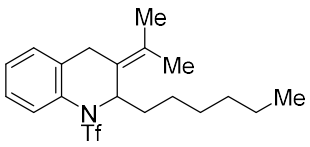

5al'

(2.8:1 ratio of **3ai** and **3ai'**, inseparable mixture (27.5 mg, 42% yield), obtained as a transparent oil). **^{1}H NMR** (500 MHz, $CDCl_3$) δ 7.33 (d, J = 7.1 Hz, 0.58H), 7.23 – 7.08 (m, 3.25H), 5.33 (t, J = 7.1 Hz, 0.74H), 5.03 (t, J = 7.2 Hz, 0.26H), 3.50 – 3.43 (m, 2H), 2.00 (q, J = 7.3 Hz, 1.58H), 1.70 (s, 0.88H), 1.66 (s, 0.88H), 1.48 (s, 4.43H), 1.28 – 1.11 (m, 8.67H), 0.82 (t, J = 6.6 Hz, 2.25H), 0.77 (t, J = 7.0 Hz,

1.02H). **^{19}F NMR** (282 MHz, $CDCl_3$) δ -74.48, -74.57. **^{13}C NMR** (126 MHz, $CDCl_3$) δ 139.2 (C), 137.1 (C), 134.5 (C), 133.0 (C), 132.4 (C), 129.0 (CH), 128.2 (CH), 128.0 (CH), 127.7 (CH), 127.4 (CH), 127.0 (C), 126.9 (CH), 126.8 (CH), 126.3 (CH), 126.1 (C), 123.9 (CH), 120.2 (d, J = 325.6 Hz, C), 120.0 (d, J = 324.9 Hz, C), 67.9 (C), 59.3 (CH), 32.8 (CH_2), 31.8 (CH_2), 31.7 (CH_2), 30.0 (CH_2), 29.8 (CH_2), 29.33 (CH_3), 29.27 (CH_2), 29.1 (CH_2), 28.6 (CH_2), 27.8 (CH_2), 25.7 (CH_2), 22.7 (CH_2), 22.6 (CH_2), 20.3 (CH_3), 20.2 (CH_3), 14.2 (CH_3), 14.1 (CH_3). **HRMS** [APCI]: *m/z* calculated for $C_{19}H_{26}F_3NO_2S$ $[M]^+$: 389.1636, found 389.1633.

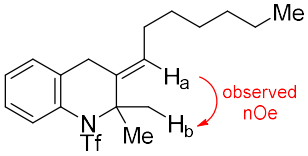

Assignment of stereochemistry of **5al** was based on a NOESY experiment. Qualitative nOe was observed between the H_a (5.33 ppm) with the H_b (1.48 ppm).

5-Methoxy-3-(nonan-5-ylidene)-1-((trifluoromethyl)sulfonyl)-1,2,3,4-tetrahydroquinoline (5bb)

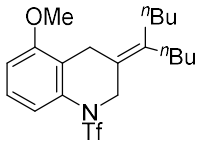

5bb

(48.6 mg, 69% yield), obtained as a yellow oil. **^{1}H NMR** (300 MHz, $CDCl_3$) δ 7.21 – 7.14 (m, 2H), 6.84 – 6.72 (m, 1H), 4.40 (s, 2H), 3.87 (s, 3H), 3.49 (s, 2H), 2.19 – 2.04 (m, 4H), 1.46 – 1.25 (m, 8H), 1.01 – 0.85 (m, 6H). **^{19}F NMR (**282 MHz, $CDCl_3$) δ -75.23. **^{13}C NMR** (75 MHz, $CDCl_3$) δ 157.0 (C), 137.4 (C), 136.9 (C), 126.8 (CH), 122.3 (C), 121.3 (C), 120.1 (d, *J* = 325.4 Hz, C), 116.7 (CH), 108.4 (CH), 55.7 (CH_3), 49.7 (CH_2), 32.0 (CH_2), 31.9 (CH_2), 31.1 (CH_2), 30.0 (CH_2), 24.5 (CH_2), 23.1 (CH_2), 23.0 (CH_2), 14.2 (CH_3), 14.1 (CH_3). **HRMS** [APCI]: *m/z* calculated for $C_{20}H_{29}F_3NO_3S$ $[M+H]^+$: 390.1709, found 390.1704.

5-Chloro-3-(nonan-5-ylidene)-1-((trifluoromethyl)sulfonyl)-1,2,3,4-tetrahydroquinoline (5cb)

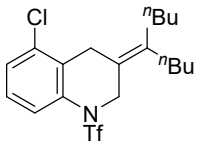

5cb

(35.7 mg, 50% yield), obtained as a white solid. **^{1}H NMR** (500 MHz, $CDCl_3$) δ 7.40 (d, *J* = 8.2 Hz, 1H), 7.25 (d, *J* = 8.0 Hz, 1H), 7.10 (t, *J* = 8.2 Hz, 1H), 4.34 (brs, 2H), 3.55 (s, 2H), 2.04 (dt, *J* = 22.1, 7.5 Hz, 4H), 1.40 – 1.15 (m, 8H), 0.95 – 0.81 (m, 6H). **^{19}F NMR** (282 MHz, $CDCl_3$) δ -75.25. **^{13}C NMR** (126 MHz, $CDCl_3$) δ 138.3 (C), 137.5 (C), 134.0 (C), 130.9 (C), 128.0 (CH), 127.2 (CH), 123.3 (CH), 121.7 (C), 120.1 (q, *J* = 324.9 Hz, C), 49.7 (CH_2), 32.00 (CH_2), 31.98 (CH_2), 31.0 (CH_2), 30.1 (CH_2), 28.8 (CH_2), 23.1 (CH_2), 23.0 (CH_2), 14.12 (CH_3), 14.09 (CH_3). **HRMS** [APCI]: *m/z* calculated for $C_{19}H_{24}ClF_3NO_2S$ $[M-H]^+$: 422.1163, found 422.1163.

3-(nonan-5-ylidene)-5-(trifluoromethyl)-1-((trifluoromethyl)sulfonyl)-1,2,3,4-tetrahydroquinoline (5db)

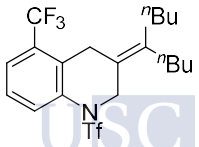

5db

(26.2 mg, 34% yield), obtained as a white solid. **^{1}H NMR** (300 MHz, $CDCl_3$) δ 7.71 (d, *J* = 8.2 Hz, 1H), 7.60 (d, *J* = 7.9 Hz, 1H), 7.35 (t, *J* = 8.1 Hz, 1H), 4.46 (s, 2H), 3.68 (s, 2H), 2.10 (t, *J* = 7.7 Hz, 2H), 2.02 (t, *J* = 7.2 Hz, 2H), 1.41 – 1.27 (m, 8H), 0.93 (q, *J* = 6.8 Hz, 6H). **^{19}F NMR** (282 MHz, $CDCl_3$) δ -60.46, -75.22. **^{13}C NMR** (75 MHz, $CDCl_3$) δ 137.7 (C), 133.0 (C), 128.8 (CH), 126.8 (CH), 125.0 (q, *J* = 5.6 Hz, C), 122.1 (C), 119.4 (d, *J* = 324.8 Hz, C), 50.0 (CH_2), 32.2 (CH_2), 31.7 (CH_2), 30.5 (CH_2), 30.3 (CH_2), 27.3 (CH_2), 23.0 (CH_2), 14.1 (CH_3), 14.0 (CH_3). **HRMS** [APCI]: *m/z* calculated for $C_{20}H_{25}F_6NO_2S$ $[M]^+$: 457.1510, found 457.1512.

6-Chloro-3-(nonan-5-ylidene)-1-((trifluoromethyl)sulfonyl)-1,2,3,4-tetrahydroquinoline (5eb)

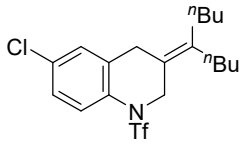

5eb

(39.7 mg, 56% yield), obtained as a yellow oil. **^{1}H NMR** (300 MHz, $CDCl_3$) δ 7.39 (d, *J* = 8.4 Hz, 1H), 7.19 – 7.09 (m, 2H), 4.34 (s, 2H), 3.45 (s, 2H), 2.10 – 1.90 (m, 4H), 1.34 – 1.21 (m, 8H), 0.90 – 0.76 (m, 6H). **^{19}F NMR** (282 MHz, $CDCl_3$) δ -75.49. **^{13}C NMR** (75 MHz, $CDCl_3$) δ 137.7 (C), 134.81 (C), 134.78 (C), 133.0 (C), 128.9 (CH), 127.2 (CH), 126.0 (CH), 122.3 (C), 120.1 (d, *J* = 325.0 Hz, C), 50.0 (CH_2), 32.1 (CH_2), 32.0 (CH_2), 30.8 (CH_2), 30.1 (CH_2), 23.1 (CH_2), 23.0 (CH_2), 14.14 (CH_3), 14.08 (CH_3). **HRMS** [APCI]: *m/z* calculated for $C_{19}H_{24}ClF_3NO_2S$ $[M-H]^+$: 422.1163, found 422.1161.

6-Bromo-3-(nonan-5-ylidene)-1-((trifluoromethyl)sulfonyl)-1,2,3,4-tetrahydroquinoline (5fb)

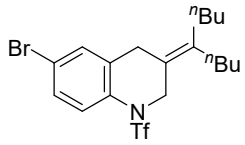

5fb

(49.1 mg, 63% yield), obtained as a yellow oil. **^{1}H NMR** (300 MHz, $CDCl_3$) δ 7.45 – 7.29 (m, 3H), 4.41 (s, 2H), 3.53 (s, 2H), 2.16 – 1.95 (m, 4H), 1.46 – 1.23 (m, 8H), 1.02 – 0.82 (m, 6H). **^{19}F NMR** (282 MHz, $CDCl_3$) δ -75.49. **^{13}C NMR** (75 MHz, $CDCl_3$) δ 137.8 (C), 135.3 (C), 135.1 (C), 131.8 (CH), 130.1 (CH), 126.3 (CH), 122.3 (C), 120.9 (C), 120.1 (d, *J* = 324.9 Hz, C), 50.0 (CH_2), 32.04 (CH_2), 31.98 (CH_2), 30.8 (CH_2), 30.7 (CH_2), 30.1 (CH_2), 23.1 (CH_2), 23.0 (CH_2), 14.14 (CH_3), 14.08 (CH_3). **HRMS** [APCI]: *m/z* calculated for $C_{19}H_{26}BrF_3NO_2S$ $[M+H]^+$: 468.0814, found 468.0813.

3-(Nonan-5-ylidene)-6-phenyl-1-((trifluoromethyl)sulfonyl)-1,2,3,4-tetrahydroquinoline (5gb)

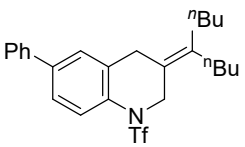

5gb

(56.5 mg, 73% yield), obtained as a white solid. **^{1}H NMR** (300 MHz, $CDCl_3$) δ 7.66 – 7.54 (m, 3H), 7.51 – 7.42 (m, 4H), 7.42 – 7.34 (m, 1H), 4.49 (s, 2H), 3.64 (s, 2H), 2.20 – 2.03 (m, 4H), 1.46 – 1.31 (m, 8H), 1.04 – 0.89 (m, 6H). **^{19}F NMR** (282 MHz, $CDCl_3$) δ -75.46. **^{13}C NMR** (75 MHz, $CDCl_3$) δ 140.4 (C), 140.2 (C), 137.2 (C), 133.3 (C), 129.0 (CH), 127.8 (CH), 127.6 (CH), 127.2 (CH), 125.7 (CH), 125.0 (CH), 123.1 (C), 120.2 (d, *J* = 325.0 Hz, C), 50.2 (CH_2), 32.1 (CH_2), 32.0 (CH_2), 31.1 (CH_2), 30.8 (CH_2), 30.2 (CH_2), 23.1 (CH_2), 23.0 (CH_2), 14.2 (CH_3), 14.1 (CH_3). **HRMS** [APCI]: *m/z* calculated for $C_{25}H_{29}F_3NO_2S$ $[M-H]^+$: 464.1866, found 464.1859.

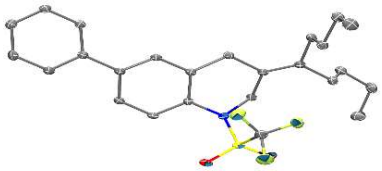

The structure of this compound was confirmed by X-Ray diffraction analysis (CCDC: 2026002).

6-Methoxy-3-(nonan-5-ylidene)-1-((trifluoromethyl)sulfonyl)-1,2,3,4-tetrahydroquinoline (5hb)

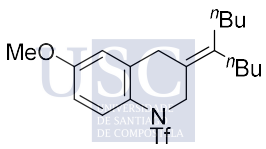

5hb

(47.0 mg, 67% yield), obtained as a white solid. **^{1}H NMR** (300 MHz, $CDCl_3$) δ 7.43 (d, *J* = 8.6 Hz, 1H), 6.80 – 6.71 (m, 2H), 4.41 (brs, 2H), 3.80 (s, 3H), 3.52 (s, 2H), 2.14 – 1.97 (m, 4H), 1.42 – 1.28 (m, 8H), 1.01 – 0.84 (m, 6H). **^{19}F NMR** (282 MHz, $CDCl_3$) δ -75.46. **^{13}C NMR** (75 MHz, $CDCl_3$) δ 158.7 (C), 136.9 (C), 134.7 (C), 129.0 (C), 126.0 (CH), 123.2 (C), 120.2 (d, *J* = 325.1 Hz, C), 113.8 (CH), 112.4 (CH), 55.6 (CH_3), 50.3 (CH_2), 32.1 (CH_2), 32.0 (CH_2), 31.2 (CH_2), 30.7 (CH_2), 30.1 (CH_2), 23.1 (CH_2), 23.0 (CH_2), 14.2 (CH_3), 14.10 (CH_3). **HRMS** [APCI]: *m/z* calculated for $C_{20}H_{29}F_3NO_3S$ $[M+H]^+$: 420.1815, found 420.1803.

3-(nonan-5-ylidene)-1-((trifluoromethyl)sulfonyl)-1,2,3,4-tetrahydroquinoline-6-carbonitrile (5ib)

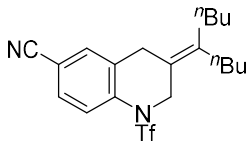

5ib

(11.2 mg, 16% yield), obtained as a white solid**. ^{1}H NMR** (300 MHz, $CDCl_3$) δ 7.66 (d, *J* = 9.2 Hz, 1H), 7.53 (d, *J* = 7.2 Hz, 2H), 4.44 (brs, 2H), 3.58 (s, 2H), 2.08 (q, *J* = 7.5 Hz, 4H), 1.44 – 1.25 (m, 8H), 0.93 (q, *J* = 6.9 Hz, 6H). **^{19}F NMR** (282 MHz, $CDCl_3$) δ -75.01. **^{13}C NMR** (75 MHz, $CDCl_3$) δ 140.3 (C), 138.7 (C), 134.0 (C), 132.9 (CH), 130.8 (CH), 125.2 (CH), 121.3 (C), 120.0 (d, *J* = 324.5 Hz, C), 118.2 (C), 111.0, 49.9 (CH_2), 32.0 (CH_2), 30.8 (CH_2), 30.7 (CH_2), 30.1 (CH_2), 23.1 (CH_2), 23.0 (CH_2), 14.2 (CH_3), 14.1 (CH_3). **HRMS** [APCI]: *m/z* calculated for $C_{20}H_{25}F_3N_2O_2S$ $[M]^+$: 414.1589, found 414.1586.

7-Chloro-3-(nonan-5-ylidene)-1-((trifluoromethyl)sulfonyl)-1,2,3,4-tetrahydroquinoline (5jb)

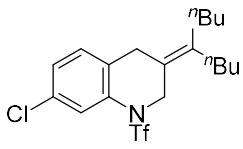

5jb

(40.6 mg, 57% yield), obtained as a yellow solid. **^{1}H NMR** (300 MHz, $CDCl_3$) δ 7.55 (d, *J* = 2.0 Hz, 1H), 7.26 – 7.10 (m, 2H), 4.41 (brs, 2H), 3.52 (s, 2H), 2.16 – 1.97 (m, 4H), 1.44 – 1.21 (m, 8H), 1.02 – 0.81 (m, 6H). **^{19}F NMR** (282 MHz, $CDCl_3$) δ -75.51. **^{13}C NMR** (75 MHz, $CDCl_3$) δ 137.7 (C), 137.1 (C), 132.3 (C), 131.4 (C), 129.9 (CH), 127.6 (CH), 124.8 (CH), 122.5 (C), 120.1 (d, *J* = 324.8 Hz, C), 50.0 (CH_2), 32.05 (CH_2), 31.98 (CH_2), 30.8 (CH_2), 30.5 (CH_2), 30.1 (CH_2), 23.1 (CH_2), 23.0 (CH_2), 14.2 (CH_3), 14.1 (CH_3). **HRMS** [APCI]: *m/z* calculated for $C_{19}H_{24}ClF_3NO_2S$ $[M-H]^+$: 422.1163, found 422.1160.

Methyl 3-(nonan-5-ylidene)-1-((trifluoromethyl)sulfonyl)-1,2,3,4-tetrahydroquinoline-7-carboxylate (5kb)

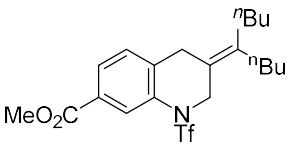

5kb

(37.2 mg, 50% yield), obtained as a white solid. **^{1}H NMR** (500 MHz, $CDCl_3$) δ 8.19 (d, *J* = 1.6 Hz, 1H), 7.91 (dd, *J* = 8.0, 1.6 Hz, 1H), 7.29 (d, *J* = 8.1 Hz, 1H), 4.44 (s, 2H), 3.92 (s, 3H), 3.60 (s, 2H), 2.13 – 2.01 (m, 4H), 1.41 – 1.26 (m, 8H), 0.99 – 0.88 (m, 6H). **^{19}F NMR** (282 MHz, $CDCl_3$) δ -75.52. **^{13}C NMR** (126 MHz, $CDCl_3$) δ 166.2 (C), 138.3 (C), 137.8 (C), 136.4 (C), 129.4 (C), 129.1 (CH), 128.5 (CH), 125.9 (CH), 122.4 (C), 120.1 (q, *J* = 324.6 Hz, C), 52.5 (CH_3), 50.0 (CH_2), 32.1 (CH_2), 32.0 (CH_2), 31.2 (CH_2), 30.8 (CH_2), 30.1 (CH_2), 23.1 (CH_2), 23.0 (CH_2), 14.14 (CH_3), 14.08 (CH_3). **HRMS** [APCI]: *m/z* calculated for $C_{21}H_{29}F_3NO_4S$ $[M+H]^+$: 448.1764, found 448.1766.

7-Methoxy-3-(nonan-5-ylidene)-1-((trifluoromethyl)sulfonyl)-1,2,3,4-tetrahydroquinoline (5lb)

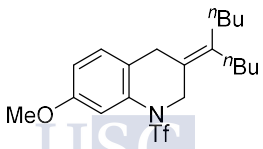

5lb

(44.7 mg, 64% yield), obtained as a white solid. **^{1}H NMR** (500 MHz, $CDCl_3$) δ 7.10 (dd, *J* = 5.6, 3.0 Hz, 2H), 6.80 (dd, *J* = 8.5, 2.6 Hz, 1H), 4.42 (brs, 2H), 3.80 (s, 3H), 3.49 (s, 2H), 2.16 – 1.99 (m, 4H), 1.49 – 1.18 (m, 8H), 1.05 – 0.77 (m, 6H). **^{19}F NMR** (282 MHz, $CDCl_3$) δ -75.52. **^{13}C NMR** (126 MHz, $CDCl_3$) δ 158.4 (C), 136.86 (C), 136.88 (C), 129.5 (CH), 124.8 (C), 123.4 (C), 120.2 (q, *J* = 325.0 Hz, C), 114.0 (CH), 109.9 (CH), 55.6 (CH_3), 50.2 (CH_2), 31.97 (CH_2), 32.01 (CH_2), 30.9 (CH_2), 30.1 (CH_2), 23.1 (CH_2), 23.0 (CH_2), 14.2 (CH_3), 14.1 (CH_3). **HRMS** [APCI]: *m/z* calculated for $C_{20}H_{29}F_3NO_3S$ $[M+H]^+$: 420.1815, found 420.1812.

7-Fluoro-3-(nonan-5-ylidene)-1-((trifluoromethyl)sulfonyl)-1,2,3,4-tetrahydroquinoline (5mb)

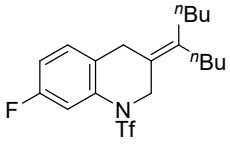

5mb

(47.0 mg, 69% yield), obtained as a yellow oil. **^{1}H NMR** (300 MHz, $CDCl_3$) δ 7.30 (dd, *J* = 9.8, 2.6 Hz, 1H), 7.21 – 7.13 (m, 1H), 6.95 (td, *J* = 8.3, 2.6 Hz, 1H), 4.42 (s, 2H), 3.52 (s, 2H), 2.16 – 1.98 (m, 4H), 1.46 – 1.28 (m, 8H), 1.00 – 0.84 (m, 6H). **^{19}F NMR** (282 MHz, $CDCl_3$) δ -75.57, -114.62 (q, *J* = 8.1 Hz). **^{13}C NMR** (75 MHz, $CDCl_3$) δ 161.0 (d, *J* = 245.6 Hz, C), 137.5 (C), 137.0 (d, *J* = 10.6 Hz, C), 129.9 (d, *J* = 8.9 Hz, CH), 128.5 (d, *J* = 3.2 Hz, C), 122.6 (C), 120.1 (d, *J* = 324.5 Hz, C), 114.6 (d, *J* = 21.4 Hz, CH), 112.1 (d, *J* = 25.5 Hz, CH), 50.0 (CH_2), 32.03 (CH_2), 31.97 (CH_2), 30.9 (CH_2), 30.3 (CH_2), 30.1 (CH_2), 23.1 (CH_2), 23.0 (CH_2), 14.2 (CH_3), 14.1 (CH_3). **HRMS** [APCI]: *m/z* calculated for $C_{19}H_{25}F_4NO_2S$ $[M]^+$: 407.1542, found 407.1544.

8-Methyl-3-(nonan-5-ylidene)-6-phenyl-1-((trifluoromethyl)sulfonyl)-1,2,3,4-tetrahydroquinoline (5nb)

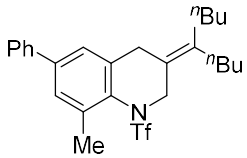

5nb

(42.2 mg, 53% yield), obtained as a brown oil. **^{1}H NMR** (500 MHz, $CDCl_3$) δ 7.52 – 7.45 (m, 2H), 7.39 – 7.33 (m, 2H), 7.32 – 7.24 (m, 2H), 7.20 – 7.17 (m, 1H), 4.82 (d, *J* = 16.7 Hz, 1H), 3.87 (d, *J* = 16.7 Hz, 1H), 3.59 (d, *J* = 18.2 Hz, 1H), 3.45 (d, *J* = 18.2 Hz, 1H), 2.41 (s, 3H), 2.09 – 1.95 (m, 2H), 1.97 – 1.84 (m, 2H), 1.36 – 1.18 (m, 8H), 0.91 – 0.79 (m, 6H). **^{19}F NMR** (282 MHz, $CDCl_3$) δ -74.69. **^{13}C NMR** (126 MHz, $CDCl_3$) δ 141.4 (C), 140.3 (C), 136.8 (C), 136.4 (C), 136.1 (C), 134.8 (C), 128.9 (CH), 128.6 (CH), 127.8 (CH), 127.3 (CH), 124.9 (CH), 124.3 (C), 120.2 (q, *J* = 325.2 Hz, C), 51.4 (CH_2), 32.4 (CH_2), 32.0 (CH_2), 31.8 (CH_2), 30.3 (CH_2), 30.2 (CH_2), 23.1 (CH_2), 19.5 (CH_3), 14.2 (CH_3), 14.1 (CH_3). **HRMS** [APCI]: *m/z* calculated for $C_{26}H_{32}F_3NO_2S$ $[M]^+$: 479.2100, found 479.2098.

6,8-Dimethyl-3-(nonan-5-ylidene)-1-((trifluoromethyl)sulfonyl)-1,2,3,4-tetrahydroquinoline (5ob)

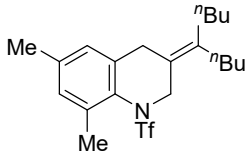

5ob

(36.1 mg, 52% yield), obtained as a yellow oil. **^{1}H NMR** (500 MHz, $CDCl_3$) δ 6.96 (s, 1H), 6.87 (s, 1H), 4.85 (d, *J* = 16.7 Hz, 1H), 3.88 (d, *J* = 16.7 Hz, 1H), 3.54 (d, *J* = 18.1 Hz, 1H), 3.43 (d, *J* = 18.2 Hz, 1H), 2.38 (s, 3H), 2.30 (s, 3H), 2.13 – 2.01 (m, 2H), 2.03 – 1.90 (m, 2H), 1.40 – 1.23 (m, 8H), 1.00 – 0.86 (m, 6H). **^{19}F NMR** (282 MHz, $CDCl_3$) δ -74.42. **^{13}C NMR** (126 MHz, $CDCl_3$) δ 138.3 (C), 136.2 (C), 135.8 (C), 135.7 (C), 133.0 (C), 130.5 (CH), 126.8 (CH), 124.5 (C), 120.2 (q, *J* = 325.3 Hz, C), 51.4 (CH_2), 32.3 (CH_2), 32.0 (CH_2), 31.7 (CH_2), 31.5 (CH_2), 30.3 (CH_2), 30.2 (CH_2), 23.0 (CH_3), 21.1 (CH_3), 19.1 (CH_2), 14.2 (CH_3), 14.1 (CH_3). **HRMS** [APCI]: *m/z* calculated for $C_{21}H_{31}F_3NO_2S$ $[M+H]^+$: 418.2022, found 418.2023.

3-(Nonan-5-ylidene)-1-((trifluoromethyl)sulfonyl)-1,2,3,4-tetrahydrobenzo[g]quinoline (5pb)

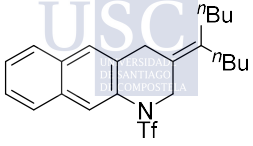

5pb

(49.0 mg, 67% yield), obtained as a black oil. **^{1}H NMR** (300 MHz, $CDCl_3$) δ 8.01 (s, 1H), 7.87 – 7.75 (m, 2H), 7.68 (s, 1H), 7.53 – 7.44 (m, 2H), 4.54 (s, 2H), 3.70 (s, 2H), 2.19 – 1.98 (m, 4H), 1.45 – 1.28 (m, 8H), 1.00 – 0.87 (m, 6H). **^{19}F NMR** (282 MHz, $CHCl_3$) δ -75.63. **^{13}C NMR** (75 MHz, $CHCl_3$) δ 136.6 (C), 134.3 (C), 132.5 (C), 132.3 (C), 131.8 (C), 128.3 (CH), 127.2 (CH), 127.0 (CH), 126.8 (CH), 126.3 (CH), 123.4 (C), 123.2 (CH), 120.2 (d, *J* = 324.2 Hz, C), 50.7 (CH_2), 32.1

(CH_2), 32.0 (CH_2), 31.3 (CH_2), 30.6 (CH_2), 30.4 (CH_2), 23.1 (CH_2), 23.0 (CH_2), 14.2 (CH_3), 14.1 (CH_3). **HRMS** [APCI]: *m/z* calculated for $C_{23}H_{28}F_3NO_2S$ $[M]^+$: 439.1793, found 439.1796.

(*E*)-3-Benzylidene-2,2-dimethyl-6-phenyl-1-((trifluoromethyl)sulfonyl)-1,2,3,4-tetrahydroquinoline (5gg)

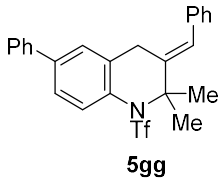

5gg

(62.4 mg, 82% yield), obtained as a yellow solid. **^{1}H NMR** (500 MHz, $CDCl_3$) δ 7.50 – 7.13 (m, 13H), 6.42 (s, 1H), 3.73 (s, 2H), 1.66 (s, 6H). **^{19}F NMR** (282 MHz, $CDCl_3$) δ -75.09. **^{13}C NMR** (126 MHz, $CDCl_3$) δ 143.0 (C), 141.2 (C), 140.0 (C), 136.8 (C), 136.2 (C), 134.6 (C), 128.99 (CH), 128.95 (CH), 128.6 (CH), 128.3 (CH), 127.8 (CH), 127.3 (CH), 127.2 (CH), 126.2 (CH), 125.8 (CH), 123.7 (CH), 120.1 (q, *J* = 324.8 Hz, C), 68.7 (C), 31.5 (CH_2), 29.7 (CH_3). **HRMS** [APCI]: *m/z* calculated for $C_{25}H_{22}F_3NO_2S$ $[M]^+$: 457.1323, found 457.1326.

3.7 Procedure for the gram scale synthesis of 5aj and 5aj'

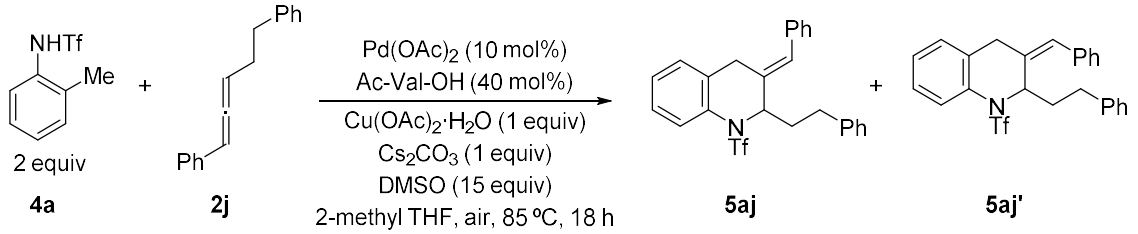

To a solution of $Pd(OAc)_2$ (51.0 mg, 10 mol%), Ac-Val-OH (144.5 mg, 40 mol%), $Cu(OAc)_2.H_2O$ (453.1 mg, 1 equiv), Cs_2CO_3 (739.4 mg, 1 equiv) and **4a** (1.09 g, 4.54 mmol, 2 equiv) in 2-methyl THF (7 mL) and DMSO (2.4 mL, 15 equiv), under air atmosphere, heated at 85 °C, in a Schlenk tube sealed with a rubber septum was slowly added the allene **2j** (500.0 mg, 2.27 mmol) with a syringe pump during 1h. The reaction was stirred at 85 °C during 18 h and then cooled to room temperature. Evaporation and column chromatography on silica gel (hexanes:diethylether; 99:1) afforded **3-benzylidene-2-phenethyl-1-((trifluoromethyl)sulfonyl)-1,2,3,4-tetra hydro quinoline** (1.8:1 E/Z ratio of **5aj** and **5aj'**, inseparable mixture (706.2 mg, 68% yield), obtained as a yellow solid).

3.8 Synthesis of the deuterated analogue in the methyl position of substrate 4a

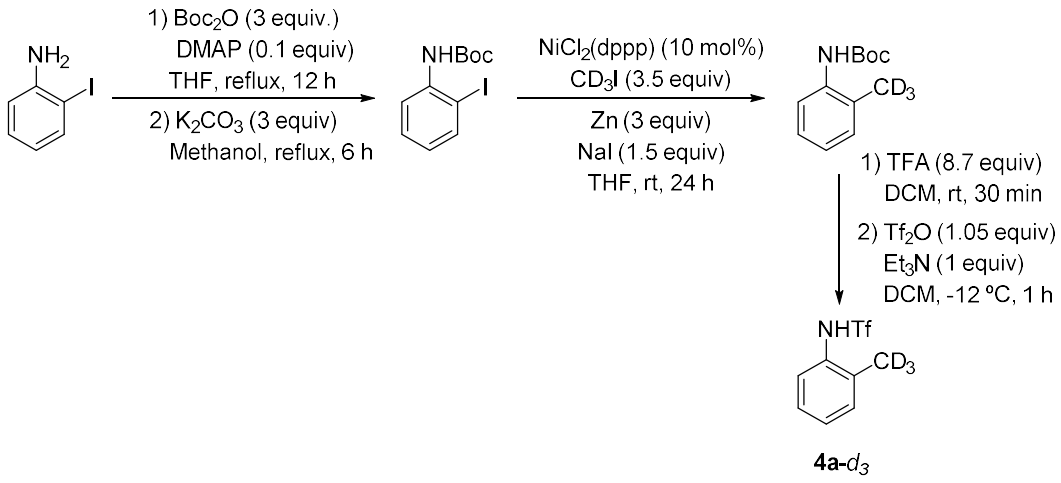

4a-*d*$_3$

Following a reported procedure,[177] in a flame-dried round flask under argon atmosphere, 2-iodoaniline (1.00 g, 4.57 mmol) was added. Then, it was dissolved in anhydrous THF (50 mL), followed by the addition of Boc_2O (2.98 g, 3 equiv) and DMAP (56 mg, 0.1 equiv). The solution was stirred at reflux for 12 h and then cooled to room temperature. The solvent was evaporated and the crude was partitioned between 40 mL of HCl (0.5 N) and 40 mL of EtOAc. The aqueous phase was extracted with EtOAc (2x40 mL) and the organic phases were washed with brine (40 mL), dried over Na_2SO_4, filtered and concentrated to afford the crude di-Boc product as a brown solid. The crude was redissolved in methanol (50 mL), followed by the addition of K_2CO_3 (1.89g, 3 equiv.). The solution was stirred at reflux for 6 h. The solvent was evaporated and the crude was purified by column chromatography on silica gel (hexanes:ethyl acetate; 95:5), affording **tert-butyl (2-iodophenyl)carbamate** as a white solid (1.04 g, 71% yield). All the spectral data recorded were in agreement with those found in the corresponding literature.

Following a previously reported procedure,[178] to a flame-dried Schlenk under argon atmosphere was added $NiCl_2$(dppp) (147 mg, 0.1 equiv), zinc powder (534 mg, 3 equiv), NaI (613 mg, 1.5 equiv) and tert-butyl (2-iodophenyl)carbamate (870 mg, 2.73 mmol). Then, anhydrous THF (27 mL) and CD_3I (619 µL, 3.5 equiv) were sequentially added. The reaction was stirred at room temperature for 24h. Then, 20 mL of NH_4Cl (sat.) was added to destroy all remaining CD_3I, and the solution was stirred during 2 h. After that, the solution was filtered through a pad of Celite©, eluted with DCM. The volatiles were evaporated, followed by a purification by column chromatography on silica gel (hexanes:diethyl ether; 95:5), affording **tert-butyl (2-(methyl-d3)phenyl)carbamate** as a white solid (451 mg, 79% yield, 100% deuterated). **^{1}H NMR** (300 MHz, $CDCl_3$) δ 7.80 (d, *J* = 8.1 Hz, 1H), 7.26 – 7.10 (m, 2H), 7.00 (td, *J* = 7.4, 1.3 Hz, 1H), 6.28 (s, 1H), 1.53 (s, 9H). **^{2}D NMR** (46 MHz, $CDCl_3$) δ 2.23 (brs). **^{13}C NMR** (75 MHz, $CDCl_3$) δ 153.2 (C), 136.5 (C), 130.4 (CH), 126.9 (CH), 123.8 (CH), 121.0 (CH), 80.5 (C), 28.5 (CH_3).

Following a general procedure for N-Boc deprotection,[179] to a solution of tert-butyl (2-(methyl-d3)phenyl)carbamate (440 mg, 2.09 mmol) in DCM (7 mL) was added TFA (1.4 mL, 8.7 equiv).

[177] S. Jana, A. Verma, R. Kadu, S. Kumar, *Chem. Sci.* **2017**, *8*, 6633.
[178] L. Hu, X. Liu, X. Liao, *Angew. Chem. Int. Ed.* **2016**, *55*, 9743.
[179] Y. So, J. H. Song, D. Il. Jung, *J. Org. Chem.* **2008**, *73*, 5658.

The reaction was stirred at rt during 30 min. After the reaction was completed, the residue was diluted with DCM, basified with $NaHCO_3$ (sat.) until pH 8, extracted with DCM (3x10 mL), dried over Na_2SO_4, filtered and concentrated. The crude amine (228 mg) was used in the next step without further purification.

To a solution of the crude amine (220 mg, 2.00 mmol) in dichloromethane (4 mL) under argon atmosphere was added triethylamine (278 µL, 2.00 mmol) at -12°C. After the solution was stirred 5 minutes at that temperature, trifluoromethanesulfonic anhydride (353 µL, 1.05 equiv) was added dropwise. The reaction was stirred for 1 h at that temperature before being quenched with water. The organic layer was separated and the aqueous layer extracted with dichloromethane. The combined organic phases were washed with brine and then dried over Na_2SO_4. Evaporation and column chromatography on silica gel (hexanes:diethylether; 80:20) afforded **1,1,1-trifluoro-N-(2-(methyl-d3)phenyl)methanesulfonamide (4a-*d*$_3$)** as a white solid (370 mg, 77%). **^{1}H NMR** (300 MHz, $CDCl_3$) δ 7.42 – 7.35 (m, 1H), 7.31 – 7.19 (m, 3H), 6.82 (s, 1H). **^{2}D NMR** (46 MHz, $CDCl_3$) δ 2.36. **^{19}F NMR** (282 MHz, $CDCl_3$) δ -76.51. **^{13}C NMR** (75 MHz, $CDCl_3$) δ 133.8 (C), 132.1 (C), 131.4 (CH), 128.6 (CH), 127.4 (CH), 126.4 (CH), 119.9 (d, *J* = 322.3 Hz, C).

3.9 Measure of the kinetic isotopic effect (KIE) by a competition test

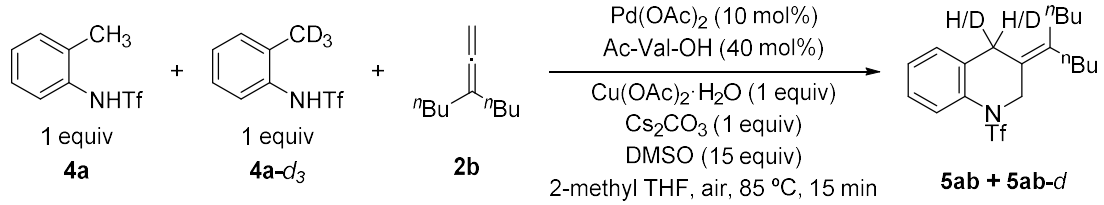

To a solution of $Pd(OAc)_2$ (3.7 mg, 10 mol%), Ac-Val-OH (10.6 mg, 40 mol%), $Cu(OAc)_2{\cdot}H_2O$ (33.3 mg, 1 equiv), Cs_2CO_3 (54.4 mg, 1 equiv), **4a** (39.9 mg, 0.167 mmol) and **4a-*d*$_3$** (40.5 mg, 0.167 mmol) in 2-methyl THF (2 mL) and DMSO (0.178 µL, 15 equiv), under air atmosphere, in a Schlenk tube was added the allene **2b** (25.4 mg, 0.167 mmol). The tube was sealed with a rubber septum and an air atmosphere was injected in the flask with a balloon and a needle. The reaction was heated at 85 °C, stirred during 15 min and then cooled to room temperature. Evaporation and column chromatography on silica gel (hexanes:diethylether; 99:1) afforded 23.5 mg of a mixture of **5ab** and **5ab**-*d*. The KIE value (approximately **7.3**) was obtained by integrating the H_a signal and the H^4/D signal of compound **5ab**.

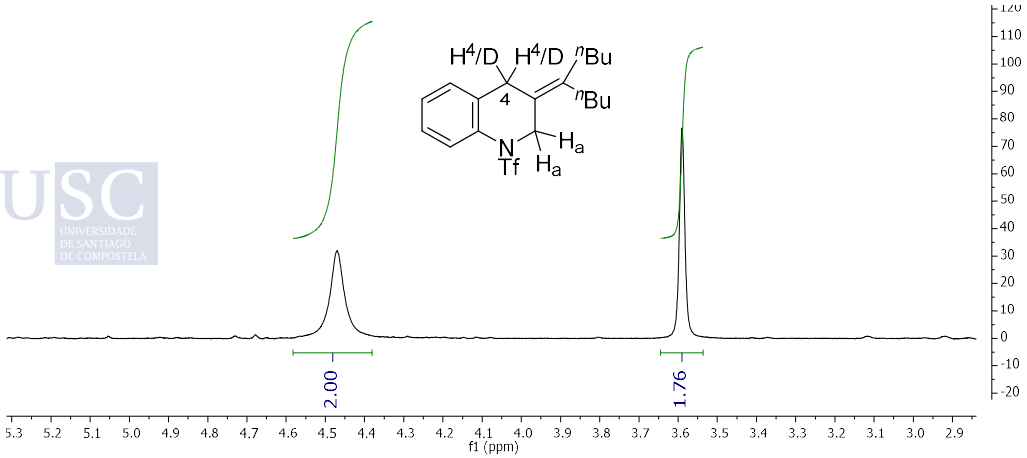

3.10 Measure of the kinetic isotopic effect (KIE) by a parallel test

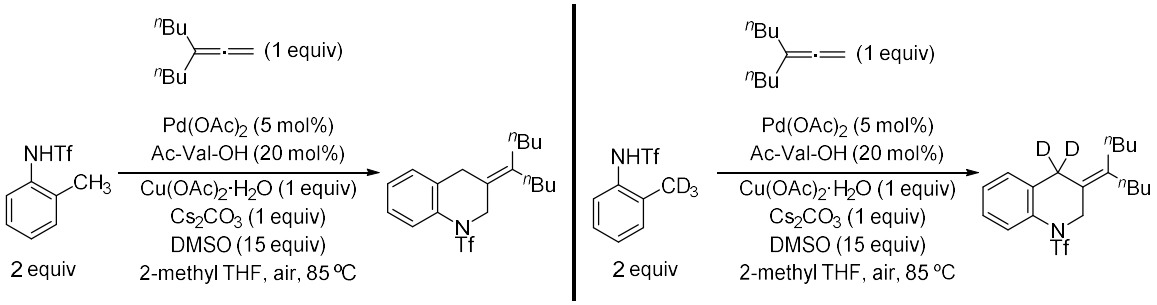

Following the general procedure for the synthesis of compounds **5**, two reactions were set using two separated Schlenk tubes under air atmosphere. $Pd(OAc)_2$ (1.9 mg, 5 mol%), Ac-Val-OH (5.3 mg, 20 mol%), $Cu(OAc)_2$·H2O (33.3 mg, 1 equiv), Cs_2CO_3 (54.4 mg, 1 equiv) were added in each Schlenk. Then, in the first Schlenk, **4a** (39.9 mg, 0.167 mmol) was added, and in the second Schlenk, **4a**-d_3 (40.5 mg, 0.167 mmol) was added. After that, 2-methyl THF (2 mL), DMSO (0.178 µL, 15 equiv) and the allene **2b** (25.4 mg, 0.167 mmol) were added. The tubes were sealed with a rubber septum and stirred at 85 °C. Both tests were set up with 3 minutes of delay. Aliquots of 250 µL of the reaction were taken at 5, 10, 20 and 60 min, filtered through a Florisil© pad and eluted with ethyl acetate. The volatiles were evaporated and the crude residues were analyzed with ^{19}F NMR spectrometry. The parallel tests were repeated, taking from the non-deuterated experiments, aliquots of 250 µL at 10, 30, 60 and 120 min, and from the deuterated experiment, aliquots of 250 µL at 20, 40, 60 and 90 min.

To calculate KIE, the linear regression method was used. The quotient between the integral of the product signal and the integral of the remaining starting material signal was plotted as a function of time, so that the slope can be calculated with a least squares approximation. Duplicate points were calculated with the mean between the two points. KIE was calculated as the quotient between the slope of the non-deuterated experiment and the deuterated experiment, resulting in an approximate value of **2.7**.

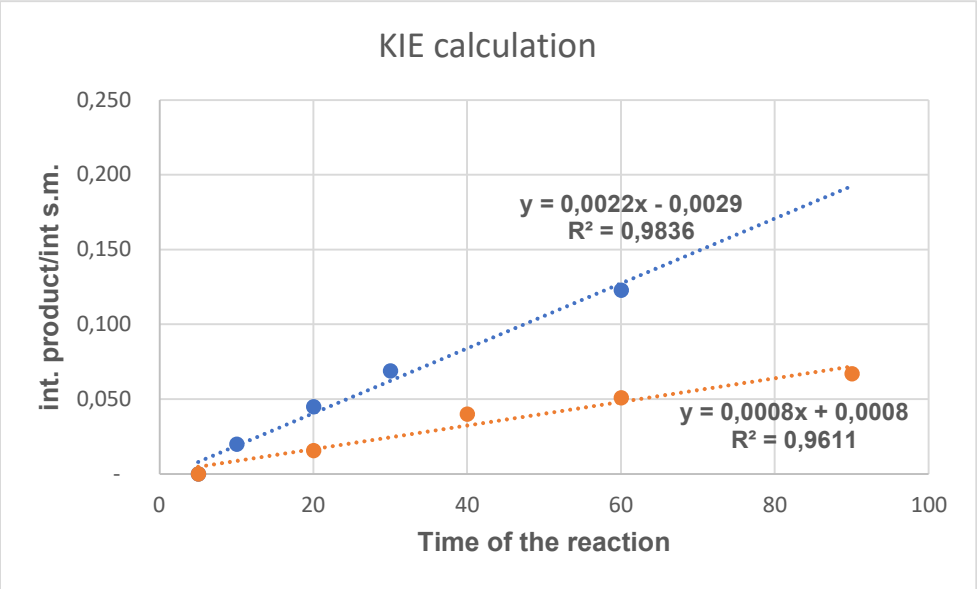

Time (min)	Ratio
5	0.000
10	0.020
20	0.045
30	0.069
60	0.123

Time (min)	Ratio
5	0.000
20	0.016
40	0.040
60	0.051
90	0.067

3.11 General procedure for the Pd-catalyzed formal (4+2) annulation of triflyl-protected *o*-methylaniline 4a with chiral allene (*S*)-2e, exemplified by entry 1 of Table 8

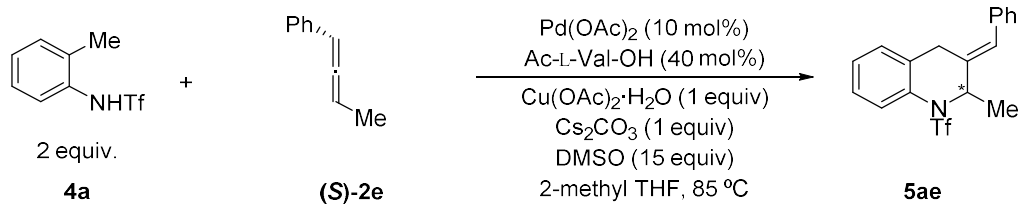

To a solution of $Pd(OAc)_2$ (3.7 mg, 10 mol%), Ac-Val-OH (10.6 mg, 40 mol%), $Cu(OAc)_2{\cdot}H_2O$ (33.3 mg, 1 equiv), Cs_2CO_3 (54.4 mg, 1 equiv) and **4a** (79.9 mg, 0.333 mmol, 2 equiv) in 2-methyl THF (1 mL) and DMSO (0.178 µL, 15 equiv), under air atmosphere, heated at 85 °C, in a Schlenk tube sealed with a rubber septum was slowly added the allene **(*S*)-2e** (25.4 mg, 0.167 mmol) with a syringe pump during 1 h. The reaction was stirred at 85 °C during 18 h and then cooled to room temperature. Evaporation and column chromatography on silica gel (hexanes:diethylether; 99:1) afforded **(*E*)-3-Benzylidene-2-methyl-1-((trifluoromethyl)sulfonyl)-1,2,3,4-tetrahydro quinoline (5ae)** as a white solid (41.3 mg, 67% yield).

Enantioselectivity was determined by chiral SFC analysis on Phenomenex Cellulose-1 at 40 °C (CO_2 : MeOH = 98:02, 0.5 mL/min).

Racemic sample

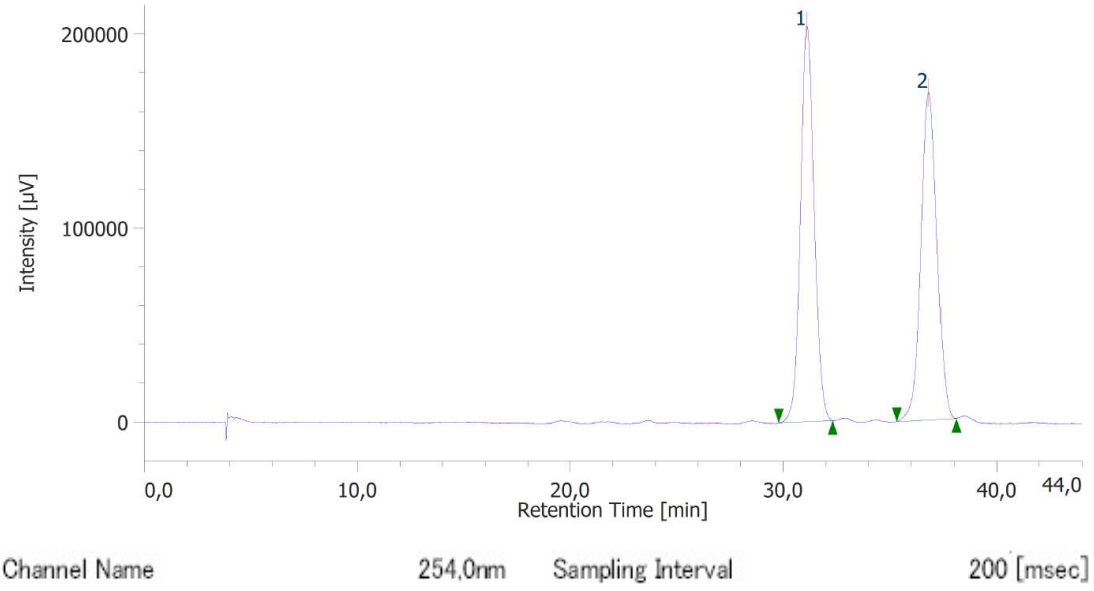

#	Peak Name	CH	tR [min]	Area [μV·sec]	Height [μV]	Area%	Height%	Quantity	NTP	Resolution	Symmetry Factor	Warning
1	Unknown	7	31,110	9077191	204021	51,085	54,733	N/A	11599	4,574	1,076	
2	Unknown	7	36,820	8691599	168739	48,915	45,267	N/A	11934	N/A	1,018	

Asymmetric sample (58:42 er)

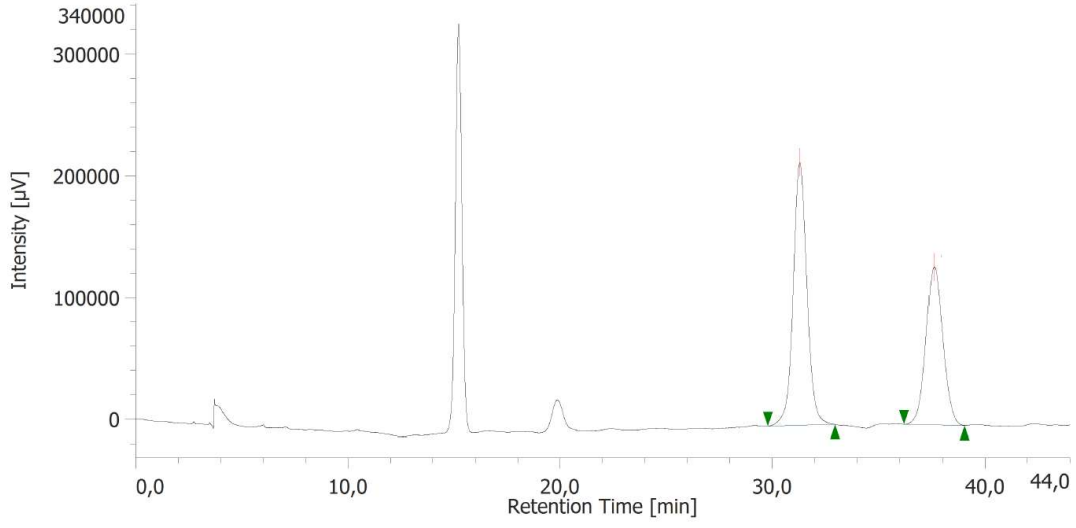

#	Peak Name	CH	tR [min]	Area [μV·sec]	Height [μV]	Area%	Height%	Quantity	NTP	Resolution	Symmetry Factor	Warning
1	Unknown	5	31,290	9724299	215953	58,047	62,478	N/A	12012	4,951	1,053	
2	Unknown	5	37,603	7028075	129691	41,953	37,522	N/A	11299	N/A	1,051	

3.12 Test of chiral allene (*S*)-2e in absence of substrate 4a

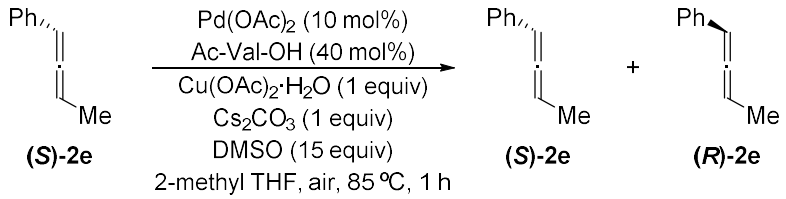

To a solution of $Pd(OAc)_2$ (3.7 mg, 10 mol%), Ac-Val-OH (10.6 mg, 40 mol%), $Cu(OAc)_2{\cdot}H_2O$ (33.3 mg, 1 equiv), Cs_2CO_3 (54.4 mg, 1 equiv) in 2-methyl THF (2 mL) and DMSO (0.178 µL, 15 equiv), under air atmosphere in a Schlenk tube sealed with a rubber septum, allene **(*S*)-2e** was added (24.1 mg, 0.167 mmol). The reaction was stirred at 85 °C during 1 h and then cooled to room temperature, filtered through a silica/Florisil© pad and eluted with pentane. The crude was analyzed by chiral GC chromatography on Chiraldex G-TA.

Chiral starting material (>99% ee)

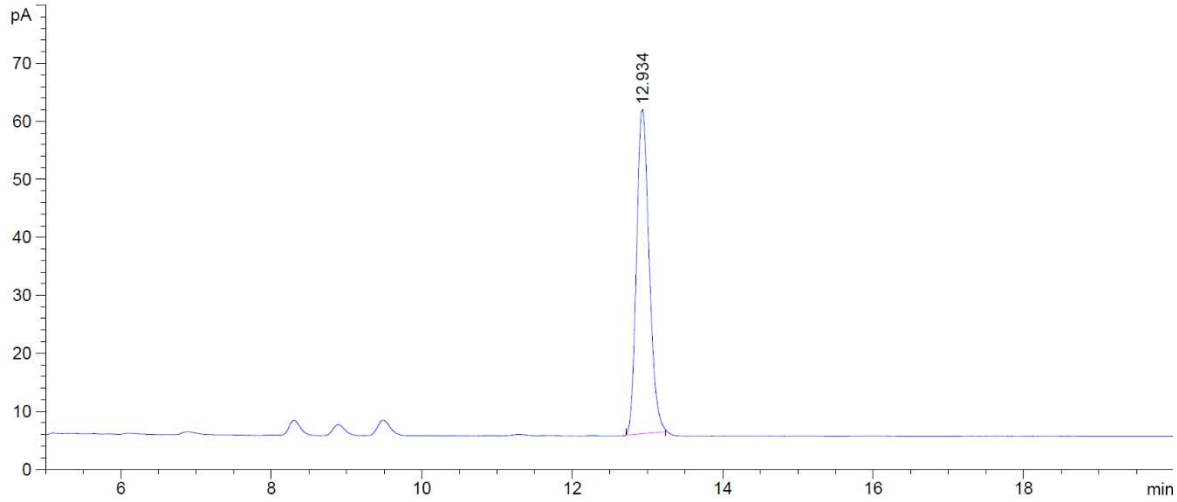

Peak #	RetTime [min]	Type	Width [min]	Area [pA*s]	Height [pA]	Area %
1	12.934	BB	0.1409	652.41986	55.91862	1.000e2
Totals :				652.41986	55.91862	

Crude (61:39 er)

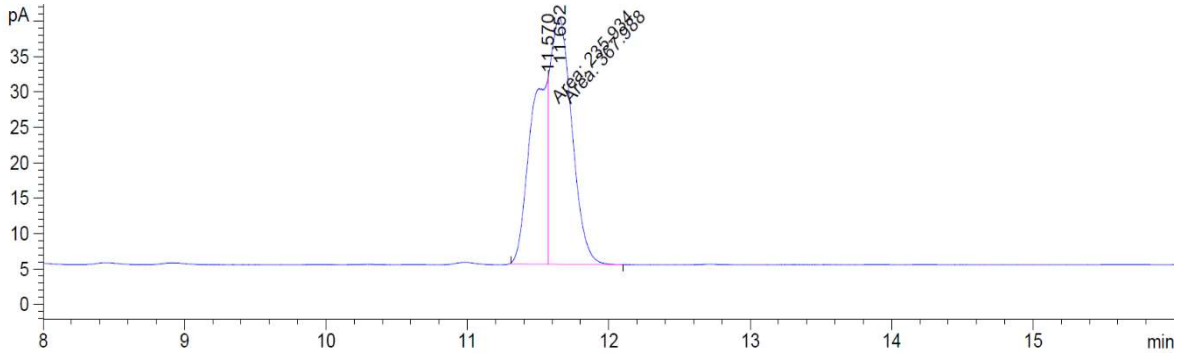

Peak #	RetTime [min]	Type	Width [min]	Area [pA*s]	Height [pA]	Area %
1	11.570	MF	0.1498	235.93372	26.24906	39.06697
2	11.652	FM	0.1766	367.98752	34.72678	60.93303
Totals :				603.92123	60.97584	

3.13 General procedure for the Pd-catalyzed formal (5+2) annulation of triflyl-protected *o*-methylbenzylamines with allenes, exemplified with 7ab

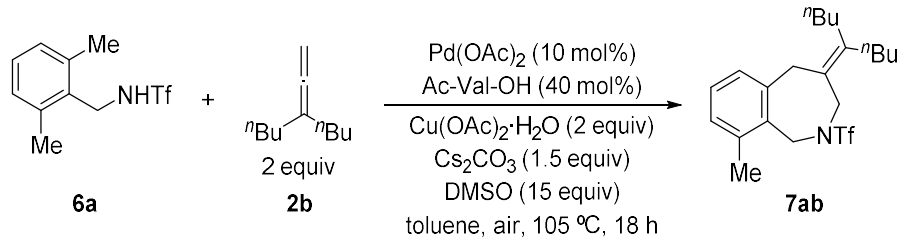

To a solution of $Pd(OAc)_2$ (3.7 mg, 10 mol%), Ac-Val-OH (10.6 mg, 40 mol%), $Cu(OAc)_2{\cdot}H_2O$ (66.7 mg, 2 equiv.), Cs_2CO_3 (81.6 mg, 1.5 equiv) and **6a** (44.6 mg, 0.167 mmol) in toluene (2 mL) and DMSO (0.178 µL, 15 equiv), under air atmosphere, in a Schlenk tube was added the allene **2b** (50.9 mg, 0.333 mmol, 2 equiv.). The tube was sealed with a rubber septum and an air atmosphere was injected in the flask with a balloon and a needle. The reaction was heated at 105 °C, stirred during 18 h and then cooled to room temperature. Evaporation and column chromatography on silica gel (hexanes:diethylether; 99:1) afforded **9-methyl-4-(nonan-5-ylidene)-2-((trifluoromethyl)sulfonyl)-2,3,4,5-tetrahydro-1H-benzo[c]azepine (7ab)** as a white solid (60.2 mg, 86% yield). **^{1}H NMR** (300 MHz, $CDCl_3$) δ 7.17 – 7.06 (m, 1H), 7.03 (d, *J* = 7.5 Hz, 2H), 4.64 (brs, 2H), 4.24 (brs, 2H), 3.62 (s, 2H), 2.34 (s, 3H), 2.14 – 2.02 (m, 4H), 1.36 – 1.21 (m, 8H), 0.98 – 0.85 (m, 6H). **^{19}F NMR** (282 MHz, $CDCl_3$) δ -76.17. **^{13}C NMR** (75 MHz, $CDCl_3$) δ 141.7 (C), 139.4 (C), 135.7 (C), 132.6 (C), 128.9 (CH), 127.9 (CH), 127.8 (CH), 124.4 (C), 120.3 (d, *J* = 323.7 Hz, C), 52.5 (CH_2), 48.3 (CH_2), 37.2 (CH_2), 32.7 (CH_2), 32.0 (CH_2), 31.5 (CH_2), 30.8 (CH_2), 23.2 (CH_2), 23.0 (CH_2), 19.8 (CH_3), 14.10 (CH_3), 14.05 (CH_3). **HRMS** [APCI]: *m/z* calculated for $C_{21}H_{31}F_3NO_2S$ $[M+H]^+$: 418.2022, found 418.2018.

9-Fluoro-4-(nonan-5-ylidene)-2-((trifluoromethyl)sulfonyl)-2,3,4,5-tetrahydro-1*H*-benzo[*c*]azepine (7bb)

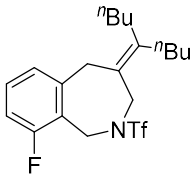

7bb

(52.7 mg, 75% yield), obtained as a yellow oil. **^{1}H NMR** (300 MHz, $CDCl_3$) δ 7.18 (q, *J* = 7.3 Hz, 1H), 7.00 – 6.85 (m, 2H), 4.68 (brs, 2H), 4.26 (brs, 2H), 3.64 (s, 2H), 2.15 – 2.01 (m, 4H), 1.38 – 1.16 (m, 8H), 0.99 – 0.80 (m, 6H). **^{19}F NMR** (282 MHz, $CDCl_3$) δ -76.35, -118.85 (dd, *J* = 9.9, 5.7 Hz). **^{13}C NMR** (75 MHz, $CDCl_3$) δ 160.0 (d, *J* = 246.4 Hz, C), 142.9 (C), 141.5 (C), 129.1 (d, *J* = 9.1 Hz, CH), 125.2 (d, *J* = 3.1 Hz, CH), 123.9 (C), 121.9 (d, *J* = 13.9 Hz, C), 120.2 (d, *J* = 323.5 Hz, C), 113.5 (d, *J* = 22.6 Hz, CH), 52.6 (CH_2), 44.3 (d, *J* = 8.4 Hz, CH_2), 36.4 (CH_2), 32.8 (CH_2), 31.9 (CH_2), 31.4 (CH_2), 30.7 (CH_2), 23.1 (CH_2), 23.0 (CH_2), 14.1 (CH_3). **HRMS** [APCI]: *m/z* calculated for $C_{20}H_{28}F_4NO_2S$ $[M+H]^+$: 422.1771, found 422.1771.

9-Methoxy-4-(nonan-5-ylidene)-2-((trifluoromethyl)sulfonyl)-2,3,4,5-tetrahydro-1*H*-benzo[*c*]azepine (7cb)

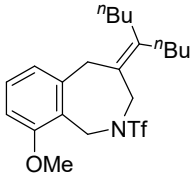

7cb

(65.4 mg, 90% yield), obtained as a white solid. **^{1}H NMR** (500 MHz, $CDCl_3$) δ 7.16 (t, *J* = 7.9 Hz, 1H), 6.75 (dd, *J* = 15.8, 7.9 Hz, 2H), 4.71 (brs, 2H), 4.23 (brs, 2H), 3.81 (s, 3H), 3.60 (s, 2H), 2.10 – 2.00 (m, 4H), 1.35 – 1.19 (m, 8H), 0.95 – 0.82 (m, 6H). **^{19}F NMR** (282 MHz, $CDCl_3$) δ -76.15. **^{13}C NMR** (126 MHz, $CDCl_3$) δ 156.6 (C), 141.4 (C), 140.4 (C), 128.5 (CH), 124.8 (C), 122.7 (C), 122.2 (CH), 120.3 (q, *J* = 323.8 Hz, C), 108.8 (CH), 55.8 (CH_3), 52.4 (CH_2), 45.4 (CH_2), 36.3 (CH_2), 32.8 (CH_2), 31.9 (CH_2), 31.4 (CH_2), 30.8 (CH_2), 23.1 (CH_2), 23.0 (CH_2), 14.09 (CH_3), 14.07 (CH_3). **HRMS** [APCI]: *m/z* calculated for $C_{21}H_{31}F_3NO_3S$ $[M+H]^+$: 434.1971, found 434.1971.

7-Methoxy-9-methyl-4-(nonan-5-ylidene)-2-((trifluoromethyl)sulfonyl)-2,3,4,5-tetrahydro-1*H*-benzo[*c*]azepine (7db)

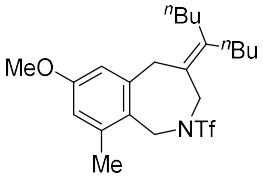

7db

(52.7 mg, 71% yield), obtained as a yellow solid. **^{1}H NMR** (300 MHz, $CDCl_3$) δ 6.58 (s, 2H), 4.59 (brs, 2H), 4.20 (brs, 2H), 3.78 (s, 3H), 3.57 (s, 2H), 2.33 (s, 3H), 2.09 (q, *J* = 7.9 Hz, 4H), 1.37 – 1.24 (m, 8H), 0.96 – 0.85 (m, 6H). **^{19}F NMR** (282 MHz, $CDCl_3$) δ -76.21. **^{13}C NMR** (75 MHz, $CDCl_3$) δ 158.8 (C), 141.9 (C), 141.1 (C), 137.4 (C), 125.0 (C), 124.1 (C), 120.2 (d, *J* = 324.2 Hz, C), 113.7 (CH), 113.4 (CH), 55.3 (CH_3), 52.3 (CH_2), 47.7 (CH_2), 37.7 (CH_2), 32.7 (CH_2), 32.0 (CH_2), 31.5 (CH_2), 30.8 (CH_2), 23.2 (CH_2), 23.0 (CH_2), 20.1 (CH_3), 14.12 (CH_3), 14.06 (CH_3). **HRMS** [APCI]: *m/z* calculated for $C_{22}H_{33}F_3NO_3S$ $[M+H]^+$: 448.2128, found 448.2126.

1-Ethyl-7,9-dimethyl-4-(nonan-5-ylidene)-2-((trifluoromethyl)sulfonyl)-2,3,4,5-tetrahydro-1*H*-benzo[*c*]azepine (7eb)

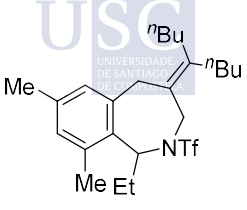

7eb

(66.6 mg, 87% yield), obtained as a yellow oil. NMR characterization performed at 50 °C. **^{1}H NMR** (500 MHz, $CDCl_3$) δ 6.84 (s, 2H), 5.24 – 5.14 (m, 1H), 4.40 (d, *J* = 14.9 Hz, 1H), 4.19 (d, *J* = 14.9 Hz, 1H), 3.60 (q, *J* = 15.6 Hz, 2H), 2.28 (s, 3H), 2.26 (s, 3H), 2.20 – 2.03 (m, 4H), 1.95 – 1.83 (m, 1H), 1.73 – 1.60 (m, 1H), 1.45 – 1.23 (m, 8H), 1.09 (t, J = 7.4 Hz, 3H), 1.00 – 0.91 (m, 3H), 0.88 (t, *J* = 7.1 Hz, 3H). **^{19}F NMR** (282 MHz, $CDCl_3$) δ -76.45. **^{13}C NMR** (126 MHz, $CDCl_3$) δ 139.7 (C), 137.8 (C), 136.6 (C), 134.9 (C), 134.8 (C), 130.1 (CH), 129.6

(CH), 126.9 (C), 120.2 (q, *J* = 323.4 Hz, C), 62.0 (CH), 48.1 (CH_2), 37.4 (CH_2), 33.1 (CH_2), 32.4 (CH_2), 31.2 (CH_2), 30.6 (CH_2), 26.7 (CH_2), 23.13 (CH_2), 23.11 (CH_2), 20.8 (CH_3), 19.6 (CH_3), 14.0 (CH_3), 13.9 (CH_3), 11.7 (CH_3). **HRMS** [APCI]: *m/z* calculated for $C_{24}H_{37}F_3NO_2S$ $[M+H]^+$: 460.2492, found 460.2496.

1,7,9-trimethyl-4-(nonan-5-ylidene)-2-((trifluoromethyl)sulfonyl)-2,3,4,5-tetrahydro-1H-benzo[c]azepine (7fb)

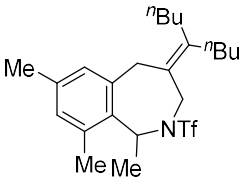

7fb

(50.7 mg, 68% yield), obtained as a yellow oil. **^{1}H NMR** (300 MHz, $CDCl_3$) δ 6.84 (s, 2H), 5.53 – 5.38 (m, 1H), 4.37 (d, *J* = 14.7 Hz, 1H), 4.24 (d, *J* = 14.8 Hz, 1H), 3.57 (s, 2H), 2.27 (d, *J* = 9.1 Hz, 6H), 2.21 – 1.90 (m, 4H), 1.45 (d, *J* = 7.3 Hz, 3H), 1.41 – 1.17 (m, 8H), 0.89 (dt, *J* = 21.3, 6.9 Hz, 6H). **^{19}F NMR** (282 MHz, $CDCl_3$) δ -76.04. **^{13}C NMR** (75 MHz, $CDCl_3$) δ 139.5 (C), 137.8 (C), 136.6 (C), 135.3 (C), 134.2 (C), 130.0 (CH), 129.5 (CH), 126.5 (C), 120.3 (d, *J* = 323.8 Hz, C), 55.6 (CH), 48.1 (CH_2), 37.1 (CH_2), 33.1 (CH_2), 32.5 (CH_2), 31.2 (CH_2), 30.6 (CH_2), 23.1 (CH_2), 20.8 (CH_3), 19.5 (CH_3), 19.4 (CH_3), 14.1 (CH_3), 14.0 (CH_3). **HRMS** [APCI]: *m/z* calculated for $C_{23}H_{35}F_3NO_2S$ $[M+H]^+$: 446.2335, found 446.2350.

(*E*)-4-Benzylidene-9-methoxy-3,3-dimethyl-2-((trifluoromethyl)sulfonyl)-2,3,4,5-tetrahydro-1*H*-benzo[*c*]azepine (7cg)

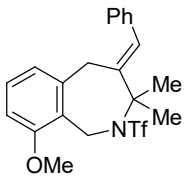

7cg

(43.5 mg, 61% yield), obtained as a white solid. **^{1}H NMR** (300 MHz, $CDCl_3$) δ 7.34 – 7.18 (m, 4H), 7.15 – 7.02 (m, 2H), 6.81 (t, *J* = 8.1 Hz, 2H), 6.66 (s, 1H), 5.42 – 4.49 (m, 2H), 3.90 – 3.79 (m, 5H), 1.87 (s, 6H). **^{19}F NMR** (282 MHz, $CDCl_3$) δ -77.21. **^{13}C NMR** (75 MHz, $CDCl_3$) δ 156.5 (C), 144.3 (C), 140.1 (C), 136.5 (C), 128.9 (CH), 128.7 (CH), 128.3 (CH), 127.3 (CH), 127.1 (CH), 124.5 (C), 121.5 (CH), 119.6 (d, *J* = 323.4 Hz, C), 108.7 (CH), 70.5 (C), 56.0 (CH_3), 44.3 (C), 35.0 (CH_2), 26.7 (CH_3). **HRMS** [APCI]: *m/z* calculated for $C_{21}H_{22}F_3NO_3S$ $[M]^+$: 425.1272, found 425.1274.

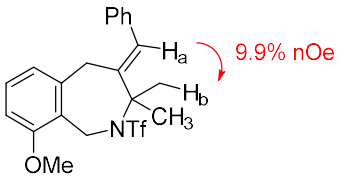

Assignment of stereochemistry of **5ch** was based on the observed nOe between the H_a (6.66 ppm, 100%) with H_b (1.87 ppm, 9.9%).

3.14 Test with monosubstituted *o*-methylbenzyltriflamide 4g

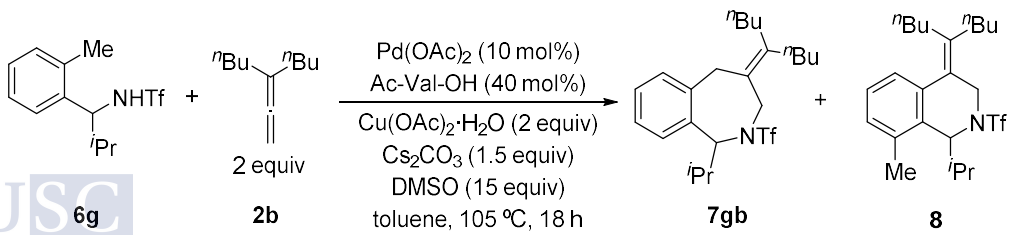

To a solution of $Pd(OAc)_2$ (3.7 mg, 10 mol%), Ac-Val-OH (10.6 mg, 40 mol%), $Cu(OAc)_2{\cdot}H_2O$ (66.7 mg, 2 equiv.), Cs_2CO_3 (81.6 mg, 1.5 equiv.) and **6g** (50.9 mg, 0.167 mmol) in toluene (2 mL) and DMSO (0.178 µL, 15 equiv.), under air atmosphere, in a Schlenk tube was added the allene **2b** (50.9 mg, 0.333 mmol, 2 equiv.). The tube was sealed with a rubber septum and an air atmosphere was injected in the flask with a balloon and a needle. The reaction was heated at

105 °C, stirred during 18 h and then cooled to room temperature. Evaporation and column chromatography on silica gel (hexanes:diethylether; 99:1) afforded **8-methyl-4-(nonan-5-ylidene)-2-((trifluoromethyl)sulfonyl)-1,2,3,4-tetrahydroisoquinoline (8)** as a yellow oil (66.2 mg, 89% yield). **^{1}H NMR** (500 MHz, $CDCl_3$) δ 7.20 – 6.98 (m, 3H), 4.55 (d, *J* = 10.7 Hz, 1H), 4.44 (d, *J* = 11.6 Hz, 1H), 4.07 (brs, 1H), 2.23 (s, 3H), 2.12 – 2.02 (m, 4H), 1.37 – 1.29 (m, 6H), 1.26 – 1.15 (m, 3H), 1.09 (d, *J* = 6.6 Hz, 3H), 0.89 (t, *J* = 7.1 Hz, 3H), 0.79 (t, *J* = 7.3 Hz, 3H), 0.72 (d, *J* = 6.8 Hz, 3H). **^{19}F NMR** (282 MHz, $CDCl_3$) δ -75.46. **^{13}C NMR** (126 MHz, $CDCl_3$) δ 140.4 (C), 137.0 (C), 134.12 (C), 134.05 (C), 129.1 (CH), 127.1 (CH), 124.0 (C), 120.1 (d, *J* = 324.7 Hz, C), 62.6 (CH), 46.4 (CH_2), 33.2 (CH_2), 31.5 (CH_2), 31.0 (CH_2), 30.3 (CH_2), 23.2 (CH_2), 23.0 (CH_2), 20.8 (CH), 19.4 (CH_3), 19.2 (CH_3), 14.1 (CH_3), 14.0 (CH_3). **HRMS** [APCI]: *m/z* calculated for $C_{23}H_{35}F_3NO_2S$ $[M+H]^+$: 446.2335, found 446.2324. Product **7gb** was not observed.

3.15 General procedure for the enantioselective formal (5+2) annulation based on a kinetic resolution of triflyl-protected o-methylbenzylamines, and selected chromatograms

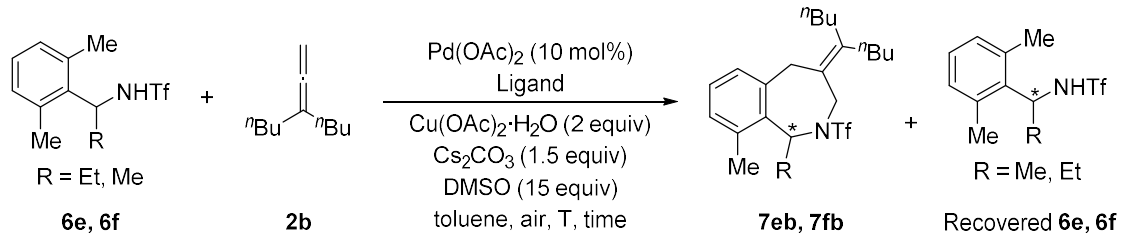

To a solution of $Pd(OAc)_2$ (2.2 mg, 10 mol%), ligand (15 or 40 mol%), $Cu(OAc)_2{\cdot}H_2O$ (39.9 mg, 2 equiv), Cs_2CO_3 (48.9 mg, 1.5 equiv) and **6e** (R = Et, 30.9 mg, 0.1 mmol) or **6f** (R = Me, 30.9 mg, 0.1 mmol) in toluene (1.5 mL) and DMSO (0.107 µL, 15 equiv), under air atmosphere, in a Schlenk tube was added the allene **2b** (15.2 mg, 0.1 mmol, 1 equiv. or 30.4 mg, 0.2 mmol, 2 equiv.). The tube was sealed with a rubber septum and an air atmosphere was injected in the flask with a balloon and a needle. The reaction was heated at the corresponding temperature, stirred during 4-72 h and then cooled to room temperature. Evaporation and column chromatography on silica gel (hexanes:diethylether; 99:1 – 70:30) afforded the corresponding cycloadduct **7eb** or **7fb** and the recovered starting material **6e** or **6f**.

*Enantioselectivity of **7eb** was determined by chiral HPLC analysis on Chiralpak IF-3 at 40 ºC (Hexane, 0.5 mL/min). Enantioselectivity of **6e** was determined by chiral HPLC analysis on Chiralpak IA at 40 ºC (Hexane : iPrOH = 99:1, 0.5 mL/min). Enantioselectivity of **7fb** was determined by chiral SFC analysis on Phenomenex i-Cellulose-5 at 40 ºC (CO_2 : MeOH = 99:01, 0.5 mL/min). Enantioselectivity of **6f** was determined by chiral SFC analysis on Phenomenex Cellulose-1 at 40 ºC (CO_2 : MeOH = 98:02, 0.5 mL/min).*

Selectivity (*s*) was calculated with the following equation: (s) = ln[(1 − *C*)(1 − ee_{SM})]/ln[(1 − *C*)(1 + ee_{SM})], where *C* = ee_{SM}/(ee_{SM} + ee_{PR})

Racemic samples

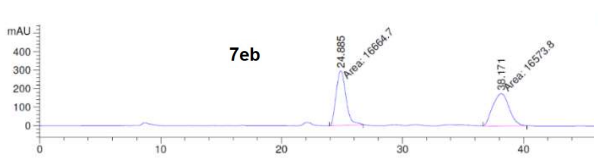

Signal 1: DAD1 A, Sig=220,8 Ref=360,100

Peak #	RetTime [min]	Type	Width [min]	Area [mAU*s]	Height [mAU]	Area %
1	24.885	MM	0.9390	1.66647e4	295.79361	50.1368
2	38.171	MM	1.5681	1.65738e4	176.16078	49.8632
Totals :				3.32385e4	471.95439	

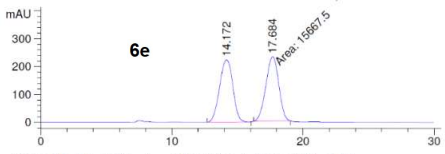

Signal 1: DAD1 A, Sig=220,8 Ref=600,100

Peak #	RetTime [min]	Type	Width [min]	Area [mAU*s]	Height [mAU]	Area %
1	14.172	BB	1.1000	1.57048e4	223.43663	50.0594
2	17.684	MM	1.1316	1.56675e4	230.75403	49.9406
Totals :				3.13722e4	454.19066	

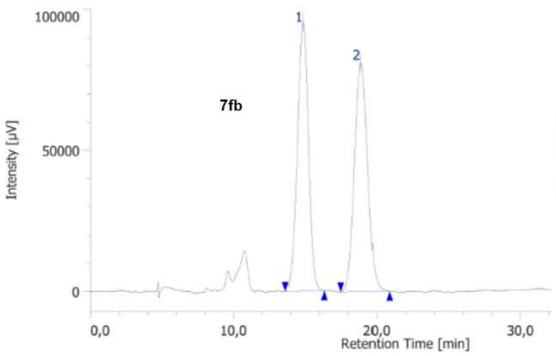

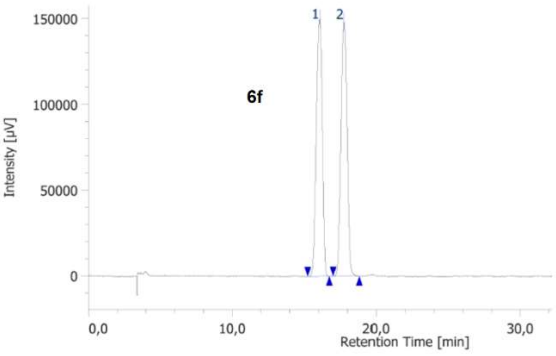

Channel Name 220,0nm

Channel Name 222,0nm

#	Peak Name	CH	tR [min]	Area [µV·sec]	Height [µV]	Area%	Height%
1	Unknown	5	14,863	5111224	95253	49,806	54,040
2	Unknown	5	18,887	5151065	81010	50,194	45,960

#	Peak Name	CH	tR [min]	Area [µV·sec]	Height [µV]	Area%	Height%
1	Unknown	6	16,077	4394782	150093	49,840	50,318
2	Unknown	6	17,783	4422936	148197	50,160	49,682

Asymmetric selected examples

Using **6e** to synthesize **7eb**.

Entries 3 and 5 of Table 10:

Entry	Ligand (mol%)	Temp.	Time	Yield	Conversion	er **7eb**	er rec. **6e**
3	Boc-Phe-NHOMe (15)	70 °C	48 h	33%	42%	83:17	69:31
5	Boc-Leu-NHOMe (15)	80 °C	48 h	48%	57%	78:22	82:18

Entry 3: (**5ea:** 83 : 17 e.r.; **4e:** 69 : 31 e.r., *s* = 7)

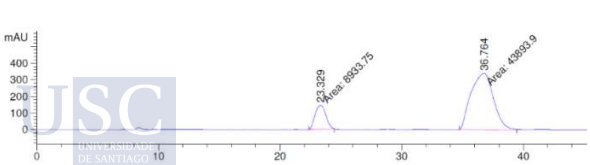

Signal 1: DAD1 A, Sig=220,8 Ref=360,100

Peak #	RetTime [min]	Type	Width [min]	Area [mAU*s]	Height [mAU]	Area %
1	23.329	MM	1.0239	8933.75195	145.41899	16.9111
2	36.764	MM	2.1518	4.38939e4	339.97278	83.0889
Totals :				5.28276e4	485.39177	

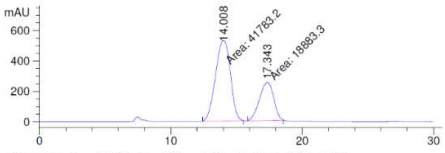

Signal 1: DAD1 A, Sig=220,8 Ref=600,100

Peak #	RetTime [min]	Type	Width [min]	Area [mAU*s]	Height [mAU]	Area %
1	14.008	MM	1.3121	4.17832e4	530.74652	68.8735
2	17.343	MM	1.2565	1.88833e4	250.48181	31.1265
Totals :				6.06665e4	781.22833	

Entry 5: (**5ea:** 78 : 22 e.r.; **4e:** 82 : 18 e.r., *s* = 7)

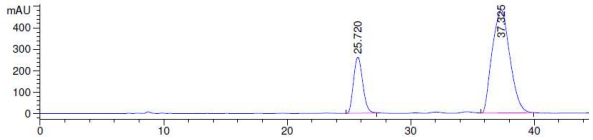

Signal 1: DAD1 A, Sig=220,8 Ref=360,100

Peak #	RetTime [min]	Type	Width [min]	Area [mAU*s]	Height [mAU]	Area %
1	25.720	PB	0.8121	1.34255e4	261.01547	21.9972
2	37.325	VB	1.3953	4.76070e4	480.75317	78.0028
Totals :				6.10325e4	741.76865	

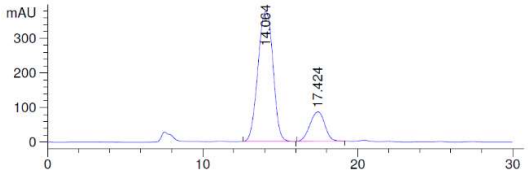

Signal 1: DAD1 A, Sig=220,8 Ref=600,100

Peak #	RetTime [min]	Type	Width [min]	Area [mAU*s]	Height [mAU]	Area %
1	14.064	BP	1.0807	2.53633e4	376.12076	81.7360
2	17.424	BB	1.0019	5667.44531	84.99376	18.2640
Totals :				3.10307e4	461.11452	

Using **6f** to synthesize **7fb**

Table 11

Entry	Ligand (mol%)	Temp.	Time	Yield	Conversion	er **7fb**	er rec. **6f**
1	Boc-Phe-NHOMe (15)	70 °C	48 h	38%	43%	86:14	75:25
2	Boc-Leu-NHOMe (15)	70 °C	72 h	42%	59%	88:12	78:22
3	Boc-Leu-NHOMe (15)	60 °C	72 h	20%	21%	90:10	60:40

Entry 1: (**7fb:** 86 : 14 e.r. ; **6f**: 74 : 26 e.r., *s* = 10)

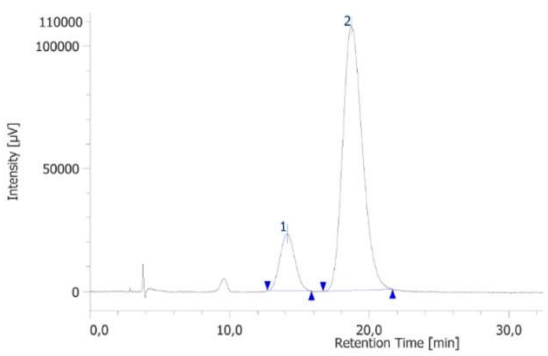

Channel Name 220,0nm

#	Peak Name	CH	tR [min]	Area [μV·sec]	Height [μV]	Area%	Height%
1	Unknown	5	14,130	1696557	22909	13,908	17,558
2	Unknown	5	18,727	10501544	107570	86,092	82,442

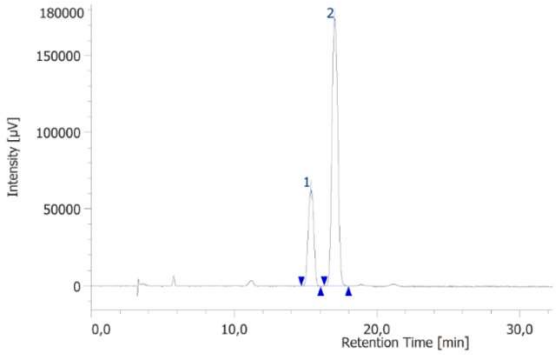

Channel Name 222,0nm

#	Peak Name	CH	tR [min]	Area [μV·sec]	Height [μV]	Area%	Height%
1	Unknown	6	15,373	1706298	62492	25,677	26,399
2	Unknown	6	17,037	4939069	174228	74,323	73,601

Entry 2: (**7fb**: 88 : 12 e.r. $[\alpha]_D^{19.8}$ = -19.3 (*c* 1.0, CH_2Cl_2); **6f:** 78 : 22 e.r. $[\alpha]_D^{19.8}$ = -10.3 (*c* 1.0, CH_2Cl_2), *s* = 13).

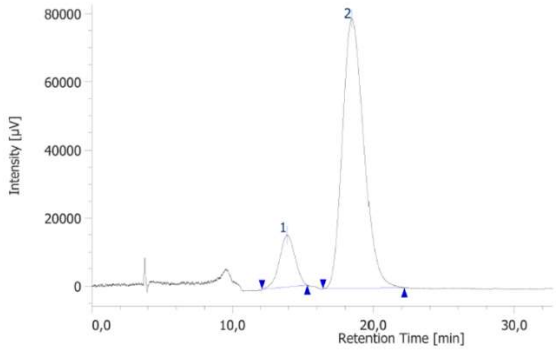

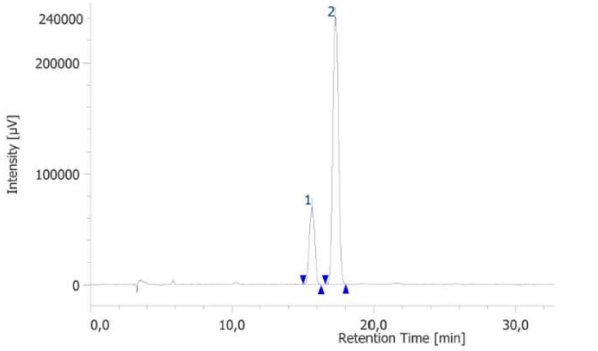

#	Peak Name	CH	tR [min]	Area [μV·sec]	Height [μV]	Area%	Height%
1	Unknown	5	13.890	1165617	15296	12.267	16.173
2	Unknown	5	18.480	8336394	79284	87.733	83.827

#	Peak Name	CH	tR [min]	Area [μV·sec]	Height [μV]	Area%	Height%
1	Unknown	6	15.657	1905173	69542	21.900	22.398
2	Unknown	6	17.310	6794155	240942	78.100	77.602

Entry 3: (**7fb**: 90 : 10 e.r.; **6f:** 59 : 41, *s* = 11)

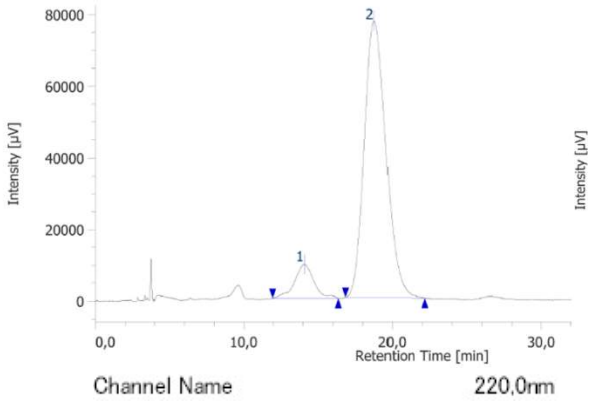

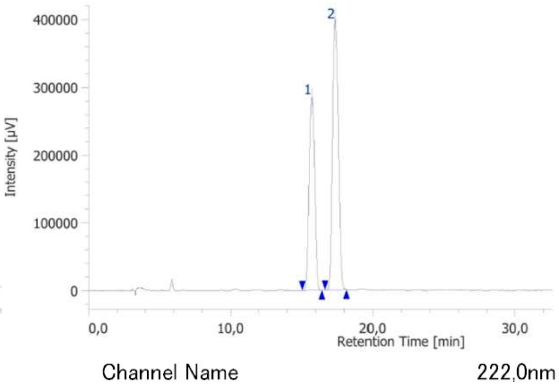

#	Peak Name	CH	tR [min]	Area [μV·sec]	Height [μV]	Area%	Height%
1	Unknown	5	14.077	867122	9522	10.022	10.973
2	Unknown	5	18.763	7785395	77254	89.978	89.027

#	Peak Name	CH	tR [min]	Area [μV·sec]	Height [μV]	Area%	Height%
1	Unknown	6	15.730	7886958	284579	40.754	41.586
2	Unknown	6	17.370	11465740	399738	59.246	58.414

3.16 Derivatization of tetrahydro-2-benzazepine products

*3.16.1 General procedure for the hydrogenation of compounds **7cg** and **5aa**, exemplified for **7cg***

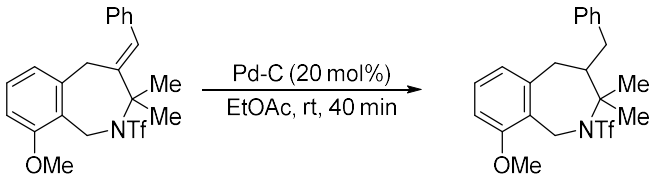

7cg **9**

To a suspension of Pd-C (20.0 mg, 20 mol%, 10% purity) in ethyl acetate (2 mL) was added **7cg** (40.0 mg, 0.094 mmol). Then, the solution was saturated with H_2 and stirred under H_2 pressure (balloon) during 40 min. Then, the solution was filtered through a Florisil© pad and eluted with ethyl acetate. The solvent was removed under reduced pressure. Flash chromatography on silica gel (hexanes:diethyl ether 99:1 – 95:5) afforded **4-benzyl-9-methoxy-3,3-dimethyl-2-((trifluoromethyl)sulfonyl)-2,3,4,5-tetrahydro-1H-benzo[c]azepine (9)** as a white solid (29.2 mg, 73% yield). **^{1}H NMR** (300 MHz, $CDCl_3$) δ 7.35 – 7.09 (m, 5H), 7.03 (t, *J* = 7.6 Hz, 1H), 6.68 (d, *J* = 8.2 Hz, 1H), 6.50 (d, *J* = 7.6 Hz, 1H), 5.38 (d, *J* = 18.0 Hz, 1H), 4.44 (d, *J* = 18.0 Hz, 1H), 3.80 (s, 3H), 3.09 (dd, *J* = 16.8, 7.6 Hz, 1H), 2.87 – 2.73 (m, 2H), 2.49 – 2.31 (m, 2H), 1.64 (s, 6H). **^{19}F NMR** (282 MHz, $CDCl_3$) δ -76.77. **^{13}C NMR** (75 MHz, $CDCl_3$) δ 156.2 (C), 139.97 (C), 139.95 (C), 129.1 (CH), 128.7 (CH), 127.8 (CH), 126.5 (CH), 124.7 (C), 122.6 (CH), 119.9 (d, *J* = 324.2 Hz, C), 108.5 (CH), 67.9 (C), 55.9 (CH_3), 49.8 (CH), 43.5 (CH_2), 37.7 (CH_2), 34.0 (CH_2), 26.3 (CH_3), 21.8 (CH_3). **HRMS** [APCI]: *m/z* calculated for $C_{21}H_{23}F_3NO_3S$ $[M-H]^+$: 426.1345, found 426.1346.

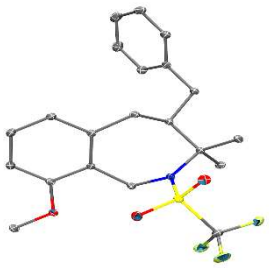

The structure of this compound was confirmed by X-ray diffraction analysis (CCDC: 2025994).

*3.16.2 Procedure for the deprotection of triflate of compound **9***

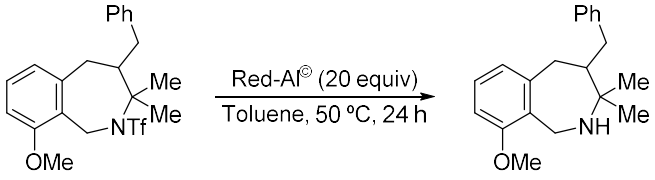

9 **10**

To a stirred solution of **9** (40.0 mg, 0.094 mmol) in toluene (1 mL) was added sodium bis(2-methoxyethoxy)-aluminum dihydride (0.28 mL, 10 equiv., 65% wt in toluene) dropwise at rt. Then, the reaction was heated at 50 °C overnight. After that, another portion of bis(2-methoxyethoxy)-aluminum dihydride (0.28 mL, 10 equiv., 65% wt in toluene) was added and the reaction was monitored by TLC. After complete conversion of the starting material, the reaction was carefully quenched at 0 °C with 5% aqueous ammonium chloride (2 mL). The mixture was extracted with DCM (3x5 mL). The organic phases were washed with brine and dried over Na_2SO_4. Evaporation and column chromatography on silica gel (DCM:MeOH:Et_3N; 98:1:1)

afforded **4-benzyl-9-methoxy-3,3-dimethyl-2,3,4,5-tetrahydro-1H-benzo[c]azepine (10)** as a white solid (21.1 mg, 76% yield). **^{1}H NMR** (300 MHz, $CDCl_3$) δ 7.36 – 7.11 (m, 5H), 6.98 (t, *J* = 7.9 Hz, 1H), 6.68 (d, *J* = 7.9 Hz, 1H), 6.43 (d, *J* = 7.5 Hz, 1H), 4.20 (d, *J* = 16.8 Hz, 1H), 4.04 (d, *J* = 16.7 Hz, 1H), 3.79 (s, 3H), 3.06 – 2.79 (m, 2H), 2.65 (d, *J* = 15.5 Hz, 1H), 2.26 (dd, *J* = 13.8, 11.4 Hz, 1H), 2.09 – 1.99 (m, 1H), 1.40 (s, 3H), 1.24 (s, 3H). **^{13}C NMR** (75 MHz, $CDCl_3$) δ 156.4 (C), 142.1 (C), 141.3 (C), 129.5 (C), 129.2 (CH), 128.4 (CH), 126.8 (CH), 125.9 (CH), 122.7 (CH), 108.2 (CH), 56.3 (C), 55.6 (CH_3), 48.8 (CH), 38.5 (CH_2), 37.8 (CH_2), 33.9 (CH_2), 27.6 (CH_3), 23.8 (CH_3). **HRMS** [APCI]: *m/z* calculated for $C_{20}H_{26}NO$ $[M+H]^+$: 296.2009, found 296.2008.

*3.16.3 Procedure for the removal of methoxy group of compound **9***

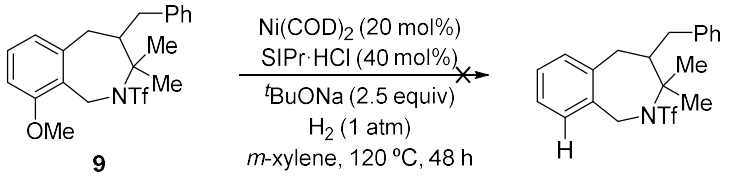

Following a reported procedure,[157] inside a glovebox, a sealed tube equipped with a stirring bar was loaded with $Ni(COD)_2$ (2.6 mg, 20 mol%), 1,3-bis-(2,6-diisopropylphenyl)imidazolinium chloride (8.0 mg, 40 mol%), sodium *tert*-butoxide (11.2 mg, 2.5 equiv) and substrate **9** (20.0 mg, 0.047 mmol). The sealed tube was taken out the glovebox and filled with *m*-xylene (0.5 mL). The reaction mixture was degassed with a vacuum pump, saturated with H_2 and stirred under H_2 pressure (balloon) at 120 °C during 48 h. The reaction was then warmed to room temperature, diluted with diethyl ether and quenched with 1.5 M aqueous HCl. After stirring for 15 min, the organic layer was separated and the aqueous layer was extracted with diethyl ether. The combined organic layers were filtered through a short pad of Celite© and the solvent was removed under reduced pressure. Analysis of the reaction crude showed no conversion of the starting material.

4- Addendum: Preliminary studies on Pd-catalyzed cyclization of o-methylbenzylamines to isoindolines involving a C(sp^3)–H activation

4.1 Procedure for the synthesis of nosyl-protected 1-mesitylpropan-1-amine (6e')

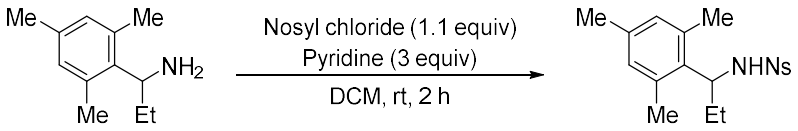

6e'

To a solution of nosyl chloride (0.69 g, 1.1 equiv) in dichloromethane (6.6 mL) under argon atmosphere was added 1-mesitylpropan-1-amine (500 mg, 2.82 mmol). The reaction was stirred during 2 h at rt. After that, the reaction was quenched with HCl (10%) until pH ≈ 2. The aqueous phase was extracted three times with dichloromethane. The combined organic phases were washed with brine and then dried over Na_2SO_4. Evaporation and column chromatography on silica gel (hexanes:ethyl acetate; 70:30) afforded **N-(1-mesitylpropyl)-4-nitrobenzenesulfonamide (6e')** as a white solid (349 mg, 34% yield). **^{1}H NMR** (300 MHz, $CDCl_3$) δ 7.99 (d, *J* = 8.8 Hz, 2H), 7.57 (d, *J* = 8.8 Hz, 2H), 6.71 (brs, 1H), 6.36 (brs, 1H), 5.07 (brs, 1H), 4.88 (q, *J* = 7.6 Hz, 1H), 2.37 – 1.76 (m, 11H), 0.92 (t, *J* = 7.4 Hz, 3H). **^{13}C NMR** (75 MHz, $CDCl_3$) δ 149.4 (C), 146.1 (C), 137.6 (C), 132.2 (C), 127.8 (CH), 123.4 (CH), 56.0 (CH), 27.7 (CH_2), 20.8 (CH_3), 20.6 (CH_3), 11.2 (CH_3). **HRMS** [APCI]: *m/z* calculated for $C_{18}H_{22}N_2O_4S$ $[M]^+$: 362.1300, found 362.1304.

4.2 General procedure for the Pd-catalyzed cyclization of α-unsubstituted *o*-methylbenzyltriflamides

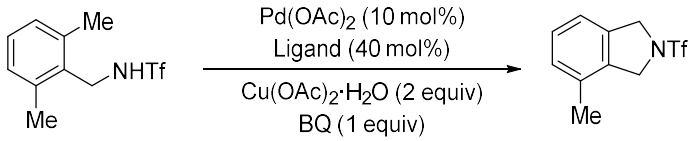

6a **11**

To a Schlenk tube, under air atmosphere, $Pd(OAc)_2$ (2.2 mg, 10 mol%), ligand (40 mol%), $Cu(OAc)_2{\cdot}H_2O$ (39.9 mg, 2 equiv), *p*-benzoquinone (10.8 mg, 1 equiv), Cs_2CO_3 (48.9 mg, 1.5 equiv) and **6a** (32.0 mg, 0.1 mmol) were added. The solids were solved in toluene (1.5 mL) and DMSO (0.107 µL, 15 equiv). The tube was sealed with a rubber septum and an air atmosphere was injected in the flask with a balloon and a needle. The reaction was heated at 105 °C, stirred during 16 h and then cooled to room temperature. Evaporation and column chromatography on silica gel (hexanes:diethylether; 99:1) afforded **4-methyl-2-((trifluoromethyl)sulfonyl) isoindoline (11)**. **^{1}H NMR** (500 MHz, $CDCl_3$) δ 7.21 – 7.17 (m, 2H), 7.06 (d, *J* = 7.6 Hz, 1H), 7.01 (d, *J* = 7.7 Hz, 1H), 4.84 (s, 2H), 4.76 (s, 2H), 2.20 (s, 3H). **^{19}F NMR** (282 MHz, $CDCl_3$) δ -76.88. **^{13}C NMR** (126 MHz, $CDCl_3$) δ 134.7 (C), 134.1 (C), 133.0 (C), 129.2 (CH), 128.8 (CH), 120.6 (d, *J* = 323.7 Hz, C), 120.0 (CH), 55.1 (CH_2), 54.2 (CH_2), 18.8 (CH_3). **HRMS** [APCI]: *m/z* calculated for $C_{10}H_{10}F_3NO_2S$ $[M]^+$: 265.0384, found 265.0383.

4.3 Procedure for the Pd-catalyzed cyclization of α-ethyl *o*-methylbenzylnosylamide (6e')

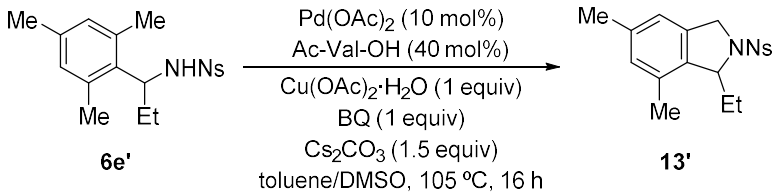

To a Schlenk tube, under air atmosphere, $Pd(OAc)_2$ (2.2 mg, 10 mol%), Ac-Val-OH (6.7 mg, 40 mol%), $Cu(OAc)_2 \cdot H_2O$ (39.9 mg, 2 equiv), *p*-benzoquinone (10.8 mg, 1 equiv), Cs_2CO_3 (48.9 mg, 1.5 equiv) and **6e'** (36.2 mg, 0.1 mmol) were added. The solids were solved in toluene (1.5 mL) and DMSO (0.107 µL, 15 equiv). The tube was sealed with a rubber septum and an air atmosphere was injected in the flask with a balloon and a needle. The reaction was heated at 105 °C, stirred during 16h and then cooled to room temperature. Evaporation and column chromatography on silica gel (hexanes:diethylether; 99:1) afforded **1-ethyl-5,7-dimethyl-2-((4-nitrophenyl)sulfonyl)isoindoline (13')** as a white solid (5.1 mg, 10% yield). **^{1}H NMR** (500 MHz, $CDCl_3$) δ 8.26 (d, *J* = 7.8 Hz, 2H), 7.98 (d, *J* = 7.6 Hz, 2H), 6.81 (s, 1H), 6.75 (s, 1H), 5.11 (s, 1H), 4.66 (d, *J* = 14.4 Hz, 2H), 4.59 (d, *J* = 14.5 Hz, 2H), 2.25 (s, 3H), 2.18 (s, 3H), 2.16 – 2.10 (m, 1H), 1.94 – 1.78 (m, 1H), 0.73 (t, *J* = 7.1 Hz, 3H). **^{13}C NMR** (126 MHz, $CDCl_3$) δ 150.1 (C), 144.6 (C), 138.3 (C), 136.1 (C), 134.7 (C), 132.1 (C), 130.6 (CH), 128.3 (CH), 124.4 (CH), 120.4 (CH), 67.0 (CH), 54.3 (CH_2), 27.9 (CH_2), 21.2 (CH_3), 18.9 (CH_3), 8.0 (CH_3). **HRMS** [APCI]: *m/z* calculated for $C_{18}H_{20}N_2O_4S$ $[M]^+$: 360.1144, found 360.1147.

Selected spectra

1-Selected spectra from Chapter II

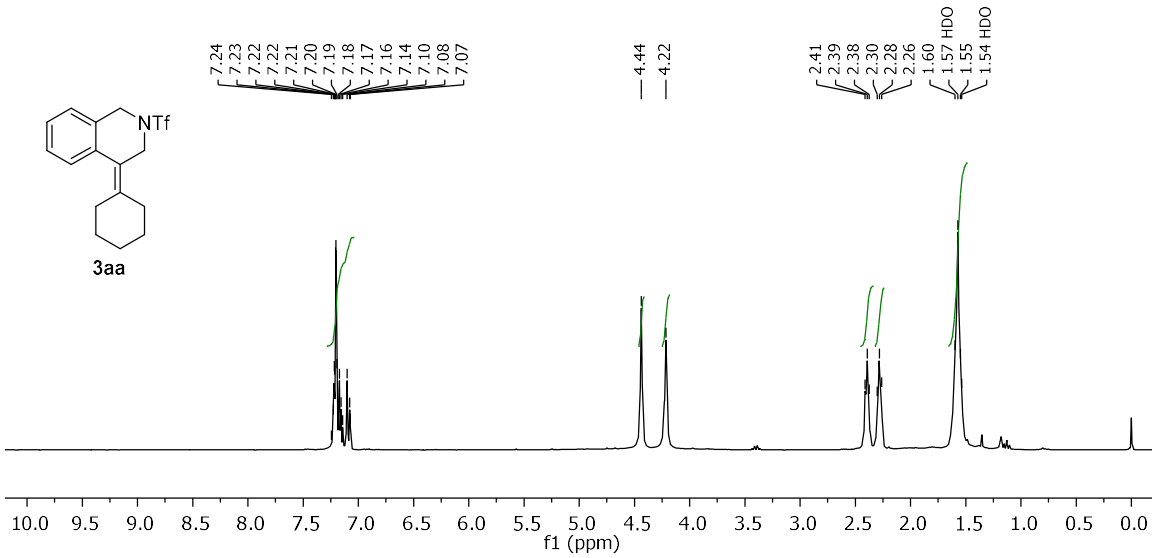

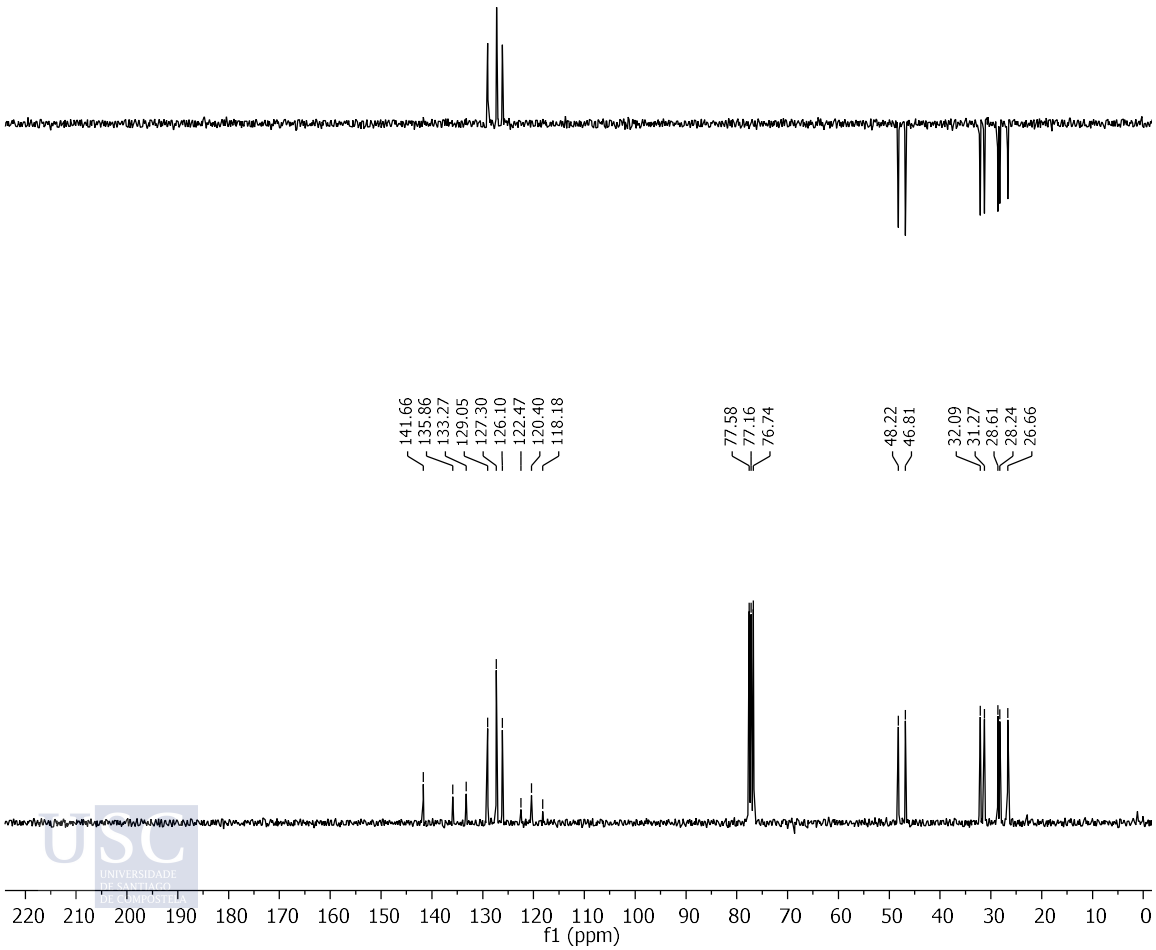

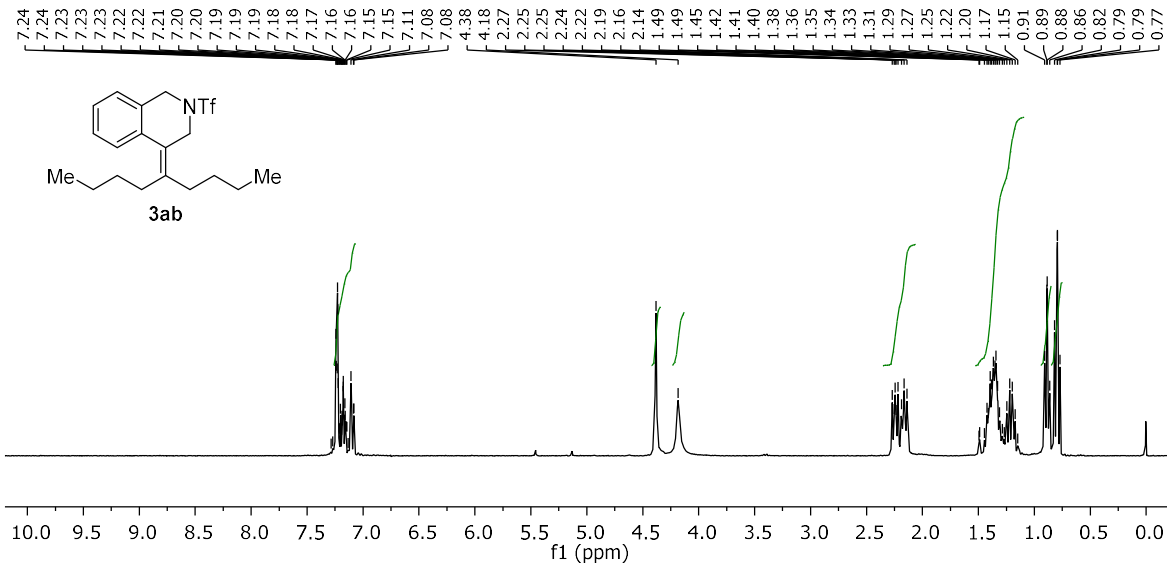
7.24 7.24 7.23 7.23 7.23 7.22 7.22 7.21 7.20 7.20 7.19 7.19 7.19 7.18 7.18 7.17 7.16 7.16 7.15 7.15 7.11 7.08 7.08 4.38 4.18 2.27 2.25 2.25 2.24 2.22 2.19 2.16 2.14 1.49 1.49 1.45 1.42 1.41 1.40 1.38 1.36 1.35 1.34 1.33 1.31 1.29 1.27 1.25 1.22 1.20 1.17 1.15 0.91 0.89 0.88 0.86 0.82 0.79 0.79 0.77
NTf
Me
Me
3ab
10.0 9.5 9.0 8.5 8.0 7.5 7.0 6.5 6.0 5.5 5.0 4.5 4.0 3.5 3.0 2.5 2.0 1.5 1.0 0.5 0.0
f1 (ppm)

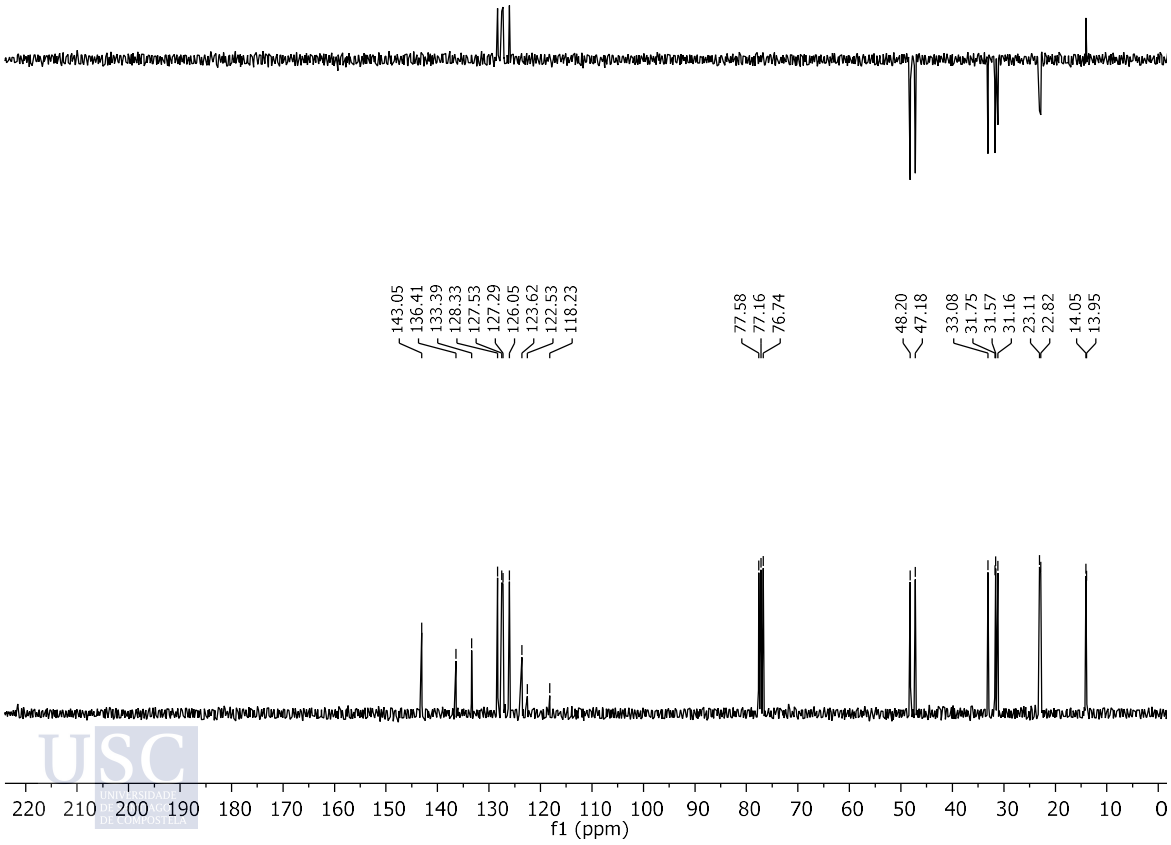
143.05 136.41 133.39 128.33 127.53 127.29 126.05 123.62 122.53 118.23
77.58 77.16 76.74
48.20 47.18
33.08 31.75 31.57 31.16 23.11 22.82
14.05 13.95
220 210 200 190 180 170 160 150 140 130 120 110 100 90 80 70 60 50 40 30 20 10 0
f1 (ppm)

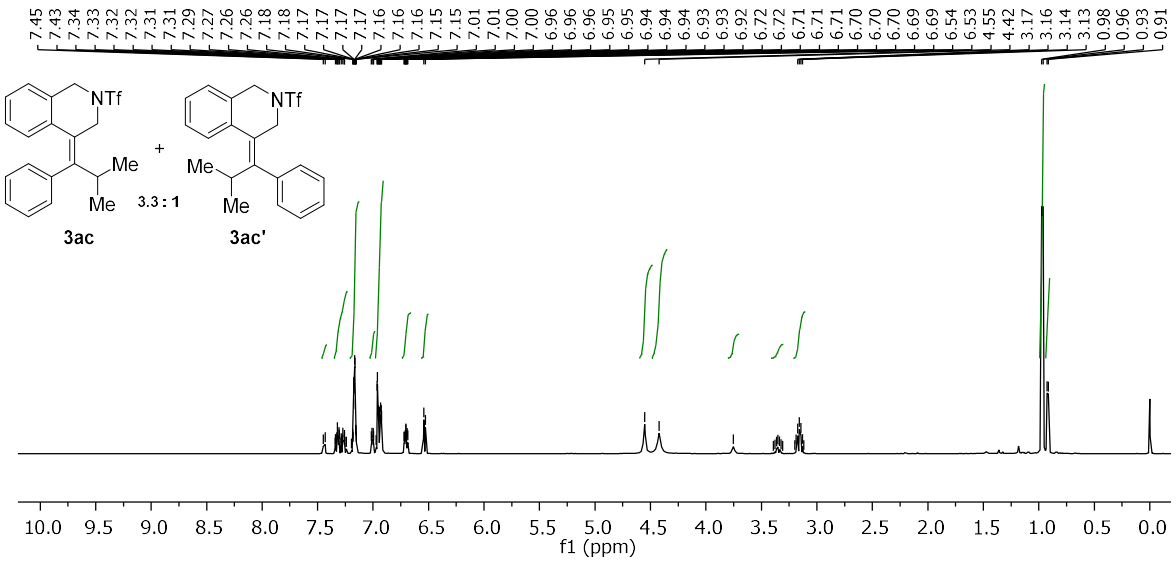

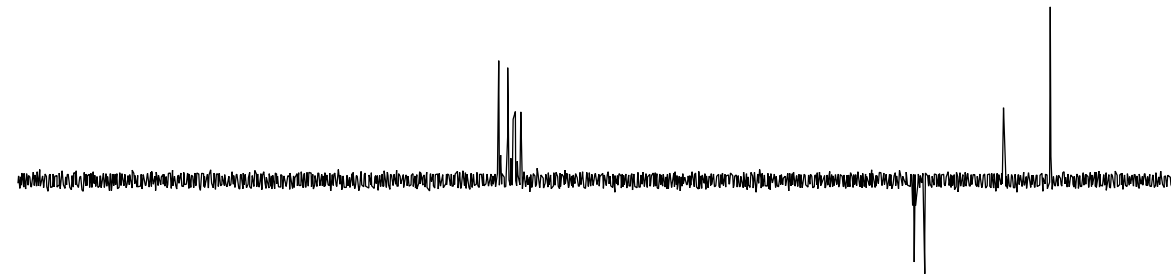

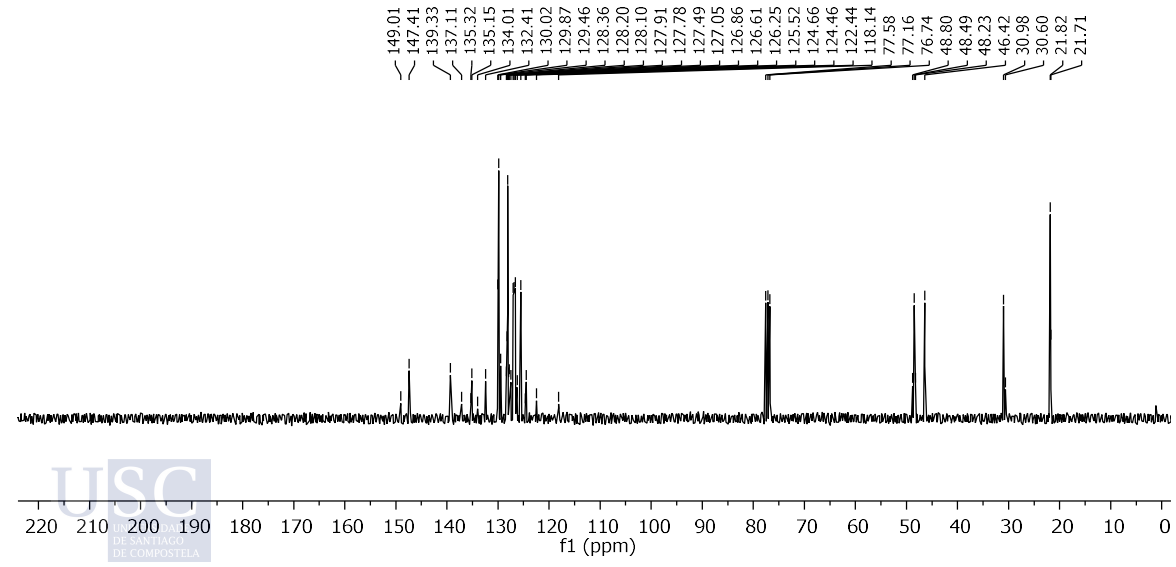

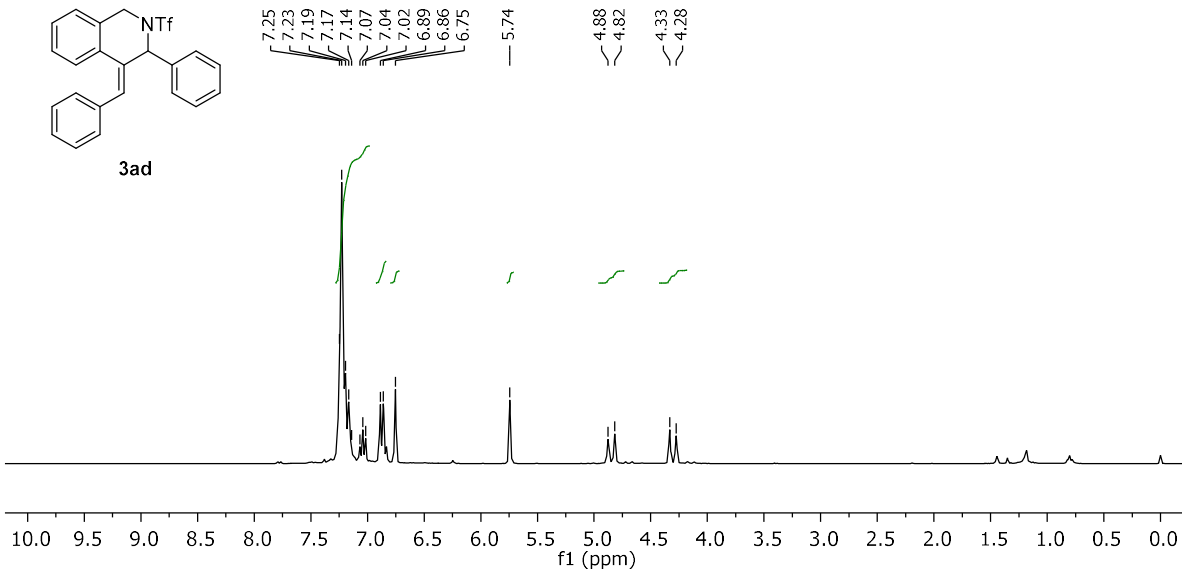
NTf
3ad
7.25
7.23
7.19
7.17
7.14
7.07
7.04
7.02
6.89
6.86
6.75
5.74
4.88
4.82
4.33
4.28
10.0 9.5 9.0 8.5 8.0 7.5 7.0 6.5 6.0 5.5 5.0 4.5 4.0 3.5 3.0 2.5 2.0 1.5 1.0 0.5 0.0
f1 (ppm)

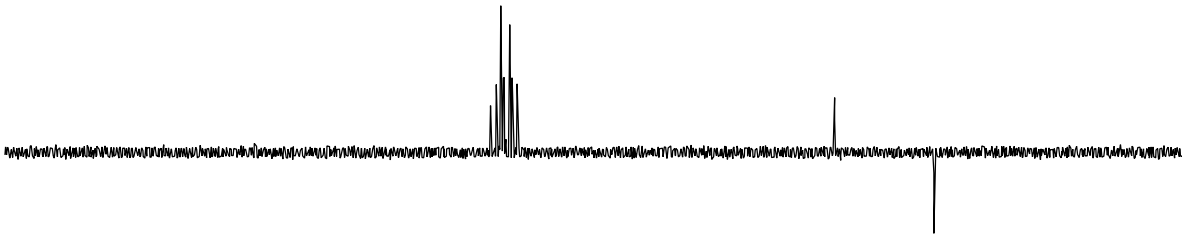

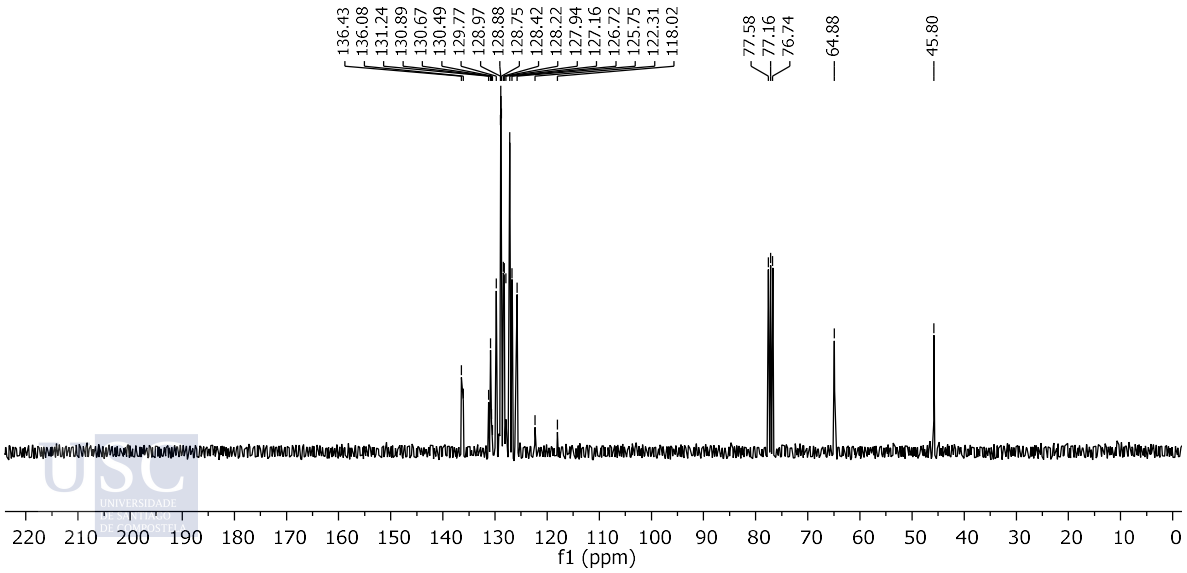
136.43
136.08
131.24
130.89
130.67
130.49
129.77
128.97
128.88
128.75
128.42
128.22
127.94
127.16
126.72
125.75
122.31
118.02
77.58
77.16
76.74
64.88
45.80
220 210 200 190 180 170 160 150 140 130 120 110 100 90 80 70 60 50 40 30 20 10 0
f1 (ppm)

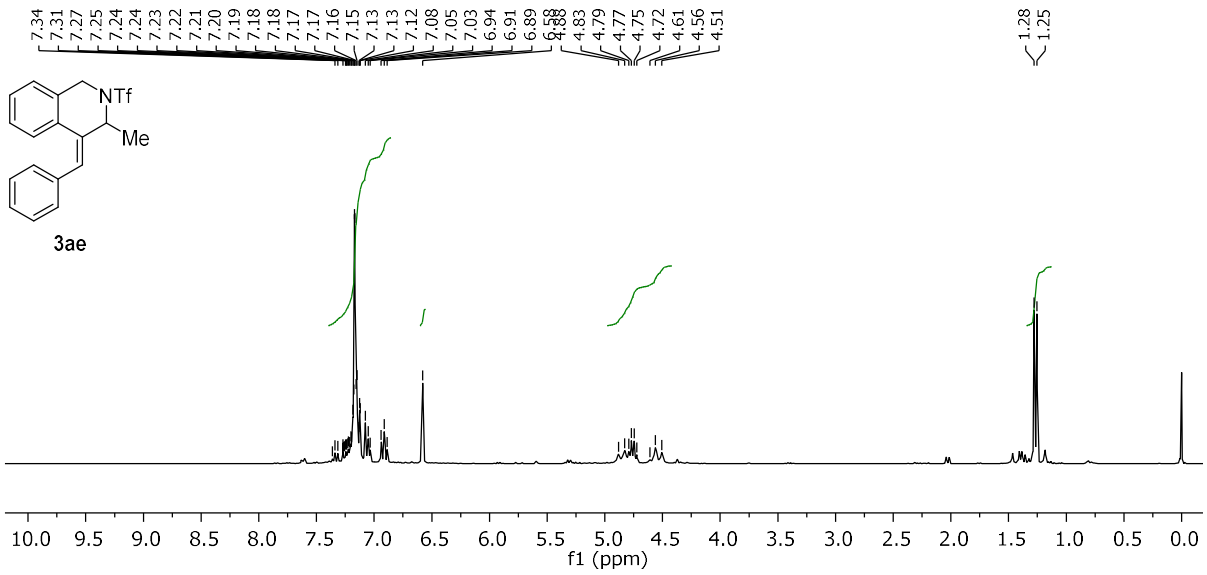
7.34
7.31
7.27
7.25
7.24
7.24
7.23
7.22
7.21
7.20
7.19
7.18
7.18
7.17
7.17
7.16
7.15
7.13
7.12
7.08
7.05
7.03
6.94
6.91
6.89
4.83
4.79
4.77
4.75
4.72
4.61
4.56
4.51
1.28
1.25
NTf
Me
3ae
10.0 9.5 9.0 8.5 8.0 7.5 7.0 6.5 6.0 5.5 5.0 4.5 4.0 3.5 3.0 2.5 2.0 1.5 1.0 0.5 0.0
f1 (ppm)

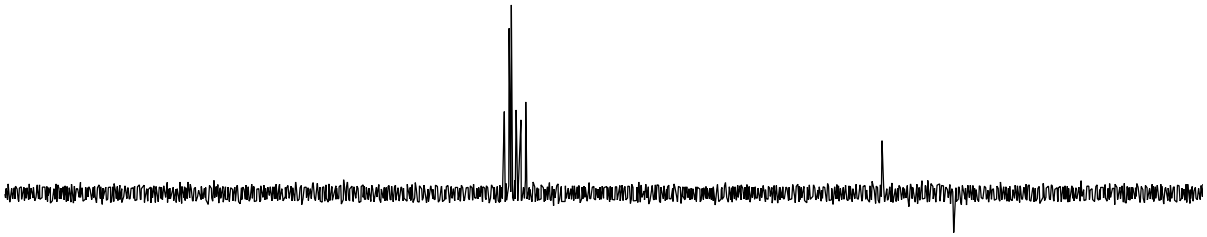

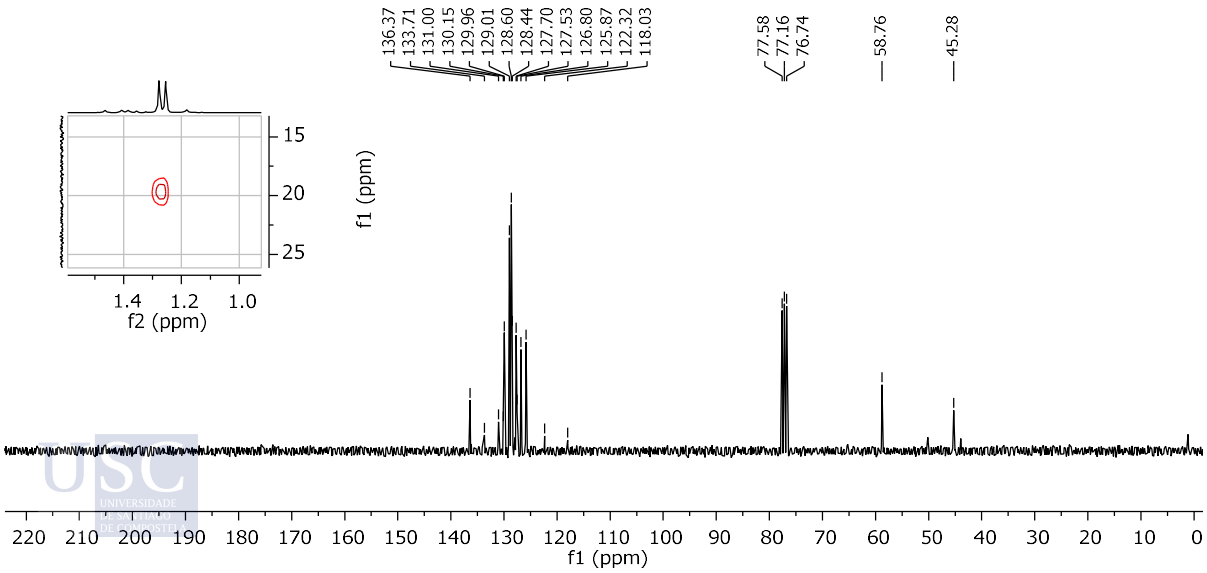
136.37
133.71
131.00
130.15
129.96
129.01
128.60
128.44
127.70
127.53
126.80
125.87
122.32
118.03
77.58
77.16
76.74
58.76
45.28
15
20
25
1.4 1.2 1.0
f2 (ppm)
f1 (ppm)
220 210 200 190 180 170 160 150 140 130 120 110 100 90 80 70 60 50 40 30 20 10 0
f1 (ppm)

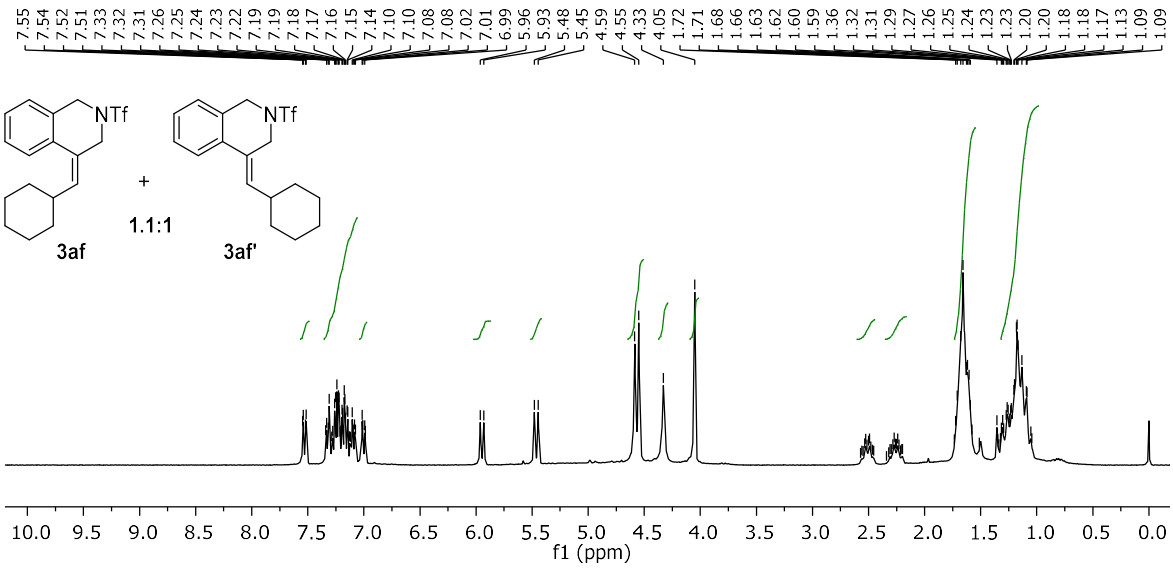
7.55 7.54 7.52 7.51 7.33 7.32 7.31 7.26 7.25 7.24 7.23 7.22 7.19 7.19 7.18 7.17 7.16 7.15 7.14 7.10 7.10 7.08 7.08 7.02 7.01 6.99 5.96 5.93 5.48 5.45 4.59 4.55 4.33 4.05 1.72 1.71 1.68 1.66 1.63 1.62 1.60 1.59 1.36 1.32 1.31 1.29 1.27 1.26 1.25 1.24 1.23 1.23 1.20 1.20 1.18 1.18 1.17 1.13 1.09 1.09
NTf
NTf
+
1.1:1
3af
3af'
10.0 9.5 9.0 8.5 8.0 7.5 7.0 6.5 6.0 5.5 5.0 4.5 4.0 3.5 3.0 2.5 2.0 1.5 1.0 0.5 0.0
f1 (ppm)

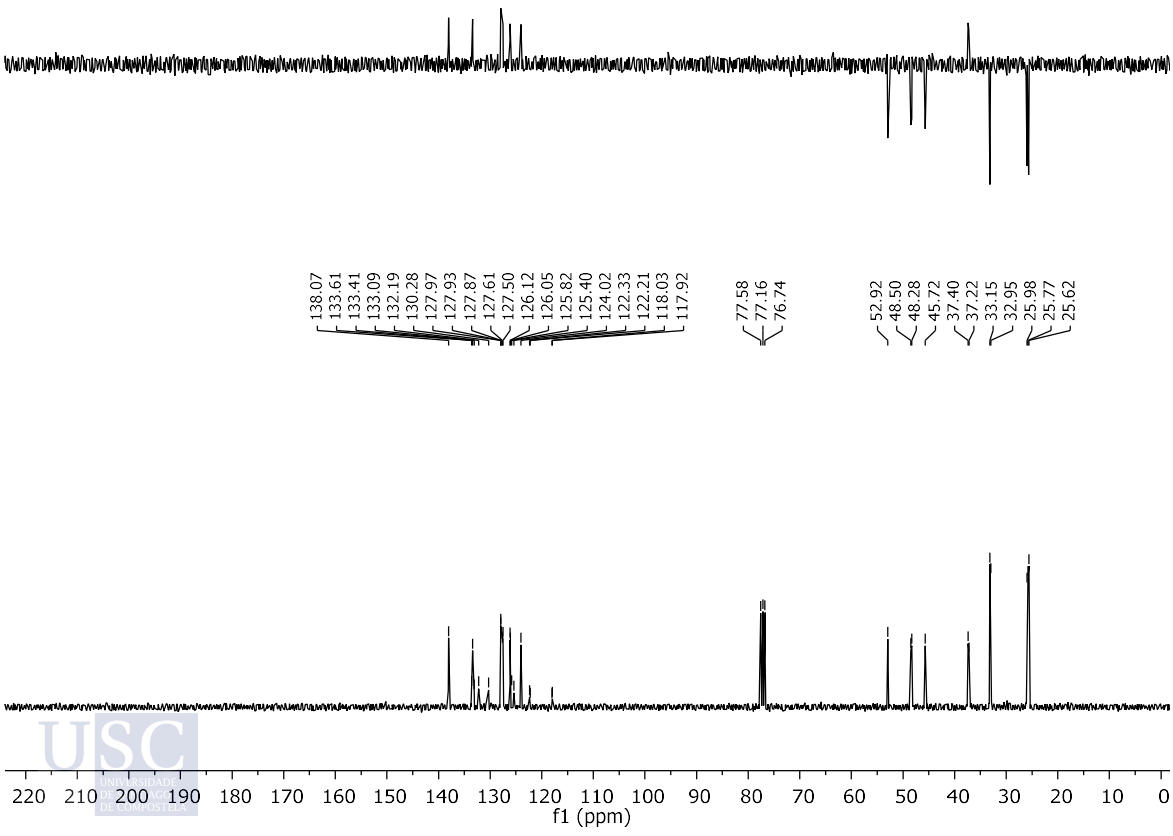
138.07 133.61 133.41 133.09 132.19 130.28 127.97 127.93 127.87 127.61 127.50 126.12 126.05 125.82 125.40 124.02 122.33 122.21 118.03 117.92
77.58 77.16 76.74
52.92 48.50 48.28 45.72 37.40 37.22 33.15 32.95 25.98 25.77 25.62
220 210 200 190 180 170 160 150 140 130 120 110 100 90 80 70 60 50 40 30 20 10 0
f1 (ppm)

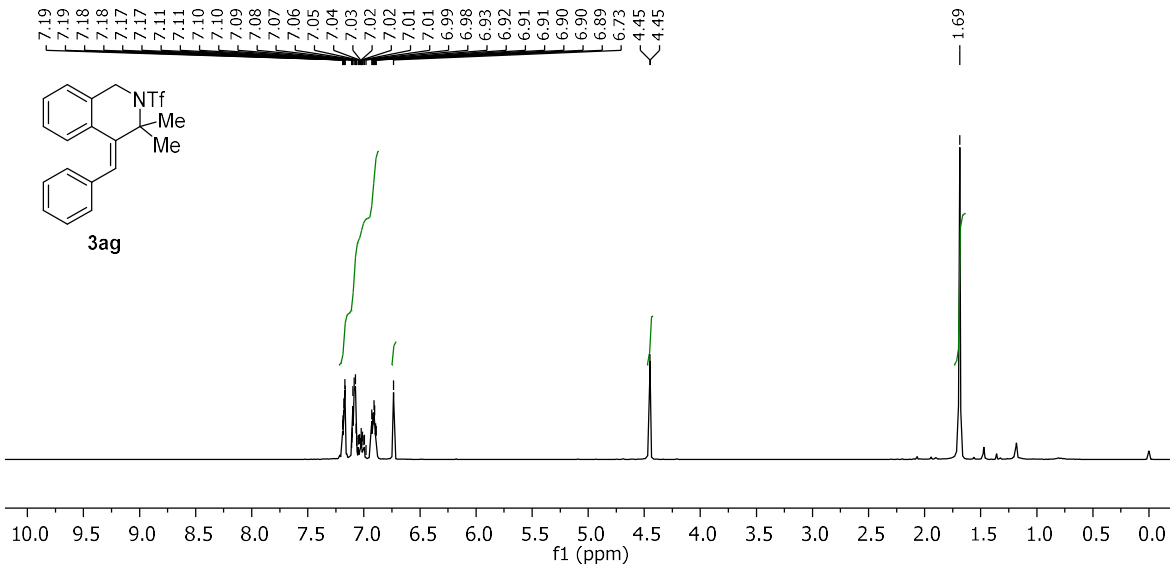
7.19
7.19
7.18
7.18
7.17
7.17
7.11
7.11
7.10
7.10
7.09
7.08
7.07
7.06
7.05
7.04
7.03
7.02
7.02
7.01
7.01
6.99
6.98
6.93
6.92
6.91
6.91
6.90
6.90
6.89
6.73
4.45
4.45
1.69
NTf
Me
Me
3ag
10.0 9.5 9.0 8.5 8.0 7.5 7.0 6.5 6.0 5.5 5.0 4.5 4.0 3.5 3.0 2.5 2.0 1.5 1.0 0.5 0.0
f1 (ppm)

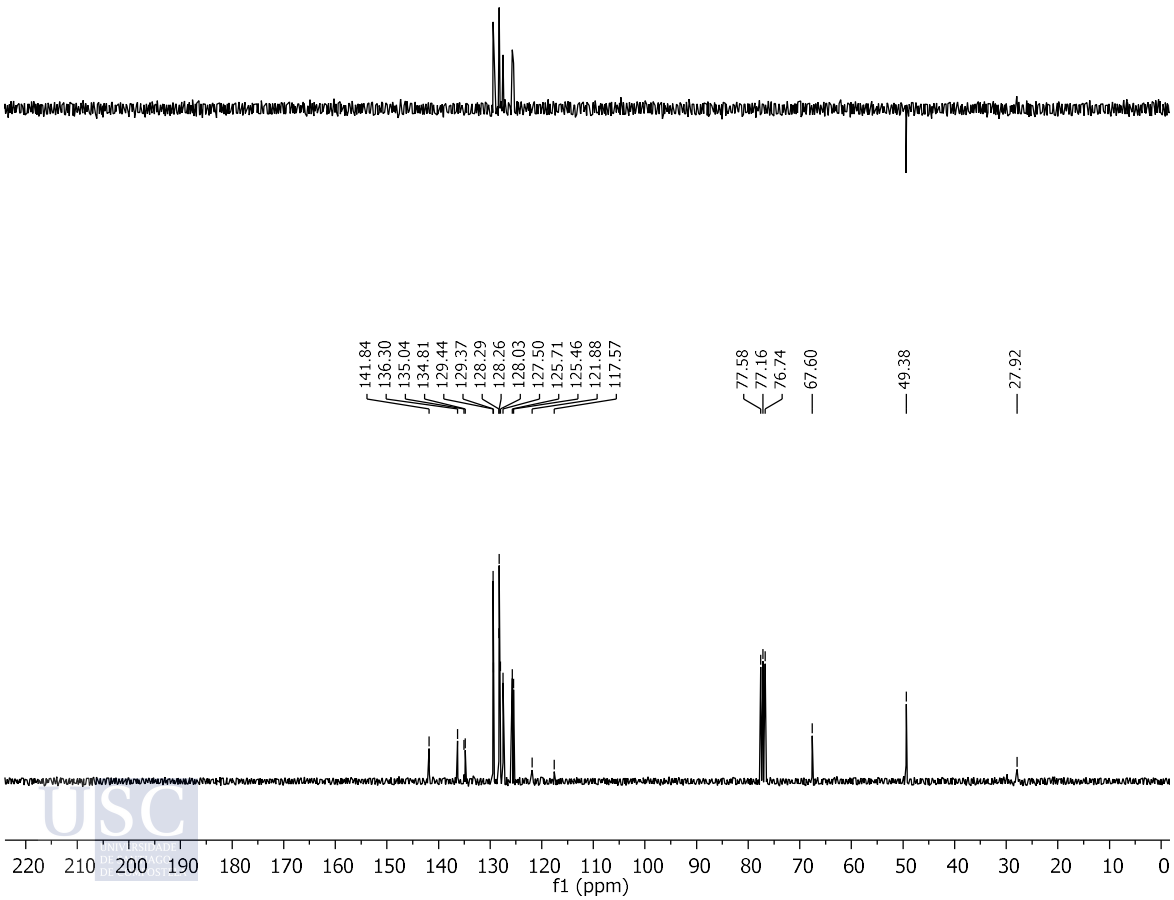
141.84
136.30
135.04
134.81
129.44
129.37
128.29
128.26
128.03
127.50
125.71
125.46
121.88
117.57
77.58
77.16
76.74
67.60
49.38
27.92
220 210 200 190 180 170 160 150 140 130 120 110 100 90 80 70 60 50 40 30 20 10 0
f1 (ppm)

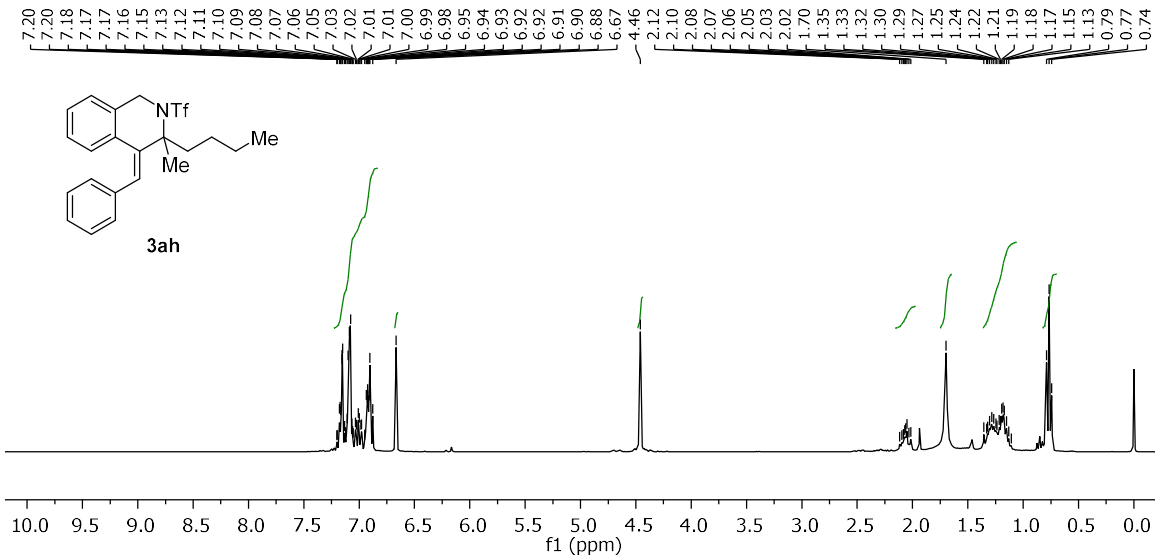

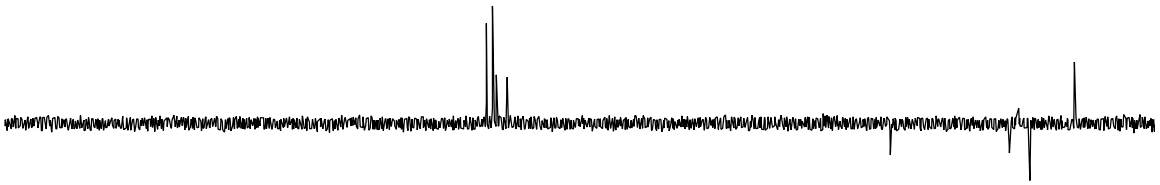

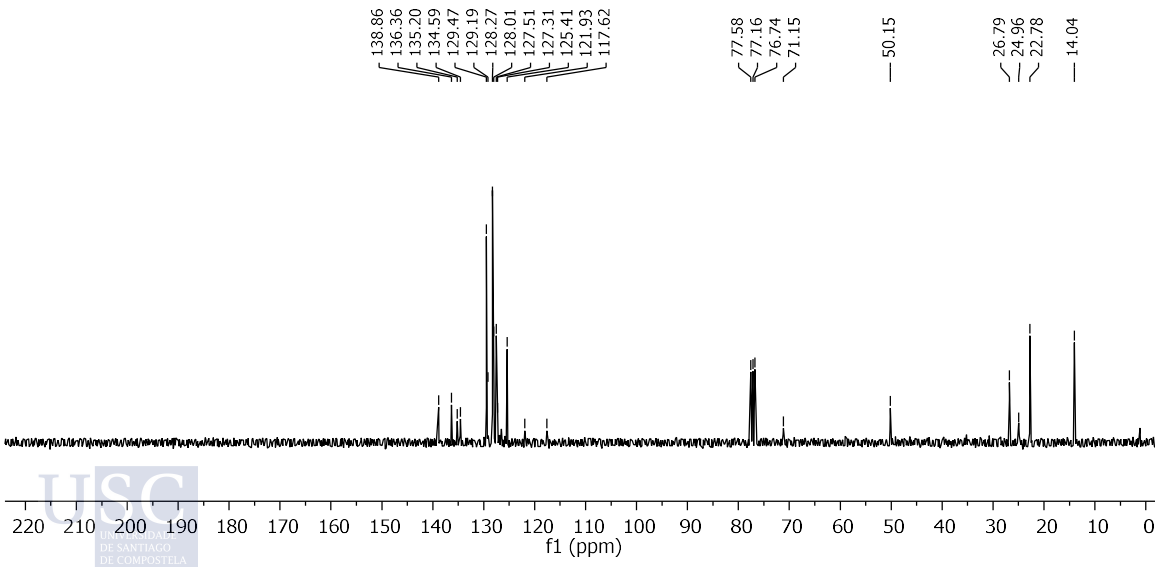

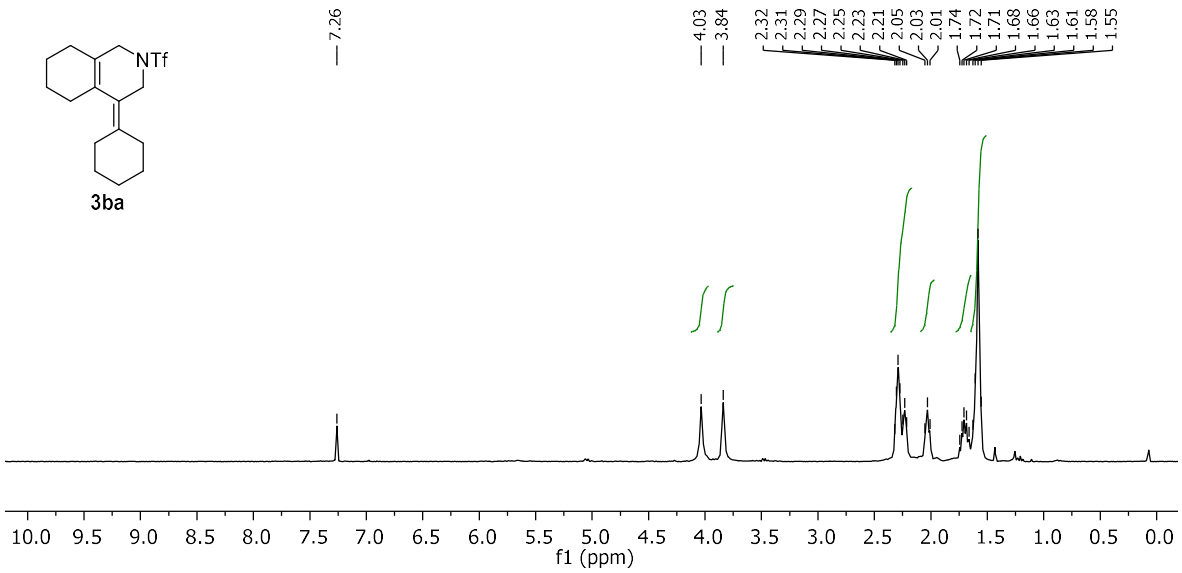
NTf
3ba
7.26
4.03
3.84
2.32
2.31
2.29
2.27
2.25
2.23
2.21
2.05
2.03
2.01
1.74
1.72
1.71
1.68
1.66
1.63
1.61
1.58
1.55
10.0 9.5 9.0 8.5 8.0 7.5 7.0 6.5 6.0 5.5 5.0 4.5 4.0 3.5 3.0 2.5 2.0 1.5 1.0 0.5 0.0
f1 (ppm)

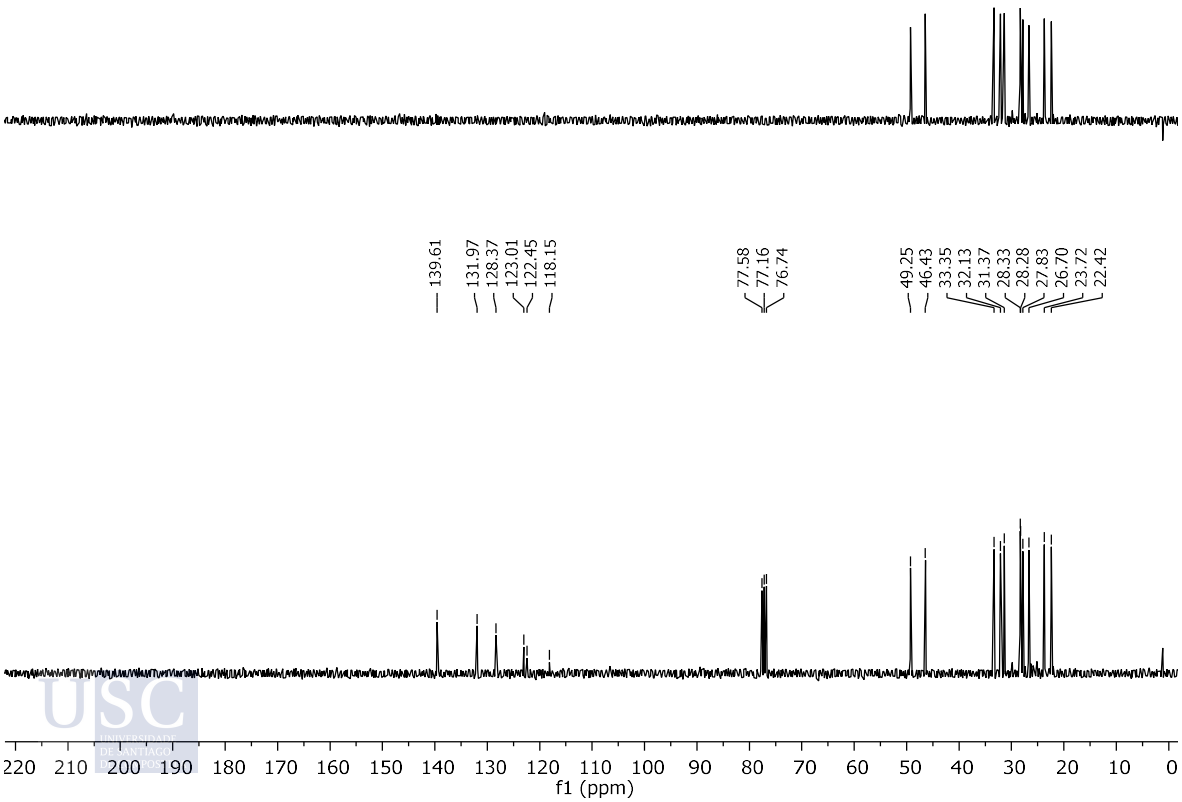
139.61
131.97
128.37
123.01
122.45
118.15
77.58
77.16
76.74
49.25
46.43
33.35
32.13
31.37
28.33
28.28
27.83
26.70
23.72
22.42
220 210 200 190 180 170 160 150 140 130 120 110 100 90 80 70 60 50 40 30 20 10 0
f1 (ppm)

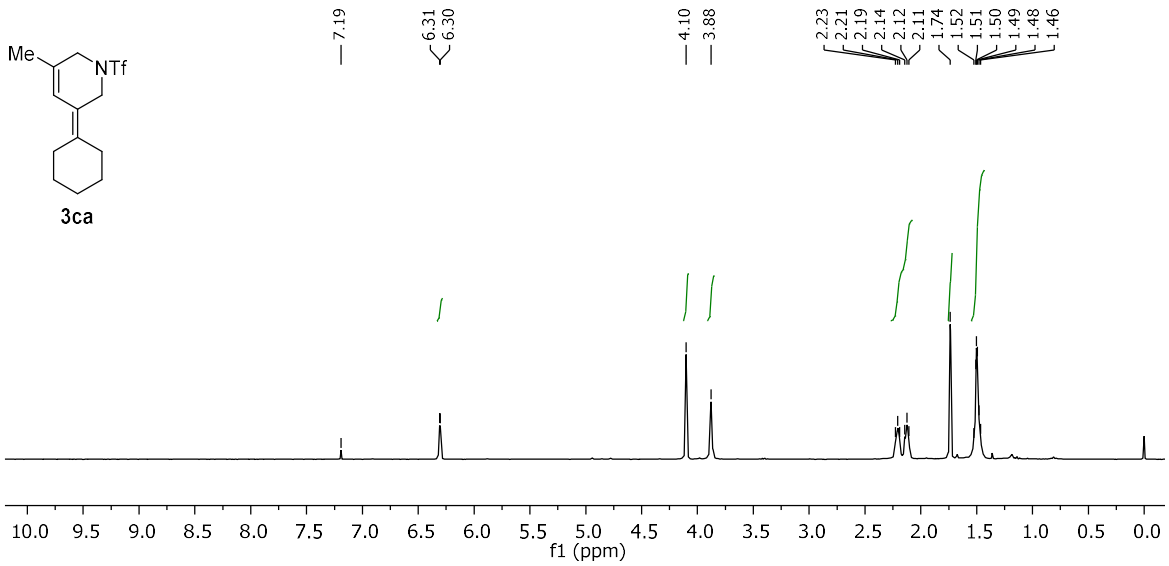

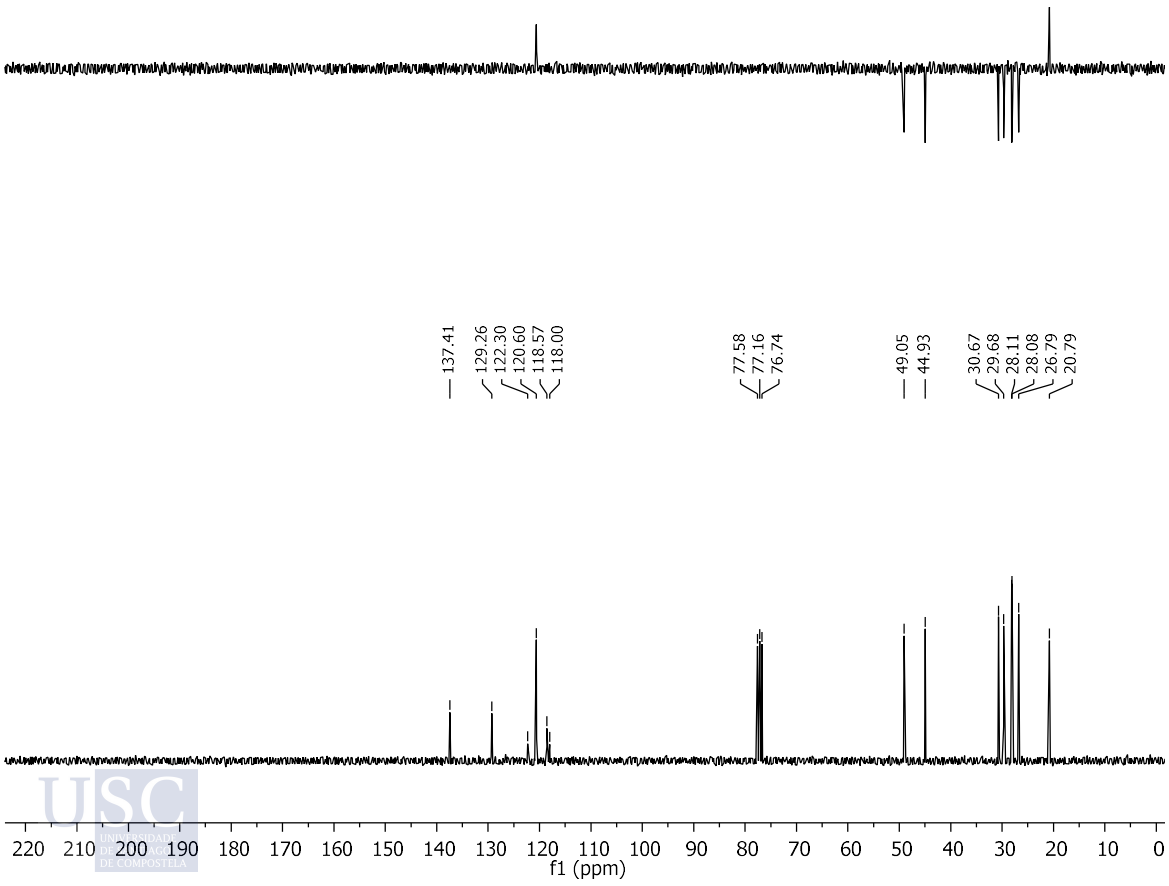

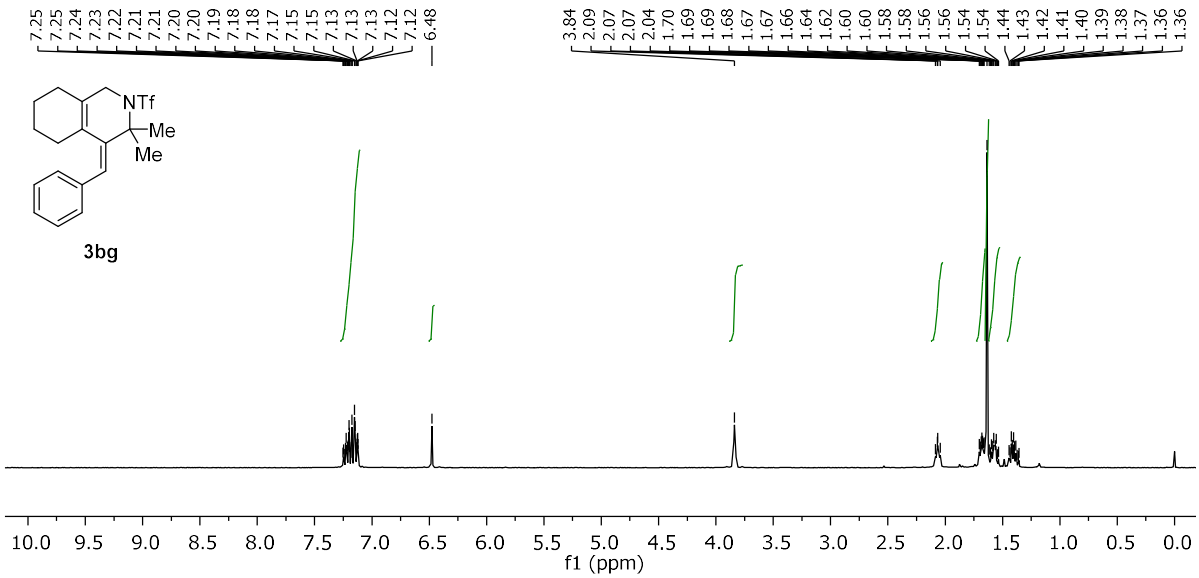

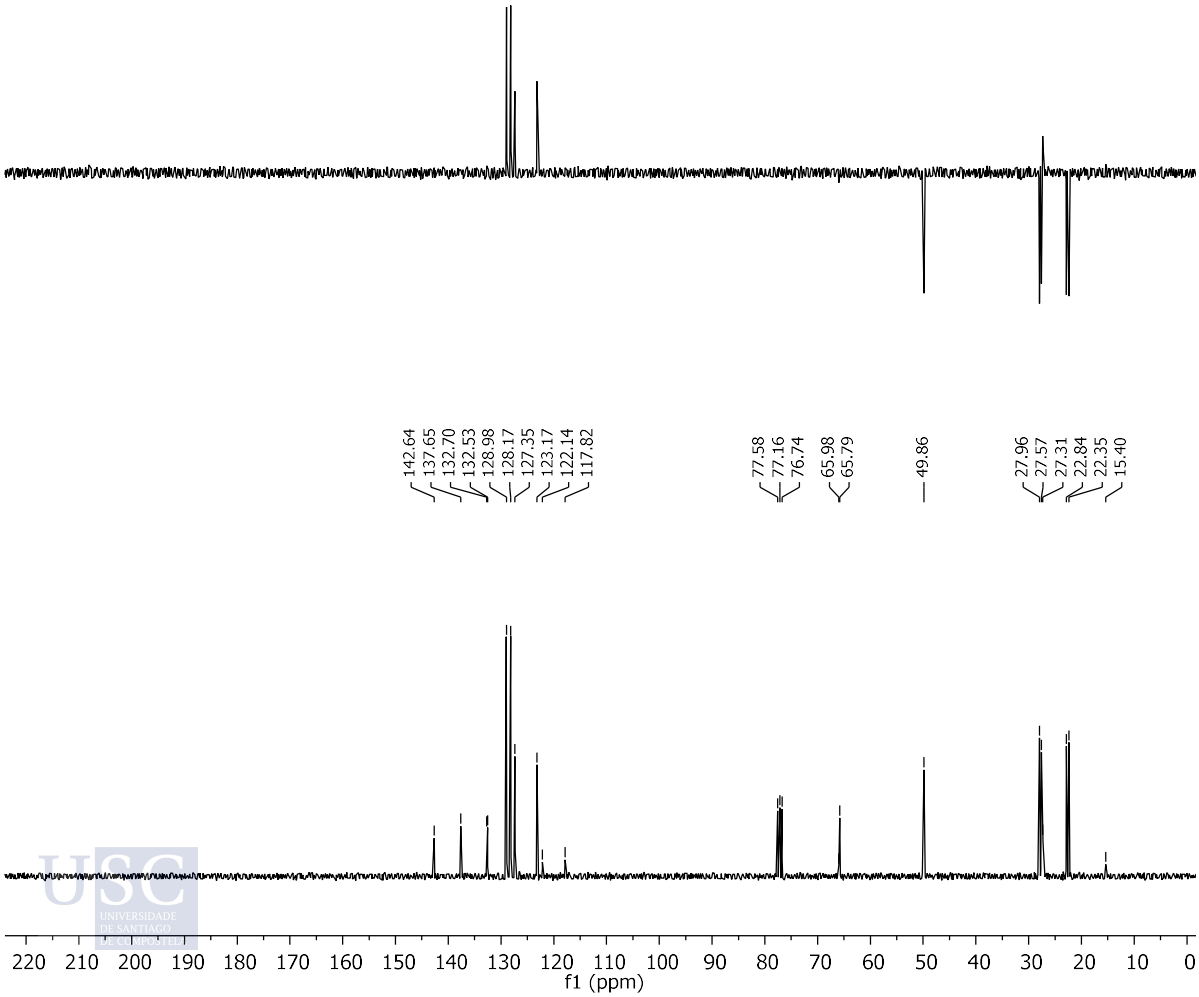

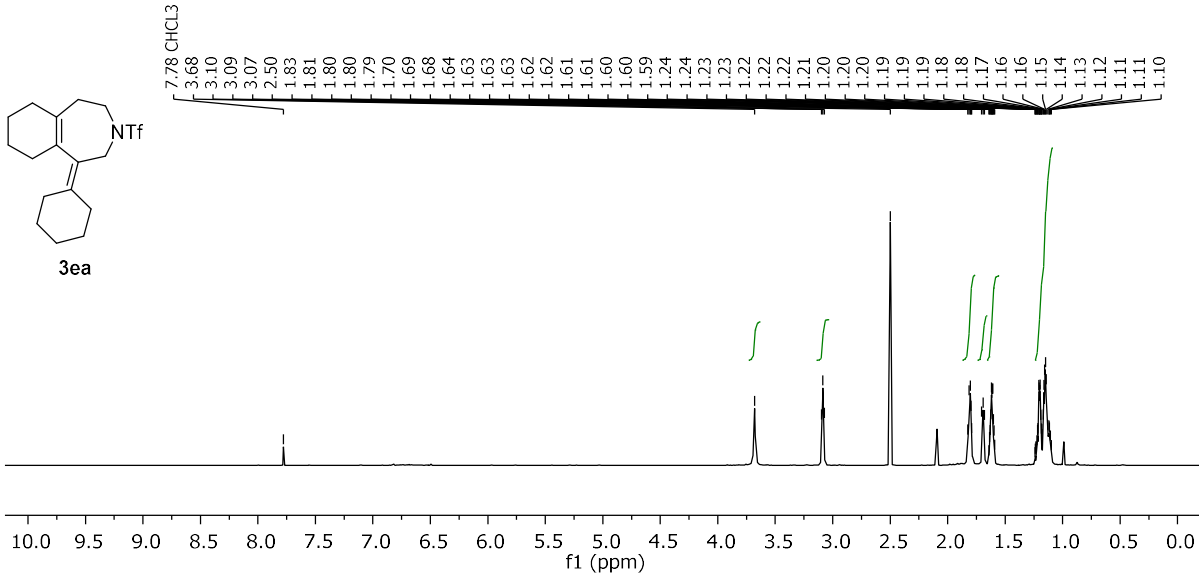

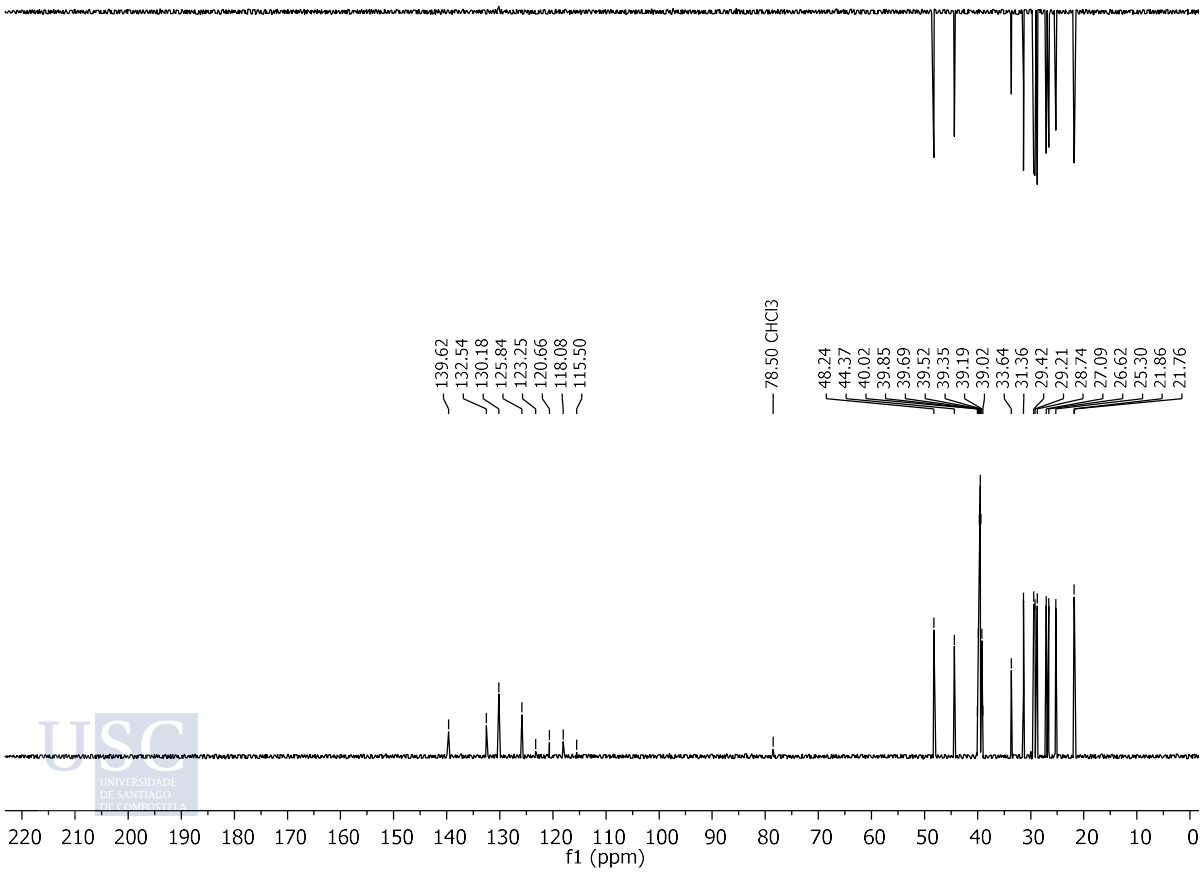

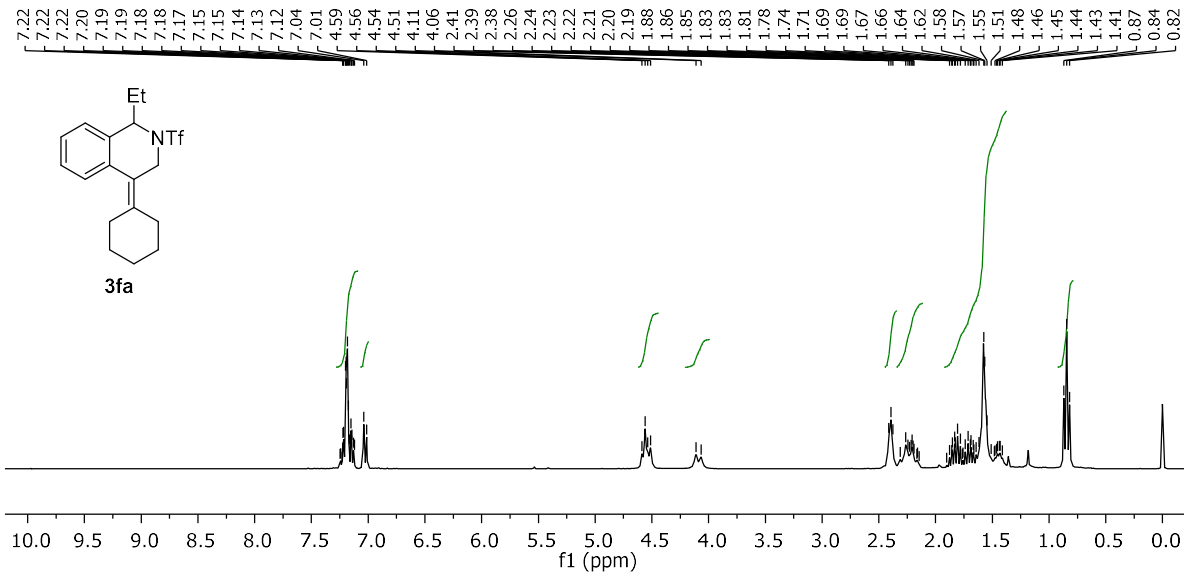
7.22
7.22
7.22
7.20
7.19
7.19
7.18
7.18
7.17
7.15
7.15
7.14
7.13
7.12
7.04
7.01
4.59
4.56
4.54
4.51
4.11
4.06
2.41
2.39
2.38
2.26
2.24
2.23
2.22
2.21
2.20
2.19
1.88
1.86
1.85
1.83
1.83
1.81
1.78
1.74
1.71
1.69
1.69
1.67
1.66
1.64
1.62
1.58
1.57
1.55
1.51
1.48
1.46
1.45
1.44
1.43
1.41
0.87
0.84
0.82
Et
NTf
3fa
10.0 9.5 9.0 8.5 8.0 7.5 7.0 6.5 6.0 5.5 5.0 4.5 4.0 3.5 3.0 2.5 2.0 1.5 1.0 0.5 0.0
f1 (ppm)

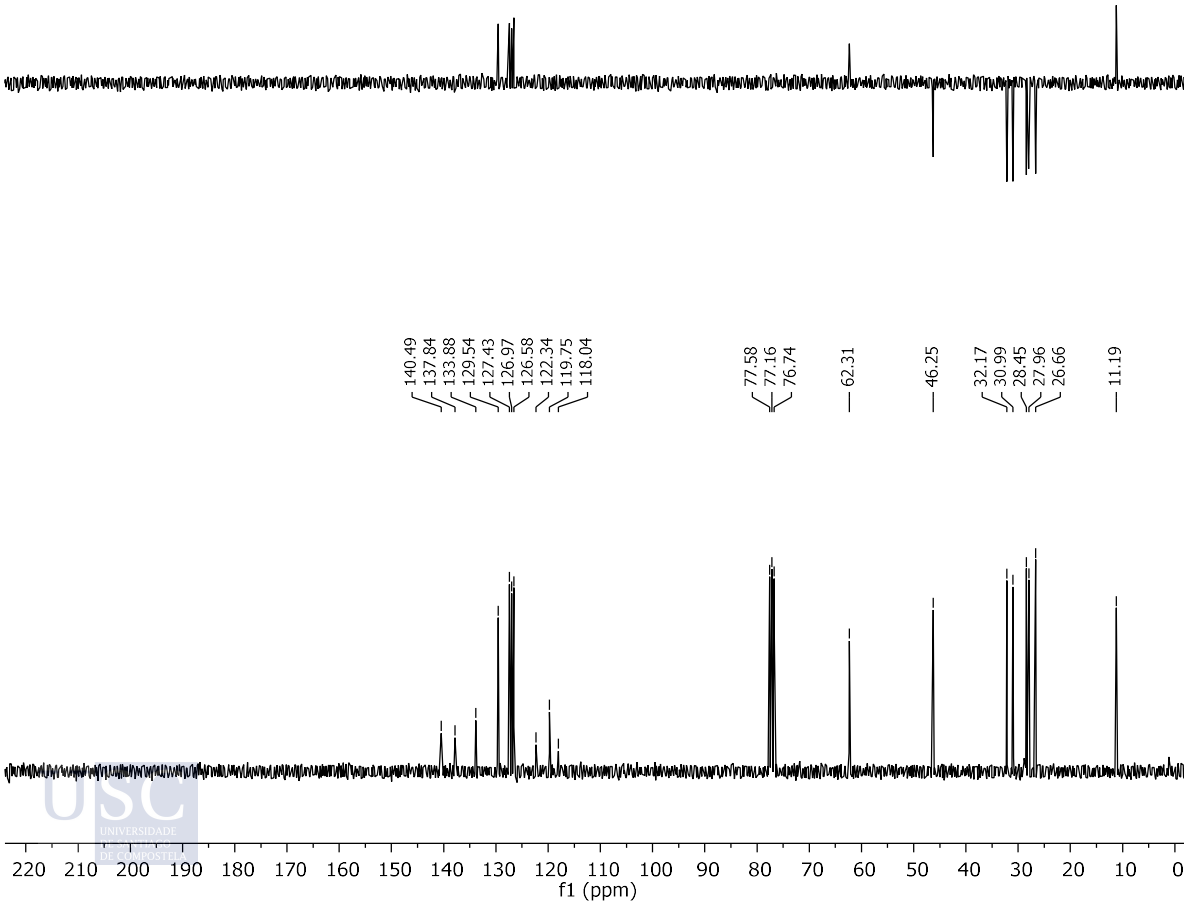
140.49
137.84
133.88
129.54
127.43
126.97
126.58
122.34
119.75
118.04
77.58
77.16
76.74
62.31
46.25
32.17
30.99
28.45
27.96
26.66
11.19
220 210 200 190 180 170 160 150 140 130 120 110 100 90 80 70 60 50 40 30 20 10 0
f1 (ppm)

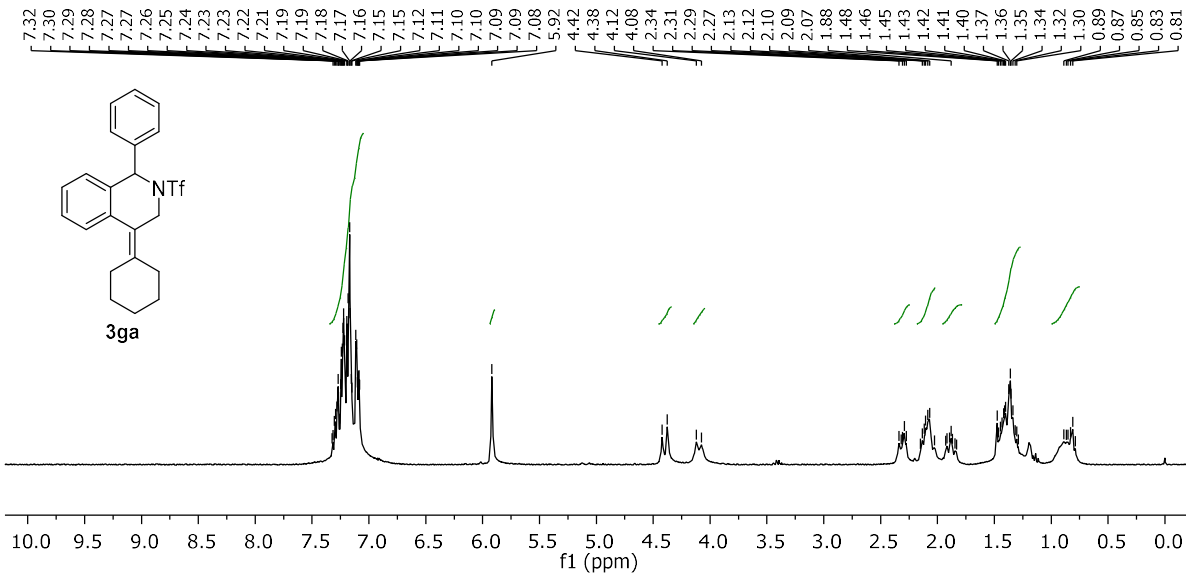

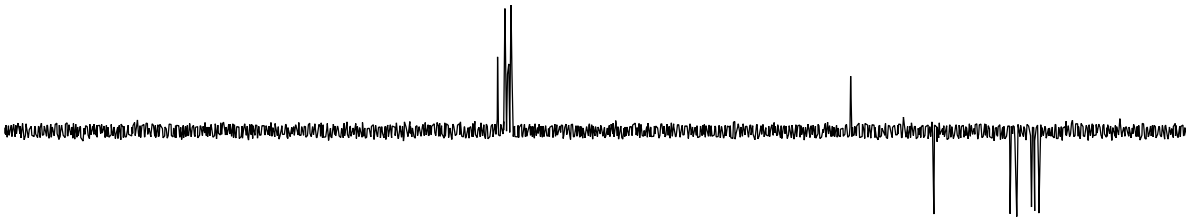

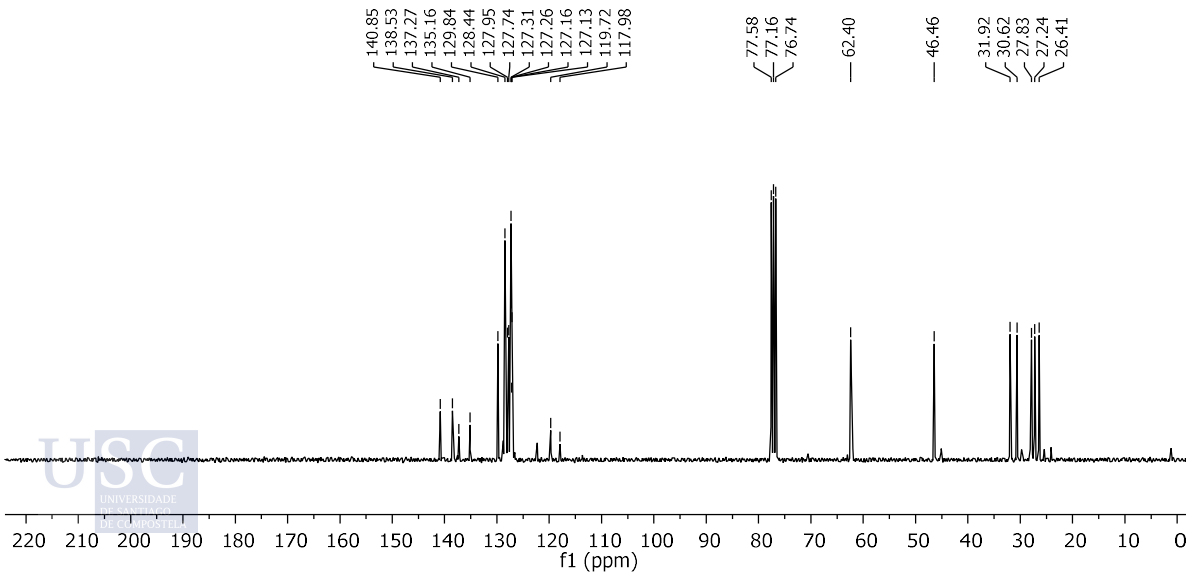

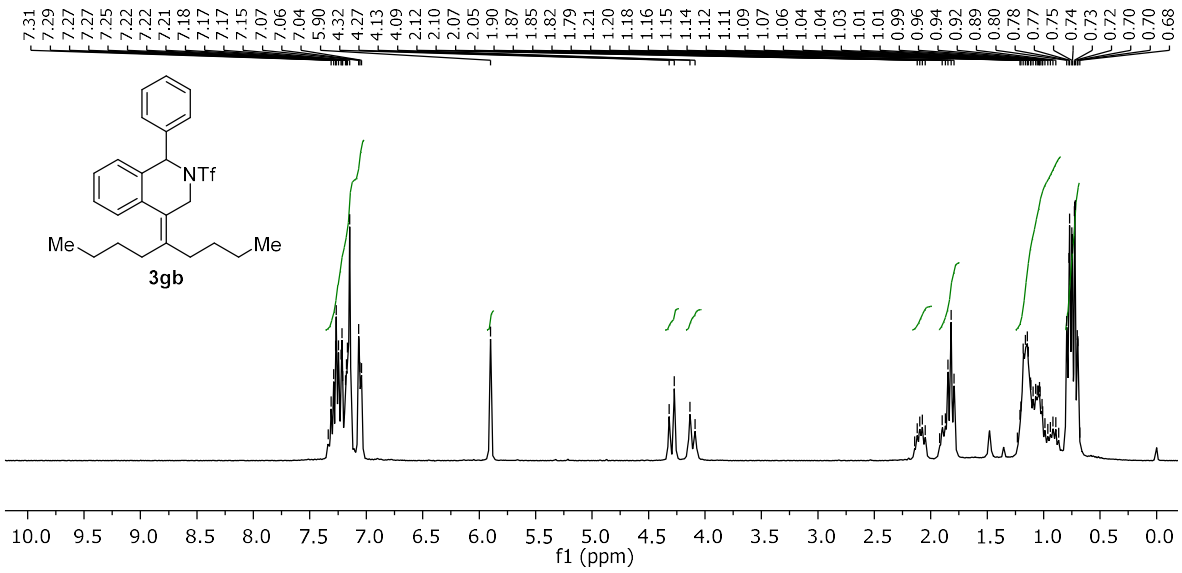
7.31 7.29 7.27 7.27 7.25 7.22 7.22 7.21 7.18 7.17 7.17 7.15 7.07 7.06 7.04 5.90 4.32 4.27 4.13 4.09 2.12 2.10 2.07 2.05 1.90 1.87 1.85 1.82 1.79 1.21 1.20 1.18 1.16 1.15 1.14 1.12 1.11 1.09 1.07 1.06 1.04 1.04 1.03 1.01 1.01 0.99 0.96 0.94 0.92 0.89 0.80 0.78 0.77 0.75 0.74 0.73 0.72 0.70 0.70 0.68
NTf
Me
Me
3gb
10.0 9.5 9.0 8.5 8.0 7.5 7.0 6.5 6.0 5.5 5.0 4.5 4.0 3.5 3.0 2.5 2.0 1.5 1.0 0.5 0.0
f1 (ppm)

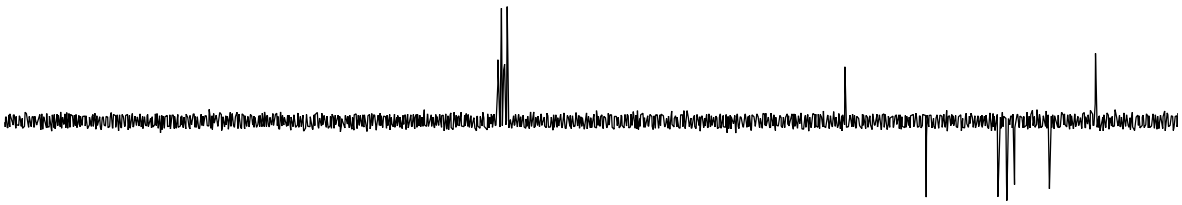

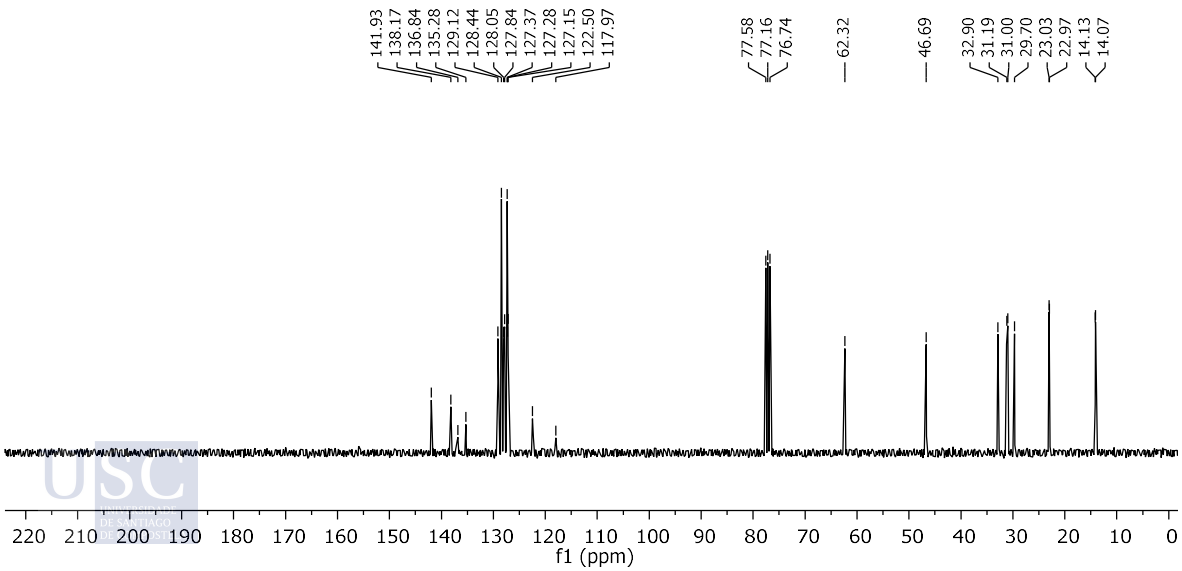
141.93 138.17 136.84 135.28 129.12 128.44 128.05 127.84 127.37 127.28 127.15 122.50 117.97
77.58 77.16 76.74
62.32
46.69
32.90 31.19 31.00 29.70 23.03 22.97 14.13 14.07
220 210 200 190 180 170 160 150 140 130 120 110 100 90 80 70 60 50 40 30 20 10 0
f1 (ppm)

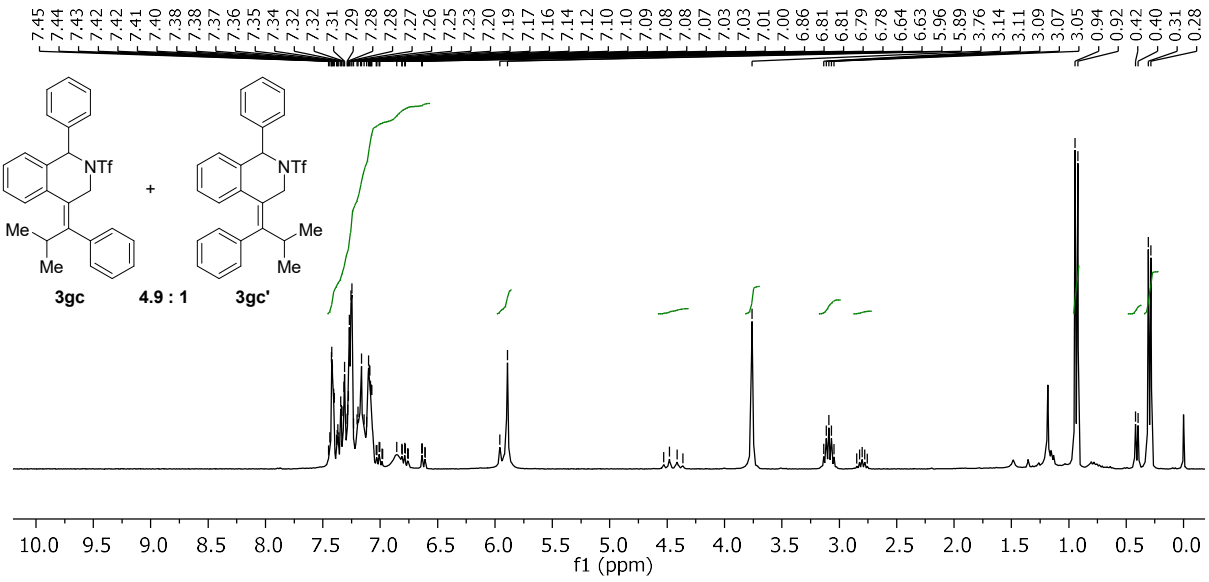

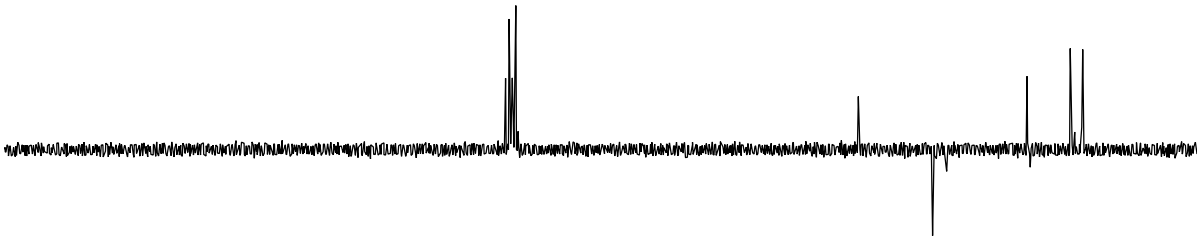

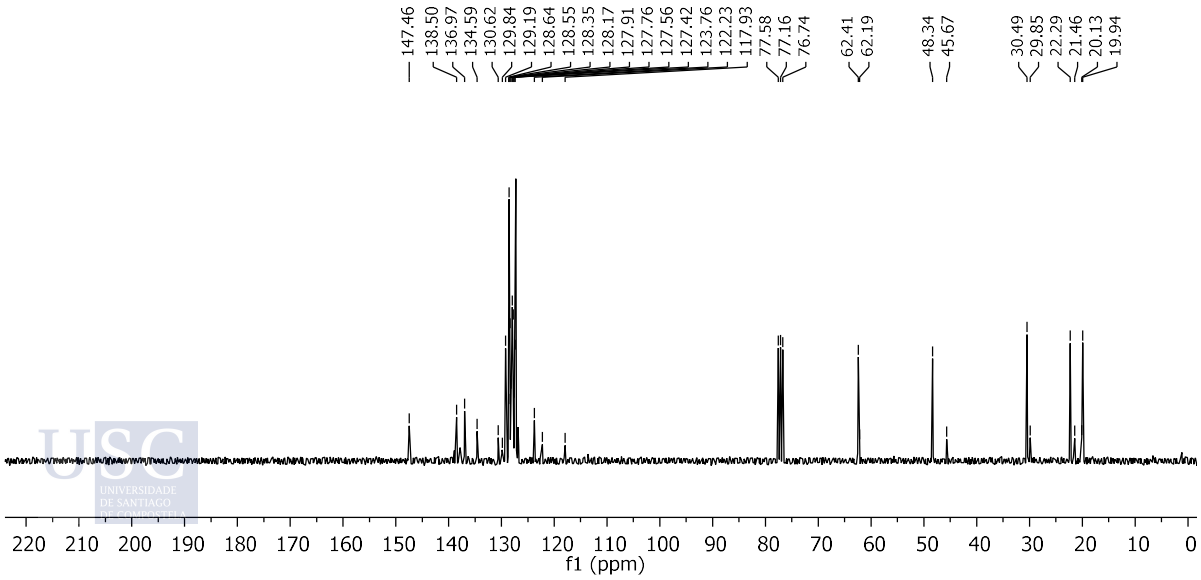

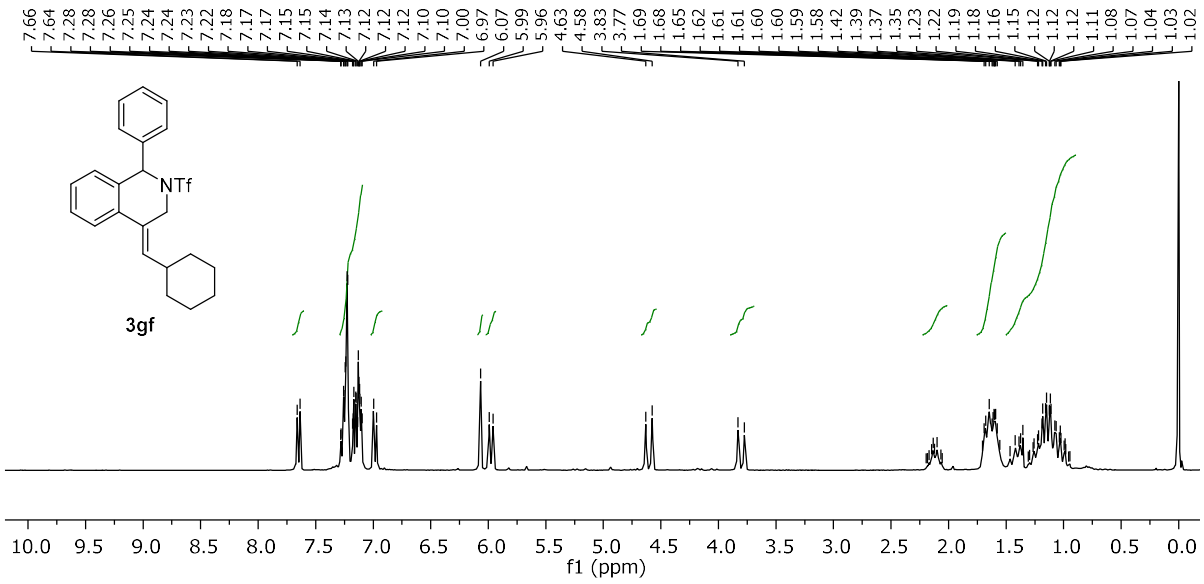

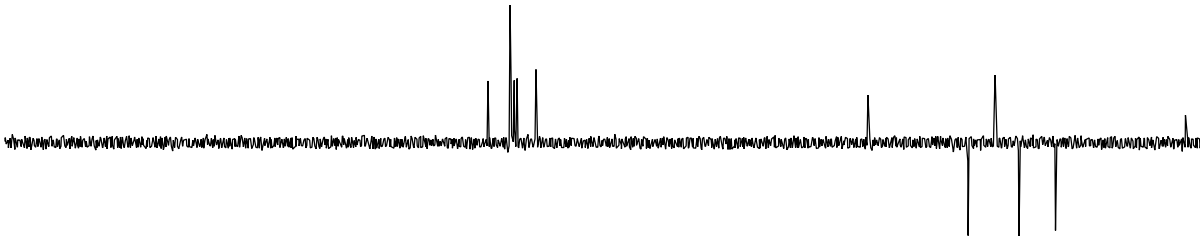

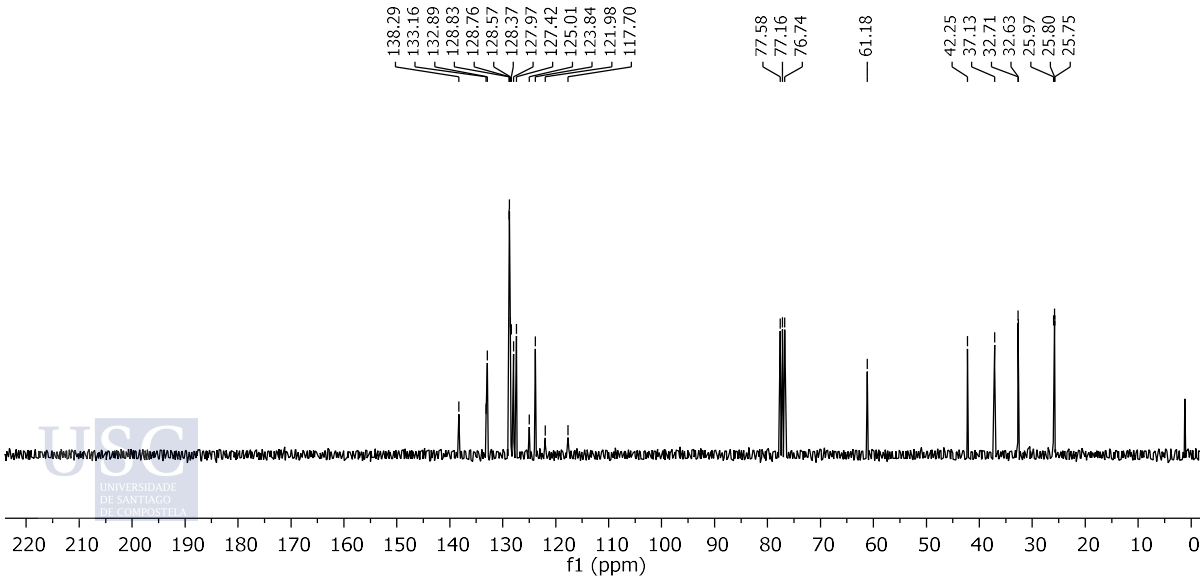

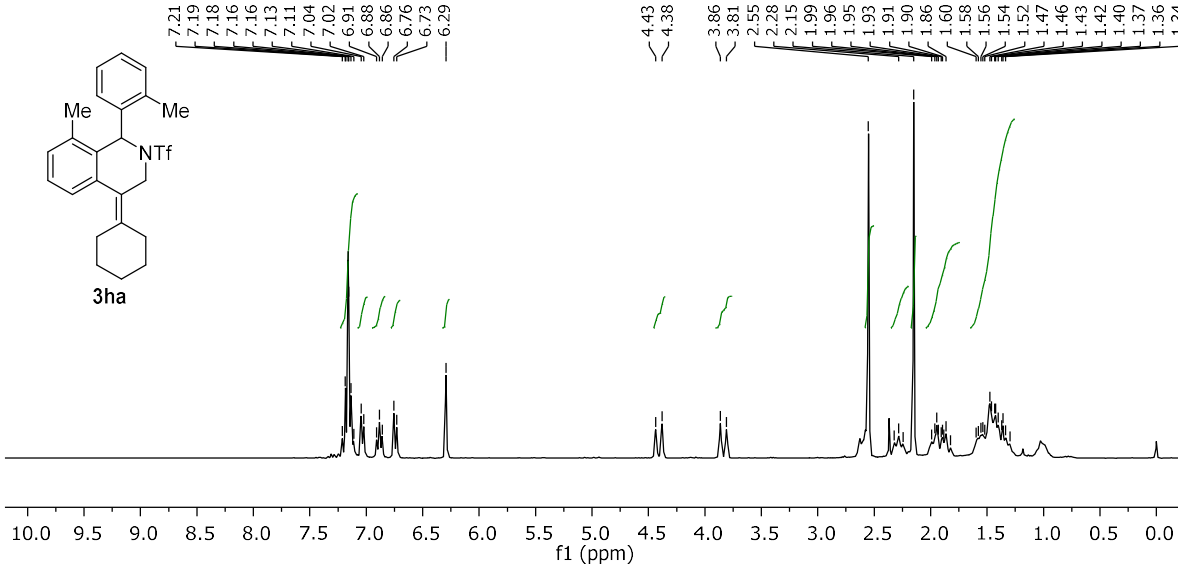
7.21
7.19
7.18
7.16
7.16
7.13
7.11
7.04
7.02
6.91
6.88
6.86
6.76
6.73
6.29
4.43
4.38
3.86
3.81
2.55
2.28
2.15
1.99
1.96
1.95
1.93
1.91
1.90
1.86
1.60
1.58
1.56
1.54
1.52
1.47
1.46
1.43
1.42
1.40
1.37
1.36
Me
Me
NTf
3ha
10.0 9.5 9.0 8.5 8.0 7.5 7.0 6.5 6.0 5.5 5.0 4.5 4.0 3.5 3.0 2.5 2.0 1.5 1.0 0.5 0.0
f1 (ppm)

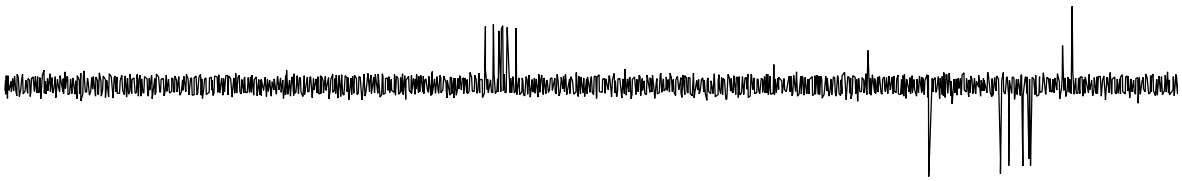

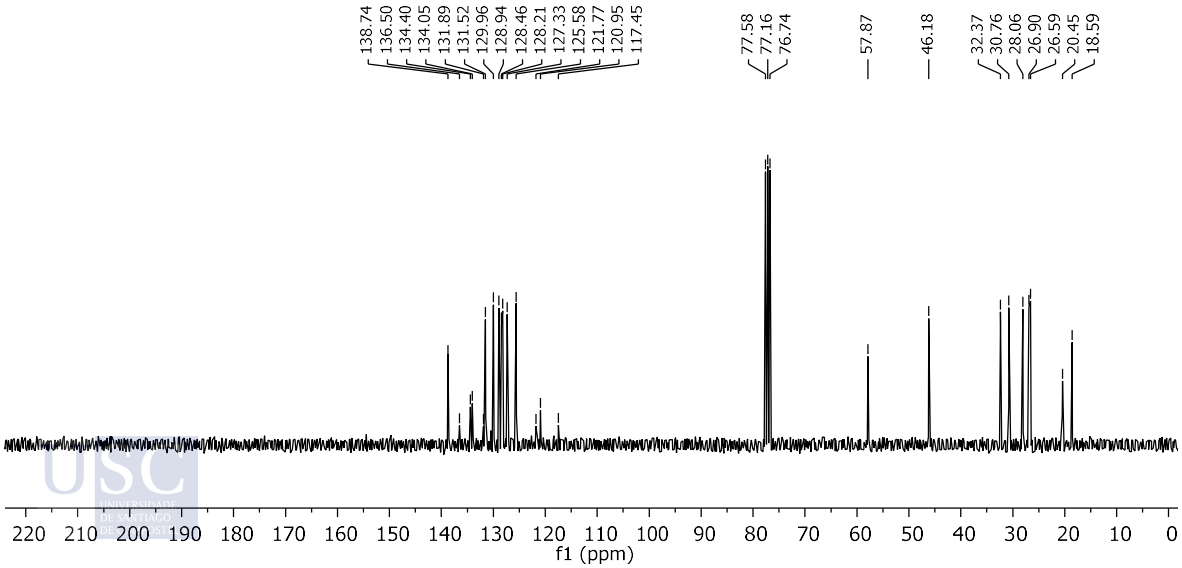
138.74
136.50
134.40
134.05
131.89
131.52
129.96
128.94
128.46
128.21
127.33
125.58
121.77
120.95
117.45
77.58
77.16
76.74
57.87
46.18
32.37
30.76
28.06
26.90
26.59
20.45
18.59
220 210 200 190 180 170 160 150 140 130 120 110 100 90 80 70 60 50 40 30 20 10 0
f1 (ppm)

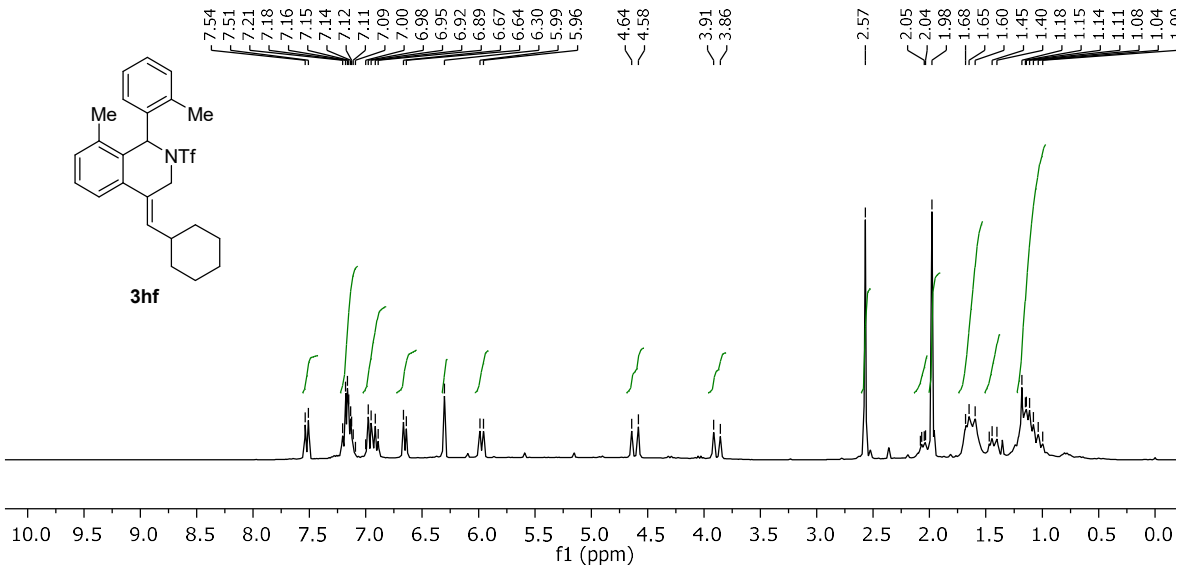

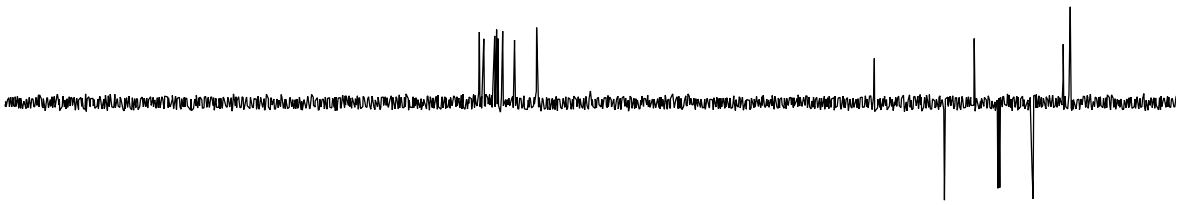

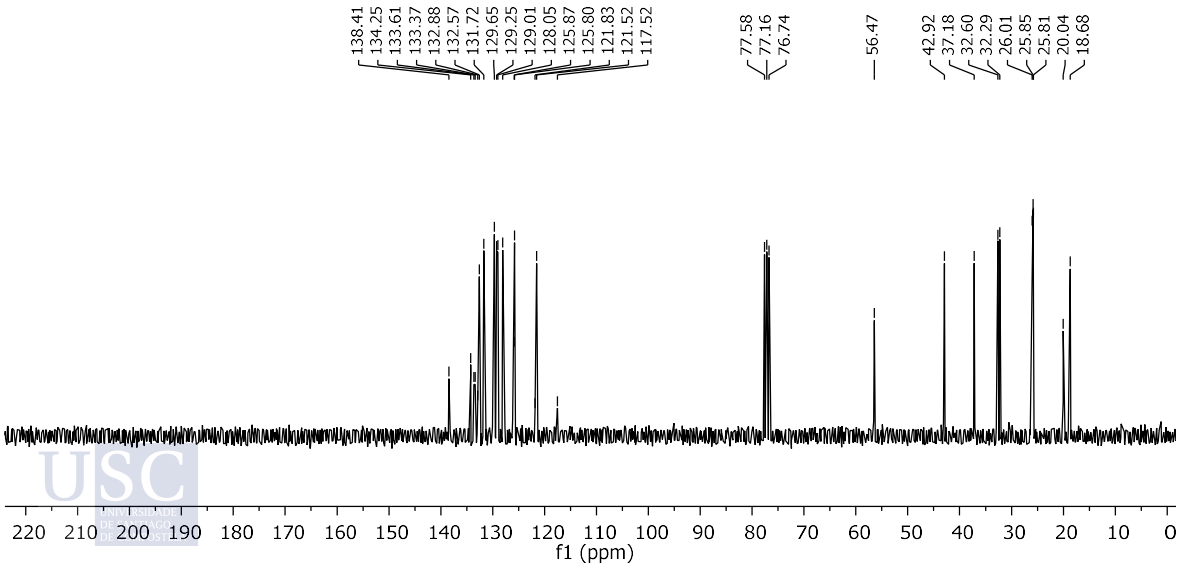

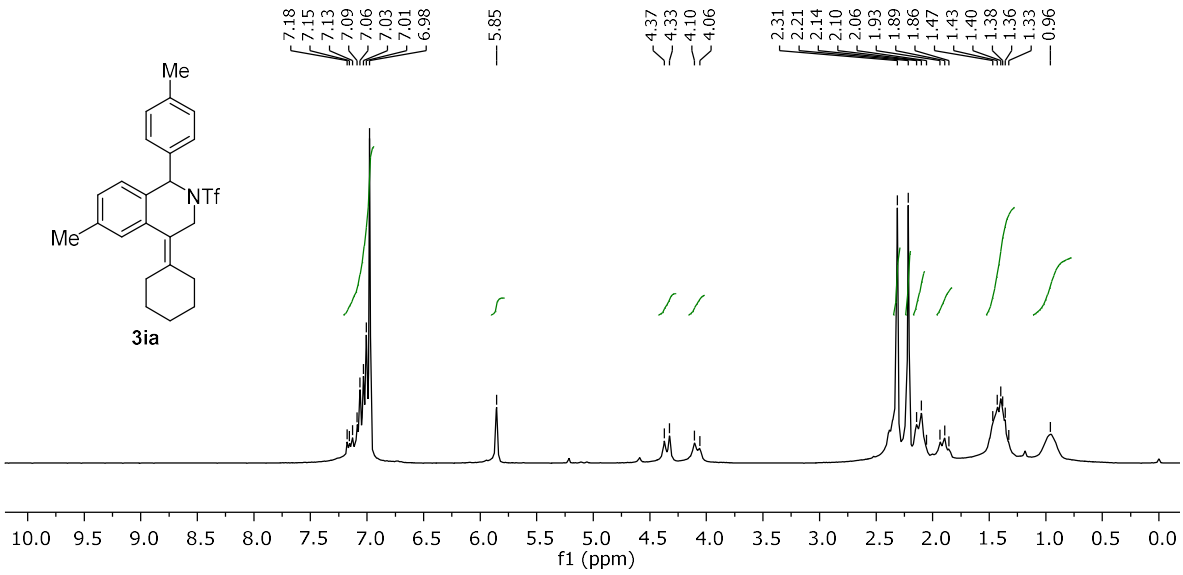
7.18
7.15
7.13
7.09
7.06
7.03
7.01
6.98
5.85
4.37
4.33
4.10
4.06
2.31
2.21
2.14
2.10
2.06
1.93
1.89
1.86
1.47
1.43
1.40
1.38
1.36
1.33
0.96
Me
NTf
Me
3ia
10.0 9.5 9.0 8.5 8.0 7.5 7.0 6.5 6.0 5.5 5.0 4.5 4.0 3.5 3.0 2.5 2.0 1.5 1.0 0.5 0.0
f1 (ppm)

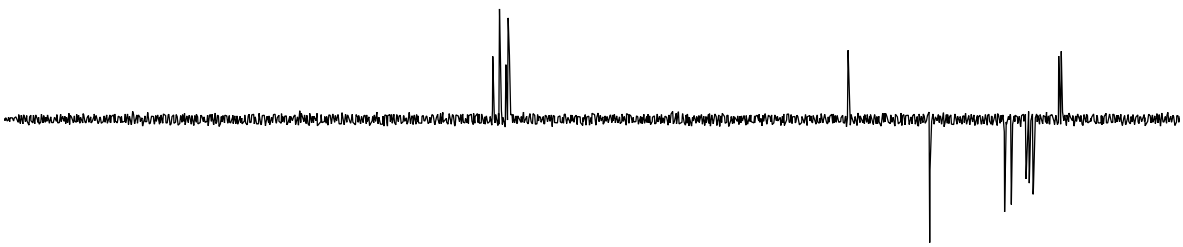

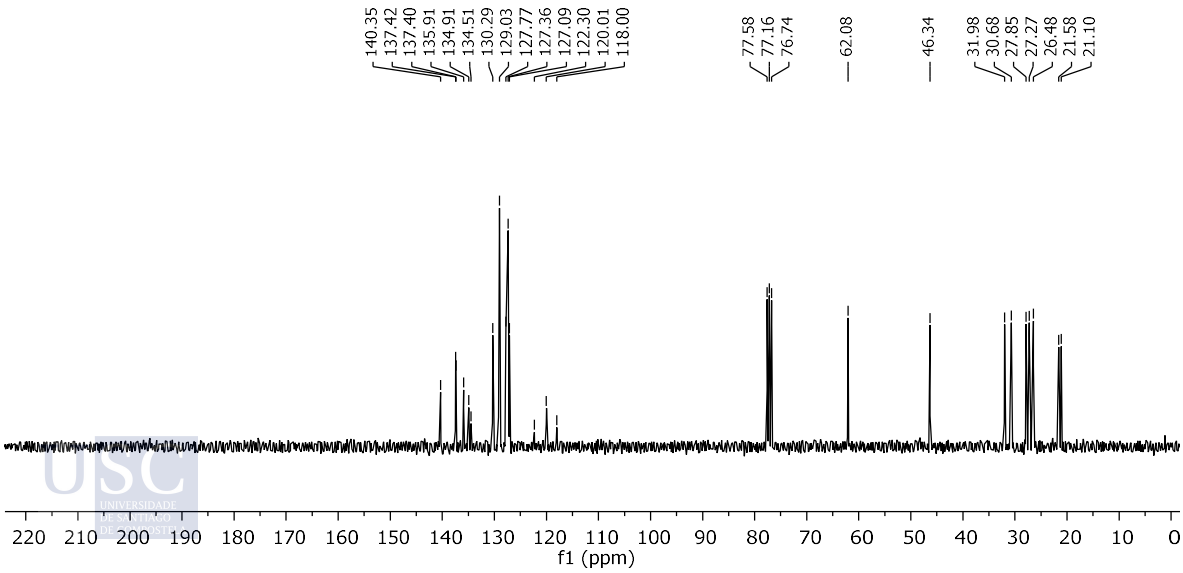
140.35
137.42
137.40
135.91
134.91
134.51
130.29
129.03
127.77
127.36
127.09
122.30
120.01
118.00
77.58
77.16
76.74
62.08
46.34
31.98
30.68
27.85
27.27
26.48
21.58
21.10
220 210 200 190 180 170 160 150 140 130 120 110 100 90 80 70 60 50 40 30 20 10 0
f1 (ppm)

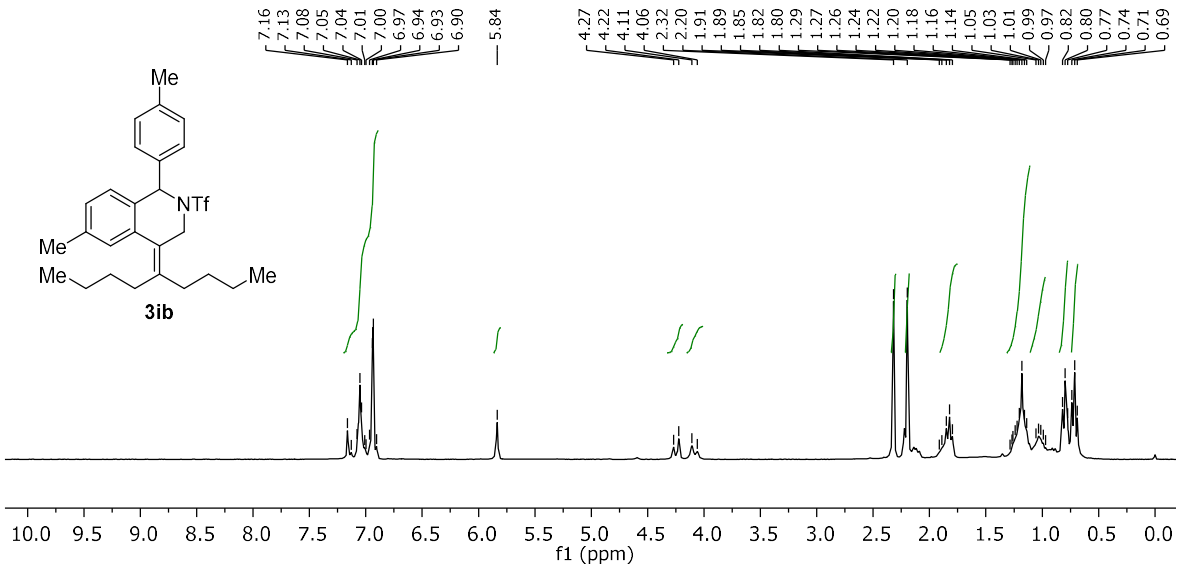
7.16
7.13
7.08
7.05
7.04
7.01
7.00
6.97
6.94
6.93
6.90
5.84
4.27
4.22
4.11
4.06
2.32
2.20
1.91
1.89
1.85
1.82
1.80
1.29
1.27
1.26
1.24
1.22
1.20
1.18
1.16
1.14
1.05
1.03
1.01
0.99
0.97
0.82
0.80
0.77
0.74
0.71
0.69
Me
NTf
Me
Me
Me
3ib
10.0 9.5 9.0 8.5 8.0 7.5 7.0 6.5 6.0 5.5 5.0 4.5 4.0 3.5 3.0 2.5 2.0 1.5 1.0 0.5 0.0
f1 (ppm)

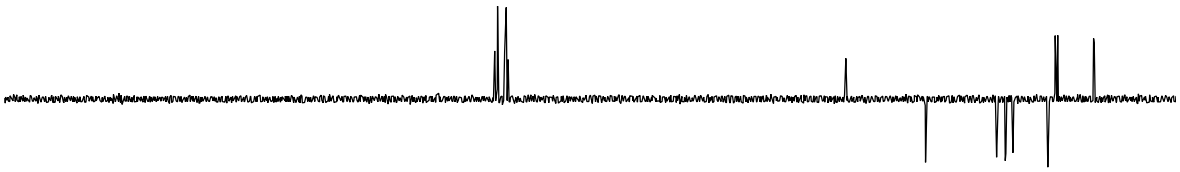

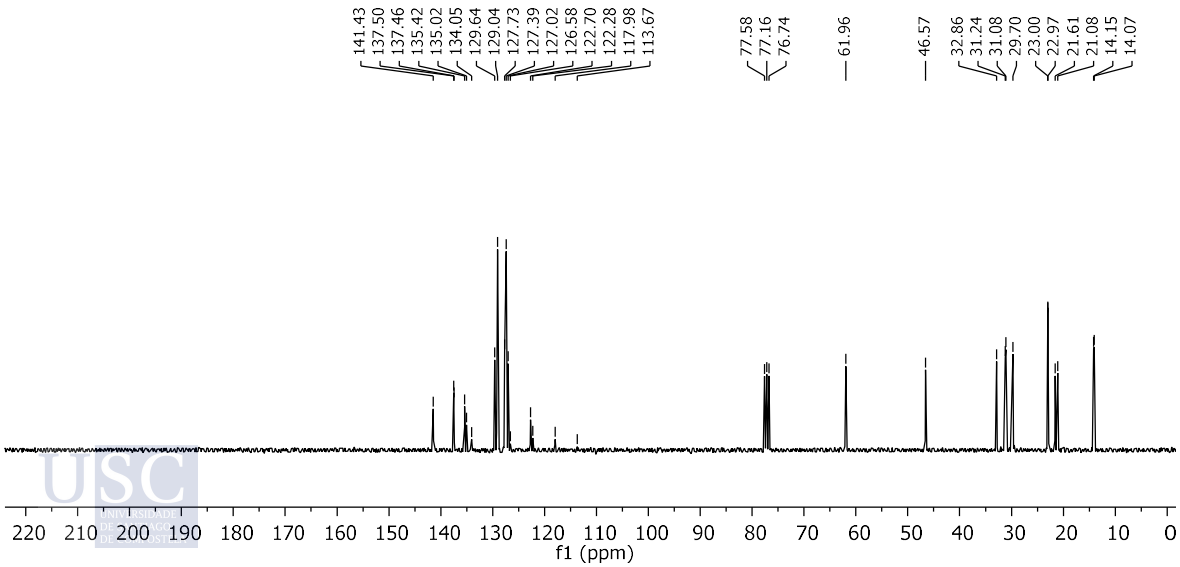
141.43
137.50
137.46
135.42
135.02
134.05
129.64
129.04
127.73
127.39
127.02
126.58
122.70
122.28
117.98
113.67
77.58
77.16
76.74
61.96
46.57
32.86
31.24
31.08
29.70
23.00
22.97
21.61
21.08
14.15
14.07
220 210 200 190 180 170 160 150 140 130 120 110 100 90 80 70 60 50 40 30 20 10 0
f1 (ppm)

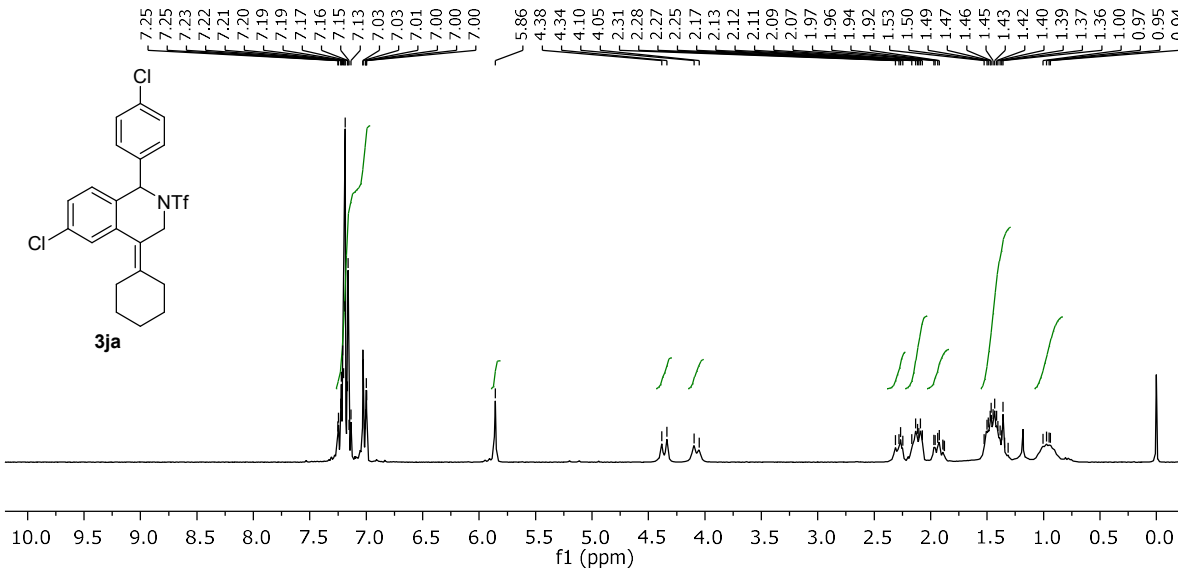
7.25
7.25
7.23
7.22
7.21
7.20
7.19
7.19
7.17
7.16
7.15
7.13
7.03
7.03
7.01
7.00
7.00
7.00
5.86
4.38
4.34
4.10
4.05
2.31
2.28
2.27
2.25
2.17
2.13
2.12
2.11
2.09
2.07
1.97
1.96
1.94
1.92
1.53
1.50
1.49
1.47
1.46
1.45
1.43
1.42
1.40
1.39
1.37
1.36
1.00
0.97
0.95
Cl
NTf
Cl
3ja
10.0 9.5 9.0 8.5 8.0 7.5 7.0 6.5 6.0 5.5 5.0 4.5 4.0 3.5 3.0 2.5 2.0 1.5 1.0 0.5 0.0
f1 (ppm)

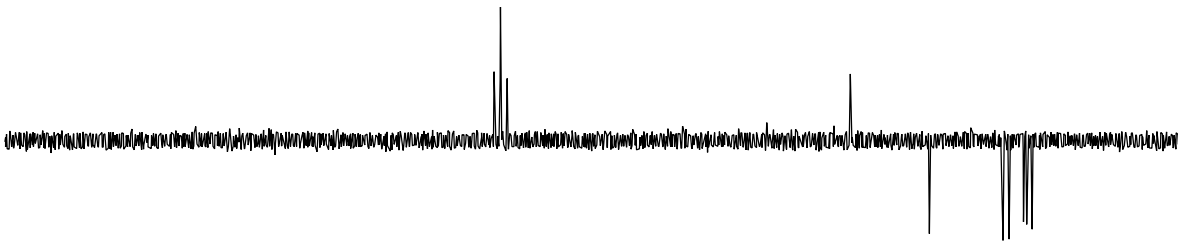

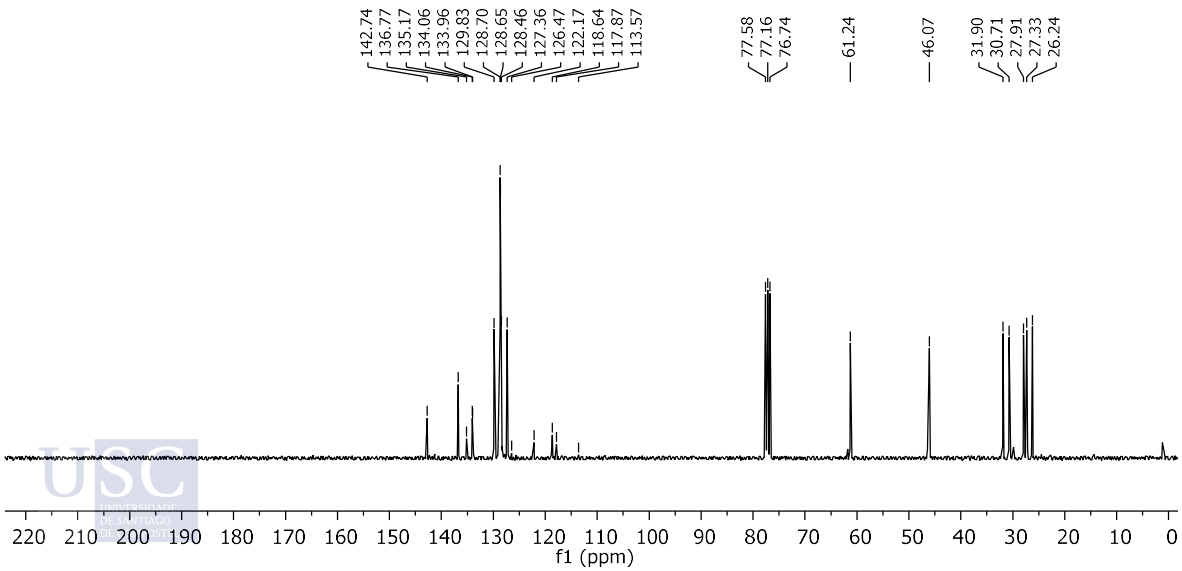
142.74
136.77
135.17
134.06
133.96
129.83
128.70
128.65
128.46
127.36
126.47
122.17
118.64
117.87
113.57
77.58
77.16
76.74
61.24
46.07
31.90
30.71
27.91
27.33
26.24
220 210 200 190 180 170 160 150 140 130 120 110 100 90 80 70 60 50 40 30 20 10 0
f1 (ppm)

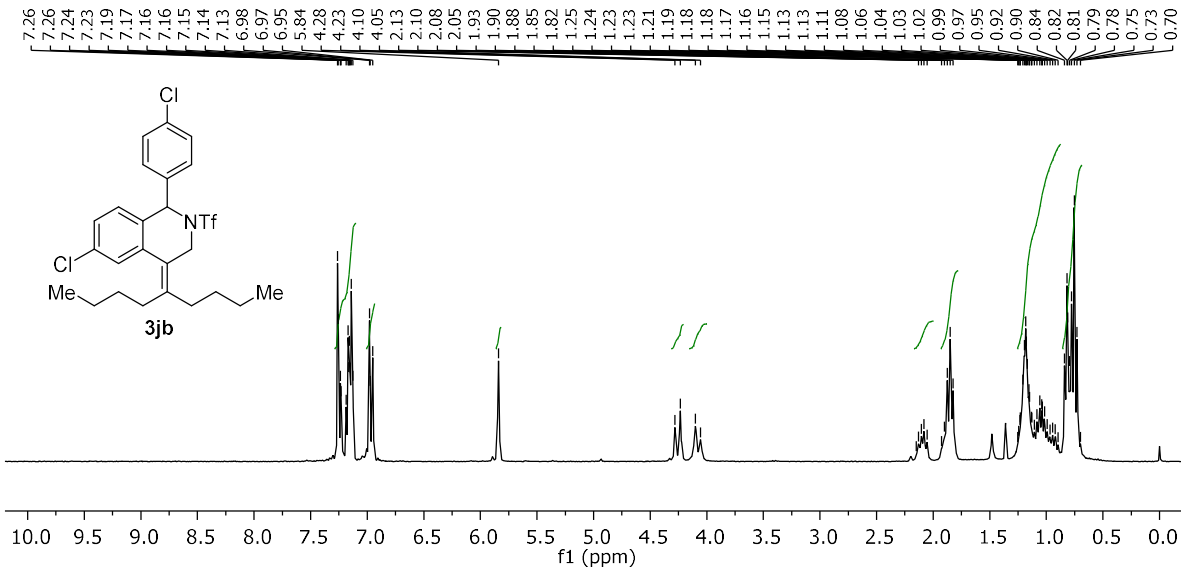
7.26 7.26 7.24 7.23 7.19 7.17 7.16 7.16 7.15 7.14 7.13 6.98 6.97 6.95 5.84 4.28 4.23 4.10 4.05 2.13 2.10 2.08 2.05 1.93 1.90 1.88 1.85 1.82 1.25 1.24 1.23 1.23 1.21 1.19 1.18 1.17 1.16 1.15 1.13 1.13 1.11 1.08 1.06 1.04 1.03 1.02 0.99 0.97 0.95 0.92 0.90 0.84 0.82 0.81 0.79 0.78 0.75 0.73 0.70
Cl
NTf
Cl
Me
Me
3jb
10.0 9.5 9.0 8.5 8.0 7.5 7.0 6.5 6.0 5.5 5.0 4.5 4.0 3.5 3.0 2.5 2.0 1.5 1.0 0.5 0.0
f1 (ppm)

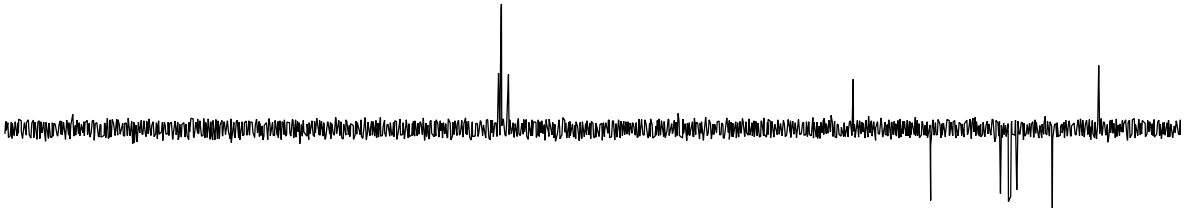

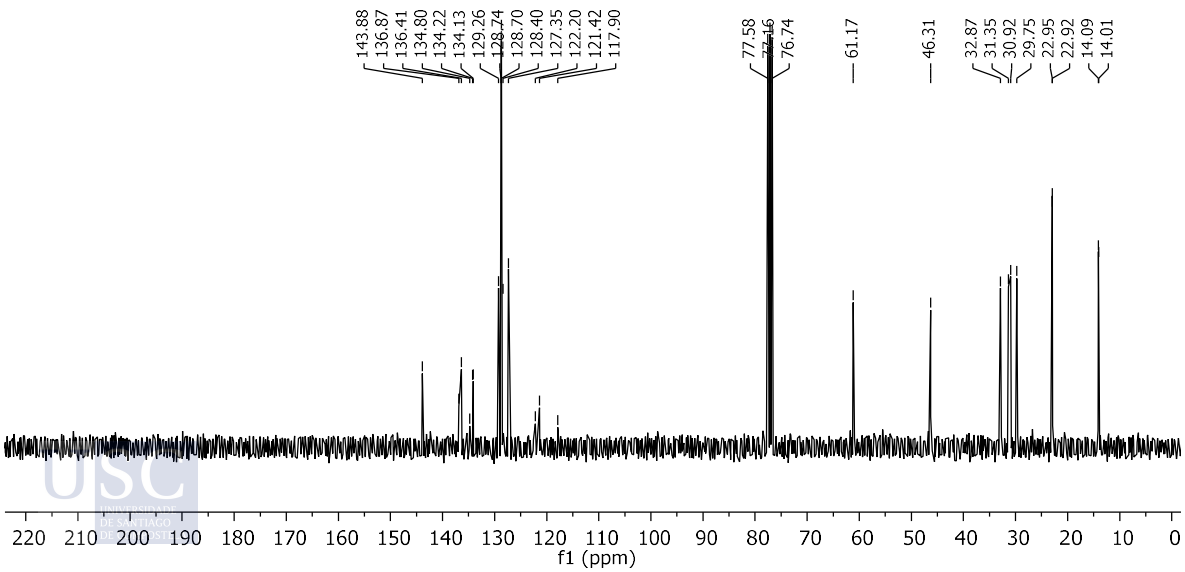
143.88 136.87 136.41 134.80 134.22 134.13 129.26 128.74 128.70 128.40 127.35 122.20 121.42 117.90
77.58 77.16 76.74
61.17
46.31
32.87 31.35 30.92 29.75 22.95 22.92 14.09 14.01
220 210 200 190 180 170 160 150 140 130 120 110 100 90 80 70 60 50 40 30 20 10 0
f1 (ppm)

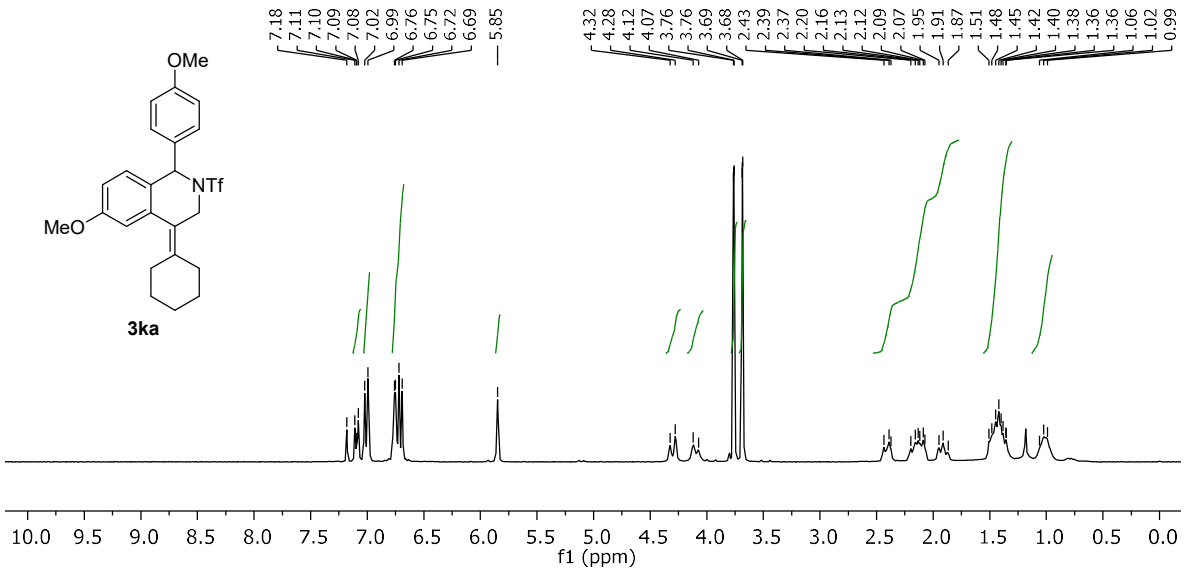
7.18
7.11
7.10
7.09
7.08
7.02
6.99
6.76
6.75
6.72
6.69
5.85
4.32
4.28
4.12
4.07
3.76
3.76
3.69
3.68
2.43
2.39
2.37
2.20
2.16
2.13
2.12
2.09
2.07
1.95
1.91
1.87
1.51
1.48
1.45
1.42
1.40
1.38
1.36
1.36
1.06
1.02
0.99
OMe
NTf
MeO
3ka
10.0 9.5 9.0 8.5 8.0 7.5 7.0 6.5 6.0 5.5 5.0 4.5 4.0 3.5 3.0 2.5 2.0 1.5 1.0 0.5 0.0
f1 (ppm)

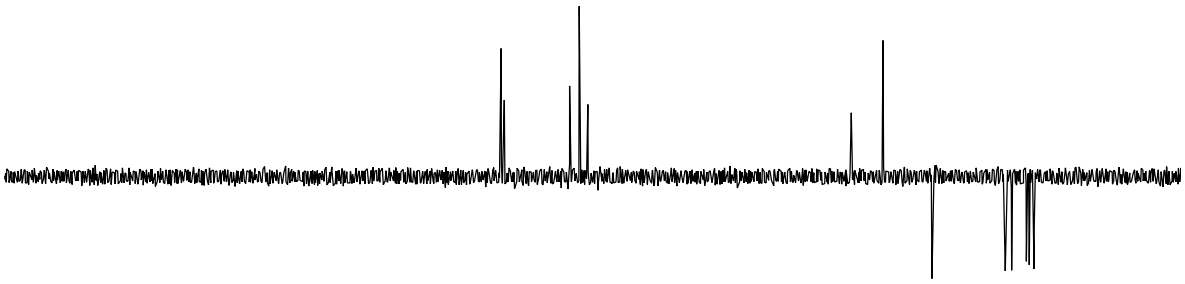

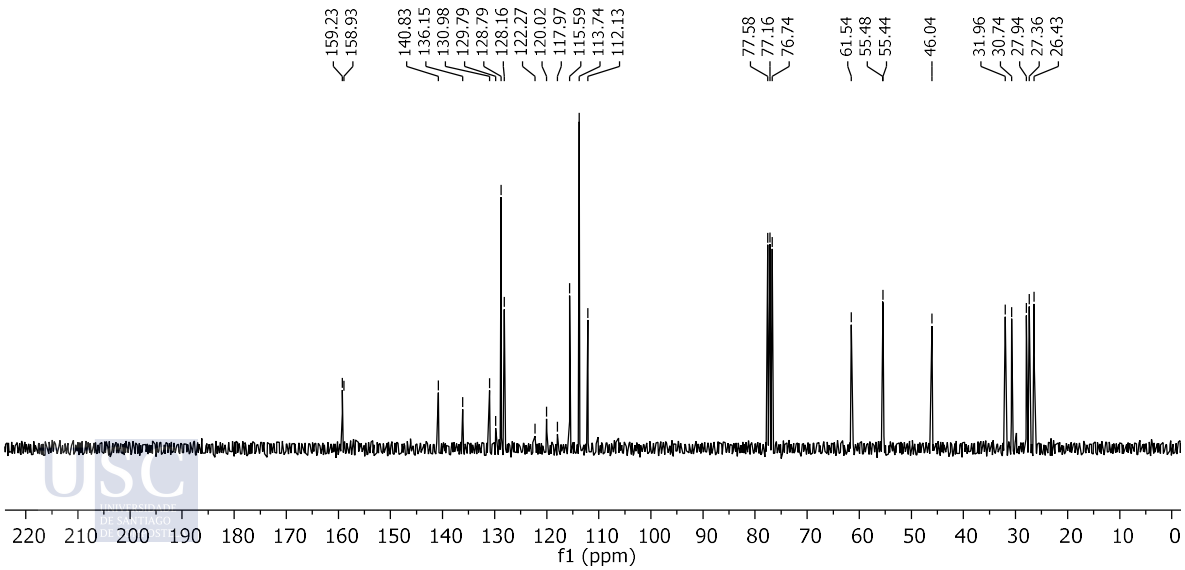
159.23
158.93
140.83
136.15
130.98
129.79
128.79
128.16
122.27
120.02
117.97
115.59
113.74
112.13
77.58
77.16
76.74
61.54
55.48
55.44
46.04
31.96
30.74
27.94
27.36
26.43
220 210 200 190 180 170 160 150 140 130 120 110 100 90 80 70 60 50 40 30 20 10 0
f1 (ppm)

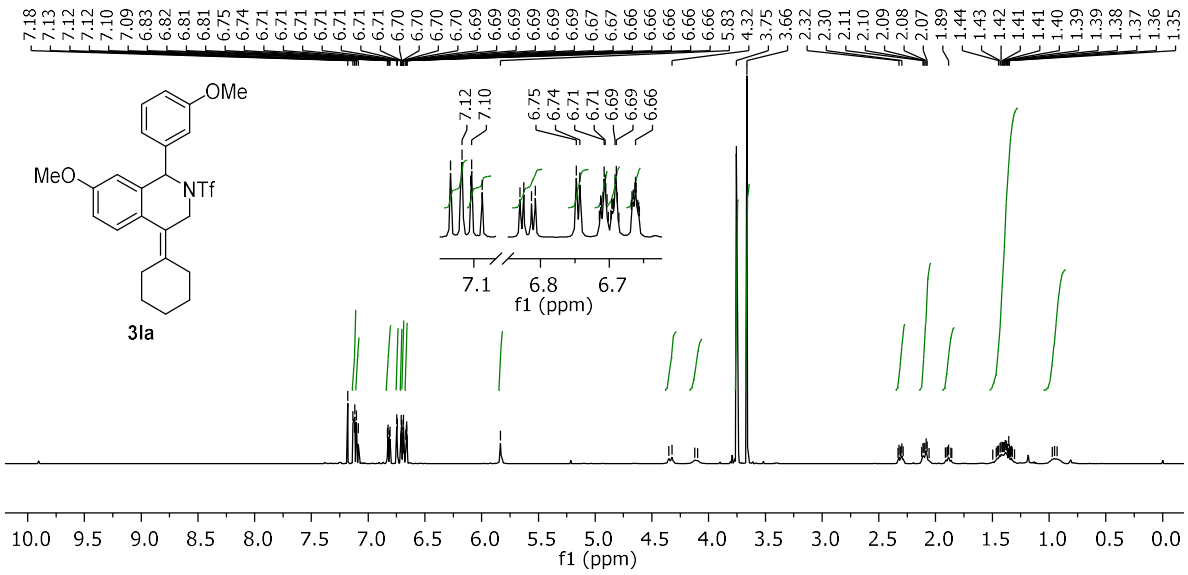
7.18 7.13 7.12 7.12 7.10 7.09 6.83 6.82 6.81 6.81 6.75 6.74 6.71 6.71 6.71 6.71 6.71 6.71 6.70 6.70 6.70 6.70 6.69 6.69 6.69 6.69 6.69 6.69 6.67 6.67 6.66 6.66 6.66 6.66 6.66 6.66 5.83 4.32 3.75 3.66 2.32 2.30 2.11 2.10 2.09 2.08 2.07 1.89 1.44 1.43 1.42 1.41 1.41 1.40 1.39 1.39 1.38 1.37 1.36 1.35
OMe
MeO
NTf
3la
7.12 7.10 6.75 6.74 6.71 6.69 6.69 6.66
7.1 6.8 6.7
f1 (ppm)
10.0 9.5 9.0 8.5 8.0 7.5 7.0 6.5 6.0 5.5 5.0 4.5 4.0 3.5 3.0 2.5 2.0 1.5 1.0 0.5 0.0
f1 (ppm)

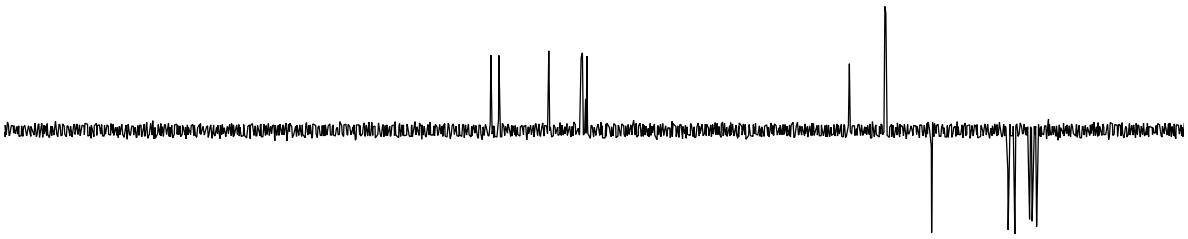

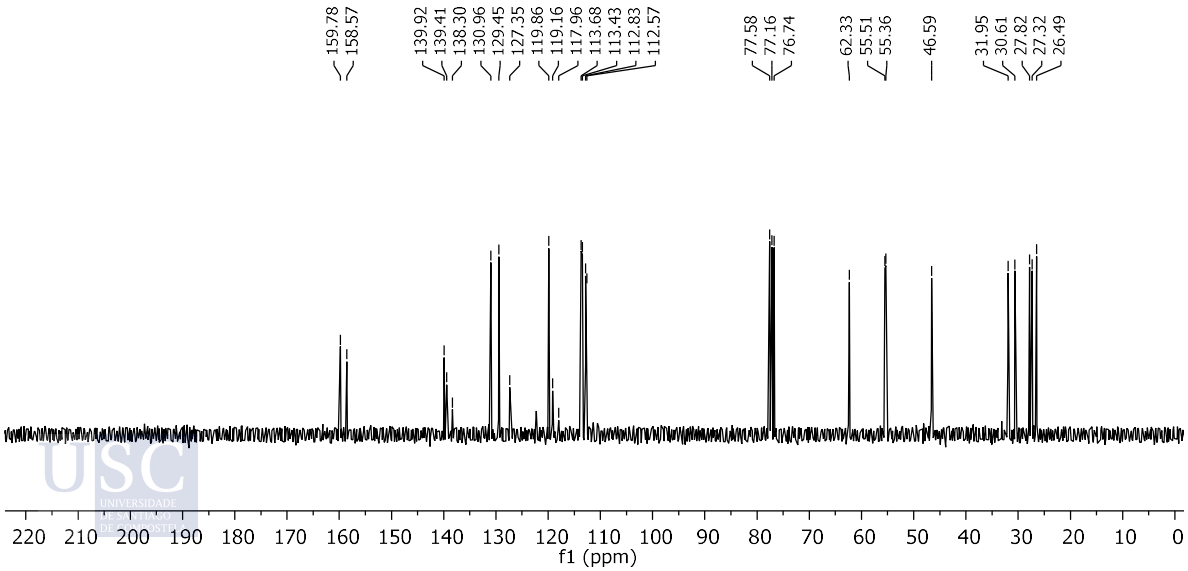
159.78 158.57 139.92 139.41 138.30 130.96 129.45 127.35 119.86 119.16 117.96 113.68 113.43 112.83 112.57 77.58 77.16 76.74 62.33 55.51 55.36 46.59 31.95 30.61 27.82 27.32 26.49
220 210 200 190 180 170 160 150 140 130 120 110 100 90 80 70 60 50 40 30 20 10 0
f1 (ppm)

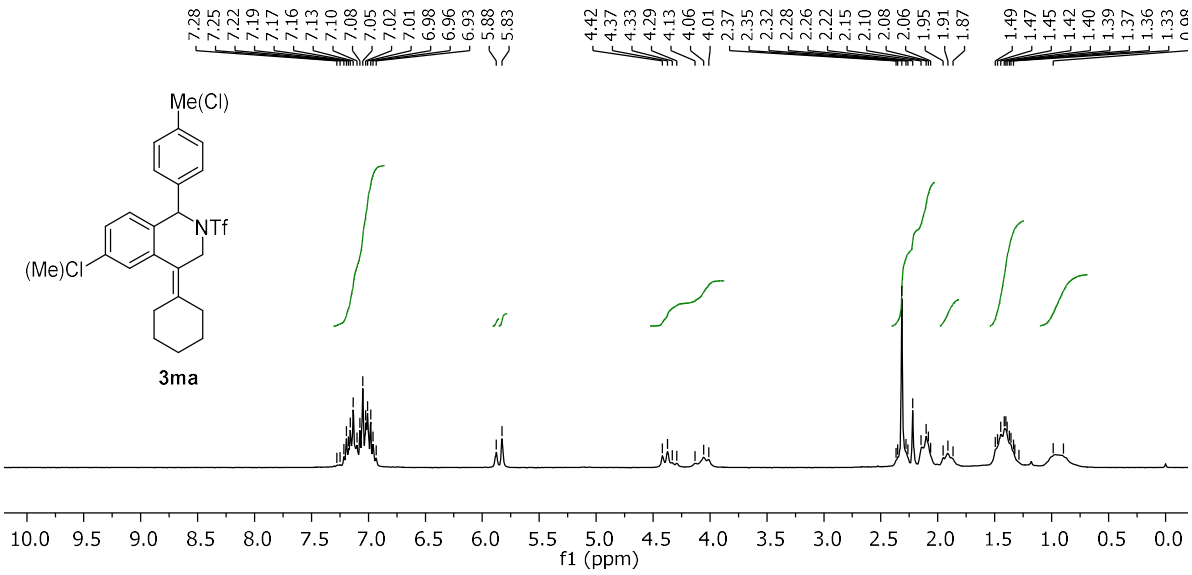
7.28
7.25
7.22
7.19
7.17
7.16
7.13
7.10
7.08
7.05
7.02
7.01
6.98
6.96
6.93
5.88
5.83
4.42
4.37
4.33
4.29
4.13
4.06
4.01
2.37
2.35
2.32
2.28
2.26
2.22
2.15
2.10
2.08
2.06
1.95
1.91
1.87
1.49
1.47
1.45
1.42
1.40
1.39
1.37
1.36
1.33
Me(Cl)
NTf
(Me)Cl
3ma
10.0 9.5 9.0 8.5 8.0 7.5 7.0 6.5 6.0 5.5 5.0 4.5 4.0 3.5 3.0 2.5 2.0 1.5 1.0 0.5 0.0
f1 (ppm)

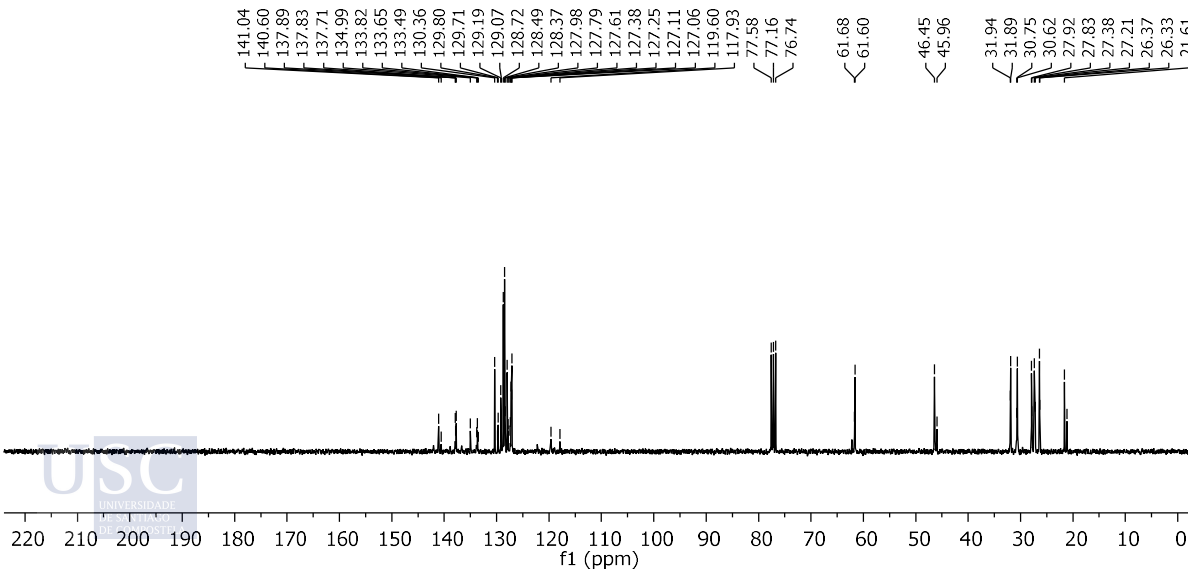
141.04
140.60
137.89
137.83
137.71
134.99
133.82
133.65
133.49
130.36
129.80
129.71
129.19
129.07
128.72
128.49
128.37
127.98
127.79
127.61
127.38
127.25
127.11
127.06
119.60
117.93
77.58
77.16
76.74
61.68
61.60
46.45
45.96
31.94
31.89
30.75
30.62
27.92
27.83
27.38
27.21
26.37
26.33
220 210 200 190 180 170 160 150 140 130 120 110 100 90 80 70 60 50 40 30 20 10 0
f1 (ppm)

2-Selected spectra from Chapter III

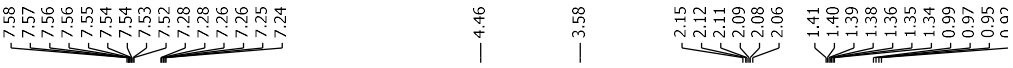

^{1}H NMR (300 MHz, $CDCl_3$)

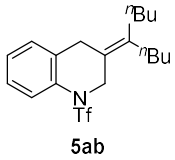

5ab

DEPT-135

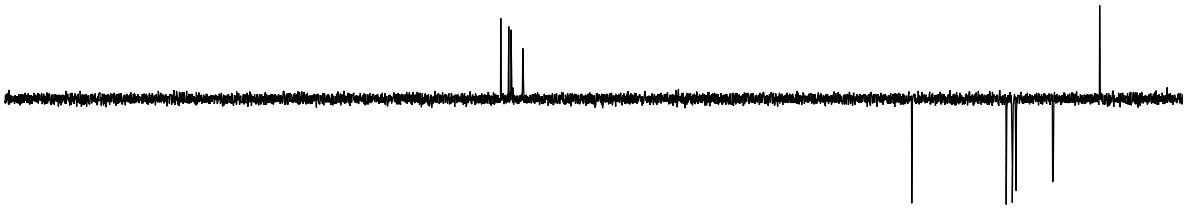

^{13}C NMR (75 MHz, $CDCl_3$)

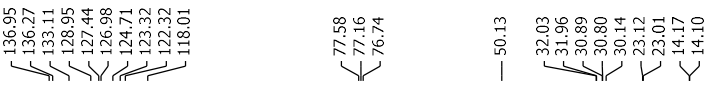

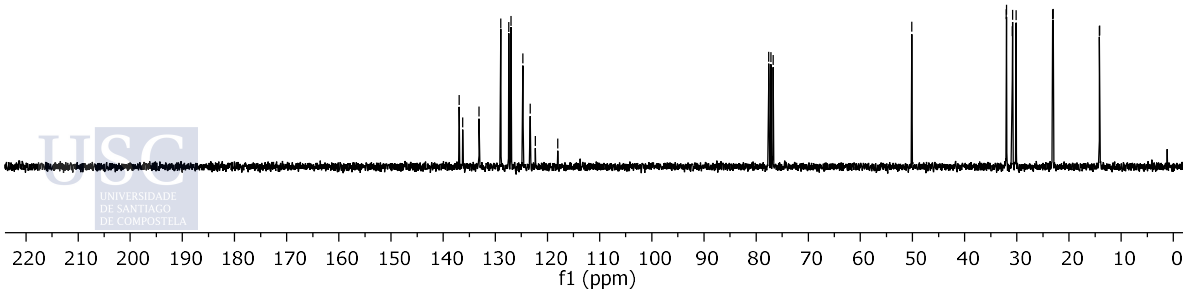

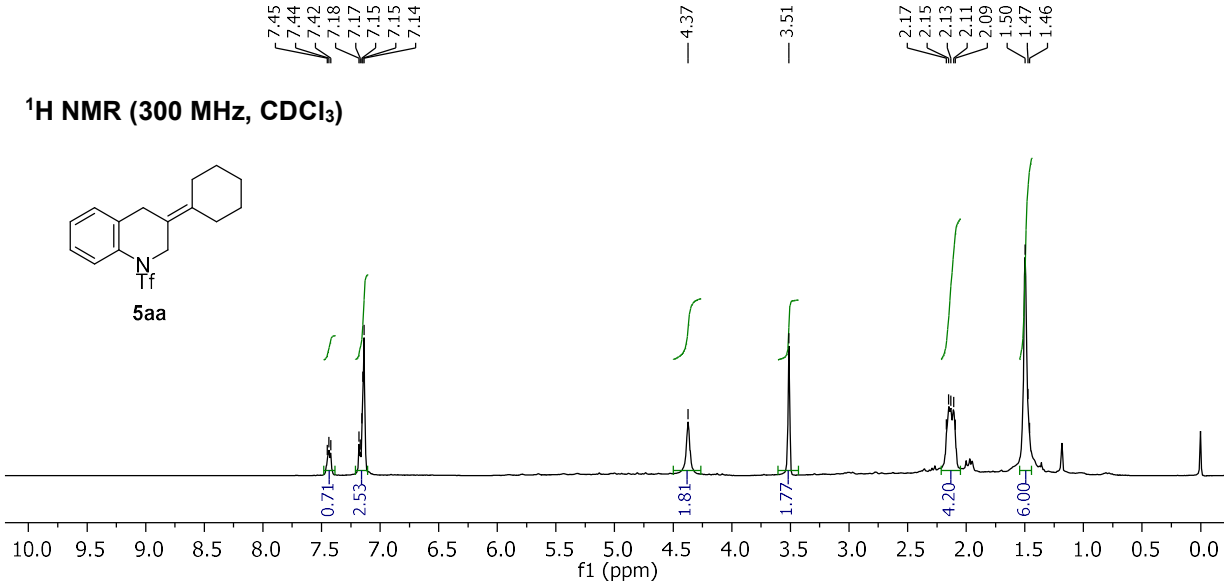

^{1}H NMR (300 MHz, $CDCl_3$)

5aa

DEPT-135

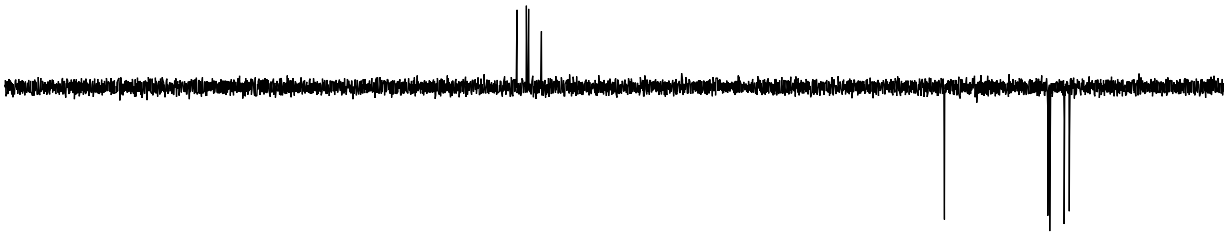

^{13}C NMR (75 MHz, $CDCl_3$)

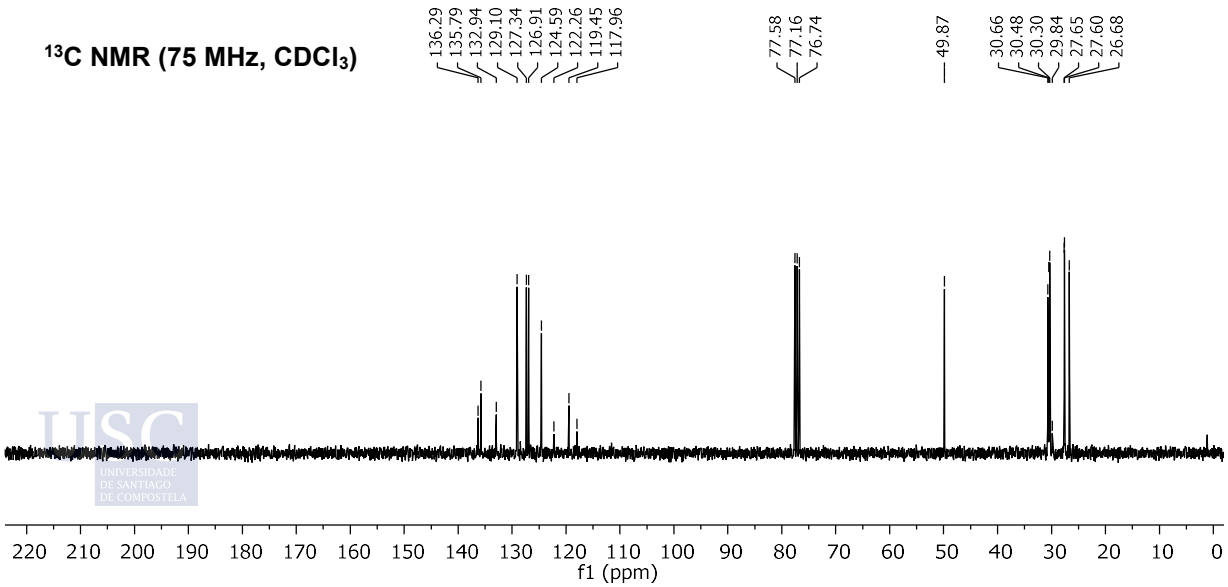

^{1}H NMR (500 MHz, $CDCl_3$)

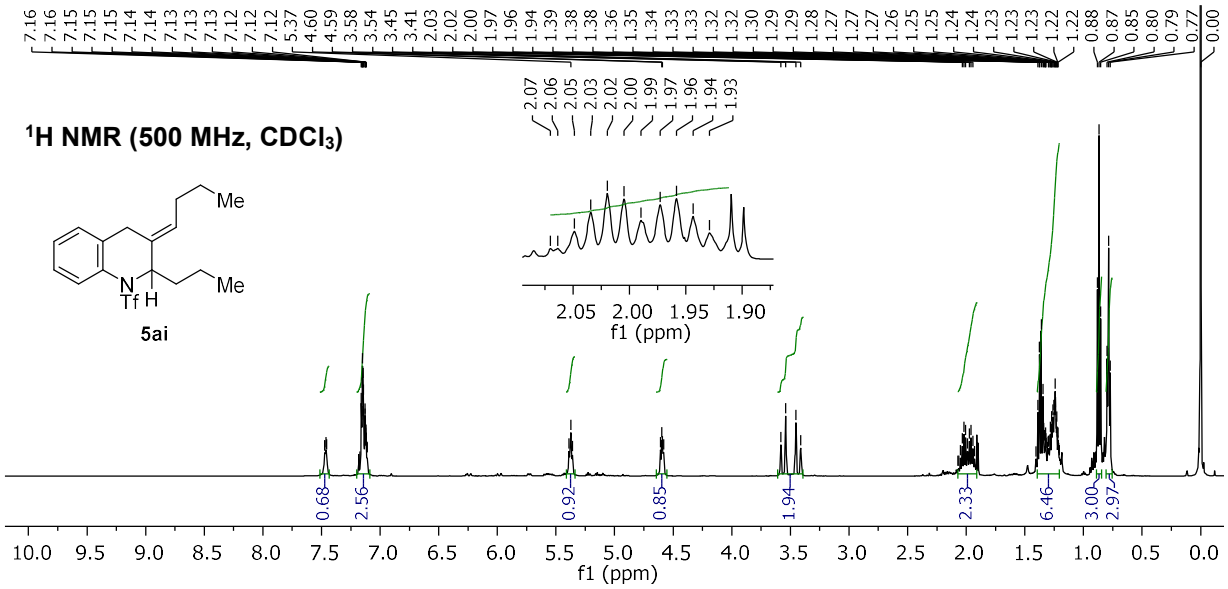

DEPT-135

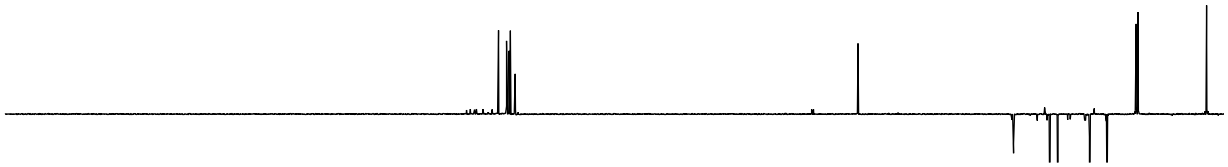

^{13}C NMR (126 MHz, $CDCl_3$)

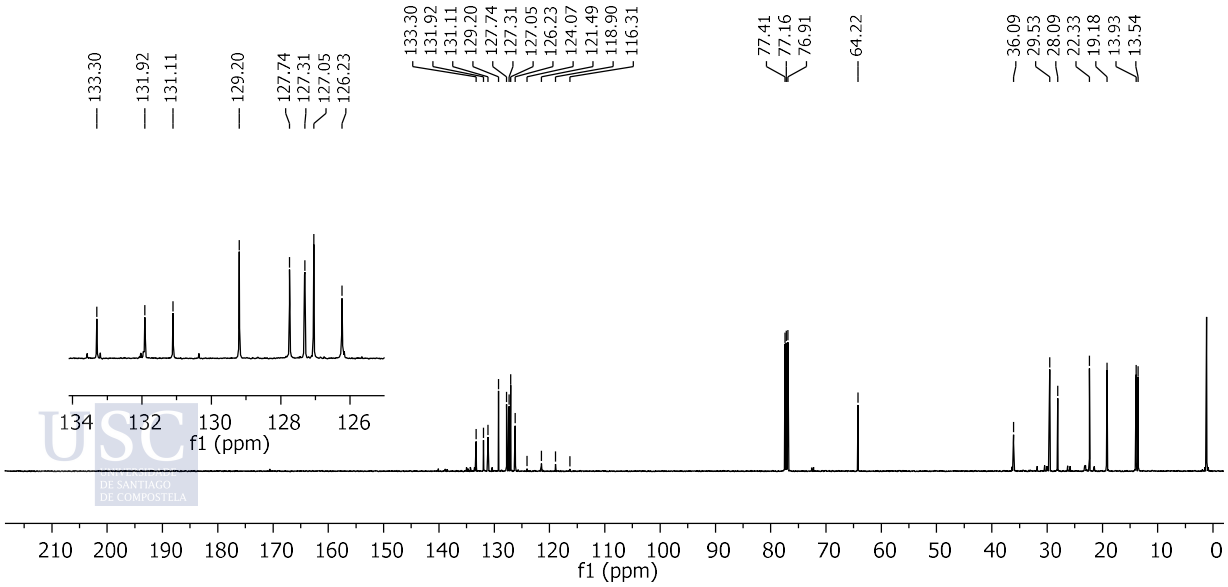

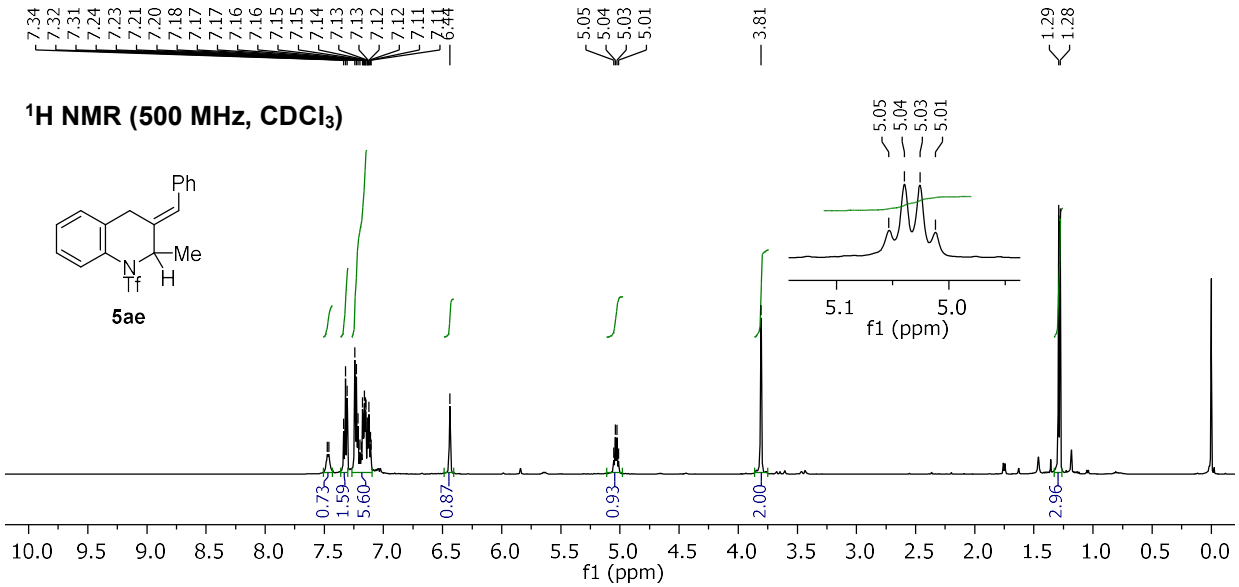

DEPT-135

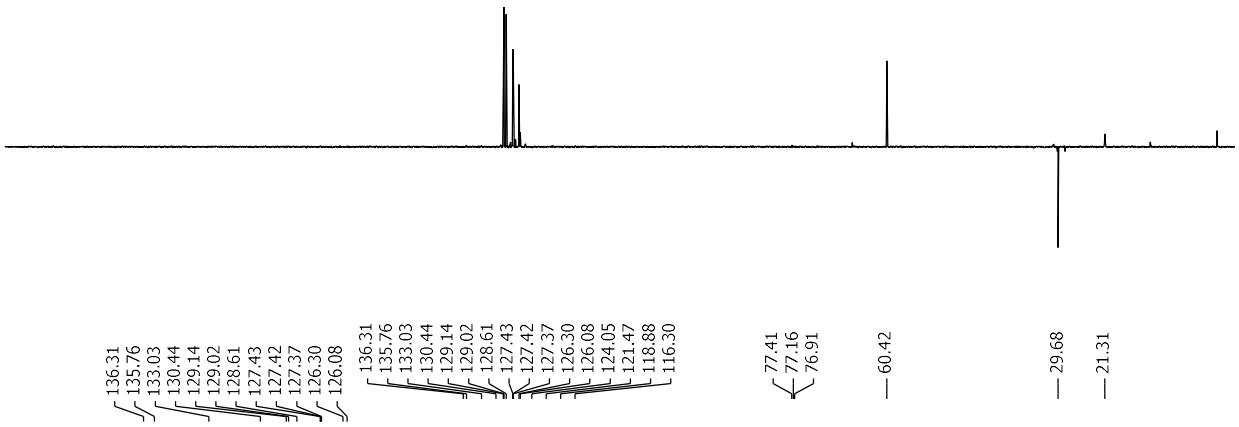

¹³C NMR (126 MHz, CDCl₃)

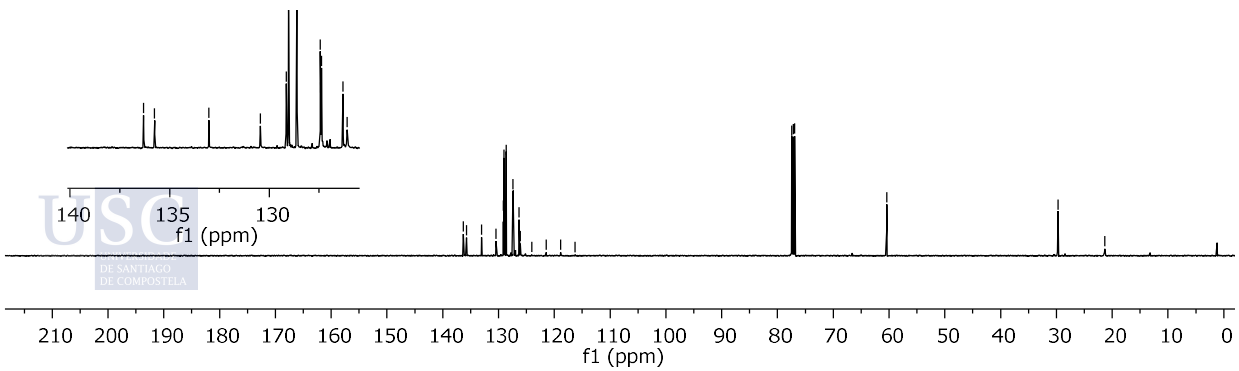

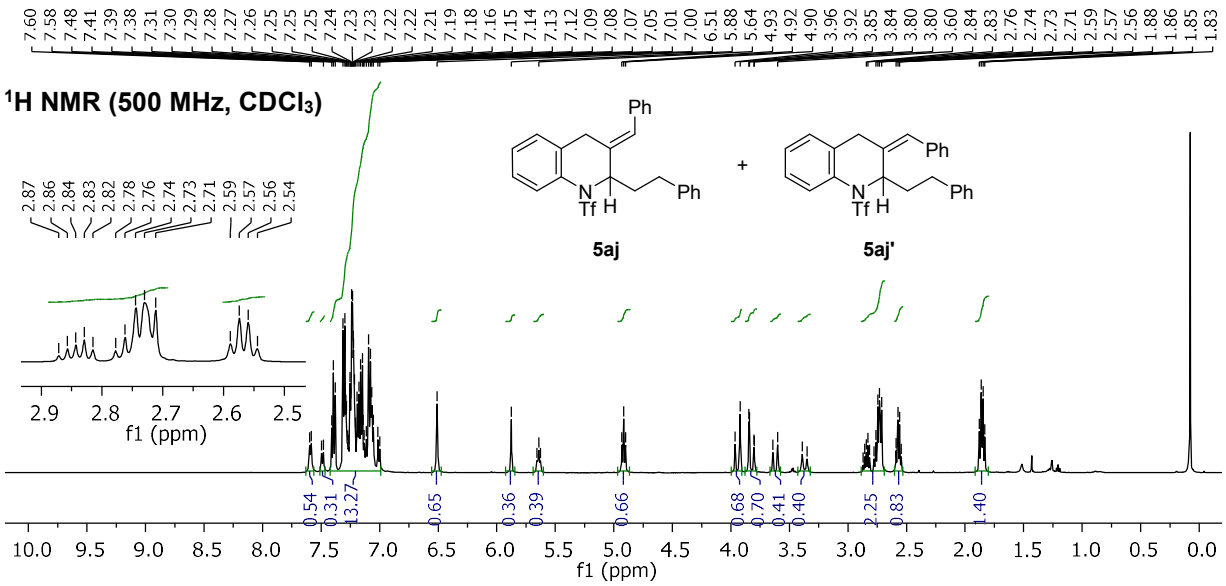

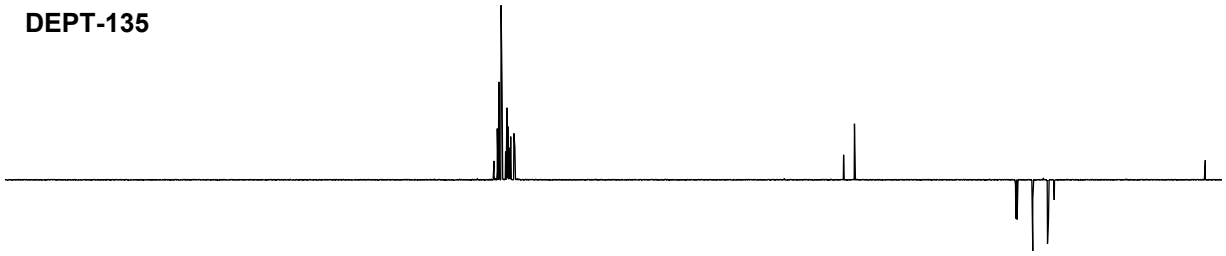

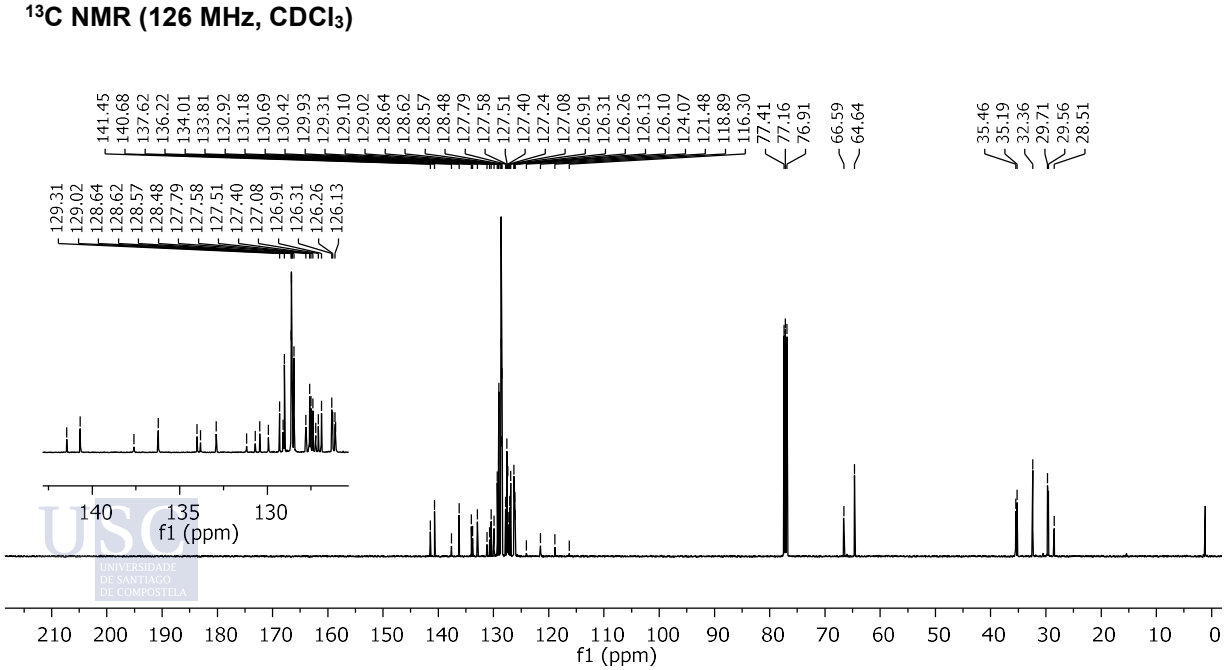

^{1}H NMR (500 MHz, $CDCl_3$)

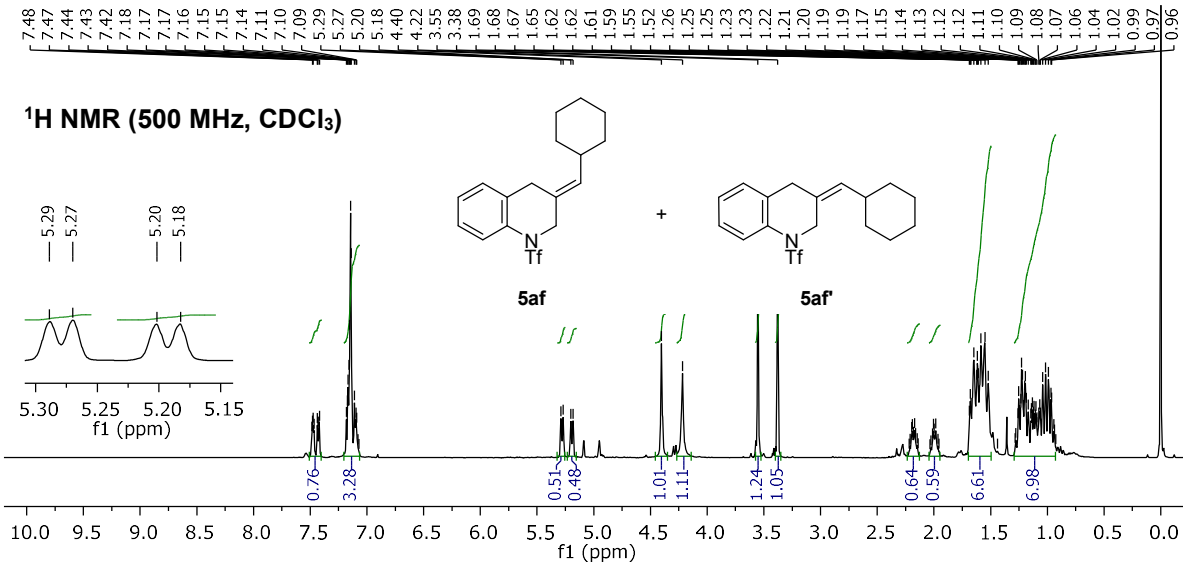

DEPT-135

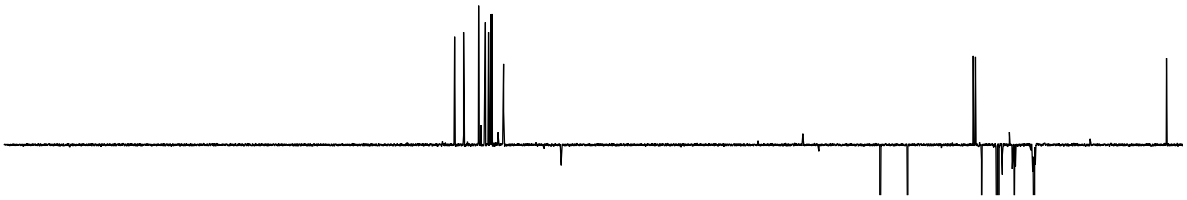

^{13}C NMR (126 MHz, $CDCl_3$)

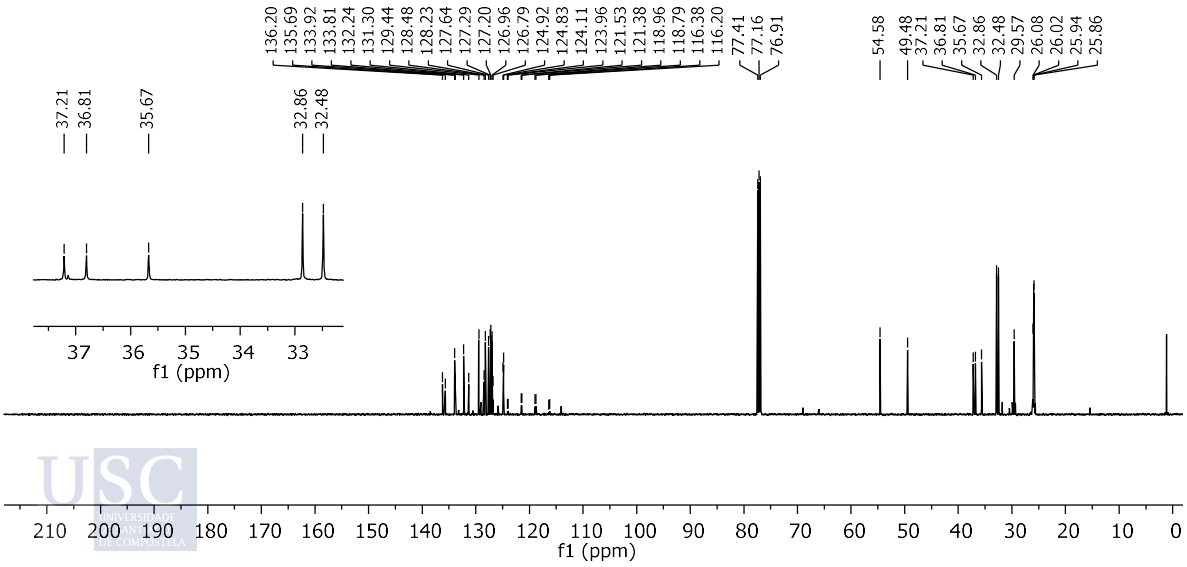

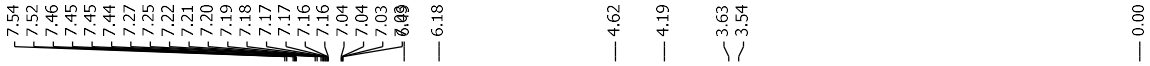

^{1}H NMR (500 MHz, $CDCl_3$)

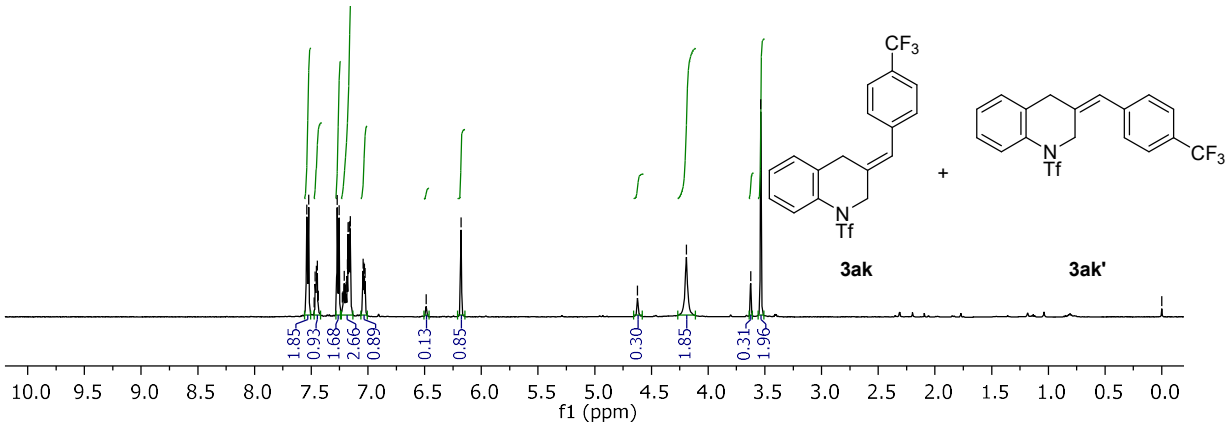

DEPT-135

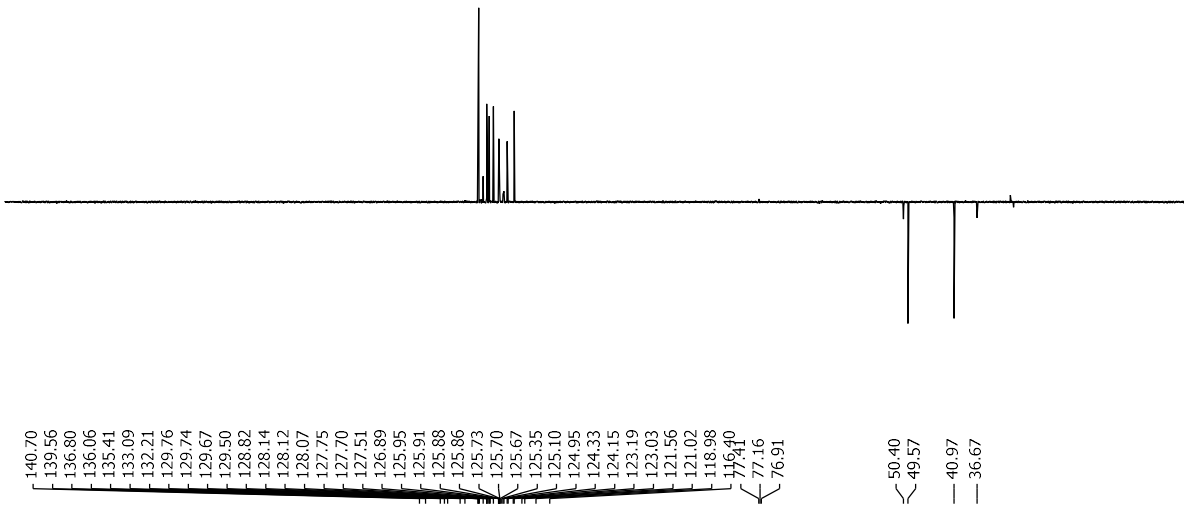

^{13}C NMR (126 MHz, $CDCl_3$)

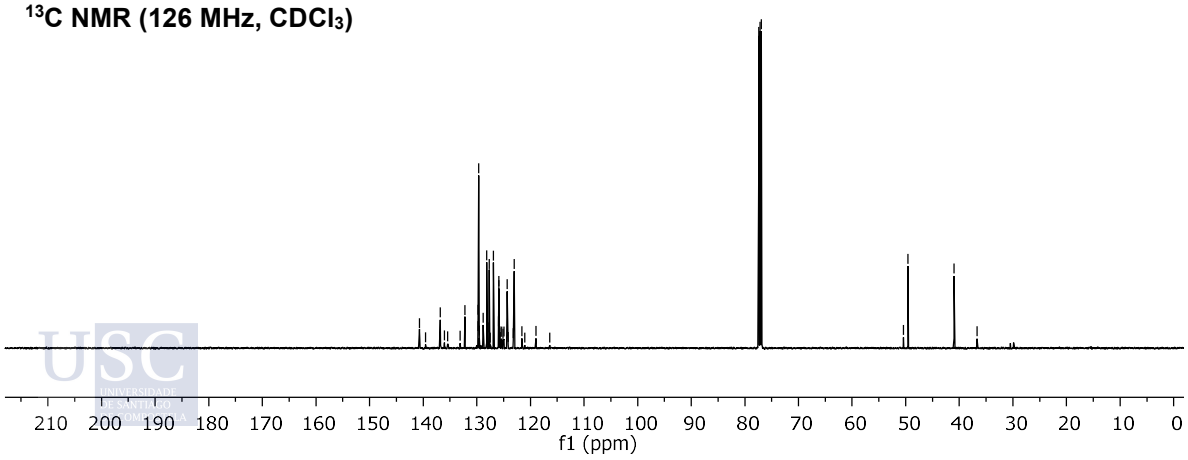

^{1}H NMR (300 MHz, $CDCl_3$)

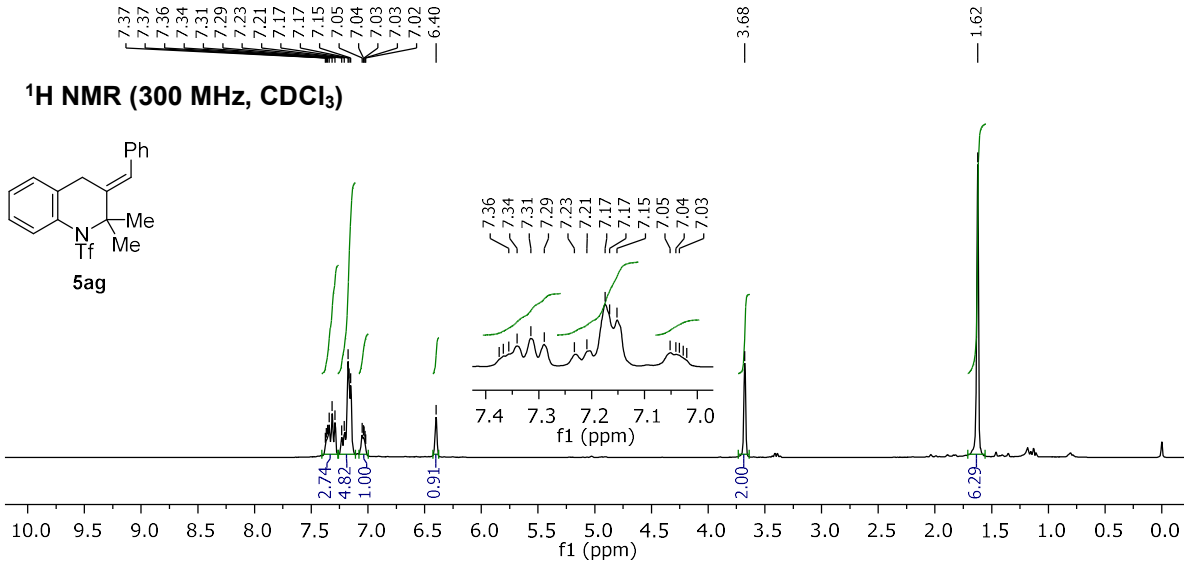

DEPT-135

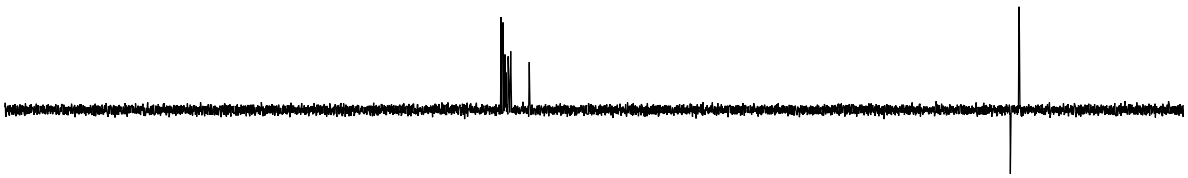

^{13}C NMR (75 MHz, $CDCl_3$)

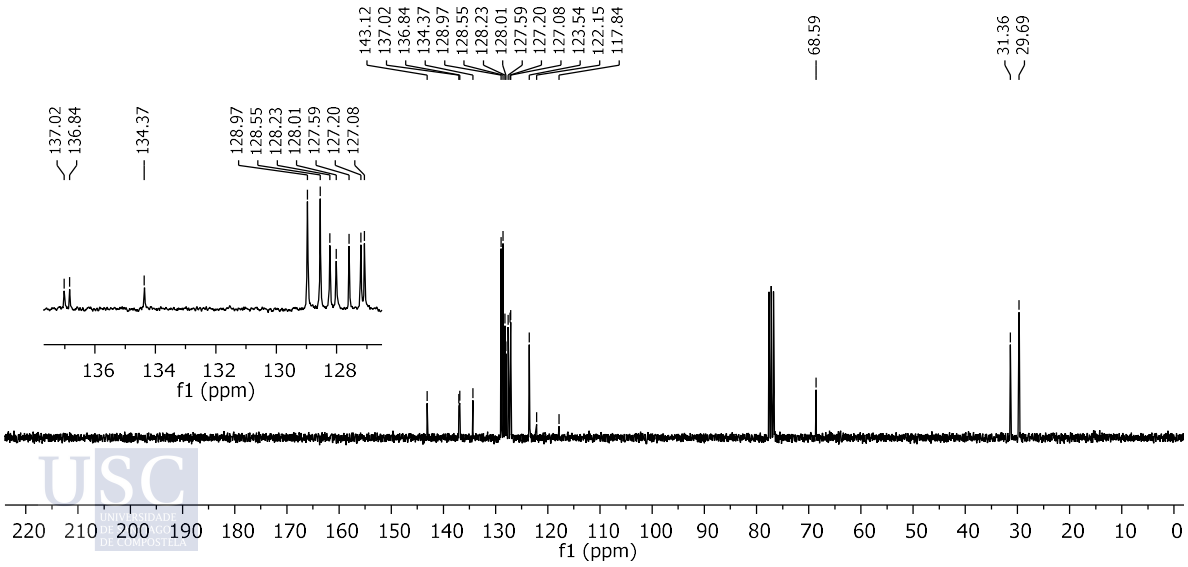

^{1}H NMR (300 MHz, $CDCl_3$)

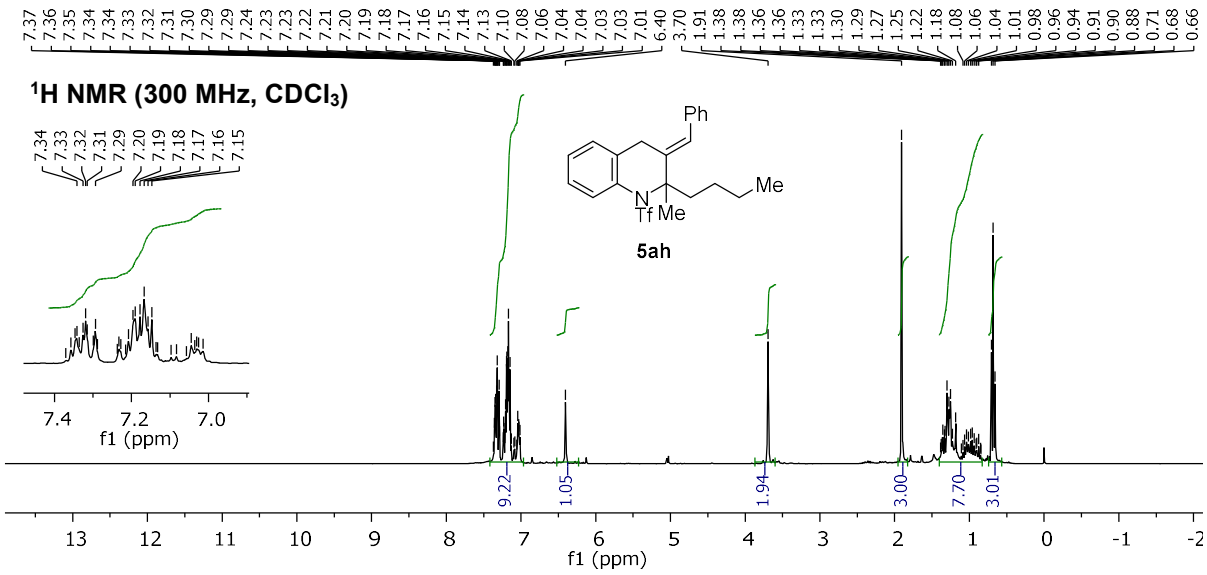

DEPT-135

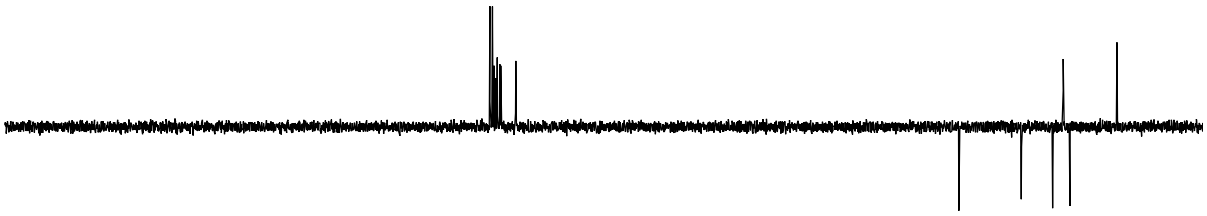

^{13}C NMR (75 MHz, $CDCl_3$)

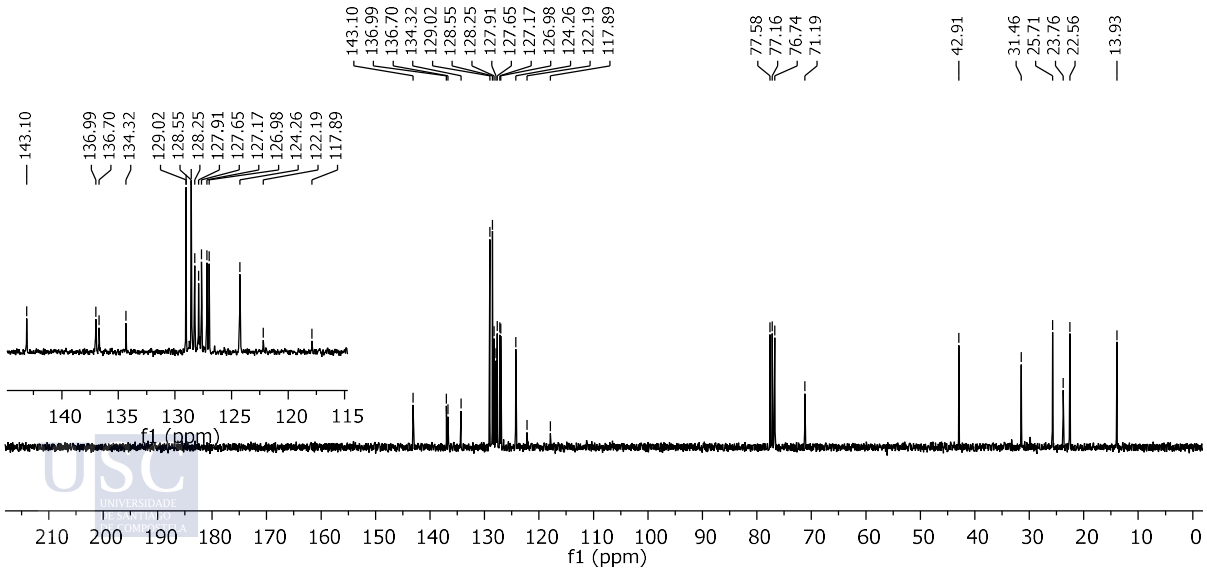

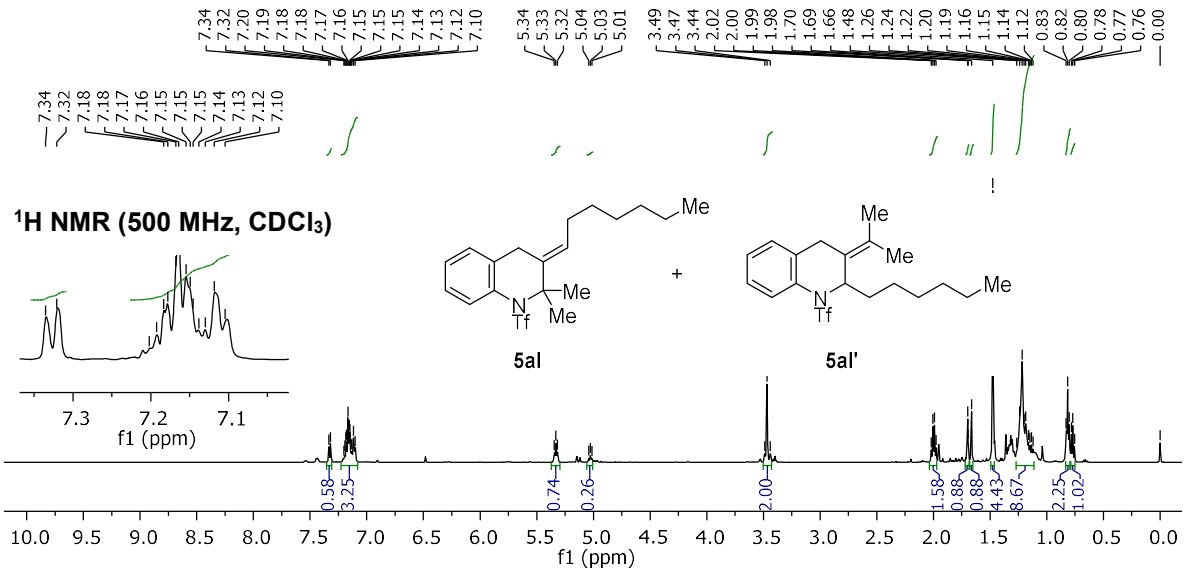
7.34 7.32 7.20 7.19 7.18 7.18 7.17 7.16 7.15 7.15 7.14 7.13 7.12 7.10
5.34 5.33 5.32 5.04 5.03 5.01
3.49 3.47 3.44 2.02 2.00 1.99 1.98 1.70 1.69 1.66 1.48 1.26 1.24 1.22 1.20 1.19 1.16 1.15 1.14 1.12 0.83 0.82 0.80 0.78 0.77 0.76 0.00
7.34 7.32 7.18 7.18 7.17 7.16 7.15 7.15 7.14 7.13 7.12 7.10
¹H NMR (500 MHz, CDCl₃)
Me
Me
N
Tf
Me
+
Me
Me
N
Tf
Me
5al
5al'
7.3 7.2 7.1
f1 (ppm)
0.58 3.25 0.74 0.26 2.00 1.58 0.88 0.88 4.43 8.67 2.25 1.02
10.0 9.5 9.0 8.5 8.0 7.5 7.0 6.5 6.0 5.5 5.0 4.5 4.0 3.5 3.0 2.5 2.0 1.5 1.0 0.5 0.0
f1 (ppm)

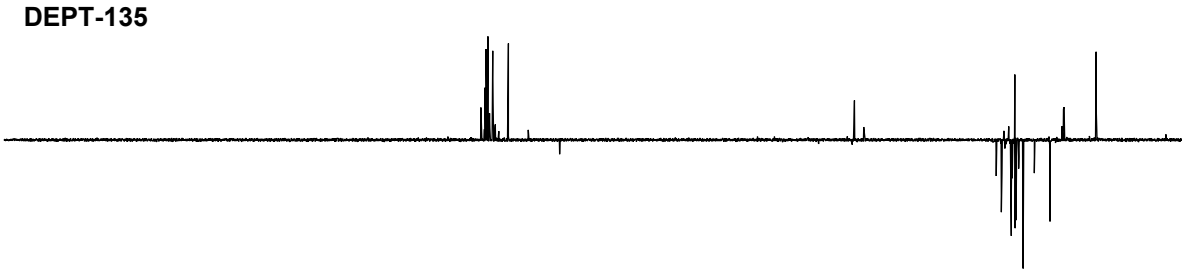
DEPT-135

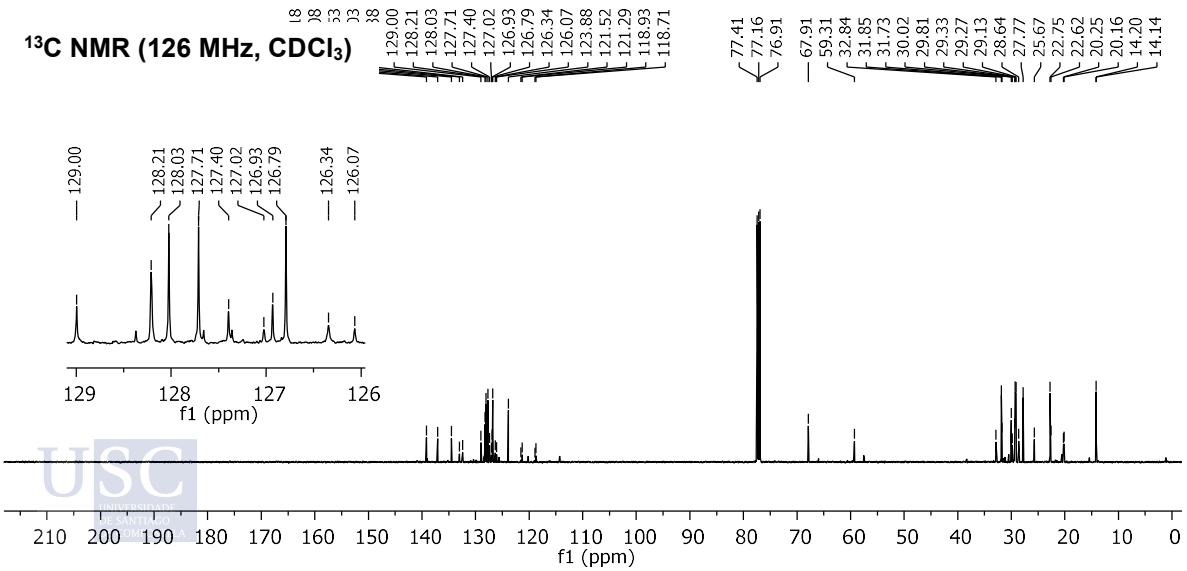
¹³C NMR (126 MHz, CDCl₃)
129.00 128.21 128.03 127.71 127.40 127.02 126.93 126.79 126.34 126.07 123.88 121.52 121.29 118.93 118.71
77.41 77.16 76.91
67.91 59.31 32.84 31.85 31.73 30.02 29.81 29.33 29.27 29.13 28.64 27.77 25.67 22.75 22.62 20.25 20.16 14.20 14.14
129.00 128.21 128.03 127.71 127.40 127.02 126.93 126.79 126.34 126.07
129 128 127 126
f1 (ppm)
210 200 190 180 170 160 150 140 130 120 110 100 90 80 70 60 50 40 30 20 10 0
f1 (ppm)

HSQC spectrum ($CDCl_3$)

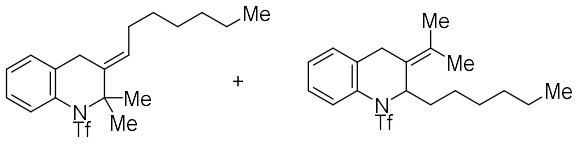

5al **5al'**

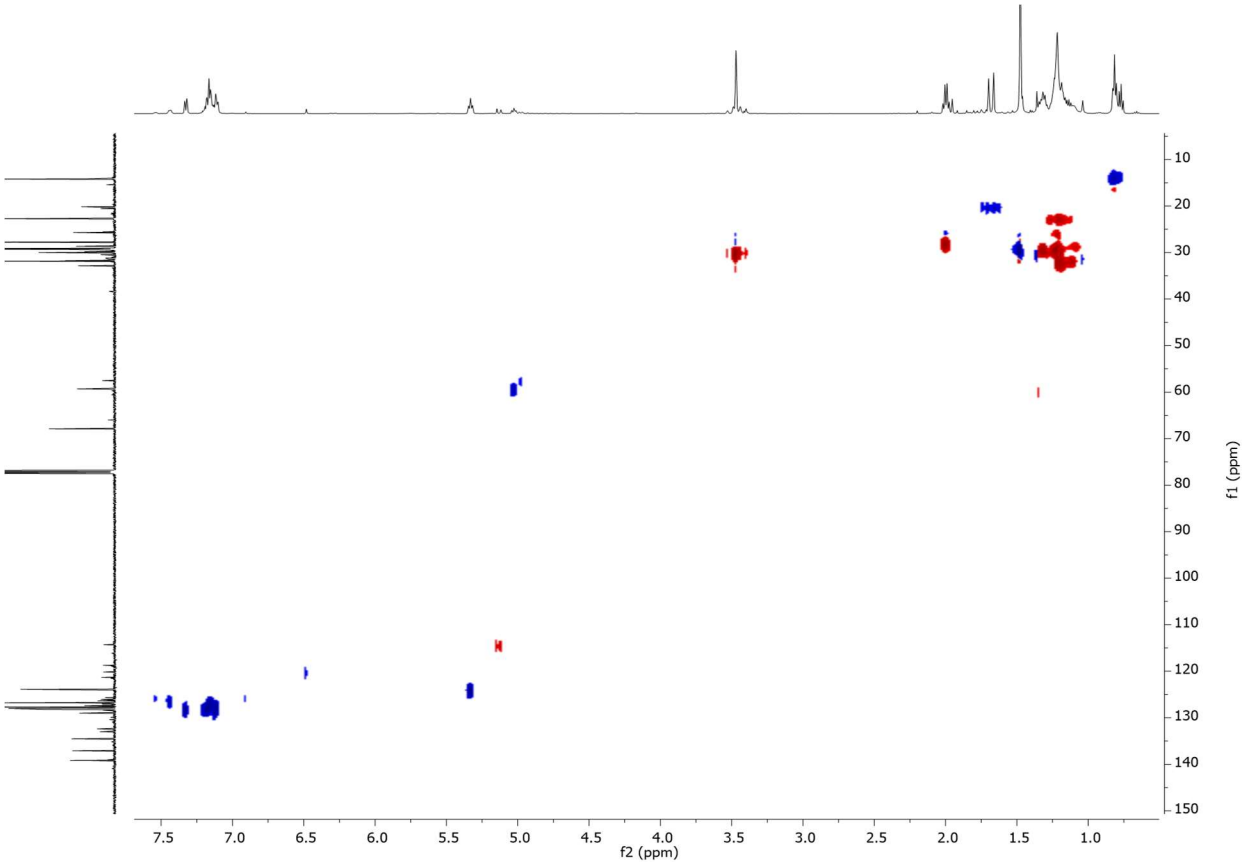

^{1}H NMR (300 MHz, $CDCl_3$)

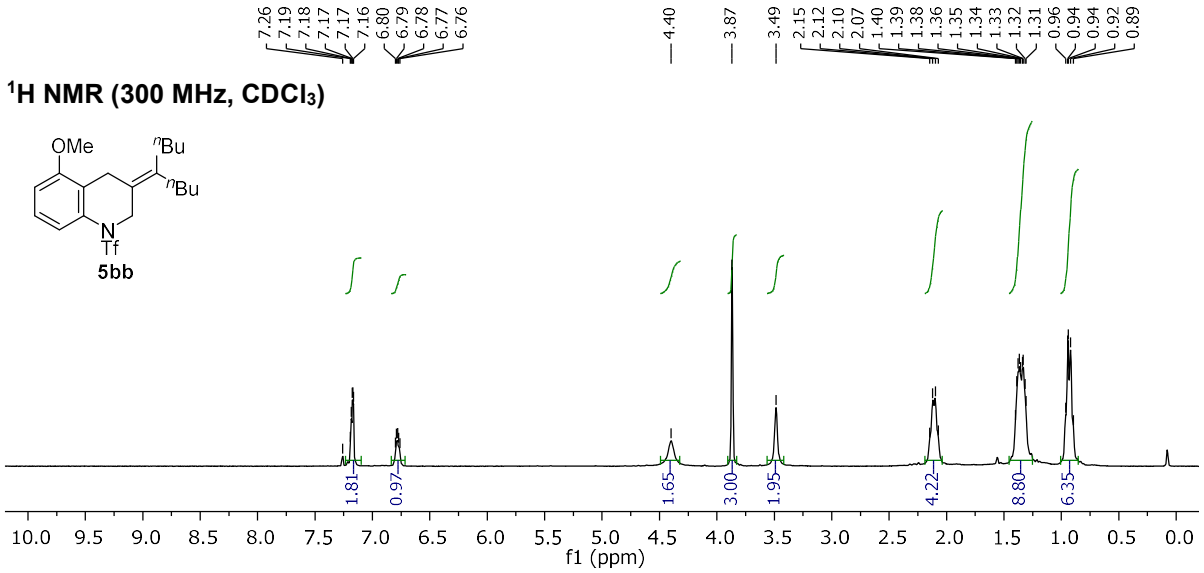

DEPT-135

^{13}C NMR (75 MHz, $CDCl_3$)

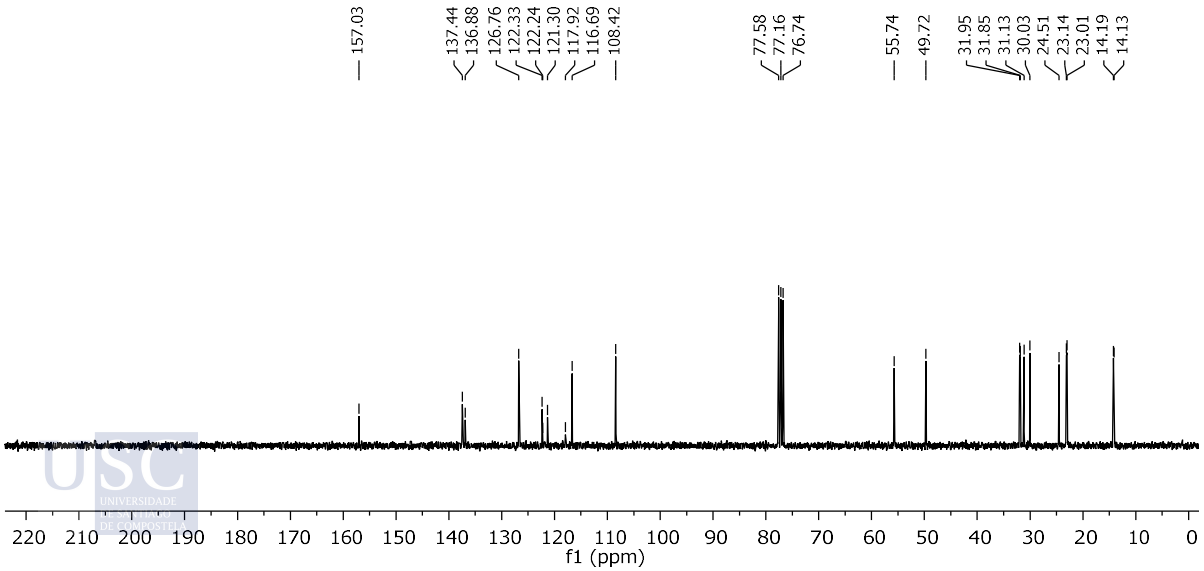

^{1}H NMR (500 MHz, $CDCl_3$)

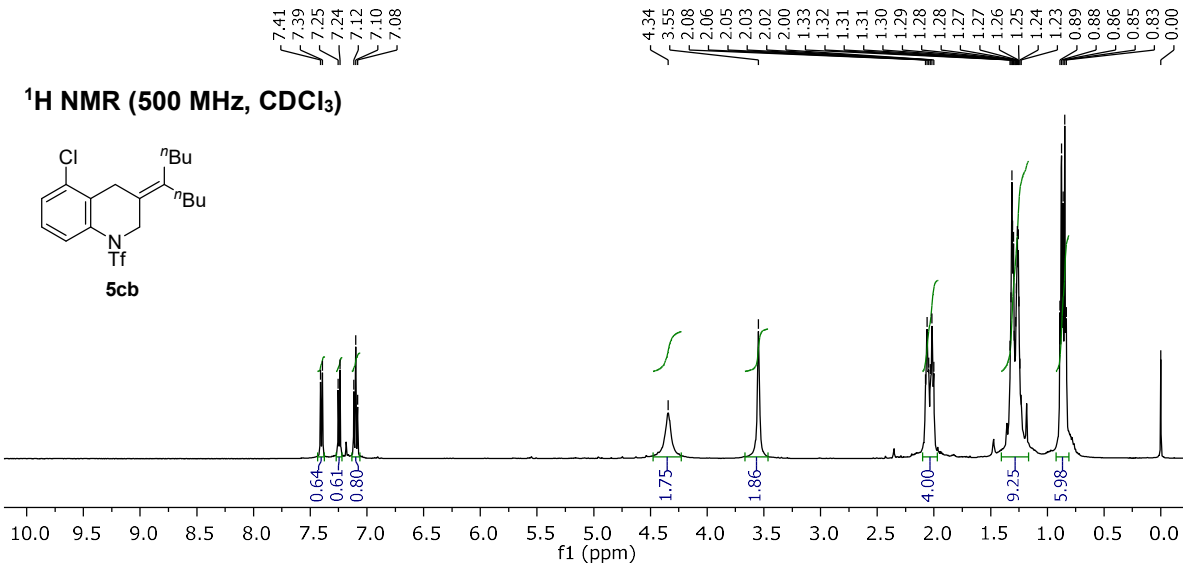

DEPT-135

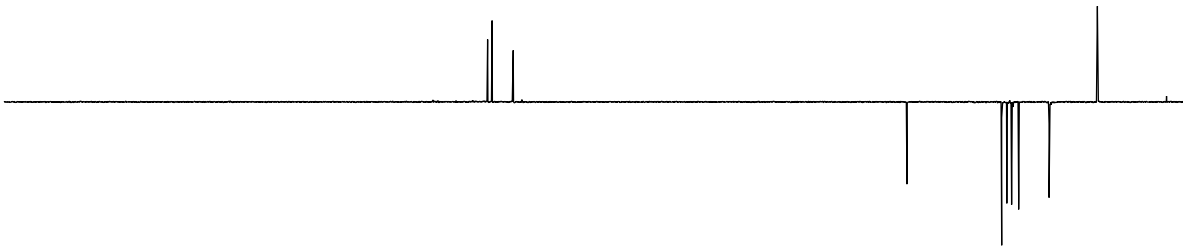

^{13}C NMR (126 MHz, $CDCl_3$)

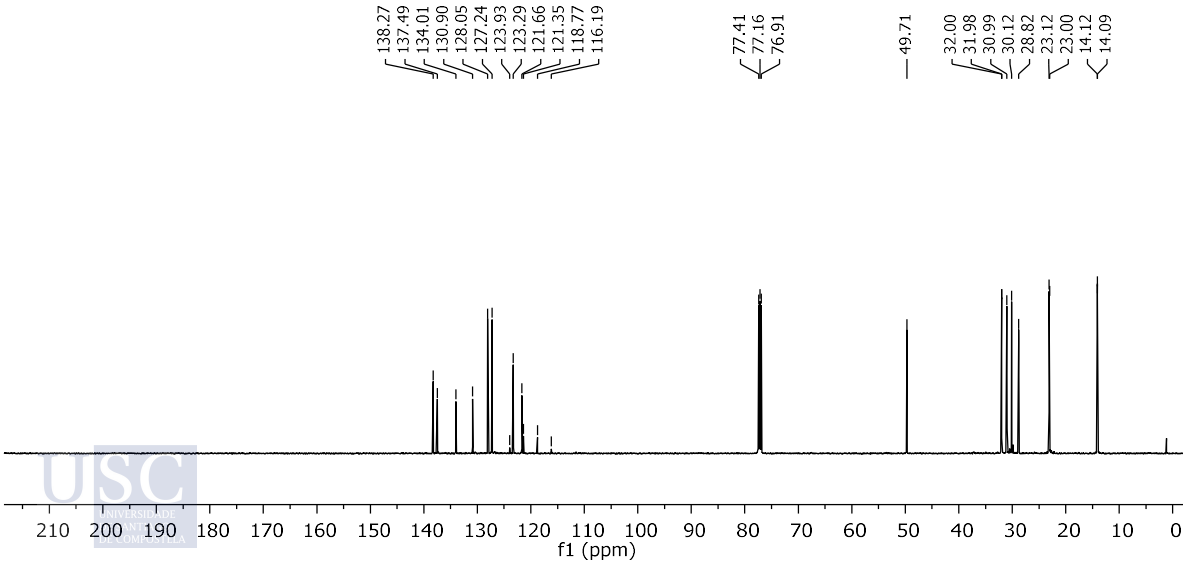

^{1}H NMR (500 MHz, $CDCl_3$)

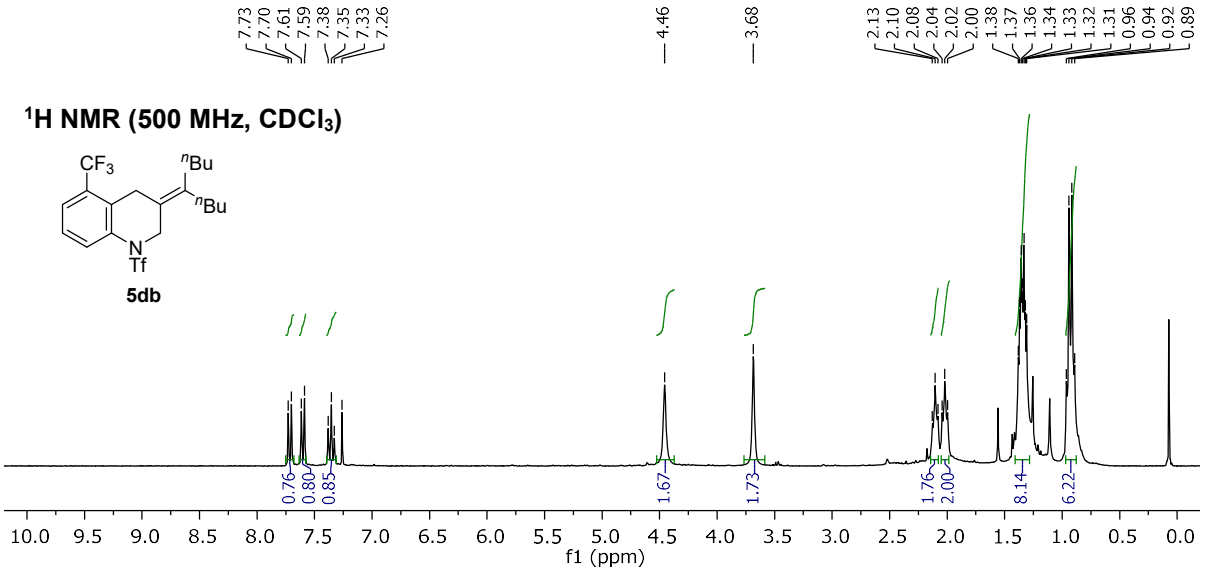

DEPT-135

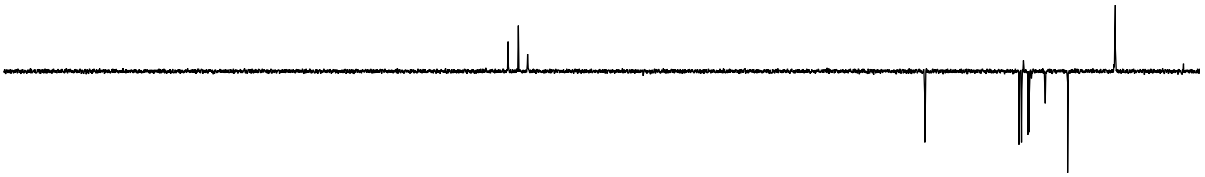

^{13}C NMR (126 MHz, $CDCl_3$)

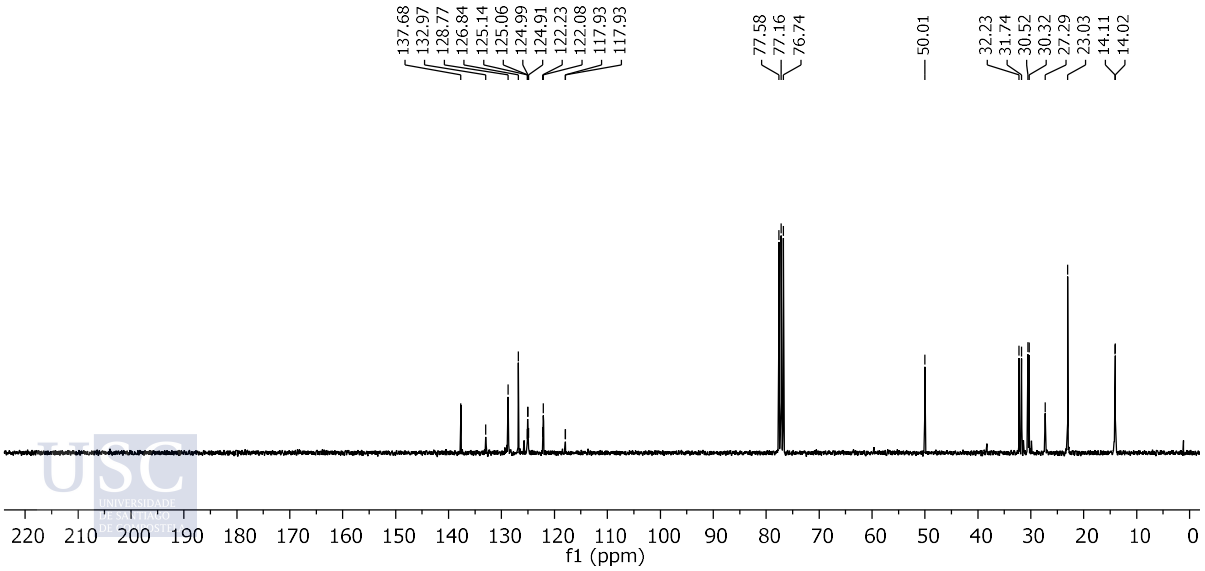

^{1}H NMR (300 MHz, $CDCl_3$)

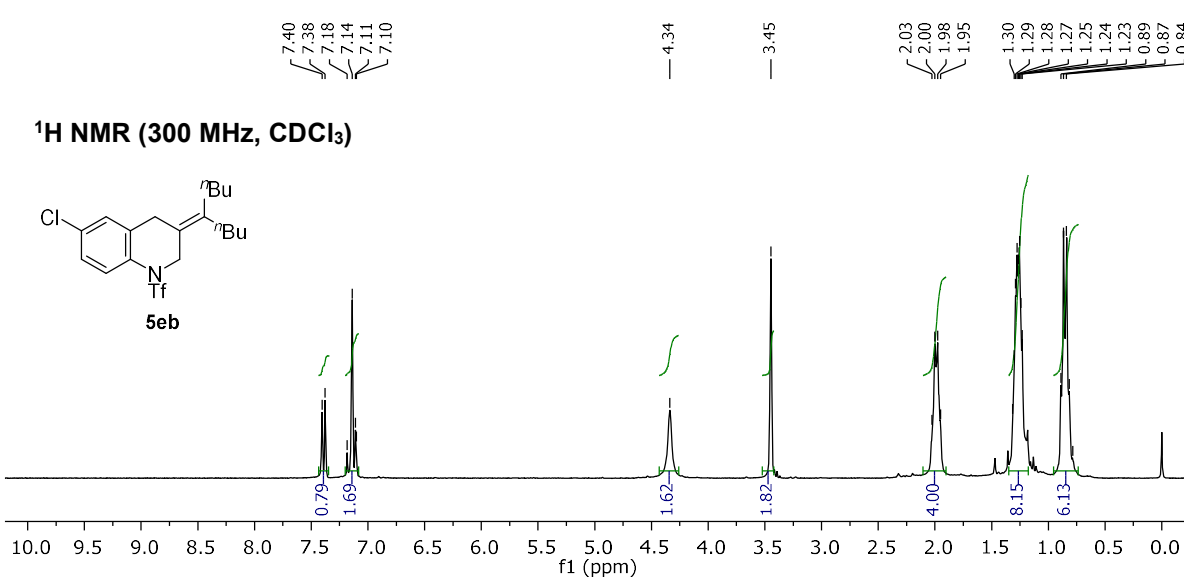

DEPT-135

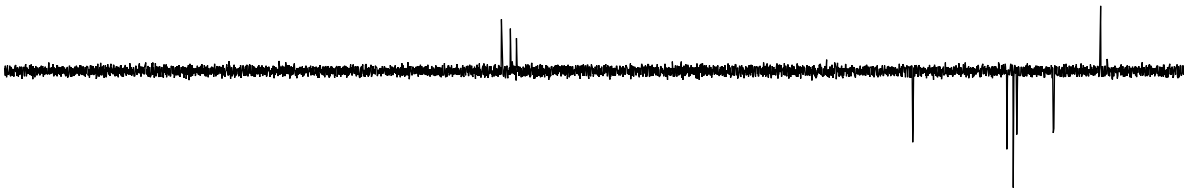

^{13}C NMR (75 MHz, $CDCl_3$)

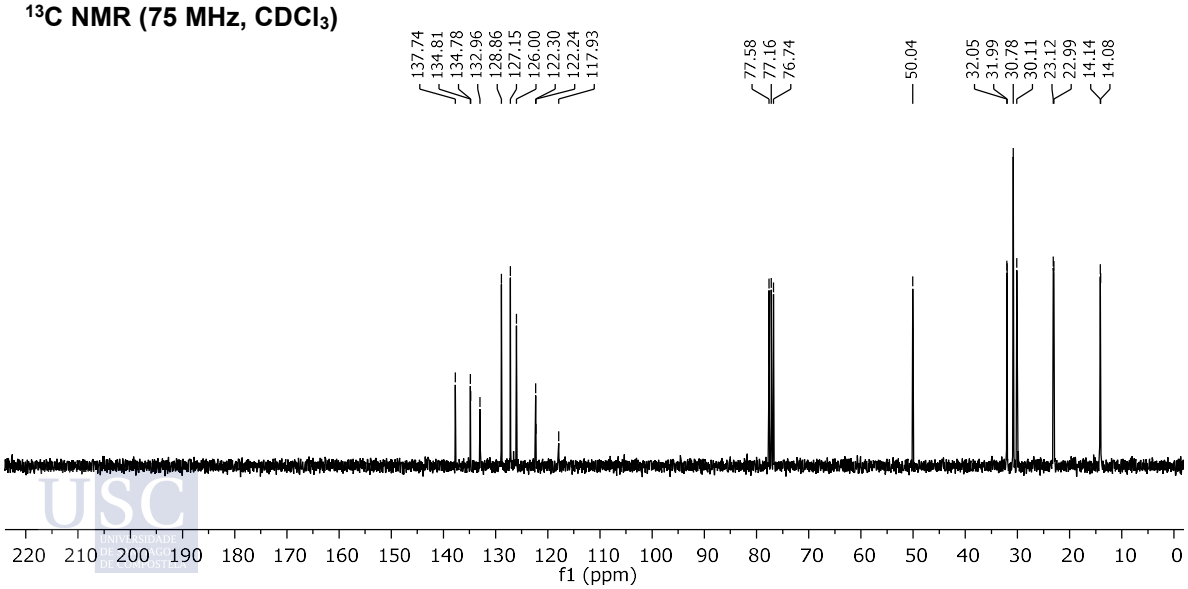

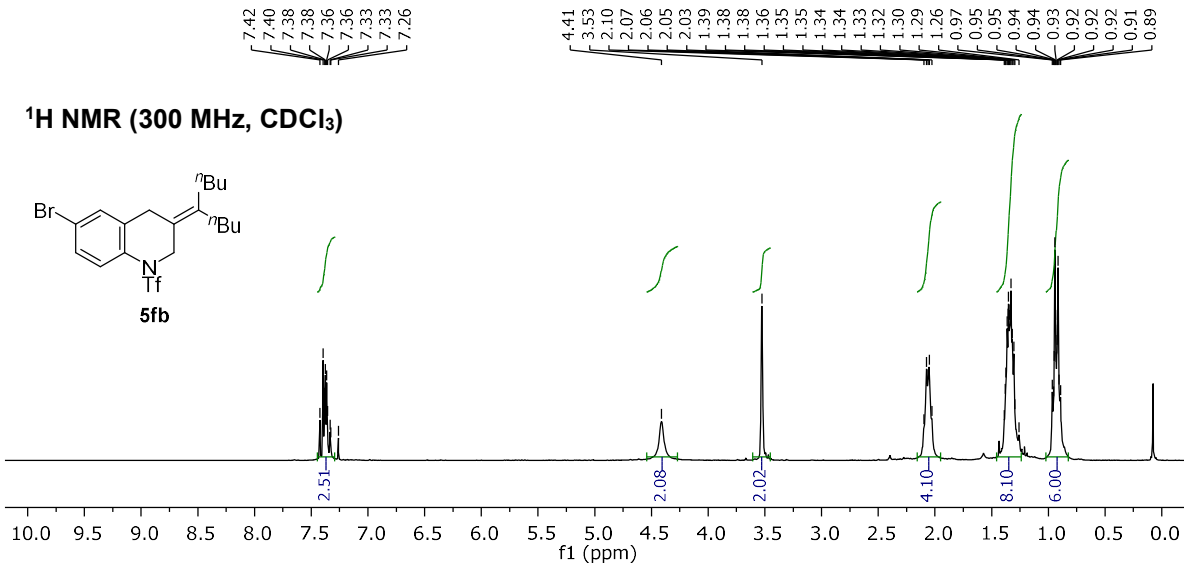

DEPT-135

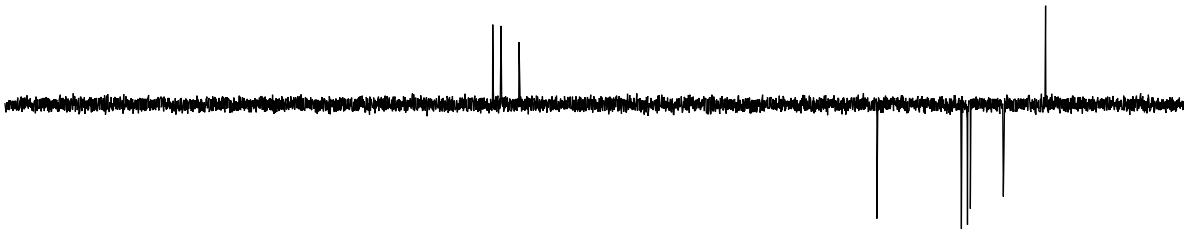

^{13}C NMR (75 MHz, $CDCl_3$)

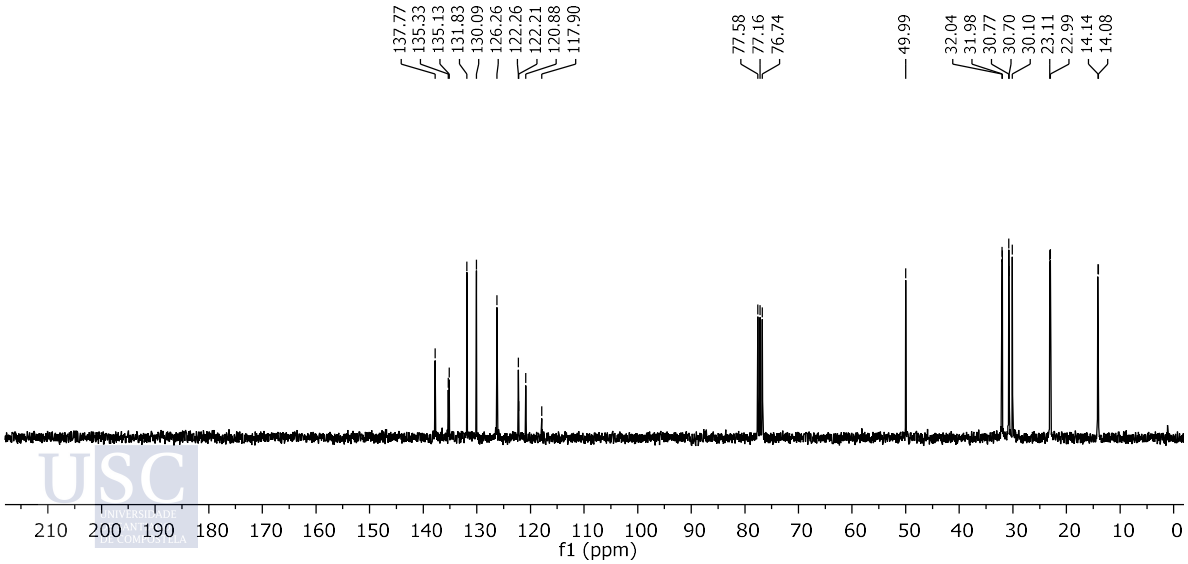

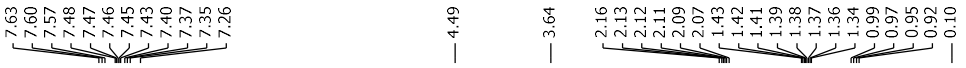

^{1}H NMR (300 MHz, $CDCl_3$)

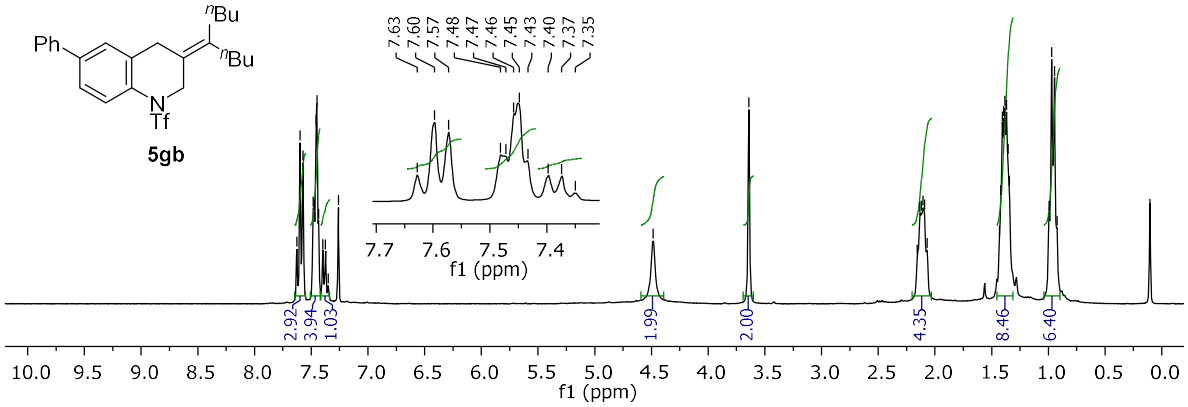

DEPT-135

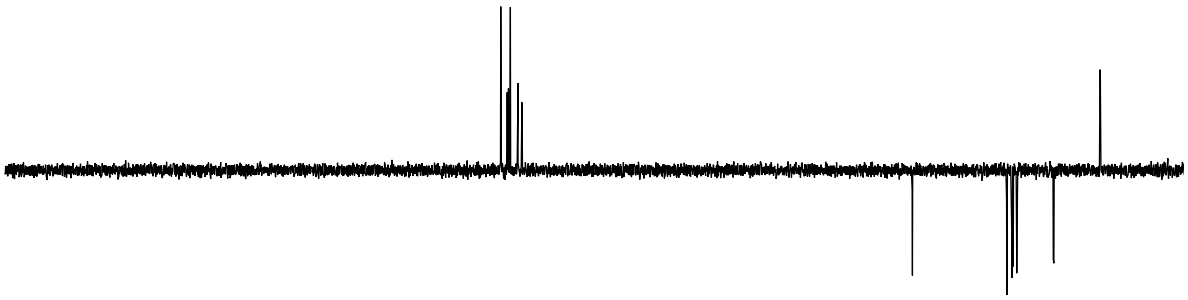

^{13}C NMR (75 MHz, $CDCl_3$)

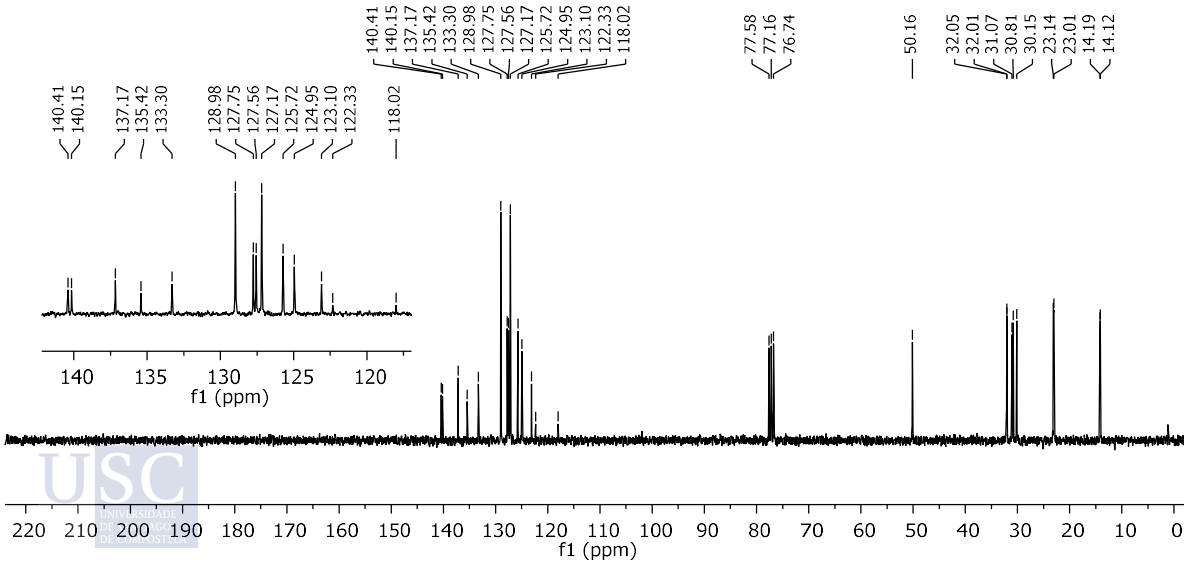

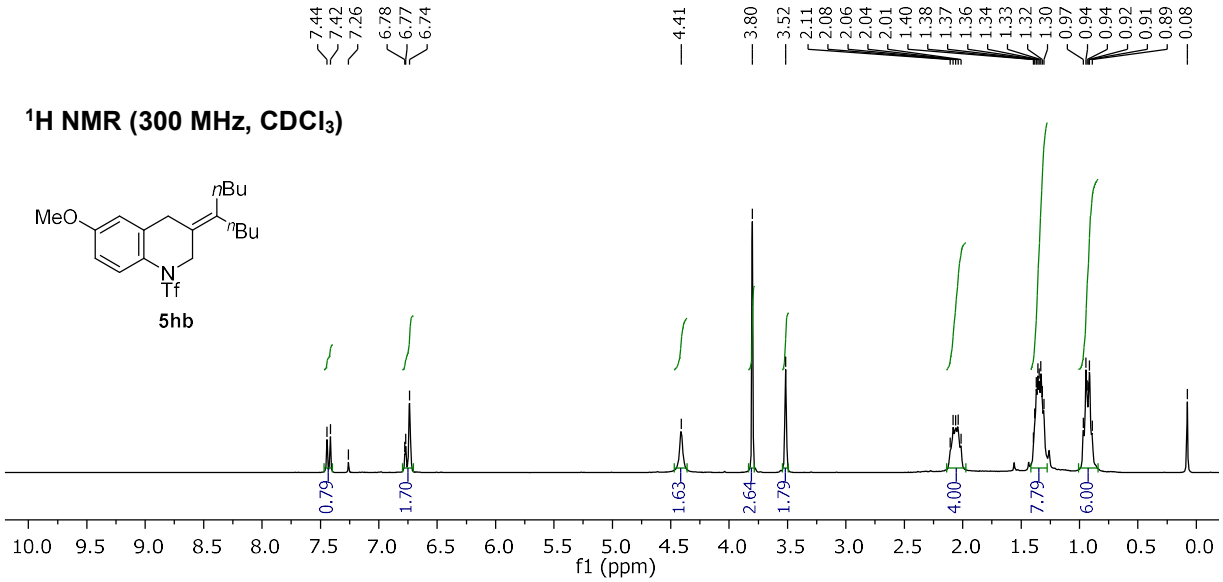

DEPT-135

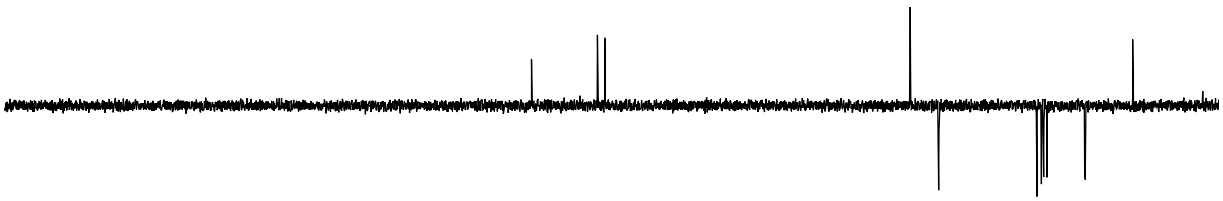

^{13}C NMR (75 MHz, $CDCl_3$)

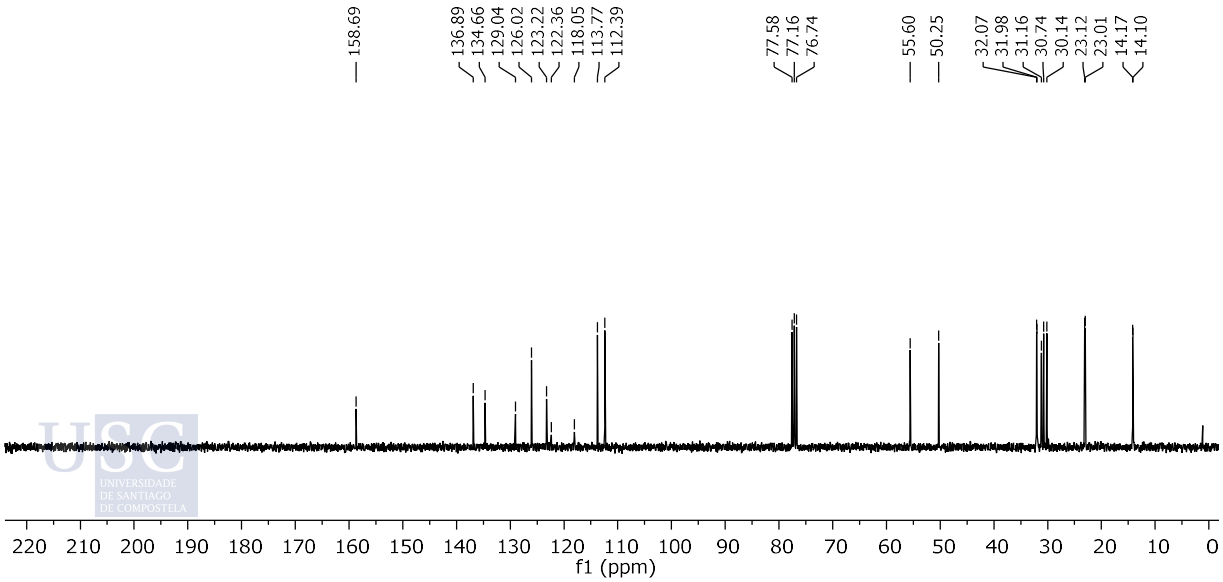

^{1}H NMR (300 MHz, $CDCl_3$)

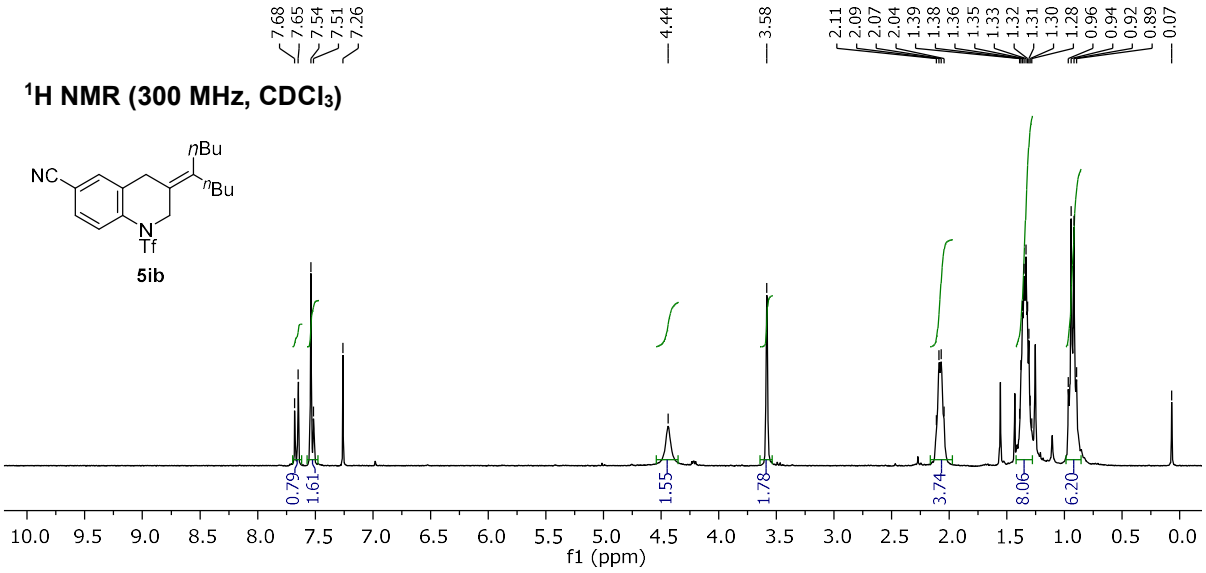

DEPT-135

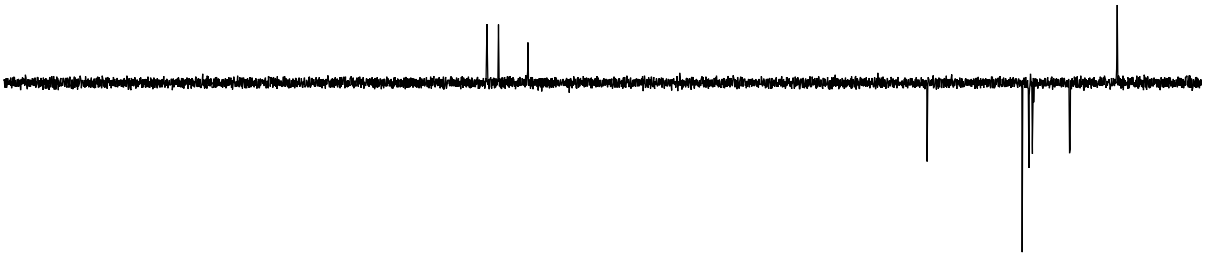

^{13}C NMR (75 MHz, $CDCl_3$)

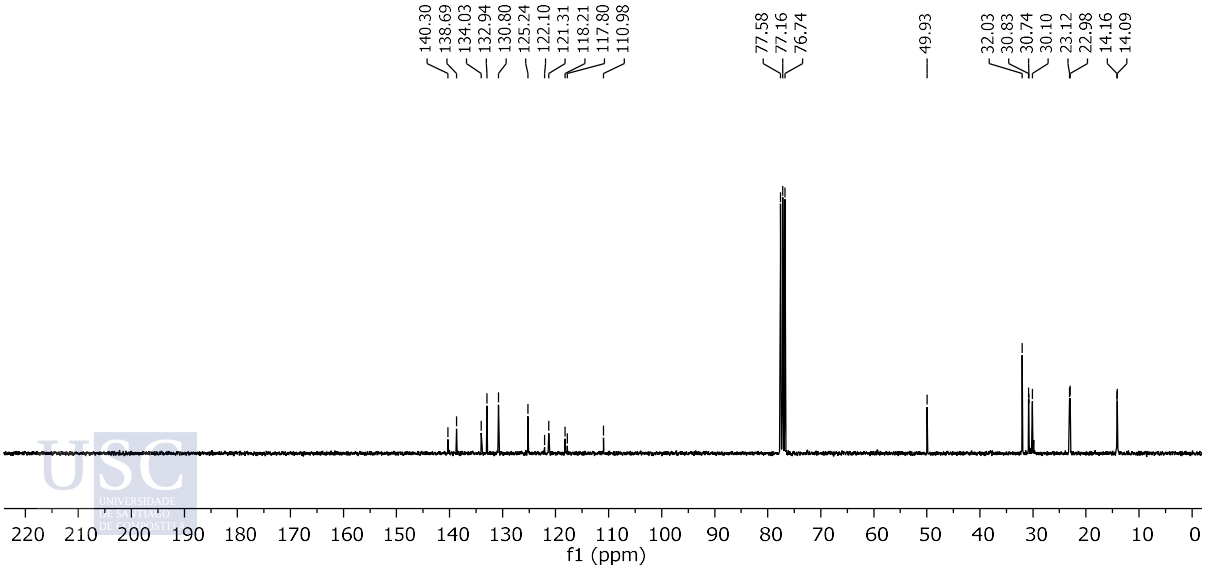

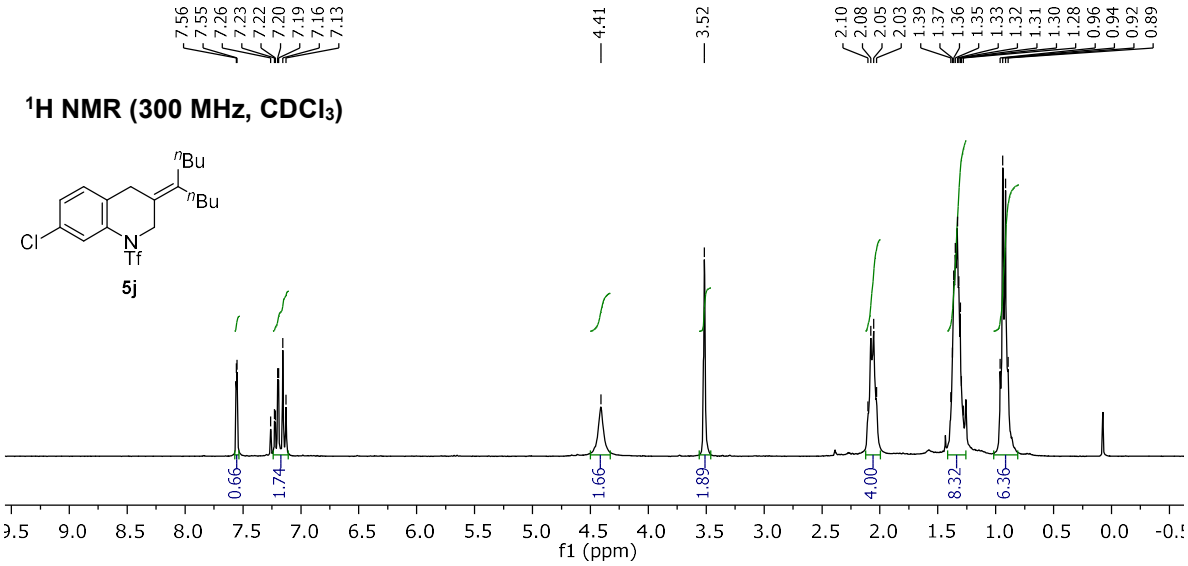

^{1}H NMR (300 MHz, $CDCl_3$)

5j

DEPT-135

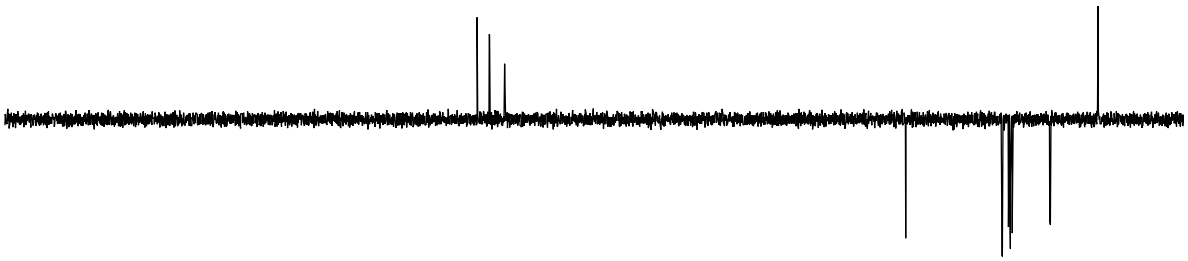

^{13}C NMR (75 MHz, $CDCl_3$)

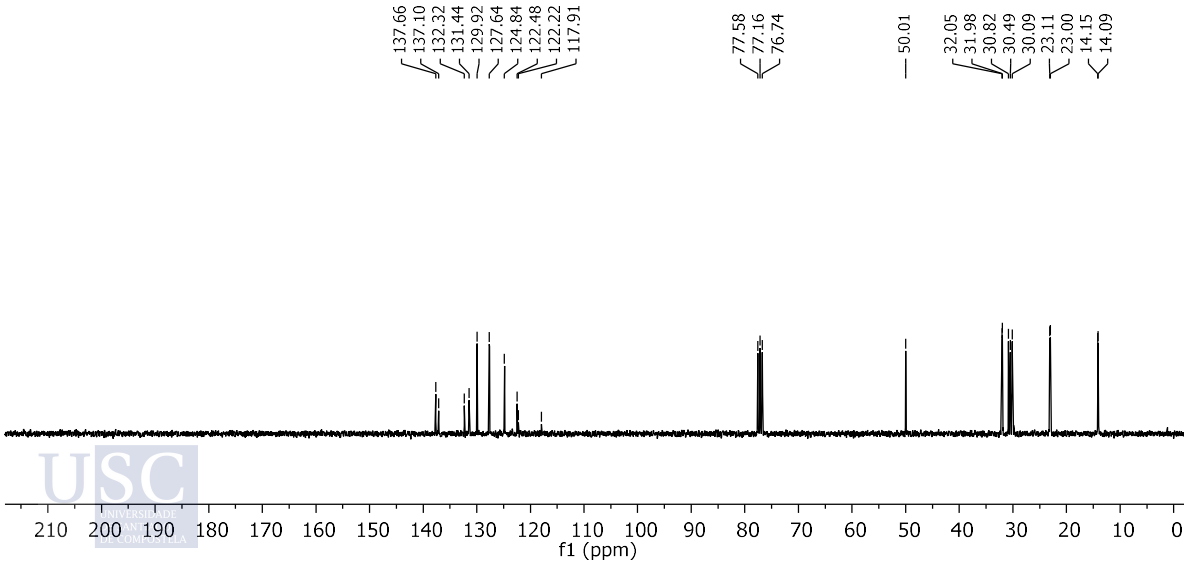

^{1}H NMR (500 MHz, $CDCl_3$)

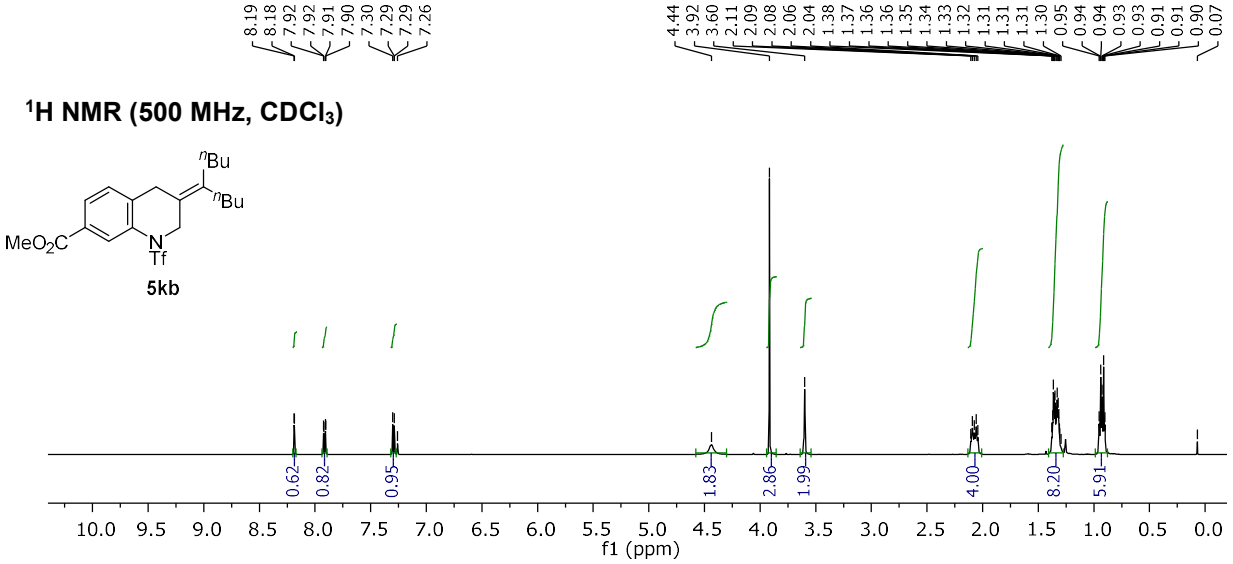

DEPT-135

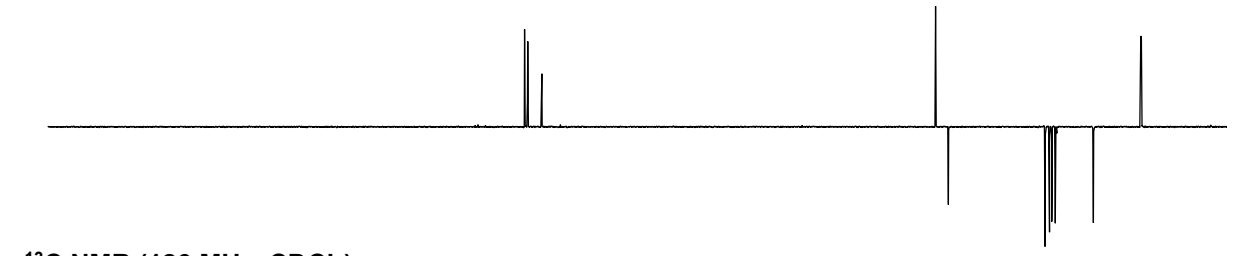

^{13}C NMR (126 MHz, $CDCl_3$)

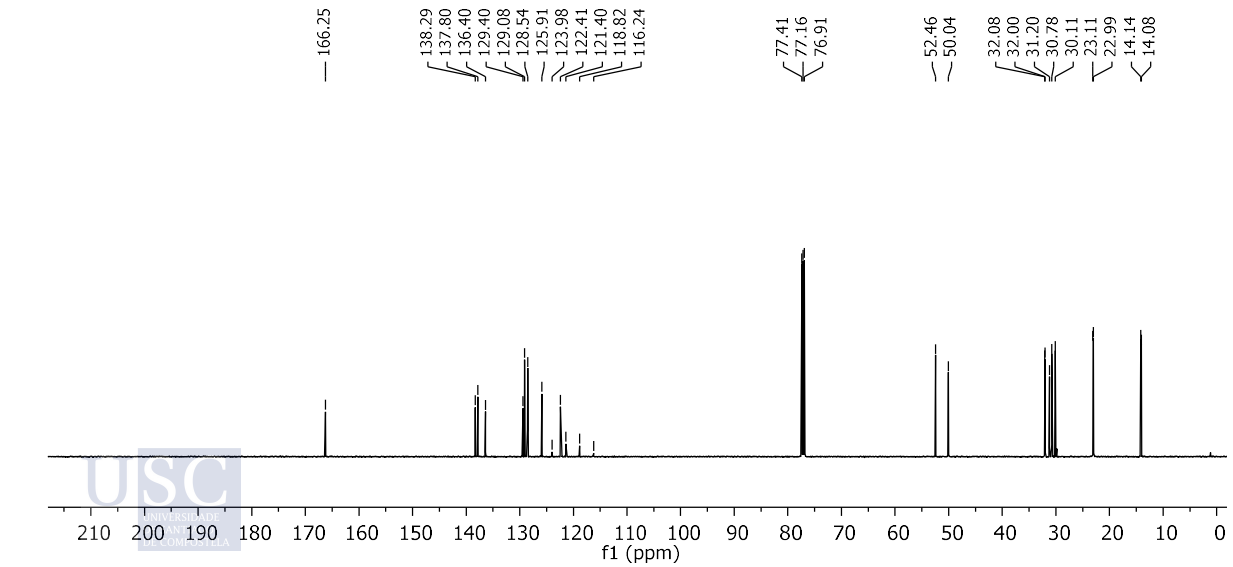

^{1}H NMR (500 MHz, $CDCl_3$)

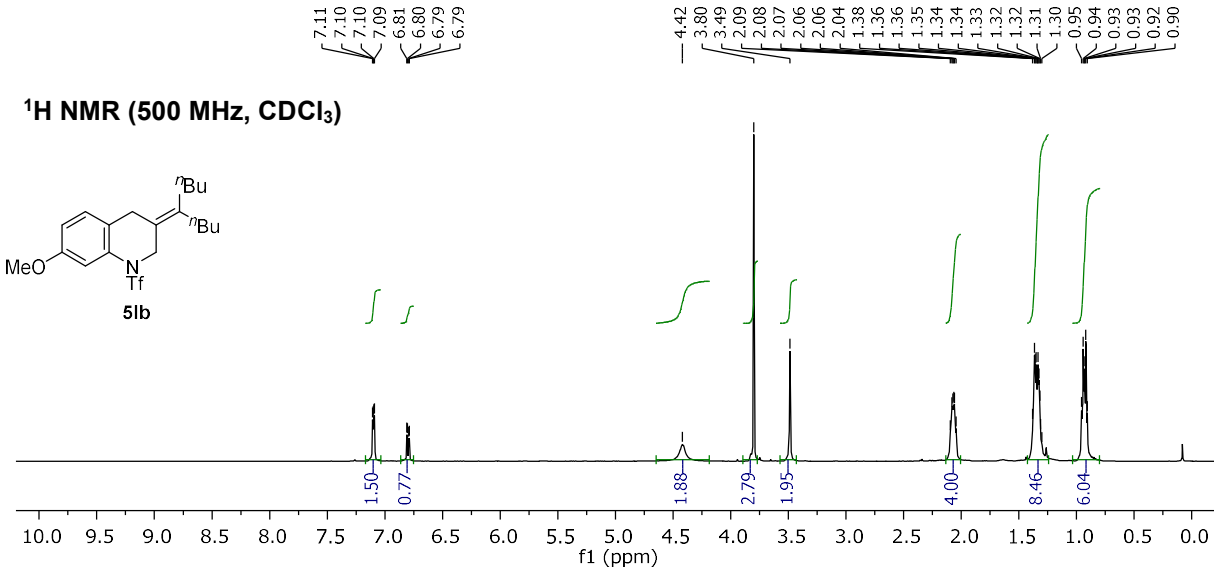

DEPT-135

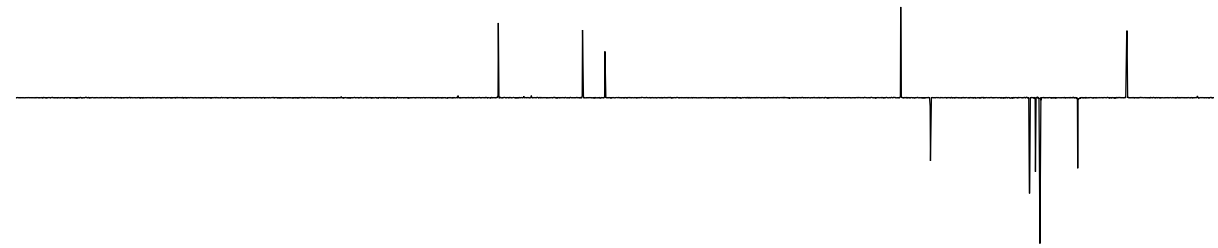

^{13}C NMR (126 MHz, $CDCl_3$)

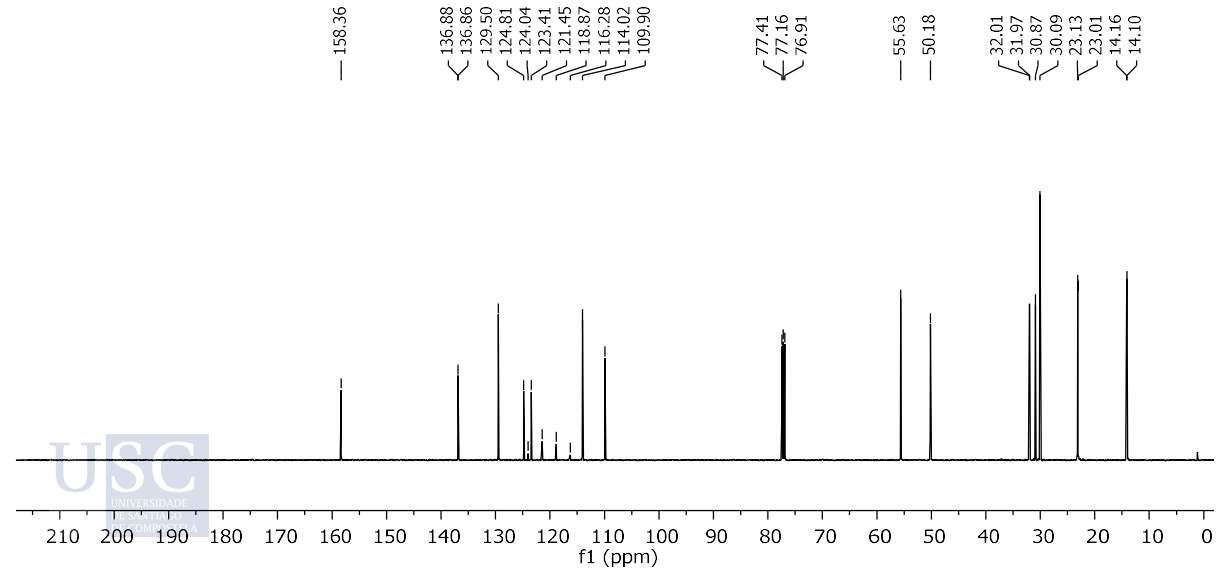

^{1}H NMR (300 MHz, $CDCl_3$)

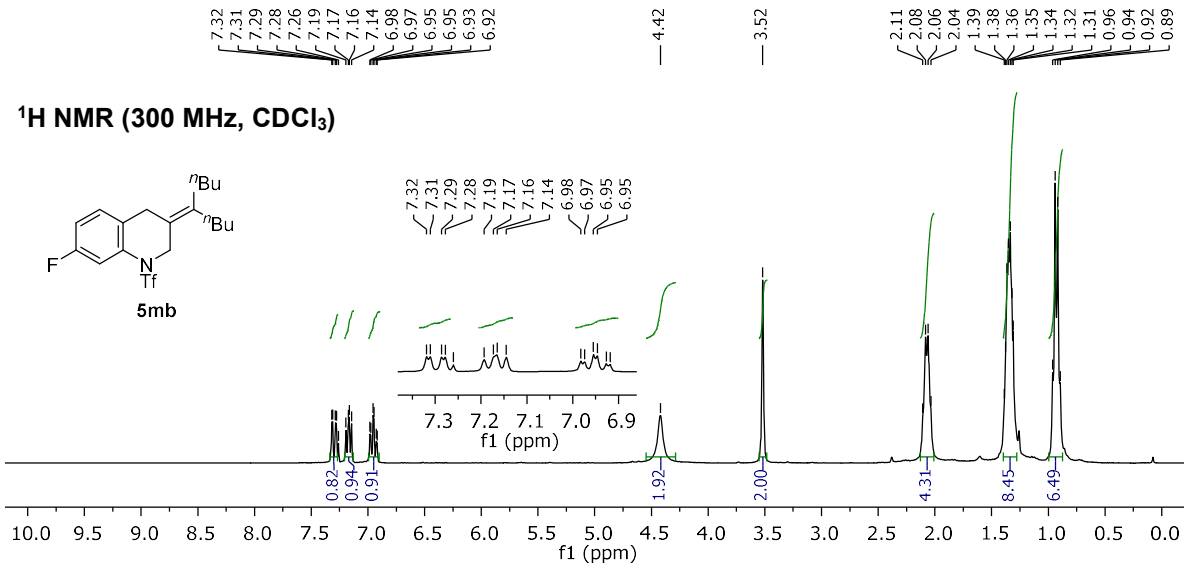

DEPT-135

^{13}C NMR (75 MHz, $CDCl_3$)

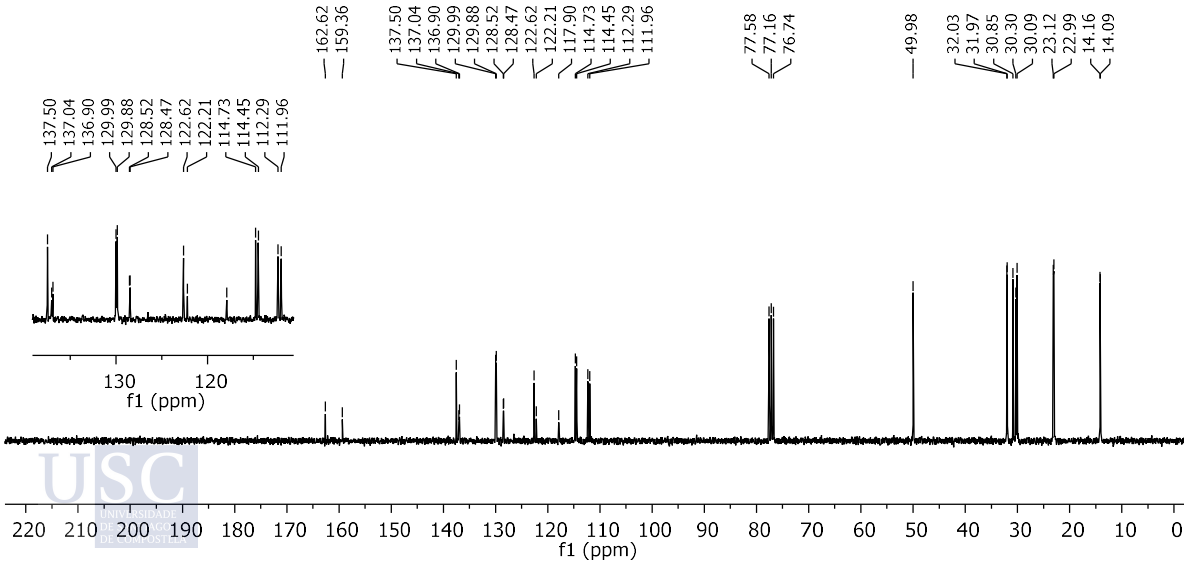

^{1}H NMR (500 MHz, $CDCl_3$)

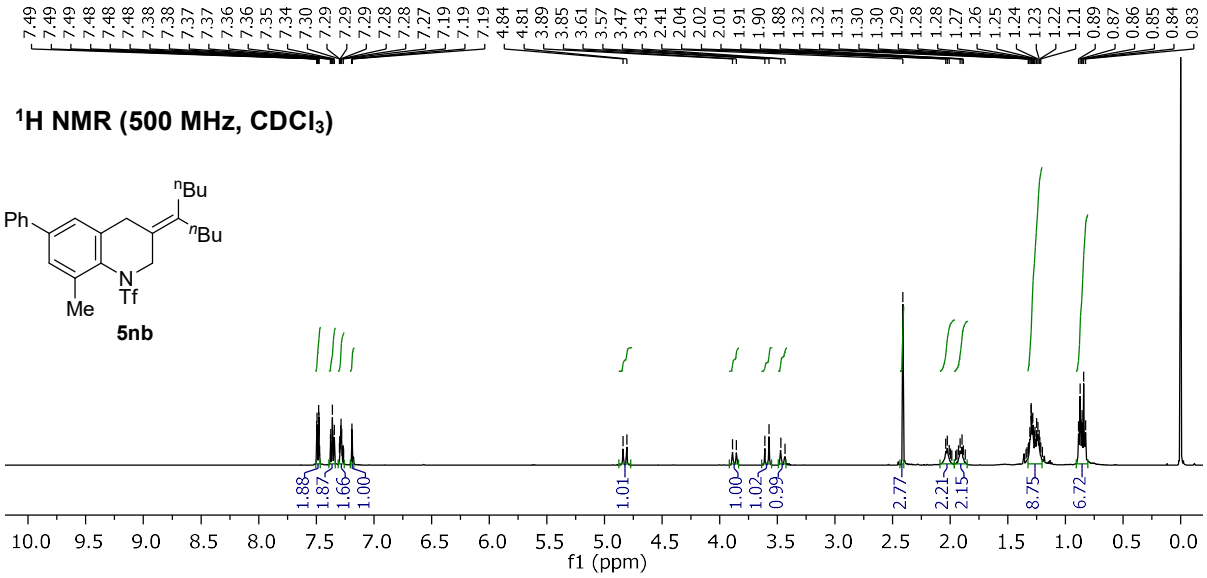

DEPT-135

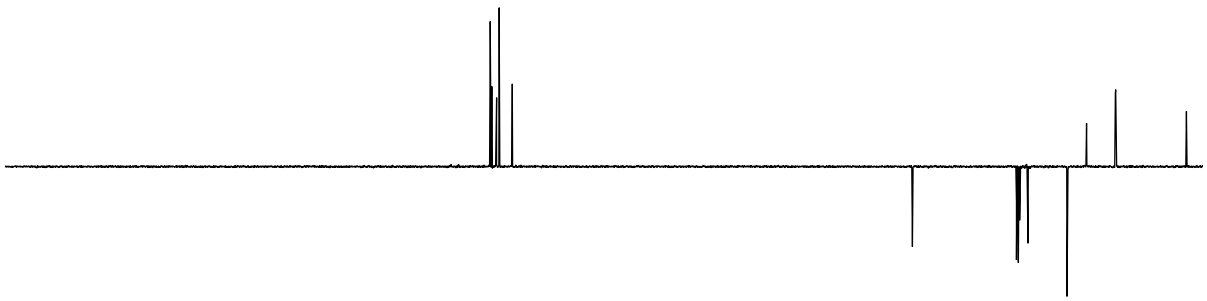

^{13}C NMR (126 MHz, $CDCl_3$)

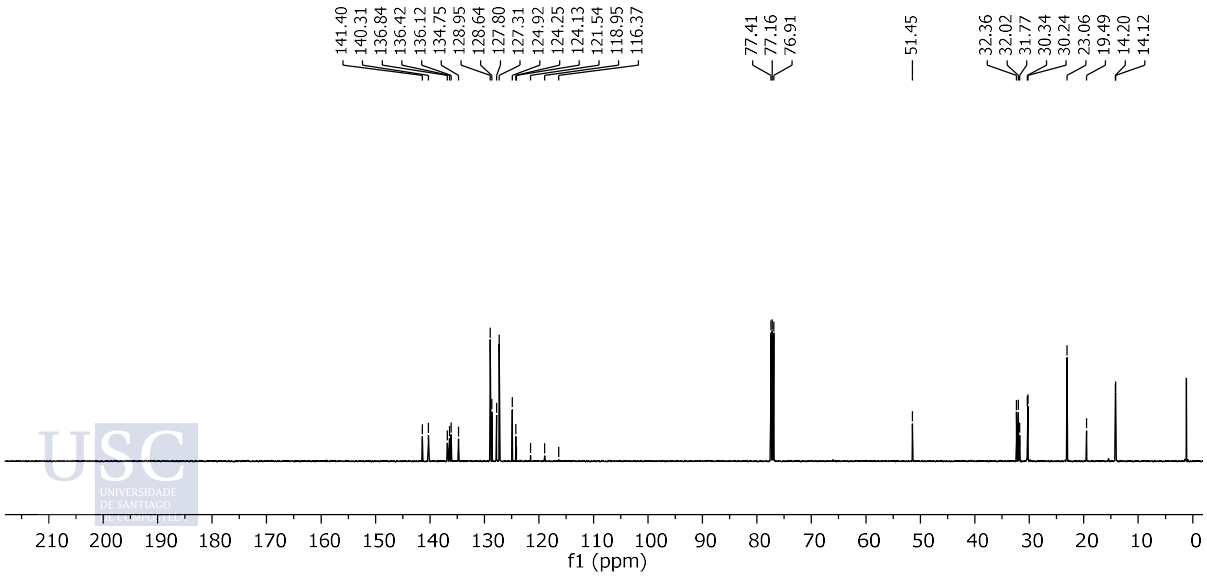

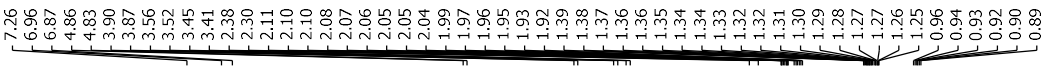

^{1}H NMR (500 MHz, $CDCl_3$)

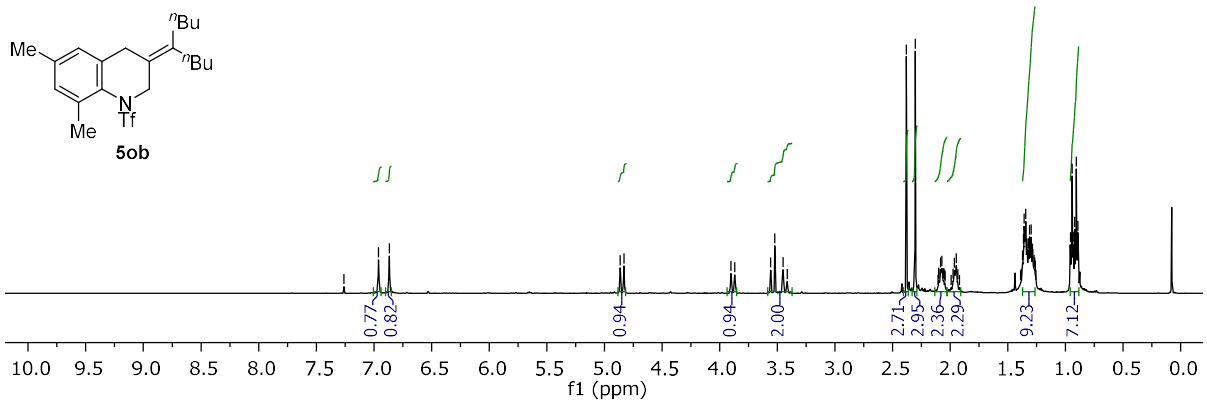

DEPT-135

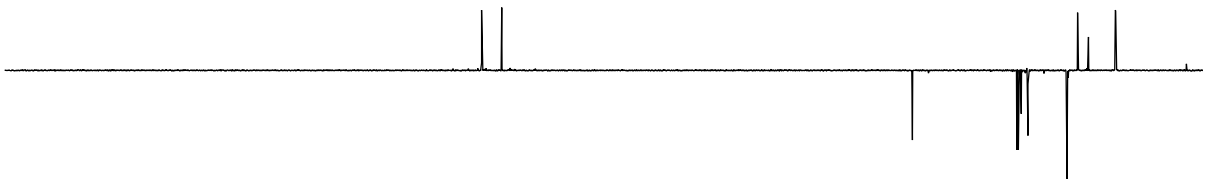

^{13}C NMR (126 MHz, $CDCl_3$)

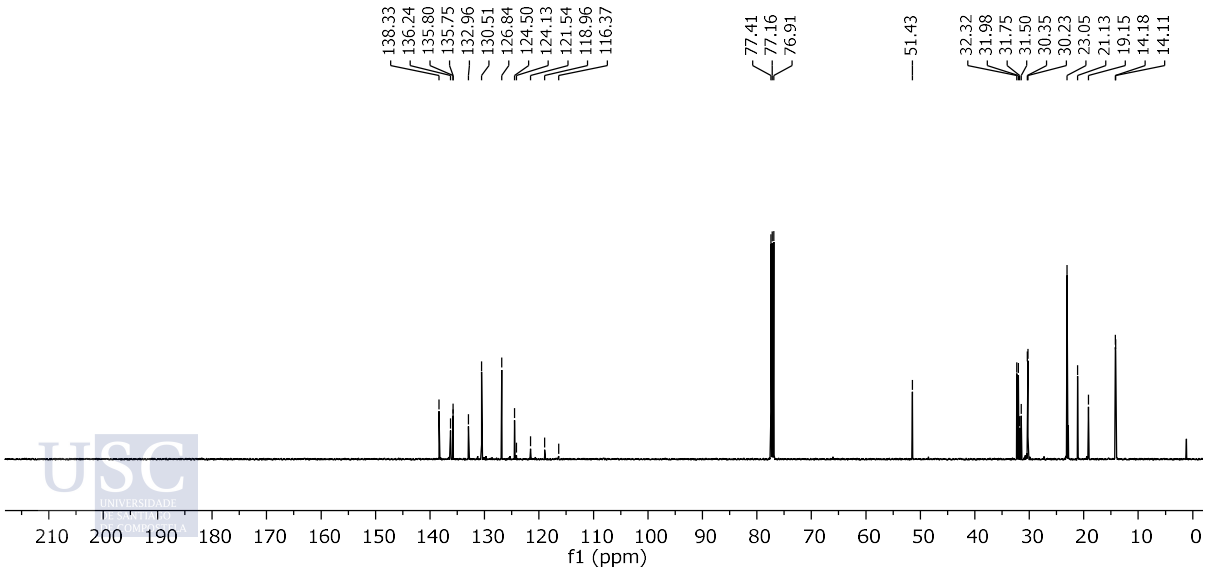

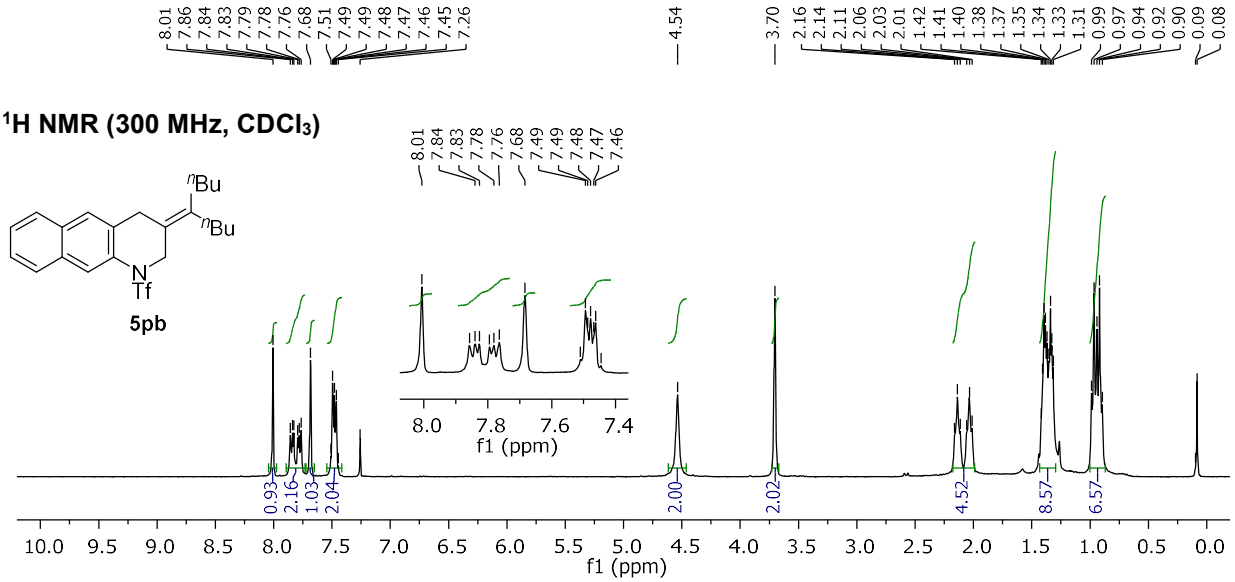

DEPT-135

^{13}C NMR (75 MHz, CDCl$_3$)

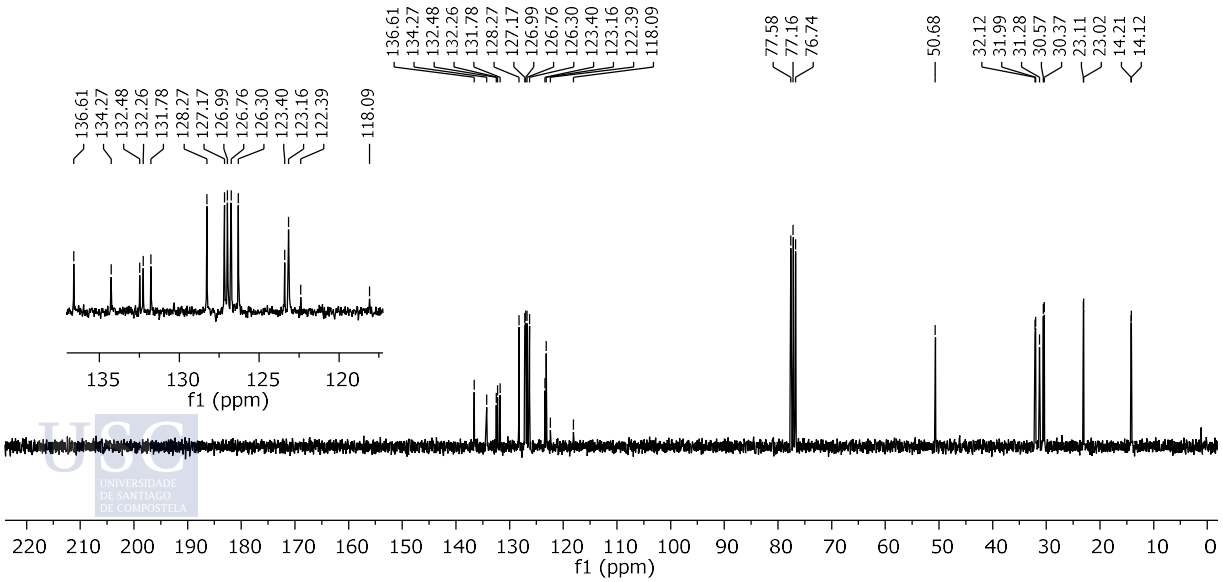

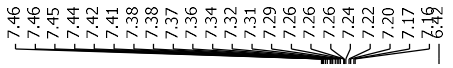

^{1}H NMR (500 MHz, $CDCl_3$)

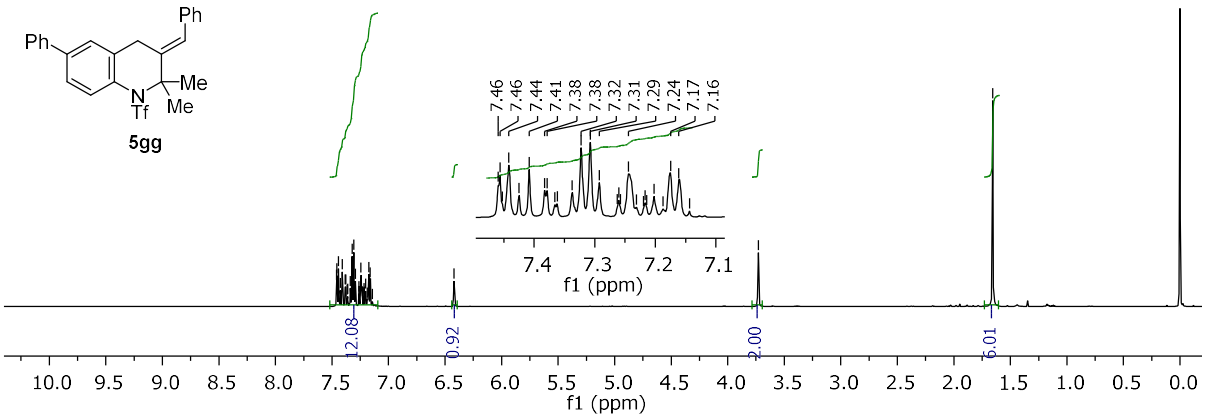

DEPT-135

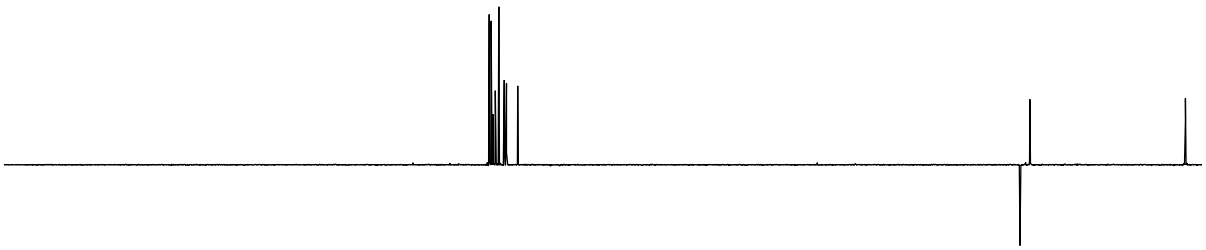

^{13}C NMR (126 MHz, $CDCl_3$)

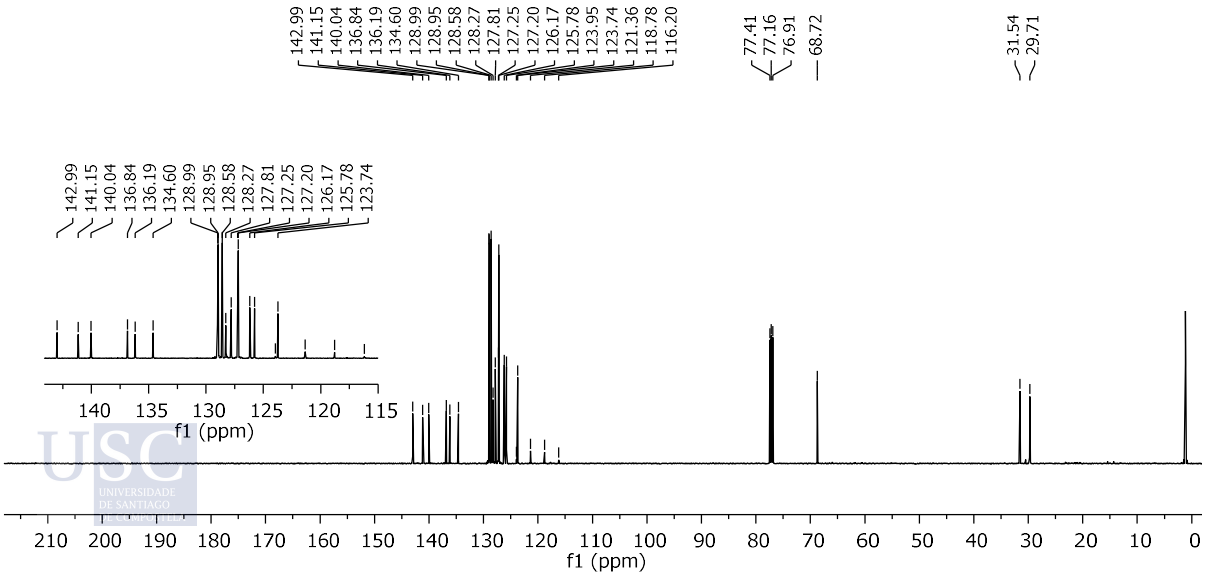

^{1}H NMR (300 MHz, $CDCl_3$)

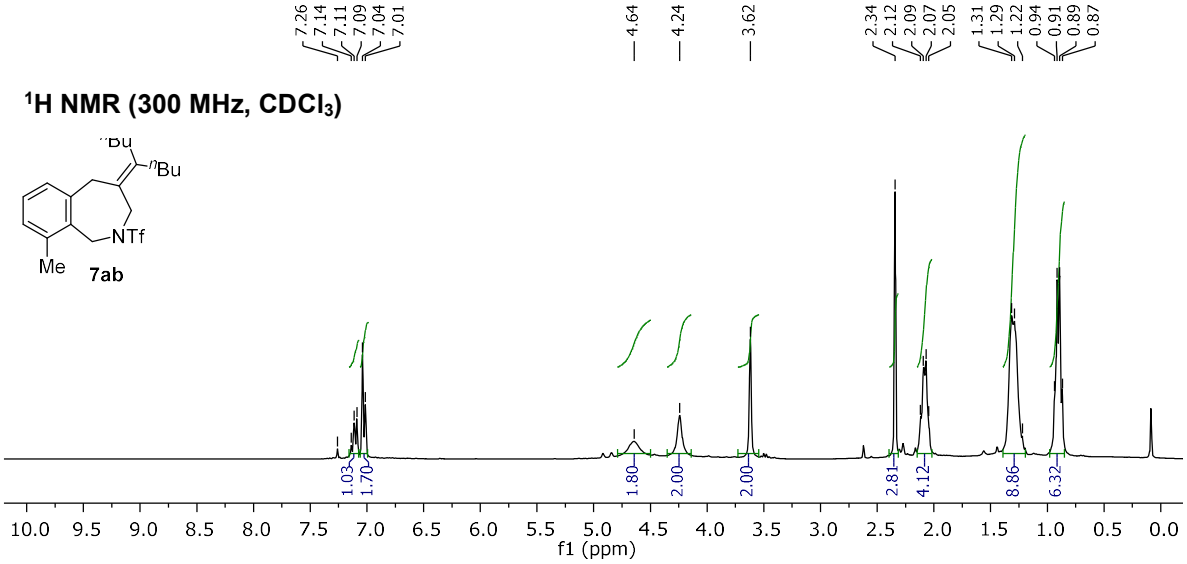

DEPT-135

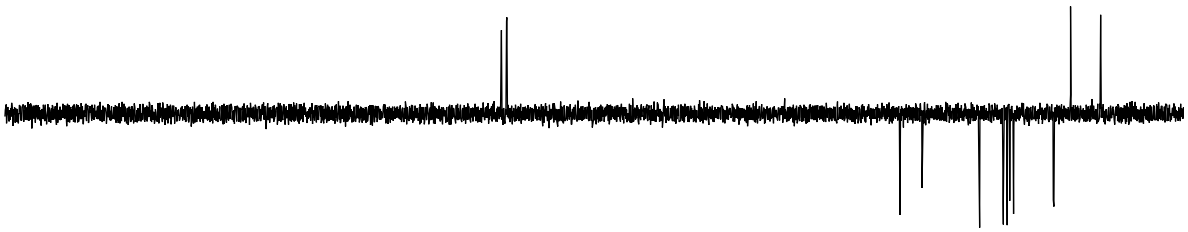

^{13}C NMR (75 MHz, $CDCl_3$)

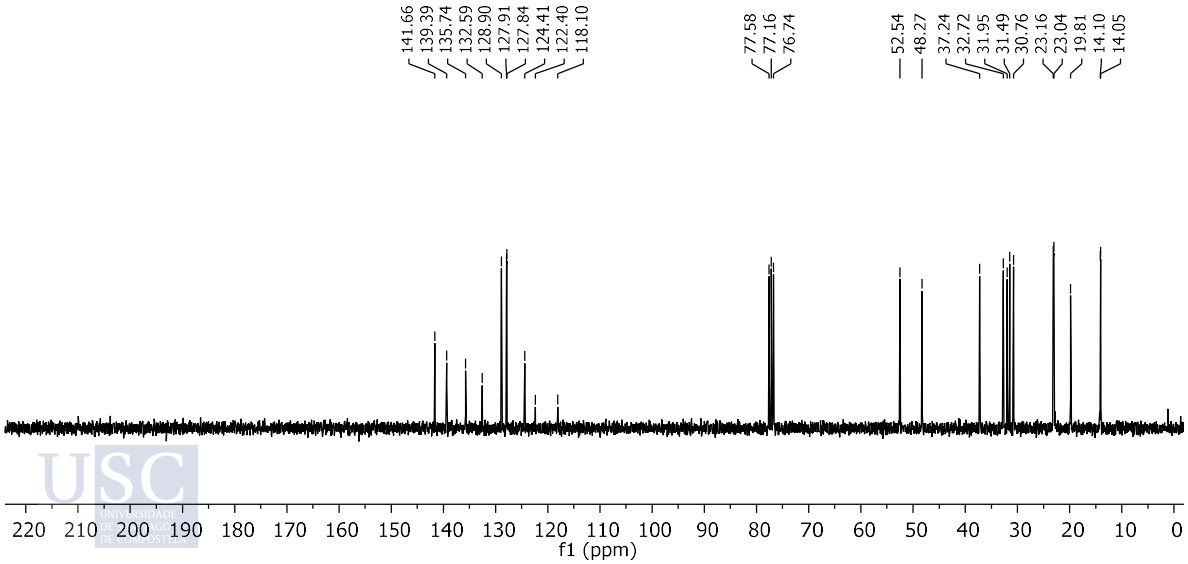

^{1}H NMR (300 MHz, $CDCl_3$)

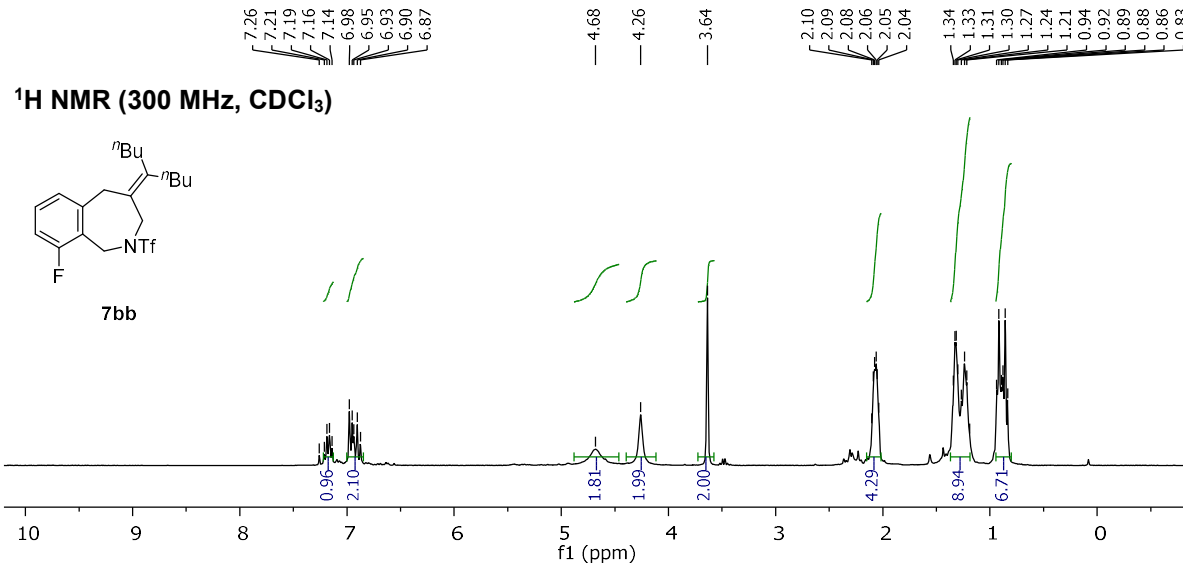

DEPT-135

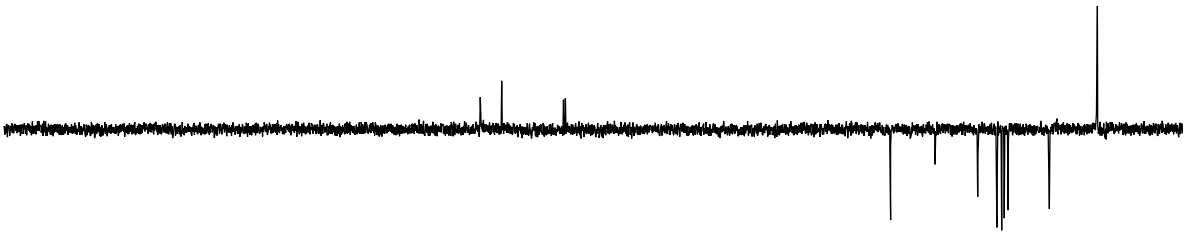

^{13}C NMR (75 MHz, $CDCl_3$)

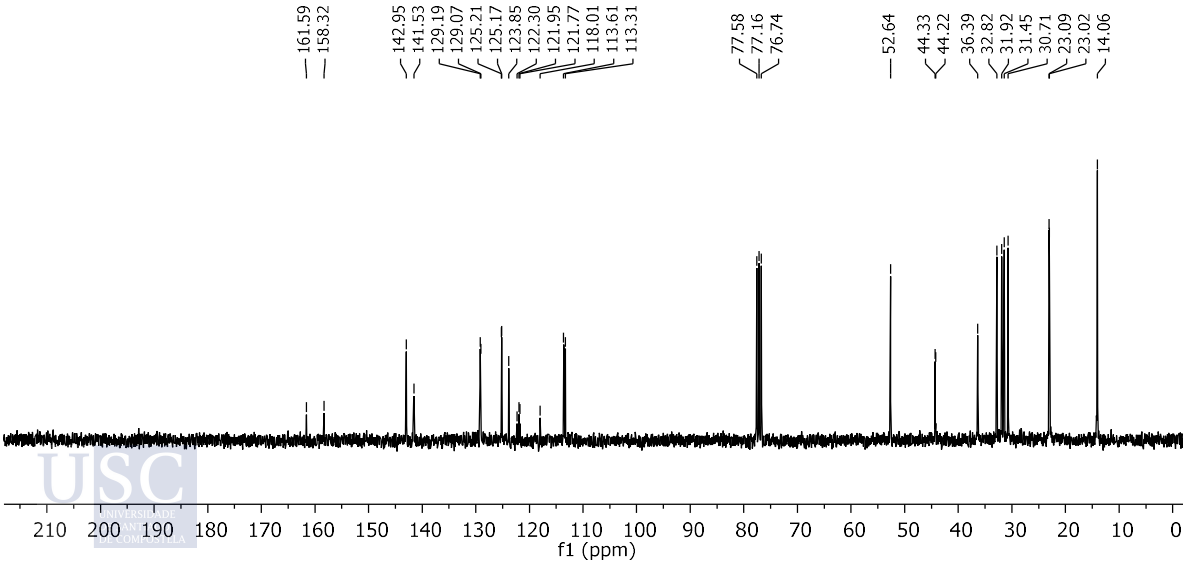

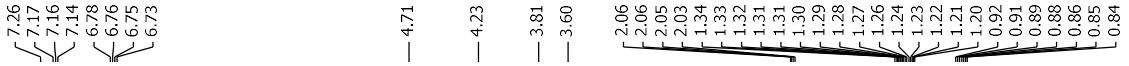

^{1}H NMR (500 MHz, $CDCl_3$)

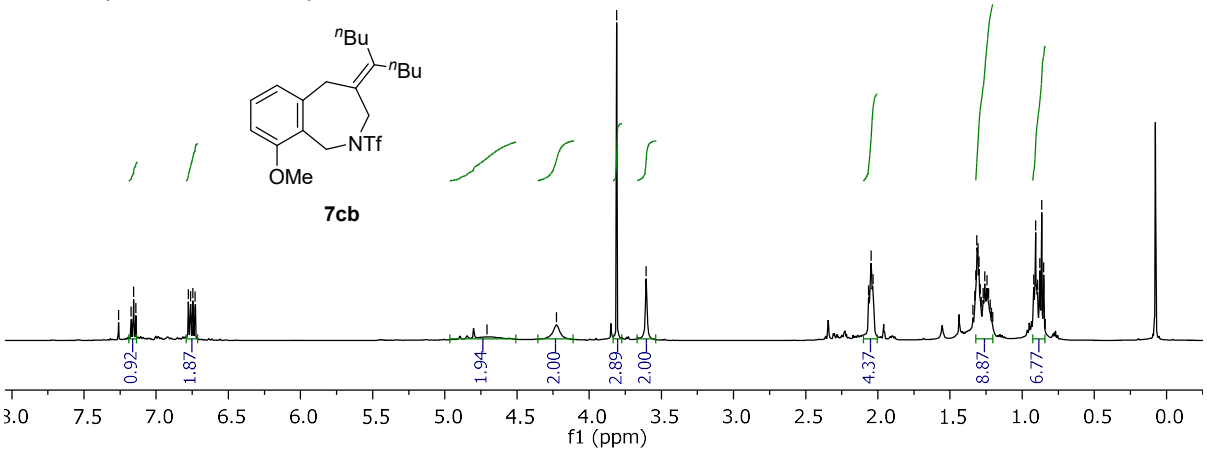

DEPT-135

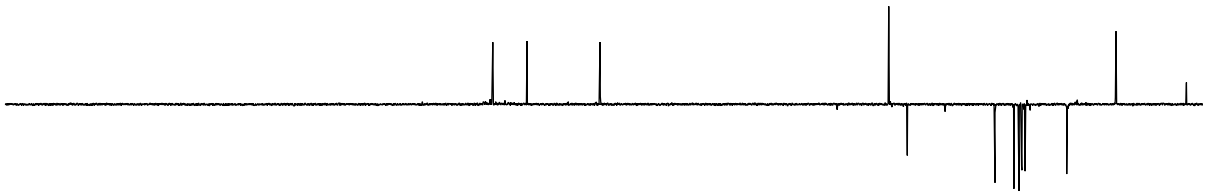

^{13}C NMR (126 MHz, $CDCl_3$)

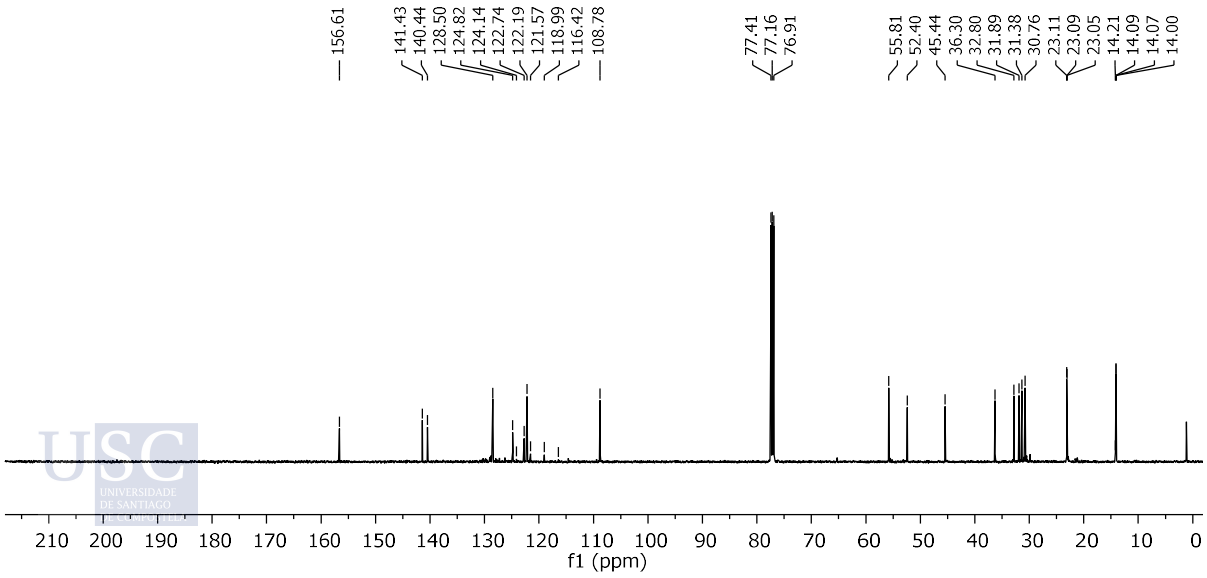

^{1}H NMR (300 MHz, $CDCl_3$)

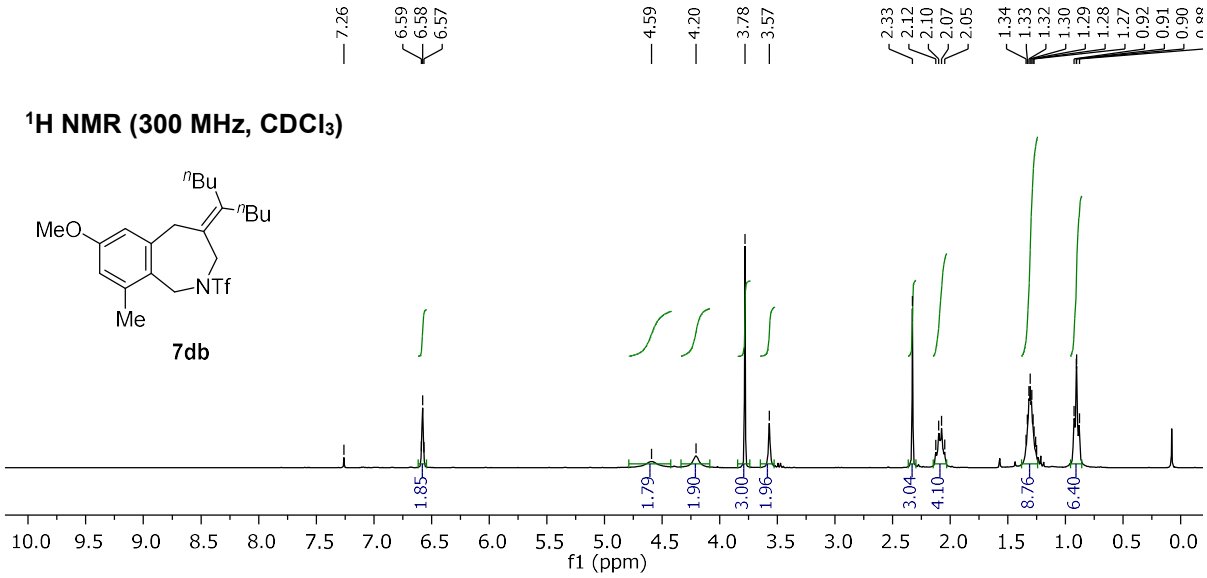

DEPT-135

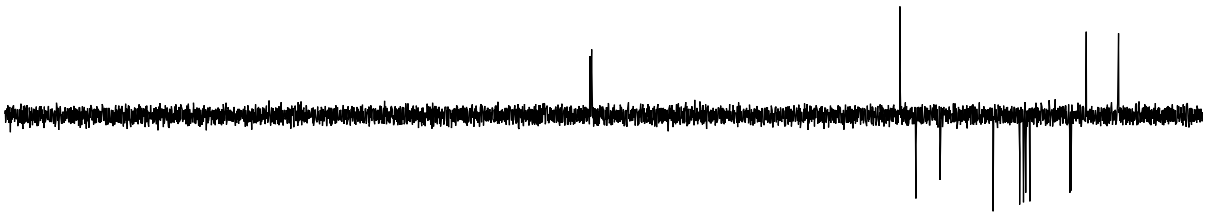

^{13}C NMR (75 MHz, $CDCl_3$)

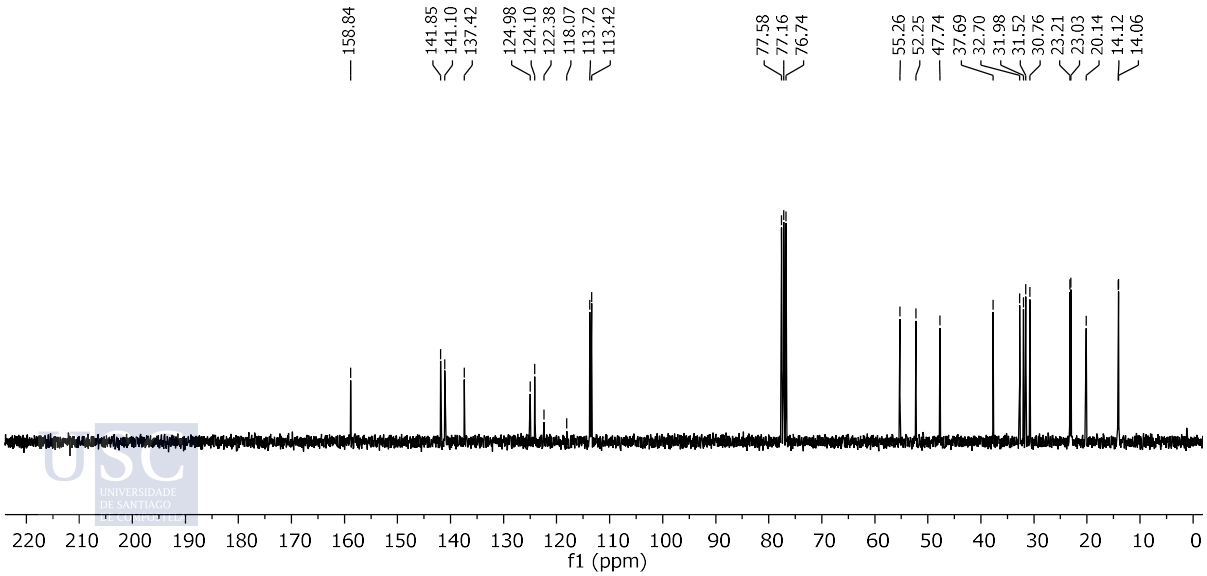

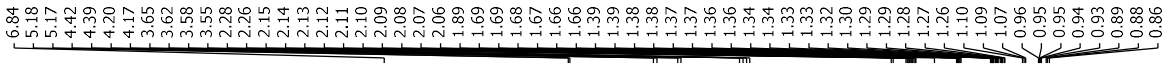

^{1}H NMR (500 MHz, $CDCl_3$)

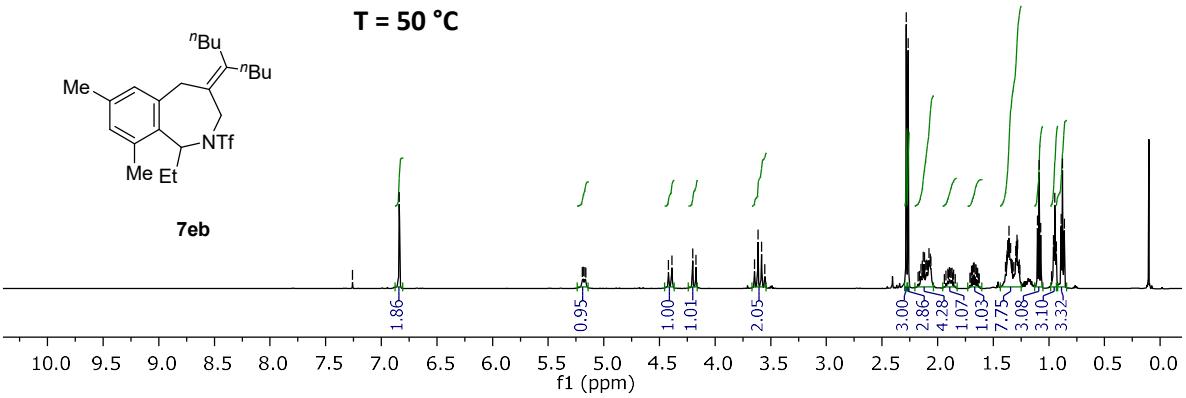

DEPT-135

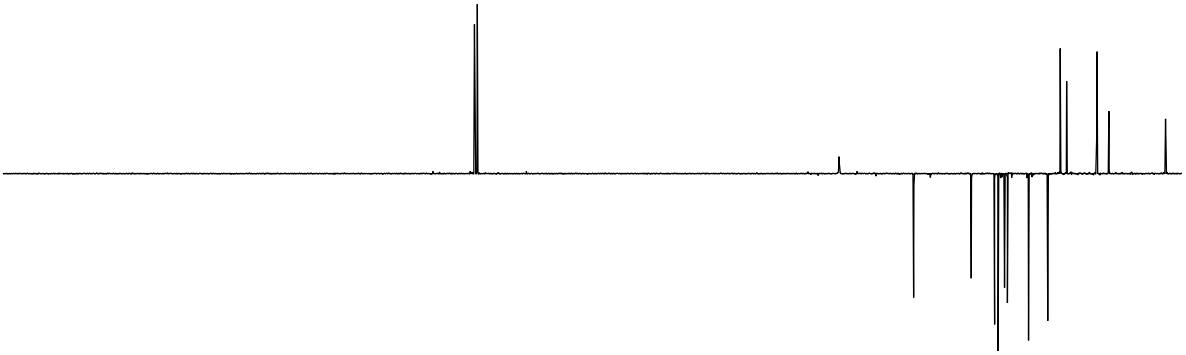

^{13}C NMR (126 MHz, $CDCl_3$)

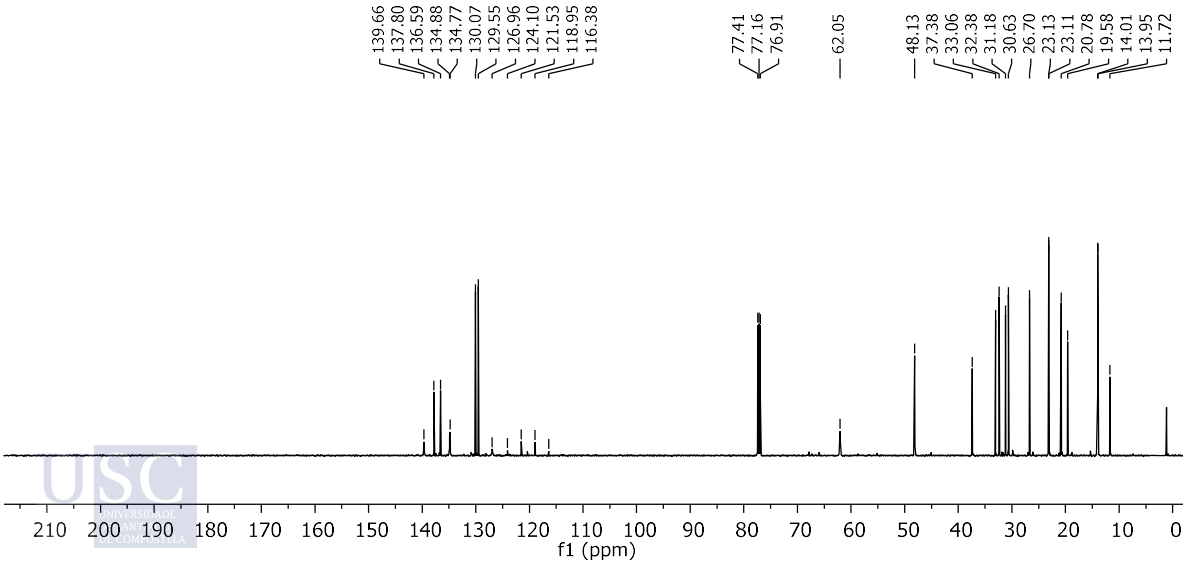

^{1}H NMR (300 MHz, $CDCl_3$)

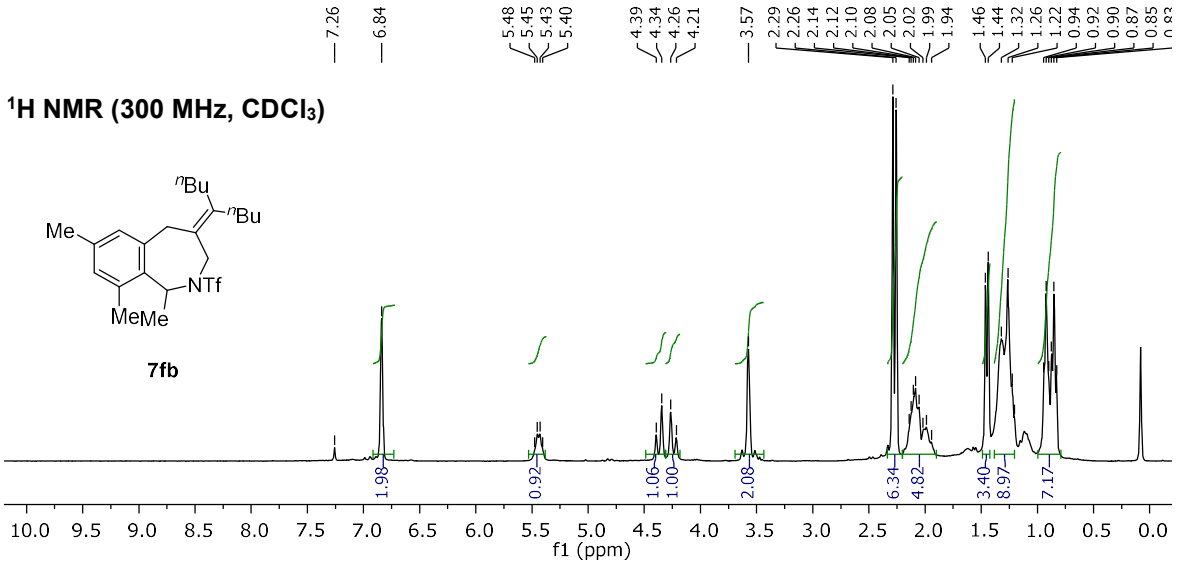

7fb

DEPT-135

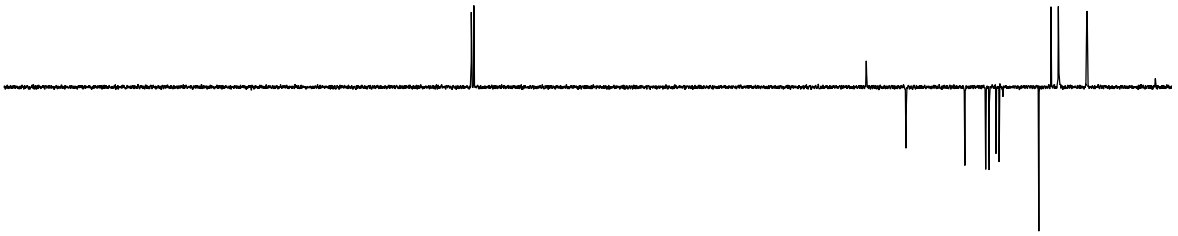

^{13}C NMR (75 MHz, $CDCl_3$)

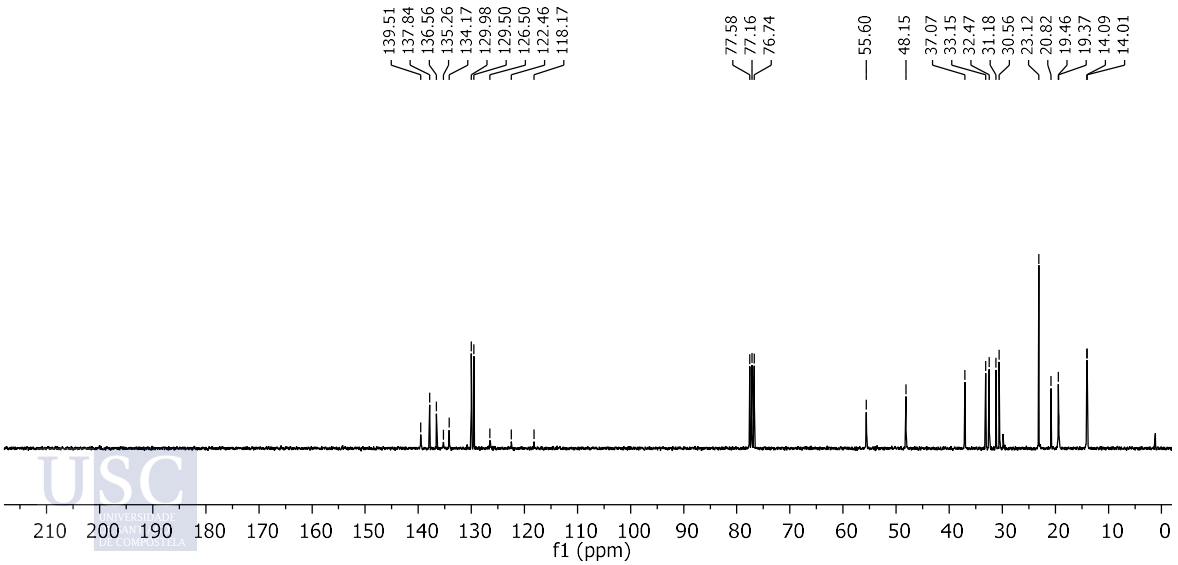

^{1}H NMR (300 MHz, $CDCl_3$)

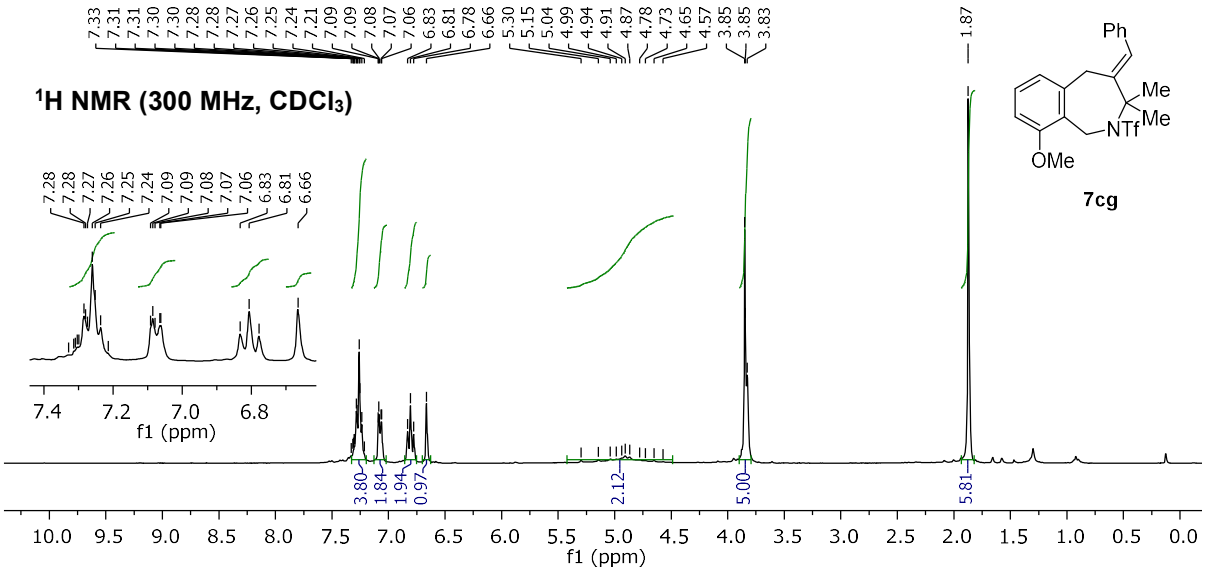

DEPT-135

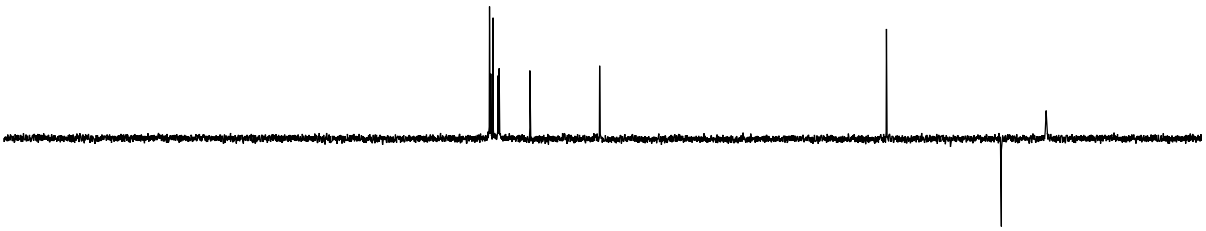

^{13}C NMR (75 MHz, $CDCl_3$)

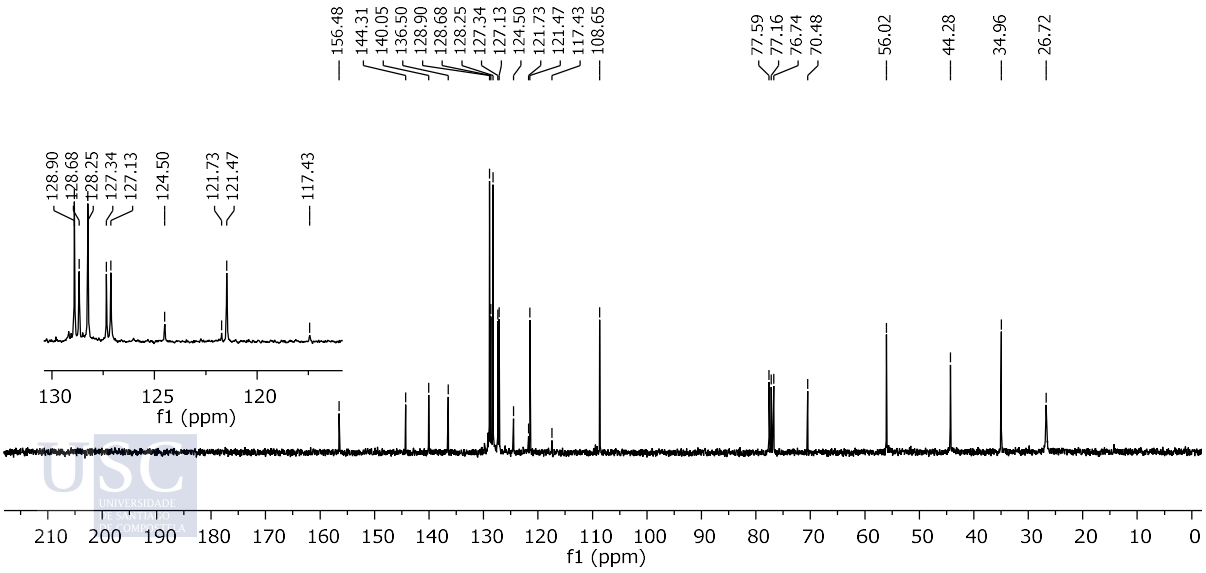

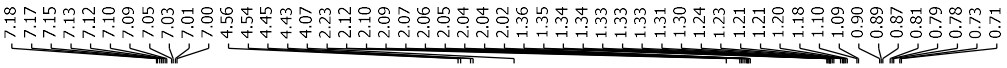

^{1}H NMR (500 MHz, $CDCl_3$)

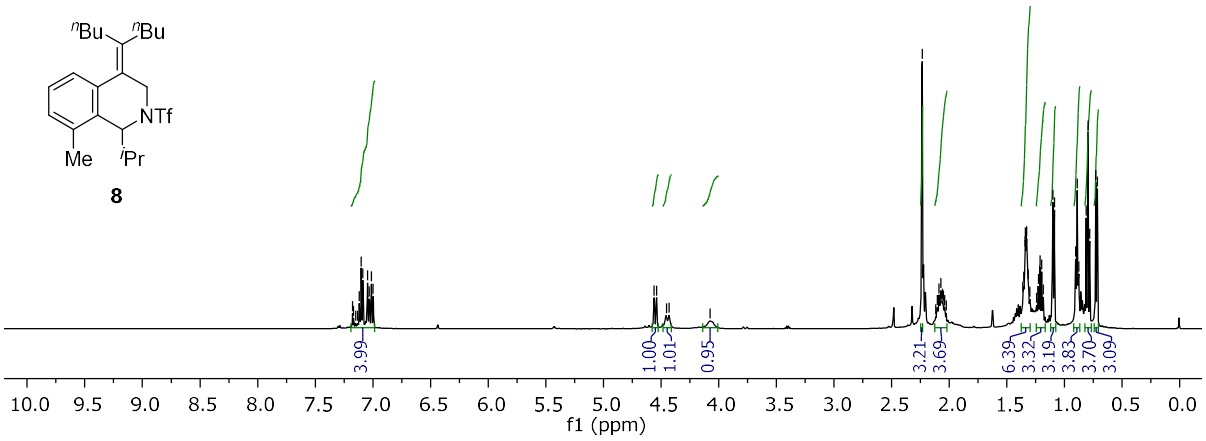

DEPT-135

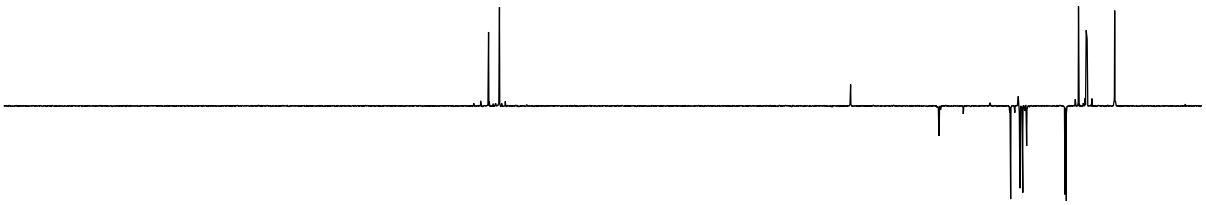

^{13}C NMR (126 MHz, $CDCl_3$)

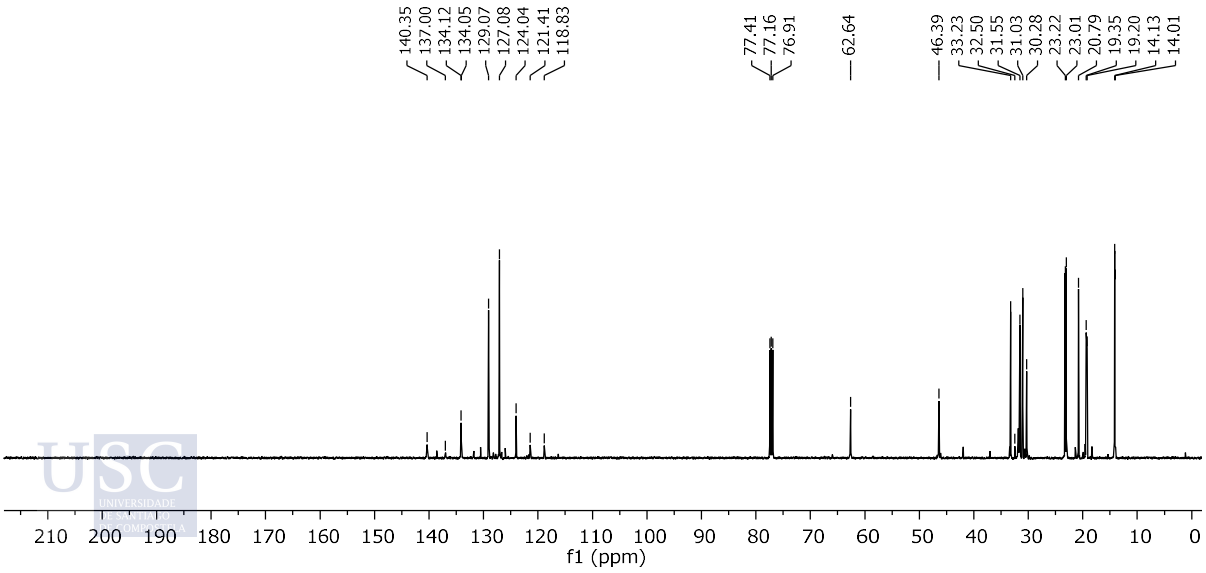

^{1}H NMR (300 MHz, $CDCl_3$)

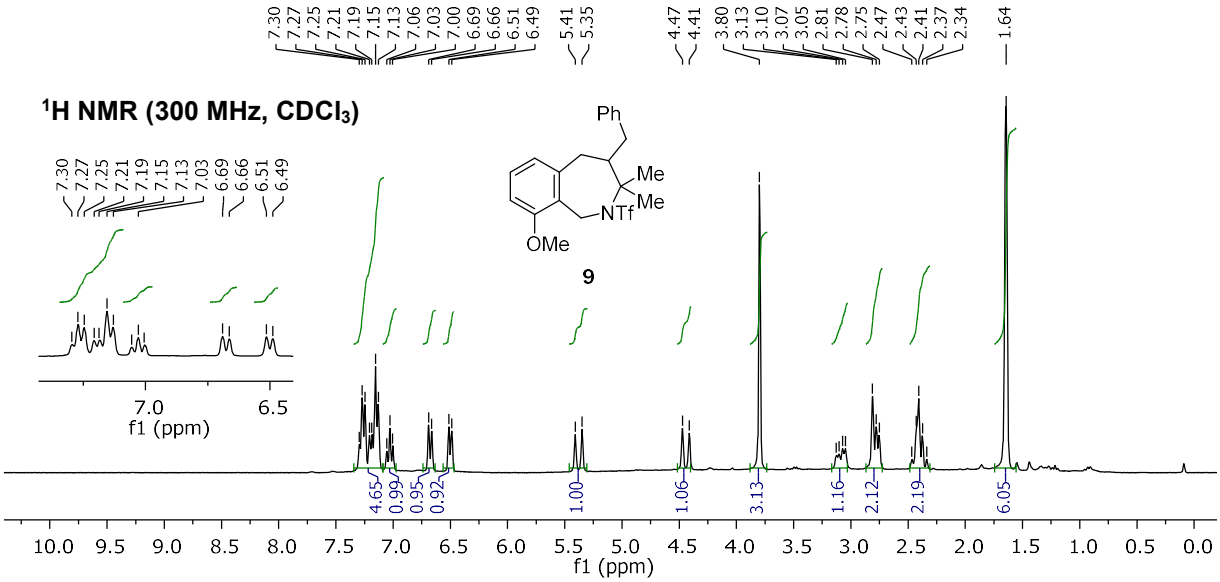

DEPT-135

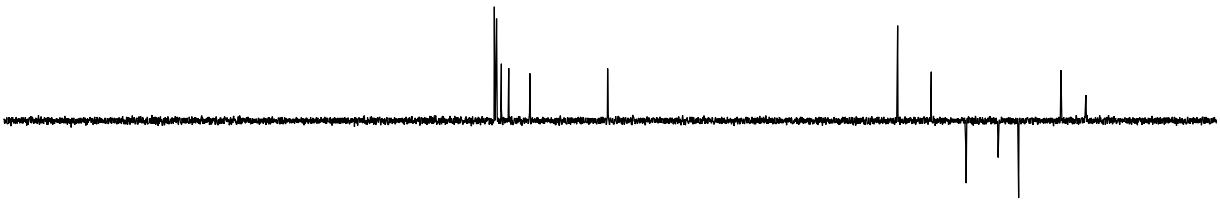

^{13}C NMR (75 MHz, $CDCl_3$)

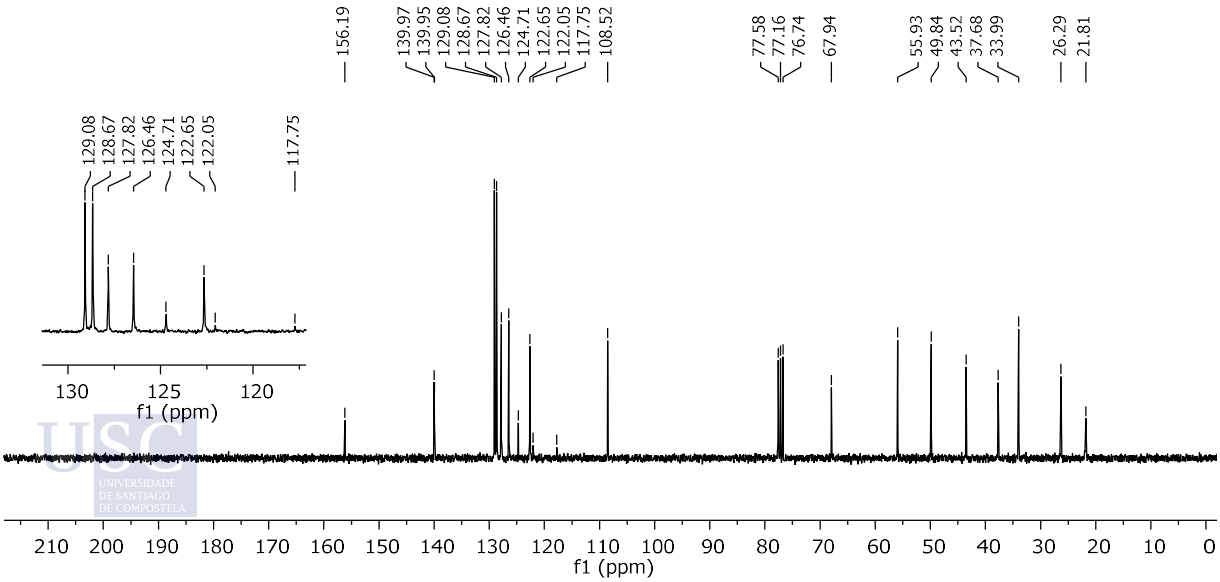

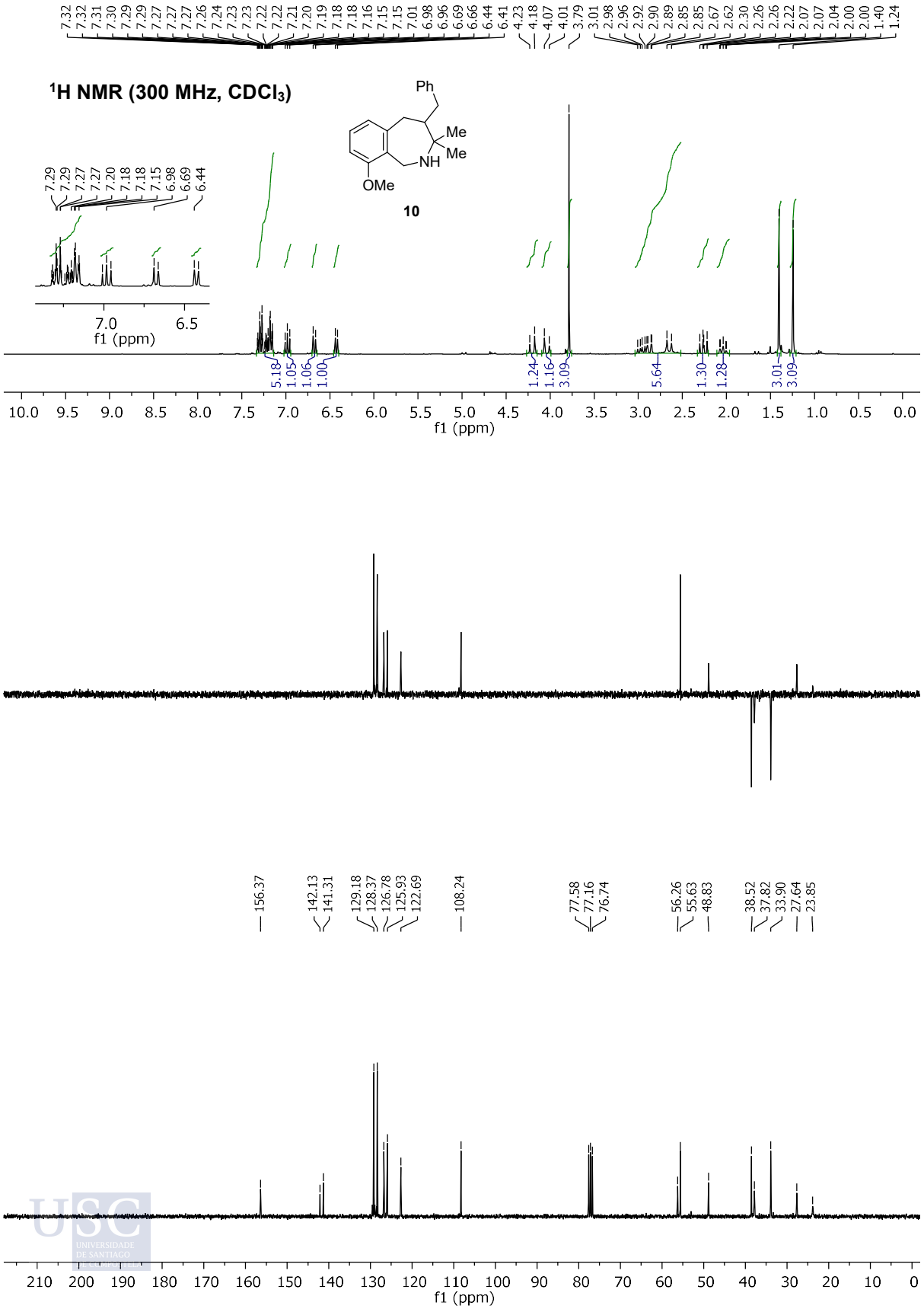

3-Selected spectra from Addendum

^{1}H NMR (500 MHz, $CDCl_3$)

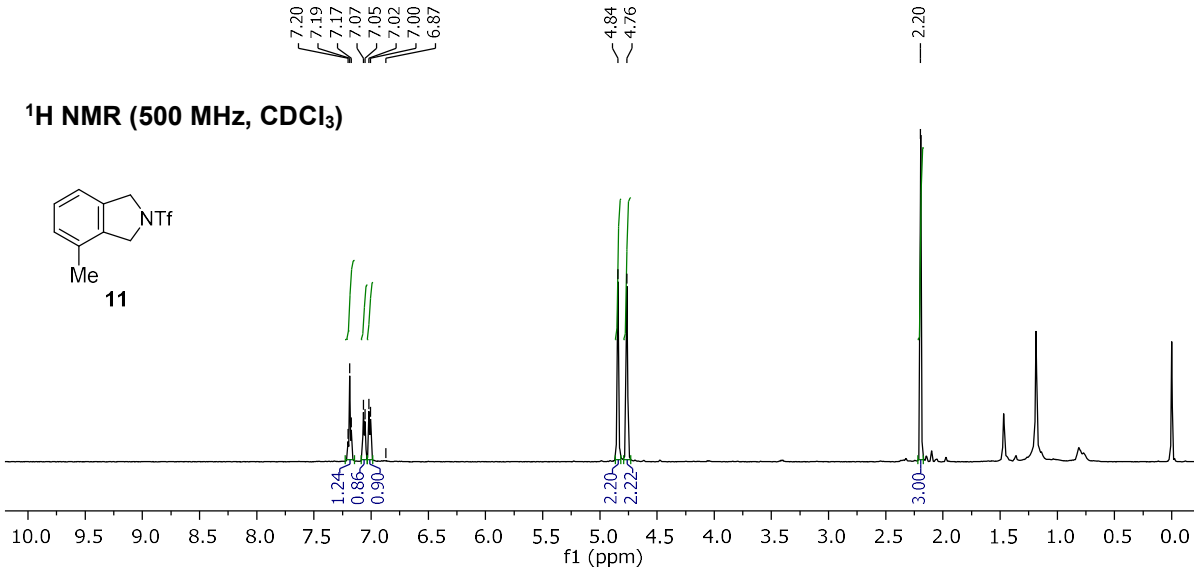

DEPT-135

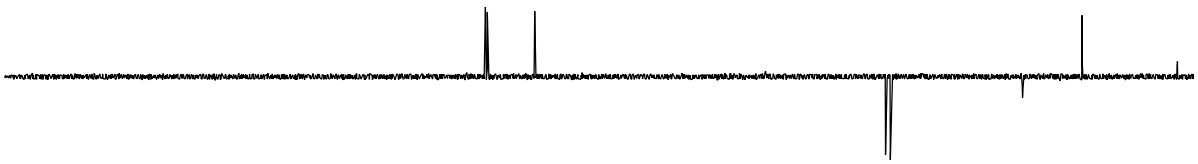

^{13}C NMR (126 MHz, $CDCl_3$)

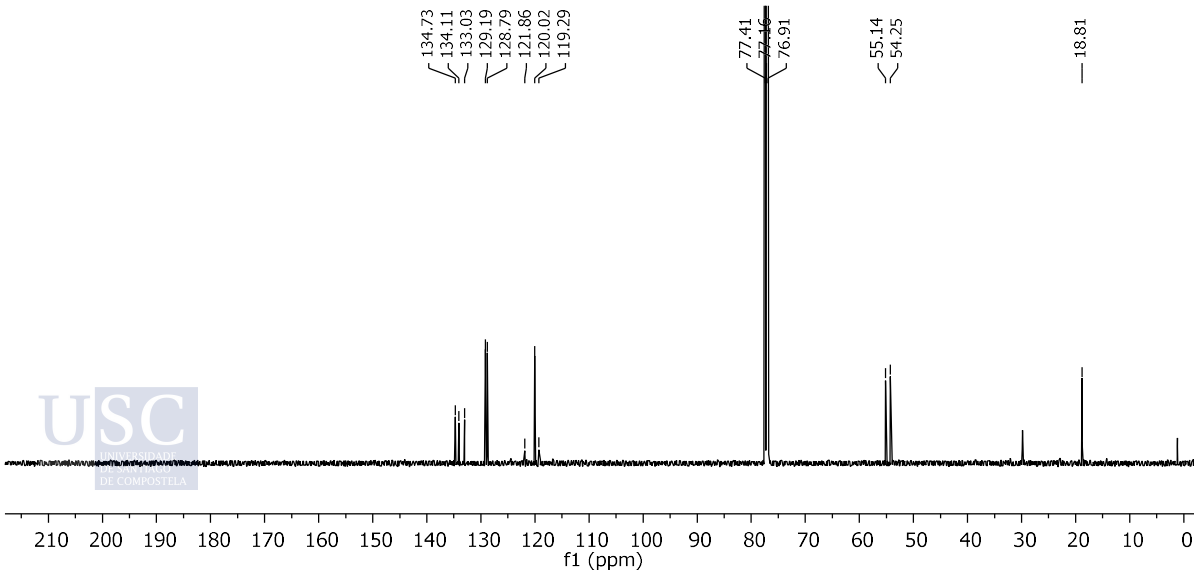

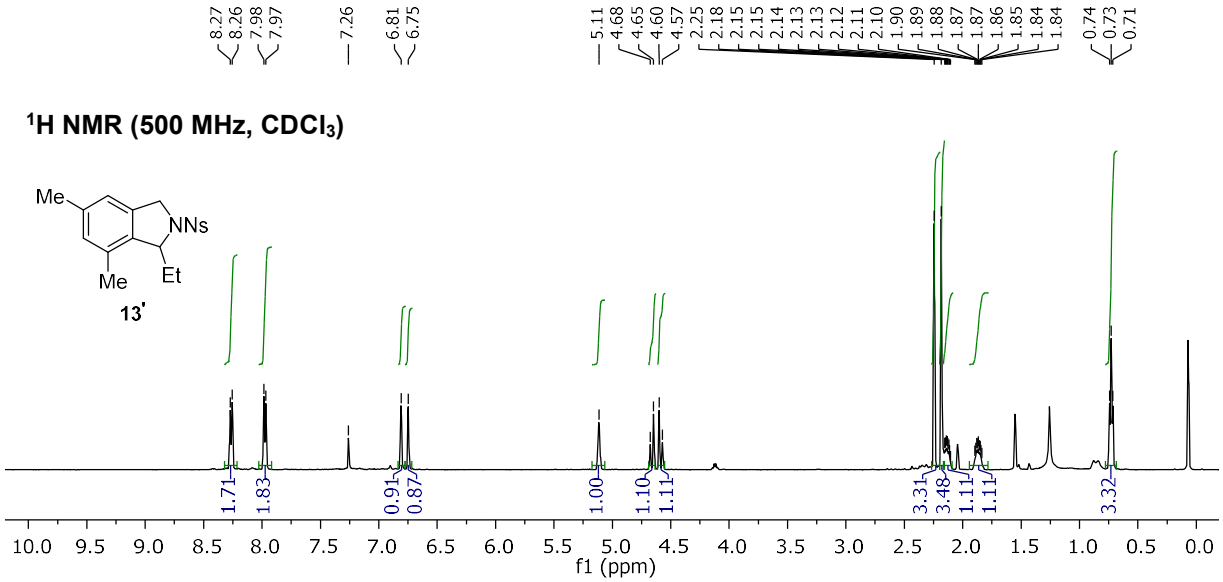

^{1}H NMR (500 MHz, $CDCl_3$)

DEPT-135

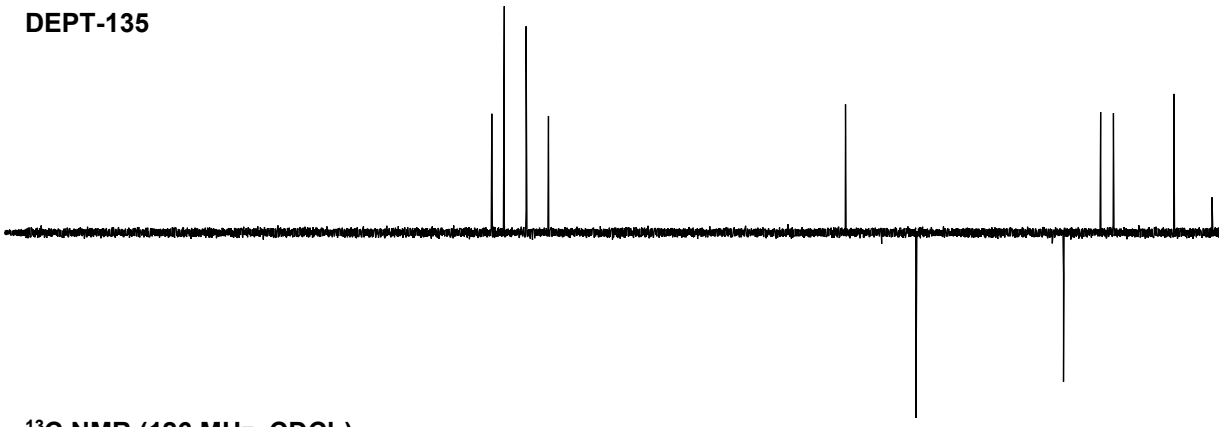

^{13}C NMR (126 MHz, $CDCl_3$)

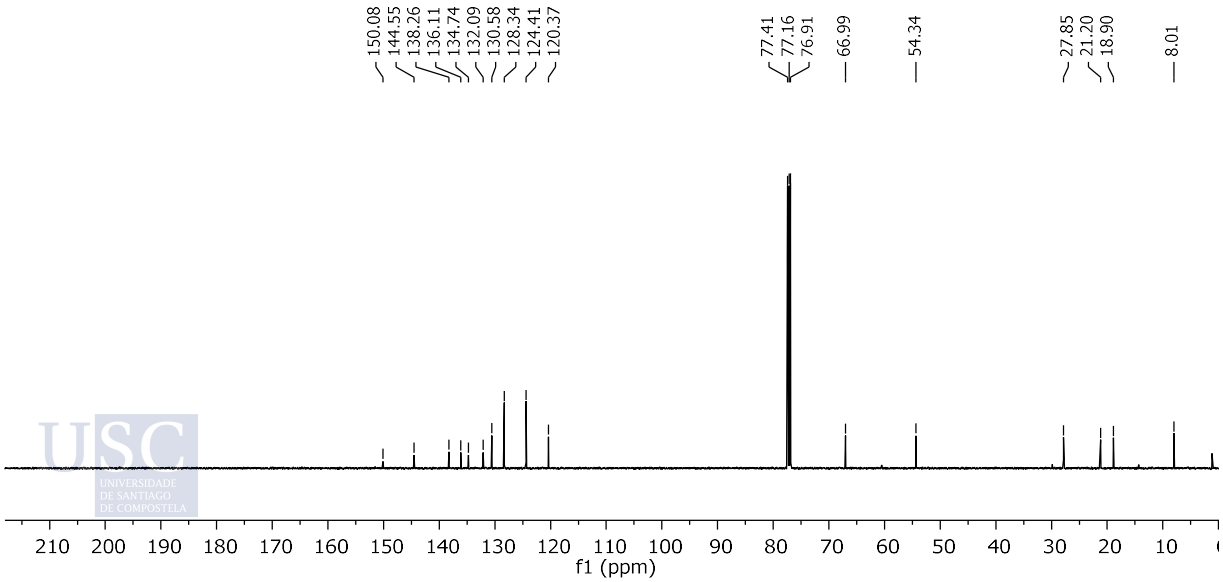

List of publications

Title	Palladium-Catalyzed, Enantioselective Formal Cycloaddition between Benzyltriflamides and Allenes: Straightforward Access to Enantioenriched Isoquinolines
Authors	Xandro Vidal, José Luis Mascareñas and Moisés Gulías
Year	2019
Journal	Journal of the American Chemical Society (*JACS*)
Volume, pages…	141, 1862-1866
Impact Factor	14.695
PhD student contribution	All the experimental data (yields and enantiomeric ratios) and synthesis and characterization of all the compounds.
Copyright	Open-access article (ACS AutorChoice article with CC-BY-NC-ND)

Title	Assembly of Tetrahydroquinolines and 2-Benzazepines by Pd-Catalyzed Cycloadditions Involving the Activation of C(sp^3)–H Bonds
Authors	Xandro Vidal, José Luis Mascareñas and Moisés Gulías
Year	2021
Journal	Organic Letters
Volume, pages…	23, 5323-5328
Impact Factor	6.005
PhD student contribution	All the experimental data (yields and enantiomeric ratios) and synthesis and characterization of all the compounds.
Copyright	Open-access article (ACS AutorChoice article with CC-BY)

Don't regret anything you do

because in the end

it makes you who you are

-Closer To The Edge, 30STM

During this PhD thesis we have developed several palladium-catalyzed formal cycloadditions involving the activation of both C(sp^2)–H and C(sp^3)–H bonds, using allenes as cycloaddition partners. These transformations allow to access highly valuable azaheterocyclic skeletons from simple starting materials in good yields. Moreover, asymmetric versions of these reactions have also been developed, making possible to achieve the corresponding cycloadducts with high enantioselectivities.